



INTERNATIONAL CONFERENCE ON

# HYDROLOGY AND WATER RESOURCES

ICHWR-2021

LAHORE-PAKISTAN, MARCH 25, 2021

## Conference Proceedings

Organized By:

Center Of Excellence in Water Resources Engineering  
University of Engineering and Technology, Lahore-Pakistan



*International Conference on*

# **HYDROLOGY AND WATER RESOURCES**

*ichwr-2021*

*Lahore-Pakistan, March 25, 2021*

## **Conference Proceedings**

**CENTRE OF EXCELLENCE IN WATER RESOURCES ENGINEERING**  
University of Engineering and Technology, Lahore-Pakistan

**Suggested citation:**

AUTHOR, A. (2021), Title of the Paper. In: International Conference on Hydrology and Water Resources 2021. Centre of Excellence in Water Resources Engineering: UET Lahore-Pakistan, pp. xx-xx. ISBN: [978-969-8670-06-01](#)

© 2021 Centre of Excellence on Water Resources Engineering, UET Lahore-Pakistan.

All rights reserved. Published 2021.

**ISBN: 978-969-8670-06-01**

The views expressed in this publication are those of the authors and do not necessarily reflect the views and policies of the Centre of Excellence in Water Resources Engineering (CEWRE), its Board of Governors, or any official.

CEWRE does not guarantee the accuracy and originality of the data included in this publication and accepts no responsibility for any consequence of their use.

CEWRE encourages printing or copying information exclusively for personal and noncommercial use with proper acknowledgment of CEWRE. Users are restricted from reselling, redistributing, or creating derivative works for commercial purposes without the express, written consent of CEWRE.

**Organizing Committee:**

Prof. Dr. Noor Muhammad Khan  
Dr. Muhammad Kaleem Sarwar  
Dr. Ijaz Ahmad  
Engr. Faraz-ul-Haq  
Engr. M. Awais Zafar

Chairman  
Coordinator  
Secretary  
Member  
Member

**Editors:**


- Dr. Ijaz Ahmad
- Engr. Faraz-ul-Haq

**Compiled By:**

- Engr. M. Awais Zafar
- Engr. Faraz-ul-Haq
- Engr. Rana Zain Nabi Khan

Centre of Excellence on Water Resources  
Engineering  
UET, G.T. Rd, Lahore- Pakistan. 54890  
Tel: +92 42 99250257  
Fax: +92-42-99250259  
Email: [cewre@cewre.edu.pk](mailto:cewre@cewre.edu.pk)  
[www.cewre.edu.pk](http://www.cewre.edu.pk)

For orders, please contact:  
Conference Organizing Committee  
Tel: +92 42 99250257  
Email: [ichwr@cewre.edu.pk](mailto:ichwr@cewre.edu.pk)

 Printed on recycled paper.

# FOREWORD



Since the establishment of the Centre of Excellence in Water Resources Engineering (CEWRE) in 1976, we have contributed to the nation through highly qualified professionals in the field of water resources. Over the forty years period, needs of the nation have changed from the fighting the twin menace of water logging and salinity to assuring the availability of water to stakeholders especially the irrigation and hydropower sectors of Pakistan. This Centre has contributed to bring an end to the water logging-salinity menace by imparting relevant engineering knowledge and technologies to the graduate engineers of the country and preparing them to combat the debacle successfully.

Maintaining its tradition of imparting knowledge, skill and aptitude, the Centre has successfully conducted conferences, seminars, symposia, training workshops, webinars and trained over 300 professionals through continued professional development (CPD) drive in water resources and allied disciplines in year 2020. During the year 2020, marked with COVID-19 Pandemic, with extended months long curfews and lockdowns been initiated by Governments all across the globe, all conference activities including academic learning and growth has come to a halt. Therefore, in this critical period of pandemic to promote educational and research activities, CEWRE had decided to organize the International Conference on Hydrology and Water Resources (ICHWR). The aim of this conference was to provide a stage for exchanging the latest research results and sharing the advanced research methods in related fields.

Despite the COVID -19 closures of educational institutes all over the country, the Centre has maintained its standard of high performance without sacrificing the regular academic curriculum and the quality aspects, through shifting to online cum distance learning (ODL) way of teaching. I am personally thankful to Centre's faculty and staff, and the University management for their cooperation in the stress period of COVID -19 pandemics. Without their contribution, this gigantic task of delivering high quality education, trainings and research was not possible.

We wish to continue this conference at least once in a year so that the knowledge which we gathered could be shared. I hope and believe that we shall overcome the issues of water stress, floods, energy shortages, and food issues through our continuous efforts and resolve to make a better sustainable Pakistan for our future generations before it is too late.

**Director**



# Vice Chancellor's Message



## Prof. Dr. Syed Mansoor Sarwar

Vice Chancellor

University of Engineering & Technology, Lahore

It is my profound privilege and honour to welcome you all, at the inaugural session of the international conference on **Hydrology and Water Resources** organized by the Centre of Excellence in Water Resources Engineering at University of Engineering and Technology Lahore, Pakistan.

Respected Minister, I am grateful to you for sparing time out of your extremely busy schedule to grace this occasion. Your presence here in the galaxy of researchers, engineers and scientists in water sector truly signifies the importance of the subject.

Ladies and gentlemen, we all know that Water is vital resource for human well-being and functioning of the ecosystem. But the availability of fresh water is stressed due to factors like population growth, enhanced living standards, and continuous degradation of freshwater resources. Sustainable water resources management is only possible through concerted efforts of the political leadership and the research community.

In this context, the prime objective of this conference is to provide a platform for sharing the knowledge and recent research gathered at individual water related institutes around the world and to come up with agenda for future research and action.

UET Lahore, the pioneer institute of higher learning in the country has several departments dealing with various aspects of water development, water quality and quantity issues. Centre of Excellence in Water Resources is one of such platforms imparting high quality teaching and learning in the field of water resources. UET Lahore is playing its role in resolving the water related issues through human resource development and research activities. Hundreds of UET graduates are managing the water resources of country in Public and Private Sectors including but not limited to Punjab Irrigation Department, WAPDA, Federal Flood Commission, UNESCO, etc.,

Finally, I sincerely hope that there will be a fruitful exchange of ideas and experiences among the scientists and engineers of Pakistan and foreign countries.

Respected Chief Guest, Speakers, and Participants, I once again extend sincere gratitude on my behalf and on behalf of the Organizing Committee of the Conference for your presence in the inaugural session of this International Conference on Hydrology and Water Resources. This is a source of immense encouragement for all of us.

Also I would like to acknowledge the efforts of the Faculty and Staff of the Centre of Excellence for arranging this important conference, and I expect a very knowledge full and fruitful event today.

Thanks a lot.

## Chief Guest



### Muhammad Mohsin Khan Leghari

Minister of Punjab for Irrigation  
Government of Punjab

Water is life and life cannot be imagined without it. When there is a shortage of electricity, new plants can be installed, if there is a gas or petroleum shortage, it can be imported but for water, it has what nature has given to us and we must use it wisely. Water is meant differently for different people. As the population increases, the value of water increases. At one time, Pakistan was water abundant with an availability of 6000 m<sup>3</sup> per person but now its availability is limited to 800-1000 m<sup>3</sup> per person. Pakistan is ranked 17<sup>th</sup> among the countries with the availability of freshwater. However, we need to tap and use it efficiently. Efforts were made in the past, but their pace needs to be increased. We must share research with actual users of society. Unless we share the knowledge and interact with each other, we cannot be useful to society. The water sector is facing problems due to its aging infrastructure. Governance is the main issue in the management of water resources rather than the water shortage. Therefore, the interaction between Government, industry, and academia is necessary and government cannot survive without taking help from academia. Government and academia must engage with each other to come up with the solution for better productivity. They must research how we can use the limited water we have.

Therefore, I request to University of Engineering and Technology, Lahore to come up with the issues and their feasible solutions. Thank you for giving me the opportunity to be with you.

# Organizing Committee



**Dr. Noor Muhammad Khan**  
Conference Chairman



**Dr. Muhammad Kaleem Sarwar**  
Conference Coordinator



**Dr. Ijaz Ahmad**  
Conference Secretary



**Engr. Faraz ul Haq**  
Member



**Engr. Muhammad Awais Zafar**  
Member

<b>Inaugural Session</b>		
08:30 AM - 09:00 AM	Online Joining	MS Teams
9:00 AM - 09:05 AM	Recitation of Holy Quran	Hafiz Hammad Ahmad
9:05 AM - 09:15 AM	Welcome to Distinguished Guests, Keynote speakers, Authors and Participants	Prof. Dr. Noor Muhammad Khan, Director, CEWRE
09:15 AM - 09:25 AM	Welcome address by Vice Chancellor, UET Lahore	Prof. Dr. Syed Mansoor Sarwar, VC, UET, Lahore
09:25 AM - 09:35 AM	Opening Speech by Chief Guest	Muhammad Mohsin Khan Leghari, Minister for Irrigation, Punjab, Pakistan
09:35 AM - 09:50 AM	Keynote Lecture	Prof. Dr. Habib-ur-Rehman, UET Lahore, Pakistan
09:50 AM - 10:05 AM	Keynote Lecture IoT Applications in Flash Flood Control Systems	Prof. Dr. Zahiraniza Mustaffa, University Teknologi PETRONAS, Malaysia
10:05 AM - 10:20 AM	Keynote Lecture	Engr. Shahid Hameed, GM WAPDA
<b>Technical Session-I</b> <b>Session Chair: Dr. Ghulam Nabi</b> <i>Repporteour: Engr. Muhammad Awais Zafar</i>		
10:30 AM - 10:45 AM	Special Lecture Role of Water Resources in Sustainable Development	Dr. Ali Asghar Iraqpoor, Islamic Azaad University, Iran
10:45 AM - 10:55 AM	Auto-calibration and uncertainty analysis of SWAT Model for Haro River Watershed using Sequential Uncertainty Fitting (SUFI-2) algorithm.	Saima Nauman, University of Lahore
10:55 AM – 11:05 AM	Laboratory Measurements of Velocity and Hydrodynamic Force Over Coarse Fixed Rough Bed	Muhammad Zain bin Riaz, Uni of Wollongong, Australia
11:05 AM – 11:15 AM	Revitalizing Dying Karezes of Tehsil Karezat, Balochistan, Pakistan	Hamayun Khan, BUIT, Engineering and Management Sciences, Quetta
11:15 AM – 11:25 AM	Performance Evaluation of Various Models for the Assessment of Reference Evapotranspiration in Arid and Semi-Arid Zones of Pakistan	Rabeeya Noor, BZU Multan
11:25 AM – 11:35 AM	Application of Multispectral Images Using R-Studio Package to Estimate Canal Water Deficit: A Comprehensive Study of Multan Irrigation Zone	Qamar Iqbal, BZU Multan
11:35 AM - 11:45 AM	Participatory Environmental Socio-Economic Modelling Complexity Issues and Solution. A case study of the Rechna Doab	Muhammad Asif, BZU Multan
11:45 AM - 11:55 AM	Optimization of Water Allocation Based on Irrigation Water Supply and Demand in Chaj Doab, Pakistan	Muhammad Abdul Wajid, Uni of Agri, Faisalabad
11:55 AM - 12:05 PM	Q & A session and concluding remarks by the Session Chair	Dr. Ghulam Nabi



<b>Technical Session-II</b> <b>Session Chair: Prof. Dr. Noor Muhammad Khan</b> <i>Repporteour: Dr. Muhammad Waseem</i>		
12:15 PM - 12:30 PM	Keynote Lecture	Prof. Dr. Asit K. Biswas, Uni of Glasgow, Scotland
12:30 PM - 12:45 PM	Special Lecture Flood Management in Pakistan	Dr. Ejaz Tanveer, Federal Flood Commission, Pakistan
12:45 PM - 12:55 PM	Evaluation of Low Impact Development (Lids) Drainage Control Measures Using PCSWMM in an Urban Watershed	Qaiser Abbas, BZU Multan
12:55 PM - 01:05 PM	Experimental Study of a Flow Through Permeable Spur Dikes in a Rectangular Channel	Rana Shahid Asghar, UET Taxila
01:05 PM - 01:15 PM	Quantifying Potential Impact of Temperature Variations on Water Demand in Multan Irrigation Zone	Hafiz Muhammad Kamran
01:15 PM - 01:25 PM	Estimation of Water Budget for Selected Irrigation Canal: A Case Study of LBDC Sahiwal	Asim Qayyum Butt, Quaid e Azam College of Engineering and Technology, Sahiwal
01:25 PM - 01:35 PM	Evaluation of Various Soft Computing Approaches to Estimate Reference Evapotranspiration of three Cities of South Punjab	Aarish Maqsood, BZU Multan
01:35 PM - 01:45 PM	Role of Oblique Vegetation in Flood Mitigation	Shahbaz Khalid, UET Taxila
01:45 PM - 01:55 PM	Experimental Study of Soil Erosion on Steep Hills with Varying Tree Patterns	Wali Ahmed, UET Taxila
01:55 PM - 02:05 PM	Q & A session and concluding remarks by the Session Chair	Prof. Dr. Noor Muhammad Khan
<b>Technical Session-III</b> <b>Session Chair: Prof. Dr. Shahid Ali</b> <i>Repporteour: Dr. Mudassir Iqbal</i>		
02:15 PM - 02:30 PM	Special Lecture	Dr. Raza-ul-Mustsfa, University Teknologi PETRONAS, Malaysia
02:30 PM - 02:40 PM	Management of Surface Water Resources to Mitigate the Water Stress in Karachi	Tayyab, Nespak Karachi
02:40 PM - 02:50 PM	Spatiotemporal Variations in Snow Cover Using Google Earth Engine in Gilgit-Baltistan, Pakistan	Hania Arif, University of the Punjab
02:50 PM -03:00 PM	Modelling of Rainfall-Runoff Process by GEP, RBF-SVM and M5 Model Tree in Jhelum River Basin, Pakistan	Dr. Saifullah, BZU Multan
03:00 PM - 03:10 PM	Meteorological Droughts to Hydrological Droughts: A Case Study of the Soan Basin, Pakistan	Dr. Muhammad Waseem, CEWRE

# Schedule

03:10 PM - 03:20 PM	Investigation of Extreme Hydrologic Events Using Innovative Trend Analysis Method Over Upper Indus River Basin	Muhammad Shehzad Ashraf, CEWRE
03:20 PM - 03:30 PM	Evaporation Simulation for a Reservoir Using ANN Technique	Taqi Leghari UET Taxila
03:30 PM - 03:40 PM	Q & A session and concluding remarks by the Session Chair	Prof. Dr. Shahid Ali

## Concluding Session

03:50 PM - 04:10 PM	Keynote Lecture	Mr. Peter Kovács, Water Director, Hungary
04:10 PM - 04:25 PM	Special lecture Modernizing Hydro Operation - improving efficiency and mitigating operational and safety risks	Dr. Mubasher Hussain, Global Hydropower & Dams Envision Digital, United Kingdom
04:25 PM - 04:35 PM	Vote of thanks by Director CEWRE, UET Lahore	Prof. Dr. Noor Muhammad Khan

## Table of Contents

Sr. No.	Title of Paper	Page No.
1	Development of scour equations around bridge piers using simple linear regression analysis. <b>Authors:</b> Muhammad Arif, Abdul Razzaq Ghumman, Usman Ali Naeem, Faraz ul Haq	1-4
2	Experimental study on scour around spur dikes in a channel bend <b>Authors:</b> Salman Masood, Ghufran Ahmed Pasha, Usman Ghani, Afzal Ahmed	5-8
3	Study of clear water local scour phenomenon around bridge pier groups <b>Authors:</b> Ali Iftikhar, Kaleem Sarwar, Muhammad Fahim Aslam	9-15
4	Experimental study of a flow through permeable spur dikes in a rectangular channel <b>Authors:</b> Rana Shahid Asghar, Ghufran Ahmed Pasha, Usman Ghani, Shahbaz Khalid	16-22
5	Estimation of Water Budget for Selected Irrigation Canal: A Case Study of LBDC Sahiwal <b>Authors:</b> Asim Qayyum Butt, Khadija Khan, Saiqa Mushtaq, Aqsa Zahoor, Syeda Aqsa Gillani	23-32
6	Evaluation of Various Soft Computing Approaches to Estimate Reference Evapotranspiration of three Cities of South Punjab <b>Authors:</b> Aarish Maqsood, Muhammad Shoaib, Hamza Salaudin	33-40
7	Performance evaluation of various models for the assessment of reference evapotranspiration in arid and semi-arid zones of Pakistan <b>Authors:</b> Rabeea Noor, Aarish Maqsood, Azhar Inam	41-47
8	Investigation of Extreme Hydrologic Events using Innovative Trend Analysis Method over Upper Indus River Basin <b>Authors:</b> Muhammad Shehzad Ashraf, Ijaz Ahmad, Muhammad Waseem, Faraz-ul-Haq, Muhammad Jawad Ashraf	48-56
9	Streamflow Forecasting at Mangla Reservoir in the Jhelum River by Using ARIMA Model <b>Authors:</b> Hammad-ur-Rehman, Ijaz Ahmad, Muhammad Waseem	57-63
10	Meteorological droughts to hydrological droughts: a case study of the Soan Basin, Pakistan <b>Authors:</b> Awais Naeem Sarwar, Muhammad Waseem, Ijaz Ahmad, Muhammad Azam, Muhammad Nouman Sattar	64-76
11	Assessing, Mapping and Optimizing the Potential Dam Site Selection Using ArcGIS <b>Authors:</b> Muhammad Sohail Jameel, Muhammad Farjad Sami, Afra Siab khattak, Ali Raza , Sohail Iqbal, Umer Shahzad	77-85
12	Evaporation Simulation for a reservoir Using ANN Technique <b>Authors:</b> Muhammad Taqi, Usman Ali Naeem, Mujahid Iqbal, Akhtar Abbas, Zeeshan Akbar, Salman Masood	86-90

13	Design and Development of Irrigation Schedule and Sowing Techniques to Enhance Cucumber Yield <b>Authors:</b> Muhammad Zeeshan Khan, Muhammad Zaman, Junaid Nawaz Chauhdary, Muhammad Umair, Malik Mubashar Ishaq, Shabana Kausar	91-95
14	Impact of Bio Slurry on Soil Physical Properties and Crop Yield <b>Authors:</b> Shabana Kausar, Muhammad Zaman, Muhammad Tayyab, Muhammad Umair, Malik Mubashar Ishaq, Muhammad Zeeshan Khan	96-100
15	Evaluation of Root Zone Behavior and Cucumber Yield under Different Mulch Materials <b>Authors:</b> Malik Mubashar Ishaq, Muhammad Zaman, Junaid Nawaz Chauhdary, Muhammad Zeeshan Khan, Shabana Kausar	101-104
16	Modelling of Rainfall-runoff process by GEP, RBF-SVM and M5 model tree in Jhelum River Basin, Pakistan <b>Authors:</b> Muhammad Waqas, Muhammad Saifullah, Sarfraz Hashim, Muhammad Shoaib, Adila Naseem, Mohsin Khan	105-112
17	Auto-calibration and uncertainty analysis of SWAT Model for Haro River Watershed using Sequential Uncertainty Fitting (SUFI-2) algorithm. <b>Authors:</b> Saima Nauman, Zed Zulkafli	113-118
18	A Participatory Socioeconomic Environmental Modelling Framework for Groundwater Management <b>Authors:</b> Rabeea Noor, Muhammad Azhar Inam, Qaiser Abbas, Muhammad Asif	119-124
19	Participatory Environmental Socio-Economic Modelling Complexity Issues and Solution. A case study of the Rechna Doab <b>Authors:</b> Muhammad Asif, Azhar Inam, Qaiser Abbas, Rabeea Noor	125-132
20	Reuse of Wastewater for Irrigation Purposes in Pakistan <b>Authors:</b> Asim Qayyum Butt, Allah Bachaya, Abid Latif, Amna, Aleeza Kainat, Sarfaraz Ali, Muhammad Arif	133-146
21	Application of Geostatistical Algorithms to Investigate Groundwater Quality Zones for Irrigated Agriculture <b>Authors:</b> Imran Rasheed, Aamir Shakoor, Zahid Mahmood Khan, Hafiz Umar Farid, Ijaz Ahmad, Naveed Ahmad, Qamar Iqbal, Hafiz Muhammad Kamran, Muhammad Abdul Wajid	147-154
22	Revitalizing Dying Karezes of Tehsil Karezat, Balochistan, Pakistan <b>Authors:</b> Hamayun Khan, Syed Mobasher Aftab	155-174
23	Subsurface investigation for Groundwater formation in District Rahim Yar Khan (Pakistan) using Vertical Electrical Techniques <b>Authors:</b> Hafiz Umar Farid, Akhtar Ali, Zahid Mehmood Khan, Ijaz Ahmad, Aamir Shakoor	175-182
24	Assessment of Groundwater Vulnerability and Aquifer Protective Capacity Using Vertical Electrical Resistivity Method	183-191



	<b>Authors:</b> Muhammad Rizwan Shahid, Hafiz Umar Farid, Zahid Mahmood Khan, Muhammad Naveed Anjum, Saddam Hussain	
25	Evaluation of Low Impact Development (Lids) Drainage Control Measures Using Pcswm in an Urban Watershed <b>Authors:</b> Qaiser Abbas, Muhammad Azhar Inam <sup>1</sup> , Rabea Noo , Muhammad Asif	192-195
26	Management of Surface Water Resources to Mitigate the Water Stress in Karachi <b>Author:</b> Muhammad Tayyab	196-204
27	Comparison of Treaties/Agreements Signed Between Major Transboundary River Basins <b>Authors:</b> Faraz ul Haq, Ijaz Ahmad, Noor Muhammad Khan	205-208
28	Optimization of Water Allocation Based on Irrigation Water Supply and Demand in Chaj Doab, Pakistan <b>Authors:</b> Muhammad Abdul Wajid, Syed Hamid Hussain Shah, Aamir Shakoor, Hafiz Umar Farid, Ijaz Ahmad, Naveed Ahmad, Muhammad Adnan Shahid, Aroosa Jabeen	209-217
29	Application of Multispectral images using R-Studio package to Estimate Canal Water Deficit: A comprehensive study of Multan Irrigation Zone <b>Authors:</b> Qamar Iqbal, Aamir Shakoor, Zahid Mahmood Khan, Hafiz Umar Farid, Ijaz Ahmad, Muhammad Awais, Imran Rasheed, Hafiz Muhammad Kamran, Muhammad Abdul Wajid	218-225
30	Formulation of Precision Input Management Strategy for Wheat using Handheld Crop Sensor <b>Authors:</b> Huzaifa Shahzad, Hafiz Umar Farid, Zahid Mahmood Khan, Aamir Shakoor, Rana Muhammad Asif Kanwar, Khawar Abbas	226-232
31	Role of oblique vegetation in flood mitigation <b>Authors:</b> Shahbaz Khalid, Ghufraan Ahmed Pasha, Usman Ghani, Afzal Ahmed, Muhammad Asghar, Ammar Sabir	233-240
32	Comparative Study of Total Dissolved Solids (TDS) Between Sand Absorption Media and Silica Absorption Media for Ganglion Trap of Non-Aqueous Phase Liquid (NAPL), Using Flow Visualization Channel. <b>Authors:</b> Musaab Habib Bangash, Naeem Ejaz, Muhammad Zeeshan Ahad, M. Mahboob Alam	241-244
33	Laboratory measurements of velocity and hydrodynamic force over coarse fixed rough bed <b>Authors:</b> Muhammad Zain Bin Riaz, Shu-Qing Yang, Muttucumarar Sivakumar	245-251
34	Experimental study of soil erosion on steep hills with varying tree patterns <b>Authors:</b> Walli Ahmed, Ghufraan Ahmed Pasha, Usman Ghani , Afzal Ahmad	252-256
35	Soil Mapping of Inaccessible Sites using Remote Sensing and GIS <b>Authors:</b> Tariq Ahmed Awan, Muhammad Usman Arshid	257-263

36	Quantifying Potential Impact of Temperature Variations on Water Demand in Multan Irrigation Zone <b>Authors:</b> Hafiz Muhammad Kamran, Aamir Shakoor, Zahid Mahmood Khan, Hafiz Umar Farid, Ijaz Ahmad, Hafiz Muhammad Awais, Qamar Iqbal, Imran Rasheed, Muhammad Abdul Wajid	264-271
37	Climate Change Impact Assessment on Irrigation Water Supply and Demand in Rechna Doab, Pakistan <b>Authors:</b> Aroosa Jabeen, Syed Hamid Hussain Shah, Aamir Shakoor, Muhammad Abdul Wajid, Muhammad Adnan Shahi, Hafiz Umar Farid	272-279
38	Spatiotemporal Variations in Snow Cover using Google Earth Engine in Gilgit-Baltistan, Pakistan <b>Authors:</b> Hania Arif, Syed Amer Mehmood, Hafiz Haroon Ahmad	280-286
39	Impact of climate variation on hydrological behavior of snow fed catchment in Chitral basin, Pakistan. <b>Authors:</b> Muhammad Muneeb, Muhammad Waseem, Muhammad Awais Zafar, Faraz ul Haq	287-299

## Development of scour equations around bridge piers using simple linear regression analysis

Muhammad Arif<sup>1</sup>, Abdul Razzaq Ghumman<sup>2</sup>, Usman Ali Naeem<sup>1</sup>, Faraz ul Haq<sup>3\*</sup>

<sup>1</sup> Civil Engineering Department, University of Engineering and Technology Taxila, Pakistan

<sup>2</sup> Civil Engineering, Qassim University College of Engineering: Buraidah, Al Qassim, SA

<sup>3</sup> Centre of Excellence in Water Resources, University of Engineering and Technology 54890, Pakistan

Corresponding author email: [engrfaraz@uet.edu.pk](mailto:engrfaraz@uet.edu.pk)

**Abstract:** The aim of this research work was to study the scouring phenomenon for different shapes of bridge piers. Experiments were performed by altering velocity and depth of water in a horizontal sediment circulatory loop. The total number of experiments performed were eighteen having six experiments for each three different shapes of piers. To check the velocity of flow, the apparatus used was velocity sensor. It was controlled by using selector switch. After collecting the data, various scour equations were developed by using linear regression analysis. The comparison of experimentally observed scour was done with calculated scour. The comparison showed that both the shape of pier and flow velocity are very sensitive for scour depth.

**Keywords:** Scour; Sediment circulatory loop; Regression analysis; Velocity Sensor

### Introduction

Due to turbulent flows action, removal of sediments occurs near the structures which is known as scouring. At bridges, this diminishes the elevation of bed near the abutments and piers, exposing the bridge foundations, due to which collapse as well as loss of both property and life may occur. The collapse of bridges is a common phenomenon resulting due to scour at piers and abutments. Flow depth, velocity of water flow, sediment as well as pier characteristics all contributes to bridge pier scouring. The bearing capacity of the surrounding bed material can be reduced due to scour around the structure and if not properly designed, it can lead to the failure of the structure. The structure may even fail under normal flow conditions if the depth of foundation is not sufficient. A lot of money will be wasted in construction of a bridge if the foundation is placed too deep. Therefore, the precise estimation of maximum scour depth at bridge piers must be done which is vital for both cost-effective as well as safe design of bridges.

Beg and Mubeen (2010) presented detailed work on scouring covering all the possible aspects such as flow field scour process, time variation and parameters affecting depth of scour.

A. Keshavarzi and Reza Ghazi (2012) used Adaptive Neuro Fuzzy Interference System (ANFIS) to model depth of local and pattern scouring around convex and concave arch shape bed sills. Another method adopted by Coleman (2005) to predict depth of local scouring at a

complex pier presents combine existing expressions for scour respectively at uniform piers, piles in group with debris rafts, caisson-founded piles, and piles group alone. Bozkus and Yildiz (2004) observed effects of piers of bridge inclination on scouring depths around bridge piers. The method proposed by Mia (2004) includes the estimation of the depth of local scour with time. Several laboratories and numerical research have been used to measure the maximum scour depth of bridge piers. Most of the research work has been focused on equilibrium scour depth in alluvial sand beds, such as Melville and Sutherland (1998) and Breusers, et al. (1977). Many researchers have worked on the estimation of time related scour such as Dey (2007), Oliveto and Hager (2002). For measuring the scour depth of other shapes of pier and alignments the procedures of Hoffmans and Verheij (1997), Melville and Chiew (1997), Richardson (1993) are based on the study of local scour at circular ones and its correction factors. The aim of this research work was to study the scouring phenomenon for different shapes of bridge piers.

### Research Methodology

Experimental work was carried out in “Sediment Circulatory Loop” as shown in Figure 1. Plastic transparent bridge piers having Square, Circular and elliptical shape were used. Each pier had length of 450mm and width of 50.80mm. Sand having specific gravity of 2.802 and particle size

of  $D_{50}=0.28\text{mm}$  was used as bed material. Pier was fixed on the bed of channel with the help of bolt fixed in the bottom of sediment box. Sand was filled up to a depth of 203mm into sediment box fixed in the sediment loop. A wheel of 2ft diameter attached with an electric motor was installed in sediment loop to circulate water at required velocity. Velocity was controlled with the help of selector switch fixed at motor. The velocity of water was measured by using velocity sensor. Scouring pattern was observed continuously. Time duration for each experiment was 10 minutes. Slope of channel was fixed at zero in the whole experimentation. Scour was calculated from graduated scale fixed at piers and also by using point gauge as shown in Figure 1. Dimension and specifications of the channel are demonstrated in Table 1.



**Fig. 1** Sediment circulatory loop for measurement of scour depth using graduated scale.

**Table 1.** Salient specifications of the Circulatory Sediment Flume

Mean Flow Depth	120 mm
Length of Flume	2700 mm
Width of Flume	300 mm
Depth of Flume	450 mm
Pier Width	50.80 mm

Each pier was tested with three different velocity and three different depths of flow. In this way total 18 experiments were performed to observe the phenomenon of scour affected by shape of pier.

### Results and discussions

Simple regression analysis is performed for the scour values against velocity and depth of flow. Scour depth against the flow depth at the constant velocity 0.2 m/s, for the circular pier is shown in Figure 2.  $R^2=0.871$  is linear regression value for circular pier. “X” is the flow depth in mm and “Y” is the scour depth in mm. From linear

regression, we can see that scour depth decreases as flow depth increases. This regression value is better reliable.

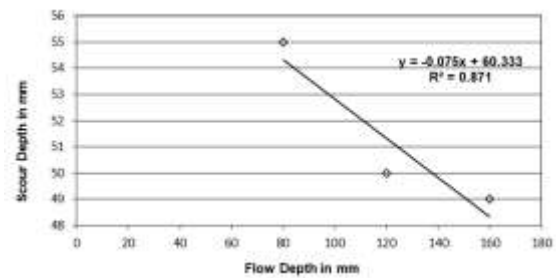


**Figure 2:** Scouring for circular pier keeping velocity constant 0.20 m/s

Regression analysis of scour depth against the velocity of flow, keeping the flow depth constant, for circular pier is carried out in Figure 3. In this condition  $R^2=0.9453$  having most reliable linear regression. “Y” is the scour depth in mm and “X” is the flow velocity. Flow velocity is directly proportional to the scour depth.

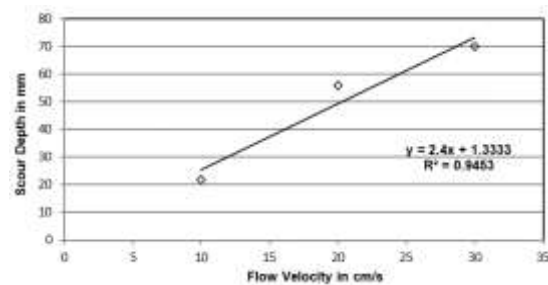


**Figure 3:** Scouring for circular pier keeping depth constant  $D=120\text{mm}$

For the elliptical pier, scour depth is plotted against the flow depth, keeping the velocity of flow constant as shown in Figure 4. “X” is the flow depth in mm and “Y” is the scour depth in mm.  $R^2=0.9643$  is the linear regression value in case of elliptical pier. This is the most reliable regression value. As the flow depth increases the scour depth decreases.

Scour depth, in case of elliptical pier is observed and is plotted against flow velocity keeping the depth of flow constant as shown in Figure 5. In this condition  $R^2=0.9992$  which is approximately equal to one. This regression value is the most suitable from all other values. “X” is the flow velocity and “Y” is the scouring depth. As velocity increases the scour depth also increases in the same way.



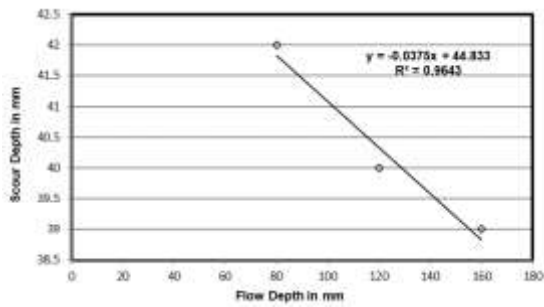


**Figure 4:** Scouring for elliptical pier keeping velocity constant 0.20m/s

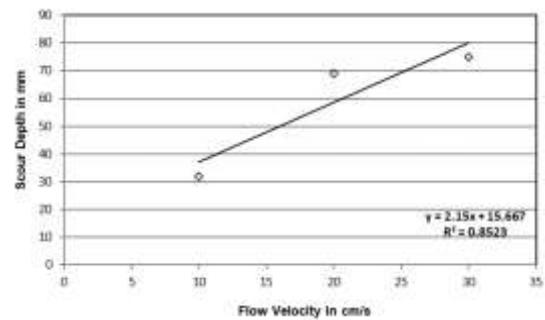


**Figure 7:** Scouring for square pier keeping depth constant D=120mm

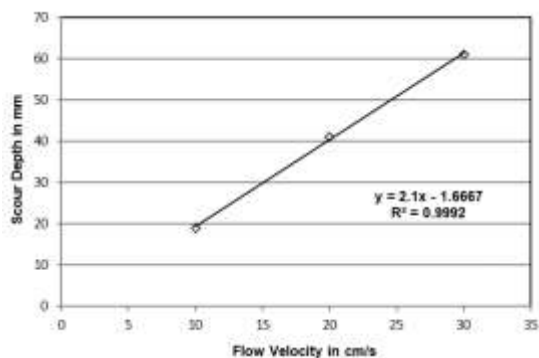


**Figure 5:** Scouring for elliptical pier keeping depth constant D=120mm

Experiments were carried out for square pier too and scour depth is observed for different flow depth at constant velocity, Results of the observation are shown in Figure 6. “Y” is the scouring depth in mm and “X” is the flow depth in mm.  $R^2=0.9231$  is the linear regression value in case of square pier. Flow depth is inversely proportional to the scour depth keeping velocity constant 0.20 m/s.

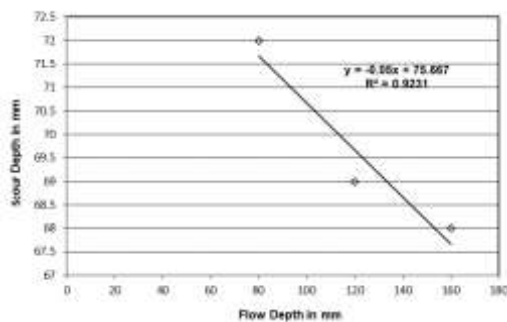


**Figure 6:** Scouring for square pier keeping velocity constant 0.20m/s

In Case of Square pier, Relation between scour depth and flow velocity at constant depth of flow is shown in Figure 7. In this condition  $R^2$  have regression value 0.8523. While “X” is the flow velocity in cm/s and “Y” is the scour depth in mm keeping flow depth constant  $d=120$ mm.

## Conclusions

From comparison of developed models, we have concluded that scour depth is directly proportional to the flow velocity and inversely proportional to the depth of water flow. Pier shape and flow velocity both are very sensitive for scour depth. Elliptical pier is the most suitable (square, circular and elliptical) for design of hydraulic bridges. The developed equations will be useful for measuring scour depth around bridge piers under various flow depths with constant velocity. Similarly, the scour depth studies will also be carried out by considering various flow velocities with constant depth. From developed models we can check the percentage reliability of scouring for all three shapes. The research will be helpful for safe designing of the bridge piers constructed overflowing water. Further this research will be helpful while deciding the depth of the foundations of the piers having different shapes.

## Acknowledgments

The authors are highly obliged to University of Engineering and Technology Taxila for providing sufficient funds to purchase the sediment circulatory loop without which the research would have not been possible. Also, the authors fully acknowledge Civil Engineering Department for issuing Velocity Sensor to measure velocities.

## References

- Beg, Mubeen. "Characteristics of developing scour holes around two piers placed in transverse arrangement." In *Scour and Erosion*, pp 76-85, 2010.
- A. Keshavarzi, R. Gazni, and S. R. Homayoon, "Prediction of scouring around an arch-shaped bed sill using Neuro-Fuzzy model," *Applied Soft Computing*, Volume 12 , pp. 486-493, 2012.

- S. E. Coleman, "Clearwater local scour at complex piers," *Journal of Hydraulic Engineering*, Volume 131, pp. 330-334, 2005.
- Z. Bozkus and O. Yildiz, "Effects of inclination of bridge piers on scouring depth," *Journal of Hydraulic Engineering*, Volume 130, pp. 827-832, 2004.
- Mia, Md Faruque, and Hiroshi Nago. "Closure to "Design Method of Time-Dependent Local Scour at Circular Bridge Pier" by Md. Faruque Mia and Hiroshi Nago." *Journal of Hydraulic Engineering*, Volume 130, No. 12, pp. 1213-1213, 2004.
- Melville, B. W., and A. J. Sutherland. "Design method for local scour at bridge piers." *Journal of Hydraulic Engineering*, Volume 114, No. 10, pp. 1210-1226, 1998.
- H. Breusers, G. Nicollet, and H. Shen, "Local scour around cylindrical piers," *Journal of Hydraulic Research*, Volume 15, pp. 211-252, 1977.
- S. Dey and R. V. Raikar, "Characteristics of horseshoe vortex in developing scour holes at piers," *Journal of Hydraulic Engineering*, Volume 133 pp. 399-413, 2007.
- G. Oliveto and W. H. Hager, "Temporal evolution of clear-water pier and abutment scour," *Journal of Hydraulic Engineering*, Volume 128, pp.811-820, 2002.
- G. J. Hoffmans and H. Verheij, *Scour manual*: CRC press, Volume 96,1997.
- B. W. Melville and Y.-M. Chiew, "Time scale for local scour at bridge piers," *Journal of Hydraulic Engineering*, , Volume 125, pp. 59-65, 1999.
- E. V. Richardson, L. J. Harrison, J. Richardson, and S. Davis, "Evaluating scour at bridges," 1993.
- E. M. Laursen and A. Toch, *Scour around bridge piers and abutments: Iowa Highway Research Board Ames, IA*, Volume 4, 1956.
- B. W. Melville and S. E. Coleman, *Bridge scour*: Water Resources Publication, 2000.
- Johnson, Peggy A. "Reliability-based pier scour engineering." *Journal of Hydraulic engineering*, Volume 118, No.10, pp.1344-1358,1992.
- Melville, B. W. "Local scour at bridge abutments." *Journal of Hydraulic Engineering*, Volume 118, No.4, pp.615-631,1992.
- Kandasamy, J. K., and B. W. Melville. "Maximum local scour depth at bridge piers and abutments." *Journal of hydraulic research*, Volume 36, No.2, pp.183-198,1998.
- Raudkivi, A. J. "Scour at bridge piers." *Scouring: IAHR hydraulic structures design manual 2*, pp.61-98,1991.

## Experimental study on scour around spur dikes in a channel bend

Salman Masood<sup>1\*</sup>, Ghufuran Ahmed Pasha<sup>1</sup>, Usman Ghani<sup>1</sup>, Afzal Ahmed<sup>1</sup>

<sup>1</sup> Civil Engineering Department, University of Engineering and Technology, Taxila, Pakistan

Corresponding author email: [14-ce-137@students.uettaxila.edu.pk](mailto:14-ce-137@students.uettaxila.edu.pk)

**Abstract:** Scouring is one of the main reasons for damaging the spur dike due to the shearing action of water in a channel bend. Once a spur dike is damaged, it may affect the other spur dikes (placed in the line of it) thus, failing the riverbank. The present laboratory work deals with the study of scour hole geometry under clear water scour conditions around the non-submerged and impermeable spur dikes. Multiple rectangular spur dikes were constructed at 90-degree and other inclinations on the two physically designed bend models including mild and sharp bends placed in an open rectangular channel. The slope of the channel bed is uniform and having sediments of the average diameter of 0.71 mm. The laboratory analysis was carried to study scour around spur dikes and the effect of location of spur dike on scour pattern in the bends. These experimental findings are significant in interpreting the design of multiple spur dikes in the channel bend.

**Keywords:** Spur dike; Scour depth; Mild and sharp bend; Location of spur dike

### Introduction

River-bank stabilization problems are solved with the help of a proper design of the spur dikes dealing with river training structures to enhance navigation, improve the flow depth for irrigation purposes, improve flood control and protect the erodible banks having either sharp bend or mild bend. Spur dikes are used to train river in favorable condition and stabilize its course. The property, the land and the embankments from erosion are protected by spur dikes (Garde et al., 1961). Spur dikes are the hydraulic structures that project either perpendicular or at some orientation from the bank towards the center of the channel. Spur dikes are used widely in the field of river engineering for riverbank stabilization and protection from erosion. Spur dikes in the field of navigation has increased the sediment transportation rate in the water channels and these structures have minimized the channel dredging cost too for improving the channel depth of flow and channel alignment (Pagliara & Kurdistani, 2017).

According to the orientation point of view, the spur dikes are of three types including attracting, deflecting and repelling. Maximum work has been done on angled spur dikes and on this basis, spur dikes are classified into attracting (towards upstream), repelling (towards downstream) and deflecting (normal to flowing water) ones. Spur dikes are used to fix the lower limits of confluence of a distributary with the main river. The flow in the channel is restricted into a constricted bridge waterway opening (I. Khassaf

& A. Abbas, 2018). The maximum scour hole depth and volume around the spur dyke normal to flow and at any inclination, are of great concern in the bends. Scour hole depth depends upon location of the spur dike in the bend, length of the spur dike, radius of curvature and length of the wing of the spur dike (Vaghefi et al., 2015). The prime parameters for scour depth variation are contraction ratio, the angle of spur dyke, the Froude number and drag coefficient are determined from dimensional analysis that affect the scour hole depth around the spur dikes (Kuhnle et al., 2002). The flow parameters including velocity, discharge, Froude number and flow depth are the controlling tools of scouring in the channel. By varying one or several parameters mentioned above, local scour and contraction scour both are changed (Garde et al., 1961; omenzadeh et al., 2019). The spur dike length is primarily based on diverting the water currents away from the channel embankments. The spacing of 2.5 times the length of spur dyke was recommended in concave bends and spacing of 1 times for convex bend (Klump & Baird, 1992). On the Mississippi river, the corps of engineers spaced 2 times the spur dike length and 1.5 times the spur dike length. For concave bends, the spacing was 1.5 times the dyke length and 2.5 times for convex bends (Klump & Baird, 1992; Shields Jr, 1995). While designing the crest of the submerged spur dike, it must have a constant elevation instead of being variable and is equal to low water conditions. To protect the banks of the channel, the crest of the spur dyke

should not less than the elevation of the banks and greater than any high surge (Elawady et al., 2000). A spur dyke that is made up of erodible material, should be protected against the local scour by providing riprap or a layer of stone pitching at the nose of the spur dyke associated with the bank of the channel for protection against erosion (Zaghloul, 1983). The flowing water in the channel creates vortices including primary and intermittent vortices at and around spur dikes. The primary vortices flow occurs at the nose of the sour dyke while the intermittent flows are usually found on the upstream side and downstream side of the spur dykes (Kuhnle et al., 2002). The undisturbed approach velocity has influenced on the local scour hole depth and volume around the spur dykes. The channel flow width is contracted or decreased due to installation of spur dike causing a change in the velocity profile in the area around the spur dikes. The flow conditions including flow velocity and Froude number play a significant role towards scour hole depth around the spur dikes. The increase in the flow velocity as well as in Froude number of the channel causes the increase in the scour hole properties. There is a linear relationship between approach velocity and scour depth around the spur dikes under clear water conditions and at critical flow velocity, maximum scour depth is achieved (Ettema & Muste, 2004).

It may be concluded that a lot of work has been performed on spur dikes after the perusal of above cited literature review. Still less attention has been paid particularly on number of multiple spur dikes in series (both in the outer and inner banks) and orientations in a mild as well as on sharp channel bends. The shape of the bend whether concave or convex requires a different number of spur dikes in series and hence these parameters do require some more investigations. Therefore, an experimental attempt has been made to investigate the study on scour around the spur dikes in a channel bend by considering location and inclinations of spur dikes.

### Research Methodology

In this study, a smooth rectangular flume channel (20m length, 1m width and 0.75m depth) equipped with a recirculating water facility was used to execute the laboratory work on scour. The rectangular channel was used, a smooth and straight entrance, a concrete base along with side walls that were made of thick glass for observing the scouring mechanism. The length of the spur

dike was used as 1/5<sup>th</sup> of the channel width (Alsawaf et al., 2019). The total number of spur dikes were five in the complete experimental work (the spur dikes were given designation as S1, S2, S3, S4 and S5 from left to right). Non-submerged and impermeable rectangular spur dikes made up of wood, were constructed at designed bend models including mild and sharp bend. The rectangular channel was divided into three equal portions.

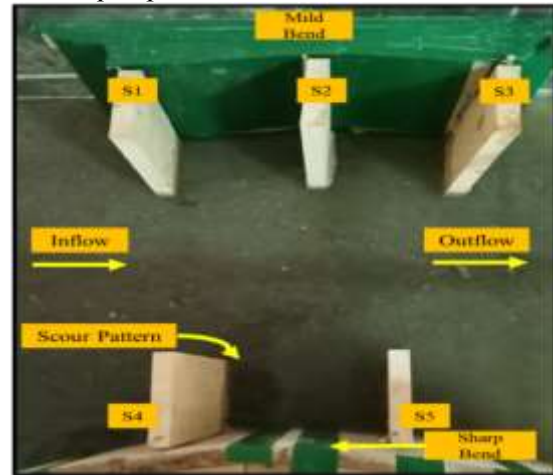


**Fig. 1** Schematic view of channel bend

The middle portion was used for the experimental work. The length of the middle portion was 6m long along with 0.3 m thick fine sand bed of uniformly graded sediments of the average diameter ( $d_{50}$ ) of 0.71mm. The standard deviation,  $S_d = (d_{84}/d_{16})^{0.5}$  was 1.20 against  $d_{50}$  of 0.71mm used for all experiments. The discharge had been controlled, maintained, and quantified with the help of a gated rectangular weir at the end of the flume channel. All experiments were carried out against 3 hours duration (Elawady et al., 2000). Table 1 elaborates all the parameters that were involved in all experiments.

**Table 1** Flow Parameters

Discharge( $m^3/s$ )	0.074
Flow depth, $F_d(m)$	0.231
Median Grain Size, $d_{50}(m)$	0.0007
Approach Flow Velocity, $V(m/s)$	0.333
Critical Velocity, $V_c(m/s)$	0.4871
Critical Shear Velocity, $V_{*c}(m/s)$	0.025
Water Flow Intensity, $V/V_c$	0.61
Froude Number, $F_r$	0.29



## Results and Discussion

### Scour Pattern around Spur Dikes

The observation of scour pattern around multiple spur dikes was quite complex. The shape of the bend and location of the spur dike had a significant role towards scour depth. The flowing water was scouring the front spur dikes at both bend models first but scour pattern with maximum scour depth was seen at the outer spur dike on sharp bend. The scour depth on the other spur dike at the same sharp bend model lied ahead of it was minimum. Streamlines were generated from spur dike position S4 that affect the scouring mechanism on spur dike at mild bend model at position S3. The longitudinal and traverse profiles of multiple spur dikes operated simultaneously on both bend models were diagrammed (Fig. 2).

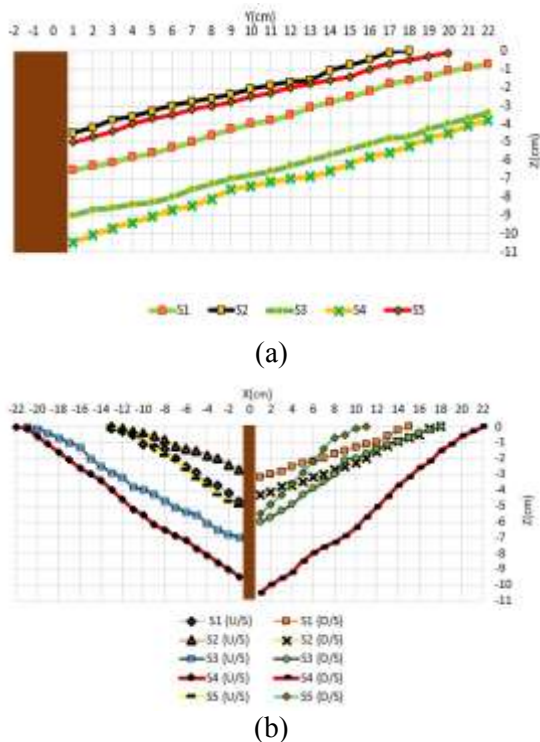


**Fig. 2** Scour profiles around 90-degree spur dikes; (a) and (b) are longitudinal and cross-sectional profiles respectively from nose of spur dike.

### Scour Depth Versus Spur Dike Position

Each spur dike in the deigned bend models were represented by two sides including upstream and downstream. The fig.3 represented the scour depth at upstream and downstream side of a single spur dike owing to variation in the values of scour depth. The maximum scour depth was significant at position S4 due to direct conflicting

with the flowing water. The direction of the streamlines produced at S4 was from S4 to S3 diagonally and had influenced further scouring at S3. The parameters (listed in table 1) were the same in the complete experiments but scour depth on each spur dike was found different. It was concluded that maximum and minimum scour depth was achieved at S4 and S5 on sharp bend and at S3 and S2 on mild bend.

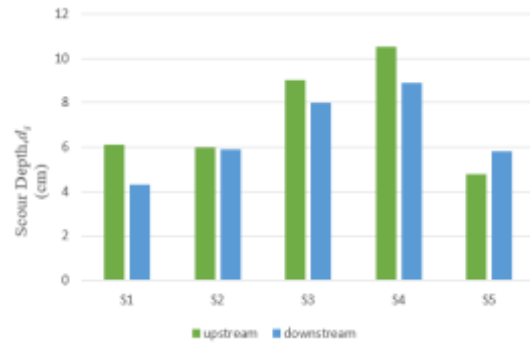


**Fig. 3** Comparison of scour depth for different position of spur dikes in the bends.

### Time Variation of Scour Depth

The scouring phenomenon was started around the nose of the multiple spur dikes constructed on both bend types including mild and sharp bend. From the nose, the scour was started and then moved towards the center of the rectangular channel.

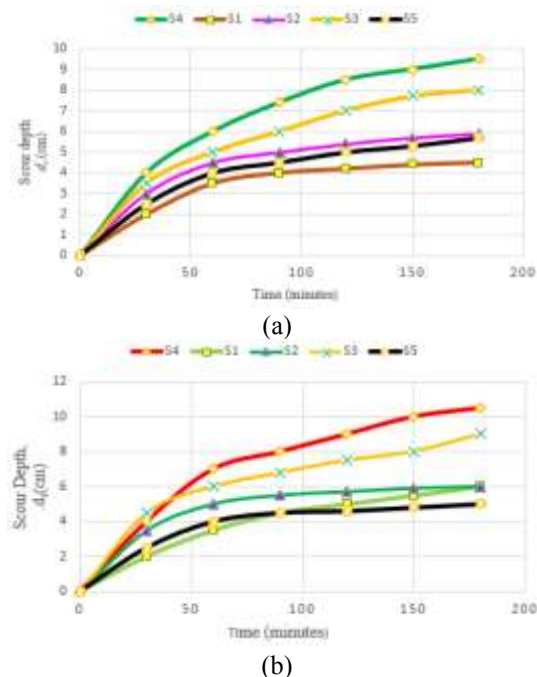


**Fig. 4** Time evaluation of scour depth around spur dikes; (a) and (b) are the upstream and downstream scour depth of all positions of spur dikes.

The scour depth was found maximum at upstream side of S1, S2, S3, S4 as compared to downstream sides, respectively. But at downstream side of S5, the scour depth was observed maximum as compared to upstream side. Initially, the scour depth was increased during the first hour of the experimental duration. After the second hour, it was observed that 75% of scouring had been done and the remaining scour depth was achieved stably in the remaining last hour of laboratory work.

### Conclusions

Experiments were performed to investigate scouring phenomenon around spur dikes in a channel bend. It was concluded that scour depth was increased by 23.5% at S4 and reduced by 21%, 49.2%, 50%, 36% on S4, S3, S3, S1, respectively. The experimental execution of multiple spur dikes was found to be more efficient to reduce scour in a channel bend.

### References

- Alsawaf, M., Ghazali, A. H., Mohammad, T. A., Ab Ghani, A., & Yusuf, B. (2019). Movable-bed experiments using spur dike to concentrate flow in one channel of multithreaded channel model. *Journal of Hydraulic Engineering*, 145(5), 06019006(1-8).
- Elawady, E., Michiue, M., & Hinokidani, O. (2000). Experimental study of flow behavior around submerged spur-dike on rigid bed. *Proceedings of Hydraulic Engineering*, 44, 539-544.
- Ettema, R., & Muste, M. (2004). Scale effects in flume experiments on flow around a spur dike in flatbed channel. *Journal of Hydraulic Engineering*, 130(7), 635-646.
- Garde, R. J., Subramanya, K. S., & Nambudripad, K. D. (1961). Study of scour around spur-dikes. *Journal of the Hydraulics Division*, 87(6), 23-37.
- Khassaf, I. S., & Abbas, A., H. (2018). Study of the local scour around L-shape groynes in clear water conditions. *International Journal of Engineering & Technology*, 7(4.20), 271.
- Klump, C., & Baird, D. (1992). Recent criteria for design of groins. *Journal of Hydraulic Engineering*.
- Kuhnle, R. A., Alonso, C. V., & Shields, F. D. (2002). Local scour associated with angled spur dikes. *Journal of Hydraulic Engineering*, 128(12), 1087-1093.
- Omenzadeh, R. M., Makvandi, A., & Aghamajidi, R. (2019). Investigation of the effect of spur dike length on the scour depth near the spur dike at the 90 degree position and the 180 degree bend of the rivers. *International Journal of Engineering and Technology*, 11(1), 35-40.
- Pagliara, S., & Kurdistani, S. M. (2017). Flume experiments on scour downstream of wood stream restoration structures. *Geomorphology*, 279, 141-149.
- Shields Jr, F. D. (1995). Fate of Lower Mississippi River habitats associated with river training dikes. *Aquatic Conservation: Marine and Freshwater Ecosystems*, 5(2), 97-108.
- Vaghefi, M., Ahmadi, A., & Faraji, B. (2015). The effect of support structure on flow patterns around T-shape spur dike in 90° bend channel. *Arabian Journal for Science and Engineering*, 40(5), 1299-1307.
- Zaghloul, N. A. (1983). Local scour around spur-dikes. *Journal of Hydrology*, 60(1-4), 123-140.

## Study of clear water local scour phenomenon around bridge pier groups

Ali Iftikhar<sup>1\*</sup>, Kaleem Sarwar<sup>2</sup>, Muhammad Fahim Aslam<sup>3</sup>

<sup>1</sup> Centre of Excellence in Water Resources Engineering, University of Engineering and Technology, Main GT Road Lahore.

Corresponding author email: [ranaaliiftikhar999@gmail.com](mailto:ranaaliiftikhar999@gmail.com)

**Abstract:** Local scour around bridge piers is one of the major factors behind collapsing of bridges throughout the world. Various studies and experiments have been performed to study the effect of local scour in this regard. Material used for the experiments was consist of PVC pipe as bridge piers and the sand of River Ravi. For the current study the impact of local scour was studied by changing the pier spacing, grouping of piers and their inclination angles in the model prepared in the open channel flume in the laboratory. Total 36 experiments were performed to investigate the impact of parameters discussed above. Time to achieve equilibrium scour depth graph was plotted to determine the time required for the determination of time required for the occurrence of maximum scour depth. It was concluded from the experiments that when the flow intensity was increased, depth of scour also increased for all inclination angles. Moreover, when inclination of the pier was increased, depth of scour decreased. Comparison of results was done with different other methods and techniques and trend line was plotted.

**Keywords:** Local scour; Bridge pier; Inclination; Pier spacing.

### Introduction

Scouring around the bridge pier leads to bridge failure. Shape of bridge abutment or pier or piles are one of the major contributors behind scouring. The amount of sediment that is removed from the edge of bridge pier is called bridge pier scouring. Total depth from NSL upto the point of sediment removal is called as scour depth. Erosion is the process where natural forces like water erodes the bed and bank materials of channel, as well as the proximity of the bridge abutment or pier. Local scour is a result of the erosive action of the current flowing in the alluvial beds and removes sediments around or near the structures in the flowing water. (Padmini et. al, 2009).

According to types of sediment transport, two types of local scour (clear water and live bed scour) is occurred by the potential flow. Clear water scour takes place when the bed material around the pier is static. Whereas, live bed scour takes place when the material from the bed is generally eroded by the flow. The erosive behavior of the potential flow around bridge columns affects the structure stability. It leads to very high costs (direct and indirect) along with the loss of human lives. (Toth et al. 2011). A pier or an abutment will locally change the flow directions and cause erosion or deposition in the vicinity of the structure. (Walter et al. 2016).

The mechanism that creates scour around the bridge columns was due to vortices that are developed around the column when water flows through them. The vortices have been divided into modules known as downward flow in front of the Column. Two general types of the vortices (Horseshoe Vortex & Wake Vortex) formed when the column of bridge is entirely immersed in water. In the event of horseshoe vortex, cross-stream strands of the periphery layer on the underside are advected towards and are twisted around the bridge column. Primarily horseshoe vortex is small and approximately rounded in cross-section and relatively feeble. The horseshoe vortex travels down the generated scour hole and develops if the hole expands. The hole of scour with increasing size, the spread of the vortex of horseshoe increases because of increasing cross-sectional area and decrease in velocity.

Wake vortex framework is shaped by moving up of the unbalanced shear deposits created on column surface due to flowing water which are separated from any side of the column at the line of separation just behind the column. Wake vortex frameworks performs like a void in eradicating the material of bed, which is often transported downstream by vortexes generated from the column or pier.

Since 1950 in the USA, due to result of channel instability and channel bed scour sixty percent

out of eight hundred and twenty three bridges have been collapsed. According to US Federal Highway Association report, every year, almost fifty bridges collapse in United State of America.

### **Problem Statement**

Scouring causes the Exposure of foundation, which eventually leads to failures in bridge. The assessment of the maximum range of the scour that can be faced by pier plays the crucial role in the planning and designing of bridge sub-structure. Various techniques are used to reduce the scouring effect to avoid the bridge failure.

Keeping in view very complex nature of local scour phenomenon and its negative impacts, researchers have conducted many studies. Vaghefi et al. (2016) did a lot of experiments to calculate the scour around the laterally inclined circular pier and establish that depth of scour around inclined bridge column is four percent less as compared to vertical bridge pier. Bozkus et al. (2010) did a lot of research on inclined double rounded bridge columns. The results of experiments showed significant reduction in depth of scour around inclined piers than to vertical rounded bridge columns or piers.

Structurally group of piers are normally used instead of using single massive pier and also the construction of massive pier is not possible in flowing rivers or channels. Back water flow conditions may take place due to effect of group pier and causes the intrusion of the flow around the bridge columns or piers and caused different scour patterns and equilibrium scour depth. Due to presence of piers group their effect is generated, which are placed either in line with flow or vertical to it. The effect of group mostly relays upon the number of piers, the distance among them, their direction, skew angle and position of piers. (Lança et al. 2013).

Scouring around bridge foundations due to flowing water is major reason for collapsing of bridges. These failures occur without any warning and led to deaths of human lives. Moreover, huge amount of money is spent by the departments every year for their rehabilitation. (Wang et al. 2017) Soil scouring due to flow of water around the bridge piles is the one major cause regarding bridge failure. While designing the foundation of the bridge it is mandatory to calculate the scour depth. (Briaud et al. 2015) Research study is required to explore the clear water local scour phenomenon near bridge columns or piers groups at different inclination

angles by varying pier spacing and using non-uniform river bed material.

### **Objective**

The study was carried out to investigate local scours around bridge pier groups for various pier spacing and inclination angles.

### **Literature Review**

Bozkus et al. (2018) performed many experiments to study scours near the piers of bridge with different groups of pier making an angel with the vertical plane. In his investigation, he utilized two different groups of piers. In every pier group he placed piers or columns upstream & downstream at an angel of 10° and 15° with respect to vertical plane. He performed seventy-two (72) observations everyone comprising of 6 hour using uniform and clear-water flow conditions. The results demonstrated that circular pier situated at upstream & downstream of bridge pier influences the local scour in an effective way, with considerable decrease in the local scour, mainly around the upstream column or pier. Besides the intensity of flow, depth of flow is the significant variable which causes the local scour.

Yang et al. (2018) performed many experiments to study clear-water local scour nearby piers of bridge. He performed experiments by using two typical pier models, nine pile-cap elevations, and seven pier skew angles from 0° to 90° with a 15° interval. Results showed that a slight skew angle on an originally aligned pier can significantly increase the equilibrium scour depth. When a pier was skewed to the flow, the column made the largest contribution to the scour depth because its wide-pier feature became dominant. Also, for highly skewed piers with fully submerged pile cap, the equilibrium scour holes tended to equally expose the pier components.

Khan et al. (2017) in his research study, tried to find the scouring patterns in terms of scour depth and its extent in lateral direction for different shape of piers. He used square and circular pier in his study. For this purpose, in physical modeling lab, a number of experiments were performed. Through his study showed that the column or pier scour increases with increase of pier size. By increase in size of pier affected area due to scour also increases. The study further demonstrates that the square pier contributes more than the circular pier in scouring.

Elnikhely et al. (2017) investigated to explore the minimization of the local scour near the bridge

pile. He utilized perforated piles with gaps in various directions. Study results indicated eighty nine percent decrease in depth of scour because of utilizing the group of piles with angle of 45° and perforated piles with gap edge of 45°.

Guemou et. al. (2018) examined bridge pier having a longitudinal biconcave shape. Guemou et.al. (2018) noted that the concave shape of pier decreased the bed shear upto 12 %. Whereas, this shape increased the bed shear around 20 % downstream of bridge pier.

Das et al. (2017) studied a comparative scour condition around the group of three piers. He showed upstream & downstream scour conditions when two pair of piers are set aligned and 3rd pier is set in middle of coupled piers. Lab scale tests were actually done by fluctuating the halfway longitudinal space between the coupled piers or columns. It was observed that the erosion near single pier was most extreme and around couple downstream piers was discovered least. It establishes the moving of residue load far from coupled piers.

Helmy et al. (2017) studied the pier of bridge located in curved channel. A curved channel of 30 degrees was investigated with several forms of pillars that were placed in the middle of the curved part of the canal. The channel wall was made of glass with a rectangular cross section (30x60 cm). Different discharges were considered and three (3) angles were evaluated. It was deduced that the pillars could be implemented in curved channels. Helmy et al. (2017) concluded that the angle of inclination of the spring has a good effect in reducing the depth of scour. The polygon (Hexagonal) was better in the ability to decrease the scour depth at a rate of approximately 36% of the maximum depth of scour. In addition, the zero tilt angle is the finest in the ability to decrease the depth of scour.

Khaple et al. (2014), discovered the effect of pier/column in front of a bridge pier as a protection tool to decrease local scour in the bridge. Khaple et.al. (2014) noted that mutual intrusion of the pier in the local scour depends on its shape, their spacing's, the flow speed, the flow depth, the comparative diameters of the piers, the size of the sediment and the oblique angle of flow and skew distance between piers. Two same piers with serial arrangement and deviation with numerous diameters of separation between them were analyzed. It was detected in the ongoing experimentations that the equilibrium of the scour depth in the downstream pier increases as the distance between the downstream & upstream

piers enhances. However, the equilibrium of scour depth at the upstream column/pier was not depended on the spacing.

### **Data description**

Riverbed Material from River Ravi was collected for the research. Riverbed material was used for bed formation at pier section.

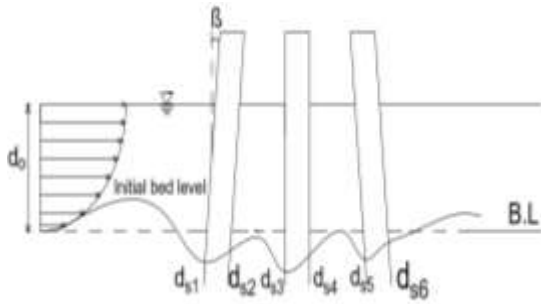
### **Research Methodology**

Model was prepared in the hydraulic laboratory of the Centre of Excellence in Water Resources Engineering, University of Engineering and Technology Lahore. For the model preparation at upstream and downstream section bed was made up of lean/varnished concrete to avoid sediment flow or to make clear water flow. A section of loose material in between upstream and downstream sections was formed with the sand collected from river Ravi. Bridge Pier of 50 mm diameter (D) made of PVC was used. Bridge pier were placed in open flume to carry out experiments. Sieve analysis of the bed material was carried out.

To examine local scours around bridge column/pier groups, pier group of two different combinations C1 (group of three piers), C2 (group of four piers) were used with inclined piers at upstream and downstream. For each pier group, variation in scoured depth “ds” by varying the flow depth “do”, flow intensity “V/Vc” and pier spacing (3D, 4D, 5D) was noted and compared with each other. Experiments were done under clear-water and steady conditions. To maintain the steady clear water conditions, no sediment inflow downstream of channel was ensured.

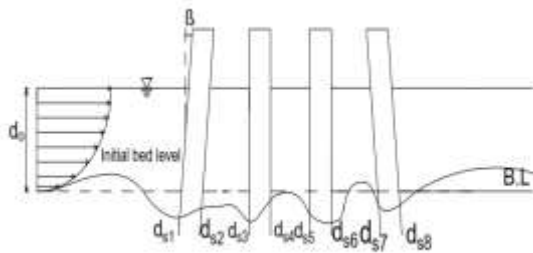
Working section of the apparatus was allowed to dry before starting of next experiment Piers were installed and sand bed was levelled by the help of steel screed. Flow depth was maintained and measured with the help of point gauge. Magnitude of scour depth was noted after drying. Scour depth on the u/s and d/s of each pier were measured with the help of point gauge.

Figure 1 represent that the arrangement for 3 piers whereas figure 2 depicts the arrangement for four piers used in experiments. Table 1 shows the results of the sieve analysis performed for the sand. Figure 3 shows the local scour in the bed after performing of the experiment.



**Fig. 1** Arrangement of 3 Piers

Where,  $d_0$  is flow depth, B.L is bed level,  $\beta$  is pier Inclination Angle,  $d_{s1}, d_{s2}, d_{s3}, d_{s4}, d_{s5}, d_{s6}$  is scour depth measured at different Points



**Fig. 2** Arrangement of 4 Piers

**Table 1** Sieve Analysis Results

Description	Values
Medium Sand	1.1%
Fine Sand	97.1%
Clay	1.8%
$D_{50}$	0.22 mm
$D/d_{50}$	$227 > 50$
Geometric SD	0.23



**Fig. 3** Observed floor after performing of experiment

**Table 2** Experiments performed for three piers arrangement.

Group C1 (Group of Three Piers)							
Depth of Flow (In)	3D (Pier Spacing)		4D (Pier Spacing)		5D (Pier Spacing)		Experiments
	$\beta = 0^\circ$	$\beta = 10^\circ$	$\beta = 0^\circ$	$\beta = 10^\circ$	$\beta = 0^\circ$	$\beta = 10^\circ$	
$d1 = 9''$	1	1	1	1	1	1	6
$d2 = 12''$	1	1	1	1	1	1	6
$d3 = 15''$	1	1	1	1	1	1	6
Total No of Experiments							18

**Table 3** Experiments performed for four piers arrangement.

Group C2 (Group of Four Piers)							
Depth of Flow (In)	3D (Pier Spacing)		4D (Pier Spacing)		5D (Pier Spacing)		Experiments
	$\beta = 0^\circ$	$\beta = 10^\circ$	$\beta = 0^\circ$	$\beta = 10^\circ$	$\beta = 0^\circ$	$\beta = 10^\circ$	
$d1 = 9''$	1	1	1	1	1	1	6
$d2 = 12''$	1	1	1	1	1	1	6
$d3 = 15''$	1	1	1	1	1	1	6
Total No of Experiments							18

## Results

The Figure 4 represents that maximum scour formation takes place in first two hours i-e,  $t/t_e=2$ . So the time duration for subsequent experimental series was limited to 2 hrs considering that the maximum scour would have

been achieved in this time duration. From the Figures 5, 6,7,8,9 and 10, it is evident that the scouring started from the upstream side of the pier, sediments get removed from this side and would be then deposited on the downstream side. Large amount of uplift takes place at the front



piers due to high velocity, direct impact and generation of vortices.

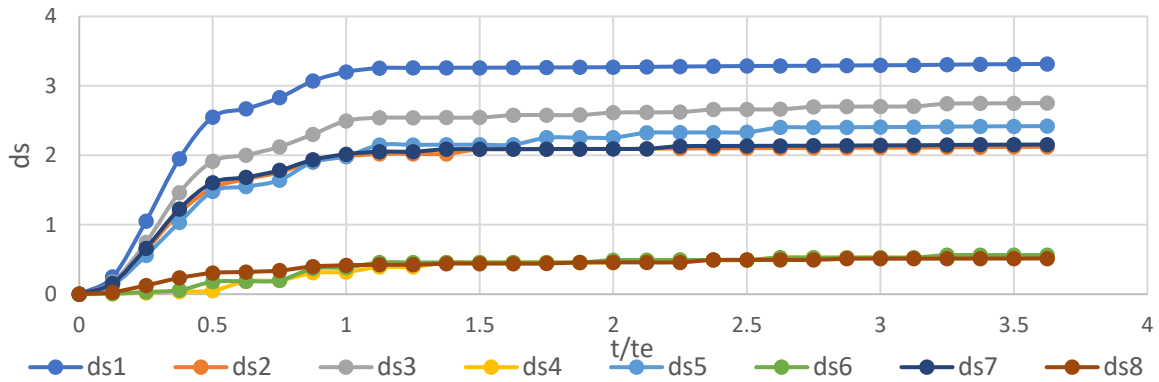


**Fig. 4** Time to achieve equilibrium scour depth graph

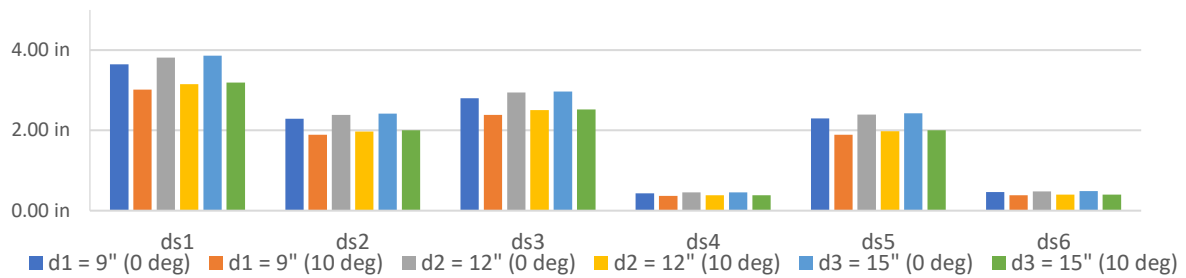


**Fig. 5** Scour depth at pier spacing 3D (C1)

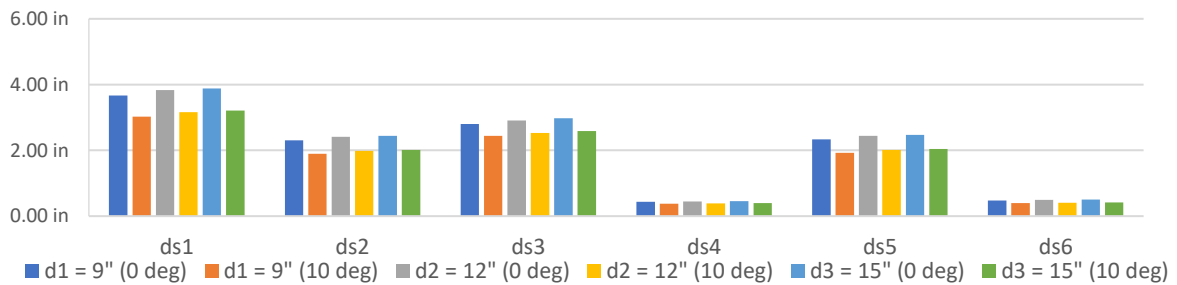


**Fig. 6** Scour depth at pier spacing 4D (C1)

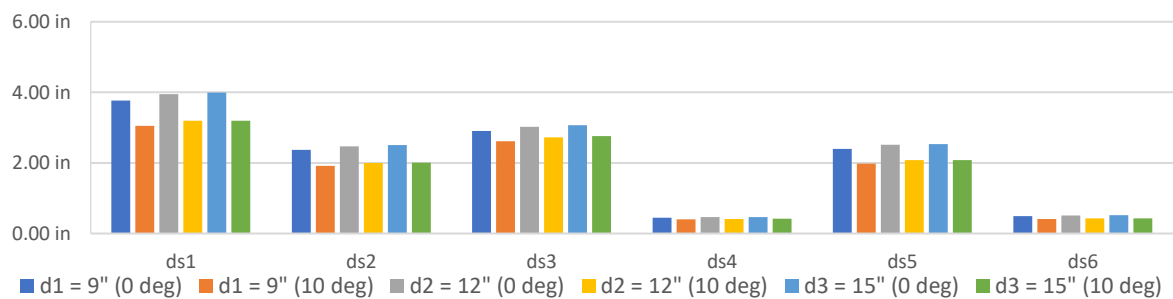


**Fig. 7** Scour depth at pier spacing 5D (C1)

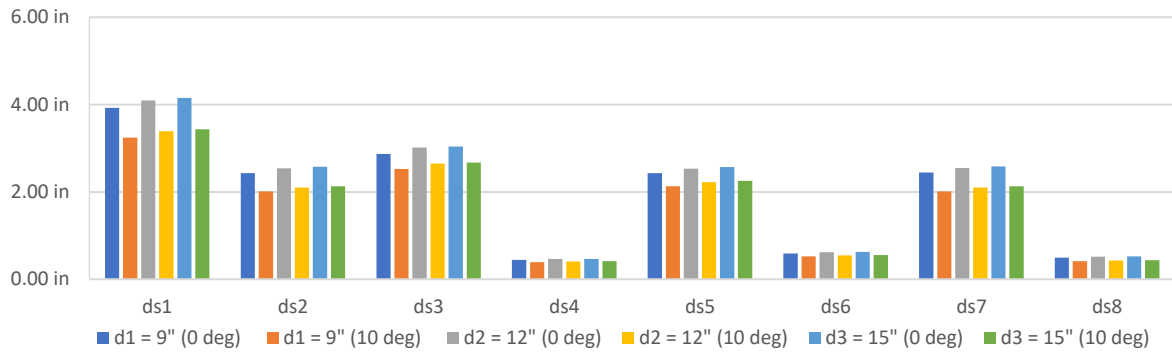


**Fig. 8** Scour depth at pier spacing 3D (C2)

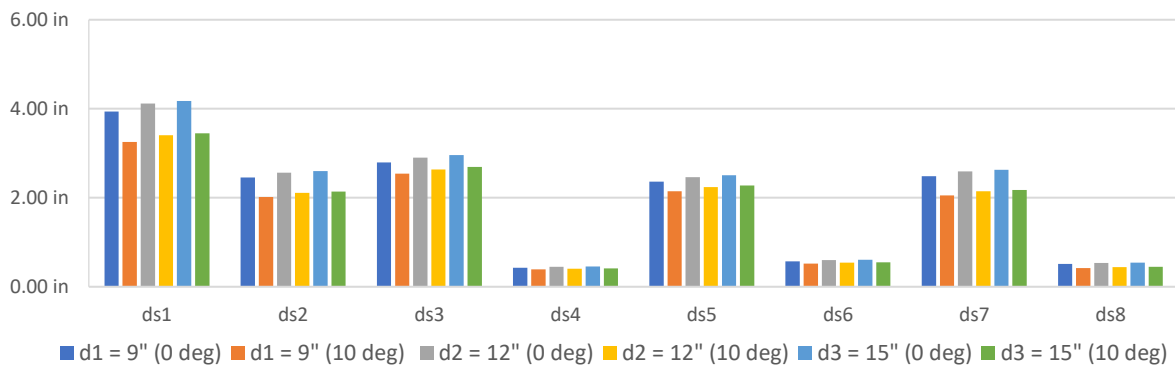


**Fig. 9** Scour depth at pier spacing 4D (C2)

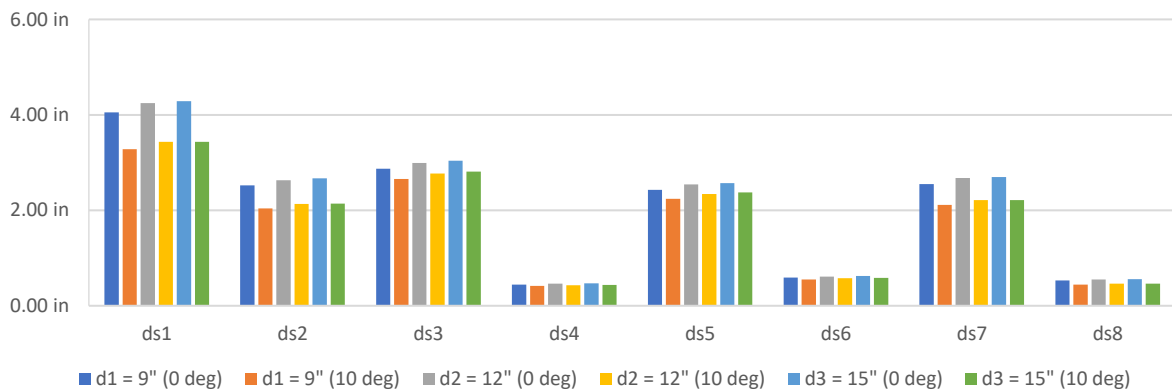


**Fig. 10** Scour depth at pier spacing 5D (C2)

### Conclusions

Considerable reduction was noted in scour around u/s and d/s pier by providing inclination. U/s and d/s scour reduced by 18 to 25% by changing the inclination angles. Centre piers scour also reduced by 10 to 15%. By increasing spacing between piers scour around u/s and d/s pier decreases by 2 to 3% and 7 to 8 % around middle piers. Also, by increasing discharge scour depth increases. Further experiments performed

by increasing number of piers in group, decreased the scour up to 4% around centre piers.

### Recommendations

Inclined pier arrangement should be preferred for the construction of bridges to reduce scour. More studies should be conducted by changing the inclination angle and their affects must be studied. Comparison of stability and cost analysis between inclined and straight piers should be done.

## Acknowledgements

This work was jointly funded by the authors and Centre of Excellence in Water Resources Engineering, University of Engineering and Technology Lahore.

## References

- Bozkuş, Z., Özalp, M. C., & Dinçer, A. E. (2018). Effect of Pier Inclination Angle on Local Scour Depth around Bridge Pier Groups. *Arabian Journal for Science and Engineering*, 43(10), 5413–5421. <https://doi.org/10.1007/s13369-018-3141-2>
- Briaud, J.-L. (2015). Scour Depth at Bridges: Method Including Soil Properties. I: Maximum Scour Depth Prediction. *Journal of Geotechnical and Geoenvironmental Engineering*, 141(2), 04014104. [https://doi.org/10.1061/\(ASCE\)GT.1943-5606.0001222](https://doi.org/10.1061/(ASCE)GT.1943-5606.0001222)
- Elnikhely, E.A. 2017. “Minimizing Scour around Bridge Pile Using Holes.” *Ain Shams Engineering Journal* 8(4): 499–506.
- Guemou, B., Seddini, A., & Ghenim, A. N. (2018). Scour around Bridge Piers: Numerical Investigations of the Longitudinal Biconcave Pier Shape. *Periodica Polytechnica Mechanical Engineering*, 62(4), 298–304. <https://doi.org/10.3311/PPme.12263>
- Helmy, Ahmed, Mostafa Ali, and Hany Ahmed. (2017). “An Experimental Study Of Local Scour Around Piers In The Curved Channels.” 4(1): 6
- Jaman, H., Das, S., Das, R., & Mazumdar, A. (2017). Hydrodynamics of Flow Obstructed by Inline and Eccentrically-Arranged Circular Piers on a Horizontal Bed Surface. *Journal of The Institution of Engineers (India): Series A*, 98(1–2), 77–83.
- Khan, M., Tufail, M., Fahad, M., Azmathullah, H. M., Aslam, M. S., Khan, F. A., & Khan, A. (2017). “experimental analysis of bridge pier scour pattern”. <https://doi.org/10.1007/s40030-017-0187-1>
- Khaple, S., Hanmaiahgari, P., & Dey, S. (2014). Studies on the effect of an upstream pier as a scour protection measure of a downstream bridge pier. In A. Schleiss, G. de Cesare, M. Franca, & M. Pfister (Eds.), *River Flow 2014* (pp. 2047–2052). <https://doi.org/10.1201/b17133-273>.
- Lança, R., Fael, C., Maia, R., Pêgo, J. P., & Cardoso, A. H. (2013). Clear-Water Scour at Pile Groups. *Journal of Hydraulic Engineering*, 139(10), 1089–1098. [https://doi.org/10.1061/\(ASCE\)HY.1943-7900.0000770](https://doi.org/10.1061/(ASCE)HY.1943-7900.0000770)
- Toth, E., & Brandimarte, L. (2011). Prediction of local scour depth at bridge piers under clear-water and live-bed conditions: Comparison of literature formulae and artificial neural networks. *Journal of Hydroinformatics*, 13(4), 812–824. <https://doi.org/10.2166/hydro.2011.065>
- Vaghefi, M.; Ghodsian, M.; Salimi, S.: Scour formation due to laterally inclined circular pier. *Arab. J. Sci. Eng.* 41(4), 13111318(2016). <https://doi.org/10.1007/s13369-015-1920-6>
- Wang, C., Yu, X., & Liang, F. (2017). A review of bridge scour: Mechanism, estimation, monitoring and countermeasures. *Natural Hazards*, 87(3), 1881–1906. <https://doi.org/10.1007/s11069-017-2842-2>
- Yang, Yifan, Bruce W. Melville, D. M. Sheppard, and Asaad Y. Shamseldin. 2018. “Clear-Water Local Scour at Skewed Complex Bridge Piers.” *Journal of Hydraulic Engineering* 144(6): 04018019.

## Experimental study of a flow through permeable spur dikes in a rectangular channel

Rana Shahid Asghar<sup>1\*</sup>, Ghufran Ahmed Pasha<sup>1</sup>, Usman Ghani<sup>1</sup>, Shahbaz Khalid<sup>1</sup>

<sup>1</sup> Department of Civil Engineering, University of Engineering and Technology, Taxila, Pakistan.

Corresponding author email: [enr.shahid272@gmail.com](mailto:enr.shahid272@gmail.com)

**Abstract:** Spur dikes are the structures placed in rivers to divert the flow, but during floods mostly floodwater damages the head of the impermeable spur dike or washes away the whole spur dike. The upper part of the impermeable spur dike also got damage because floodwater overtops from the impermeable spur dikes. In this study, lab experiments were performed to investigate the flow behavior through permeable spur dikes of varying porosities. The study was conducted on a fixed bed rectangular channel with all the spur dikes placed at a right angle to the main flow and on one side. In this research, experiments were performed both on permeable and impermeable spur dikes of varying porosities (4%, 8%, 12%, and 16%) with varying distances between the two dikes (1.5L, 2.5L, and 3.5L, where L is the length of spur dike). This paper addressed the findings of experimental analysis on a framework to measure the water depth profile at each spur dike head. It also analyzed the water depth profile in the second and third spur dike fields across the flow both in impermeable and permeable cases of spur dikes. Moreover, a trend of recirculation zone was also observed in the third spur dike field by using both impermeable and permeable spur dikes of varying porosities and distances. The results show that water depth at each spur dike head decreases with an increase in porosities. It also shows that the water depth profile in the second spur dike field decreases 0.58% by increasing 4% porosity, 3.5% decrease in water depth by increasing 8% porosity, 5.3% decrease in water depth by increasing 12% porosity, and 7.18% decrease in water depth by increasing 16% porosity. Results also show that in the case of the third spur dike field, water depth profile decreases 0.60% by increasing 4% porosity, 6.5% decrease in water depth by increasing 8% porosity, 9.5% decrease in water depth by increasing 12% porosity, and 10.7% decrease in water depth by increasing 16% porosity. The trend of the recirculation zone also changes with the increases of porosity of spur dikes.

**Keywords:** Spur dikes, Spur dike field, Porosity, Water surface profile, Recirculation zone, Fixed bed.

### Introduction

Spur dikes are structures constructed on rivers to protect riverbanks from erosion and cutting by deflecting the flow away from the banks towards the center of the river [1]. However, the construction of spur dikes causes scouring in their vicinity due to the formation of wake vortices and horseshoe which leads to failure of the spur dike itself [2]. Construction of spur dikes on the riverbanks mainly depends upon the design parameters such as hydraulic properties (discharge, water level, velocity, etc), length and width of spur dike, angle of construction of spur dike, and spacing between spur dikes [3]. Depending upon construction material spur dikes are made of stones, timber, concrete, and clay [4]. Spur dikes can be impermeable, permeable, emerged, and submerged type. In the case of permeable spur dikes, flow partly penetrates through the structure which results in velocity reduction, vortex strength in the spur dike field as compared to impermeable spur dikes [5]. Permeable spur dike also has the advantage of

being more stable and requires easy maintenance as compared to impermeable spur dikes [6].

A number of studies have investigated the details of the flow near spur dikes (Kurzke et al. 2002; Tominaga et al. 2001; Uijtewaal et al. 2001) and cases similar to spur dikes, embayment, cavities, and river harbors were studied by, e.g., Kawahara et al. (1995), Van Schijndel and Kranenburg (1998), Bijvelds et al. (1999), Muto et al. (2002, 2000). Field measurements were carried out by Sukhodolov et al. (2004, 2002), and numerical investigations by Tingsanchali and Maheswaran (1990), Nassiri and Babarutsi (1997), Ouillon and Dartus (1997), and Tang et al. (2006) [7]. The key elements of most previous studies on spur dikes were concentrated on erosion and sedimentation processes of the channel due to the installation of spur dikes [8].

The hydrodynamics of the flow near spur dikes have been explained, but detailed dynamics of the flow near a series of spur dikes remain to be fully understood [9]. The main objective of this study was water depth profiles at each spur dike

head by installing series of permeable spur dikes of varying porosity, water surface profile across the flow in each spur dike field, and trend of recirculation zone by increasing porosities of spur dikes [10].

**Flume characteristics and experimental procedure**

In a glass-sided water flume (constant bed slope 1/500) that is 11 m in length, 0.30 m in width, and 0.34 m in height, laboratory tests were performed under different conditions at the University of Engineering and Technology Taxila. The spur

dikes that were used in the channel were 0.1 m in length, 0.08 m in height, and 0.02 m in thickness, and spacing between spur dikes was 1.5L, where L is the length of spur dike. A small scale (1/3000) of wooden spur dikes were designed to analyze the water depths across the flow, water depths on each spur dike head along the flow. A high-speed digital camera was used to monitor the recirculation zone in each spur dike field with varying porosity. The schematic diagram of the water channel is shown in Fig.1 (a)

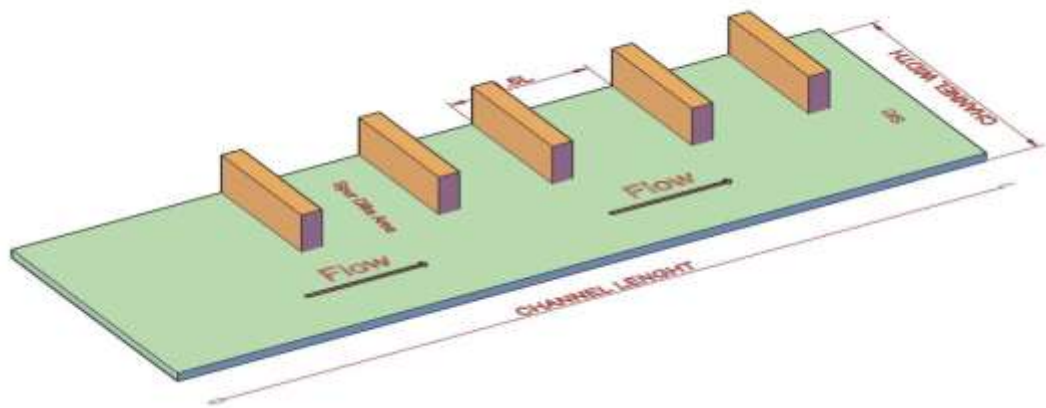


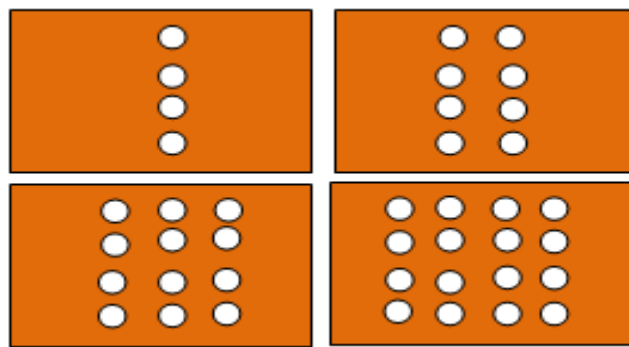
**Fig.1** The schematic diagram of the water channel

**Table 1:** Experimental conditions

Porosity(P) (%) of Spur dike	Case no	Angle of spur dike to U/S flow (Degree)	Installation Arrangement	Flow conditions	No of spur dikes
0	1	90	1.5L	Emergent	5
4	2	90	1.5L	Emergent	5
8	3	90	1.5L	Emergent	5
12	4	90	1.5L	Emergent	5
16	5	90	1.5L	Emergent	5



(a)



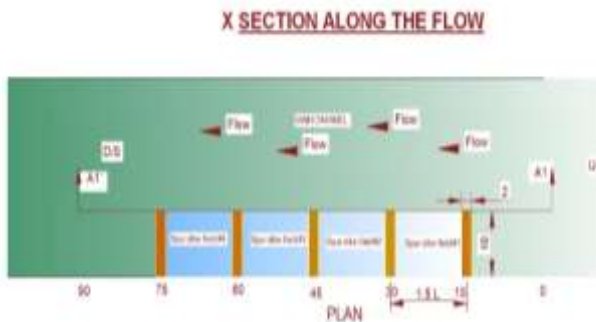
(b)

**Fig.2** Spur dike arrangements in the channel. (a) Top view of spur dike placing which is at 1.5L distance from each other (b) spur dikes with 4%,8%, 12%, 16% porosities.

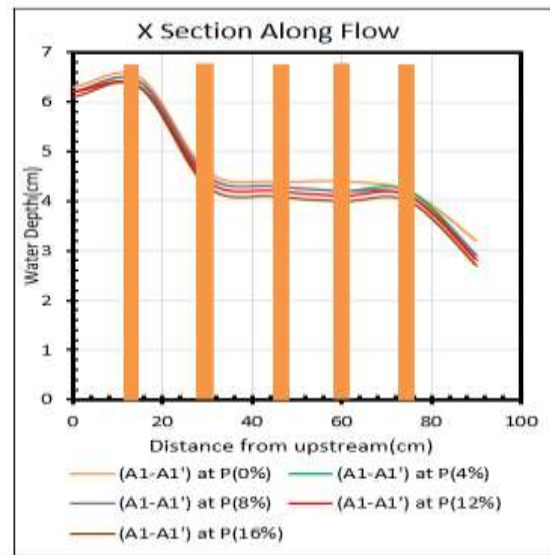
**Results and Discussion**

**Calculation of water surface profile along the flow at the head of spur dikes**

Fig.3 shows water surface profile at head of spur dikes w.r.t porosity changes. Fig. 3(a) shows a typical plan of spur dikes arrangements in the channel along with the flow. Fig. 3(b) shows the water depth profile at each of five spur dike heads for five different values of porosities (0%, 4%, 8%,12 & and 16%).



(a)



(b)

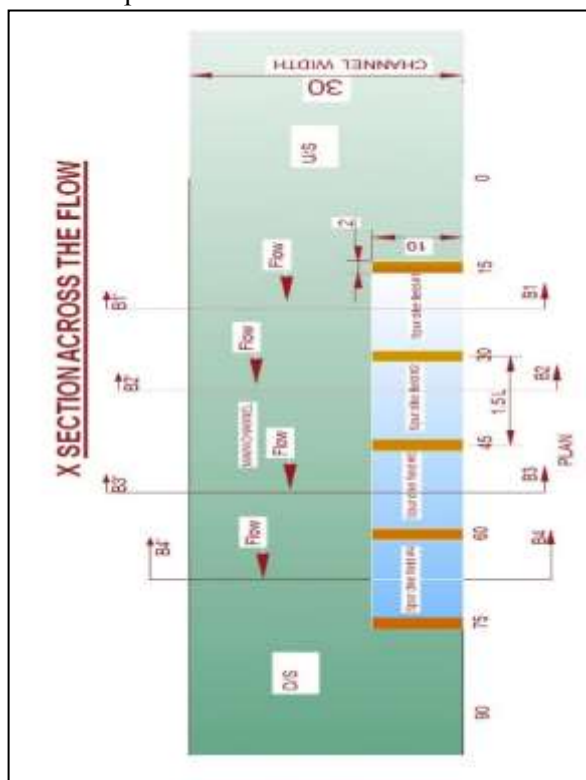
**Fig. 3** water surface profile at head of spur dikes w.r.t porosity changes (a) Typical plan of spur dike arrangements along flow (b) water depth profile at each of five spur dike heads for five different values of porosities. (0%, 4%, 8%, 12 & and 16%).



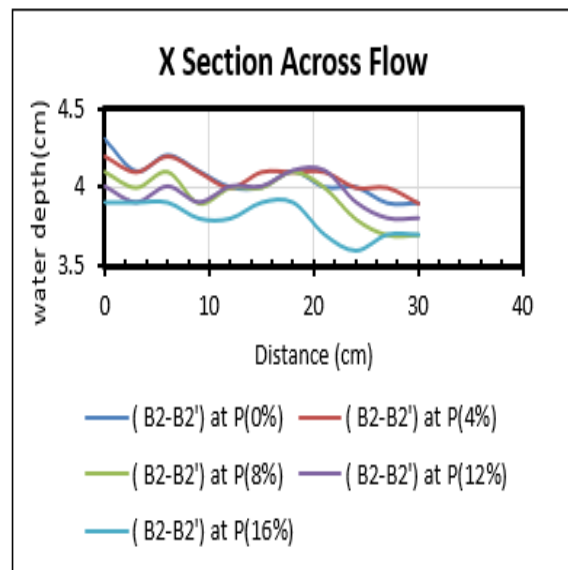
If we observe Fig.3(b) we can see that water depth in case of impermeable spur dikes(0% porosity) is high and it goes on decreasing as we increase the porosity values of permeable spur dikes(4%,8%,12%, and 16%). This clearly shows that with a decrease in water depth, turbulence on each spur dike head decreases so during floods it has been observed that the head of impermeable spur dikes damages or vanishes away. Permeable spur dikes in flood conditions are most suitable because results show that it can bear the thrust by passing wave of the flood through pores so minimizes the turbulence generated on the spur dike head.

### Calculation of water surface profile across the flow in spur dike field.

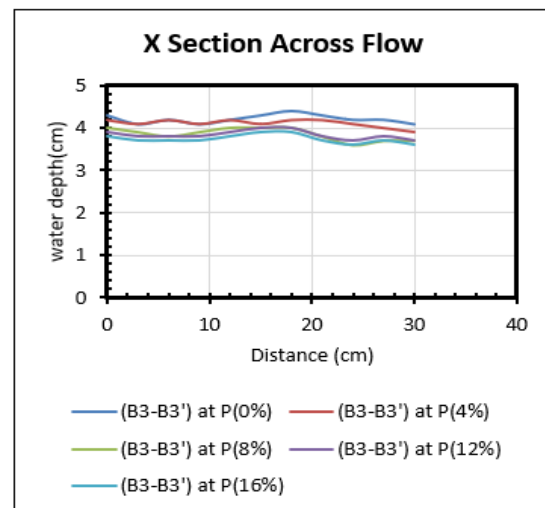
Fig.4 shows the water surface profile across the flow in the second and third spur dike fields. Fig. (4a) shows a typical plan of spur dikes in each spur dike field across the flow. Fig. 4(b) shows the water depth profile in the second spur dike field. Fig. 4(c) shows the water depth profile in the third spur dike field.



(a)



(b)



(c)

**Fig. 4** Water surface profile across the flow in second and third spur dike field. (a) A typical plan of spur dikes in each spur dike field across the flow (b) the water depth profile in the second spur dike field(c) water depth profile in the third spur dike field.

If we see the Fig 4(b) and Fig. 4(c) we can easily observe that in the second and third spur dike field, the water depth profile in case of impermeable spur dikes(0% porosity) is high and it tends to decrease in case of permeable spur dikes. Water depth profiles continue to decrease as we increase porosity levels from 4% to 16%. In the second spur dike field, the water depth profile decreases 0.58% by increasing 4% porosity, 3.5% decrease in water depth by increasing 8% porosity, 5.3% decrease in water depth by increasing 12% porosity, and 7.2%

decrease in water depth by increasing 16% porosity.

In the case of the third spur dike field, depth profile decreases 0.60% by increasing 4% porosity, 6.5% decrease in water depth by increasing 8% porosity, 9.5% decrease in water depth by increasing 12% porosity, and 10.7% decrease in water depth by increasing 16% porosity.

This decrease in water depths is due to the increased porosity of spur dikes. In the case of permeable spur dikes water continues to flow through pores from one spur dike to another and so water depth decreases.

In the case of impermeable spur dike, the undulation of the water surface in the spur dike field is greater than permeable spur dikes. In the case of permeable spur dikes results clearly shows that as the porosity of spur dikes increases undulation of the water surface in the spur dike field goes on decreasing. This happens because water waves coming through the pores encounter the waves coming from the main channel towards the spur dike field. So as the porosity of spur dikes goes on increasing, we can witness a stilling pond in spur dike field which is good for aquatic habitat.

#### **Trend of Recirculation Zone w.r.t Porosity Variation in Spur dike field.**

Fig.5 shows the trend of the recirculation zone in the third spur dike field. Fig. 5(a) shows the recirculation zone in impermeable spur dike field while Figure 5(b), 5(c), 5(d) and 5(e) shows the recirculation zone changes in permeable spur dike field.



(a)



(b)



(c)



(d)



(e)

**Fig.5.** Recirculation zone variations in the third spur dike field of impermeable and permeable spur dikes. (a) Recirculation zone in third spur dike field of impermeable spur dikes(0% porosity), Fig 5(b),5(c),(5d),and 5(e) Recirculation zone in third spur dike field of permeable spur dikes (4%,8%,12%, 16%porosity).

We can easily observe that recirculation zone in impermeable (0% porosity) spur dike field extends on entire spur dike field while with increase porosity, recirculation zone compresses and also moves in the forward direction. Figure 5(e) clearly shows that at (16% porosity) Recirculation zone in case of impermeable spur dike in third spur dike field extends throughout the spur dike field because water waves coming from the main channel extend throughout the spur dike field and these waves produce vortex flow in the entire spur dike field. In the case of permeable spur dike with increasing porosity, the recirculation zone compresses and also moves towards the forward direction within the spur dike field. This happens because, with increase porosity of spur dikes, water layers coming through the pores intersect the layers coming from the main channel towards the spur dike field due to which the recirculation zone compresses and also moves in the forward direction with an increase in porosity values which can be seen in Fig.5(e).

### Conclusion

During floods, the stability of the spur dikes is the main concern. Results show that by using permeable spur dikes we can easily pass the flood without causing any damage to the spur dikes

because due to holes in permeable spur dikes turbulence at the head of the spur dike can be minimized by lowering the water level at the head and results also shows that overtopping of floodwater can be also prevented in permeable spur dikes because water depth in spur dike fields continues to decrease by increasing porosity values.

### Acknowledgment

All authors are very thankful to the University of Engineering and Technology Taxila for providing a well-equipped hydraulics lab. The anonymous reviews are gratefully thanked for their close analysis and positive feedback

### Reference

- Fukuoka, S., Watanabe, A., Kawaguchi, H. & Yasutake, Y. 2000. A study of permeable groins in series installed in a straight channel. *Proceedings of Hydraulic Engineering* 44, 1047–1052.
- Kang, J., Yeo, H., Kim, S. & Ji, U. 2011. Permeability effects of single groin on flow characteristics. *Journal of Hydraulic Research* 49 (6), 1–8.
- K., Maeno, S., Ushita, T. & Fujii, A. 2005. Hydraulic characteristics of a group of permeable groins constructed in an open channel. *Flow. Journal of Applied Mechanics* 8, 773–782.
- Mohamed F.M. Yossef and Huib J de. Vriend. Flow details near River Groins: Experimental Investigation.
- Duan, G.D., He, L., Fu, X., Wang, Q.: Mean flow and turbulent flow around experimental spur dike. *Adv. Water Resour.* 32, 1717-1725 (2009).
- Acharya, A., Acharya, A., Duan, J.G.: Three dimensional simulation of flow field around series of spur dikes. *Int. Reff. J. of Eng. and Sci.* 2 36-57 (2013).
- Zhou, Y., Qian, S., Sun, N.: Application of permeable spur dike in mountain river training *Appl. Mech. Mater.* 641 236–240 (2014).
- Mostafa, M.M., Ahmed, H.S., Ahmed, A.A., Abdel-Raheem, G.A., Ali, N.A. Experimental study of flow characteristics around floodplain single groyne. *J. Hydro-23 Environment Res.* 22 1–13.

- Ouillon, S., and Dartus, D. (1997). "Three-dimensional computation of flow around groyne." *J. Hydraul. Eng.*, 123(11), 962–970
- Uijtewaal, W. S. J. (2005). "Effects of groyne layout on the flow in groyne fields: Laboratory experiments." *J. Hydraul. Eng.*, 131(9), 782–791.
- Tominaga, A., Ijima, K., and Nakano, Y.. (2001). "Flow structures around submerged spur dikes with various relative height." *Proc.*, 29th IAHR Congress, Beijing, 421–427.



## Estimation of Water Budget for Selected Irrigation Canal: A Case Study of LBDC Sahiwal

Asim Qayyum Butt<sup>1\*</sup>, Khadija Khan<sup>1</sup>, Saiqa Mushtaq<sup>1</sup>, Aqsa Zahoor<sup>1</sup>, Syeda Aqsa Gillani<sup>1</sup>

<sup>1</sup> Civil Engineering Department, Quaid-e-Azam College of Engineering and Technology, Sahiwal.

Corresponding author email: [asimbutt7891@gmail.com](mailto:asimbutt7891@gmail.com)

**Abstract:** In Pakistan, about half of the population is directly related to agriculture. The essential element for urban, rural, water supply, industrial use, and sanitation use is water. For domestic use in urban areas, people have about 84% access to water, and in rural areas, 0.8 MAF is estimated. This paper studies the Estimation of Water Budget for Irrigation Canal Lower Bari Doab Canal Sahiwal via identification of groundwater fluctuation by placing the piezometers at different locations of the selected site and analyzed simply by graphs on MS Excel, evapotranspiration by Cropwat 8.0 model uses Penman-Montieth method, Rainfall-Runoff by SCS curve number method, and crop water requirement by Cropwat software. This qualitative analysis strategy adopted to undertake this research has provided valuable data and information. It is observed that Groundwater fluctuation varies from 63.43ft to 65.62ft on average. Canal water supply and rainfall are less as compared to the requirement in that area. Over pumping, results decrease in groundwater budget by 14.75% from 2000 to 2019. Groundwater is decreasing continuously every year, which causes a problem for drinking purposes of humans and animals. Crop growth may also be affected by the decrease in groundwater levels in the study area. It is concluded that Proper management techniques should be adopted for the efficient use of groundwater. Groundwater recharge should be assumed in monsoon seasons because excess water is available during this season.

**Keywords:** Water Budget, Crop Water Requirement, Evapotranspiration, Groundwater, Lower Bari Doab Canal, monsoon seasons etc.

### Introduction

Water is the universal solvent; the earth is approximately 71% of water, out of which oceans hold 96.5% of water. Over total freshwater, 68 % consists of surface water, and 30% consists of groundwater. Agriculture is a driving force in the management of water use. Irrigation systems have been under pressure to produce more with lower supplies of water. Agriculture is a central part of Pakistan's budget, which pays 24.7 % of Gross National Products (GNP). During the last 30 years, groundwater has to be an essential source to canal supplies, specifically in such areas where groundwater quality is good, like in the Upper Indus Plain. In Pakistan, about half of the population is directly related to agriculture. Water plays a vital role for them. The necessary elements for urban, rural, water supply, industrial use, and sanitation use are water. Out of which 58.5% of people get their water through piped supply, and 7.6% get their water through stand posts, and the rest of people use hand pumps, wells, etc.

The future of Pakistan's agriculture depends on its irrigation and drainage system, which faces significant problems. Over-exploitation of fresh groundwater, low efficiency in delivering and

use, inequitable distribution, unreliable delivery, and insufficient cost recovery are some of these problems. The canal system being almost a century old is facing severe operational and maintenance issues. There is an inadequate capacity of the canal to pass designed discharge. Groundwater level usually fluctuates due to canal seepage: rainfall, percolation or irrigation, etc., water table level fluctuation varies seasonally and time by time. Its status varies by changes in precipitation, ETo, crop water requirement, etc. This fluctuation causes many problems regarding extraction; groundwater level rises, then salinity problems occur, which is considered a big problem. Similarly, when extraction exceeds the recharging, then the

groundwater level lowers down, then crops growth will be affected, drinking water supplies will also be affected. This paper studies the identification of groundwater fluctuation, evapotranspiration estimation, Rainfall-Runoff estimation, calculations of Crop Water Requirements, and estimation of the water budget of selected canals.

Salim Yaykiran et al. (2019) used WEAP-PGM (Water Evaluation and Planning System-Plant Growth Model) to estimate water budget

components of the Sakarya River Basin. General model performance ratings indicated that model simulations represent streamflow variations at acceptable levels. Model results revealed that runoff was 4747 million m<sup>3</sup>, groundwater flow was 3065 million m<sup>3</sup>, and ETo was 23,011 million m<sup>3</sup>.

Chuanjuan Wang et al. (2018) studied water-storage and water-saving potential for paddy fields in Gaoyou, China, using a water-balance model that was calibrated and validated using a 2-year field experimental data-set collected from an irrigated area in Gaoyou, China, in 2014–2015. Results showed that paddy fields effectively retain rainfall with utilization rates greater than 70% for shallow wet irrigation (SWI) and shallow humidity-regulated irrigation (SHRI) scenarios.

L.N. Thakuralet. al. (2009) explained water balance components by using the Thornthwaite and Mather's technique of water balance computations for the Dhasan River basin. The study revealed that on a normal basis, the basin has an annual water requirement of 1770 mm whereas the rainfall and actual evapotranspiration were 1149 mm and 821 mm. They concluded that the total water deficit in the basin was in the order of 948 mm, which was a matter of great concern.

Cuthbert M. O. (2009) presented a logical explanation to a Boussinesq equation, which is prolonged to present an expression for groundwater drainage using approximations of water table parameters. It was analyzed to make a modified groundwater fluctuation technique for the estimation of recharging of groundwater. This method/technique is mainly used where the groundwater level is variable, but on a small scale. Groundwater levels were used to estimate the recharge in the study area. Estimating recharge by using groundwater levels is a well standard and famous method.

He presented a seven-step method to determine the recharge by using groundwater levels.

Mobin-ud-Din Ahmad (2002) analyzed net groundwater use in irrigated river basins using Geo-information techniques at Rechna Doab, Pakistan. A 10-day interval to represent the conditions after a complete water turn within a watercourse was chosen. A deviation of 0.82% from field measurements was observed over the 10-day interval. The higher errors occurred in October when a canal was occasionally closed due to a water shortage.

Chung-Yu Wu (2008) predicted the water table fluctuations using the artificial neural network. He talked about two types of models (groundwater prediction model) using ANN (Artificial Neural Network) technology in his study. For measuring the brightness temperature, Advanced Microwave Scanning Radiometer (AMSR) was used. For the validation of the model, soil moisture data was used and measured by using Assimilation System. All the models gave values between 0.043m and 0.047m. These results showed that high-resolution data was not available; thus, the ANN model can be used.

Ijaz Hussain et al. (2011) estimated the water supply and demand joined with projections for the future in various sectors of the economy. The study provided information on water balance and water use efficiency estimates in the competing sectors. The total water available was 274 BCM, of which 130 BCM was available for use; however, 62 BCM was lost in the system. The empirical results further revealed that the gross water supply for agriculture was nearly 190 BCM, while its demand was 210 BCM showed a shortfall of about 20 BCM.

Maceo et al. (2009) used the White and Eddy covariance method to study the groundwater fluctuations and evapotranspiration by using seven years of observed groundwater level data. At one site, ET ranges from 91 to 164 percent averagely, but it changes from 57 to 254 percent on the remaining sites. There was an improvement in comparing all the water table methods with deeper depth by comprising a connection between groundwater and river.

Karamat et al. (2012) studied groundwater's physicochemical profile in Bahawalpur City to evaluate its adoption for domestic use. The physicochemical investigation was applied to the water samples, which were taken from all over the city. According to WHO standards, different parameters were graphically drawn with the pH to check their changes with respect to limit. This study suggests the proper treatment of groundwater to be treated appropriately from hazardous effects and may become useful for humans.

Aarti et al. (2013) used data of 20 years of approximately 100 wells to study groundwater level fluctuations on a seasonally and annually basis in Valsad district (VD) and Navsari District (ND) of Gujrat. The result of their study showed that the groundwater level fluctuates on a seasonal basis. The average water level trend variation is increasing in VD while it is



decreasing in ND. On the other hand, the intermediate groundwater level is decreasing in VD and Navsari district both.

Pingwang and Sergey (2014) developed a relation between daily groundwater levels and evapotranspiration, which was used to estimate the reduction in groundwater by phreatophytes. The standard deviation of daily groundwater levels and evapotranspiration of a short period were used in this study. A comparison was established between groundwater evapotranspiration resulted from daily groundwater level fluctuation with already predefined values.

Shao-feng et al. (2014) selected the Coastal plain region of Jiangsu Province, China, by constructing nine shallow monitoring wells to study seasonal variations in groundwater levels and salinity. According to results, precipitation has more effect than evaporation, which has more effect than the river stage. In the rainy season, salinity increases as the water level decrease. Musa and Iliyasu (2015) selected Terengganu, Malaysia, to study groundwater level fluctuations due to change in rainfall by using the climatic parameters and groundwater fluctuation data. By using excel and GIS, results were drawn in graphs that maximum rainfall was from Sep to Dec. But max groundwater level was measured in Jan and Feb.

Kuldeep and Upasana (2016) estimated the groundwater balance and resource by using geospatial technology. They made their study by raster-based modeling in ArcGIS. According to this study, the results were 786.56, 379.29, 1165.85 MCM for net annual groundwater availability, annual groundwater draft, and total groundwater potential, respectively.

Scot et al. (2007) studied the water budget at a forested plain watershed in South Carolina. The result showed that Hamon estimation and Penman-Monteith (PM) estimation methods performed well with avg deviations of 12.6mm and 13.9mm, respectively. An error of 9% was estimated for the years 2003 and 2004 and seasonal water budgets too.

Keith Edwin (2009) studied hydrological processes inferred from water table fluctuations at selected sites. He said that groundwater recharge, baseflow, and ETo are expressed as:

$$R = \Delta S + Et + BF$$

The study's result indicates an essential amount of information about hydrological processes for measuring water table levels at high frequency.

Ritesh et al. (2011) selected Puri city located on India's coast. For the estimation of topography, the Geographic Information system was used and using the digital elevation model (DEM) and by developing groundwater contours with respect to space and time.

Hasan et al. (2013) selected the Chapai Nawabgonj district to assess the rainfall effect on groundwater level fluctuations. They collected rainfall and groundwater data from the Bismarck-Mandan Development Association (BMDA) and ETo from the Water Modeling (IWM), Dhaka. The result shows that rainfall usually started from May to Sep, and during the rest of the year, there was just a little bit or no rain in the area. The study also showed that max rainfall occurs from Jun to Aug, and due to this, the max water table was observed from July to Sep.

Dinesh et al. (2013) predicted the water table elevation fluctuation using 10 Artificial Neural Networks (ANN) models. MATLAB was used to develop both the Fuzzy logic and ANN models. The conclusion was that these techniques are easier and reliable as compared to other methods. This paper shows that ANN is suitable for more inputs, and Fuzzy models show better performance for a few.

Rocio et al. (2016) studied the water budget analysis in the United Arab Emirates (UAE), where there is low precipitation, but humans and animals' growth rate is high. The estimated Water budget represented the variation in groundwater storage, which was calculated by GRACE satellite compared with total rainfall, evapotranspiration, and desalinated water. Results showed a deficiency in groundwater every year, so there should be adopted some recharging techniques to balance it.

### **Study area and data description**

Lower Bari Doab Canal (LBDC) off-takes from Balloki barrage, located southwest of Lahore at a distance of about 65 km. LBDC and BS link feed about 23% of the irrigated area of Punjab. The LBDC serves a cultivable command area of about 1.7 million acres in Kasur, Okara, Sahiwal, and Khanewal.

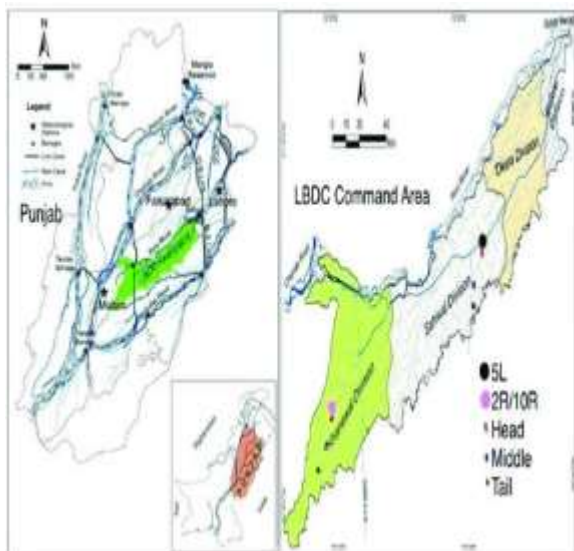


Figure 11 Study Area (LBDC Sahiwal)

## Research Methodology



Figure 12 Research Methodology Data Required Historical data of some parameters is required to conduct this research, including the precipitation data, climatic data, and canal discharges. Some other data include crop data, evapotranspiration, crop water requirement, periodic water level fluctuations, and groundwater levels.

### Data Collection

The discharge data is collected from Irrigation Department Punjab. Rainfall data will also be collected from the Punjab Irrigation Department. The different piezometers installed in the study area are named differently according to their specific location or some other famous places like Sahiwal, Balloki, Okara, Gamber, Harrapa, Chichawatni, Mianchanu, khanewal. Precipitation data, climatic data, canal discharge, crop data, and evapotranspiration will be

collected from the Pakistan Meteorological Department (PMD).

### Data Analysis

By acquiring the required or calculated rainfall data, crops, and climatic data, the crop water requirement will be determined using Cropwat software—Wells and Tubewells for determining the groundwater levels near LBDC Sahiwal. WWF has a project in which they have installed 25 Piezometric groundwater levels will be determined for which there would be a clear estimation about recharging and discharging of that area. After estimating the recharging or discharging impact on that area, fluctuations in the groundwater level will be determined. Then by subtracting total discharge from total recharge, the water budget of groundwater flow will be determined.

### Groundwater Fluctuation:

Groundwater level data is measured from different piezometers at different sites of the study area. This data was analyzed using MS Excel by making graphs between months and their other locations' groundwater levels.

### Evapotranspiration Estimation:

Cropwat 8.0 model uses the Penman-Montieth method for estimation of evapotranspiration, Equation used in this method is as follows.

$$E_{to} = (0.408\Delta (R_n - G) + \gamma (900 / T + 273) u_2 (V_s - V_a)) / \Delta + \gamma (1 + 0.34u_2)$$

Where,

$E_{t0}$  = Reference evapotranspiration (mm / day)

$R_n$  = Net radiations at crop surface (MJ / m<sup>2</sup> / day)

$G$  = soil heat flux density (MJ / m<sup>2</sup> / day)

$T$  = mean daily air temperature at 2 m height (0C)

$U_2$  = wind speed at 2 m height (m / s)

$V_s$  = saturated vapor pressure (k Pa)

$V_a$  = actual vapor pressure (k Pa)

### Rainfall-Runoff Estimation:

The rainfall-runoff was estimated by SCS method. The general equation is as follows:

$$Q = \frac{(P - 0.2S)^2}{(P + 0.8S)}$$

$$S = \frac{1000}{CN} - 10 \quad (24)$$

Where,

$Q$  = Runoff (inch),  $P$  = Rainfall (inch)

$S$  = Potential maximum retention,  $CN$  = Curve number

### **Crop Water Requirement:**

The amount of water required to compensate for the evapotranspiration loss from the cropped field is defined as crop water requirements. The Blanney-Criddle method had been used for estimating ETo by the meteorological department. The total canal command area was divided into eight subareas called HSUs, assuming similar hydrological conditions, i.e., rainfall and ETo within the HSUs. For interpolation of these hydrological parameters (rainfall and ETo), the most commonly used method called IDW (Inverse Distance Weighting) interpolation was used as given in the Equation.

$$Z_p = \frac{\sum_{i=1}^n Z_i W_i}{\sum_{i=1}^n W_i}$$

$Z_p$  = interpolated value at the desired location

$Z_i$  = parameter value at the known point

$W_i$  = weight assigned to the known location

The weighting function used for the above equation is given in Equation.

$W_i = 1/(d_i)^2$

### **Streamflow Recharge Estimation:**

Streamflow recharge was calculated for LBDC Sahiwal. Authorized discharge, depth, and length were available for LBDC. Cross-sectional area was calculated by dividing authorized discharge by its velocity, a width of the channel was calculated by dividing the cross-sectional area to a depth of water, by multiplying wetted perimeter to the length of distributary, the wetted area was calculated, and finally, streamflow recharge was calculated by multiplying permeability to the wetted area.

### **Water Budget Estimation:**

Total precipitation recharge is calculated by subtracting evapotranspiration and runoff into total rainfall. Recharge through rainfall and streamflow recharge is sum up to give total recharge. The water budget equation can be explained as follows:

$$\Delta S = \pm SRO \pm GF - E + P - ET$$

Where,

$P$  = Precipitation

$ET$  = Evapotranspiration

$SRO$  = Surface Runoff

$GF$  = Groundwater Flow

### **Results:**

#### **Groundwater Fluctuation:**

Data collected from different piezometers at different sites in the study area is analyzed by making their graph on MS Excel, which is shown in the figure 3.

It was observed from the graph that the groundwater level from January to May decreases because of high water usage in the summer season, and groundwater level increases from June to December due to the monsoon season.

#### **Evapotranspiration Estimation:**

Evapotranspiration measured by Cropwat 8.0 model is shown in the following table from 2000 to 2019, which shows that maximum values are in summer months and minimum values are in winter months.

#### **Rainfall-Runoff Estimation:**

Direct runoff volume from the year 2000 to 2019 is shown in the above figure 4, which represents 24.85 (in) as the maximum peak value of direct runoff in the year 2012 and 4.1(in) as the peak minimum value of direct runoff in the year 2000.

#### **Crop Water Requirements Estimation:**

The above analysis shows an increasing crop water requirement continuously from head to tail of the canal command due to climatic variation (Figure 4).

#### **Stream flow Recharge Estimation:**

Streamflow recharge is calculated for LBDC Sahiwal. A detailed description of LBDC is shown in the following table 2.

It was concluded that the total streamflow recharge calculated for LBDC Sahiwal was 73.83mm.

#### **Water Budget:**

Recharge through precipitation is calculated by subtracting evapotranspiration and runoff through total rainfall. Streamflow recharge is added up into recharge through rainfall to give total recharge in the study area. Then total recharge is subtracted through well withdrawals, which gives the net budget as shown in the table 3.

**Table 4** Detailed Description of Evapotranspiration.

Year	Jan	Feb	Mar	Apr	May	Jun	Jul	Aug	Sep	Oct	Nov	Dec
2000	1.67	2.56	3.51	4.93	6.43	6.64	7.32	5.93	5.14	3.85	2.16	1.54
2001	1.6	2.73	3.36	5.09	6.36	7.2	7.44	7.04	6.3	3.56	2.38	1.74
2002	1.65	2.86	3.40	5.76	6.97	7.65	7.89	7.63	5.46	4.23	2.23	1.62
2003	1.71	2.19	3.61	5.08	7.81	8.91	8.10	7.23	5.88	3.49	2.59	1.81
2004	1.88	2.47	4.18	5.25	11.34	12.43	8.06	7.85	6.15	3.39	2.29	1.94
2005	1.68	2.51	3.88	5.09	8.08	7.25	6.16	6.50	5.31	3.36	2.50	1.68
2006	1.67	2.33	3.67	5.19	8.31	7.77	10.60	6.79	4.67	3.19	2.40	1.45
2007	1.63	2.28	3.53	5.59	5.32	8.75	5.88	5.81	5.82	3.78	2.02	1.48
2008	1.55	2.33	3.70	6.24	8.02	8.11	9.22	5.97	5.77	3.52	1.98	1.76
2009	1.45	1.96	3.43	5.15	5.65	8.24	6.50	8.24	5.51	4.53	2.21	1.50
2010	1.34	2.19	3.68	5.35	7.24	6.97	7.24	5.62	5.09	3.82	2.13	1.55
2011	1.31	2.26	3.02	4.84	4.30	11.91	7.63	7.61	5.06	3.17	2.10	1.32
2012	1.42	2.45	3.51	4.83	7.92	8.97	8.06	6.29	5.59	4.10	2.24	1.65
2013	1.55	2.42	3.84	5.04	5.81	7.13	6.9	7.73	5.41	3.54	1.82	1.28
2014	1.33	1.98	2.96	4.32	5.6	7.8	6.87	5.22	5.14	3.47	2	1.34
2015	1.19	1.88	3.06	4.69	6.81	7.82	6.66	5.49	4.79	3.67	2.26	1.34
2016	1.2	1.98	2.91	4.03	6.27	8.32	8.36	6.14	4.62	2.93	1.99	1.3
2017	1.3	2.09	2.37	4.77	6.21	6.81	6.95	5.9	5.46	3.34	1.96	1.27
2018	1.15	2.14	2.72	4.85	4.9	9.57	8.03	7.41	6.34	3.45	1.87	1.41
2019	1.18	1.91	2.82	4.08	5.47	5.98	5.73	6.67	5.84	3.57	2.03	1.51

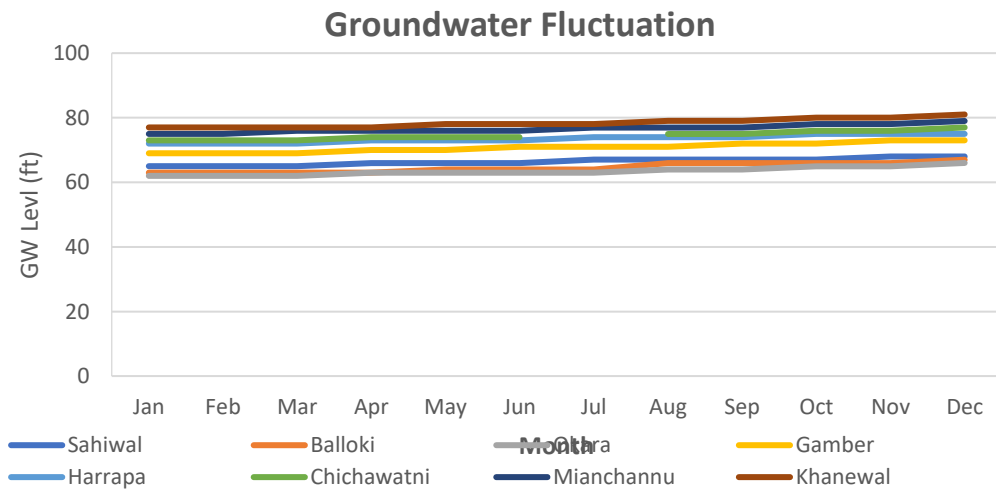


**Figure 13** Ground water Levels at Different Piezometers Locations

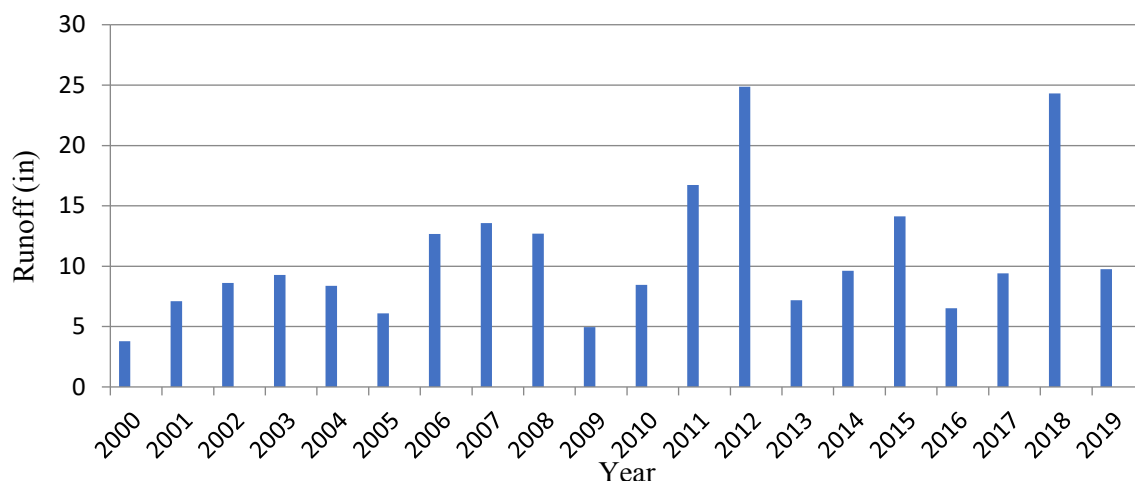


**Figure 14** Direct Runoff Estimated Using CN Method

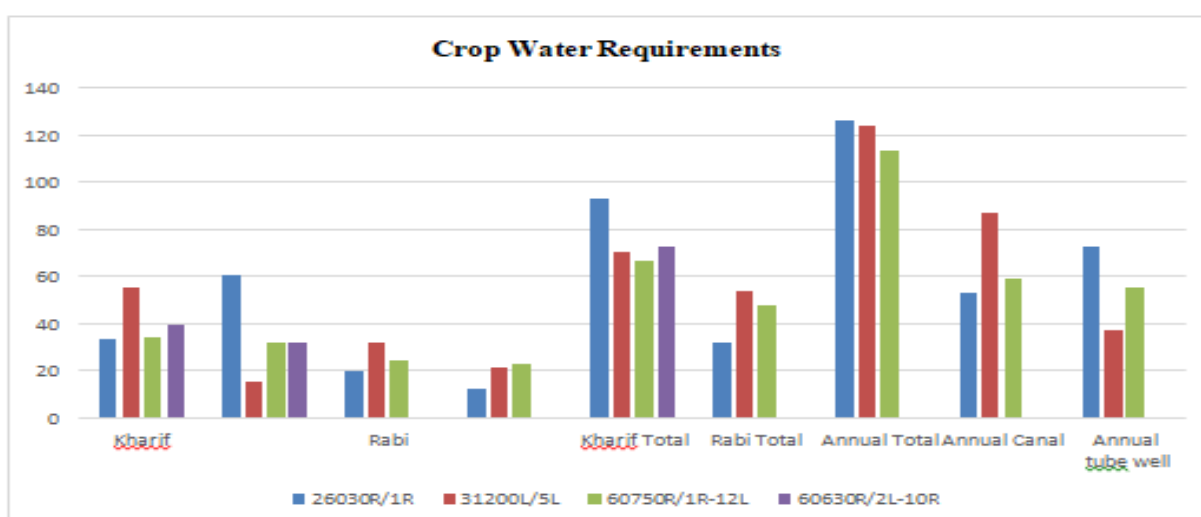


**Figure 15** Crop Water Requirements (Water Usage at Watercourse Level of Four Watercourses)

**Table 5** Detailed Description of LBDC

Sr. No.	Description	Units	LBDC
1	Authorized Discharge	Cusecs	278
2	Velocity	feet per sec	6.5
3	Depth of water	ft	4.2
4	Length	km	75
5	Cross Sectional Area	square ft	42.77
6	Width of channel	ft	10.18
7	Wetted perimeter	ft	18.58
8	Wetted Area	ft	4570680
9	Permeability	feet per sec	0.0000164
10	Total Seepage	cusec	74.96
11	Total Study Area	square km	985
12	Stream flow recharge	mm	73.83

**Table 6** Detailed Water Budget

Year	Rainfall (mm)	ET0 (mm)	Runoff (mm)	Precipitation Recharge (mm)	Stream flow Recharge	Total Recharge	Well Withdrawals (mm)	Net Deficit (mm)
2000	158.75	1571.93	94.66	-1507.84	73.83	-1434.01	267.26	-
2001	248.75	1666.83	177.22	-1595.30	73.83	-1521.47	280.62	1701.27
2002	288.75	1744.4	215.14	-1670.79	73.83	-1596.96	294.65	-
2003	306.25	1776.64	231.88	-1702.27	73.83	-1628.44	309.38	-
2004	282.5	2044.91	209.18	-1971.59	73.83	-1897.76	324.85	1937.82
2005	222.25	1642.5	152.41	-1572.66	73.83	-1498.83	341.1	-
2006	394.25	1765.38	316.92	-1688.05	73.83	-1614.22	358.15	-
2007	417	1578.32	339.09	-1500.41	73.83	-1426.58	376.06	1972.37
2008	395	1769.34	317.65	-1691.99	73.83	-1618.16	394.86	-
2009	191.25	1653.75	123.86	-1586.36	73.83	-1512.53	414.6	-
2010	285	1588.36	211.57	-1514.93	73.83	-1441.10	435.33	1927.13
2011	497.5	1658.62	417.90	-1579.02	73.83	-1505.19	457.1	-
2012	703.75	1734.66	621.44	-1652.35	73.83	-1578.52	479.96	-
2013	251.25	1595.96	179.57	-1524.28	73.83	-1450.45	503.95	2058.48
2014	315	1460.91	240.27	-1386.18	73.83	-1312.35	529.15	-
2015	431.75	1510.49	353.49	-1432.23	73.83	-1358.40	555.61	-
2016	233.75	1522.35	163.14	-1451.74	73.83	-1377.91	583.39	1914.01
2017	310	1473.08	235.47	-1398.55	73.83	-1324.72	612.56	-
2018	689.75	1637.63	607.58	-1555.46	73.83	-1481.63	643.19	-
2019	318.75	1423.2	243.87	-1348.32	73.83	-1274.49	675.35	-

This budget shows a net deficit starting from -1728.32mm in 2000 to -2027.94 in 2019. This deficit can be increased if proper management techniques are not done in that area. The total net deficit, along with their recharge, is shown in the figure.

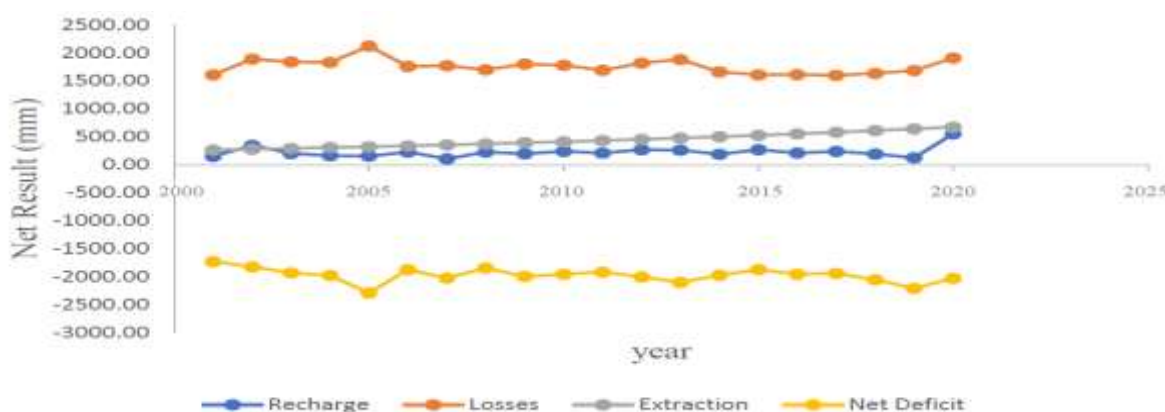


**Figure 16** Water Budget (Different Parameters used in Water Budget)

**Conclusions**

The conclusion drawn from the conducted research was that Groundwater fluctuation varies from 63.43 ft to 65.62 ft on average. Canal water supply and rainfall are less as compared to the requirement in that area. It causes an excess reduction in the groundwater level. Over pumping shows result in a decrease in

groundwater budget by 14.75% from 2000 to 2019. Crop growth may also be affected by a decrease in groundwater levels in the study area. In the future, this study helps that Proper management techniques should be adopted for efficient use of groundwater. High delta crops should be replaced with low delta crops. In this way, the crop water requirement of different crops will be less than high delta crops. So, their



growth will not be affected. Groundwater recharge should be adopted in monsoon seasons because excess water is available during this season.

### Acknowledgements

We are highly indebted and grateful to our creator and the Lord of the universe, Allah Almighty, who granted us with the best of health and courage to undertake this responsibility and complete it in the best feasible way in minimum time. Without ALLAH's help and love of our Holy Prophet Hazrat Muhammad (Peace be upon Him) with us, this was never possible for ordinary persons like us.

How can we forget to thank our B.Sc. fellows and seniors for being there to help me whenever and whatever we needed?

At last, but definitely not the least, we would like to thank our parents and family for their prayers. Engr. Asim Qayyum Butt, Khadija Khan, Saiqa Mushtaq, Aqsa Zahoor, Syeda Aqsa Gillani

### References

- United States Geological Survey. (2016, Dec 2). Global water volume. Available from: [https://www.usgs.gov/special-topic/water-science-school/science/how-much-water-there-earth?qt-science\\_center\\_objects=0#qt-science\\_center\\_objects](https://www.usgs.gov/special-topic/water-science-school/science/how-much-water-there-earth?qt-science_center_objects=0#qt-science_center_objects)
- Ping Wang<sup>1</sup> and Sergey P. Pozdniakov<sup>2</sup>. Water Resources Research. 2014;(1):2276–92.
- Olowu TO, Sundararajan A, Moghaddami M, Sarwat AI, Unigwe O, Okekunle D, et al. [http://www.eskom.co.za/CustomerCare/TariffsAndCharges/Documents/RSA\\_Distribution\\_Tariff\\_Code\\_Vers\\_6.pdf%0Ahttp://www.nersa.org.za/lbdcip.irrigation.punjab.gov.pk](http://www.eskom.co.za/CustomerCare/TariffsAndCharges/Documents/RSA_Distribution_Tariff_Code_Vers_6.pdf%0Ahttp://www.nersa.org.za/lbdcip.irrigation.punjab.gov.pk) - Lower Bari Doab Canal Improvem... - LBDCIP Irrigation Punjab Available from:<http://sur.ly/i/lbdcip.irrigation.punjab.gov.pk/>
- Yaykiran S, Cuceloglu G, Ekdal A. Estimation of water budget components of the Sakarya River basin by using the WEAP-PGM model. Vol. 11, Water (Switzerland). 2019.
- Wang C, Wang S, Chen H, Wang J, Tao Y, Liu J. Evaluation of water-storage and water-saving potential for paddy fields in Gaoyou, China. Water (Switzerland). 2018;10(9).
- Thakural LN, Kumar S, Singh S, Kumar R, Jain SK, Thomas T. Estimation of Water Balance Components in the Dhasan River Basin. Indian Journals. 2009;19(3):2–8.
- Cuthbert MO. An improved time series approach for estimating groundwater recharge from groundwater level fluctuations. 2010;46(September):1–11.
- Ahmad M. Estimation of net groundwater use in irrigated river basins using geo-information techniques: a case study in Rechna Doab, Pakistan. [Internet]. 2002. Available from: <http://www.cabdirect.org/abstracts/20046798467.html>
- Bisht D, Jain S, Raju MM. Prediction of Water Table Elevation Fluctuation through Fuzzy Logic & Artificial Neural Networks. 2013;51:107–20.
- Hussain I, Hussain Z, Sial MH, Akram W, Farhan MF. Water Balance , Supply and Demand and Irrigation Efficiency of Indus Basin. Water. 2011;49(1):13–38.
- Martinet MC, Vivoni ER, Cleverly JR, Thibault JR, Schuetz JF, Dahm CN. On groundwater fluctuations , evapotranspiration , and understory removal in riparian corridors. 2009;45:1–19.
- Mehmood K, Younas U, Iqbal S, Shaheen MA, Samad A, Hassan SI. Physicochemical profile of ground water in Bahawalpur city, Pakistan: hazardous aspects. J Chem Soc Pakistan. 2012;34(5).
- Avalkar A. Engineering A Study of Groundwater Fluctuation in Coastal Region , Valsad and Navsari District . Surat Aarti Avalkar Dr . S . M . Yadav Sahita Waikhom. Glob Res Anal. 2013;2(4):81–5.
- Yan S, Yu S, Wu Y, Pan D, She D, Ji J. Seasonal Variations in Groundwater Level and Salinity in Coastal Plain of Eastern China Influenced by Climate. 2015;2015.
- Abdullahi MG, Garba I. Effect of Rainfall on Groundwater Level Fluctuation in Terengganu , Malaysia Effect of Rainfall on Groundwater Level Fluctuation in Terengganu ., 2016;(January).
- Pareta K, Ph D, Pareta U. Ground Water Balance And Resource Estimation. 048:1–18.
- Harder S V, Amatya DM, Callahan Tj, Trettin Cc, Hakkila J. Hydrology And Water Budget For A Forested Atlantic Coastal Plain Watershed , South Carolina 1. 2007;43(3).
- Schilling KE, Schilling KE. Hydrological processes inferred from water table fluctuations , Walnut Creek , Iowa. 2009;
- Vijay R, Sharma A, Ramya SS, Gupta A. Fluctuation of groundwater in an urban coastal city of India: a GIS-based approach. Hydrol Process 2011 Apr 30;25(9):1479–85.

- Available from:  
<http://doi.wiley.com/10.1002/hyp.7914>
- Hasan MR, Mostafa MG, Matin I. Effect Of Rainfall On Groundwater Level Fluctuations In Chapai Nawabgonj District. 2013;2(4):2800–7.
- Gonzalez R, Ouarda TBMJ, Marpu PR, Allam MM, Eltahir EAB, Pearson S. Water Budget Analysis in Arid Regions , Application to the United Arab Emirates. 2016;
- Admasu W, Tadesse K, Abstract DH. Evaluation of reference evapotranspiration estimated from limited climatic parameters using CROPWAT 8.0 model under humid condition of Arsi Zone. Merit Res J Environ Sci Toxicol [Internet]. 2014;2(7):2350–2266. Available from:  
<http://www.meritresearchjournals.org/est/index.htm>
- More Information - SCS Curve Number Method Available from:  
<https://engineering.purdue.edu/mapserve/LTHIA7/documentation/scs.htm>
- Streamflow Routing - Section Four: Stream Properties & Manning’s Equation Available from:  
[http://stream1.cmatc.cn/pub/comet/HydrologyFlooding/streamflow/comet/hydro/basic/Routing/print\\_version/04-stream\\_properties.htm](http://stream1.cmatc.cn/pub/comet/HydrologyFlooding/streamflow/comet/hydro/basic/Routing/print_version/04-stream_properties.htm)
- Division WR. General Guidelines for Calculating a Water Budget Water Resources Division (WRD).

## Evaluation of Various Soft Computing Approaches to Estimate Reference Evapotranspiration of three Cities of South Punjab

Aarish Maqsood<sup>1\*</sup>, Muhammad Shoaib<sup>1</sup>, Hamza Salaudin<sup>1</sup>

<sup>1</sup> Department of Agricultural Engineering, Bahauddin Zakariya University, Multan 60800, Pakistan

Corresponding author email: [aarishmaqsood@gmail.com](mailto:aarishmaqsood@gmail.com)

**Abstract:** Numerous soft computing approaches can be utilized to estimate reference evapotranspiration ( $ET_o$ ) for a particular region. Precise measurement of  $ET_o$  is crucial in various disciplines including agriculture applications, water resources arrangement and management, and hydrologic water balance as well. In this study five supervised learning algorithms/models, namely, probabilistic neural network (PNN), radial base function (RBF), group method of data handling (GMDH), cascade correlation (CC), support vector machines (SVM) are used to estimate  $ET_o$  using eight climatic parameters comprising of temperature (maximum, minimum and mean), relative humidity (maximum, minimum and mean) wind speed and sunshine hours. All the predictor variables were grouped into eight different combinations. The results of the developed models were compared with the standard method of Penman Monteith (PM56), which was developed by the food and agriculture organization (FAO) of the United Nations. The result shows that SVM is the best model for the computation of  $ET_o$  in all three selected cities. The statistical performance parameters of correlation coefficient ( $R^2$ ) and root mean square error (RSME) were found to be in the range of 97 to 98% and 0.28 to 0.31, respectively. Moreover, all supervised learning algorithms show enough the disparity from arid to humid climate aside from SVM which shows relatively indistinguishable outcomes for all the climatic zones in correlation with the standard PM56 method. Therefore, SVM is concluded to be a reliable soft computing approach for the estimation of  $ET_o$ .

**Keywords:** Reference evapotranspiration; soft computing approaches; weather stations; cross-validation

### Introduction

Reference evapotranspiration is an important parameter in hydrology, water resources, and particularly in agriculture for irrigation purposes (Wang and Cai, 2009). Reference evapotranspiration is denoted as  $ET_o$  and it is defined as the estimation of evapotranspiration from a reference crop or surface.  $ET_o$  can be accurately measured with the Penman-Monteith (PM56) model (Allen et al., 1998). It has been proved to be more accurate as compared to other strategies that are frequently utilized as the reference equation maintaining perfection and uniformity of estimation of  $ET_o$  for agrometeorological purposes (Gavilán et al., 2007; López-Urrea et al., 2006; Pereira et al., 2015). This method needs many climatic and aerodynamic parameters includes maximum and minimum temperature, maximum and minimum relative humidity, wind speed and solar radiation, saturation vapor pressure deficit, slope vapor pressure curve, and psychometric constant, which are mostly not easily available.

Alternatively, numerous other methods are available to estimate  $ET_o$ . At present, soft computing approaches are gaining popularity in various applications of Water Resources

Engineering due to fewer data requirements while sustaining accuracy and minimize computational costs (Huang et al., 2010; intelligence and 2008, n.d.). Soft computing is a cutting-edge approach to building computationally intelligent frameworks. It is an emerging approach for an estimation that competes up to the massive capacity of human knowledge to apprehend in a climate of imprecision and vulnerability (ZADEH, 1996).

Soft computing approaches have an advantage over conventional methods, as they can solve non-linear problems and easily formalized. It is based on backpropagation, quick prop, genetic algorithms (GA), fuzzy logic (FL), artificial neural networking (ANN). Moreover, the ANN model can be improvised by learning algorithms of generalized regression neural networks (GRNN), backpropagation (Kışı, 2006), and genetic algorithms (Kim and Kim, 2008). Numerous studies carried out on these approaches to estimate evapotranspiration and found the best results as a comparison to conventional methods (Kim et al., n.d.; Kumar et al., 2002; Sudheer et al., 2003; Trajkovic, 2005; Traore et al., n.d.)

It is obvious from the beyond references that the implementation of soft computing approaches for ET assessment is simply restricted to not a few methodologies of ANN, FL, and GA. Nevertheless, some other non-traditional soft computing approaches do present which have not been utilized at this point. This investigation is then intended to apply several of the non-traditional approaches for  $ET_0$  assessment.

In the present study, five soft computing approaches PNN, RBF, GMDH, CCNN, and SVM are used to estimate  $ET_0$ . These approaches have never been used before in the present study area of Punjab, Pakistan. The results acquired from the soft computing models were compared with the FAO56-PM along with the mentioned models. Thus, the objectives of the present study are given as (1) Prediction of  $ET_0$  by utilizing the strong predicting modeling approaches; (2) determination of the most appropriate approach for estimating  $ET_0$  by comparing the results of selected approaches.

The rest of the paper is coordinated as follows. To start with, the study area and data description are clarified in detail followed by the discussion of different approaches used in this paper. After that, the results sum up and explains the significant finding of the study. A short conclusion is brief toward the end.

### Study area and data description

The study area includes three cities of Punjab (Bhakkar, Dera Ghazi Khan, and Jhang). Bhakkar is located in the west of Punjab. The weather of Bhakkar is desert-like climate categorize with almost no rainfall. Dera Ghazi Khan is abbreviated as D.G. Khan and is in the south of Punjab. It is the 19th largest city in Pakistan by population. The climate of D.G. Khan is semi-arid. Jhang is the capital city of Jhang district and is located on the east bank of the Chenab river. Table 1 summarizes the geographical location of these stations. The average annual rainfall for Bhakkar, D.G. Khan, and Jhang received is 213, 236, and 532 mm, respectively.

The monthly climatic data for all the selected stations have been acquired from the Pakistan Meteorological Department (PMD). The duration of the data used in this study is 1996-2015. Fig. 1 illustrates the topographical map of metrological stations used in this study. **Error! Reference source not found.** The monthly metrological data consist of six parameters of maximum ( $T_{max}$ ) and minimum ( $T_{min}$ )

temperature, maximum ( $RH_{max}$ ) and minimum ( $RH_{min}$ ) relative humidity, wind speed ( $U$ ), and sunshine hours ( $n$ ). Average temperature and relative humidity ( $T_{avg}$ ,  $R_{avg}$ ) can be computed from maximum and minimum values. The data has been divided into two groups for training and testing purposes.

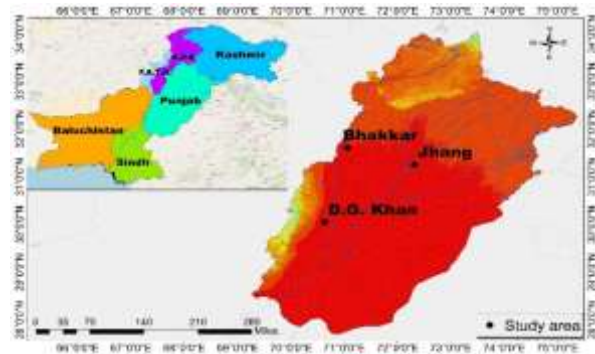


**Fig. 1** Location of meteorological station in Pakistan

**Table 7** The location of metrological stations

Station name	Longitude (E)	Latitude (N)	Elevation (m)
Bhakkar	71.06	31.61	159
D.G. Khan	70.63	30.05	390
Jhang	72.31	31.26	158

70 % of the data is utilized for training. While the remaining 30 % data is utilized for testing of the developed models. Table 2 sums up the statistical parameters such as minimum and maximum values, standard deviation, coefficient of variation, skewness, and kurtosis of training and testing data test.

pattern recognition. It consists of three layers. In the primary layer, PNN is comprised of  $n$  nodes that are the elements of the input layer. The subsequent layer is called the pattern layer. These patterns are classified, and each pattern unit is the dot product of weight and input layer neurons. Then performs non-linear operation instead of using back-propagation. After that, the summation sums of the inputs from the primary layer units. At last, the output or decision units come out with a single weighted variable. The sketch of the PNN classification network is shown in Fig. 2.

### Radial base function (RBF)

RBF is the most used approach in artificial neural networks for solving approximate problems. It has an advantage over other approaches because

of its speed and fast learning. It is also a feed-forward network composed of three layers.

**Table 8** Statistical parameter utilized in training and testing monthly data.

Variable	Data set	Maximum	Minimum	Mean ( $\mu$ )	Standard deviation ( $\sigma$ )	Co-efficient of variation (CV)	Skewness ( $C_s$ )	Kurtosis ( $C_k$ )
$T_{max}$	Training	44.7	16.9	32.141	7.494	23.32	-0.39	-1.14
	Testing	44.1	17.6	32.558	7.425	22.8	-0.42	-1.19
$T_{min}$	Training	30.2	3.2	18.282	8.219	44.96	-0.3	-1.34
	Testing	29.9	3.6	18.039	8.263	45.81	-0.23	-1.49
$T_{mean}$	Training	36.4	10.6	25.211	7.768	30.81	-0.37	-1.3
	Testing	36.8	11.15	25.298	7.729	30.55	-0.33	-1.41
$RH_{max}$	Training	98	34	73.759	13.05	17.69	-0.71	-0.32
	Testing	94	46	74.519	11.591	15.55	-0.44	-0.45
$RH_{min}$	Training	76	15	44.863	11.381	25.37	-0.26	-0.5
	Testing	66	21	46.926	9.641	20.55	-0.4	-0.24
$RH_{mean}$	Training	87	24.5	59.311	11.707	19.74	-0.62	-0.31
	Testing	80	34	60.722	9.911	16.32	-0.55	-0.11
U	Training	5.9	0	1.8681	1.2916	69.14	0.55	-0.49
	Testing	6.1	0	2.042	1.698	83.17	0.67	-0.75
n	Training	11.34	4.18	8.3686	1.3793	16.48	-0.49	-0.13
	Testing	10.24	3.44	7.701	1.52	19.74	-0.65	-0.1

**Research Methodology Probabilistic neural network (PNN)**

PNN is a feedforward neural network proposed by Specht (Specht, 1990). It is used in various applications for solving non-linear problems and The first layer consists of input networks, the second layer also name a hidden layer, composed of non-linear activation units and the output layer. All layers of the RBF model shown in Fig. 3. When the error is reached at a predetermined desired number or number of epochs performed, training of the RBF model is terminated. After that number of nodes is selected for the hidden layer. The Gaussian function is used as a computational function. Then model predictions and observations are evaluated, and the final model is chosen based on the least computation error.

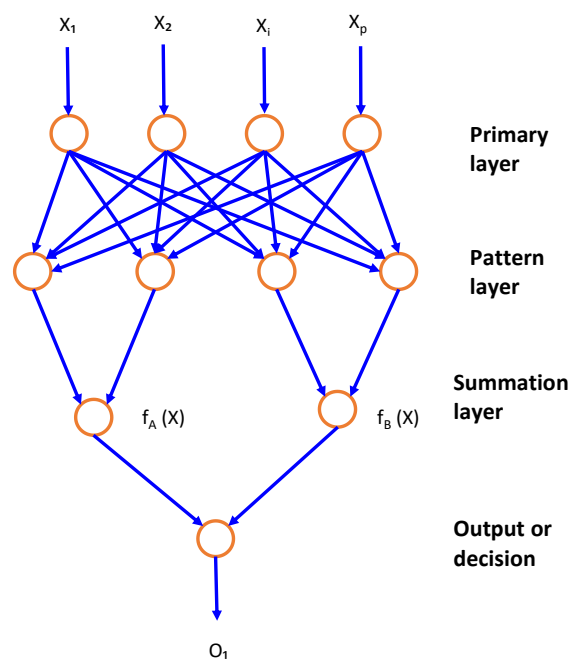


**Fig. 2** Classification of pattern for PNN

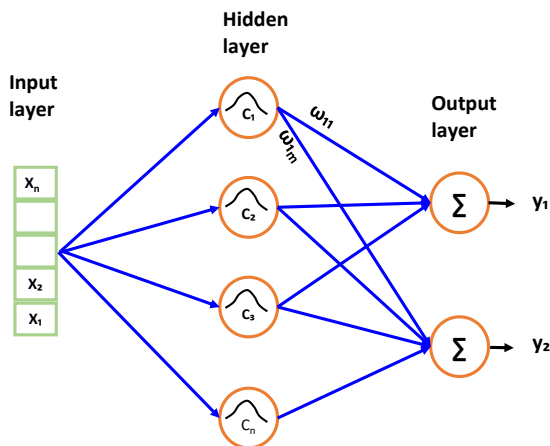


**Fig. 3** Typical structure of RBF network

### Group method of data handling (GMDH)

GMDH is another approach used in neural networks, which was proposed by Ivakhnenko (Ivakhnenko, 1968). It can be applied in various applications of deep learning i.e., forecasting, data mining, optimization, and pattern recognition. The primary aim behind the GMDH network is really to build a capacity in a feed-forward network based on a second-degree transfer function. The number of layers and neurons inside the hidden layers, shown in Fig. 4, the predictor variables, and the ideal model structure is naturally decided in this model calculation. The structure between the input and output variables finished through a GMDH neural organization is a nonlinear function called the Volterra series. The main purpose of the GMDH algorithm is to find the  $\alpha_i$  unknown coefficients in the Volterra series.

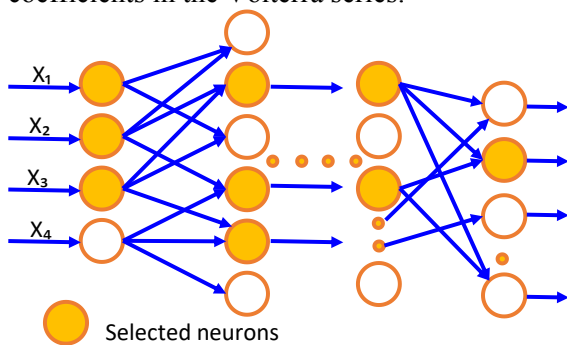


**Fig. 4** Typical structure of GMDH network

### Cascade correlation neural network (CCNN)

Course Correlation is another supervised learning approach used frequently in artificial neural networking, published by Fahlman (Fahlman and Lebiere, 1990). It used the perceptron learning algorithm for the single-layer and for simulation it uses a quick prop algorithm. It has an advantage backpropagation algorithm

because it overcomes the problem of step size and moving target. In the start, it needs a minimal network, and every input is associated with the output layer with an adjustable weight. As the learning begins, neurons are added one by one. Once hidden neurons are added then it is unchangeable, and all weights are frozen, hidden layers are trained according to the output layer. For every new layer of hidden neurons, it increased the magnitude of correlation and minimizes the loss function. Every time, the hidden neuron is added, it receives information from the subsequent hidden layers. The iteration continues until the desired value is reached. Its structure is demonstrated in Fig. 5

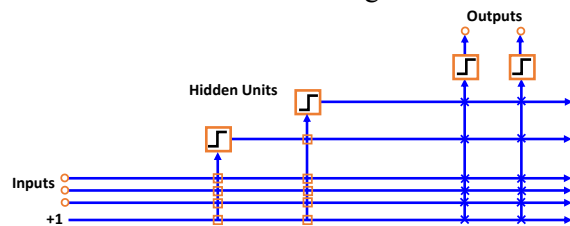


**Fig. 5** Typical structure of CCNN model

### Support vector machines (SVM)

SVM is a supervised machine learning algorithm. It is a powerful tool for pattern recognition and is widely used for classification. The line of classification should be picked in quite a way that it is having the most extreme speculation capacity. To make separable classes, it changes the element into a higher dimensional feature space utilizing kernels i.e., Gaussian, polynomial, and sigmoid. The basic principle uses in the SVM algorithm is to grasp the relationship between input and output datasets. The relationship developed based on training data sets i.e.  $(x_k, y_k)$ ;  $k = 1, \dots, N$ . If  $y$  is continuous then it is linear regression and it is class-mark, then it is a classification problem. The classification is based on datasets shown in Fig. 6 (Samsudin et al., 2010).

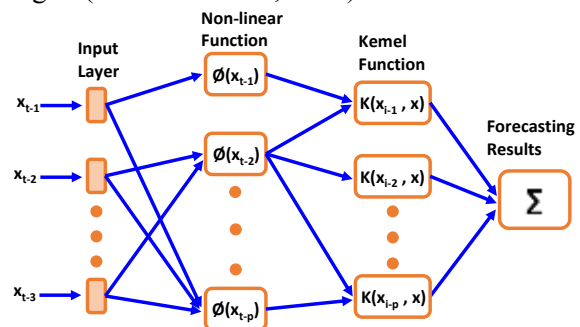


**Fig. 6** Typical structure of SVM network



## Evaluation criteria

The reliability of these soft computing approaches was evaluated based on simulation results and statistical indicators such as Root mean square error (RMSE) and the correlation coefficient ( $R^2$ ) against the FAO-56 PM model. The RMSE and  $R^2$  are as follows:

$$RMSE = \sqrt{\frac{1}{n} \sum_{i=1}^n (ET_{iQ} - ET_{ip})^2} \quad (1)$$

$$R^2 = \left[ \frac{\sum_{i=1}^n (ET_{ip} - \overline{ET_p}) (ET_{iQ} - \overline{ET_Q})}{\sqrt{\sum_{i=1}^n (ET_{ip} - \overline{ET_p})^2 \sum_{i=1}^n (ET_{iQ} - \overline{ET_Q})^2}} \right]^2 \quad (2)$$

Where  $ET_{ip}$  is the  $ET_o$  value noticed using soft computing approach at the  $i^{th}$  step;  $ET_{iQ}$  is the corresponding  $ET_o$  value acquired from PM56;  $n$  is the number of data set;  $ET_Q$  is the mean values acquired from FAO-56 PM and  $ET_p$  is the mean of estimated  $ET_o$  value noticed using machine learning approaches.

## Results

At the starting point, soft computing models are played with the data that is calculated using the FAO-56 PM equation. As a guideline for evaluating the execution of data-driven models, the alike set data of testing was assumed for 3 regions of south Punjab, Pakistan. To evaluate the results of the developed models, the coefficient of determination/ correlation Coefficient ( $R^2$ ) and root mean square error (RMSE) is used. The performing indicators,  $R^2$  and RMSE of testing data set for a selected region of south Punjab is presented in Fig. 7 (a, b, c, d, e, f, g, h, i, j) respectively.

Fig. 7 shows the  $R^2$  and RMSE computation for selected regions using the five models with 17 combinations of predictor variables. In Bhakkar, all models show the  $R^2$  and RMSE between 0.95 to 0.97 and 0.31 to 0.38 mm/day. Overall, the SVM model shows the highest  $R^2$  value (0.9697), and CCNN shows the lowest  $R^2$  value (0.9614). While SVM model show the lowest RMSE value (0.312 mm/day) and PNN show the highest RMSE value (0.3776 mm/day). On the other hand,  $T_{mean}$ , U combination of predictor variables was found to be

the best combination for evaluating the  $ET_o$  in this region.

In DG Khan,  $R^2$  and RMSE values of all models observe between 0.94 to 0.98 and 0.31 to 0.48 mm/day. Overall, the high value of  $R^2$  (0.981) is obtained when computed using SVM and PNN shows the lowest  $R^2$  value (0.9445). While SVM model show the lowest RMSE value (0.3103 mm/day) and PNN show the highest RMSE value (0.489 mm/day). Rather,  $T_{min}$ ,  $R_{mean}$ , U combination of predictor variables was found fit for this region for statistical analysis.  $R^2$  and RMSE values of all models notice between 0.97 to 0.98 and 0.28 to 0.32 mm/day in Jhang. Overall, SVM show the high value of  $R^2$ , and CNN shows the highest RMSE value (0.3264mm/day). Rather,  $T_{min}$ ,  $R_{mean}$ , U combination of predictor variables found fit for this region for statistical analysis just like DG khan.

From the above results, it can be noticed that the SVM model performs well as compared to other supervised learning models in all elected regions of south Punjab. However, PNN and CCNN models show almost equal results in contrast to the GMDH model. Also, all models generate low  $R^2$  values in DG. Khan except for the SVM model. It is obvious from Figure 1 that all models have an allowable coefficient of determination ( $R^2$ ), which is greater than 90% for selected regions. It can be observed that the testing data of supervised learning models is no over placed. Alternatively states that the soft computing models show all non-linearity of  $ET_o$ , which is the major merit of soft computing models. Same as, it can be observed in Figure 1 that the SVM model brings less value of RMSE for the elected regions of south Punjab which ranges from 0.28 – 0.31 mm/day, respectively. On the other hand, PNN, RBF, GMDH, and CCNN models indicate the high value of RMSE. Although, It can be concluded from the performance of RMSE and  $R^2$  that the SVM model has the extra ability as compared to other models for the evaluation of  $ET_o$  in elected regions of south Punjab.

Fig. 7 (a, b, c) indicates  $ET_o$  evaluation of all soft computing models in the hydrographical form for elected regions.

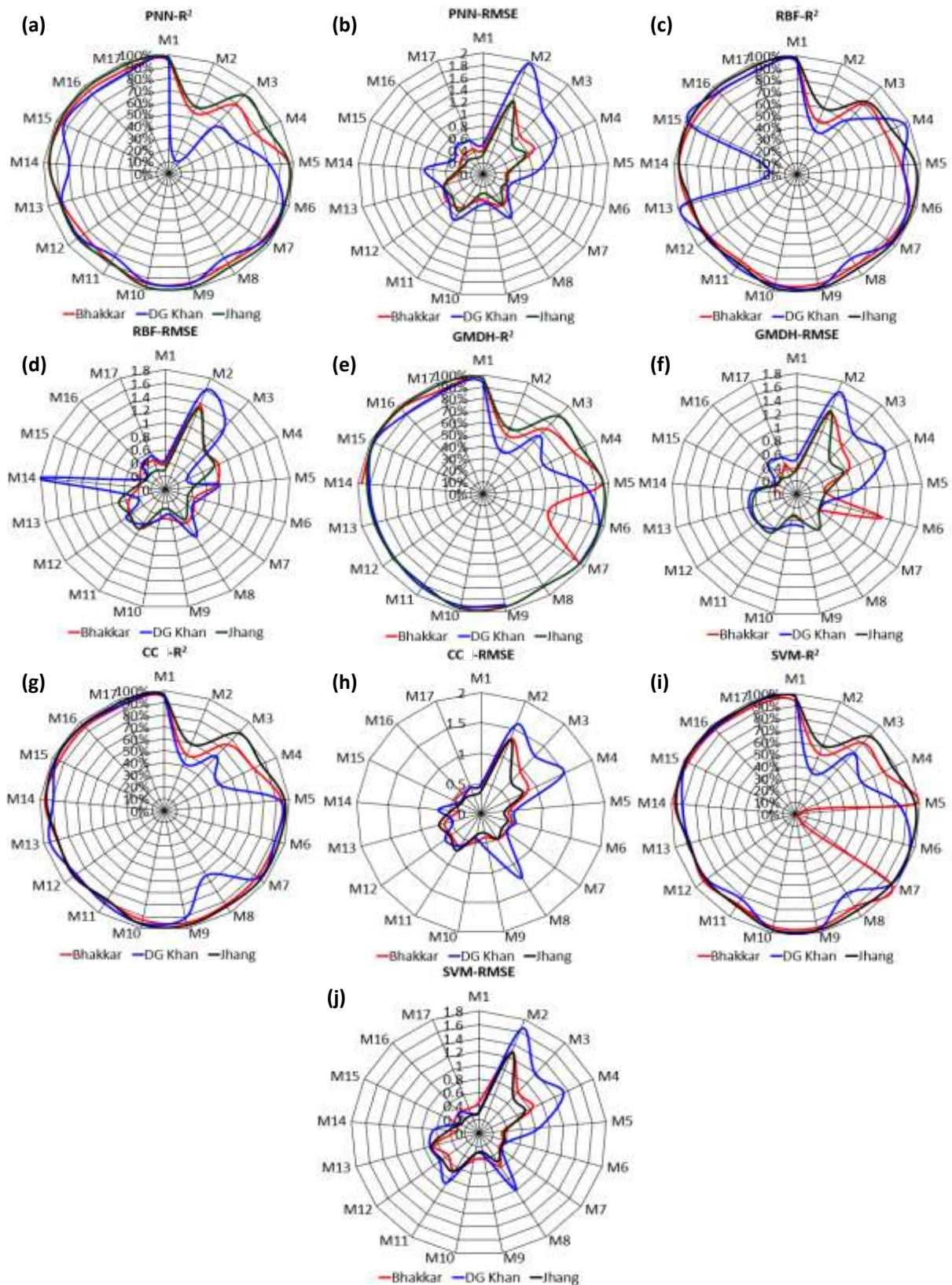


**Fig. 7**  $R^2$  and RMSE estimation using PNN, RBF, GMDH, CC, and SVM for selected stations of Pakistan

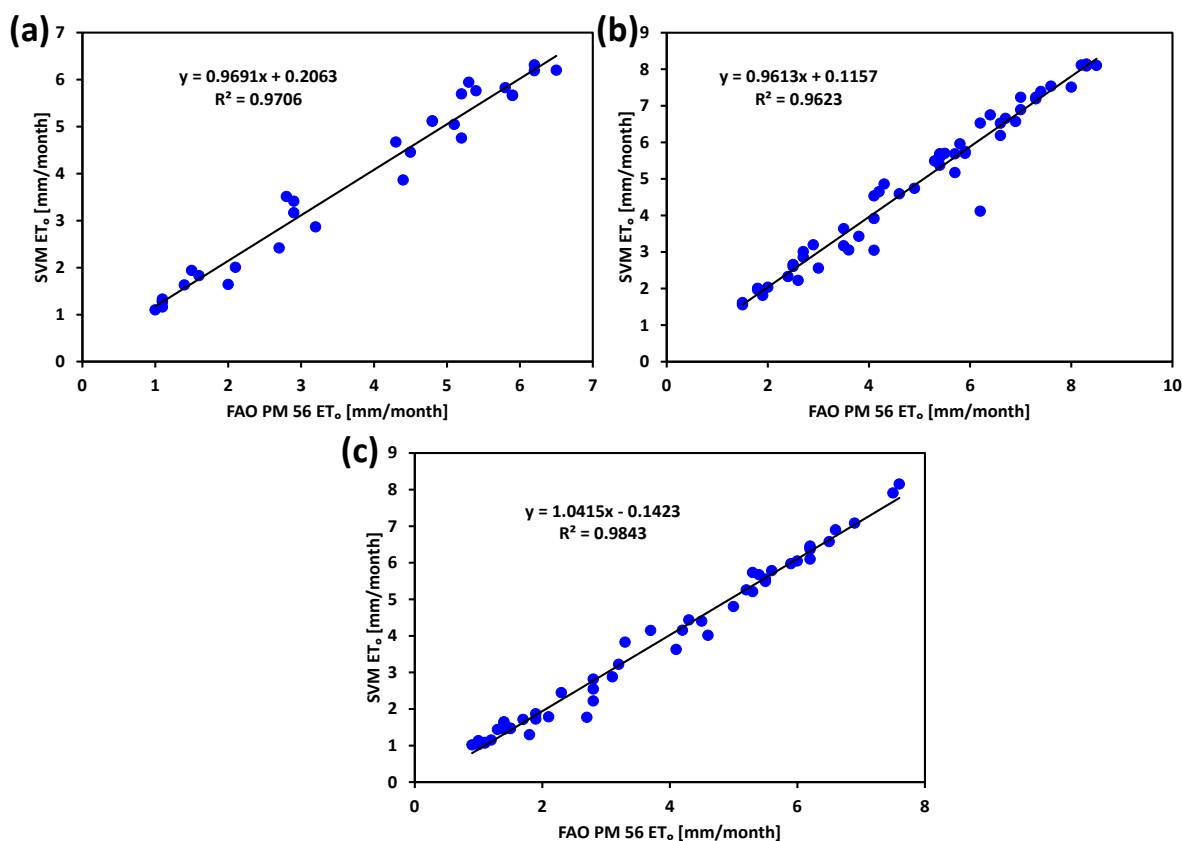


**Fig. 7** ET<sub>0</sub> comparison between SVM and PM56 (a) Bhakkar (b) DG Khan (c) Jhang

This may be because of the reality that SVM always looks for global improved solutions, avoid overfitting, and no physical influence which finally guides to the top performance over other data-driven models.

### Conclusions

The present study provides the prediction of ET<sub>0</sub> using five soft computing approaches (PNN, RBF, GMDH, CCNN, and SVM). The computed ET<sub>0</sub> from FAO-56 recommends PM equation was used as reference values for the comparison. Soft computing models were evaluated based on statistical parameters i.e., R<sup>2</sup> and RMSE. The monthly mean ET<sub>0</sub> was accurately estimated using soft computing methods and was found to be in the acceptable range for all selected climatic stations. To estimate the contribution of different predictor variables for ET<sub>0</sub> estimation, the parameters of mean temperature and wind speed are found more critical for effective results.

### Acknowledgments

This research work has been carried out in the Department of Agricultural Engineering, Bahauddin Zakariya University, Multan-Pakistan.

### References

- Allen, R.G., Allen, R.G., Pereira, L.S., Raes, D., Smith, M., Organization, (FAO) Food and Agriculture, 1998. Crop evapotranspiration, FAO irrigation and drainage paper. FAO, Rome.
- Fahlman, S.E., Lebiere, C., 1990. The cascade-correlation learning architecture, in: Advances in Neural Information Processing Systems. pp. 524–532.
- Gavilán, P., Berengena, J., Allen, R.G., 2007. Measuring versus estimating net radiation and soil heat flux: Impact on Penman-Monteith reference ET estimates in semiarid regions. *Agric. Water Manag.* 89, 275–286. <https://doi.org/10.1016/j.agwat.2007.01.014>
- Huang, Y., Lan, Y., Thomson, S.J., Fang, A., Hoffmann, W.C., Lacey, R.E., 2010. Development of soft computing and applications in agricultural and biological engineering. *Comput. Electron. Agric.* <https://doi.org/10.1016/j.compag.2010.01.001>
- intelligence, D.C.-S. in C., 2008, undefined, n.d. Soft computing. Springer.

- Ivakhnenko, A.G., 1968. The group method of data of handling; a rival of the method of stochastic approximation. *Sov. Autom. Control* 13, 43–55.
- Kim, S., hydrology, H.K.-J. of, 2008, undefined, n.d. Neural networks and genetic algorithm approach for nonlinear evaporation and evapotranspiration modeling. Elsevier.
- Kim, S., Kim, H.S., 2008. Neural networks and genetic algorithm approach for nonlinear evaporation and evapotranspiration modeling. *J. Hydrol.* 351, 299–317. <https://doi.org/10.1016/j.jhydrol.2007.12.014>
- Kiş, Ö., 2006. Generalized regression neural networks for evapotranspiration modelling. *Hydrol. Sci. J.* 51, 1092–1105. <https://doi.org/10.1623/hysj.51.6.1092>
- Kumar, M., Raghuwanshi, N.S., Singh, R., Wallender, W.W., Pruitt, W.O., 2002. Estimating Evapotranspiration using Artificial Neural Network. *J. Irrig. Drain. Eng.* 128, 224–233. [https://doi.org/10.1061/\(asce\)0733-9437\(2002\)128:4\(224\)](https://doi.org/10.1061/(asce)0733-9437(2002)128:4(224))
- López-Urrea, R., Olalla, F.M. de S., Fabeiro, C., Moratalla, A., 2006. An evaluation of two hourly reference evapotranspiration equations for semiarid conditions. *Agric. Water Manag.* 86, 277–282. <https://doi.org/10.1016/j.agwat.2006.05.017>
- Pereira, L.S., Allen, R.G., Smith, M., Raes, D., 2015. Crop evapotranspiration estimation with FAO56: Past and future. *Agric. Water Manag.* <https://doi.org/10.1016/j.agwat.2014.07.031>
- Samsudin, R., Saad, P., Shabri, A., 2010. A hybrid least squares support vector machines and GMDH approach for river flow forecasting. *Hydrol. Earth Syst. Sci. Discuss.* 7, 3691–3731. <https://doi.org/10.5194/hessd-7-3691-2010>
- Specht, D.F., 1990. Probabilistic neural networks. *Neural networks* 3, 109–118.
- Sudheer, K.P., Gosain, A.K., Ramasastri, K.S., 2003. Estimating Actual Evapotranspiration from Limited Climatic Data Using Neural Computing Approach. *J. Irrig. Drain. Eng.* 129, 214–218. [https://doi.org/10.1061/\(ASCE\)0733-9437\(2003\)129:3\(214\)](https://doi.org/10.1061/(ASCE)0733-9437(2003)129:3(214))
- Trajkovic, S., 2005. Temperature-Based Approaches for Estimating Reference Evapotranspiration. *J. Irrig. Drain. Eng.* 131, 316–323. [https://doi.org/10.1061/\(ASCE\)0733-9437\(2005\)131:4\(316\)](https://doi.org/10.1061/(ASCE)0733-9437(2005)131:4(316))
- Traore, S., Wang, Y., management, T.K.-A. water, 2010, undefined, n.d. Artificial neural network for modeling reference evapotranspiration complex process in Sudano-Sahelian zone. Elsevier.
- Wang, D., Cai, X., 2009. Irrigation Scheduling—Role of Weather Forecasting and Farmers’ Behavior. *J. Water Resour. Plan. Manag.* 135, 364–372. [https://doi.org/10.1061/\(asce\)0733-9496\(2009\)135:5\(364\)](https://doi.org/10.1061/(asce)0733-9496(2009)135:5(364))
- ZADEH, L.A., 1996. Fuzzy Logic, Neural Networks, and Soft Computing. pp. 775–782. [https://doi.org/10.1142/9789814261302\\_0040](https://doi.org/10.1142/9789814261302_0040)

## Performance evaluation of various models for the assessment of reference evapotranspiration in arid and semi-arid zones of Pakistan

Rabeea Noor<sup>1\*</sup>, Aarish Maqsood<sup>1</sup>, Azhar Inam<sup>1</sup>

<sup>1</sup> Department of Agricultural Engineering, Bahauddin Zakariya University Multan, Pakistan

Corresponding author email: [rabeeanoor123@gmail.com](mailto:rabeeanoor123@gmail.com)

**Abstract:** Reference Evapotranspiration ( $ET_0$ ) plays an essential part in well-organized irrigation and water resource management. It can be computed by FAO56 Penman-Monteith (PM), a well-known reference model for  $ET_0$  evaluation. However, this model needs extra comprehensive meteorological data. Such data usually not available at every climatic station. An alternative approach needs to investigate daily  $ET_0$  with the fewer parameter, sustaining the precision. The study focuses to assess the performance of models against the FAO-56 Penman-Monteith model using the climatic data. The study evaluates the most reliable  $ET_0$  model for the arid and semi-arid region that needs fewer input data (temperature, solar radiation) compared with the FAO-56 PM model of  $ET_0$ . The research was conducted to compare the two models including the Hargreaves and Jensen-Haise model for the evaluation of  $ET_0$  under arid and semi-arid regions such as Faisalabad and Multan. The statistical analysis showed that the computed RMSE, MSE and MAE values ranged from 0.0345 to 0.0405, 0.0418 to 0.0202 and 0.1440 to 0.1692 mm/day for Hargreaves and from 0.0678 to 0.3243, 0.0422 to 0.3681 and 0.1458 to 0.4945 mm/day for Jensen-Haise model, respectively. The calculated  $R^2$  for Hargreaves and Jensen-Haise model were varying from 0.9447 to 0.9811 and 0.9311 to 0.9778 respectively. The endpoint results indicated that the Hargreaves model gave better results in the semi-arid region while the Jensen-Haise model gave better results in an arid region.

**Keywords:** FAO-56 Penman-Monteith, Hargreaves, Jensen-Haise, Reference Evapotranspiration, Arid -Semi-arid region

### Introduction

Reference Evapotranspiration ( $ET_0$ ) is considered the most indispensable parameter of hydrology and has a significant part in the field of irrigated agriculture. Usually, the most commonly used method for  $ET_0$  is Penman-Monteith (PM) equation developed by the Food and Agriculture Organization (FAO) (Doorenbos and Pruitt, 1977). It is extensively applied in irrigated farms for crop water requirement estimation and scheme the utilization of water resources proficiently. It is the major component of water balance because of vast applications i.e. the hydrological cycle, managing water resources, water forecasting, and reservoir performance (Allen, Richard G., pereira, Luis s., raes, dirk and smith, 1998). Moreover, the exact assessment of  $ET_0$  is essential in the computation of water demand, water allocation, and water budget estimation. An accurate evaluation of the irrigation water demand is necessary to prevent further damage to water resources.

FAO-56 PM has been recommended globally for the assessment of  $ET_0$ . However, it needs large climatic data, e.g., solar radiation, wind speed, relative humidity minimum & maximum

temperature, saturation vapor pressure deficit, slope vapor pressure curve, and psychrometric constant (**Table 3**). Such a dataset is usually not available for all climatic stations. Under the condition of restricted availability of data (mostly in developing countries like Pakistan) equations developed by Hargreaves can be utilized after regional reconciliation in parameters. Some models need only confined weather parameters such as Hargreaves requires only air temperature data and radiation as shown in **Table 3**. Hargreaves method requires less amount and time for the assessment of crop water demand.

In arid and semi-arid zones the actual application of water in canal command areas is essential, as a key portion, such as 71 percent of allocated canal water, is lost as conveyance losses (Khan, 2015). So, the water application efficiency in the command area could be increased if the volume of water is applied as per the requirements of crops.

Various equations have been suggested for the assessment of  $ET_0$  and applied on specific sites especially in moderate zones of the world. Although, there is no general accord on the appropriateness of a model for given weather



(Smith et al., 1998). Therefore, the equations need careful regional calibration before using it for the assessment of  $ET_0$ . The regional calibration and validation are more essential in hot semi-arid and arid regions than the moderate weather because several of the equations have already been tested in a moderate environment (DehghaniSanij et al., 2004).

In several of the assessment studies in a moderate environment, the PM equation, and a modified version (PM Equation of FAO-56) of it, outperformed the other equations.

Pakistan is facing the issue of water scarcity and the requirement of water for irrigation is also enhanced due to the requirement of nourishment and fiber (Khoso et al., 2015). In Pakistan, out of the total geographical area of 79.6 million hectares, 70% of the area is arid and semi-arid (Farooq et al., 2007) and hence the assessment of  $ET_0$  is necessary to ensure the optimum utilization of available water resources.

The objective of this research is to assess the performance of equations namely: Hargreaves (HG) and Jensen-Haise (JH) model against the FAO-56 PM model in computing daily reference evapotranspiration in the arid and semi-arid region of Pakistan and to evaluate the reliable  $ET_0$  model that needs least input climatic data compared with the FAO-56 Penman-Monteith model of  $ET_0$ .

### Study area and data description

In this study, data of three stations such as Multan from South Punjab and Faisalabad from North Punjab was used to compute the  $ET_0$ . The geographical and climatic features of the station shown in **Table 1**. The topographical map of the study area is shown in **Fig. 1**.

The climatic data such as maximum daily temperature, minimum daily temperature, wind speed, sunshine hours, and relative humidity for the city of Multan is taken from Central Cotton Research Institute (CCRI) and for the city of Faisalabad is taken from University of Agriculture Faisalabad (UAF). Statistical parameters of data used in this study i.e., maximum, minimum, mean, standard deviation, coefficient of variation, skewness, and kurtosis are shown in **Table.2**

## Research Methodology

### Computation of reference Evapotranspiration

Three evapotranspiration models such as FAO-56 PM, HG and JH model were used to compute reference evapotranspiration. These two models were utilized to assess  $ET_0$  using daily climatic data **Table 3**.

### Penman-Monteith Model of FAO56

CROPWAT 8.0 was used for the computation of Penman-Monteith as proposed by the Food and Agriculture Organization (FAO) (Allen, Richard G., PEREIRA, Luis S., RAES, Dirk and SMITH, 1998). The following FAO56 Penman-Monteith (PM) equation is given by (Allen, Richard G., PEREIRA, Luis S., RAES, Dirk and SMITH, 1998).

$$ET_0 = \frac{0.408\Delta(R_n - G) + \frac{900U_2\gamma}{T+273}(e_s - e_a)}{\Delta + \gamma(1+0.34U_2)} \quad (1)$$

**Where,**  $ET_0$  = daily reference evapotranspiration [mm/day];  $R_n$  = net radiation at the crop surface [ $MJm^{-2}/day$ ];  $G$  = soil heat flux density [ $MJm^{-2}/day$ ];  $T$  = daily air temperature at 2 m height [ $^{\circ}C$ ];  $U_2$  = wind speed at 2 m height [m/s];  $e_s$  = saturation vapor pressure [kPa];  $e_a$  = actual vapor pressure [kPa];  $\Delta$  = slope vapor pressure curve [ $kPa/^{\circ}C$ ];  $\gamma$  = psychrometric constant [ $kPa/^{\circ}C$ ].

### Hargreaves Model (HG):

$ET_0$  computed by using HG  $ET_0$  equation (HG) proposed by (Hargreaves and Samani, 1985) and it is described as:

$$ET_0 = 0.0023 R_a (T + 17.8) (T_{max} - T_{min})^{0.5} \quad (2)$$

Where,  $ET_0$  = reference evapotranspiration (mm/day);  $R_a$  = daily extraterrestrial radiation (mm/day);  $T$ ,  $T_{max}$  and  $T_{min}$  = mean, maximum and minimum temperature ( $^{\circ}C$ ) respectively. Due to the less data need, it is often used under the condition of low data availability and chiefly, when the only temperature of the air is available (Hargreaves and Allen, 2003).

### Jensen-Haise Model (JH):

$ET_0$  computed by using JH Model proposed by (James, 1988; Jensen and Allen, 2016) is given as:

$$ET_0 = C_T (T_{mean} - T_x) * R_s \quad (3)$$



Where,  $ET_0$  = daily reference evapotranspiration [mm/day];  $R_s$  = solar radiation ( $MJ\ m^{-2}\ d^{-1}$ );  $C_T$  and  $T_x$  are constants and indicated as:

$$C_T = \frac{1}{\left[ \left( 45 - \frac{h}{137} \right) + \left( \frac{365}{e(T_{max}) - e(T_{min})} \right) \right]}$$

$$T_x = -2.5 - 0.14 \times (e(T_{max}) - e(T_{min})) - \frac{h}{500}$$

**Table 9** Geographical locations of study area.

Station	Latitude	Longitude	Rain (mm)	Elevation (m)	Period data	Climate
Multan	30.19	71.47	186.8	122	2018-2020	Arid
Faisalabad	31.44	73.06	346	184.4	2018-2020	Semi-Arid

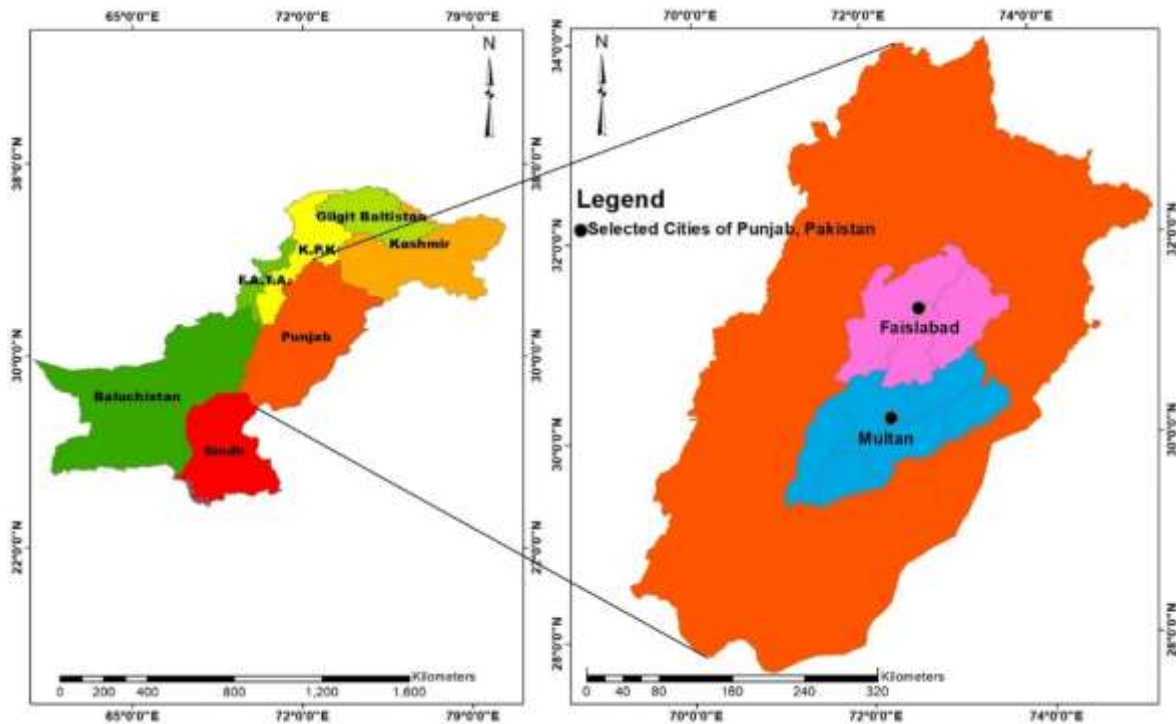


**Fig. 1** Layout map of study area

**Table 2** Statistical parameters used in this study.

Variable	Data set	Maximum	Minimum	Mean ( $\mu$ )	Standard deviation ( $\sigma$ )	Co-efficient of variation (CV)	Skewness ( $C_s$ )	Kurtosis ( $C_k$ )
$T_{max}$	Multan	34	4	19.615	7.731	39.41	-0.13	-1.34
	Faisalabad	32.2	2.1	19.019	7.825	41.14	-0.2	-1.35
$T_{min}$	Multan	49.1	12	35.821	6.633	18.52	-0.63	0.25
	Faisalabad	45.5	8.8	31.315	7.62	24.33	-0.55	-0.38
RH	Multan	88	16	54.181	16.219	29.94	-0.39	-0.32
	Faisalabad	88	16	54.181	16.219	29.94	-0.39	-0.32
U	Multan	13	1	4.074	2.178	53.47	1.23	1.84
	Faisalabad	13	1	4.074	2.178	53.47	1.23	1.84
N	Multan	15.4	0	9.068	2.606	28.74	-0.86	1.29
	Faisalabad	11.8	0	7.558	2.984	39.48	-1.08	0.43

Rad	Multan	32.9	4.9	19.824	6.098	30.76	-0.19	-0.96
	Faisalabad	27.7	4.7	17.58	5.924	33.7	-0.21	-0.91

Where:  $h$  = altitude of the location (m);  $e(T_{\max})$  and  $e(T_{\min})$  are vapor pressures (mbar) of the month with the average maximum and minimum temperature, respectively.

$R^2$  value varies from zero to one, with zero specifying that the suggested model does not match with the estimated value from the PM method and one denote complete fit. R-squared is the fraction of all sum of squares. It was calculated as:

**Table 3** Data required by different models

Parameters	FAO-56 PM	HG	JH
Maximum Temperature $^{\circ}\text{C}$	✓	✓	✓
Minimum Temperature $^{\circ}\text{C}$	✓	✓	✓
Humidity (%)	✓		
Wind Speed (m/s)	✓		
Solar radiation (MJ/m <sup>2</sup> /day)	✓	✓	✓
Sun Duration (hour)	✓		
Saturation vapor pressure deficit	✓		
Psychometric constant	✓		
Slope vapor pressure curve	✓		
Evaporation (mm)	✓		

$$R^2 = \frac{[\sum_{i=1}^n (b_i - \bar{b})(o_i - \bar{o})]^2}{[\sum_{i=1}^n (b_i - \bar{b})^2 \sum_{i=1}^n (o_i - \bar{o})^2]} \quad (4)$$

Where,  $o_i$  = approximated  $ET_o$  by the FAO-56 PM technique for a day  $i$  (mm/day);  $b_i$  = approximated  $ET_o$  by the HG or JH equation for the day  $i$  (mm/day);  $\bar{b}$  and  $\bar{o}$  = average of  $b_i$  and  $o_i$ ;  $n$  = total number of observations.

The RMSE is the square root of the variance of the residuals. Residuals are the difference between the actual values and the predicted values. It shows the exact fit of the model to the data i.e., how near the noted data points are to the model's assumed values. Whereas R-squared is a respective estimate of fit, RMSE is a definite measure of fit. Lower values of RMSE show finer fit.

$$RMSE = \sqrt{\frac{\sum_{i=1}^n (o_i - b_i)^2}{n}} \quad (5)$$

Where,  $o_i$  = approximated  $ET_o$  by the PM method for day  $i$  (mm/day);  $b_i$  = approximated  $ET_o$  by the HG or JH model for day  $i$  (mm/day);  $n$  = total no of observations.

The  $ET_o$  estimation was also evaluated using the statistical parameter such as mean absolute error (MAE) and mean squared error (MSE). These parameters are expressed as:

$$MAE = \frac{\sum_{i=1}^n |o_i - b_i|}{n}$$

$$MSE = \frac{\sum_{i=1}^n (o_i - b_i)^2}{n}$$

## Results

The HG and JH model, which are temperature and radiation dependent  $ET_o$  models, are compared with the standard FAO-56 PM model of  $ET_o$  in semi-arid (i.e., Faisalabad) and Arid climatic region (i.e., Multan) of Pakistan. According to statistical analysis that is utilized in the semi-arid region (i.e., Faisalabad) between HG and FAO-56 PM model, the HG  $ET_o$  model indicated underestimation in summer and overestimation in winter when compared with the FAO-56 PM model. The conclusions are shown in **Table 4** and **Fig. 2(a)**. The RMSE, MAE, MSE, and  $R^2$  values are shown in **Table 4**. HG  $ET_o$  model indicated underestimation in the summer season in the semi-arid region (Faisalabad) because of high wind speed and do overestimates in the winter season because of low wind speed. The FAO-56 PM model utilizes the parameter of wind speed in its computation, but the HG model does not utilize it. Because of this, the FAO-56 PM model indicated low  $ET_o$  values in winter and high  $ET_o$  values in the summer season as compared to the HG model.

**Table 4** Statistical Analysis of  $ET_o$  calculated by HG and JH compared with the FAO-56 PM model at the station of Faisalabad

Model	RMSE mm/day	MSE	MAE	$R^2$	Error
HG	0.0345	0.0418	0.1440	0.9811	7.61
JH	0.2055	0.0422	0.1458	0.9377	31.67

The statistical results between JH and FAO-56 PM model show that the JH Model indicated underestimation of  $ET_o$  by 31.67% as concluded by (Adeboye et al., 2009). This conclusion is shown in Fig. 2(b) and Table 4. The difference of variation between the JH Model and FAO-56 PM has the coefficient of determination ( $R^2 = 0.9811$ ) with an RMSE of 0.2055 mm/day, MSE with 0.0422 mm/day, and MAE with 0.1458 mm/day. The results have compiled in Table 4. FAO-56 PM model at arid region i.e., Multan station show that the  $ET_o$  estimated by HG  $ET_o$  method overestimated the PM  $ET_o$  method by 38.51% as shown in Fig. 3 (a) and compiled in Table 5.

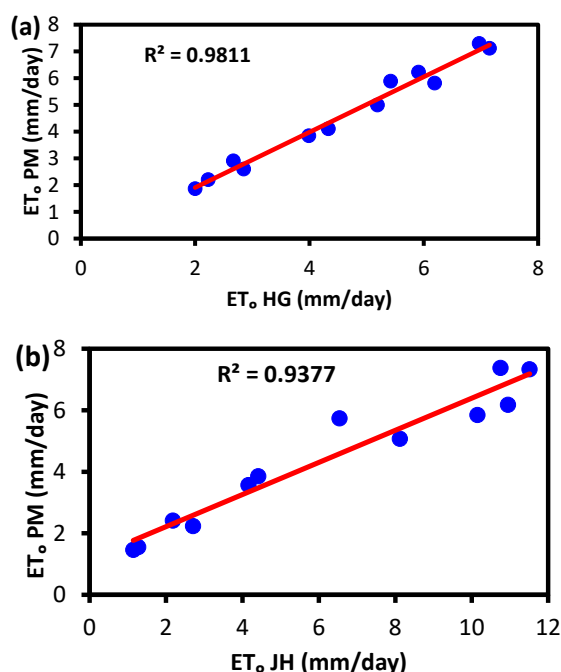


**Fig. 2** Comparison of  $ET_o$  by (a) HG and (b) JH Model against PM  $ET_o$  model at the station of Faisalabad

The difference of variation between the HG and FAO-56 PM has the coefficient of determination ( $R^2 = 0.9447$ ) with an RMSE of 0.0405 mm/day, MSE with 0.0202 mm/day, and MAE with

0.1692 mm/day as shown in **Table 5**. The comparison of  $ET_o$  estimated by HG and FAO-56 PM model at arid region i.e., Multan station show that the  $ET_o$  estimated by HG  $ET_o$  method overestimated the PM  $ET_o$  method by 38.51% as shown in Fig. 3 (a) and compiled in Table 5. The difference of variation between the JH and FAO-56 PM  $ET_o$  model has  $R^2 = 0.9778$  with RMSE of 0.3243 mm/day, MSE of 0.3681 mm/day, MAE with 0.4945 mm/day at Multan Station as shown in **Table 5**. Statistical Analysis of  $ET_o$  calculated by HG and JH compared with the FAO-56 PM model at stations of Faisalabad and Multan is shown in **Table 5**. The JH  $ET_o$  Model indicates an underestimation of  $ET_o$  in the four months (January, February; November, December) and overestimated  $ET_o$  in the remaining months of the year by 23.42% as shown in **Fig. 3 (b)** and **Table 5**.

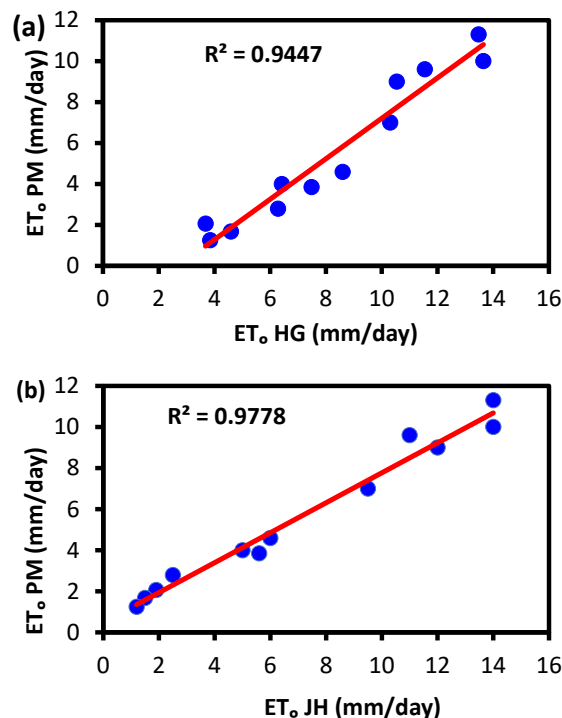


**Fig. 3** Comparison of  $ET_o$  by (a) HG and (b) JH Model against PM  $ET_o$  model at the station of Multan

**Table 5** Statistical Analysis of ET<sub>o</sub> calculated by HG and JH model compared with the FAO-56 PM model at the station of Multan

Model	RMSE mm/day	MSE	MAE	R <sup>2</sup>	Error
Hargreaves	0.0405	0.0202	0.1692	0.9447	38.51
Jensen-Haise	0.3243	0.3681	0.4945	0.9778	23.42

The semi-arid region and arid regions were slightly different. HG showed a higher R<sup>2</sup> for the semi-arid region compared with the arid region. However, this model showed the lowest RMSE, MSE, and MAE among the JH model. While the JH model tended to generate the highest RMSE, MSE and MAE and/or R<sup>2</sup> (**Table 4 and 5**) at the arid and semi-arid region.

### Conclusions

Using long-term daily climatic data (2018-2020) collected from two different sites in Pakistan, two simple models were assessed for their potential to evaluate the ET<sub>o</sub>. The results indicated that under semi-arid conditions, the Hargreaves model indicates an underestimation of ET<sub>o</sub> in summer and overestimation in winter.

Hence, it was found highly sustainable for evaluating the ET<sub>o</sub> due to less RMSE, MSE, and MAE. This model also resulted in less variation of ET<sub>o</sub> as compared to the Jensen-Haise model in a semi-arid region. While, the Jensen-Haise model showed underestimation of ET<sub>o</sub> in four months (January, February; November, December) and overestimated ET<sub>o</sub> in the remaining months of the year and it was found acceptable for the arid region for evaluating the ET<sub>o</sub>. For practical application, the simple models of the Hargreaves model and Jensen-Haise model are suggested for use within the semi-arid and arid regions of Pakistan, where daily climatic data is limited and only temperature or solar radiation data is available. Nevertheless, these can be adopted on a large scale for the planning of irrigation management. The FAO-56 PM model is assumed as one of the well-suited models, but plenty of climatic data is needed when a small level study is engrossed in irrigation command, and hence this model may not be applicable to apply in micro-irrigation command areas.

### Acknowledgments

This work is supported by the Central Cotton Research Institute (CCRI) and the University of Agriculture, Faisalabad (UAF). Climatic data of

Multan was provided by Central Cotton Research Institute (CCRI) and for Faisalabad, data is taken from the University of Agriculture, Faisalabad (UAF). Their help is greatly appreciated.

### References

- Adeboye, O.B., Osunbitan, J.A., Adekalu, K.O., Okunade, D.A., 2009. Evaluation of FAO-56 Penman-Monteith and Temperature Based Models in Estimating Reference Evapotranspiration Using Complete and Limited Data, Application to Nigeria. *Agric. Eng. Int. CIGR J.* 0, 1–25.
- Allen, Richard G., PEREIRA, Luis S., RAES, Dirk and SMITH, M., 1998. FAO Irrigation and Drainage Paper Crop by. *Irrig. Drain.* 300, 300.
- DehghaniSanij, H., Yamamoto, T., Rasiyah, V., 2004. Assessment of evapotranspiration estimation models for use in semi-arid environments. *Agric. Water Manag.* 64, 91–106. [https://doi.org/10.1016/S0378-3774\(03\)00200-2](https://doi.org/10.1016/S0378-3774(03)00200-2)
- Doorenbos, J., Pruitt, W.O., 1977. Guidelines for predicting crop water requirements. FAO *Irrig. Drain. Pap.* 24, 144.
- Farooq, U., Ahmad, M., Jasra, A.W., 2007. Natural resource conservation, poverty alleviation, and farmer partnership. *Pak. Dev. Rev.* 46, 1023–1049. <https://doi.org/10.30541/v46i4iipp.1023-1049>
- Hargreaves, G.H., Allen, R.G., 2003. History and Evaluation of Hargreaves Evapotranspiration Equation. *J. Irrig. Drain. Eng.* 129, 53–63. [https://doi.org/10.1061/\(asce\)0733-9437\(2003\)129:1\(53\)](https://doi.org/10.1061/(asce)0733-9437(2003)129:1(53))
- Hargreaves, G.H., Samani, Z.A., 1985. Reference Crop Evapotranspiration From Ambient Air Temperature. *Pap. - Am. Soc. Agric. Eng.*
- James, L., 1988. Principles of farm irrigation system design. John Wiley & Sons, New York.
- Jensen, M.E., Allen, R.G., 2016. Evaporation, evapotranspiration, and irrigation water

- requirements, Evaporation, Evapotranspiration, and Irrigation Water Requirements. American Society of Civil Engineers (ASCE). <https://doi.org/10.1061/9780784414057>
- Khan, A.A., 2015. GEOGRAPHICAL. A.A., 2015. An overview on emerging water scarcity in pakistan, its causes, impacts and remedial measures. J. Appl. Eng. Sci. 13, 35–44. <https://doi.org/10.5937/jaes13-6445>
- Smith, M., Allen, R., Pereira, L., 1998. Revised FAO methodology for crop-water requirements. Int. At. Energy Agency 51–58.
- Khoso, S., Wagan, F.H., Tunio, A.H., Ansari,

## Investigation of Extreme Hydrologic Events using Innovative Trend Analysis Method over Upper Indus River Basin

Muhammad Shehzad Ashraf<sup>1</sup>, Ijaz Ahmad<sup>1\*</sup>, Muhammad Waseem<sup>1</sup>, Faraz-ul-Haq<sup>1</sup>, Muhammad Jawad Ashraf<sup>2</sup>

<sup>1</sup> Centre of Excellence in Water Resources Engineering, University of Engineering and Technology, Lahore 54890, Pakistan

<sup>2</sup> Civil Engineering Department, University of Engineering and Technology, Lahore 54890, Pakistan

Corresponding author email: [dr.ijaz@uet.edu.pk](mailto:dr.ijaz@uet.edu.pk)

**Abstract:** Pakistan is one of those countries which are water stressed and its water resources are vulnerable to changing climatic conditions, therefore for effective planning and management of water resources investigation of variability of streamflow is very essential which provides requisite assistance for agriculture, domestic supply and hydropower generation. This paper investigated the variability in streamflow extreme values to evaluate the current and future water resources availability from UIRB using ITA method over 20 stations of UIRB. To analyze the variations in extreme values daily streamflow timeseries is divided into two categories; extremely low (<10<sup>th</sup> percentile) and extremely high (>90<sup>th</sup> percentile) flows. Extremely low streamflow timeseries manifested significant increasing trends at seven (7) stations, significant decreasing trends at three (3) stations and ten (10) stations revealed insignificant trends. For extremely high streamflow time series fifteen (15) stations showed insignificant, one (1) station significant increasing and four (4) stations revealed significant decreasing trends. From the results it is inferred that extremely low streamflow are going to be more significant over upper Indus basin as compared to extremely high streamflow in near future, which may constitute drastic danger in lower Indus basin where post population is dependent on agriculture. There may be more pressure on water resources which are already in scared situation.

**Keywords:** Extreme events; streamflow; ITA; UIRB

### Introduction

Increased concentrations of greenhouse gases in the atmosphere is inducing significant changes in the global climate (Chen et al., 2017a). The earth climate had accomplished significant change in geological history, however the current climate change is remarkable and mainly attributed to anthropogenic activities during post industrial era to meet the demands of growing population for food and other life necessities (IPCC, 2014). Variability of hydrological, meteorological and climatological variables at seasonal, annual and monthly scales have been investigated in many studies by employing parametric and non-parametric tests (Djaman et al., 2017; Gao et al., 2017; Wang et al., 2017). The Mann Kendall and Spearman's rho tests are among the most widely used trend detection tests. In any cases, the application of these methods needs some restrictive assumptions, such as independent structure of the timeseries, normality of the distribution, and length of data. For example, the existence of a positive serial correlation increases the probability that the MK test erroneously detects a trend (von Storch, 1999). Moreover, the

cited tests do not allow to identify the contribution of low and high values in the detected trend. An innovative trend analysis (ITA) method was developed and evaluated (Şen, 2012, 2017) for investigating the trends in hydrological, meteorological and environmental variables (Ay and Kisi, 2015; Haktanir and Citakoglu, 2014). For instance, (Saphoglu et al., 2014) examined the variations in monthly and annual streamflow by using linear regression, MK and ITA methods and found close relation between the results of all three methods. In another study (Elouissi et al., 2016) used ITA method to investigate the variations in monthly precipitation over 25 stations of Algeria and found that north and southern parts of Macta watershed exhibited decreasing and increasing trends, respectively. In few other studies, ITA method was used in combination with MK and SSE tests to investigate the variations in hydrometeorological variables (Ali et al., 2019; Cherinet et al., 2019) and found that as compared to other non-parametric trend methods, ITA method has a universal application, i.e., it does not require normal distribution of timeseries, serially independent data, seasonal phase and



length of timeseries. In addition, significant subseries trends (sub-trends) can be detected by using ITA method from its graphical representation of results.

UIRB is a distinctive region multiplex climate, perceptible physical and topographical features and conflicting hydrological systems (Hasson et al., 2015). The Impact of dynamics and variability of Indus river flows were investigated by employing Mann Kendall, least square estimation and multiple linear regression techniques and results showed declined trend of rainfall, rising trend of temperature in most cities and increasing trend of river flows in upper stations (Javed and Ahmad Hassan, 2019). Spatial and temporal flow variations, drought and flood periods were investigated by employing MK and SSE tests over upper Indus river basin and found that winter and spring flows presented increasing drifts while summer and autumn flows showed decreasing trends (Arfan et al., 2019). Hydrology of upper Indus River at northern areas of Pakistan over 7 stations was studied and demonstrated that Murree station received maximum amount of rainfall throughout the year and maximum flow was detected in 1993 that is 3235 cumecs and minimum flow happened in 1974 that was 1760 cumecs (Daniyal Hassan, 2016). To the best information of author there is not any study or published work in literature over upper Indus River Basin related to ITA methodology in detection of variations in extreme streamflow values and also to inspect the trends in low, medium and high flows. So this study plugs this exploration gap. This research work is conducted over the UIRB to study variations in extreme flow values, for this daily streamflow values on the basis of percentiles are divided into two categories i.e. extremely low (< 10<sup>th</sup> percentile) and extremely high flows (>90<sup>th</sup> percentile).

### Study area and data

The UIRB is one of world's most glaciated basin hosting more than 11000 glaciers and covering a surface area of 22000 Km<sup>2</sup> (Williams, 2013). The UIRB has great socio-economic importance for Pakistan because it is the main source of water for fulfilling downstream demands for various uses such as agriculture, hydropower, industry, domestic, etc. The mountainous range of the Hindu Kush-Karakoram-Himalayas spreads over more than 2000 kilometers in length from east to west and is highly vulnerable to climatic conditions including precipitation and changing

source areas of flows and it is considered as third pole of our planet (Bocchiola and Diolaiuti, 2013a). The Indus river provides water to world's largest contiguous irrigation system from which country furnish 90% of its food products; however, due to insufficient water supplies, country may face drastic food conditions (Qureshi, 2011). Therefore, investigation of variations in water resources availability has significant importance in the planning and management of future projects to meet the ever-increasing food and fiber requirements. The daily streamflow was collected from Water and Power Development Authority (WAPDA) of Pakistan and twenty stations were selected for further analysis based on homogeneity, extent and completeness of records. The data range of selected stations varies from 35 to 55 years (1961 to 2015). The locations of various stream gauge stations being operated over UIRB are presented in Fig. 1.

## Methodology

### Innovative trend analysis method

In few studies, the ITA method has been used with other trend analysis methods in detecting the variations in climatological, meteorological and hydrological data round the world because of its advantages over other non-parametric methods. In this method, the first step is to split data into two halves and place each half in ascending order individually. The first half of the data is located on the X-axis and the second half on the Y-axis of a Cartesian coordinate system as shown in Fig. 2.

A succession of clusters would categorize the deviation of each half. If the data points in a scatter plot are located on the 45o (1:1) line, it indicates no-trend in the hydrometeorological timeseries data however, if the data points accumulated in the lower and upper triangular area of the 1:1 line, it demonstrates downward or upward trends, respectively (Şen, 2012).

The magnitude of the trend presents in the data series maybe estimated by utilizing the equation given below (Wu and Qian, 2017).

$$D = \frac{1}{n} \sum_{i=1}^n \frac{10(Y_j - Y_i)}{\mu} \quad (11)$$

where  $D$  characterizes the trend indicator,  $n$  designates the number of data values of each subseries,  $Y_i$  and  $Y_j$  are the data values in the first and second subseries, respectively, and  $\mu$  represents the mean of the first subseries. A

negative or positive value of D displays a decreasing or increasing trend, respectively.

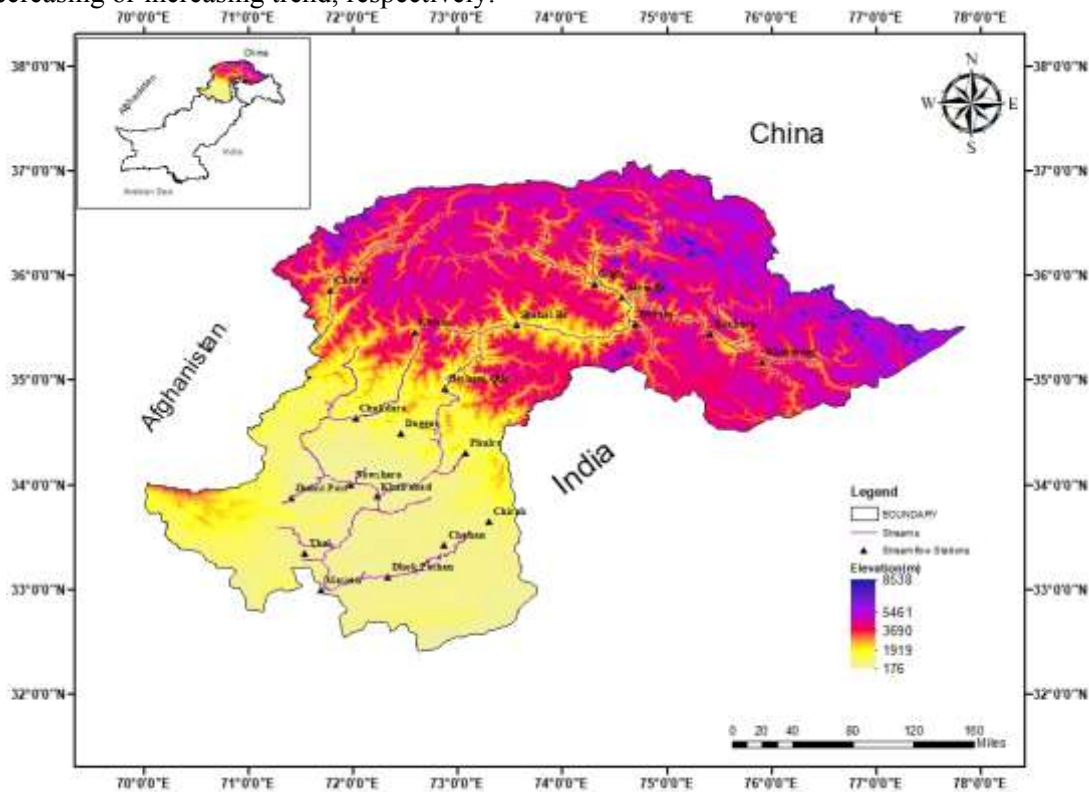


**Figure 1.** Location of selected stream gauging stations.

**Results**

**Variations in extreme values of streamflow timeseries**

Daily streamflow timeseries of various stations being selected in this study were divided into two categories, i.e., extremely low flows (< 10<sup>th</sup> percentile) and extremely high flows (> 90<sup>th</sup> percentile) as drought and flood events are considered more sensitive to variations in the extreme streamflow values (Ahmad et al., 2018; Wu and Qian, 2017). The variations in extreme values of streamflow were investigated by using the ITA method and results are presented in Figs. 3, 4 & 5. Extremely low streamflow exhibited significant increasing trends over Kharhong, Kachura, Doyain, Shatial Br., Daggar, Jhansi Post and Dhok Pathan stations as data points of these stations lies above the 1:1 line. However, Phulra, Khairabad and Thal stations exhibited significant decreasing trends because data points lie below the no-trend line. For Gilgit, Alam Br., Besham Qila, Kalam, Chakdara, Chitral, Nowshera, Chahan and Massan stations, most of the data points lies within the 10% range of 1:1 line. Extremely high flows showed that at most

of the stations, data points fall within the 10% variations from no-trend line, which exhibited insignificant trends at a 90% confidence interval. Only Doyain station exhibited a significant increasing trend for extremely high flows. The spatial distribution of extreme values is presented in Fig. 6.

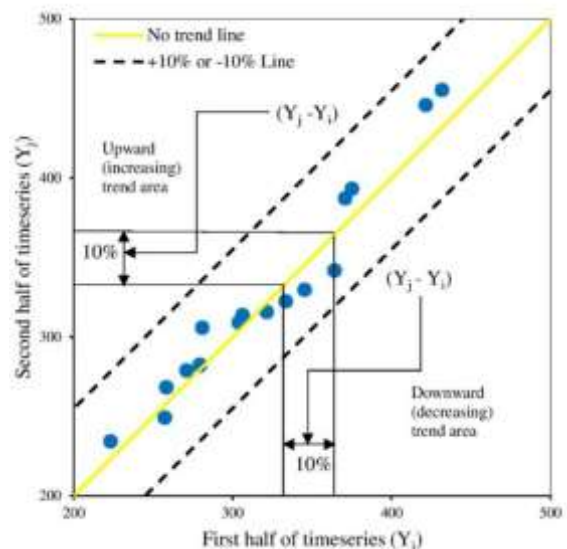


**Figure 2.** Representation of upward, downward and no trend areas in ITA methodology.

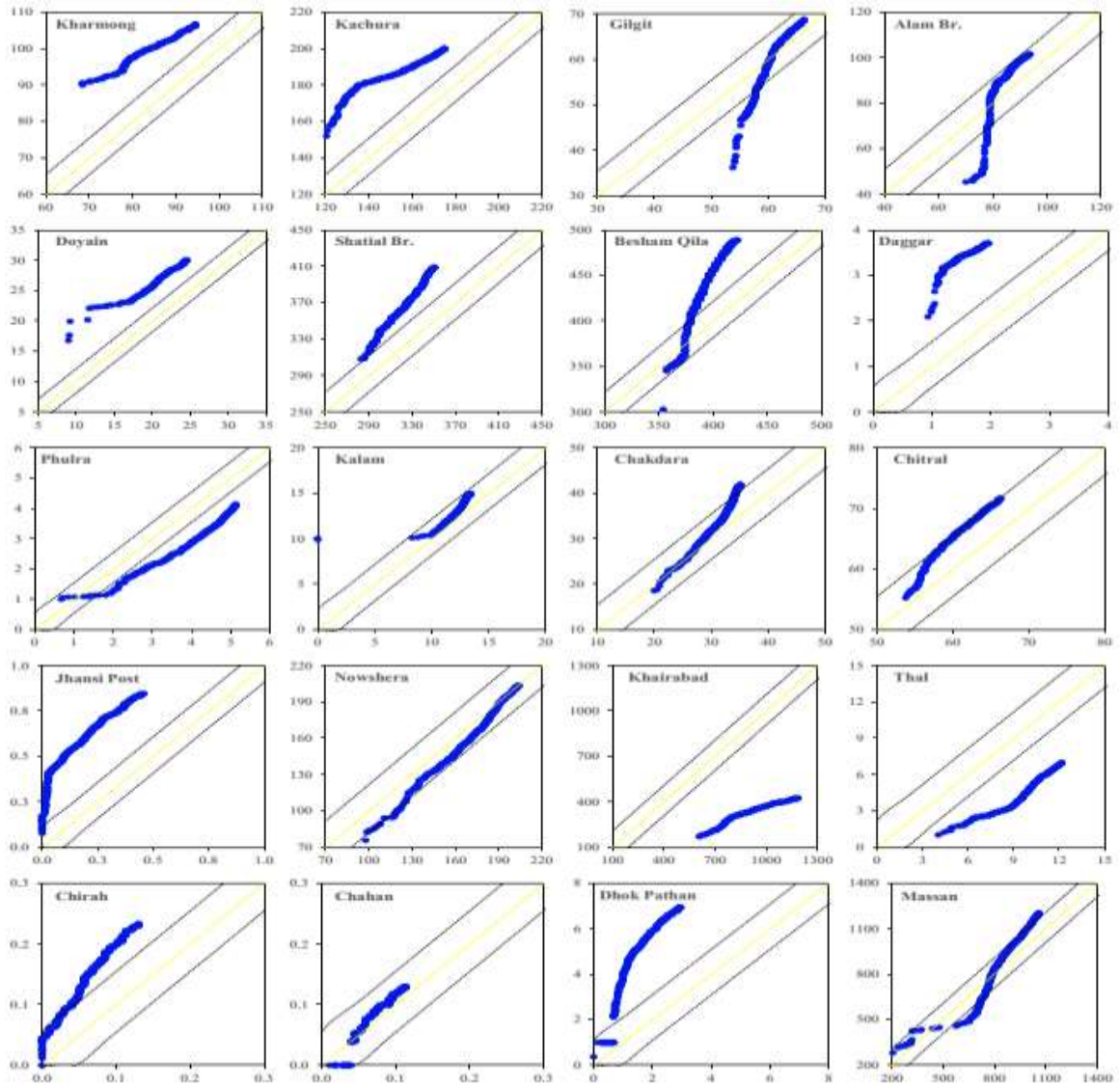


**Figure 3.** Sen's ITA method results of extremely low streamflow at 20 stations over UIRB.

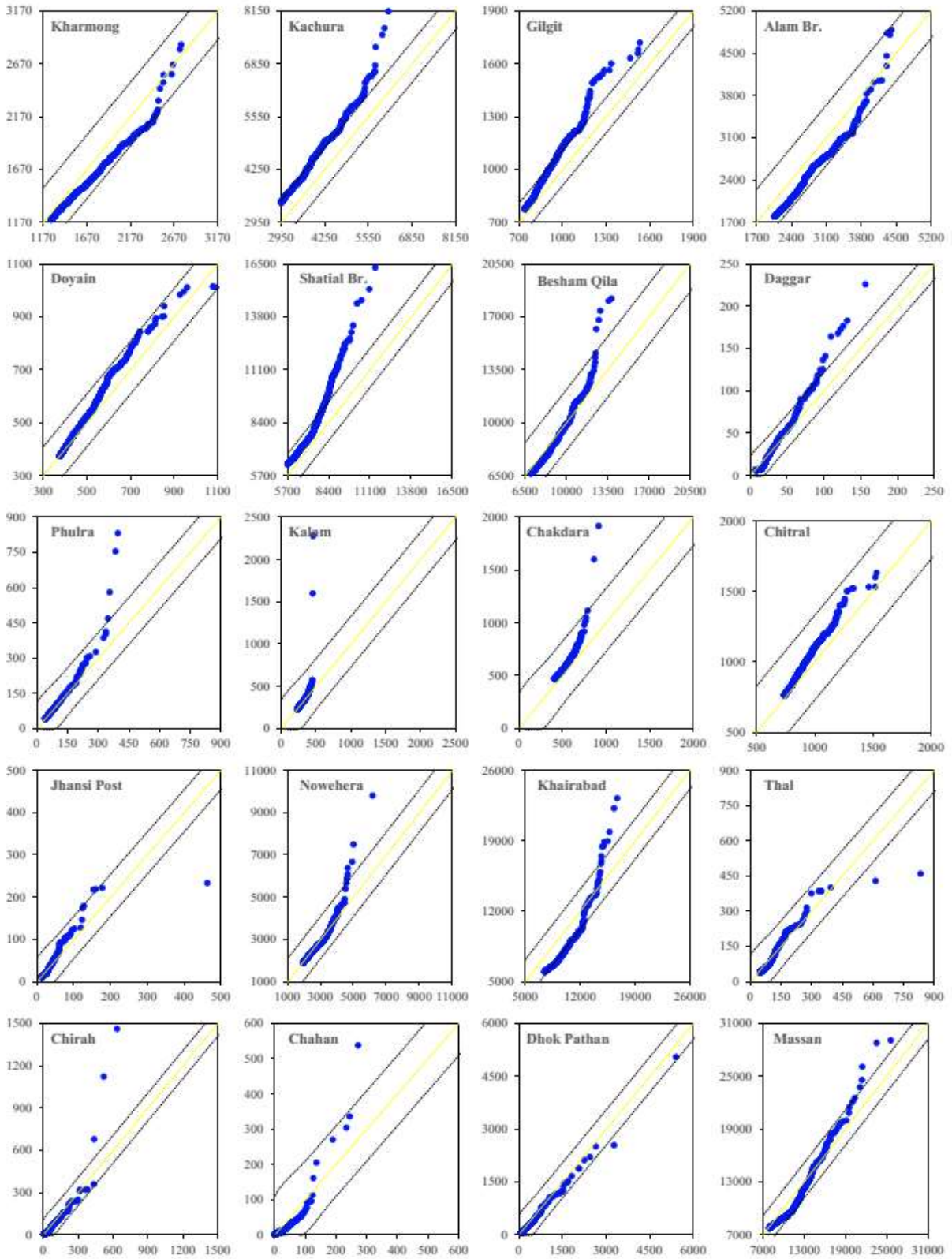


**Figure 4.** Sen's ITA method results of extremely high streamflow at 20 stations over UIRB.



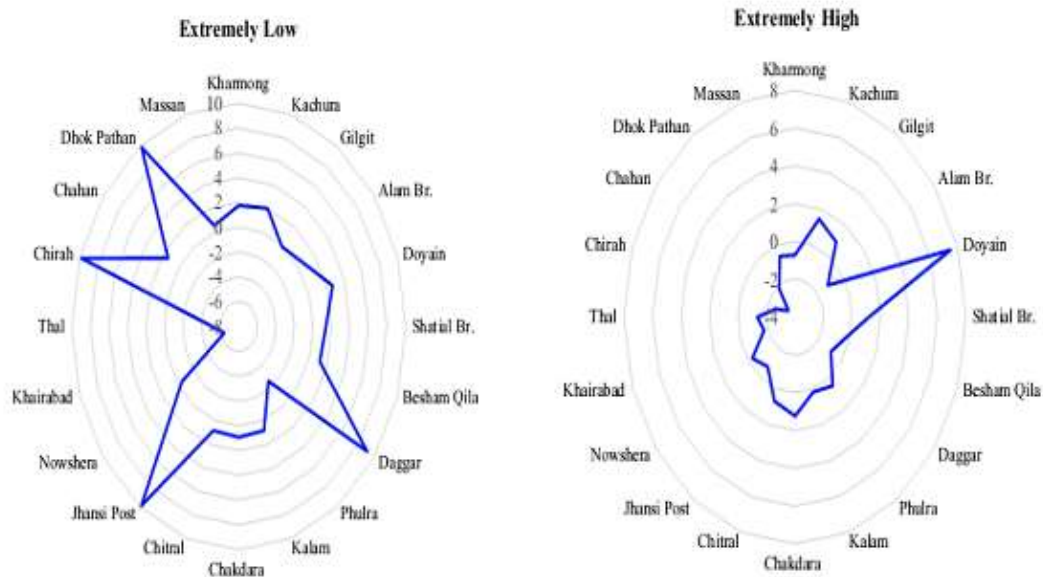


**Figure 5.** Extremely low and extremely high streamflow variations result by ITA method.

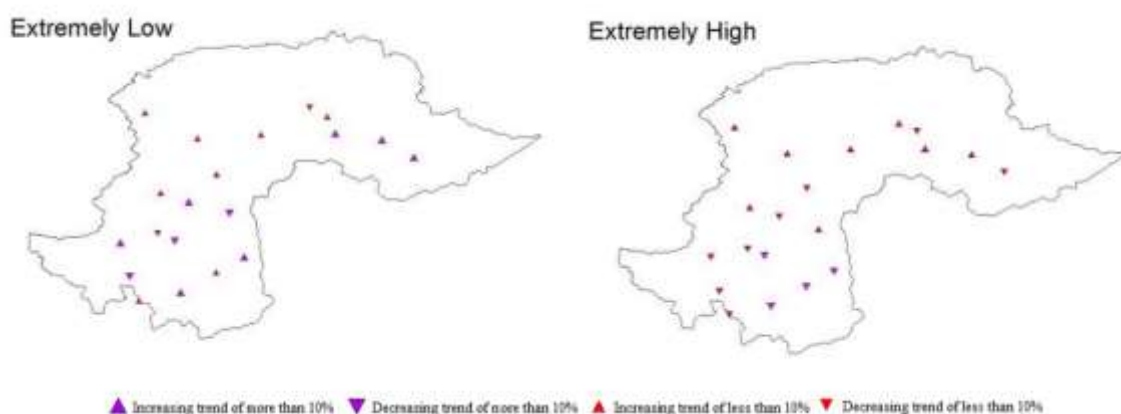


**Figure 6.** Spatial distribution of trends in extreme values of streamflow by ITA method

## Discussions

In this study, extreme streamflow values variability over the upper Indus river basin was investigated by using ITA method. Pakistan is vulnerable to extreme hydrologic events and bears a tremendous economic crisis due to variations in water availability (Basharat, 2016). Extreme events, including severe water shortages and flooding are likely to continue in the future (IPCC, 2014). Previous investigations in different regions found that the extreme hydrologic events demonstrated both expanding and diminishing patterns worldwide (Stojković et al. 2014; Vicente-Serrano et al. 2017). Therefore, variations in extreme streamflow

were also investigated to examine their impact on extreme hydrologic events, which were often observed in Pakistan in recent years.

Extremely low flows exhibited significant increasing trends at seven (07) stations and significant decreasing trends at three (03) stations. Extremely high flows exhibited significant increasing and decreasing trends at one (01) and four (04) stations, respectively. It may be concluded that extremely low flows are going to be more significant over UIRB as compared to extremely high flows which depicts a low availability of water in the near future. These trends may cause more stress on water

availability which is already at an alarming situation.

## Conclusions

Variations in extreme streamflow events were investigated by employing innovative trend analysis method. Significant increasing trends were found in the extremely low streamflow timeseries as compared to extremely high streamflow over the upper Indus basin. Extremely low streamflow showed increasing trends in upper and lower reaches of UIRB and constitute constant pressure on water resources availability in the lower Indus plains where most of the country's population is dependent on agricultural activities. Extremely high streamflow showed increasing trends in high elevated reach of UIRB which suggests probable aggravation of flooding however in the lower elevated reach extremely high streamflow exhibited significant decreasing trends showing reduction of flooding in that reach. Therefore, it is concluded that the variations in the extremely low flows will be more pronounced compared to extremely high flows in the future and put continuous pressure on water resources availability from UIRB. The results of the present study may be useful for decision-makers and practitioners of water resources for assessing extreme hydrologic events in developing future water conservation and management strategies.

## References

- Ahmad, I., Zhang, F., Tayyab, M., Anjum, M.N., Zaman, M., Liu, J., Farid, H.U., Saddique, Q., 2018. Spatiotemporal analysis of precipitation variability in annual, seasonal and extreme values over upper Indus River basin. *Atmos. Res.* 213, 346–360. <https://doi.org/10.1016/j.atmosres.2018.06.019>
- Ali, R., Kuriqi, A., Abubaker, S., Kisi, O., 2019. Long-term trends and seasonality detection of the observed flow in Yangtze River using Mann-Kendall and Sen's innovative trend method. *Water (Switzerland)* 11. <https://doi.org/10.3390/w11091855>
- Ali, R.O., Abubaker, S.R., 2019. Trend analysis using mann-kendall, sen's slope estimator test and innovative trend analysis method in Yangtze river basin, china: review. *Int. J. Eng. Technol.* 8, 110–119.
- Arfan, M., Lund, J., Hassan, D., Saleem, M., Ahmad, A., 2019. Assessment of spatial and temporal flow variability of the Indus River. *Resources* 8. <https://doi.org/10.3390/resources8020103>
- Ay, M., Kisi, O., 2015. Investigation of trend analysis of monthly total precipitation by an innovative method. *Theor. Appl. Climatol.* 120, 617–629. <https://doi.org/10.1007/s00704-014-1198-8>
- Bard, A., Renard, B., Lang, M., Giuntoli, I., Korck, J., Koboltschnig, G., Janža, M., d'Amico, M., Volken, D., 2015. Trends in the hydrologic regime of Alpine rivers. *J. Hydrol.* 529, 1823–1837. <https://doi.org/10.1016/j.jhydrol.2015.07.052>
- Basharat, M., 2016. Indus Basin Drought (1999–2002) Impact on Irrigated Agriculture – a Policy Review in the Preview of Mega Storages and Floods.
- Bocchiola, D., Diolaiuti, G., 2013. Recent (1980–2009) evidence of climate change in the upper Karakoram, Pakistan. *Theor. Appl. Climatol.* 113, 611–641. <https://doi.org/10.1007/s00704-012-0803-y>
- Chen, P.C., Wang, Y.H., You, G.J.Y., Wei, C.C., 2017a. Comparison of methods for non-stationary hydrologic frequency analysis: Case study using annual maximum daily precipitation in Taiwan. *J. Hydrol.* 545, 197–211. <https://doi.org/10.1016/j.jhydrol.2016.12.001>
- Chen, P.C., Wang, Y.H., You, G.J.Y., Wei, C.C., 2017b. Comparison of methods for non-stationary hydrologic frequency analysis: Case study using annual maximum daily precipitation in Taiwan. *J. Hydrol.* 545, 197–211. <https://doi.org/10.1016/j.jhydrol.2016.12.001>
- Cherinet, A.A., Yan, D., Wang, Hao, Song, X., Qin, T., Kassa, M.T., Girma, A., Dorjsuren, B., Gedefaw, M., Wang, Hejia, Yadamjav, O., 2019. Climate Trends of Temperature, Precipitation and River Discharge in the Abbay River Basin in Ethiopia. *J. Water Resour. Prot.* 11, 1292–1311. <https://doi.org/10.4236/jwarp.2019.1110075>
- Daniyal Hassan, R., 2016. Hydrology of Upper Indus Basin. 4th Int. Conf. Energy, Environ. Sustain. Dev. 2016 (EESD 2016).
- Djaman, K., Koudahe, K., Akinbile, C.O., Irmak, S., 2017. Evaluation of Eleven Reference Evapotranspiration Models in Semiarid Conditions. *J. Water Resour. Prot.* 09, 1469–



1490.  
<https://doi.org/10.4236/jwarp.2017.912094>
- Elouissi, A., Şen, Z., Habi, M., 2016. Algerian rainfall innovative trend analysis and its implications to Macta watershed. *Arab. J. Geosci.* 9, 1–12.  
<https://doi.org/10.1007/s12517-016-2325-x>
- Gao, T., Wang, H.J., Zhou, T., 2017. Changes of extreme precipitation and nonlinear influence of climate variables over monsoon region in China. *Atmos. Res.*  
<https://doi.org/10.1016/j.atmosres.2017.07.017>
- Hasson, S., Böhner, J., Lucarini, V., 2015. Prevailing climatic trends and runoff response from Hindukush-Karakoram-Himalaya, upper Indus basin. *Earth Syst. Dyn. Discuss.* 6, 579–653.  
<https://doi.org/10.5194/esdd-6-579-2015>
- IPCC, 2014. Part A: Global and Sectoral Aspects. (Contribution of Working Group II to the Fifth Assessment Report of the Intergovernmental Panel on Climate Change). *Clim. Chang. 2014 Impacts, Adapt. Vulnerability.* 1132.
- Javed, A., Ahmad Hassan, S., 2019. Study the Dynamics and Variability of River Indus Flow. *Int. J. Sci.* 8, 30–39.  
<https://doi.org/10.18483/ijsci.2072>
- Kehrwald, N.M., Thompson, L.G., Tandong, Y., Mosley-Thompson, E., Schotterer, U., Alfimov, V., Beer, J., Eikenberg, J., Davis, M.E., 2008. Mass loss on himalayan glacier endangers water resources. *Geophys. Res. Lett.* 35, 2–7.  
<https://doi.org/10.1029/2008GL035556>
- Latif, Y., Yaoming, M., Yaseen, M., 2018. Spatial analysis of precipitation time series over the Upper Indus Basin. *Theor. Appl. Climatol.* 131, 761–775.  
<https://doi.org/10.1007/s00704-016-2007-3>
- Lutz, A.F., Immerzeel, W.W., Kraaijenbrink, P.D.A., Shrestha, A.B., Bierkens, M.F.P., 2016. Climate change impacts on the upper indus hydrology: Sources, shifts and extremes. *PLoS One* 11, 1–33.  
<https://doi.org/10.1371/journal.pone.0165630>
- Mahajan, D.R., Dodamani, B.M., 2015. Trend Analysis of Drought Events Over Upper Krishna Basin in Maharashtra. *Aquat. Procedia* 4, 1250–1257.  
<https://doi.org/10.1016/j.aqpro.2015.02.163>
- Minora, U., Bocchiola, D., D'Agata, C., Maragno, D., Mayer, C., Lambrecht, A., Mosconi, B., Vuillermoz, E., Senese, A., Compostella, C., Smiraglia, C., Diolaiuti, G., 2013. 2001&ndash;2010 glacier changes in the Central Karakoram National Park: a contribution to evaluate the magnitude and rate of the "Karakoram anomaly" Cryosph. Discuss. 7, 2891–2941.  
<https://doi.org/10.5194/tcd-7-2891-2013>
- Momcilo, M., Misganaw, D., B., S.M., Siddhartha, V., A., C.R., 2014. Sensitivity Analysis of Annual Nitrate Loads and the Corresponding Trends in the Lower Illinois River. *J. Hydrol. Eng.* 19, 533–543.  
[https://doi.org/10.1061/\(ASCE\)HE.1943-5584.0000831](https://doi.org/10.1061/(ASCE)HE.1943-5584.0000831)
- Onyutha, C., 2016. Identification of sub-trends from hydro-meteorological series. *Stoch. Environ. Res. Risk Assess.* 30, 189–205.  
<https://doi.org/10.1007/s00477-015-1070-0>
- Qureshi, A.S., 2011. Water Management in the Indus Basin in Pakistan: Challenges and Opportunities. *Mt. Res. Dev.* 31, 252–260.  
<https://doi.org/10.1659/mrd-journal-d-11-00019.1>
- Saphoglu, K., Kilit, M., Yavuz, B.K., 2014. Trend analysis of streams in the Western Mediterranean Basin of Turkey. *Fresenius Environ. Bull.* 23, 313–324.
- Şen, Z., 2017. Innovative trend significance test and applications. *Theor. Appl. Climatol.*  
<https://doi.org/10.1007/s00704-015-1681-x>
- Şen, Z., 2012. Innovative trend analysis methodology. *J. Hydrol. Eng.* 17, 1042–1046.  
[https://doi.org/10.1061/\(ASCE\)HE.1943-5584.0000556](https://doi.org/10.1061/(ASCE)HE.1943-5584.0000556)
- Sharma, C., Panda, S., Pradhan, R., Singh, A., Kawamura, A., 2016. Precipitation and Temperature Changes in Eastern India by Multiple Trend Detection Methods. *Atmos. Res.* 180.  
<https://doi.org/10.1016/j.atmosres.2016.04.019>
- Smiraglia, C., Mayer, C., Mihalcea, C., Diolaiuti, G., Belò, M., Vassena, G., 2007. 26 Ongoing variations of Himalayan and Karakoram glaciers as witnesses of global changes: recent studies on selected glaciers, in: Baudo, R., Tartari, G., Vuillermoz, E. (Eds.), *Mountains Witnesses of Global Changes Research in the Himalaya and Karakoram: Share-Asia Project, Developments in Earth Surface Processes.* Elsevier, pp. 235–247.  
<https://doi.org/https://doi.org/10.1016/S092>

- 8-2025(06)10026-7
- Stojković, M., Ilić, A., Prohaska, S., Plavšić, J., 2014. Multi-Temporal Analysis of Mean Annual and Seasonal Stream Flow Trends, Including Periodicity and Multiple Non-Linear Regression. *Water Resour. Manag.* 28, 4319–4335. <https://doi.org/10.1007/s11269-014-0753-5>
- Tefaruk, H., Hatice, C., 2014. Trend, Independence, Stationarity, and Homogeneity Tests on Maximum Rainfall Series of Standard Durations Recorded in Turkey. *J. Hydrol. Eng.* 19, 5014009. [https://doi.org/10.1061/\(ASCE\)HE.1943-5584.0000973](https://doi.org/10.1061/(ASCE)HE.1943-5584.0000973)
- Vicente-Serrano, S.M., Zabalza-Martínez, J., Borràs, G., López-Moreno, J.I., Pla, E., Pascual, D., Savé, R., Biel, C., Funes, I., Azorin-Molina, C., Sanchez-Lorenzo, A., Martín-Hernández, N., Peña-Gallardo, M., Alonso-González, E., Tomas-Burguera, M., Kenawy, A. El, 2017. Extreme hydrological events and the influence of reservoirs in a highly regulated river basin of northeastern Spain. *J. Hydrol. Reg. Stud.* 12, 13–32. <https://doi.org/https://doi.org/10.1016/j.ejrh.2017.01.004>
- von Storch, H., 1999. Misuses of Statistical Analysis in Climate Research, in: von Storch, H., Navarra, A. (Eds.), *Analysis of Climate Variability*. Springer Berlin Heidelberg, Berlin, Heidelberg, pp. 11–26.
- Wang, X., Hou, X., Wang, Y., 2017. Spatiotemporal variations and regional differences of extreme precipitation events in the Coastal area of China from 1961 to 2014. *Atmos. Res.* 197, 94–104. <https://doi.org/10.1016/j.atmosres.2017.06.022>
- Williams, M.W., 2013. *The Status of Glaciers in the Hindu Kush–Himalayan Region*, Mountain Research and Development.
- Wu, H., Qian, H., 2017. Innovative trend analysis of annual and seasonal rainfall and extreme values in Shaanxi, China, since the 1950s. *Int. J. Climatol.* 37, 2582–2592. <https://doi.org/10.1002/joc.4866>

## Streamflow Forecasting at Mangla Reservoir in the Jhelum River by Using ARIMA Model

Hammad-ur-Rehman<sup>1</sup>, Ijaz Ahmad<sup>1\*</sup>, Muhammad Waseem<sup>1</sup>

<sup>1</sup> Centre of Excellence in Water Resources Engineering, University of Engineering and Technology, Lahore  
54890, Pakistan

Corresponding author email: [dr.ijaz@uet.edu.pk](mailto:dr.ijaz@uet.edu.pk)

**Abstract:** Precise stream flows forecasting is very important for the water management and water storage structures. In this study the ARIMA (auto regressive integrated moving average model) is used to forecast the stream flows of Jhelum river from 2016 to 2030. The fifteen-year data from 1991-2005 is used to train the model. For the testing period 2006-2015 the simulated flows were compared with the observed flows and the RMSE, MAE and NE were determined. This study concluded that the Seasonal ARIMA model  $(1,0,0) (2,1,2)_{12}$  was best fitted model for streamflow forecasting of Jhelum river at Mangla.

**Keywords:** ARIMA, forecast, streamflow, Mangla

### Introduction

Statistical models have been used to in the operational hydrology (Koutsoyiannis 2000). Some of famous linear models are AR, ARMA and ARIMA (Somchit et al. 2018). The main advantages of ARIMA model are, estimation of correlation, trend and cycles of timeseries (Gocheva-ilieva 2014). Many softwares, e.g., R, python, Minitab, MATLAB and SPSS are incorporated in the ARIMA model by using Box-Jenkins methodology (Khashei and Bijari 2011). ARIMA model is the combination of auto regressive terms and moving average terms. The time series should be stationary otherwise conversion into stationary by differencing is prerequisite (Kasyoki 2015). Differencing removes the irregular component from timeseries (Gocheva-ilieva 2014). Sometime log transformation is adopted to convert the timeseries into stationary (Somchit et al. 2018). ARIMA model is used to determine the maximum flows of Indus river at Sukkur barrage, Pakistan and found that  $(2,1,1)$  structure as best fitted at 95 percent confidence interval (Ahmad et al. 1993). The seven seasonal ARIMA models were used to forecast the mean inflows of Dokan reservoir, north of IRAQ. Forecast the mean inflows for the period October 2005, to September, 2007 (Al-masudi 2007). The annual flows of European rivers were investigated and suggested that simulated model flows can be used for the basin management. The flows timeseries was forecasted by using the SBM single beam model. The ten large rivers of Europe were used

for this purpose (Stojković et al. 2015). The two seasonal ARIMA models  $(0,1,1)(0,1,1)_{12}$  and  $(0,1,2)(0,1,1)_{12}$  for the forecasting of Haditha reservoir, middle west of Iraq is used for forecasting (Saleh 2013). The Euphrates river water quality at KUFA city has been studied and developed the ARIMA  $(1,1,1)$ , AR(1) and AR(2) models for forecasting the time series (Valipour et al. 2013). The annual inflows of krishnagiri reservoir, India forecasted and developed the ARMA  $(2,4)$  model (Vijayakumar 2017). To forecast the inflows of Srisailam reservoir India and developed the model for synthetic stream flows (Graham et al. 2019). The precipitation data of five-gauge station in the eastern part of Jordan had been studied. The lower basin of the Jordan has steep slope. The temperature variation is -3.9 degree centigrade to 34.3 degree centigrade for a year. The ARIMA model is used to forecast the data up to 2026. The ARIMA  $(3,1,3)$  was best fitted for the monthly time series forecasting. The average annual data was best fitted for  $(4,1,3)$  and seasonal time series are best fitted for ARIMA  $(4,2,4)$  (Balasmeh 2019). The ARMA, AR and ARIMA model were used for forecasting of the stream flows of Shiroro river. The 22 years (1990-2011) model simulated results were compared with the observed flows. After the analysis, some recommendations were presented to efficiently use the flows (Musa 2013). The inflows timeseries of Talog reservoir, Iran is used to forecast the timeseries. The ARMA $(2,3)$  model was used to produce artificial timeseries (Hamidi and Telvari 2018). The 48 years mean annual inflows at Karkheh reservoir

was used to develop the three ARIMA models (0,1,1), (1,1,1) and (4,1,1). The simulated models' results were compared with the observed flows based on conditional least square CLS and unconditional least square ULS for the period 2006-2015. The comparison showed the satisfactory value (Hamidi and Telvari 2018). In California, 79 reservoir operation system were studied and elaborated in these aspects. An efficient system used this temporal scale information and fulfil all the needs of related people (Hejazi and Cai 2011). The Garzan reservoir stream flows had studied. The reservoir water was released to fulfil the private and public water requirements in the downstream side. The reservoir optimization was required to utilize the reservoir water efficiently. Therefore, the stream flows were forecasted by using the ARIMA model (Yalcin and Tigrek 2017). Sangsoorakh basin (Iran) is located in the southwest sub basin of karkheh. The Sangsoorakh basin has large contributions into water supply. Its inflows were forecasted with ARIMA and de-seasonalized ARIMA. Their results were evaluated for the period of 1999-2004. Different statistical tests were performed to check the outputs of results in numerical forms. After this, simulated results were compared with observed flows which prove that ARIMA performed better than the de-seasonalized ARMA (Reza Ghanbarpour et al. 2010). In this study, fifteen years (1991-2005) of monthly timeseries of inflows is used to develop

the ARIMA models. The developed models result from (2006-2015) are compared with the observed data. After this it is extrapolate up to 2030.

### Study Area

Mangla reservoir is the second largest reservoir in Pakistan. It is located in Mirpur district of Azad Jammu and Kashmir. It is constructed on Jhelum river in 1967. Its 45% catchment lies in Pakistan occupied Kashmir and remaining in the territory of Indian occupied Kashmir. The Mangla reservoir covers an area of 329.7 km<sup>2</sup>. The gross storage capacity of reservoir is 9.22 km<sup>3</sup>. The command area of Mangla reservoir is 60,000 km<sup>2</sup>. The temperature variation of air is 18 °C to 43 °C. The primary purpose of Mangla reservoir is to irrigate the agricultural lands. The Mangla reservoir supplies water to the upper and lower Chasma-Jhelum link canal regions. During the period of December to March (Rabi season) the irrigation demands are at their peak from for upper Jhelum region for which the water supplied from Mangla reservoir. The excess water from lower and upper Jhelum region irrigates to the lower Indus basin. Hydropower is produced as by product as the water released from the reservoir for any purpose passes through the turbines and its hydropower capacity is 1000 MW (Mega Watt). Mangla domestic demand is 4.2 million gallons of water per day.

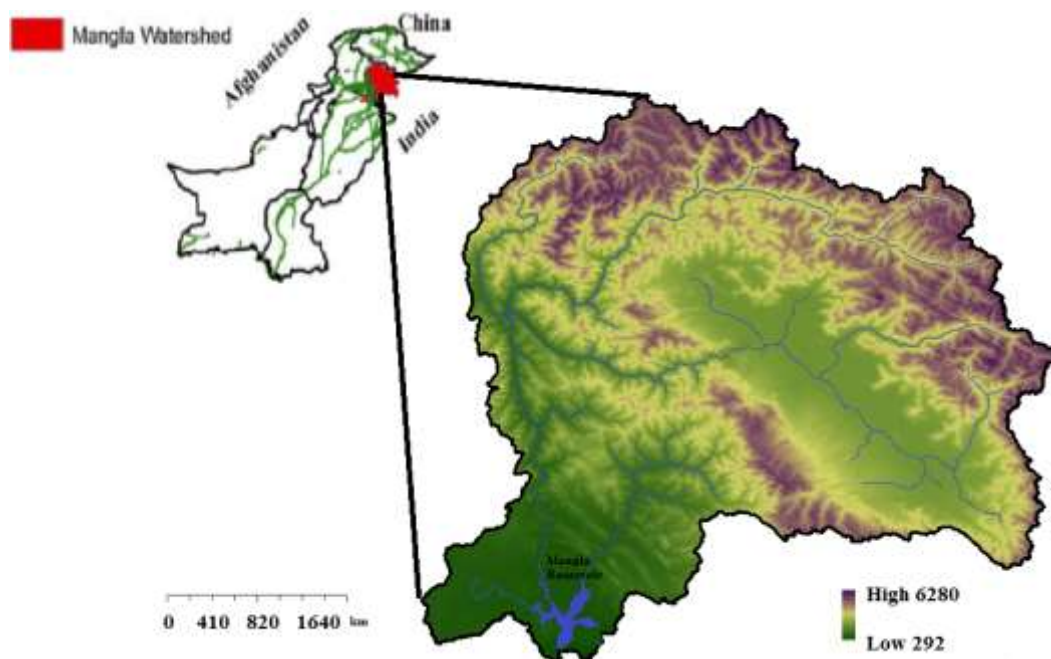


**Fig. 1** Mangla watershed and location of Mangla reservoir.

## Materials and Methods

ARIMA means the auto regressive integrated moving average model. ARIMA model assumes that the future values are linear time series and correlated with the past values with some variables and random errors (Hamidi and Telvari 2018). According to box and Jenkins methodology (1970) ARIMA model consisted of three variables p, d, and q whereas p represented the auto regressive terms ,q represented the moving average terms and d is the degree of differencing (Otok 2009; Shumway and Stoffer 2000). To develop ARIMA model the following steps are taken.

### Stationary Test

Stationary means its mean variance and covariance of time series is a constant function. A time series should be stationary otherwise convert into the stationary by differencing, log transformation and power of 10th. A white noise series  $\epsilon_t$  satisfied the stationary condition (Kasyoki 2015; Shyh-Jier Huang and Kuang-Rong Shih 2003)

### Model Identification

The model identification means to determine the value of variables p, d and q. The value of p is determined by using the ACF (auto correlation function). when the ACF value of time series reaches to zero or near to zero. It is equal to p. After plotting of PACF (partial auto correlation function) the parameter q is determined. Whereas the value of d is the degree of differencing to make the time series stationary. After the model identification the diagnostic tests are performed. it is satisfactory then it is ok. Otherwise repeat this process and select another value of parameters (Hong et al. 2016).

### Diagnostic Checking

After the model identification mostly AIC (Akaike's information criterion) and BIC (Bayesian information criterion) are performed and the least value of AIC and BIC is best fitted model.(Reza Ghanbarpour et al. 2010)

$$AIC = -2 \ln(L) + 2k$$

whereas L=likelihood function

K=number of parameters to be estimated

$$BIC = -2 \ln(\text{Max. Likelihood}) + Tp \ln(n)$$

whereas L=likelihood function

K=number of parameters to be estimated

n =number of terms

## Forecasting

The h-period ahead forecast based on an ARIMA (p, d, q) model where the d=0 is given by

$$\hat{y}_{t+h} = \hat{\delta} + \hat{\phi}_1 y_{t+h-1} + \dots + \hat{\phi}_p y_{t+h-p} + e_{t+h} - \hat{\theta}_1 e_{t+h-1} - \dots - \hat{\theta}_q e_{t+h-q}$$

$Y_{t+h}$  terms are replaced with the estimated values when the observed values finished the forecasted time series are formed. The forecasted model results are compared with the RMSE, MAE and R value (Weisang 2008)

## Results and Discussions

The historical inflow time series of Mangla reservoir from 1991 to 2005 is used to develop the ARIMA model. Mangla watershed has snow melting effect in the contribution of stream flows. The summer seasons May to July is the peak months of inflows. The mean annual flows are decreasing from 1991-2001. After this the mean annual flows are increased. The year 1991 and 1996 are the higher value of mean annual flows. Mangla inflow time series is nonstationary time series. It means that its mean, variances and covariance of time series are not constant. It is compulsory to convert into stationary because ARIMA model could not analysis the nonstationary timeseries. A number of trials is done to convert into stationary. First of all, take first difference, second order difference and so on. Unfortunately, after differencing it is not converted into stationary. Therefore, the second option log transformation is used. After log transformation the inflow time series are converted into stationary. Further analysis is performed on stationary time series. After forecasting the time series, it is reconverted into original form by taking anti-log of forecasted time series.

The Inflow time series of Mangla is divided into two periods calibration and validations.

The calibration period is selected from 1991 to 2005. whereas validation period is selected from 2006-2015. Mangla catchment has snow melting effects. In the summer seasons the temperature is high and inflows peaks are passed during this season. The inflow time series has best fitted seasonal ARIMA model structure (1,0,0)(2,1,2)<sub>12</sub>.

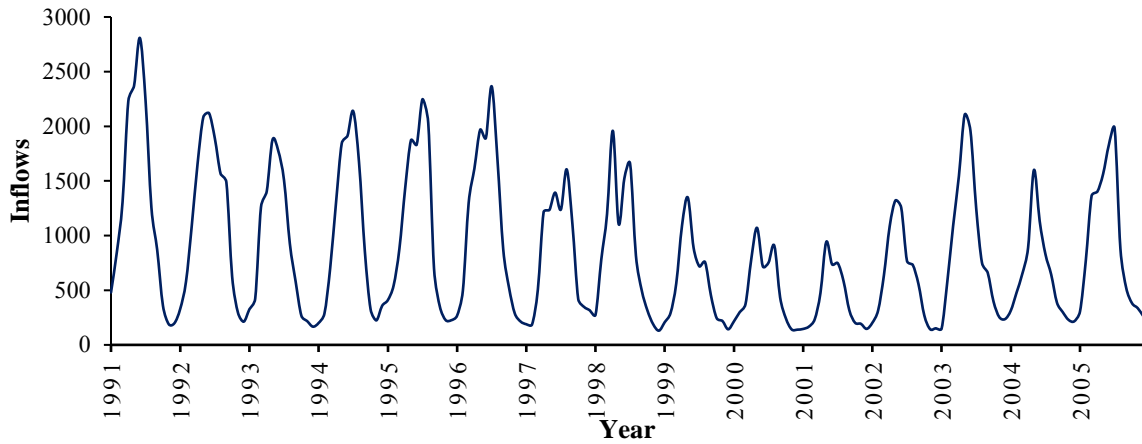


**Fig. 2** Nonstationary observed stream flows of Jhelum river at Mangla from 1991 to 2005

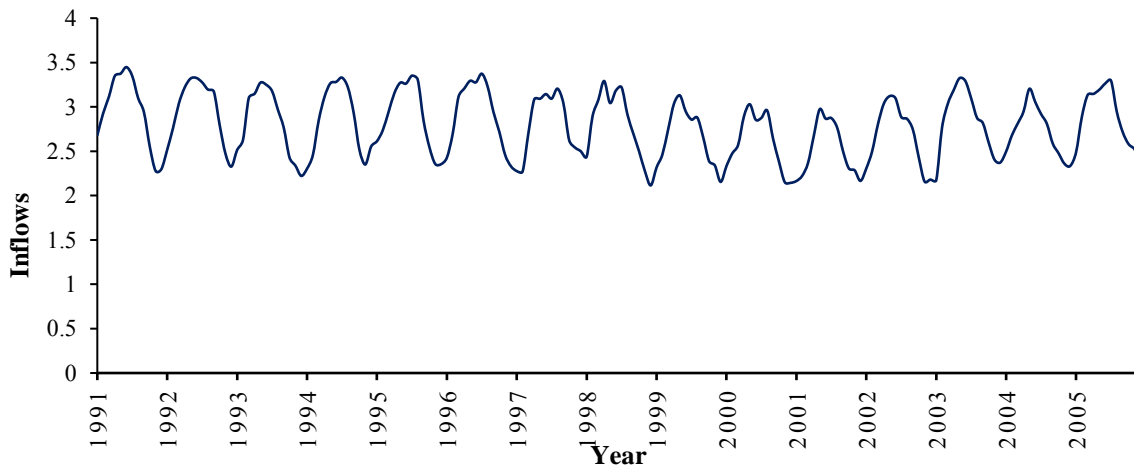


**Fig. 3** Log transferred stationary observed stream flows of Jhelum river at Mangla from 1991 to 2005

The model simulated flows are represented with the dotted lines and observed flow are presented with the solid lines.

A number of ARIMA structure is used for trial to best fit model structure. After the comparison of

observed data seasonal ARIMA model structure  $(1,0,0)(2,1,2)_{12}$  is best fitted. The simulated values are compared with the observed flows. Most of peaks are matched with the observed flows.

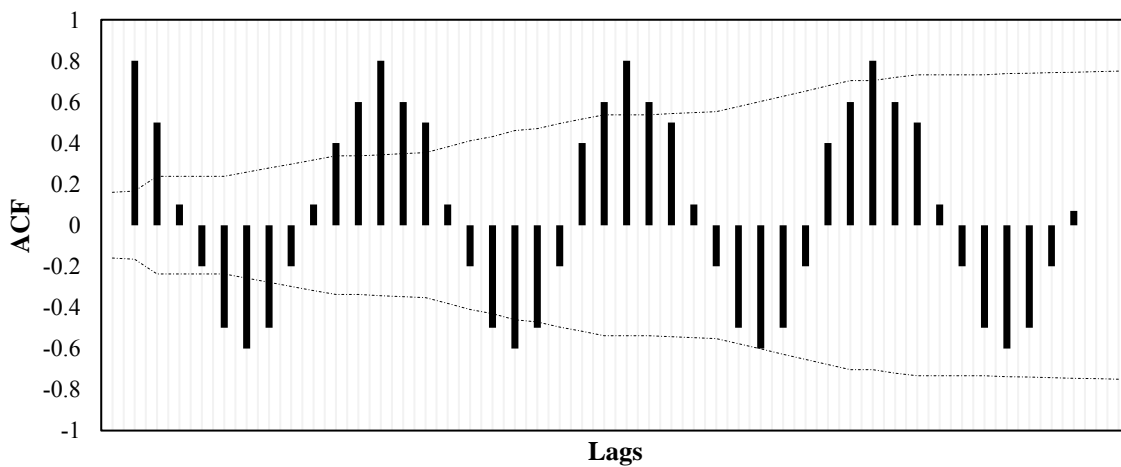


**Fig. 4** ACF of timeseries



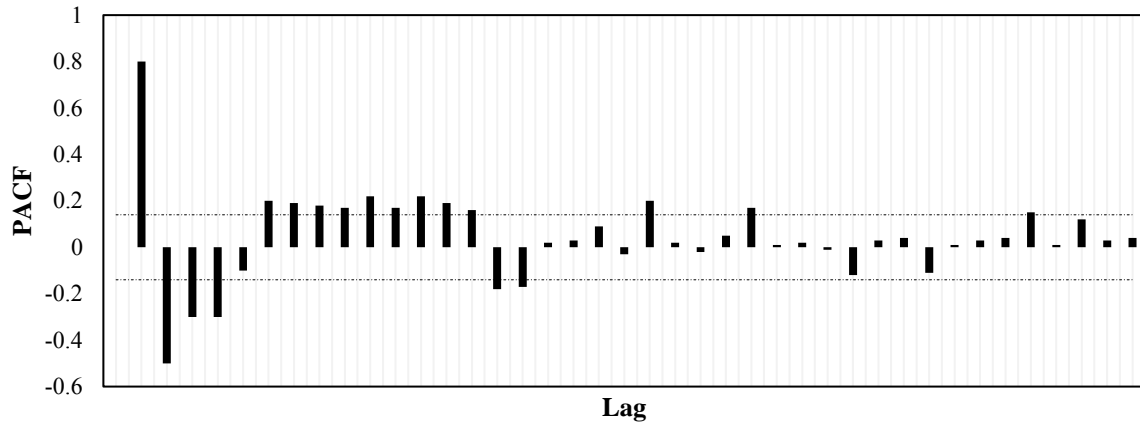


**Fig. 5** PACF of timeseries

The period of 1991-2015 is selected as the validation time period. In the validation period the most of peaks of observed date lies slightly above the observed data. In the inflow time series the seasonal trend is more prominent. Therefore seasonal ARIMA model structure is best fitted for the inflow time series. It is compared with the observed flows and evaluated the value of R square, RMSE, MAE are 0.85,195, and 145

respectively. After the validation of these results the same ARIMA model is used to forecast the inflow time series up to 2030. For the extending of times series of inflows ARIMA model is used. The simulated time series of ARIMA model is represented by the dotted lines. Most of cases the peak observed flows are same as the simulated time series. Which is shown in Fig. 6.

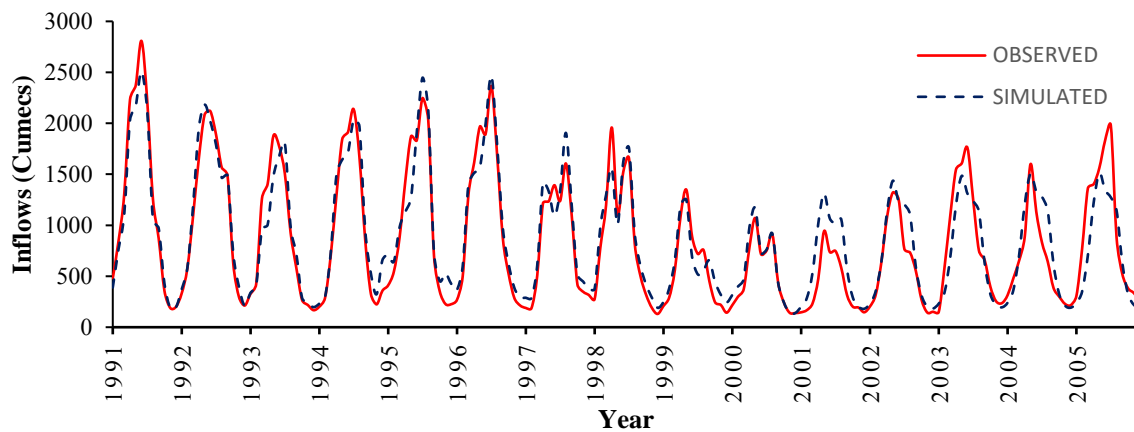


**Fig. 6** Calibration of observed and simulated streamflows of Jhelum river at Mangla using ARIMA model structure  $(1,0,0)(2,1,2)_{12}$  during period of 1991 to 2005

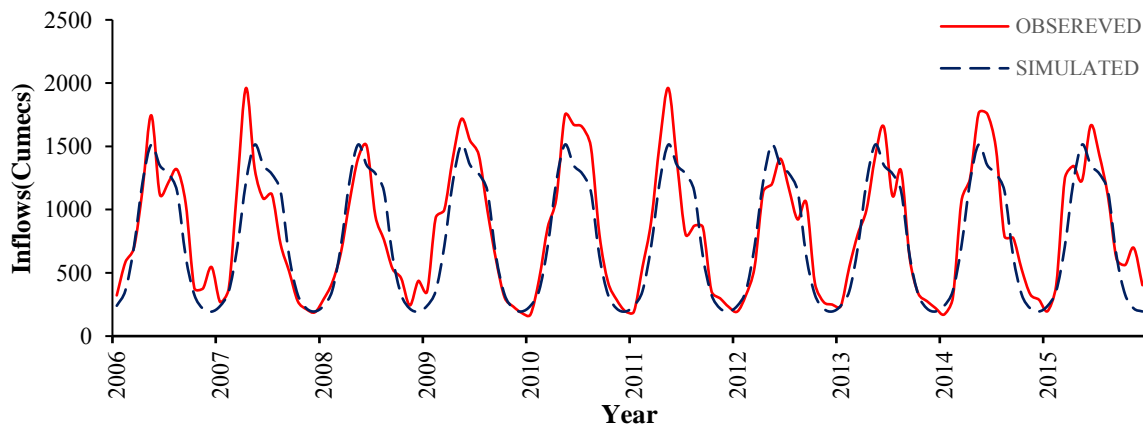


**Fig. 7** Validation of observed and simulated streamflows of Jhelum river at Mangla using ARIMA model structure  $(1,0,0)(2,1,2)_{12}$  during the period of 2006 to 2015

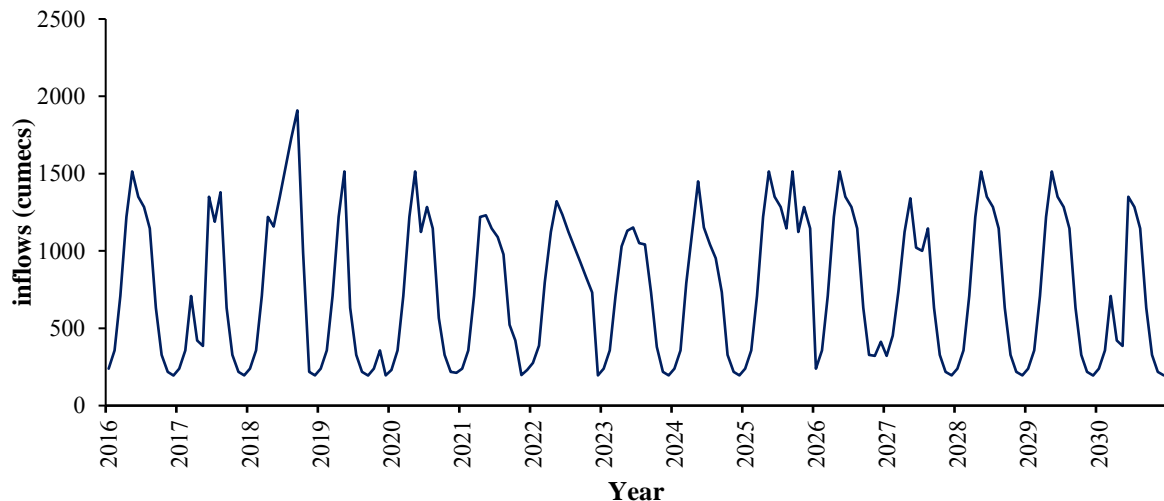


**Fig. 8** Simulated streamflow of Jhelum river at Mangla using ARIMA model structure  $(1,0,0)(2,1,2)_{12}$  during the period of 2016 to 2030

### Conclusions

In this study ARIMA model is used to forecast inflows time series of Mangla reservoir. Seasonal ARIMA model  $(1,0,0)(2,1,2)_{12}$  is best fitted for the inflow time series. For smoothening the time series (ln) log transformation is used. After comparison of results with the observed inflows it is highly accurate because their value of  $R^2$ , RMSE and MAE are 0.85, 195 and 145 .

### Acknowledgments

The authors thank the Water and Power Development Authority (WAPDA) and Pakistan Meteorological Department (PMD) for providing the data without any cost.

### References

- Ahmad, M. S., Ahmad, M. I., Naeem, H. M., and Sarwar, M. (1993). "Time Series Modelling of Annual Maximum of River Indus at Sukkur." 30(1), 36–38.
- Al-masudi, R. K. M. (2007). "Fitting ARIMA Models for Forecasting to Inflow of Dokan Reservoir." (1986), 1–10.
- Balasmeh, O. Al. (2019). "Trend analysis and ARIMA modeling for forecasting precipitation pattern in Wadi Shueib catchment area in Jordan." *Arabian Journal of Geosciences*.
- Gocheva-ilieva, S. G. (2014). "Time series analysis and forecasting for air pollution in small urban area: an SARIMA and factor analysis approach." 1045–1060.
- Graham, A., Sahu, J. K., and Sahu, Y. K. (2019). "Short communication Forecast future rainfall & temperature for the study area using seasonal auto-regressive integrated moving averages ( SARIMA ) model." 7(1), 894–897.
- Hamidi, K., and Telvari, A. (2018). "Forecasting by Stochastic Models to Inflow of Karkheh Dam at Iran Forecasting by Stochastic Models to Inflow of Karkheh Dam at Iran." (April).
- Hejazi, M. I., and Cai, X. (2011). "Building more realistic reservoir optimization models using data mining - A case study of Shelbyville Reservoir." *Advances in Water Resources*, Elsevier Ltd, 34(6), 701–717.
- Hong, X., Guo, S., Wang, L., Yang, G., Liu, D., Guo, H., and Wang, J. (2016). "Evaluating Water Supply Risk in the Middle and Lower Reaches of Hanjiang River Basin Based on an Integrated Optimal Water Resources Allocation Model." *Water*, 8(9), 364.
- Kasyoki, A. (2015). "Simple Steps for Fitting Arima Model to Time Series Data for Forecasting Using R." 4(3), 2013–2016.
- Khashei, M., and Bijari, M. (2011). "A novel hybridization of artificial neural networks and ARIMA models for time series forecasting." *Applied Soft Computing Journal*, Elsevier B.V., 11(2), 2664–2675.
- Koutsoyiannis, D. (2000). "A generalized mathematical framework for stochastic simulation and forecast of hydrologic time series." *Water Resources Research*, 36(6), 1519–1533.
- Musa, J. J. (2013). "Stochastic Modelling of Shiroro River Stream flow Process." (06), 49–54.
- Otok, B. W. (2009). "Development of Rainfall

- Forecasting Model in Indonesia by using ASTAR , Transfer Function , and ARIMA Methods.” *European Journal of Scientific Research*, 38(3), 386–395.
- Reza Ghanbarpour, M., Abbaspour, K. C., Jalalvand, G., and Moghaddam, G. A. (2010). “Stochastic modeling of surface stream flow at different time scales: Sangsoorakh karst basin, Iran.” *Journal of Cave and Karst Studies*, 72(1), 1–10.
- Saleh, Z. A. (2013). “Forecasting by Box-Jenkins ( ARIMA ) Models to Inflow of Haditha Dam.” (5).
- Shumway, R. H., and Stoffer, D. S. (2000). “Time Series Analysis and Its Applications.” 1–44.
- Shyh-Jier Huang, and Kuang-Rong Shih. (2003). “Short-term load forecasting via ARMA model identification including non-gaussian process considerations.” *IEEE Transactions on Power Systems*, 18(2), 673–679.
- Somchit, Yoshikawa, S., and Kanae, S. (2018). “Improved Forecasting of Extreme Monthly Reservoir Inflow Using an Analogue-Based Forecasting Method :”
- Stojković, M., Prohaska, S., and Plavšić, J. (2015). “Stochastic structure of annual discharges of large European rivers.” 63–70.
- Valipour, M., Banihabib, M. E., Mahmood, S., and Behbahani, R. (2013). “Comparison of the ARMA , ARIMA , and the autoregressive artificial neural network models in forecasting the monthly inflow of Dez dam reservoir.” *Journal of Hydrology*, Elsevier B.V., 476, 433–441.
- Vijayakumar, N. (2017). “A Comparative Analysis of Forecasting Reservoir Inflow using ARMA Model & Holt Winters Exponential Smoothing Technique.” (May 2016).
- Weisang, G. (2008). “Vagaries of the Euro : an Introduction to ARIMA Modeling.” 2(1), 45–55.
- Yalcin, E., and Tigrek, S. (2017). “Optimization of the Garzan Hydropower System operations.” *Arabian Journal of Geosciences*.

## Meteorological droughts to hydrological droughts: a case study of the Soan Basin, Pakistan

Awais Naeem Sarwar<sup>1</sup>, Muhammad Waseem<sup>1\*</sup>, Ijaz Ahmad<sup>1</sup>, Muhammad Azam<sup>2</sup>, Muhammad Nouman Sattar<sup>3</sup>

<sup>1</sup> Centre of Excellence in Water Resources Engineering, University of Engineering and Technology Lahore, 54890, Pakistan

<sup>2</sup> Department of Land and Water Conservation Engineering, Faculty of Agricultural Engineering and Technology, PMAS-Arid Agriculture University, Rawalpindi 46000, Pakistan

<sup>3</sup> Department of Civil Engineering, The University of Faisalabad, Faisalabad 38000, Pakistan

Corresponding author email: [waseem.jatoi@cewre.edu.pk](mailto:waseem.jatoi@cewre.edu.pk)

**Abstract:** The standard precipitation index (SPI) and stream flow drought index (SDI) were utilized in this research to investigate the relationship between meteorological and hydrological droughts in the Soan River Basin. Soan River Basin is the most important water source of Potohar region and the source of water for Islamabad. Results showed that the frequencies of both meteorological droughts and hydrological droughts has an increasing trend in the last 3 decade in the Soan River Basin. There was a strong relationship between meteorological and the hydrological droughts, which can be related with a simple linear function. The relationship between meteorological and the hydrological droughts varied in space and time. The differences between meteorological and the hydrological droughts have become more significant during the 3 decade. The presented results not only play an important reference in understanding the relationships between meteorological and hydrological droughts, but also have practical applications for regional water resource managements at catchment scale.

**Keywords:** Standard precipitation index (SPI), Stream flow drought index (SDI), Hydrological drought, Meteorological drought, Soan River Basin

### Introduction

Drought is a natural phenomenon and a natural hazard, and it occurs over most parts of the world, even in wet and humid regions (Dai 2011). Based on different disciplinary perspectives, drought can be separated into four categories (Sheffield and Wood 2012): meteorological drought, agricultural drought, hydrological drought, and socioeconomic drought. Among these different types of droughts, the hydrological cycle is the most important given the high dependence of many activities on surface water resources.

Meteorological drought is one of the important factors affecting the hydrological drought (Gumus and Algin 2017). Due to atmospheric transport of anomalously warm and dry air, spatial migration of a drought event from meteorological to hydrological drought would occur (Joseph et al. 2009). It is called drought propagation. In addition, propagation of drought is characterized by a number of features, which are related to the fact that the terrestrial part of the hydrological cycle acts as a low-pass filter to the meteorological forcing (Marković and Koch

2005). For example, a prolonged meteorological drought results into hydrological drought, and a lag occurs between meteorological and hydrological droughts. Edossa et al. (2010) analyzed drought characteristics in the Awash River Basin of Ethiopia based on meteorological and hydrological variables, and the results had shown that occurrence of hydrological drought events at Lower Awash lagged meteorological drought events in the upper Awash on average by 7 months. Tabrizi et al. (2010) found that annual time scale of meteorological drought in the upstream of the Doroodzan watershed of Iran can be used to investigate occurrence of stream flow drought in the downstream. Haslinger and Koffler (2014) have explored the linkage between meteorological drought and streamflow. Jörg-Hess et al. (2015) have quantified the effects of quality of meteorological forcing in hydrological droughts. Huang et al. (2016) have investigated the linkages between hydrological drought, climate indices, and human activities in the Columbia River basin. Gumus and Algin (2017) have analyzed the meteorological and hydrological droughts of the Seyhan-Ceyhan River Basin of Turkey. More importantly, the lag

of occurring time between meteorological and hydrological droughts is crucial in coping with drought. This time-lag issue has been addressed in some drought-prone regions in Europe and Africa (Hisdal and Tallaksen 2003). This cause-effect relationship between meteorological and hydrological droughts has been modelled with a copula-based joint meteorological-hydrological drought index by Cheraghalizadeh et al. (2018) at upstream and downstream of the Kasilian basin. Huang et al. (2017) have explored the propagation from meteorological to hydrological droughts and identified the potential influence factors. The entropy theory was used by Zhu et al. (2018) to develop a hybrid drought index, which combines meteorological, hydrological, and agricultural information and was applied to investigate the drought condition in Northwest China. Tjerdeman et al. (2018) have investigated the natural and human influences on the link between meteorological and hydrological drought indices for a large set of catchments in the contiguous United States.

The standardized precipitation index (SPI) (McKee et al.1993) and streamflow drought index (SDI) (Nalbantis 2008) are simple and effective indices for meteorological and hydrological droughts, and are also widely used in the literature due to their multiple simultaneous time scales and simplicity of calculation (Ashraf and Routray 2015; Sönmez et al. 2005). Therefore, SPI and SDI were used in this study to calculate the meteorological and hydrological drought events.

Soan River Basin is the most important water source of Potohar region. It is the source of water for the Simly Dam, which is the water reservoir for Islamabad. Soan basin plays an important role in local economic development. Its meteorological and hydrological droughts could potentially have a significant effect on regional development. However, it seems there is not a study in the literature which investigate the relationship between meteorological and hydrological droughts in the Soan River Basin.

The objectives of this paper are to investigate temporal and spatial evolutions of meteorological and hydrological droughts in the Soan River Basin by using SPI and SDI for 1983–2015 years, investigate the relationships between the meteorological and hydrological droughts including establishing a regression function between the meteorological and hydrological droughts and identifying the lag time between the two droughts, and explore the differences

between meteorological and hydrological droughts and discuss the possible reasons.

## Study Area and Data

### Study area

Soan River originating from Murree Mountains, is a major tributary of Indus River and a main hydrological unit of Potohar plateau Pakistan. Before falling into the Indus River, the Soan River runs through Chirah and Dhoke Pathan hydrological gauging stations as shown in Fig. 1. The area above the Chirah hydrological gauging station is Chirah sub-basin (hereafter sub-basin 1), and the area above Dhoke Pathan hydrological gauging station is Dhoke Pathan sub-basin (hereafter sub-basin 2). Elevation of the Soan basin ranges from 265 to 2274 m and covers an area of 6842 km<sup>2</sup>. According to the present study, mean annual precipitation of basin is 1465 mm, and the mean annual temperature varies from 8 to 18 °C for the period of 1983–2012. The slope of basin varies from gentle to steep, and almost all of the basin flow is generated from monsoon fed streams.

The Soan River provides water to the Simly Dam which is the main source of drinking water supply to Islamabad, the Capital of Pakistan. Furthermore, it is the main source of irrigation water for Potohar plateau. The 60%of basin population is rural, and agriculture is the main economic activity of the inhabitants (Ashfaq et al. 2014; Planning & Development department Government of Punjab 2015).

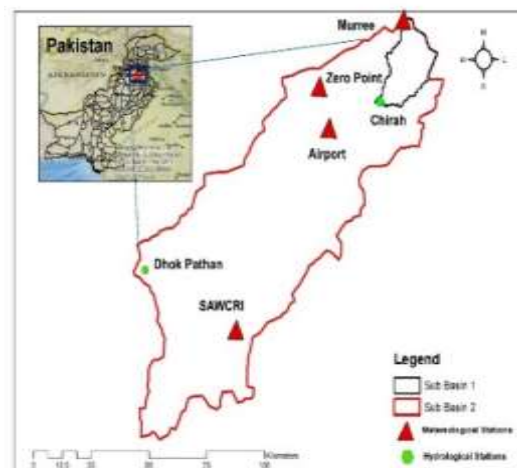


**Figure 17** Location map of the Soan basin and distribution of hydro-meteorological station

## Data sources

Daily precipitation data of 2 meteorological stations (Murree, Islamabad Zero Point) within the basin were obtained from the Pakistan Metrological Department (PMD), covering the period from 1983 to 2015. The monthly stream flow data from two hydrological gauging stations (Chirah, Dhok Pathan) were used in this study. It was obtained from the Water and Power Development Authority (WAPDA), covering the period from 1983 to 2015.

## Research Methodology

### Meteorological drought index

The SPI developed by McKee et al. (1993) was used in this study because of its popularity and easiness to use, as well as its effectiveness and suitability in this case study. Nalbantis and Tsakiris 2009 documented the meteorological drought at multiple time scales by using SPI with hydrological years. In the Soan Basin, a hydrological year is generally from October to the next September, thus the four time scales, i.e., October–December, October– March, October – June, and October –September (one complete hydrological year), were used in this study. Based on monthly precipitation, Nalbantis and Tsakiris (2009) presented the equation to calculate the cumulative precipitation depth  $R_{i,k}$ :

$$R_{i,k} = \sum_{j=1}^{3k} P_{i,j} \quad (1)$$

$$i = 1,2,3, \dots, n \quad j = 1,2, \dots, 12 \quad k = 1,2,3,4$$

Where  $P_{i,j}$  the monthly precipitation,  $i$  denotes the hydrological year,  $j$  is the month within that hydrological year, and the  $k=1$  is for October–

December, and  $k=4$  is for October –September. There are two equations, i.e., Eq. (2) and Eq. (3), to calculate SPI depending on precipitation distribution (Nalbantis and Tsakiris (2009): Eq. (2) was applied to the standardized precipitation volume, and Eq. (3) was applied to precipitation with a skewed probability distribution.

$$SPI_{i,k} = \frac{R_{i,k} - R_k}{S_k} \quad (2)$$

$$i = 1,2,3, \dots, n \quad k = 1,2,3,4$$

Where  $R_k$  and  $S_k$  are the mean and the standard deviation of the cumulative precipitation depths, respectively.

$$SPI_{i,k} = \frac{W_{i,k} - W_k}{S_k} \quad (3)$$

$$i = 1,2,3, \dots, n \quad k = 1,2,3,4$$

Where

$$W_{i,k} = \ln(R_{i,k}) \quad (4)$$

$$i = 1,2,3, \dots, n \quad k = 1,2,3,4$$

Was the natural logarithms of cumulative precipitation and  $W_k$  and  $S_k$  are the mean and the standard deviation of these logarithms, respectively.

The classification of meteorological droughts based on Nalbantis and Tsakiris (2009) was also used in this study: non-drought ( $SPI \geq 0$ ), mild drought ( $-1.0 \leq SPI < 0$ ), moderate drought ( $-1.5 \leq SPI < -1.0$ ), severe drought ( $-2.0 \leq SPI < -1.5$ ), extreme drought ( $SPI < -2.0$ ). Time series of long-term records (1960–2012) of monthly precipitation at each station was used as input to calculate SPI. Skewness coefficients of areal precipitation for all periods were calculated on original data series, as shown in Table 1.

**Table 10** Skewness coefficient of areal precipitation and their natural logarithms

Station	Calculation basis	Oct-Dec	Oct-Mar	Oct-Jun	Oct-Sep (full year)
Sub-Basin 1	Initial data	2.90740	0.59876	1.41006	1.89978
	Logarithms	0.39708	-0.21218	-0.12106	0.33679
	Final data	0.39708	-0.21218	-0.12106	0.33679
Sub-Basin 2	Initial data	1.17778	0.87367	0.79127	0.78938
	Logarithms	0.35647	0.11669	0.12089	-0.25187
	Final data	0.35647	0.11669	0.12089	-0.25187



## Hydrological drought index

Based on the SPI concepts, Nalbantis (2008) proposed the SDI which characterized hydrological droughts:

$$V_{i,k} = \sum_{j=1}^{3k} Q_{i,j} \quad (5)$$

$$i = 1,2,3, \dots, n \quad j = 1,2, \dots, 12 \quad k = 1,2,3,4$$

$$SDI_{i,k} = \frac{V_{i,k} - \bar{V}_k}{S_k} \quad (6)$$

$$i = 1,2,3, \dots, n \quad k = 1,2,3,4$$

Or

$$SDI_{i,k} = \frac{y_{i,k} - \bar{y}_k}{S_k} \quad (7)$$

$$i = 1,2,3, \dots, n \quad k = 1,2,3,4$$

$$y_{i,k} = \ln(V_{i,k}) \quad (8)$$

$$i = 1,2,3, \dots, n \quad k = 1,2,3,4$$

Where  $V_{i,k}$  is the cumulative streamflow volume for the  $i$ th hydrological year and the  $k$ th reference period;  $\bar{V}_k$  and  $S_k$  are the mean and the standard deviation of cumulative streamflow volumes of reference period  $k$  respectively. Where  $y_{i,k}$  is the log transformation of streamflow volume.

The Skewness coefficients of the raw streamflow, its natural logarithms, and the final choice dataset are shown in Table 2. Both of two Sub-Basins showed a skewed distribution, so a natural logarithm transformation was needed to estimate SDI with Eq. (7).

## Results and discussion

### Meteorological droughts

The meteorological drought index SPI, based on four time scales, are shown in

Fig. 2 for two sub-Basin. It is clear that the frequency of drought events has an increasing

trend, especially after 1999 when SPIs were always negative. These results agreed with the results previously reported droughts in Pakistan. In addition, the drought events were not the same from different computing time scales: The significant discrepancies were observed only when compared between the 3-month time scale (October–December) and the 6-month time scale (October– March), and between the 6-month time scale (October– March) and the 9-month time scale (October –June). Decent agreements were obtained between the 9-month time scale (October –June) and the hydrological year (October –September). Considering the 3-month time scale and the 12-month time scale, severe drought event ( $-2.0 \leq \text{SPI} < -1.5$ ) occurred more frequently around each station in the case of the 3-month time scale than the 12-month time scale. In addition, the fluctuation range of the 3-month time scale was bigger than those of other time scales, and the range of the 12-month time scale was the smallest.

The synthesis result indicated that the drought event state varied with the increasing of SPI time scales, generally a decline trend. It is because that computation of the SPI in the 12-month time scale aggregated total precipitation from October to September, which included both dry and wet seasons. However, SPI-3 was only accounted for the sum of precipitation from March to May, which is normally dry season in the study basin. Figure 3 shows the meteorological drought severity of two stations during 1983–2015 based on the 12-month time scale. It is found that year 1999 to 2001 was the driest year. It is also found that the meteorological drought severity was increasing in the past 33 years; the severity of meteorological droughts has the most significant trend in the downstream Sub-Basin 2.

**Table 2** Skewness coefficient of streamflow, and their natural logarithms

Station	Calculation basis	Oct-Dec	Oct-Mar	Oct-Jun	Oct-Sep (full year)
Sub-Basin 1	Initial data	1.15789	0.31284	0.46809	0.42133
	Logarithms	-0.0075	-0.77701	-.06512	0.13828
	Final data	-0.0075	-0.77701	-.06512	0.13828
Sub-Basin 2	Initial data	0.85123	0.38310	0.09603	0.26952
	Logarithms	-0.9387	-0.37564	0.52738	-0.15183
	Final data	0.85123	-0.37564	0.09603	-0.15183

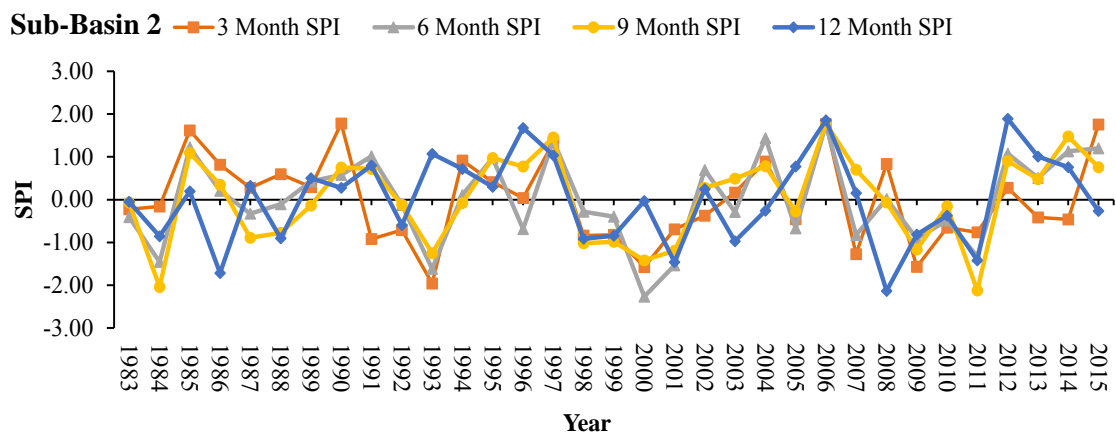
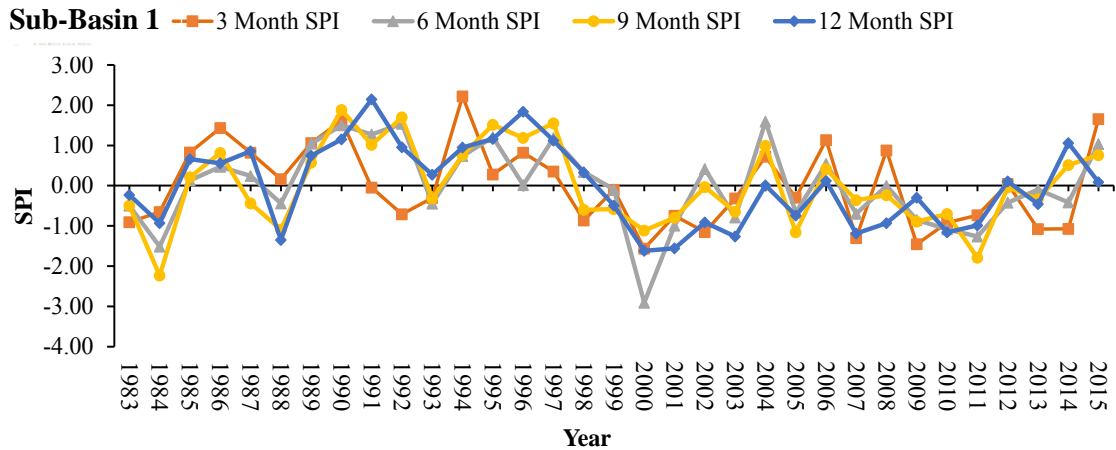


**Figure 18** Temporal variation of meteorological drought periods during 1983–2015

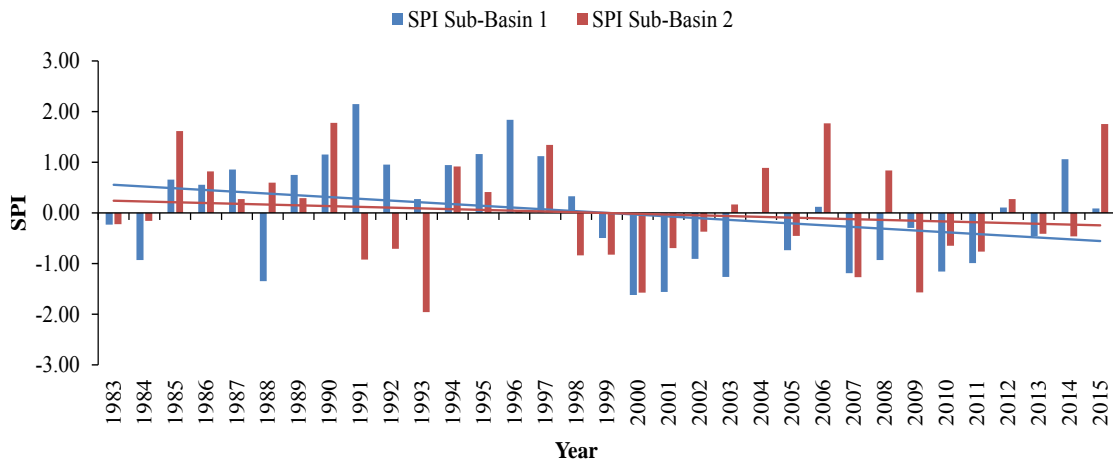


**Figure 19** Meteorological drought severity at two stations during 1983–2015 based on 12-month SPI

The Mann-Kendall method (Fu et al. 2004) was used to analyze the tendency of the meteorological drought numbers of months within a year at Sub-Basin 1 and Sub-Basin 2, based on the 12-month time scale (Fig. 4). Overall, it showed an increasing trend during

1983–2015 for two Sub-basins. However, spatial differences can be observed from upstream to downstream: The Mann-Kendall statistic Z-value was 1.78 at upstream Sub-Basin 1, and 1.71 at downstream Sub-Basin 2.

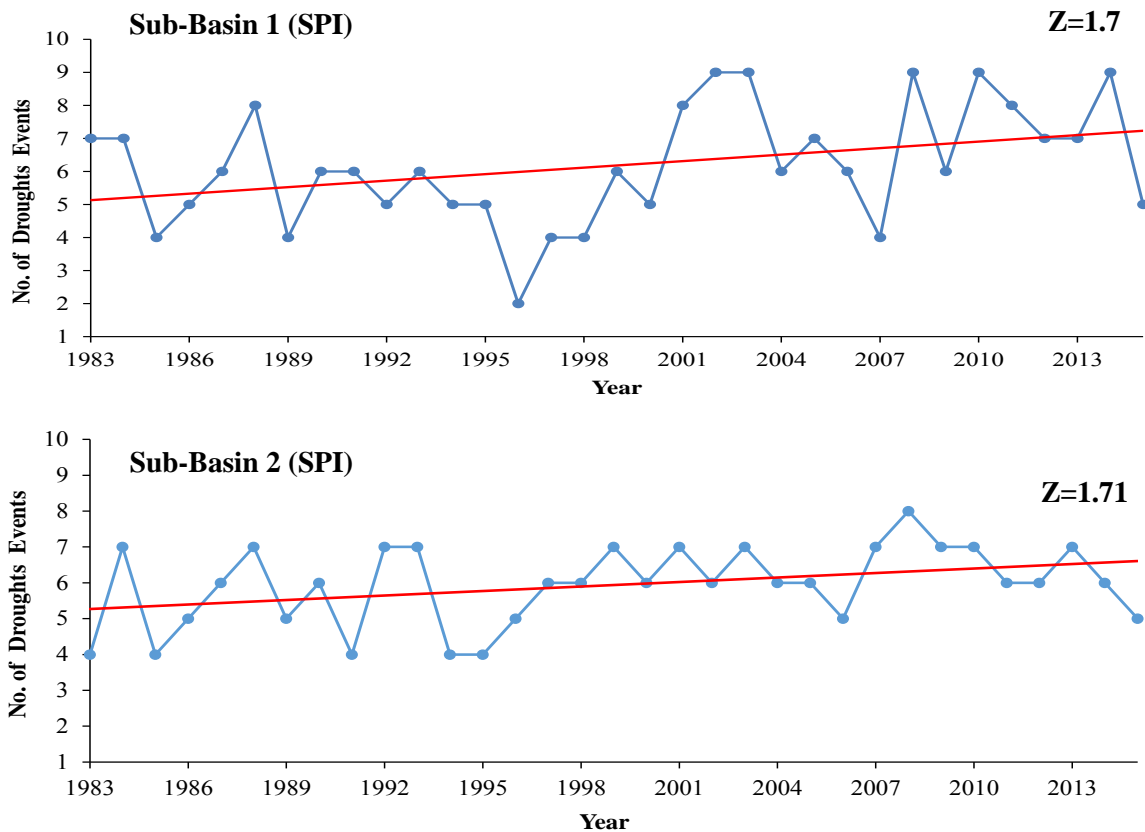
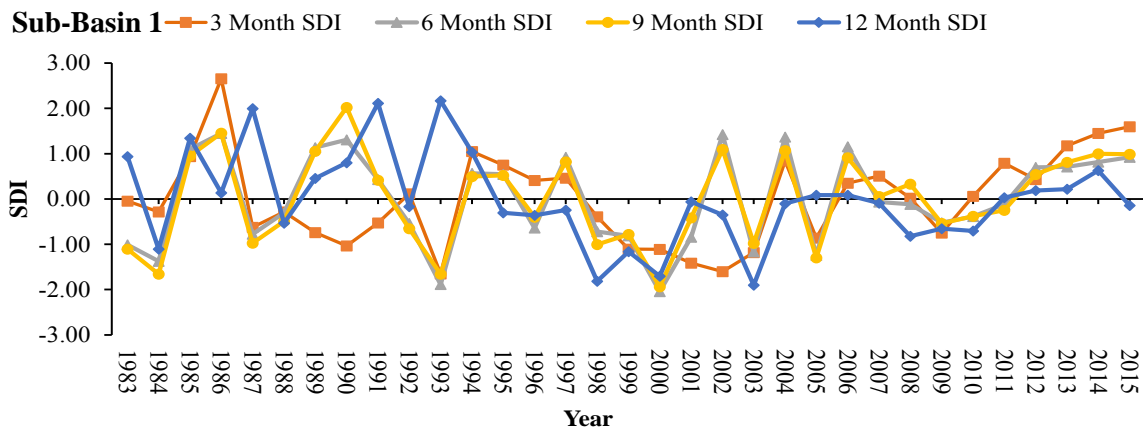


**Figure 20** Meteorological drought number of months at both Sub-Basins during 1983–2015 based on 12-month SPI

### Hydrological droughts

The SDI series for different time scales are shown in Fig. 5. It indicated that the hydrological drought occurrences had an obvious trend of increasing over the last three decades. There were more drought events in the case of the 3-month time scale than in the 12-month time scale. Figure 6 shows the hydrological drought severity of two sub-Basins during 1983–2015, based on the 12-month time scale. It was found that the

hydrological drought severity was increasing in Soan River basin. Figure 7 presents the numbers of month with hydrological drought events in a year. As a whole, it is clear that frequency (e.g., the numbers of months with a drought event) of hydrological droughts was increasing during 1983–2015 in the Soan basin. The downstream Sub-Basin 2 showed the most statistically significant trend with a Z-value of 1.83. In contrast, the trend was statistically insignificant at upstream Sub-Basin 1, although it still showed an increasing trend.



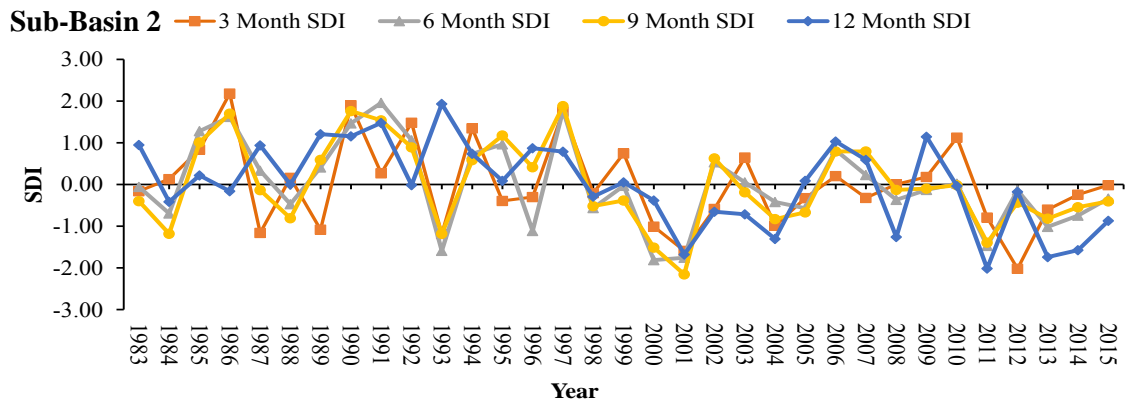


**Figure 21** SDI series for different reference periods during 1983–2015

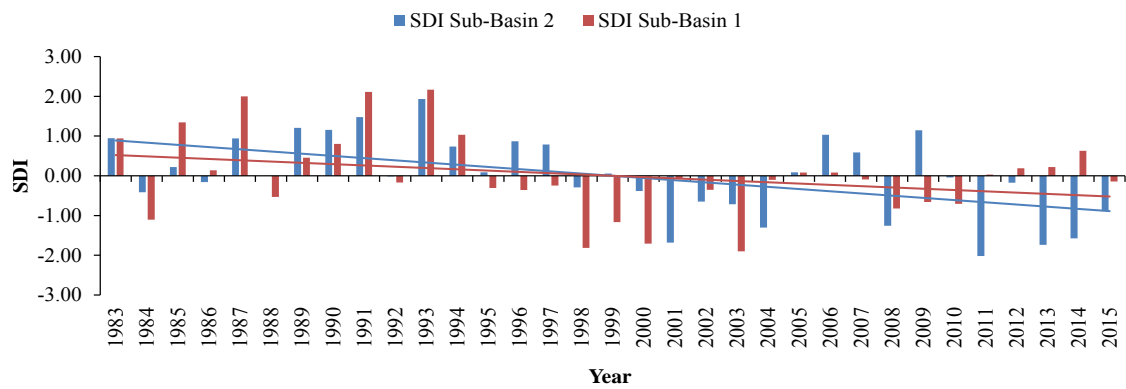


**Figure 22** Hydrological drought severity at two stations during 1983–2015 based on 12-month SDI

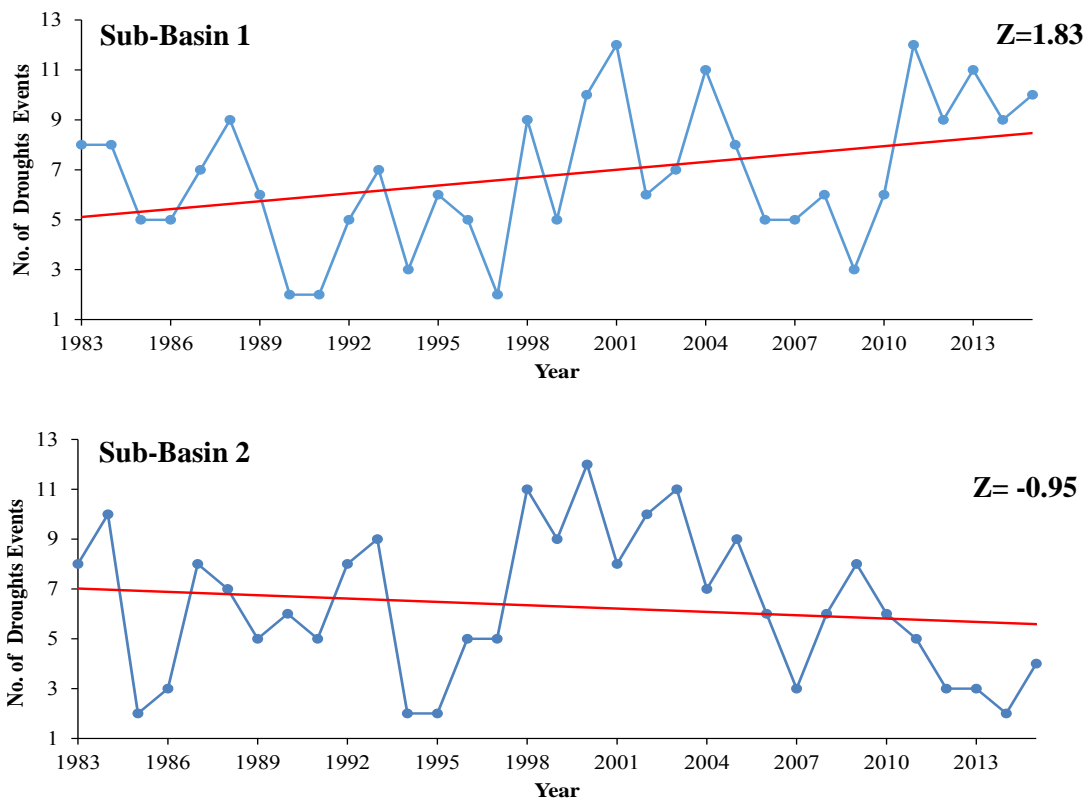


**Figure 23** Hydrological drought number of months at both Sub-Basins during 1983–2015 based on 12-month SDI

## Relationship between meteorological and hydrological droughts

### Establish regression function between SPI and SDI

From the regression coefficient (slope) and the determination coefficient ( $R^2$ ) of the linear regression equations (Table 3), it can be found that the correlations between SPI and SDI become stronger with the time scale increasing. The determination coefficients of the 6-month time scale and the 9-month time scale were higher than those of the other two time scales. For example, it was 0.4572 at the Sub-Basin 1 for the 6-month time scale. In addition, the correlation between SPI and SDI generally stronger at upstream. For example, the determination coefficients at the 9-month time scale were 0.6651, and 0.6397 at the Sub-Basin 1 and the Sub-Basin 2, respectively. Figure 8 shows the regression lines and the associated data points, which could be used to forecast the hydrological droughts based on the meteorological droughts. The linear regression models for the 6-month time scale were the best at all two stations.

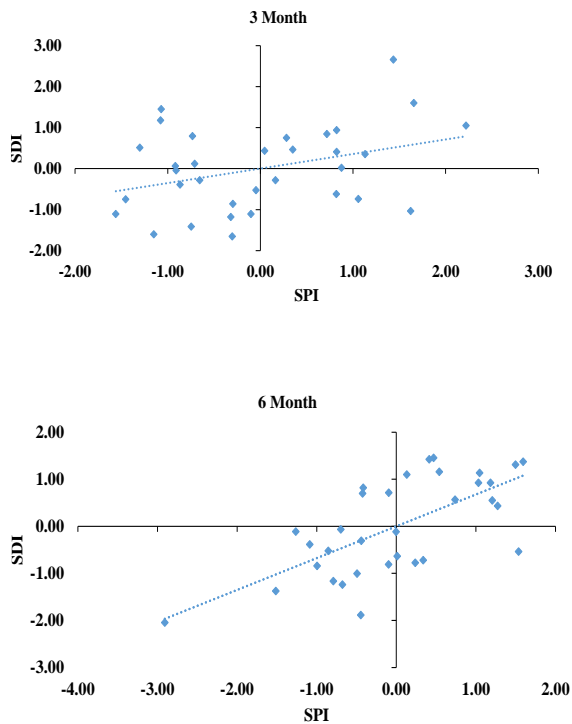
**Table 11** Regression coefficient (a) & determination coefficient ( $R^2$ ) of linear regression equations of SDI on SPI

K		Sub-Basin 1	Sub-Basin 2
October-December	a	0.3537	0.3761
	$R^2$	0.1248	0.1414
October-March	a	0.6759	0.6383
	$R^2$	0.4572	0.4076
October-June	a	0.6651	0.6397
	$R^2$	0.4424	0.4093
October-September	a	0.5469	0.4588
	$R^2$	0.2991	0.2106

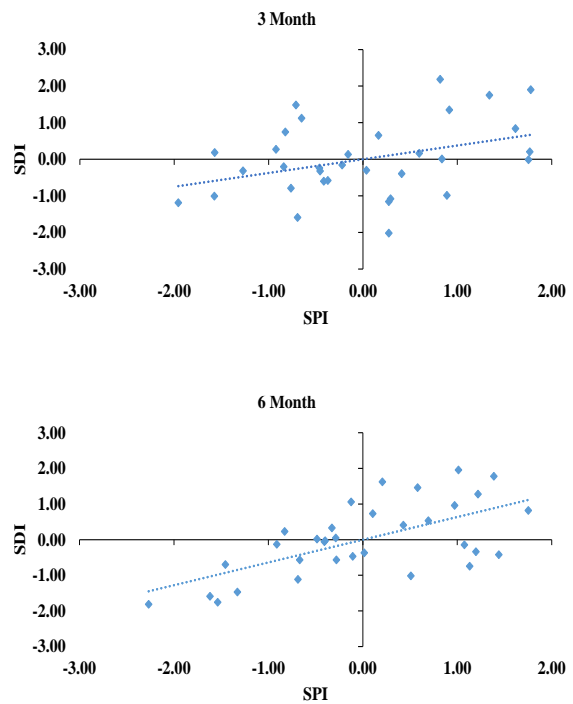
### Identification of lag time between the drought indices

To better identify the correlation between SPI and SDI, a moving average was carried out for multiple time scales (Fig. 10). Results indicated that the variations of SPI and SDI were similar during 1983–2015, and the differences between them do exist. For example, the correlation was weak at Sub-Basin 2 at 12-Month time scale. Generally speaking, the relationship between SPI and SDI was the strongest at upstream Sub-Basin 1. As a whole, the SPI was exceeding 1 month than SDI for the 3-month scale and for the 12-

#### Sub-basin 1



#### Sub-basin 1



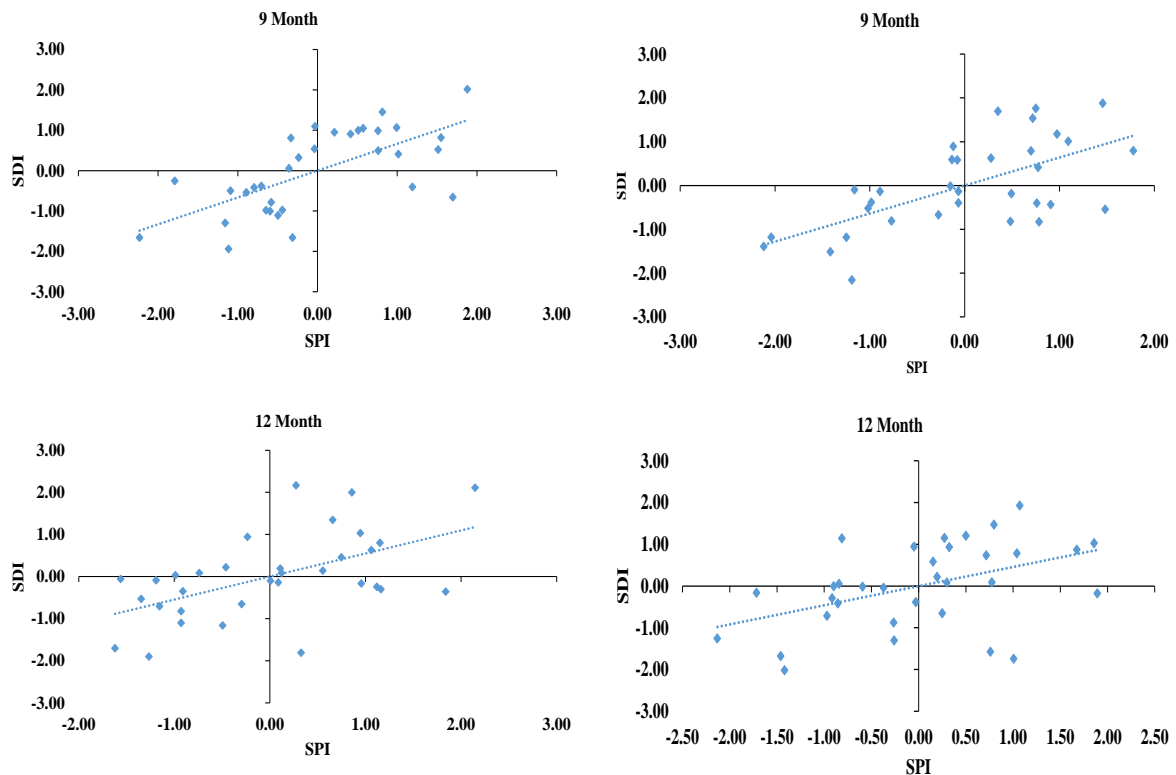


**Figure 24** Linear regression of SDI on SPI for each time scale

month scale at every station. The correlation coefficient was 0.6651 at Sub-Basin 1. For the 6-month and 9-month time scales, SDI was 2 months lagging than SPI. This timeframe of lagging time was consistent with a previous study (Tabrizi et al. 2010).

### The differences between SPI and SDI

The differences between SPI and SDI have increased during the last 33 years. The main reason was due to the decreases of precipitation and runoff, which is caused by natural climate change and variability, as well as human activities (He et al. 2015). Climate change and variability included, but is not limited to, the variation of precipitation, temperature, and potential evapotranspiration (Fu et al. 2007a), and human activity has many different aspects, such as, increased water diversion, expanded irrigation area strengthened, changed land use/cover, and soil and water conservation (Fu et al. 2004).

The precipitation had a decreasing trend during the years 1983–2015 (Fig. 9). For example, the average annual precipitation decreased from 2371.10 mm to 1385.50 mm during 1996–2007. The decreased magnitudes of precipitation were larger in Sub-Basin 1, the upper stream of the

Soan River Basin, than that in Sub-Basin 2, the lower reach. Simultaneously, the runoff coefficient also had a decline trend at both Sub-Basins expect some large values which are because of floods (Fig. 12) for example, the mean runoff coefficient was 0.94 during 1983–1992, but 0.56 during 1995–2005 at Sub-Basin 1. The annual runoff depth also had an obviously declining trend during 1983–2015 (Fig. 11). For example, the mean annual runoff was 105.44 mm during 1983–1993, while that was 32.00 mm during 1993–2003

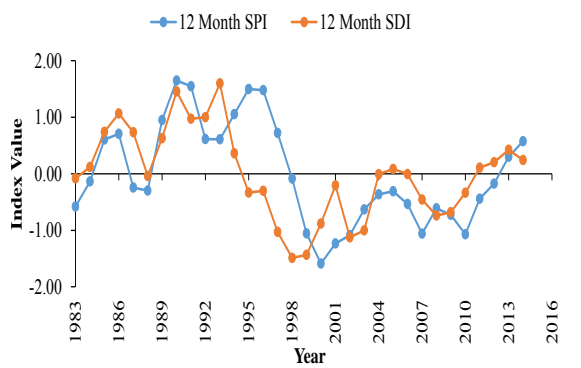
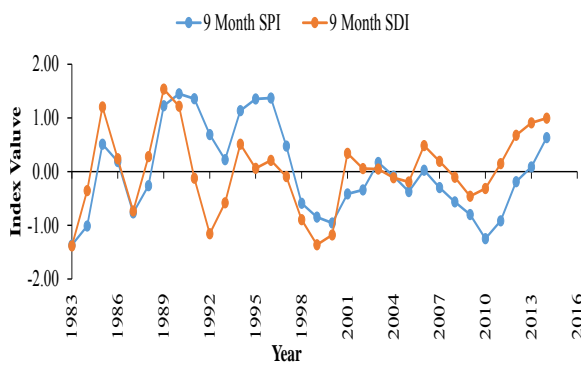
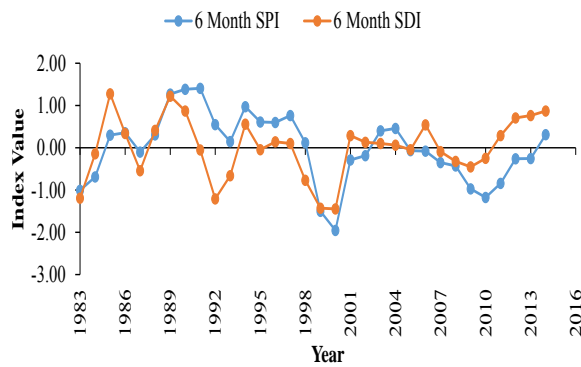
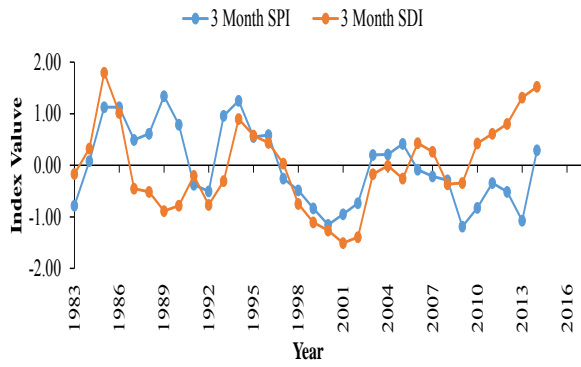
### Conclusions

The frequencies of meteorological and hydrological droughts have shown an increasing trend during the last 3 decade in the Soan River Basin. Meteorological moderate drought events and hydrological drought events occurred more frequently in the upper part of the Soan River Basin based on the 12-month time scale.

The regression coefficients of a linear regression between SPI and SDI indicated that with the time scale increasing, the regression coefficients became stronger till 9-Month. The reason for the differences between meteorological and hydrological droughts included, but were



### Sub-Basin 1



### Sub-Basin 2

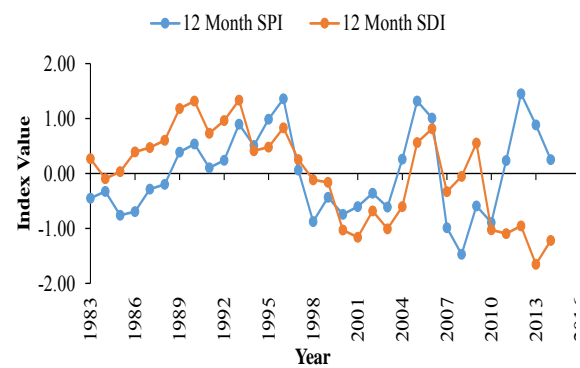
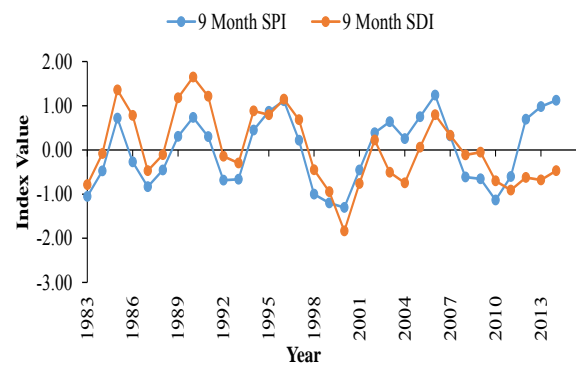
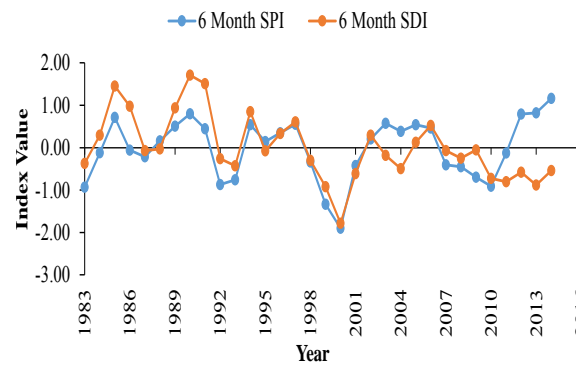
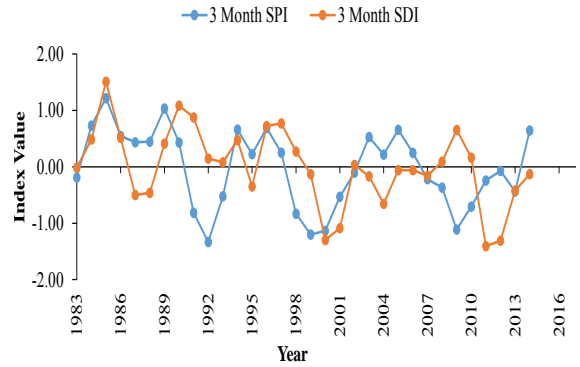


**Figure 9** The moving average of SPI and SDI at the study stations for different time scales

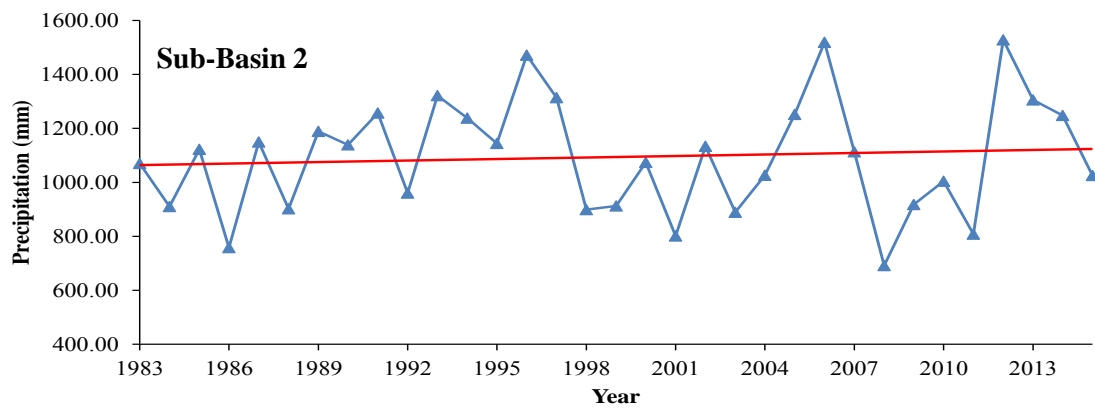
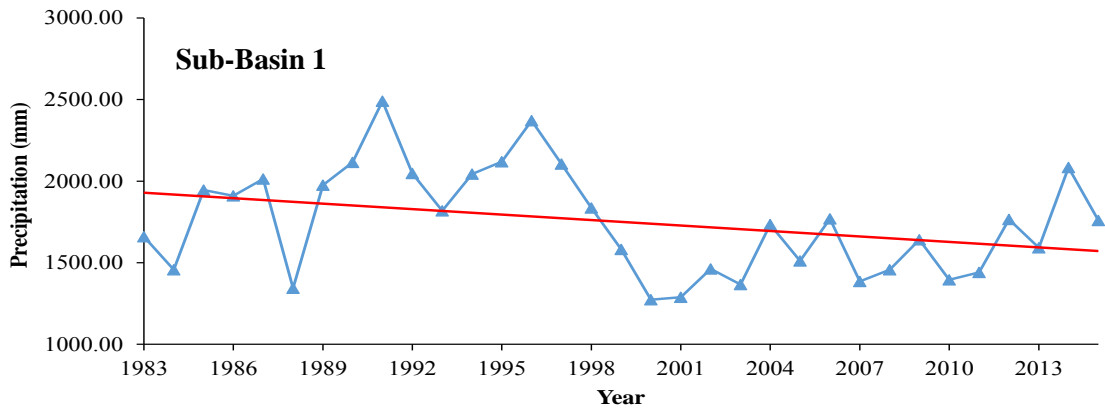


**Figure 10** Annual precipitation changing trend during the years 1983–2015

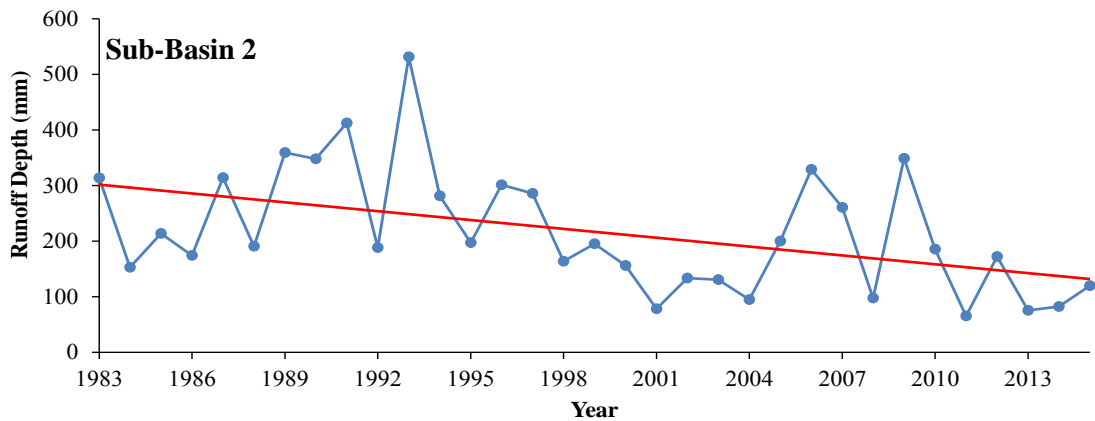
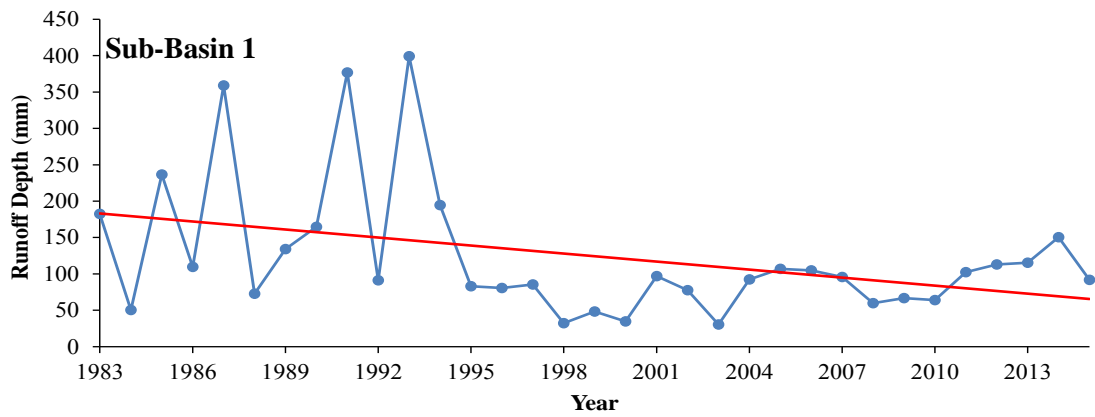


**Figure 11** Annual runoff depth during the years 1983–2015

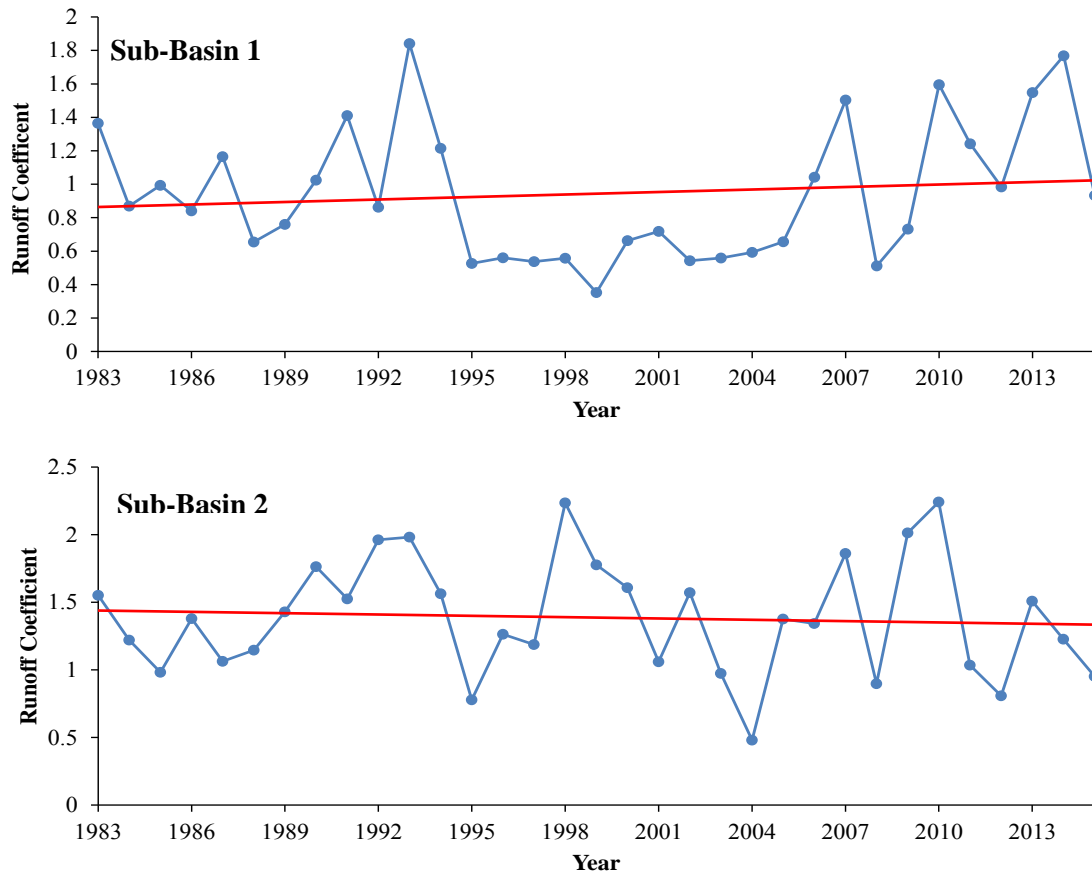


**Figure 12** The runoff coefficient during the years 1983–2

not limited to, climate change and variability, human activities, and land use/ cover changes.

This study investigated the relationships between the meteorological and hydrological drought events with SPI and SDI, and a simple linear function between them was built. The occurrence of hydrological drought events usually lagged meteorological droughts for 1–3 months depending on the calculated time scale and stations. The differences between meteorological drought and hydrological drought became larger due to climate change and human activities. One of our next step studies will explore the impacts of climate change on hydrological drought at basin scale. This relationship between meteorological and hydrological droughts presented in this study can be used for the long-term forecasting of droughts and early warning water resources management in practice.

#### Acknowledgements

Meteorological data was provided by Pakistan Meteorological Department (PMD) and Hydrological data was provided by the Water and

Power Development Authority (WAPDA), Pakistan. Their help is greatly appreciated.

#### References

- Ashfaq, M., Razzaq, A., & Hassan, S. (2015). Factors affecting the economic losses due to livestock diseases: a case study of district Faisalabad. *Pakistan journal of agricultural sciences*, 52(2).
- Ashraf, M., & Routray, J. K. (2015). Spatio-temporal characteristics of precipitation and drought in Balochistan Province, Pakistan. *Natural Hazards*, 77(1), 229-254.
- Cheraghalizadeh, M., Ghameshlou, A. N., Bazrafshan, J., & Bazrafshan, O. (2018). A copula-based joint meteorological–hydrological drought index in a humid region (Kasilian basin, North Iran). *Arabian Journal of Geosciences*, 11(12), 300.
- Dai, A. (2011). Characteristics and trends in various forms of the Palmer Drought Severity Index during 1900–2008. *Journal of Geophysical Research: Atmospheres*, 116(D12).

- Edossa, D. C., Babel, M. S., & Gupta, A. D. (2010). Drought analysis in the Awash river basin, Ethiopia. *Water resources management*, 24(7), 1441-1460.
- Fu, Q., Johanson, C. M., Warren, S. G., & Seidel, D. J. (2004). Contribution of stratospheric cooling to satellite-inferred tropospheric temperature trends. *Nature*, 429(6987), 55-58.
- Gumus, V., & Algin, H. M. (2017). Meteorological and hydrological drought analysis of the Seyhan– Ceyhan River Basins, Turkey. *Meteorological Applications*, 24(1), 62-73.
- Haslinger, K., Koffler, D., Schöner, W., & Laaha, G. (2014). Exploring the link between meteorological drought and streamflow: Effects of climate-catchment interaction. *Water Resources Research*, 50(3), 2468-2487.
- Hisdal, H., & Tallaksen, L. M. (2003). Estimation of regional meteorological and hydrological drought characteristics: a case study for Denmark. *Journal of Hydrology*, 281(3), 230-247.
- Huang, S., Huang, Q., Leng, G., & Liu, S. (2016). A nonparametric multivariate standardized drought index for characterizing socioeconomic drought: A case study in the Heihe River Basin. *Journal of Hydrology*, 542, 875-883.
- Huang, S., Li, P., Huang, Q., Leng, G., Hou, B., & Ma, L. (2017). The propagation from meteorological to hydrological drought and its potential influence factors. *Journal of Hydrology*, 547, 184-195.
- Jörg-Hess, S., Kempf, S. B., Fundel, F., & Zappa, M. (2015). The benefit of climatological and calibrated reforecast data for simulating hydrological droughts in Switzerland. *Meteorological Applications*, 22(3), 444-458.
- Joseph, S., Sahai, A. K., & Goswami, B. N. (2009). Eastward propagating MJO during boreal summer and Indian monsoon droughts. *Climate Dynamics*, 32(7-8), 1139-1153.
- Markovic, D., & Koch, M. (2005). Wavelet and scaling analysis of monthly precipitation extremes in Germany in the 20th century: Interannual to interdecadal oscillations and the North Atlantic Oscillation influence. *Water Resources Research*, 41(9).
- McKee, T. B., Doesken, N. J., & Kleist, J. (1993, January). The relationship of drought frequency and duration to time scales. In *Proceedings of the 8th Conference on Applied Climatology* (Vol. 17, No. 22, pp. 179-183).
- Nalbantis, I. (2008). Evaluation of a hydrological drought index. *European Water*, 23(24), 67-77.
- Nalbantis, I., & Tsakiris, G. (2009). Assessment of hydrological drought revisited. *Water Resources Management*, 23(5), 881-897.
- Sheffield, J., Wood, E. F., & Roderick, M. L. (2012). Little change in global drought over the past 60 years. *Nature*, 491(7424), 435-438.
- Sönmez, F. K., Koemuescue, A. U., Erkan, A., & Turgu, E. (2005). An analysis of spatial and temporal dimension of drought vulnerability in Turkey using the standardized precipitation index. *Natural Hazards*, 35(2), 243-264.
- Tabrizi, A. A., Khalili, D., Kamgar-Haghighi, A. A., & Zand-Parsa, S. (2010). Utilization of time-based meteorological droughts to investigate occurrence of streamflow droughts. *Water resources management*, 24(15), 4287-4306.
- Tijdeman, E., Hannaford, J., & Stahl, K. (2018). Human influences on streamflow drought characteristics in England and Wales. *Hydrology and Earth System Sciences*, 22(2), 1051-1064.
- Zhu, J., Zhou, L., & Huang, S. (2018). A hybrid drought index combining meteorological, hydrological, and agricultural information based on the entropy weight theory. *Arabian Journal of Geosciences*, 11(5), 91.

## Assessing, Mapping and Optimizing the Potential Dam Site Selection Using ArcGIS

Muhammad Sohail Jameel<sup>1</sup>, Muhammad Farjad Sami<sup>1</sup>, Afra Siab khattak<sup>2</sup>, Ali Raza<sup>3</sup>, Sohail Iqbal<sup>4</sup>, Umer Shahzad<sup>2</sup>

<sup>1</sup> Department of Civil Engineering, Muslim Youth University Islamabad, 47000 Pakistan

<sup>2</sup> Department of Civil Engineering, Abasyn University, Islamabad, 45710, Pakistan.

<sup>3</sup> Department of Civil Engineering, Pakistan Institute of Engineering and Technology Multan, 66000, Pakistan

<sup>4</sup> Department of Civil Engineering, University of Engineering and Technology, Taxila 47050, Pakistan

Corresponding author email: [sohailjamil10@yahoo.com](mailto:sohailjamil10@yahoo.com)

**Abstract:** Dams are the fundamental structures for the purpose of storing water and managing flash floods. Kalam in Pakistan (study area) has a hilly terrain with adequate amount of rainfall so that greater amount of water is available for utilization in various resources. In this research by using ArcGIS suitable Dam site would be selected. The project has progressed to be completed by using ArcGIS and Arc Hydro software. Further tools that are used in the project are Google Earth, Arc Scene and DIDAS software. The selected area has a total of 14 catchment areas with the addition of various factors i.e. population, Digital Elevation Model (DEM) and precipitation; 4 catchment areas have been determined in the selected area. The best suitable site among these 4 catchments is selected. In this study only precipitation data are taken into consideration while neglecting the flow of river Kalam. From the past study of precipitation showed that Matiltan site receive the maximum amount of precipitation from 2007 to 2017 at an average of 1.38m. After Matiltan the Falak Sar and Sharang Bar gets the maximum amount of precipitation, 0.9668m, 0.9744m respectively. While in case of run off, it can be seen that, Falak Sar has maximum run off. Whereas Derah Banal and Matiltan is on 2<sup>nd</sup> and 3<sup>rd</sup> number respectively. The selected site is capable of meeting all our objectives i.e. it is located far away from populated areas, can help manage flash floods, store water for agricultural as well as hydroelectric purposes and a road link is available near the site which will prove economical if the construction of the dam is carried out. The result of the study revealed that Falak Sar is the best suitable site among all four sites.

**Keywords:** ArcGIS, Arc Hydro, DEM, Kalam, Shape file, Dam, Population, Precipitation, Slope.

### Introduction

The importance of water is increasing because of the increasing population and global warming in the World. Pakistan is an agricultural country and to guarantee food security the demand for increased agricultural production has been growing. In this way, the need to construct dams has been developing limitlessly to meet the requirement of water supply, irrigation and hydroelectric energy. Different stages of dam construction, that is reconnaissance, planning and design stages require absolute, complete and up to the minute details regarding terrain surface and relief [1]. Delineation of terrain parameters like drainage system, slope and precipitation etc. are required frequently in composition of plan for development and conservation of natural resources. Recent advance in remote sensing and GIS are proving to be valuable tools in many natural resource applications such as hydrological modelling of terrain for water

harvesting, mineral exploration and dam site selection. Extensive exertion has been dedicated as of late about the capability of these techniques in assisting engineers in dam designing by permitting effective, speedy and affordable data collection and processing and analysing terrain surface contrasted with conventional design [2] [3].

The purpose of geographic information system is mainly working with geographic data and maps. ArcGIS is used to assemble geographical information, creating maps, reviewing mapped data and sharing and finding geographic information [4] [5]. Water, which is the most basic need of human life, is shrinking in quantity on daily basis. It is one of the resources that cannot be generated but only be preserved. In future water shortage will be one of the greatest difficulties in the World. Apart from water scarcity, water contamination is also a major threat to the modern world [6] [7].

In excess of 80 percent of water in Pakistan is viewed as hazardous and unsafe. Currently, 16 million individuals in Pakistan have no other choice than collecting unsafe water for drinking and cleaning purposes, prompting massive amounts of water-borne malady. Accessible water per capita has dropped from 5,600 to 903 cubic meters, as of 2016. At the present dimensions of utilization, this number is expected to drop to 500 cubic meters per person in the coming years. With 60% of Pakistan's population specifically engaged with agriculture, up to 95% of Pakistan's water is utilized in agricultural purposes. However, it is assessed that half of the water directed for agricultural use is lost, because of defective irrigation system, flawed waterways or canals, and leaking pipes. Many researchers are used GIS in their research work. Jozaghi et. al. [8] presents a comparative analysis of TOPSIS and AHP in the context of decision-making using GIS for dam site selection. Both methods were applied for selection of optimal sites for dams in the Sistani and Baluchistan province of Iran. The results show that the TOPSIS method is better suited to the problem of dam site selection for this study area. Actual locations of dams constructed in the area were used to verify the results of both methods. Noori, et. al. [9] studied the appropriate areas of dam site selection for water management. The areas were identified using remote sensing, geographic information system (GIS), and multi-criteria decision-making techniques. In addition, the proposed method of site suitability was evaluated by comparing it with the traditional analytic hierarchy process (AHP). The results of this study revealed that fuzzy logic is more accurate than AHP. Njiru and Siriba [10] study aimed to investigate hydrological information for dam site selection by integrating GIS with AHP Multi-Criteria Decision Analysis to establish hydrologic characteristics of the region suitable for a dam construction. A final suitability map was established showing four possible sites of highly suitable areas for dam construction. Ajibade et. al. [11] study the potential sites for construction of dams in Imo State, Nigeria, have been identified by using Geographical Information System (GIS) and Remote Sensing Techniques (RST) which were integrated with fuzzy logic to achieve the study objectives. The results of that study revealed that fuzzy members for all the factors were combined using the fuzzy overlay technique to produce the suitable dam site

selection map. Yildirim et. al. [13] In this study, the Geographical Information System (GIS) used with Multi Criteria Decision Making (MCDM) techniques is a useful tool for creating a model. One such MCDM is the Spatial-integrated Technique for Order Preference by Similarity to Ideal Solution (TOPSIS). TOPSIS was applied to integrate environmental, economic and sociological sensitivity into determine alternative solid waste landfill sites for Bursa Province, Turkey. Using the data obtained by comparing the geo-statistics, six of the most suitable landfill areas were determined. Adham and NabaSaiy [14] studied the Potential RWH sites were identified using a GIS-based suitability model, created with Model Builder in ArcGIS. The suitability model combined with biophysical factors i.e. slope, runoff depth, land use, soil texture, and stream order. The result of study revealed that ArcGIS was a very useful tool for integrating diverse information to find suitable sites for dams.

Globally ArcGIS is used for dam site selection. In Pakistan, a single study was done on Gilgit Baltistan area for the selection of potential dam sites. Kalam is a region with very high potential for dam sites, because of its natural terrain and environmental factors like high amount of precipitation and snow. As this area was not focused by any researcher, analysis was carried out using ArcGIS and Arc Hydro to come up with a suitable dam site in this area.

Following are the objectives of our project:

- To find several dam sites in our study area using ArcGIS.
- To find best suitable site from different sites found in our area based on population and water quantity.

### **Research Significance**

Water is the most basic necessity of human life and water scarcity itself is a major problem in the modern world. The demand for water is increasing at a rate faster than population growth. In order to overcome this problem, building dams is one of various solutions. But building dams is not an easy task as a large amount of money, people, land and many other stake holders are involved. Moreover, the selection of dam site is a cumbersome and lengthy process using traditional methods as a large number of factors have to be considered. ArcGIS software could be used for selection of a suitable dam site in the study area considering that it saves time and



money. Moreover, it is user friendly, convenient, accurate in nature, and various deciding factors could be considered simultaneously.

### Research Methodology

In this study three type data collection DEM, Shape file and precipitation. DEM collect from earth explorer which show area elevation. shape file show admin border which on national, provisional, division, district tehsil and union council level. The data were collected union council level bonders use for our study area. Precipitation data which we used from CHRS (Center for Hydrometeorology and Remote Sensing) portal data. Then we combine shape file and DEM with the help of dedas software output result in the foam of mosaic layer, that mosaic layer use in ArcGIS. Then Arc Hydro use to find drainage, accumulation and catchment. Figure 1 shows the steps involved during this research.

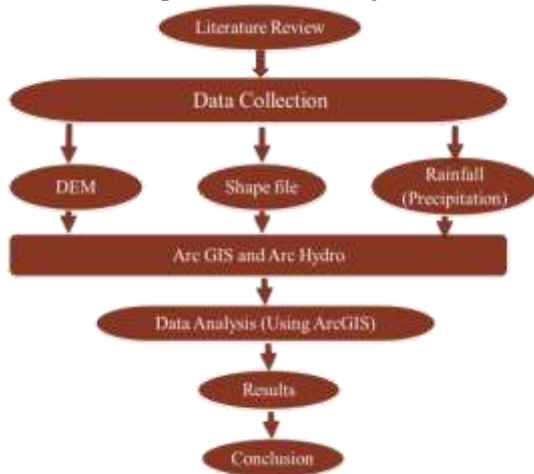


**Figure. 1** Flow chart of Research methodology

These are the following steps of Arc Hydro GIS The following processes were carried in order to achieve watersheds:

1. Fill sinks
2. Flow direction
3. Flow accumulation
4. Stream definition
5. Stream segmentation
6. Catchment grid delineation
7. Catchment polygon processing
8. Drainage line processing
9. Adjoint catchment processing
10. Drainage point processing
11. Batch watershed delineation

By getting batch watershed delineation ArcGIS is performed step by step which is given below to determine the suitable area for dam construction

1. DEM (Digital Elevation Model)
2. Shape File
3. Mosaic File
4. Google Earth and Contours
5. Slope and Arc Scene
6. Slope and Hill shade
7. Precipitation

### Results and Discussions

The steps which is performed in ArcGIS is explained below and the output which is obtained is shown in figures.

#### DEM (Digital Elevation Model)

The 2 DEMs is used to study area because study area was not compiled totally in one DEM. Their pictures are shown in Figure 2 as shown below. The colour variation shows the difference between elevation and depression, Black colour: Depression, White colour: Elevation.

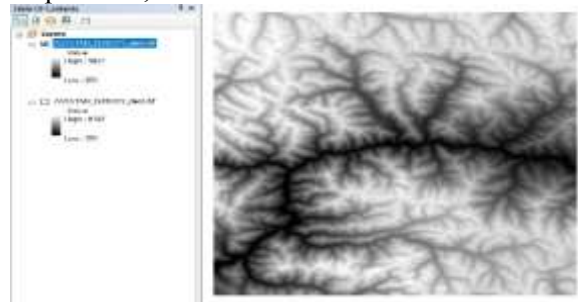


**Figure. 2** Study area which different color

#### Shape File

Shape file is the boundary of a country, province, division, district, tehsil or union council. In this study area only the union council (UC) level shape file is recommended. UC level map of the country and selected study area i.e. Kalam area from that map which is shown in Figure 3 with blue color in figure.

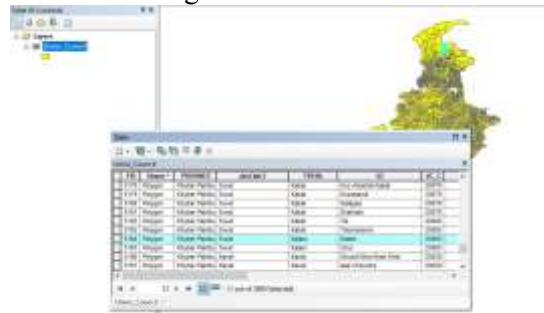


**Figure 3.** Under study area with blue color

#### Mosaic File

It is a command that merges two DEMs into one DEM. It can be done in ArcGIS as well as

ADIDAS software. In this study two DEMs merged into one DEM using ADIDAS software. After merging the two DEM, applied the shape file and selected only the area of Kalam as shown in Figure 4.

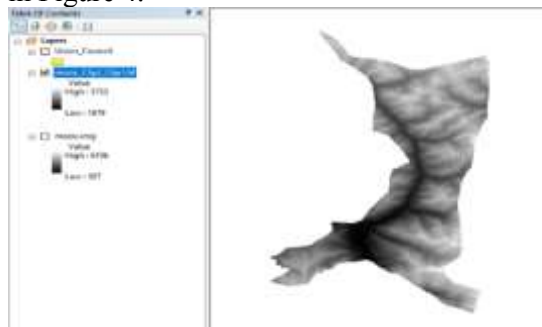


**Figure 4.** Mosaic File Study area

### Fill Sinks and Flow Direction

This function shows the depression in the ground where water can be trapped. This function can be applied as follows: the command was used to selecting Arc Hydro tool bar and selecting Terrain Pre-processing Data + Manipulation + Fill Sinks.

The picture which is obtained on ArcGIS desktop is shown in Figure 5 and 6 of our selected study area.



**Figure 5.** Picture of Fill sink

This command was used selecting Arc Hydro tool bar and selecting Terrain Pre-processing + Flow Direction. This function shows the direction of flow in a grid.

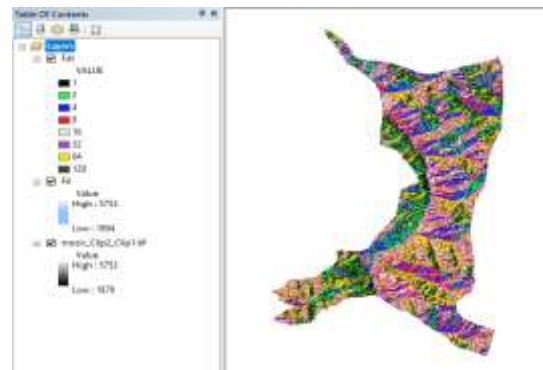


**Figure 6.** Picture of flow direction

### Flow Accumulation and Stream Definition

Flow accumulation shows that the accumulation of water upstream is less as compared to the accumulation of flow downstream. Flow accumulation is obtained by selecting the Arc Hydro toolbar, then selecting Terrain processing + Flow Accumulation.

Stream definition shows a proper streamline where flow is accumulated and starts running. This command required selecting Arc Hydro toolbar, then selecting Terrain processing + Stream Definition.

### Stream Segmentation and Catchment Grid Delineation

Stream segmentation allows assigning the same unique value to stream cells located within the same stream segment. Segments are defined as either head stream segments or segments located between two segment junctions.

Stream segmentation is obtained by selecting Arc Hydro toolbar, then selecting Terrain Pre-processing + Stream Segmentation.

Catchment grid delineation identifies the exact boundaries between different catchment areas. Catchment grid delineation is obtained by selecting Arc Hydro toolbar, then selecting Terrain Pre-processing + Catchment Grid Delineation. Figure 7 show the Catchment Grid Delineation of our selected study area.

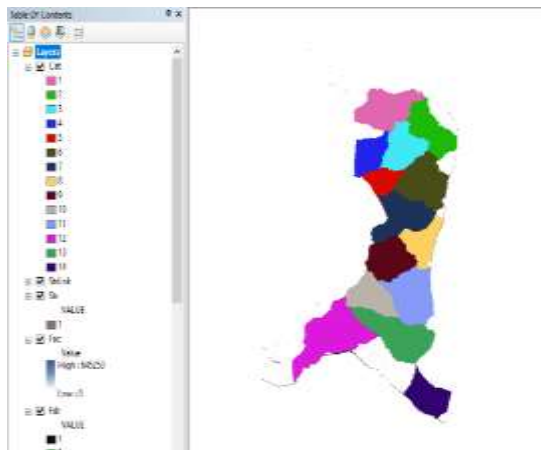


**Figure 7.** picture of Catchment Grid Delineation  
**Catchment Polygon Processing and Drainage Line Processing**

Catchment Polygon Processing converts a catchment grid into a catchment polygon feature with visible boundaries. This can be obtained by selecting Arc Hydro toolbar, then selecting Terrain Pre-processing + Catchment Polygon Processing. Drainage Line Processing shows the mainstream line in Kalam area. Drainage Line Processing was obtained by selecting Arc Hydro toolbar, then selecting Terrain Pre-processing + Drainage Line Processing. Figure 8 show the picture of drainage line process with yellow line of our selected area.



**Figure 8.** picture of drainage line with yellow line

### **Adjoint Catchment Processing and Drainage Point Processing**

Adjoint Catchment Processing generates the aggregated upstream catchments from the Catchment feature class. For each catchment that is not a head catchment, a polygon representing the whole upstream area draining to its inlet point is constructed and stored in a feature class that has an Adjoint Catchment tag. This feature class is used to speed up the point delineation process.

Drainage Point Processing was obtained by selecting the Arc Hydro toolbar, then selecting Terrain Pre-processing + Adjoint Catchment Processing.

The result of the above-mentioned processes is in the form of 14 catchment areas in Kalam region. The different colours show the different catchment areas whereas the yellow line passing throughout the Kalam region shows the drainage line. Figure 9 shows the picture of Adjoint Catchment Processing of selected study area.

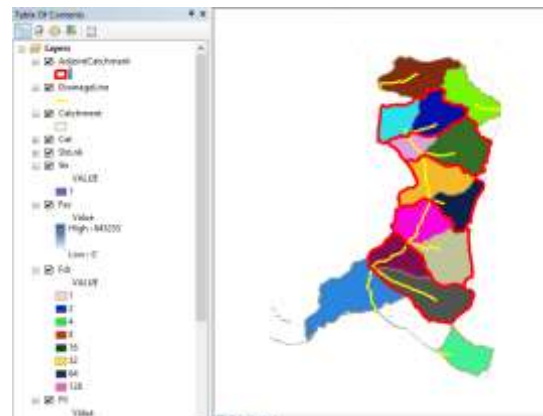


**Figure 9.** Picture of Adjoint Catchment Processing

Drainage Point Processing shows the inlet and outlet from one catchment area to the next catchment area. Drainage Point Processing was obtained by selecting Arc Hydro toolbar, then selecting Terrain Pre-processing + Drainage Point Processing. Figure 10 show the Picture of Drainage Point Processing of study area.

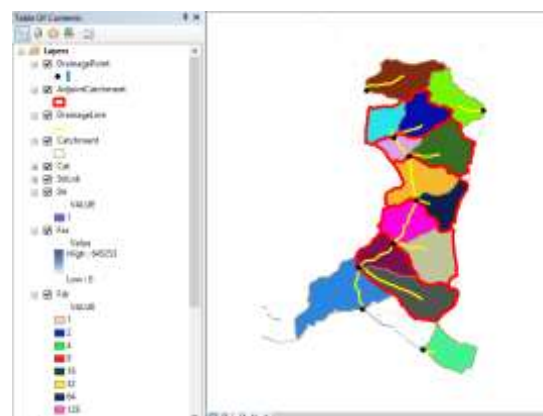


**Figure 10.** Picture of Drainage Point Processing  
**Batch Point Generation and Layer to KML**

It is also known as an outlet source for water. The selected points were taken with the help of Google Earth. The selected points were scarcely populated. We select four points for Dam site

selection in the study area. These points were selected according to our own observations using Google Earth. Figure 11 show the Picture of Batch Point Generation of study area.

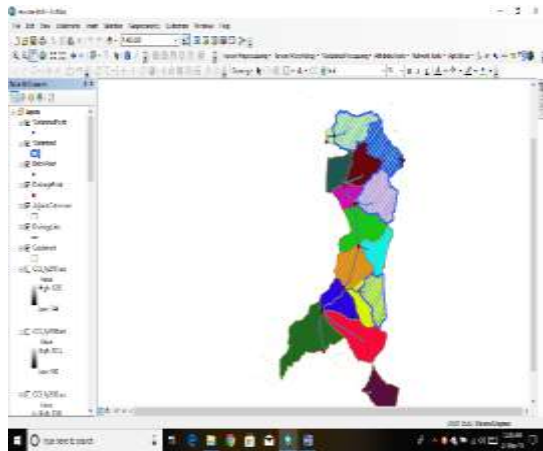


**Figure 11.** Picture of Batch Point Generation

The output of watershed layer is then converted into KML file. This KML file is then opened in Google Earth. Figure 12 Show the Picture of Layer to KML.

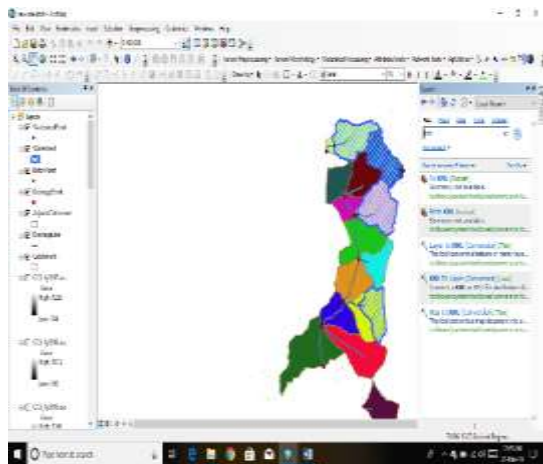


**Figure 12.** Picture of Layer to KML

### Google Earth and Contours

All the data was then compiled and exported to google earth for the selection of a suitable dam site, the study area. A contour map of the selected watershed areas was generated. The interval between two contour lines is 50 meters. Figure 13 show the picture of contour map of the selected watershed areas

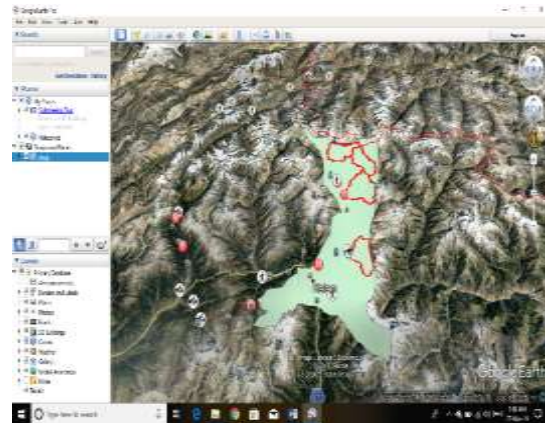


**Figure 13.** Picture of contour map of the selected watershed areas

### Slope and Arc Scene

This map was formulated to show the slope of our selected watershed areas in degrees. This software was used to represent a general and better form of study area. It requires a dimension on z-axis (elevation) that enhances the quality of DEM. The z value taken in this research was 0.000368. With the help of Arc Scene, our selected site is represented in Figure 14.

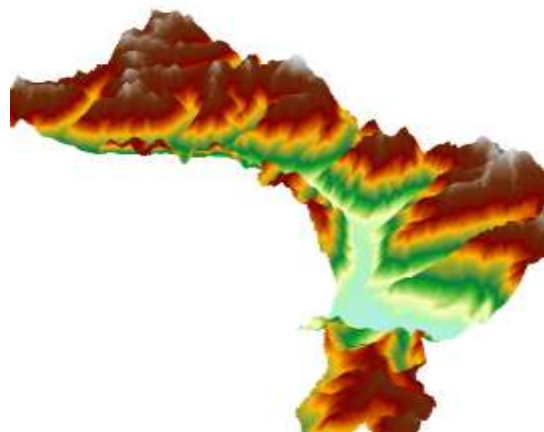


**Figure 14.** Picture Arc Scene

### Slope and Hill shade

This map shows the slope of our selected watershed areas in degrees. The slope of our selected area ranges from 0 degree to 89.72 degrees. Figure 15 show the picture of selected area Slope.



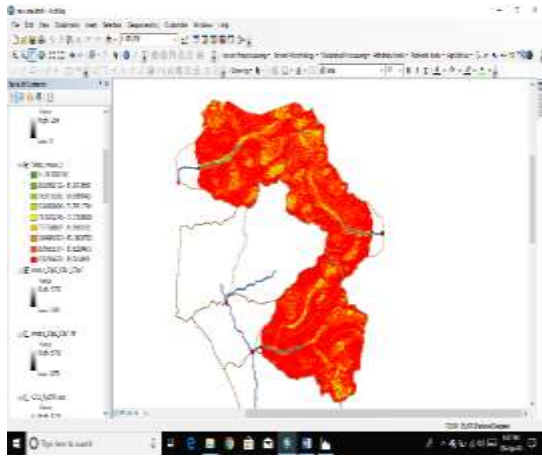


**Figure 15.** Picture of selected area Slope

This map shows the hilly terrain of our study area in general. Figure 16 show the picture of selected area Hill shade.

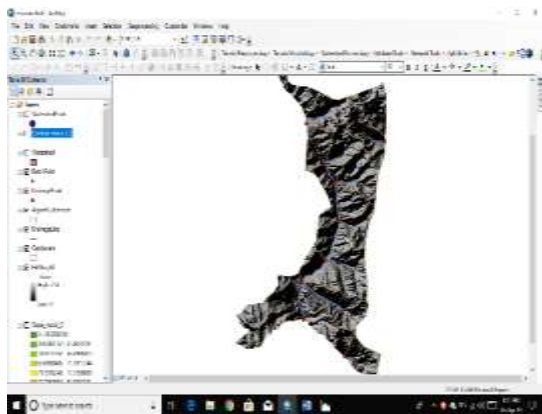


**Figure 16.** Picture of selected area Hill shade

The following 4 sites were selected for suitable dam site selection in Kalam region. The amount of water quantity was formulated from the precipitation data. Rational method was used to calculate runoff.

### Precipitation

The data we collected from Metrological Department Peshawar lacked Latitudes and Longitudes due to which this data could not be used as input for ArcGIS because this data is not reliable. So, we took precipitation data from Centre for Hydrometeorology and Remote Sensing (CHRS) data portal. This site is an archive for global satellite precipitation data and information. There are 3 licensed satellite which collect data and is available in this site for users to access. Precipitation estimation from remotely

sensed information using artificial neural networks – Cloud classification system (PERSIANN-CCS) is downloaded for data of selected site as shown in Figure 17.

Precipitation data was taken of one decade (2007-2017). This data was taken by inputting user shape file in CHRS website.

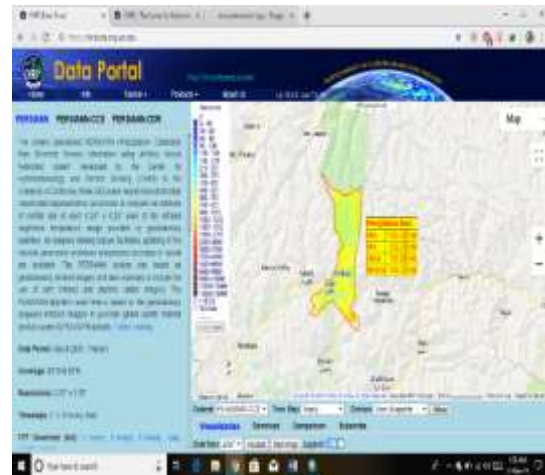


**Figure 17.** Picture of data portal of Precipitation of selected area

After taking data of individual years of 10 years in layer form, then calculate the average amount of rainfall for 10 years at the selected sites. By putting this data into ArcGIS, then calculation of the quantity of water in our selected watershed areas is done as show in in Figure 18.

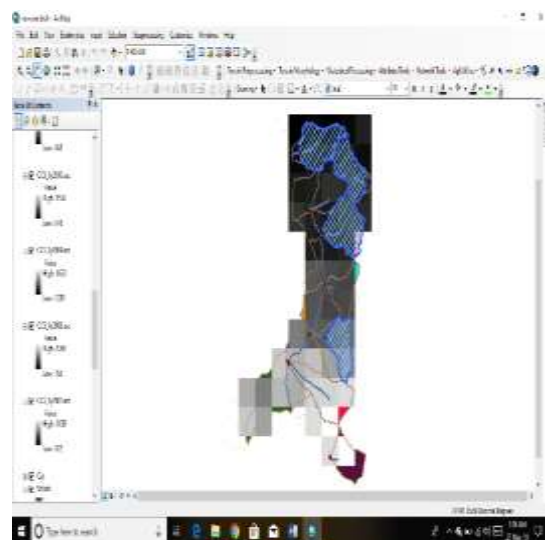


**Figure 18.** Picture of selected area Precipitation

The Precipitation data obtained for selected study area is presented in Table 1. It can be seen from the following Table 1 that Matiltan site receive

the maximum amount of precipitation from 2007 to 2017 at an average of 1.38m. After Matiltan the Derah Banal and Sharang Bar gets the maximum amount of precipitation, 0.996 0.9744 respectively. While in case of run off, it can be seen that, Falak sir has maximum run off. Whereas Derah Banal and Matiltan is on 2<sup>nd</sup> and 3<sup>rd</sup> number respectively. Also, Falak Sar is nearest to link road and with least population. Hence, overall comparison shows that Falak Sar is the best suitable site among all four sites.

### Conclusion

- ArcGIS, Arc Scene, Google earth can be used to identify potential site for a dam. It

saves a lot of time and effort. A total of 14 catchment areas were identified in Kalam region and the best suitable was identified.

- The DEM, precipitation data etc were imported from Centre for Hydrometeorology and Remote Sensing and analysed using ArcGIS and Arc Scene.
- Only two of the above sites have access to road i.e. Falak Sar and Matiltan while the other two have no road access.
- The best suitable site selected for dam is Falak Sar as it has access to road, is scarcely populated compared to Matiltan and has a greater watershed area to store water.

**Table. 1** Precipitation of four different site from 2007 to 2017 and total average Runoff.

Selected areas		Falak Sar	Matiltan	Derah Banal	Sharang Bar
Years	2007	713.67	740.50	761.14	745.83
	2008	898.00	1126.25	926.14	836.83
	2009	1303.17	1390.50	1320.57	1274.67
	2010	1047.33	1279.50	1005.71	1046.17
	2011	676.67	817.75	706.14	689.00
	2012	777.83	982.25	906.43	802.33
	2013	863.33	1092.75	907.00	917.33
	2014	830.83	1011.25	957.43	872.67
	2015	1050.17	1068.75	996.43	1058.33
	2016	681.50	891.00	710.14	698.33
2017	825.83	982.25	772.14	802.67	
Total Avg (mm)		966.833	1138.275	996.929	974.417
Total Avg (m)		0.966833	1.138275	0.996929	0.974417
Area (m <sup>2</sup> )		5337	3383	4673	3894
Coefficient (k)		0.45	0.45	0.45	0.45
Runoff (m <sup>3</sup> )		2321.995	1732.853	2096.391	1707.470
Runoff (Gallon)		613406.1847	457771.3334	553807.913	451065.8542



## REFERENCES

- Dini, B., Manconi, A., Loew, S., Chopel, J.: the punatsangchhu-i dam landslide illuminated by inSAR multitemporal analyses. *Sci. Rep.* 10, 1–10 (2020)
- Dai, X.: Dam site selection using an integrated method of AHP and GIS for decision making support in Bortala, Northwest China. Lund Univ. GEM thesis Ser. (2016)
- Iftikhar, S., Hassan, Z., Shabbir, R.: Site suitability analysis for small multipurpose dams using geospatial technologies. *J. Remote Sens. GIS.* 5, 1–13 (2016)
- Abushandi, E., Alatawi, S.: Dam site selection using remote sensing techniques and geographical information system to control flood events in Tabuk City. *Hydrol. Curr. Res.* 6, 1 (2015)
- CHEN, H.: The relationship between large reservoirs and seismicity. *Water Power Dam Constr.* (2010)
- Bishara, A., Al-Azraq, N., Alazzeah, S., Durant, J.L.: The multifaceted outcomes of community-engaged water quality management in a Palestinian refugee camp. *Environ. Plan. E Nat. Sp.* 2514848620921856 (2020)
- Hovden, L., Paasche, T., Nyanza, E.C., Bastien, S.: Water Scarcity and Water Quality: Identifying Potential Unintended Harms and Mitigation Strategies in the Implementation of the Biosand Filter in Rural Tanzania. *Qual. Health Res.* 1049732320918860 (2020)
- Jozaghi, A., Alizadeh, B., Hatami, M., Flood, I., Khorrami, M., Khodaei, N., Ghasemi Tousi, E.: A comparative study of the AHP and TOPSIS techniques for dam site selection using GIS: A case study of Sistan and Baluchestan Province, Iran. *Geosciences.* 8, 494 (2018)
- Noori, A.M., Pradhan, B., Ajaj, Q.M.: Dam site suitability assessment at the Greater Zab River in northern Iraq using remote sensing data and GIS. *J. Hydrol.* 574, 964–979 (2019)
- Njiru, F.M., Siriba, D.N.: Site Selection for an Earth Dam in Mbeere North, Embu County—Kenya. *J. Geosci. Environ. Prot.* 6, 113–133 (2018)
- Ajibade, T.F., Nwogwu, N.A., Ajibade, F.O., Adelodun, B., Idowu, T.E., Ojo, A.O., Iji, J.O., Olajire, O.O., Akinmusere, O.K.: Potential dam sites selection using integrated techniques of remote sensing and GIS in Imo State, Southeastern, Nigeria. *Sustain. Water Resour. Manag.* 6, 1–16 (2020)
- Issa, S., Al Sbakhi, R., Vakhidov, K., Khouya, S.: Geospatial technologies for dam site selection: A case study from al Ain Wadi. In: International Conference on Engineering Geophysics, Al Ain, United Arab Emirates, 9-12 October 2017. pp. 328–331. Society of Exploration Geophysicists (2017)
- Yildirim, V., Memisoglu, T., Bediroglu, S., Colak, H.E.: Municipal solid waste landfill site selection using multi-criteria decision making and GIS: case study of Bursa province. *J. Environ. Eng. Landsc. Manag.* 26, 107–119 (2018)
- Adham, A., Sayl, K.N., Abed, R., Abdeladhim, M.A., Wesseling, J.G., Riksen, M., Fleskens, L., Karim, U., Ritsema, C.J.: A GIS-based approach for identifying potential sites for harvesting rainwater in the Western Desert of Iraq. *Int. Soil Water Conserv. Res.* 6, 297–304 (2018)

## Evaporation Simulation for a reservoir Using ANN Technique

Muhammad Taqi<sup>1\*</sup>, Usman Ali Naeem<sup>1</sup>, Mujahid Iqbal<sup>1</sup>, Akhtar Abbas<sup>1</sup>, Zeeshan Akbar<sup>1</sup>, Salman Masood<sup>1</sup>

<sup>1</sup> University of Engineering and Technology Taxila

Corresponding author email: [taqi.leghari@gmail.com](mailto:taqi.leghari@gmail.com)

**Abstract:** *Evaporation models are extremely useful in planning and developing water resources. In the present study, an artificial neural network (ANN)-based evaporation model was developed and applied to a watershed in Pakistan. The model was developed to establish the conditions under which the collected data sets are short and the meteorological or hydrological parameters are missing. In this model, two scenarios were studied, one using temperatures and the second using evaporation from the previous day to assume evaporation from the following day. The cross-validation approach was applied for the generalization of ANN models. The meteorological data used for this model was collected by the Water and Power Development Authority (WAPDA). The results confirmed that the ANN model is an influential alternative to theoretical models and is applicable even when the data set of the collected data set is short and the accuracy of data is low.*

**Keywords:** Artificial neural networks; Evaporation; Meteorological data; Temperature

### Introduction

A careful approximation of the evaporation influences on water balance studies for efficient use, management, planning and design of water resources. In hydrological practices, evaporation can be estimated with conventional approaches such as direct and indirect methods that involve the use of empirical equations. The unequivocal process depends enthusiastically on noticeable calculations using pan classes A and U. Although the uninterrupted progression provides a meticulous guess of the evaporation assessment, the method is not trustworthy owing to disgusting salvation. Due to speculation, these procedures have sound effects on the time series of evaporation data. In contrast, other pragmatic methods are instigated on scrupulous quantification, the utmost commonly used comparisons designed for this sort are Penman Monteith and Priestley Taylor equation. Established on frequent aforementioned calisthenics, twain practices shown to be insufficient to cater adequate outcomes to increase evaporation statistics. Evaporation is considered one of the most problematic parameters to guess in the hydrological cycle due to the multifaceted interface between the mechanisms of the earth-plant atmosphere system (SINGH & XU, 1997). The thrifty level of certainty of the two provisions has encouraged scientists to find a new method to specify the evaporation rate more precisely. The rate of

evaporation is a nonlinear and complicated phenomenon that requires the menstruation of many factors and the change of different formulas. Therefore, given the physical constraints and the formulas, it may not be possible / realistic to estimate the rate of evaporation (Rianna et al., 2018). Over the past few decades, Artificial Intelligence (AI) techniques have been productively functional in the operations and control of physical water resources, like precipitation, sediment discharge, storage dame maneuvers, groundwater level and for the modeling of water quality constraint. Adaptive Neuro-Fuzzy Inference System (ANFIS) and ANN were used for monthly prognosis evaporation (Allawi & El-Shafie, 2016). RBF-NN neural network function applied for the prophecy of heavy metal under different weather conditions (Elzwayie et al., 2017). The Extreme Learning Machine (ELM) technique was used for flow prediction (Yaseen et al., 2016). Several artificial intelligence methods had been proposed to divide the monthly flow (Yaseen et al., 2018). Monthly sediments were conjectured using ANN techniques with different input groups (Afan et al., 2014). The operating system of the reservoir was measured using a novel AI technique from (Ehteram et al., 2017). Artificial intelligence procedures such as support RBF-NN, ANFIS and support vector regression (SVR) were jumble-sale for evaporation demonstrating (Keskin et al., 2004).

Development of Feed Forward Neural Network (FFNN) models to predict daily evaporation and found that (FFNN) works better than conventional models. Models of neural networks and genetic algorithm were used to bring bread closer to evaporation. These consequences discovered the significant competence of the systems as an effective apparatuses for appraising evaporation (Kim & Kim, 2008). Ö.Kişi (Kişi, 2009) introduced three different neural networks for guessing evaporation, he found that RBF-NN is more efficient than GRNN and (MLP) methodologies for evaporation expectations. A.Guven et.al. (Guven & Kişi, 2011) used neural network in corporation of a linearized genetic algorithm to guess the basics of the daily evaporation of the pan. Support vector machine (SVM) was castoff to enrich the expectation exactitude of daily evaporation in southeastern Iran (Kohli & Frenken, 2015). Multilayer perceptron neural network (MLP-NN) and support vector machine(SVM) was applied under several input amalgamations in lieu of weather-related constraints like air temperature, relative humidity, wind speed and precipitation to augment the level of precision for pan evaporation prediction (Eslamian et al., 2009). The above confab authorizes the significance of obligating a precise evaporation rate for handling water resources and, especially, dam and reservoir maneuvers. So, numerous researchers' efforts to ripen model and examined them with different modeling approaches, such as AI and auto regression, in directive to provide an accurate evaporation forecast. The above models require long term data series for their operation generally some parameters might be unapproachable in some study areas due several reason, so the need is to develop such models which requires less parameter for their operation. In this context, a case study on Khanpur dam Pakistan was investigated the potential of ANN models to develop a prediction model for evaporation rate with less metrological parameters.

### Research Methodology

Artificial neural networks allocate a malleable precise methodology, the architecture of the ANN has the capability to illuminate nonlinear associations. This capability of ANN marque ANN superior to recognized practices. ANN project was based on the computer or mathematical reception of data and processed

them by producing a correspondence between them. Additionally, ANN can by which it learns demo prototypes minus the need for isolated encoding reproductions for the simulation of the information's confidentially. The ANN process had several frameworks, like FFNN, RFB-NN and MLP-NN.FFNN out of which FFNN offer virtuous fastidiousness by means of best architecture by selecting the best number of neurons and hidden layers. In supplementary arguments, these procedures can deliver the outstanding presentation after numerous syntheses to choose an appropriate architectonic. In this exertion, FFNN is selected, because this is the furthestmost prominent category of ANN. The reason why this was chosen is its simplicity of work.

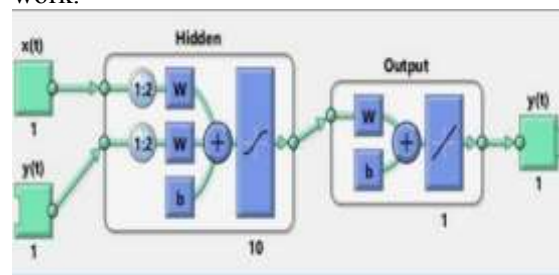


**Fig. 1** Systematic illustration of FFNN architecture

The direction of enthusiasm for connecting neurons at the entry level to neurons at the exit level. This assembly shows the calculation process in the architecture of the FFNN method. The real method of computation exists in neurons and each neuron has a collection of stimulus transmission these transmissions send the neuron and sells digs to analyze the values of the files received and deliver a result. The instigation allocation function that survives in the neurons of the input layer passes the input indicating that the input is dimension incompatible and returns the individual dimensions to the hidden layer. Therefore, the instigation transforms the function into hidden layer neurons to calculate the coming capricious arrival and produces values that embody the deductions.

### Model Structure:

The efficiency of the ANN greatly depends on the input pattern and input parameters. The input parameter is hydrological parameter they are difficult to measure due to their nonlinear behavior. So, the anticipated model was delimited by using the evaporation rate of the reservoir recorded daily and average daily air

temperature data form the period (2004-2018). For the anticipation of rate of evaporation, the model configurations were dignified into two dissimilar combinations in this investigation. The model was constructed in such a way that the target remained unchanged in both configurations, but the input combinations change according to the target requirement by using trial and error procedure. For each consequence, the first 70% of the data utilized for training the representations residual 30% were fragmented into two phases: 15% for testing and 15% for validation of the deliberated model. In first connection three model were designed by means of temperatures  $T_{max}$ ,  $T_{min}$  and  $T_{avg}$  as input to predict evaporation of the same day. Correspondingly in 2<sup>nd</sup> setup we use only the historical records of the previous day evaporation was as input and the evaporation of the next day as a target. The input data records were designed on the basis how the originator records were correlated with the prophesied results and best fitted using trial and error procedure. The All models were verified using different statistical analysis. In first setup daily maximum minimum and average temperatures are used as input and evaporation as target value (Table 1).

**Table 1** Combination of Inputs for the Models First Configuration

Representations	Inserted Combination	Target
Model-A	$T_{max}$	E(T)
Model-B	$T_{min}$	E(T)
Model-C	$T_{avg}$	E(T)

In this  $T_{max}$ ,  $T_{min}$ , and  $T_{avg}$  are maximum, minimum and average daily temperatures as input and E (T) is daily pan evaporation as output.

In the second configuration, the evaporation data was used as inputs and outputs with a different combination. Five types of models with a different ANN architecture and a combination of neurons were studied as shown in table 2.

**Table 2** Combination of Inputs and Produced Output for Second Configuration

Designation	Inputs	Target
Model-I	E(T-1)	E(T)
Model-II	E(T-2)	E(T)
Model-III	E(T-3)	E(T)
Model-IV	E(T-4)	E(T)
Model-V	E(T-5)	E(T)

In this E (T-1), E (T-2), E (T-3), E (T-4), E (T-5) are the evaporation rate of the previous 1-5 days E (T) is the current day evaporation.

### Evaluation Matrices

In general, to assess the conduct of the forecast models, it is essential to scrutinize the models by applying assured concert gauges to understand whether the planned models match the actual value. To assess the attainment of the suggested evaporation prediction models' certain statistical gauges were applied to suggested evaporation rate prediction models in this study. The indicators applied in this study correlation coefficient ( $R^2$ ), Mean Absolute error (MAE) root mean square error (RMSE) and Nash-Sutcliffe efficiency (NSE) were studied. The gauges are common to execute the designed models performance with authentic standards. For  $R^2$ , MAE, RMSE, the slighter value (near to zero) indicate superlative outcome but in case of NSE the value must lies between 0 and 1, the best performance is at 1 and 0 means no relation between the actual and predicted values.

### Results and Discussion

The models were trained using different neuron by trial and error procedure the obtained results are shown in table 3 and 4.

**Table 3** shows the values of the performance measures (RMSE,  $R^2$ , MAE and NSE) for installation no.1.

Model	RMSE	$R^2$	MAE	NSE
Model-I	4.71	0.84	3.00	0.74
Model-II	4.75	0.84	3.00	0.74
Model-III	4.79	0.82	3.19	0.73
Model-IV	4.92	0.82	3.33	0.72
Model-V	5.073	0.81	3.42	0.70

**Table 4** Demonstration of the results in the form of (RMSE,  $R^2$ , MAE and NSE) for Situation-2

Model	RMSE	MAE	$R^2$	NSE
Model-A	3.49	2.181	0.83	0.82
Model-B	3.64	2.25	0.83	0.84
Model-C	3.65	2.25	0.82	0.83

Where (RMSE) is root mean square error, MAE mean absolute error  $R^2$  is correlation co-efficient (NSE) Nash- Sutcliffe efficiency.

## Conclusions

ANN model was used for guesstimating daily evaporation in Khanpur dam watershed in Pakistan and it had been certified that ANN model has significantly accurate. The study was carried out on semi-arid region in hilly area and perform will in these environments. The investigation helps to improve an influential set up that would envisage the rate of evaporation where some of climatological, geological and hydrological features are missing. The model was tested for two set of input combination both combination shows excellent performance as shown in table. 3, 4. In the first input diagram, daily temperatures are used to find evaporation in the same way in the second digenesis, the evaporation data sets from the previous five days were used to predict evaporation after prediction, and the results are checked using the various statistical parameters to check the level of truth. We find a virtuous correspondence between the projected value and the experiential value no model from above beyond the precision limit, the consummate model in the first installation is the model-I which uses the maximum temperature of the day to predict daily evaporation. The second configuration shows that as the entry delay days increase, the depiction of the models decreases slightly, but the perfection of the five models in this particular case is appropriate. From the above results we discover that ANN model is an important substitute to the theoretical models for the evaporation and hydrological investigations. It is fairly tranquil to develop and less involve in the complete assessment of the watershed hydrological and geological considerations as are essential for the application of other kinds of physically based models.

## References

- Afan, H. A., El-Shafie, A., Yaseen, Z. M., Hameed, M. M., Wan Mohtar, W. H. M., & Hussain, A. (2014). ANN Based Sediment Prediction Model Utilizing Different Input Scenarios. *Water Resources Management*, 29(4), 1231–1245. <https://doi.org/10.1007/s11269-014-0870-1>
- Allawi, M. F., & El-Shafie, A. (2016). Utilizing RBF-NN and ANFIS Methods for Multi-Lead ahead Prediction Model of Evaporation from Reservoir. *Water Resources Management*, 30(13), 4773–4788. <https://doi.org/10.1007/s11269-016-1452-1>
- Ehteram, M., Allawi, M. F., Karami, H., Mousavi, S. F., Emami, M., El-Shafie, A., & Farzin, S. (2017). Optimization of Chain-Reservoirs' Operation with a New Approach in Artificial Intelligence. *Water Resources Management*, 31(7), 2085–2104. <https://doi.org/10.1007/s11269-017-1625-6>
- Elzwayie, A., El-shafie, A., Yaseen, Z. M., Afan, H. A., & Allawi, M. F. (2017). RBFNN-based model for heavy metal prediction for different climatic and pollution conditions. *Neural Computing and Applications*, 28(8), 1991–2003. <https://doi.org/10.1007/s00521-015-2174-7>
- Eslamian, S. S., Abedi-Koup, J., Amiri, M. J., & Gohari, S. A. (2009). Estimation of Daily Reference Evapotranspiration Using Support Vector Machines and Artificial Neural Networks in Greenhouse. *Research Journal of Environmental Sciences*, 3(4), 439–447. <https://doi.org/10.3923/rjes.2009.439.447>
- Güven, A., & Kişi, Ö. (2011). Daily pan evaporation modeling using linear genetic programming technique. *Irrigation Science*, 29(2), 135–145. <https://doi.org/10.1007/s00271-010-0225-5>
- Keskin, M. E., Terzi, Ö., & Taylan, D. (2004). Fuzzy logic model approaches to daily pan evaporation estimation in western Turkey. *Hydrological Sciences Journal*, 49(6), 1001–1010. <https://doi.org/10.1623/hysj.49.6.1001.55718>
- Kim, S., & Kim, H. (2008). Neural Networks and Genetic Algorithm Approach for Nonlinear Evaporation and Evapotranspiration Modeling. *Journal of Hydrology*, 351, 299–317. <https://doi.org/10.1016/j.jhydrol.2007.12.014>
- Kişi, Ö. (2009). Modeling monthly evaporation using two different neural computing techniques. *Irrigation Science*, 27(5), 417–430. <https://doi.org/10.1007/s00271-009-0158-z>
- Kohli, A., & Frenken, K. (2015). Evaporation from Artificial Lakes and Reservoirs. *FAO AQUASTAT Reports*, 10.
- Rianna, G., Reder, A., & Pagano, L. (2018). Estimating actual and potential bare soil evaporation from silty pyroclastic soils: Towards improved landslide prediction. *Journal of Hydrology*, 562, 193–209. <https://doi.org/10.1016/j.jhydrol.2018.05.005>

- SINGH, V. P., & XU, C.-Y. (1997). Evaluation and Generalization of 13 Mass-Transfer Equations for Determining Free Water Evaporation. *Hydrological Processes*, 11(3), 311–323. [https://doi.org/10.1002/\(sici\)1099-1085\(19970315\)11:3<311::aid-hyp446>3.3.co;2-p](https://doi.org/10.1002/(sici)1099-1085(19970315)11:3<311::aid-hyp446>3.3.co;2-p)
- Yaseen, Z. M., Allawi, M. F., Yousif, A. A., Jaafar, O., Hamzah, F. M., & El-Shafie, A. (2018). Non-tuned machine learning approach for hydrological time series forecasting. *Neural Computing and Applications*, 30(5), 1479–1491. <https://doi.org/10.1007/s00521-016-2763-0>
- Yaseen, Z. M., Jaafar, O., Deo, R. C., Kisi, O., Adamowski, J., Quilty, J., & El-Shafie, A. (2016). Stream-flow forecasting using extreme learning machines: A case study in a semi-arid region in Iraq. *Journal of Hydrology*, 542, 603–614. <https://doi.org/10.1016/j.jhydrol.2016.09.035>



## Design and Development of Irrigation Schedule and Sowing Techniques to Enhance Cucumber Yield

Muhammad Zeeshan Khan<sup>1\*</sup>, Muhammad Zaman<sup>1</sup>, Junaid Nawaz Chauhdary<sup>2</sup>, Muhammad Umair<sup>3</sup>,  
Malik Mubashar Ishaq<sup>1</sup>, Shabana Kausar<sup>1</sup>

<sup>1</sup> Department of Irrigation and Drainage, University of Agriculture, Faisalabad

<sup>2</sup> Water Management Research Centre, University of Agriculture, Faisalabad

<sup>3</sup> Department of Farm Machinery and Power, University of Agriculture, Faisalabad

Corresponding author email: [zeshaan896@gmail.com](mailto:zeshaan896@gmail.com)

**Abstract:** Agriculture is the important economic sector of Pakistan which contributes about 18.5% in GDP of Pakistan. Due to continuous climate change in Pakistan water resources are declining and country came among the water scarce countries with less than 1000 m<sup>3</sup>/capita per annum water availability. Now it's dire need to adopt new water saving techniques in agriculture to meet the water requirement of crops. Different new methods of sowing and water application should be adopted for conserving resources. So, this study is conducted to develop irrigation schedules and test various types of mulch. Randomized Complete Block design (RCBD) has been used in this experiment with 6 treatments and a control. Furthermore, every treatment has been repeated as 3 times. The treatments were T1 (black mulch+20% deficit irrigation), T2 (black mulch+40% deficit irrigation), T3 (white mulch+20% deficit irrigation), T4 (white mulch+40% deficit irrigation), T5 (wheat straw+20% deficit irrigation), T6 (wheat straw+40% deficit irrigation), Control (furrow irrigation). The results of the study revealed that among all treatments, total yield of the cucumber was maximum in 20% DI treatments than 40% DI treatments. The treatment T3 (white plastic mulch + 20% DI) had maximum yield of 47.31 tons/ha whereas the minimum yield of 31.86 tons/ha was obtained in control treatment. The water productivity of treatment T3 (white plastic mulch + 20% DI) was 28.42 kg/m<sup>3</sup>/ha. So, the treatment T3 with white mulch + 20% DI was recommended as a better technique for producing better results in terms of yield and water productivity as compared to others.

**Keyword:** deficit irrigation, mulch, evapotranspiration, yield

### Introduction

Cucumber (*Cucumis sativus*) is an important vegetable of Cucurbitaceae class (Lower and Edwards, 1986) and Fourth ranked important crop in Asia (Eifediyi *et al.*, 2010) that contains useful vitamins helpful in controlling the anxiety and stress (Amin *et al.*, 2018). Cucumber needs high soil moisture and temperature for better yield but, under hostile environmental conditions climatic extremes (Zaman *et al.*, 2020) many problems can occur such as decrease in female flowers (Cantliffe and DJ, 1981), delay in crop yield (Medany *et al.*, 1999; Marcelis *et al.*, 1993) and deficiency in minerals (Barker and Sonneveld, 1988). Therefore, the sowing of cucumber is done in tunnel farming to provide this favourable environment (Palada *et al.*, 2003). According to the report of IMF, Pakistan ranked 3rd among the water scarce countries (Nabi *et al.*, 2019). The irrigation efficiency in Pakistan is very low that is approximately 30 to 40% and only 35% water of total reaches at Nakka of the field which is actually used by the crop (Usman, 2016). Recently, use of water is exceeding

energetically that needs high water use efficiency which is feasible only under controlled environment conditions (Çakir *et al.*, 2017). Irrigation water application less than actual water requirement called as Deficit Irrigation (DI) is considered as sustainable technique in most of the world (Pereira *et al.*, 2002). Several researchers reported that insufficient irrigation technique has significant effects on productivity and growth of the crops (Karam *et al.*, 2011; Badal *et al.*, 2013; Ballester *et al.*, 2011). Mulch is a kind of material that conserve moisture content by reducing evaporation and considered as best management practice which in combination with drip irrigation improves water use efficiency and crop yield (Khurshid *et al.*, 2006; Wang *et al.*, 2014; Liu *et al.*, 2012). The use of plastic mulch can increase the soil temperature, conserve soil moisture and improve health of the soil (Gupta *et al.*, 2010; Ibarra *et al.*, 2007; Cassel Sharmasarkar *et al.*, 2001). Numerous experiments were carried out to analyse the effect of mulched drip irrigation system on the production of crops in different soil and environment conditions. The white plastic

mulch had high yield, soil temperature, WUE and moisture value than yellow, black and organic mulch (Shaikh and Fouda, 2008; Yaghi *et al.*, 2013; Mane *et al.*, 2014). The deficit irrigation levels are most suitable for irrigation of cucumber sown under greenhouse in water stress conditions (Ayas and Demirtaş, 2009; Patané *et al.*, 2011; Igbadun *et al.*, 2012).

The objective of the present work was to sow cucumber under drip irrigation and to check the effect of mulched drip irrigation system on yield and WUE under tunnel farming in semi-arid region of Pakistan. The present experiment was planned to develop the optimum irrigation schedules for cucumber based on different deficit levels under tunnel farming.

### Study area and data description

The experimental site having geographical coordinates 31.421°N (latitude) and 73.089°E (longitude) was conducted at farmer field of Sarshamir area of Faisalabad, Punjab, Pakistan on Cucumber crop during year 2019-2020 to analyze the irrigation schedule and sowing technique of Cucumber. The ground elevation of this area is 184 metre from the sea level and lies in the semi-arid area of Punjab. In winter temperature reaches below than freezing point but in summer it rises and goes upto 50 °C. The experimental area was 30 × 55ft =1650 ft<sup>2</sup> or 153.290 m<sup>2</sup> with four tunnels. The soil was sandy loam textured having pH of 8.5 and organic matter of 0.22%. The drip system was installed at 1m lateral spacing and in-line emitters having 4 lph discharge.

### Research Methodology

The field experiment was laid under Randomized complete block design (RCBD) (Zhou *et al.*, 2018). It comprises six numbers of treatments and three duplications as blocks and control as conventional farmer practice. The treatments were T1 (black mulch+20% deficit irrigation), T2 (black mulch+40% deficit irrigation), T3 (white mulch+20% deficit irrigation), T4 (white mulch+40% deficit irrigation), T5 (wheat straw+20% deficit irrigation), T6 (wheat straw+40% deficit irrigation), Control (furrow irrigation). The crop water requirement was calculated by FAO standard method (Penman-Monteith) using CROPWAT program based on FAO paper 56 (Allen *et al.*, 1998) as follows:

$$ET_c = K_c \frac{0.408 \Delta (R_n - G) + \gamma (900/T_{mean} + 273) u_2 (e_s - e_a)}{\Delta + \gamma (1 + 0.34 u_2)}$$

It is world widely use program for irrigation scheduling of different crops. The cropwater requirement values of ETo was estimated on basis of climatic parameters, but the actual ETc was calculated by multiplying reference evapotranspiration ETo with crop coefficient Kc (Bouraima *et al.*, 2015). Several parameters like number of leaves, plant height, number of fruits, fruit weight per plant, total yield and water productivity were measured to observe the growth of crop at every stage.

### Results and Discussion

The result of the CROPWAT reveals that 20% DI level had more water application value of 248mm than 40% DI level of 186mm and irrigation was applied on daily basis for the whole season. The control treatment having furrow irrigation had the highest amount of water to be applied that was 529.9mm. The water application at different deficit level and control is shown below in Fig 1:

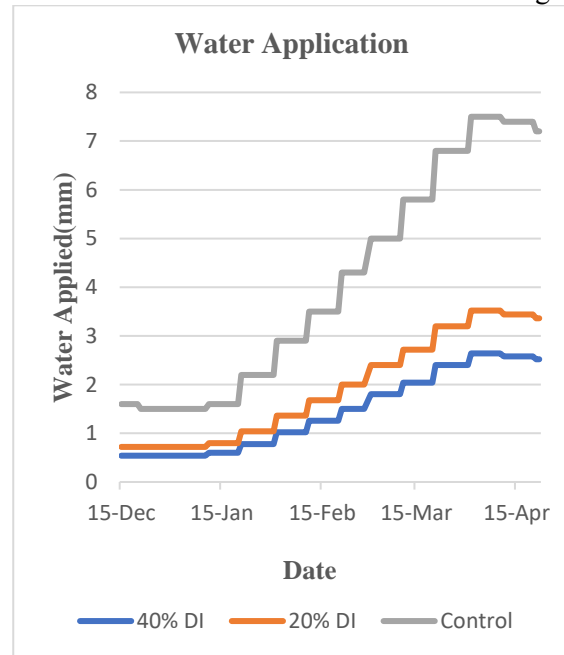


**Fig. 1** Water application graph

The results of growth parameters were also found significant. The number of leaves (44) were greater in both treatments of (white mulch + DI) than the treatments of black and wheat straw mulch due to difference in the soil temperature beneath mulch. The number of fruits per plant (36) were maximum in case of (white mulch + DI) treatments and minimum in control treatment due to difference in vegetative growth. The

comparisons between both parameters are shown below in Fig 2.

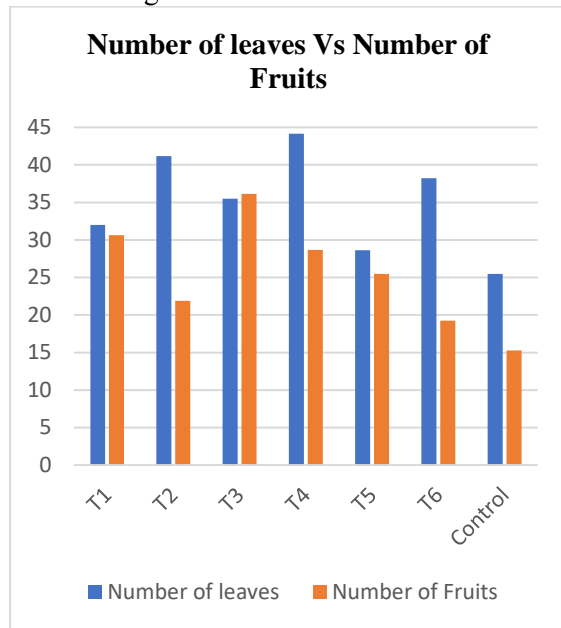


**Fig. 2** Comparison between number of leaves and fruits

The figure 3 depicts the relationship between plant height and fruit weight. The result shows the maximum in case of (white mulch + DI) treatments and minimum in (wheat straw mulch + DI) treatments. The height of plant was maximum in white mulch due to the high temperature of the soil. The fruit weight observed in this experiment was maximum in treatment T3

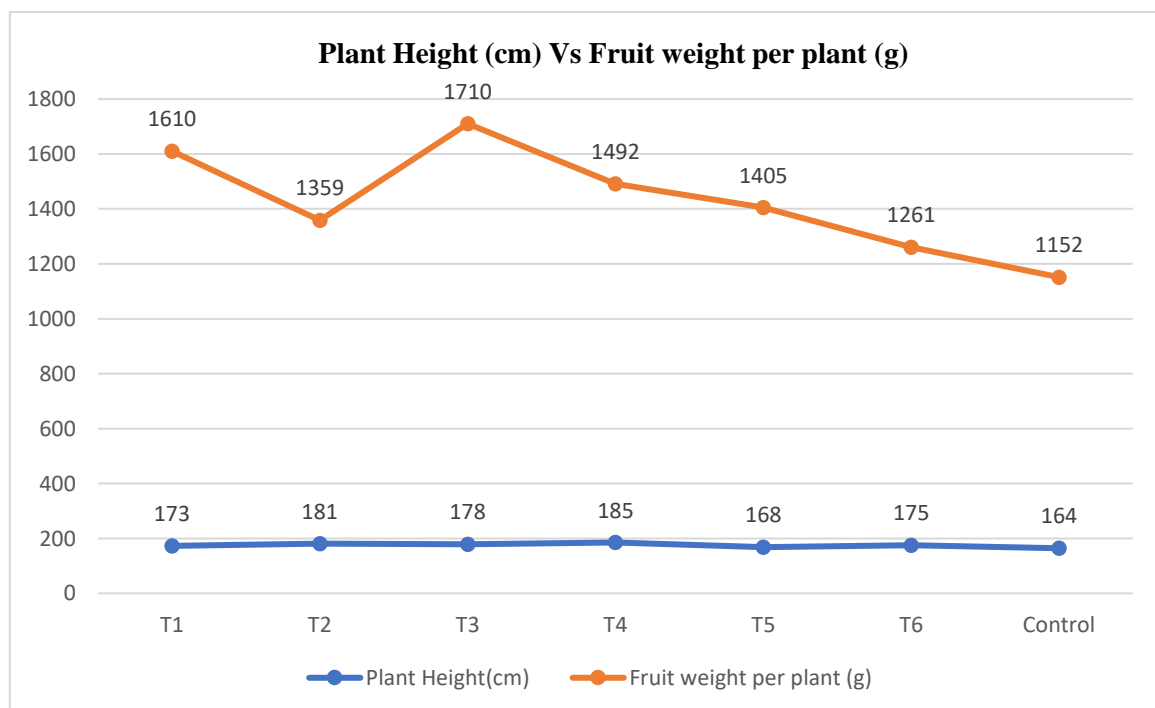


**Fig. 3** Comparison between plant height and fruits weight per plant

(white mulch + 20% DI) while the minimum yield was observed in control having furrow irrigation with no mulch condition due to better vegetative growth of the crop (Ayas and Demirtaş, 2009; Mane *et al.*, 2014; Yaghi *et al.*, 2013; Şimşek *et al.*, 2005; Shaikh and Fouda, 2008).

### Conclusion

In this field research, it has been concluded that deficit water application techniques along with best field management practices like mulching are best applicable in water stress conditions. The optimum irrigation scheduling has been developed on basis of water saving and yield of cucumber. The use of white plastic mulch along with drip irrigation has been recommended as best field management practice to get maximum yield. The water productivity of the 40% DI level was maximum than 20% DI level but 40% DI level was recommended in acute water shortage condition and 20% DI level in normal water condition.

### Acknowledgement

This research was funded and supported by the Technology Development Fund of Higher Education Commission of Pakistan grant# TDF-02-053.

## References

- Allen, R.G., L.S. Pereira, D. Raes, M. Smith and W. Ab. 1998. Fao,1998. Irrig. Drain. Pap. No. 56, FAO 300.
- Amin, E., M.M. Raza and M. Iqbal. 2018. Kheera Local : A new high yielding , well adaptable and heat tolerant cucumber ( Cucumis Sativus L .). J. Agric. Res 56:13–16.
- Ayas, S. and Ç. Demirtaş. 2009. Deficit irrigation effects on cucumber (Cucumis sativus L. Maraton) yield in unheated greenhouse condition. J. Food, Agric. Environ. 7:645–649.
- Badal, E., T.A.A. El-Mageed, I. Buesa, D. Guerra, L. Bonet and D.S. Intrigliolo. 2013. Moderate plant water stress reduces fruit drop of “ Rojo Brillante” persimmon (Diospyros kaki) in a Mediterranean climate. Agric. Water Manag. 119:154–160.
- Ballester, C., J. Castel, D.S. Intrigliolo and J.R. Castel. 2011. Response of Clementina de Nules citrus trees to summer deficit irrigation. Yield components and fruit composition. Agric. Water Manag. 98:1027–1032.
- Barker, J.C. and C. Sonneveld. 1988. Calcium deficiency of glasshouse cucumber as affected by environmental humidity and mineral nutrition. J. Hortic. Sci. 63:241–246.
- Bouraima, A.K., Z. Weihua and W. Chaofu. 2015. Irrigation water requirements of rice using Cropwat model in Northern Benin. Int. J. Agric. Biol. Eng. 8:58–64.
- Çakir, R., U. Kanburoglu-Çebi, S. Altintas and A. Ozdemir. 2017. Irrigation scheduling and water use efficiency of cucumber grown as a spring-summer cycle crop in solar greenhouse. Agric. Water Manag. 180:78–87.
- Cantliffe, D. and C. DJ. 1981. Alteration of sex expression in cucumber due to changes in temperature, light intensity, and photoperiod.
- Cassel Sharmasarkar, F., S. Sharmasarkar, S.D. Miller, G.F. Vance and R. Zhang. 2001. Assessment of drip and flood irrigation on water and fertilizer use efficiencies for sugarbeets. Agric. Water Manag. 46:241–251.
- Eifediyi, K., E.K. Eifediyi and S.U. Remison. 2010. Impact of Poultry Manure and NPK Fertilizer on Soil Physical Properties and Growth and Yield of Carrot View project
- Modelling pod growth rate of bambara groundnut (*Vigna subterranea* Verdc.) in response to photoperiod and temperature. View project Growth a. J. Plant Breed. Crop Sci. 2:216–220.
- Gupta, A.J., M.F. Ahmad and F.N. Bhat. 2010. Studies on yield, quality, water and fertilizer use efficiency of capsicum under drip irrigation and fertigation. Indian J. Hortic. 67:213–218.
- Ibarra, M.A.I., S.F.M. Moreno, E.A.C. Valencia, M.M.V. Castorena, I.S. Cohen and A.R. López. 2007. Productivity of Jalapeno pepper under drip irrigation and plastic mulch conditions. Rev. Fitotec. Mex. 30:429–436.
- Igbadun, H.E., A.A. Ramalan and E. Oiganji. 2012. Effects of regulated deficit irrigation and mulch on yield, water use and crop water productivity of onion in Samaru, Nigeria. Agric. Water Manag. 109:162–169.
- Karam, F., R. Saliba, S. Skaf, J. Breidy, Y. Rouphael and J. Balendonck. 2011. Yield and water use of eggplants (*Solanum melongena* L.) under full and deficit irrigation regimes. Agric. Water Manag. 98:1307–1316.
- Khurshid, K., M. Iqbal, M.S. Arif and A. Nawaz. 2014. Effect of Tillage and Mulch on Soil Physical Properties and Growth of Maize. Int. J. Agric. Biol. 2:122–137.
- Liu, H., H. Yang, J. Zheng, D. Jia, J. Wang, Y. Li and G. Huang. 2012. Irrigation scheduling strategies based on soil matric potential on yield and fruit quality of mulched-drip irrigated chili pepper in Northwest China. Agric. Water Manag. 115:232–241.
- Lower, R. and M. Edwards. 1986. Cucumber breeding In: M J Basset (ed.). Breeding vegetables crops. Westport, Connecticut USA: AVI Publ. Co. pp 173–203.
- Mane, M.S., S.K.Jagtap, B.L.Ayare and R.T.Thokal. 2014. RESPONSE OF CUCUMBER CROP ( *Cucumis sativus* L .) TO DRIP IRRIGATION SYSTEM UNDER VARIOUS MULCHES. J. Soils Crop. 24:193–200.
- Marcelis, L.F.M. and L.R.B. Hofman-Eijer. 1993. Effect of temperature on the growth of individual cucumber fruits. Physiol. Plant. 87:321–328.
- Nabi, G., M. Ali, S. Khan and S. Kumar. 2019. The crisis of water shortage and pollution in Pakistan: risk to public health, biodiversity,

- and ecosystem. *Environ. Sci. Pollut. Res.* 26:10443–10445.
- Palada, M.C., A.M. Davis, J.A. Kowalski and S.M.A. Crossman. 2003. Yield and irrigation water use of vegetables grown with plastic and straw mulch in the U.S. Virgin Islands. *Int. Water Irrig.* 23:21–25.
- Patanè, C., S. Tringali and O. Sortino. 2011. Effects of deficit irrigation on biomass, yield, water productivity and fruit quality of processing tomato under semi-arid Mediterranean climate conditions. *Sci. Hortic. (Amsterdam)*. 129:590–596.
- Pereira, L.S., T. Oweis and A. Zairi. 2002. Irrigation management under water scarcity. *Agric. Water Manag.* 57:175–206.
- Shaikh, A.E.- and T. Fouda. 2008. Effect of different mulching types on soil temperature and cucumber production under libyan conditions \*. *Biol. Eng.* 25:160–175.
- Şimşek, M., T. Tonkaz, M. Kaçira, N. Çömlekçioğlu and Z. Doğan. 2005. The effects of different irrigation regimes on cucumber (*Cucumis sativus* L.) yield and yield characteristics under open field conditions. *Agric. Water Manag.* 73:173–191.
- Wang, Z., M. Jin, J. Šimůnek and M.T. van Genuchten. 2014. Evaluation of mulched drip irrigation for cotton in arid Northwest China. *Irrig. Sci.* 32:15–27.
- Yaghi, T., A. Arslan and F. Naoum. 2013. Cucumber (*Cucumis sativus*, L.) water use efficiency (WUE) under plastic mulch and drip irrigation. *Agric. Water Manag.* 128:149–157.
- Zaman, M., I. Ahmad, M. Usman, M. Saifullah, M.N. Anjum, M.I. Khan and M. Uzair Qamar. 2020. Event-Based Time Distribution Patterns, Return Levels, and Their Trends of Extreme Precipitation across Indus Basin. *Water* 12:3373.
- Zhou, L., J. He, Z. Qi, M. Dyck, Y. Zou, T. Zhang and H. Feng. 2018. Effects of lateral spacing for drip irrigation and mulching on the distributions of soil water and nitrate, maize yield, and water use efficiency. *Agric. Water Manag.* 199:190–200.

## Impact of Bio Slurry on Soil Physical Properties and Crop Yield

Shabana Kausar<sup>1\*</sup>, Muhammad Zaman<sup>1</sup>, Muhammad Tayyab<sup>2</sup>, Muhammad Umair<sup>3</sup>, Malik Mubashar Ishaq<sup>1</sup>, Muhammad Zeeshan Khan<sup>1</sup>

<sup>1</sup> Department of Irrigation and Drainage, University of Agriculture Faisalabad

<sup>2</sup> Department of Energy Systems Engineering, University of Agriculture, Faisalabad

<sup>3</sup> Department of Farm Machinery and Power, University of Agriculture, Faisalabad

Corresponding author email: [shabanakausar161995@gmail.com](mailto:shabanakausar161995@gmail.com)

**Abstract:** Scarcity of water reduces the agricultural yield and may affect the GDP of the country and this issue can be mitigated by using different efficient irrigation methods like drip or sprinkler. Agricultural yield also dependent on soil fertility, which is generally enhanced by the use of chemical fertilizer (N, P, and K). These chemical fertilizers are expensive and may cause negative effects on environment. To overcome this issue, the present study is designed to use of organic fertilizer in the form of Bio Slurry instead of chemical fertilizers along with the trickle irrigation system. Four types of treatments and one control, will be used with different ratio of organic and artificial fertilizers i.e., Control: 100% artificial fertilizer, T1: 75% artificial + 25% organic fertilizer, T2: both use as 50% ratio, T3: 25% artificial + 75 % organic fertilizer, T4: 100% organic fertilizer. T2 (50%bio slurry + 50% inorganic fertilizer) has the maximum plant height, fruit weight, yield of tomato and water productivity. This study will helpful to the farmer to use appropriate ratio of fertilizers to get the better quality and maximum yield of tomato as well as maintain the soil properties.

### Introduction

Agriculture is a major ingredient of Pakistani budget and directly supports the country population and contribute 18.5% of gross domestic product (GDP). Crop yield is affected by soil fertility as well as amount and application method of watering. Tomato is one of the major ingredients that Pakistan import from India. Average yield of tomato is about 12-15 ton per acre in Pakistan with the use of inorganic fertilizers. The total area of Pakistan used for tomato crop in 2017-2018 was recorded 60600 hectares (ha) with the production of 620,100 tonnes and yield was recorded as 10.2 tonnes/hectare (t/h) (Anonymous, 2017-18). The total consumption of fertilizer during the year 2013 to 2014 in Punjab was 4,089,100 tonnes (Anonymous, 2006). Given the weak financial aptitude of small landholder growers, the chemical or synthetic fertilizers employed toward vegetable crops occur yet at incompetent frequencies which induce a decline in the magnitude of profit (Abera, 2017). In Pakistan, number of small-scale vegetable growers cannot manage to buy chemical fertilizers and big landholder vegetable growers used it in inadequate quantities, which is badly affecting soil and causing degradation. Therefore, alternative options and/or combined prospects should be employed to enhance the yield and

production of the crop for small landholder farmer's cropping systems. Tomato (*Lycopersicon esculentum* Mill) exists as a beneficial cash-crop for small landholder growers within the transboundary of Pakistan. Although, the state mean tomato capitulate exists usually very low (10.1 tonnes/ha) (Food and Agricultural Organization (FAO) (2013). Chemical or synthetic fertilizers, specifically UREA and Di-ammonium Phosphate (DAP) are utilized for better yield production during the past decades in Pakistan. The Fertilizers are the principal input in agriculture and used extensively each year. This extensive use induces a notable reduction in farmer average profit which leads to poor farming operations as well as a decline in the living standards of farmers. As usual, an accelerating inclination of chemical fertilizer application is perceived alongside the growth in the farming practice of Pakistan in the last several decades. Because of the increment in the population and the reduction in agricultural land availability. The use of fertilizer becomes the permanent source to improve crop potency per acre. Although, alternative possibilities should be attempted to promote the access of small landholder farmers to manage their soil fertility, consequently bio-slurry can become a major source which can be experimented for combined and controlled soil fertility ingredients under different irrigation frequencies. Recently, a



major developing focus is on Integrated Nutrient Management (INM) that will assist better environmental farming with diminished usage of chemical or synthesized fertilizers within the farming sector Sarker *et al.* (2020). Bio slurries are very alike to those organic matter produced after several alterations and are perceived to possess better effects on soil water-holding capacity, soil structure, and microbial exercise thus developing the chemical, physical, and biological condition of the soil over supplementing organic fertilizer and basic nutrients regarding plant requirement to the soil Goberna *et al.* (2011). The tomato crop reacts favorably to a more leading watering area. An adequate amount of applying fertilizers and suitable irrigation systems is a particularly significant determinant influencing the quality and yield of tomato crops. Irrigation application by using a drip system and better superintendence of nutrients by fertigation, improve the quality and also yield just because of the peculiar handle protecting land and water-borne infections Singh *et al.* (2002).

This research executed to estimate the impacts of the individual and combined use of fertilizers (e.g. bio-slurry and chemical fertilizer like N, P, K) and check its impact on crop germination, growth of the plant, yield, and soil properties, at the University of Agriculture Faisalabad. The proposed study will focus on monitoring soil fertility, soil texture, and soil structure, nutrient holding capacity, water holding capacity, and crop yield. A comprehensive plan will be developed to improve soil fertility and water holding capacity to increase crop production without affecting the soil.

### Study area and description

The research area is located in Faisalabad, Rachna Doab (land between two rivers Ravi and Chenab). The longitude and latitude of the experimental area were 73.06720 E and 31.43030 N correspondingly and at the height of 610ft above the sea level. The geographical location of the study area along with its soil and land use data map shown in Figure 1.

### Research methodology

The study was carried under the randomized complete block design (RCBD) with five blocks and 3 replications of each treatment. The maximum experimental area was 9.5 m<sup>2</sup>. Based on the design 5 blocks with a regular field size of

3 × 1.152m<sup>2</sup> were prepared. There was a total of 15 buckets and the average size of a single

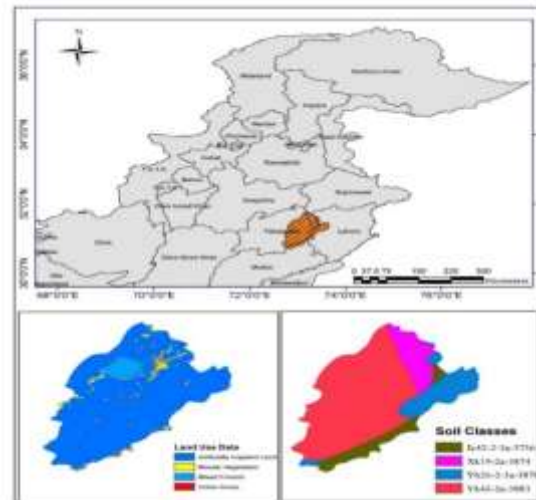


**Fig1:** Geographical location of the study area along with its soil and land use data map bucket was 1.1375ft<sup>2</sup>. The control block contains the 100% chemical fertilizer while four treatments are used under different combinations of organic and chemical fertilizer which are shown in Table 1. Field trials were conducted in a single tunnel for tomato crop and tomatoes were grown in buckets.

Each bucket contains two plants shown in Figure2.

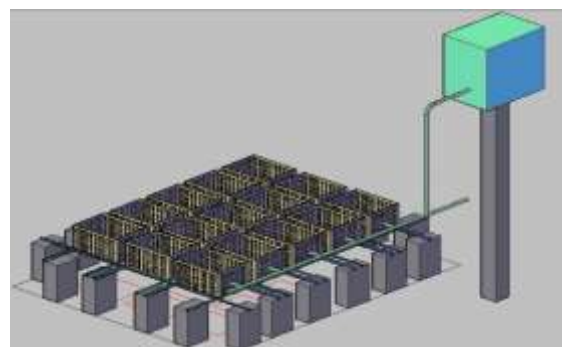


**Fig 2:** Specific layout of experiment Irrigation was done by using a drip irrigation method. Water was move by gravity, storage tank place at 4 feet height and 15 feet apart from the trial. The capacity of the storage tank was 26L. 0.5 inches' diameter of the pipe was to connect the tank to the main pipe of laterals and its length was used 18 feet. The 1-inch diameter of the pipe was used as the main pipe and its length was 8 feet. Five laterals pipe was connected to the main pipe at a spacing of 1.2 feet between each. The length of laterals was 10 feet of each and the dripper was fix at the top of every plant. PVC pipe of black color was used as laterals and the diameter of that pipe was 14 mm.

**Table 1:** Treatment description

Fertilizers	Control	T1	T2	T3	T4
Artificial	100 %	75 %	50 %	25 %	0%
Organic	0%	25 %	50 %	75 %	100 %

## Results and discussion

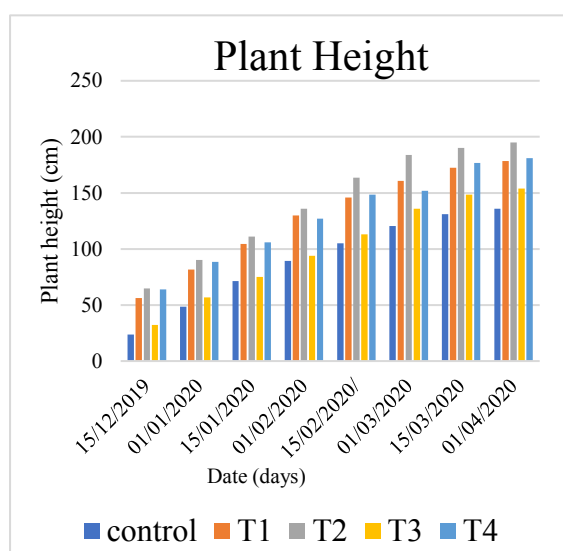
The water productivity was calculated by dividing the crop yield to water use for plant growth. It was done by using CROPWAT software, which calculate the total gross irrigation by using the climatic data of the research station (UAF), which is equal to 699.6mm.

### Statistical analysis

#### Plant height: -

The height of all experimental plants was measured by using measuring tape from the bottom up.

The column graph between different treatments and plant height (in centimeter) is shown in Figure 2. Figure 2 shows that plant height increase with time. From the graph T2 (50% bio-slurry + 50% inorganic fertilizer) shows the maximum plant height and control (or farmer practices) shows minimum plant height. The height of the plant ranges between 2.5m-5.0m tall (Adekiya, 2019).

**Fig 3:** Graphical representation of plant height

#### Fruit weight: -

The fruit weight (grams/plant) of all experimental plants was measured by using beam

balance. Statistical report for average fruit weight was done by using Minitab (analysis of variance) with the comparison of mean between treatments using the RCBD test at 5% probability. Table 2 shows that the relationship between all treatments for fruit weight was significant under the 5% significance level. The value of P is less than 0.05, hence prove that fruit weight was significant and varies for all treatment.

**Table 2:** ANOVA for fruit weight

Source	DF	Adj SS	Adj MS	F-Value	P-Value
Treatments	4	256.7	64.18	57.74	0.00*
Blocks	2	1.22	0.61	0.55	0.59
Error	8	8.89	1.11	-	-
Total	14	266.8	-	-	-

#### Yield: -

The yield of tomato (tonnes/acre) of all experimental plants was calculated. Statistical report for average yield was done by using Minitab (analysis of variance) with the comparison of mean between treatments using the RCBD test at 5% probability which is shown in Table 3.

**Table 3:** ANOVA for tomato yield

Source	DF	Adj SS	Adj MS	F-Value	P-Value
Treatments	4	1.24	0.31	60.28	0.00*
Blocks	2	0.00	0.00	0.60	0.57
Error	8	0.04	0.00	-	-
Total	14	1.29	-	-	-

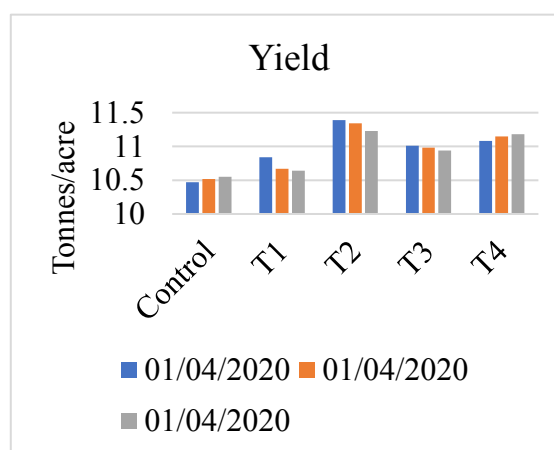
**Fig 4:** Graphical representation of yield

Table 3 shows that the relationship between all treatments for fruit yield was significant under the 5% significance level. The value of P is less than 0.05, proving that the fruit yield was significant and vary for all treatment. The graphical illustration between five treatments and

the yield at harvesting time was shown in Figure. 3, which is shown T2 (50% bio-slurry + 50% inorganic fertilizer) have a maximum yield of tomato as compared to other treatments. The minimum yield was produced in control or farmer practices (100% inorganic fertilizer). The yield per unit of irrigation moisture is between 1.09 and 1.11 kg m<sup>-3</sup> (Sarwar and Perry, 2002).

### Water productivity

The water productivity of tomato (Kg/m<sup>3</sup>/acre) of all experimental plants was calculated by dividing the crop yield to water use for plant growth. Statistical report for average yield was done by using Minitab (analysis of variance) with the comparison of mean between treatments using the RCBD test at 5% probability which is shown in Table 4. Below is the data on the yield of the plant and its graph concerning all treatments.

**Table 4:** ANOVA for water productivity

Source	DF	Adj SS	Adj MS	F-Value	P-Value
Treatments	4	1.00	0.25	61.07	0.00
Blocks	2	0.00	0.00	0.49	0.63
Error	8	0.03	0.00	-	-
Total	14	1.03	-	-	-

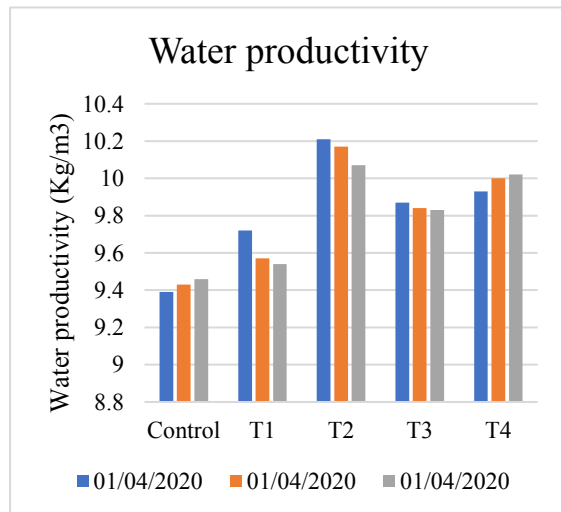


**Fig 5:** Graphical representation of WP

The ANOVA (analysis of variance) for water productivity shown in Table 4 that P for all treatments has less than 0.05. This P-value shows that all treatments were significant. The graphical illustration between five treatments and water productivity at harvesting time was shown in Figure. 4, which is shown T2 (50% bio-slurry + 50% inorganic fertilizer) have maximum water productivity of tomato as compared to other treatments. The minimum yield was produced in

control or farmer practices (100% inorganic fertilizer). The total virtual water range for crops differs widely from 491 m<sup>3</sup> / ton for vegetables to 6974 m<sup>3</sup> / ton for fluffy cotton (Ali *et al.*, 2019).

### Conclusion

We concluded that daily irrigation to tomato crops through drip irrigation enhances the water productivity of tomato crops. It is also concluded that organic fertilizer (bio-slurry) gave much better results than imported fertilizer (NPK), and made sure the economical production of tomato crop. As the locally developed fertilizer comprises all macro and micronutrients, which are important for the growth of the plant from the first day to till maturity level.

### Acknowledgement:

This research was funded and supported by the Technology Development Fund of Higher Education Commission of Pakistan grant# TDF-02-053.

### References

- Abera, G. 2017. Determination of organic materials quality based on nutrient recovery, mineral fertilizer equivalency and maize (*Zea mays* L.) allometry. *Arch. Agron. Soil Sci.* 63:48–59.
- Adekiya, A.O. 2019. Green manures and poultry feather effects on soil characteristics, growth, yield, and mineral contents of tomato. *Sci. Hortic. (Amsterdam)*. 257:108721.
- Ali, T., A.M. Nadeem, M.F. Riaz and W. Xie. 2019. Sustainable water use for international agricultural trade: The case of Pakistan. *Water (Switzerland)* 11.
- Food, F.A.O. 2013. Agricultural Organization. Production and Trade, Honey, Natural 2007–2011.
- Goberna, M., S.M. Podmirseg, S. Waldhuber, B.A. Knapp, C. Garcia and H. Insam. 2011. Pathogenic bacteria and mineral N in soils following the land spreading of biogas digestates and fresh manure. *Appl. Soil Ecol.* 49:18–25.
- Sarker, S.A., S. Wang, K.M.M. Adnan and M.N. Sattar. 2020. Economic feasibility and determinants of biogas technology adoption: Evidence from Bangladesh. *Renew. Sustain. Energy Rev.* 123:109766.

Sarwar, A. and C. Perry. 2002. Increasing water productivity through deficit irrigation: Evidence from the indus plains of Pakistan. *Irrig. Drain.* 51:87–92.

Singh, S., S. Varma and R. Singh. 2002. Integrated nutrient management in rice and its residual effect on lentil. *Indian J. Agric. Res.* 36:286–289.

## Evaluation of Root Zone Behavior and Cucumber Yield under Different Mulch Materials

Malik Mubashar Ishaq<sup>1</sup>, Muhammad Zaman<sup>2\*</sup>, Junaid Nawaz Chauhdary<sup>3</sup>, Muhammad Zeeshan Khan<sup>2</sup>, Shabana Kausar<sup>2</sup>

<sup>1</sup> Planning Commission, Government of Pakistan, Islamabad

<sup>2</sup> Department of Irrigation and Drainage, University of Agriculture, Faisalabad.

<sup>3</sup> Water Management Research Centre, University of Agriculture, Faisalabad.

Corresponding author email: [muhammad.zaman@uaf.edu.pk](mailto:muhammad.zaman@uaf.edu.pk)

**Abstract:** Nowadays water status is not up to the mark both in terms of quality and quantity as evapotranspiration causing major issues in terms of water shortage in semi-arid and arid regions, i.e. Faisalabad. This study was designed to check the impact of different mulch materials coupled with various irrigation schedules on cucumber yield and its root zone behavior. Three types of mulches; black (B), transparent (T) and coconut fiber (CF), each under two different levels of 20% and 40% DI (deficit irrigations) were used as treatments with control treatment (C) under furrow and no mulch condition. Objective was to inspect the soil moisture at different depths and root development in terms of its depth and diameter from each plot. Maximum root length was observed in case of treatment T40 (86.9 cm) followed by treatment B40 (85.4 cm) and minimum root length was observed in treatment C (67.8 cm). Maximum diameter of root was found in CF40 treatment (5.96 mm) followed by CF20 treatment (5.90 mm) and minimum diameter was found in C treatment (5.33 mm). Maximum moisture (0.273) with  $R^2=0.894$  for linear model was found after 90 days of sowing under furrow irrigation at 30 cm depth, besides, minimum moisture (0.064) with  $R^2=0.855$  for linear model was simulated after 30 days of sowing under 40% DI at 5 cm depth. Maximum yield was obtained from T20 treatment (42.3 tons/ha) followed by B20 treatment (40.2 tons/ha), while, minimum yield has been obtained from the C treatment (32.2 tons/ha).

**Keywords:** mulch, deficit irrigations, yield

### Introduction

Cucumber is from the family of cucurbitaceus that is cultivated in hot and low temperature tropics. Processing of cucumber is not much difficult as cucumber can be preserved and stored. Cucumber is assumed as one of the most economical vegetable as its consumption is increasing day by day (Anderson *et al.*, 1995). Demand of food is getting higher with each passing day and expected to be twice by 2050 (Tilman *et al.*, 2011), because of rise in the population growth and the increase in animal food. In order to compete this higher demand of food/grain and competing the food supply challenges are the main concerns of many policy makers and scientist communities (Godfray *et al.*, 2010). Keeping this scenario in mind and with decreased water available to lands, high production can be produced only by attempting the best use of precious resources like water in both arid and semi-arid areas (Haddad *et al.*, 2011). Most effective way to supply nutrients and water to plants is trickle irrigation which not only reduces the application of water but also

enhances the production of vegetables and fruits. Water is saved in this way due to less storage of water in the crop root zone and reduction in the percolation of fertilizers and water (Shehata *et al.*, 2019). Mulching is an effective method of deploying the environment of growing crop in order to enhance the production and quality of the crop by managing the temperature, conserving moisture in the soil and by reducing the evaporation from the soil (Chakraborty *et al.*, 2008). Color of covering/mulch and its transparency have a substantial effect on soil hotness and on the growth of crop. This is found that transparent mulch causes highest temperature followed by black colored mulch while no-mulch soil has lowest temperature (Salokangas, 1973). Use of mulching increases the plant growth and linked with higher yields and earliness of picking of crop (Abdul-Baki *et al.*, 2019; Ibarra *et al.*, 2001). Most famous replacement to plastic films include paper coverings, organic coverings resulting from urban and agricultural waste products and biodegradable films that are environmental friendly (Monks *et al.*, 1997; Miles *et al.*, 2012). Alternate furrow irrigation (AFI) and drip are

suitable practices for supervision of deficit irrigation in arid and semi-arid areas. In these waterings, deep infiltration and evaporation from the surface are abridged and fewer water is used (Sepaskhah and Kamgar-Haghighi, 1997; Sepaskhah and Hosseini, 2008; Ahmadi *et al.*, 2010).

It was found that many of the researches were carried out to check the parameters that exists above the ground but contrary to this only a few researches were carried out below the ground. Therefore, this study was planned to have an idea about the mechanism undergoing beneath the ground as well as above the ground. To avoid the losing of water plastic mulches are used which are good at their purpose. Major problems of these mulches are their non-biodegradability which lasts for 10 to 1000 years and causes many diseases both in animals that ingest the plastic during grazing and human beings. Moreover, plastic is going to be banned soon so, alternatives of these plastic mulches is necessary as soon as possible.

This study was carried out to cope up with all the problems mentioned above using three types of mulches including transparent plastic mulch (T), black plastic mulch (B) and coconut fiber (CF) with two different levels of irrigation at 40% deficit irrigation and 20% deficit irrigation. .

### Study area and data description

Experimental study was carried out in Faisalabad District at farmer field near Water Management Research Center (WMRC), University of Agriculture Faisalabad. Location Coordinates of the study area are 31° 21' 36'' N, 73° 00' 36'' E. Study area bears light winds and summers are found to be moist and hot while winters with cool and dry climate. Soil of the study area is mostly silty loam and very fine sand that makes a very weak subsoil. Mixed-wheat cropping system with wheat as major Rabi crop and rice and maize in Kharif season is being followed. RCBD was used for this study with 6 treatments and 3 replications with a control.

Aric CMS 81 variety of cucumber with minimum 70% germination was sown in winter at a plant to plant distance of 10 inches and row to row distance of 12 inches with conventional method. Drip line with diameter of 16 mm and emitter to emitter spacing of 9 inches with emitter discharge of 4 lph was used in the experiment.

### Research Methodology

Transparent mulch at 40% deficit irrigation (T40), Transparent mulch at 20% deficit irrigation (T20), Black plastic mulch at 40% deficit irrigation (B40), Black plastic mulch at 20% deficit irrigation (B20), coconut fibre mulch at 40% deficit irrigation (C40), coconut fibre mulch at 20% deficit irrigation (C20) and control treatment under furrow irrigation were used as treatments. CROPWAT 8.0 was used to convert sunshine hours into radiation. Hydrus-1D model was used in this study to simulate the moisture content at different depths. This uses linear finite elements to solve the Richards equation numerically for saturated, unsaturated water flow.

Hydrus-1D model was used in this experiment to model/ analyze the water movement. Moisture content measured from Time Domain Reflectometer was compared with the simulated values of moisture content for 6 different treatments. Length of root was measured for all the treatments after 30, 60, 90 and 131 days after sowing of crop with the help of Vernier Caliper. Similarly diameter of root was measured with the help of Vernier Caliper for all the treatments. At the end, yield of crop was observed to choose the best treatment for recommendation to the farmers. Methodology plan is given in the Figure 1.

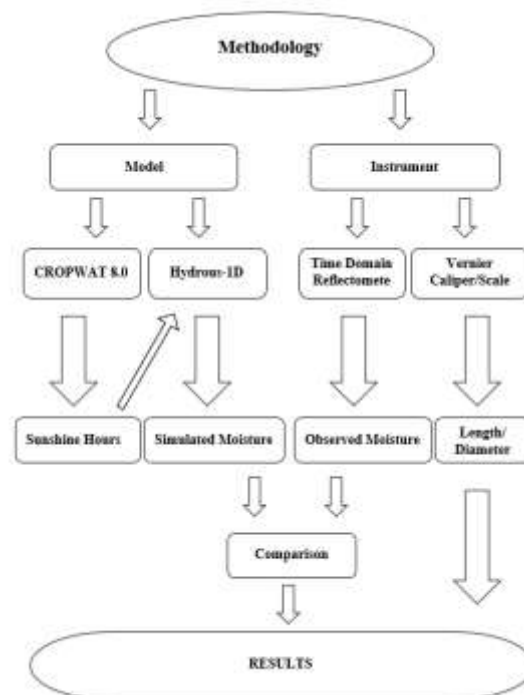


Fig. 1: Methodology Plan



## Results and Discussion

Root length was measured at different time intervals of 30, 60, 90 and 131 days after sowing of crop with the help of scale and Vernier Caliper. Maximum root length was found in case T40 treatment (86.9 cm) followed by B40 treatment (85.4 cm), T20 treatment (84.7 cm), CF40 treatment (83.4), B20 treatment (78.8 cm), CF20 treatment (75.0 cm) and C treatment (67.8 cm) respectively.

Root diameter of the crop was determined using Vernier caliper near the surface of soil. This was observed that maximum diameter of root was found in CF40 treatment (5.96 mm) followed by CF20 treatment (5.90 mm), T40 treatment (5.89 mm), B40 treatment (5.88 mm), T20 treatment (5.80 mm), B20 treatment (5.79 mm) and C treatment (5.33 mm) respectively.

Moisture content at different depths is measured with the help of time domain reflectometer (TDR) and values are compared with the moisture obtained from model. This can be seen that moisture is increasing with each passing day and with the depth. At the last stage of crop, this has been seen that moisture decreased with higher temperature at the last crop stage than the early growth stages (Choi and Jacobs, 2007).

Results depict the highest value of moisture at 30 cm depth after 90 days of sowing under furrow irrigation followed by moisture at 60 and 131 days under furrow irrigation which is same because of the difference of temperature. Minimum moisture content was observed at a depth of 5 cm with 40% deficit irrigation after 60

days of sowing which is very close to that of moisture at a depth of 5 cm with 40% deficit irrigation after 30 days of sowing. This minimum moisture content is resulted because of evaporation from the upper layers of soil.

Maximum yield has been obtained from T20 treatment (42.3 tons/ha) followed by B20 treatment (40.2 tons/ha), T40 treatment (39.8 tons/ha), CF20 treatment (38.6 tons/ha), B40 treatment (37.3 tons/ha) and CF40 treatment (36.7 tons/ha). While, minimum yield has been obtained from the C treatment (32.2 tons/ha). Combine comparison of all the treatments is given in Table: 1.

## Conclusion

It was concluded that yield of cucumber was maximum in treatment T20 (Transparent plastic mulch at 20% DI) and recommended as best technique in semi-arid region. Ranking wise results showed that T20 is best treatment and suitable treatment for the farmer revenue. It was concluded that mulch has significant effect on moisture content in the soil root zone and yield of cucumber. It is suggested that biodegradable mulches should be tested to find an alternative of plastic mulch as it is going to be banned soon.

## Acknowledgement

This research was funded and supported by the Technology Development Fund of Higher Education Commission of Pakistan grant# TDF-02-053.

**Table: 1:** Combine Comparison

Treatment	Root Diameter (mm)	Root Length (cm)	Crop Yield (t/ha)	Soil Moisture (%)	Ranking
T40	5.89	86.9	39.8	0.129	2
T20	5.80	84.7	42.3	0.139	1
B40	5.88	85.4	37.3	0.129	5
B20	5.79	78.8	40.2	0.139	4
CF40	5.96	83.4	36.7	0.129	5
CF20	5.90	75.0	38.6	0.139	3
C	5.33	67.8	32.2	0.273	6

## References

Abdul-Baki, A., C. Spence and R. Hoover. 2019. Black polyethylene mulch doubled yield of fresh market field tomatoes. Hort. Science. 27: 787-89.

Ahmadi, S.H., M.N. Andersen, F. Plauborg, R.T. Poulsen, C.R. Jensen, A.R. Sepaskhah and S. Hansen. 2010. Effects of irrigation strategies and soils on field grown potatoes: yield and water productivity. Agric. Water Manag. 97: 1923-1930.

- Anderson, D. F., M. A. Garisto, J. C. Bourrrut, M. W. Schonbeck, R. Jaye, A. Wurzberger, and R. DeGregorio. 1995. Evaluation of a paper mulch made from recycled materials as an alternative to plastic film mulch for vegetables. *J. Sustain. Dev.* 7: 39-61.
- Chakraborty, D., S. Nagarajan, P. Aggarwal, V.K. Gupta, R.K. Tomar, R.N. Garg, R.N. Sahoo, A. Sarkar, U.K. Chopra, K.S.S. Sarma and N. Kalra. 2008. Effect of mulching on soil and plant water status, and the growth and yield of wheat (*Triticum aestivum* L.) in a semi-arid environment. *Agric. Water Manag.* 95:1323–1334.
- Choi, M. and J.M. Jacobs. 2007. Soil moisture variability of root zone profiles within SMEX02 remote sensing footprints. *Adv. Water Resour.* 30:883–896.
- Godfray, H.C.J., J.R. Beddington, I.R. Crute, L. Haddad, D. Lawrence, J.F. Muir, J. Pretty, S. Robinson, S.M. Thomas and C. Toulmin. 2010. Food security: The challenge of the present. *Science* (80-. ). 327:812–818.
- Haddad, N., M. Duwayri, T. Oweis, Z. Bishaw, B. Rischkowsky, A.A. Hassan and S. Grando. 2011. The potential of small-scale rainfed agriculture to strengthen food security in Arab countries. *Food Secur.* 3:163–173.
- Ibarra, L., J. Flores and J. C. Diaz-Perez. 2001. Growth and yield of muskmelon in response to plastic mulch and row covers. *Sci. Hortic.* 87: 139-145.
- Miles, C., R. Wallace, A. Wszelaki, J. Martin, J. Cowan, T. Walters and D. Inglis. 2012. Deterioration of potentially biodegradable alternatives to black plastic mulch in three tomato production regions. *HortScience* 47:1270–1277.
- Monks, C.D., D.W. Monks, T.O.M. Basden, A. Selders, S. Poland and E. Rayburn. 1997. Soil Temperature, Soil Moisture, Weed Control, and Tomato (*Lycopersicon esculentum*) Response to Mulching. *Weed Technol.* 11:561–566.
- Salokangas, K. 1973. Effect of polyethylene and paper mulching on yield and earliness of pickling cucumber. *Acta Hortic.* 27: 223-226.
- Sepaskhah, A.R. and A.A. Kamgar-Haghighi. 1997. Water use and yields of sugarbeet grown under every-other-furrow irrigation with different irrigation intervals. *Agric. Water Manag.* 34: 71-79.
- Sepaskhah, A. R. and S. N. Hosseini. 2008. Effects of alternate furrow irrigation and nitrogen application rates on yield and water- and nitrogen-use efficiency of winter wheat (*Triticum aestivum* L.). *Plant Prod. Sci.* 11: 250-259.
- Shehata, M., M. Abd El-Hady and N. El-Magawry. 2019. Effect of Irrigation, some Plant Nutrients with Mulching on Growth and Productivity of Cucumber. *J. Plant Prod.* 10:231–239.
- Tilman, D., C. Balzer, J. Hill and B.L. Befort. 2011. Global food demand and the sustainable intensification of agriculture. *Proc. Natl. Acad. Sci. U. S. A.* 108:20260–20264.

## Modelling of Rainfall-runoff process by GEP, RBF-SVM and M5 model tree in Jhelum River Basin, Pakistan

Muhammad Waqas<sup>1</sup> Muhammad Saifullah<sup>1</sup>, Sarfraz Hashim<sup>1</sup>, Muhammad Shoaib<sup>2</sup>, Adila Naseem<sup>3</sup>,  
Mohsin Khan<sup>1</sup>

<sup>1</sup> Department of Agricultural Engineering, Muhammad Nawaz Shareef University of Agriculture, Multan  
66000, Pakistan

<sup>2</sup> Department of Agricultural Engineering, Bahauddin Zakariya University, Multan

<sup>3</sup> Department of Food Science, Bahauddin Zakariya University, Multan

Corresponding author email: [muhammad.waqas@mnsuam.edu.pk](mailto:muhammad.waqas@mnsuam.edu.pk)

**Abstract:** Globally, water management play a crucial role in economy of region and in sustainability of lives, whereas rapid growth of urbanization and irregular depths and frequencies also damaging the water storing capacity and management. This study examined the data driven model (DDM), Gene Expression Programming (GEP) for the modelling of rainfall-runoff process. According to results, in Winter Substantial downward trend was observed. Likewise, in Summer upward trend was detected at 8.03 m<sup>3</sup>/sec and downward trend of -2.48 m<sup>3</sup>/sec annually found. Flow Duration Curves (FDCs) were employed to evaluate the applied DDM against percent of Time. The FDCs revealed that GEP was better DMM for high flows and medium high flows. This study provides indication that M5 model tree is a feasible alternative to other DMMs with R<sup>2</sup>, COE, MSE and NRMSE 1.00, 1.00, 0.00, 443.76 m<sup>3</sup>/sec respectively. GEP was found more accurate DDM and highly efficient for modelling of and prediction of rainfall-runoff process.

**Keywords:** Data Driven Models, Gene expression programming, Flow Duration Curves. Prediction

### Introduction

The efficient and precise modelling of hydrological phenomenon like rainfall-runoff process is crucial in the planning of hydrological management i.e. urban sewer management, runoff prediction and irrigation and drainage systems. The rainfall-runoff process directly dependent on basin features and other meteorological components. Being a stochastic process of transformation of rainfall to runoff, many DDMs have been expressed to forecast this diverse process (Shoaib et al., 2019). According to (Penman, 1961) hydrology is a science which helps to deeply explore the question “ what happens to precipitation” furtherly, the transformation of precipitation into runoff is main feature of this query (Dariane & Karami, 2014). Runoff prediction is an important issue in hydrology and water resources management by using rainfall and other hydrological parameters. Rainfall-runoff phenomenon is one of the complex non-linear process which cannot be modeled by simple data driven models, several hydrological variables such as evaporation, infiltration, rainfall intensity, geomorphology of the basin and interaction in surface and groundwater flows plays crucial role in rainfall-

runoff process. In past few decades, data driven models (DDMs) such as Artificial Neural Network (ANN), Genetic Programming (GP), Support Vector Machines (SVMs), Decision Trees (DTs) and Adaptive Neuro Fuzzy Inference System (ANFIS) are become popular in hydrology and water resources. Thus far, the application of DDMs in prediction of rainfall-runoff and other variables are reported in several literatures (Dawson & Wilby, 1998; Hsu, Gupta, & Sorooshian, 1995; Kişi, 2009; Smith, Eli, & management, 1995; Tayfur, Moramarco, & Singh, 2007; Tokar & Johnson, 1999). In hydrology, on the concept of learning function of neurons of human brain, ANNs were progressively deployed from 1990s. The applications of ANNs in the field of hydrology a comprehensive study is mentioned in ASCE Task Committee (Engineering, 2000a, 2000b). There are many applications of ANNs by utilizing various learning algorithms in literature (Campolo, Andreussi, & Soldati, 1999; Cigizoglu & Kişi, 2005; Coulibaly, Anctil, & Bobee, 2000; Shoaib et al., 2019; Shoaib, Shamseldin, Melville, & Khan, 2015). However, ANNs have some drawbacks comprising over training, complexity, trapping in local minima and deployment of weights randomly. In this

study, GEP was used for rainfall-runoff modelling. Firstly, genetic programming (GP) was proposed by (Koza & Koza, 1992), as a generalization of Genetic Algorithms (GAs) (Goldberg, Barker, & Perez-Grau, 1989); the use of GP limited because of hypothetical examination is inhibited by norms; it is suitable where inter-relationship between the input variables are poor and require monotonous processing of huge quantity of dataset in computer understandable forms (Banzhaf, Nordin, Keller, & Francone, 1998). To model a program, a set of dependent and independent variables are referred. Initial population is first step in which it selects random population. By estimating the values of the independent and dependent variables the fitness of each program is calculated. After achieving efficient performance, the population develops from one to another generation and old models replaced by new once. At last, the program will be choosing conferring to their own fitness criteria. To achieve targeted process, the previous mentioned modelling was repeated till achievement. In this study Gene Expression Programming (GEP) is selected for rainfall-runoff modelling which is totally based on different sizes and shapes programmed in linear chromosomes of defined lengths (C. Ferreira, 2006; C. J. a. p. c. Ferreira, 2001). In GEP, two main performers namely expression trees (ETs) and chromosomes, which are expression genetic encoding of each chromosomes and each chromosomes consists of many genes of equal length (C. Ferreira, 2006). This study was arranged in such a way to employ GEP to achieve the major objective of this research as: 1) to calibrate and validate the DDM GEP for the modelling of rainfall-runoff process. To achieve these objectives, hydrological data of rainfall and runoff were employed in modelling of this process. To evaluate model performance some statistical evaluation parameters i.e. determination coefficient (R<sup>2</sup>), coefficient of efficiency (COE), mean squared error (MSE) and normalized root mean square error (NRMSE) were used.

### Study area and data description

The Jhelum river basin situated at upstream of Mangla dam, the geographical coordinates of Mangla Dam are 33.142083 °N and 73.645015 °E having total area of basin 33,867 km<sup>2</sup>. The Jhelum River originates from Pir Panjal from the North Western part of great Himalayan range and

gets significant flow from its tributaries and Jhelum river is an eastern tributary of Indus River. Jhelum River gets flows from Wular lake in Kashmir Valley and one of the main tributaries is about 130 Km downstream of Wular lake, Kunhar River and Neelum River falls into Jhelum River at Muzaffarabad. At Mangla reservoir Poonch and Kanshi joins the Jhelum River, both are important tributaries of Jhelum River. Jhelum River basin has 56% of its area about 18,966 km<sup>2</sup> lied in India like other rivers i.e. Ravi, Bias Indus and Chenab, Globally, such problems of disputed boundaries effects the other rivers in Pakistan and other river basins around the world (Bastiaanssen, Cheema, Immerzeel, Miltenburg, & Pelgrum, 2012). In this study, the area used approximately lies at elevation 2194 m with about 11,006 km<sup>2</sup> area lies above 3000 m elevation. Around 25 % of Jhelum river basin lies at in areas where maximum snow accumulation occurred. In this basin, rainfall data of previous years are accessible only below the elevation of 2800m which makes it scarcely gauged basin. The daily runoff data of Jhelum river basin are gathered from Mangla Dam with mean flow of 794 m<sup>3</sup>/s, measured from past dataset of 32 years from 1981-2012 which is provided by the Surface Water Hydrology Project, SWHP. The Jhelum river basin is mostly affected by the monsoon rainfall season whereas, the Indus Basin is not affected during Summer season due to rain shadow of Himalaya range which make Eastern Himalayan climate chronicles (Fowler & Archer, 2006; Immerzeel, Droogers, De Jong, & Bierkens, 2009; Young & Hewitt, 1990). In this Study, daily rainfall data of Nine stations lying Jhelum river basin mentioned in Table 1. There are major two rainfall sources in Jhelum river basin 1) Monsoon Rainfall 2) Western snowfall or disturbance. The monsoon season starts from June to September and Western disturbance take place from December to March of every year (Bookhagen & Burbank, 2006). Annually rainfall varies from 680-1600mm at Srinagar and Gharidupata, respectively, while it decreases from northern part towards eastern part to 870mm at Mangla region. The annual rainfall varies from 70-135% average to maximum of average (Archer & Fowler, 2008; M.J.P.P.D.T. Azmat, University of Porto, Porto, Portugal, 2015).

### Data Acquisition

The climatic data (Daily rainfall) is gathered from Surface Water Hydrology Project of the Water and Power Development Authority (SWHP- WAPDA) from year 1981-2012. Nine rainfall gauges data at different elevations within the boundary of Pakistan are described in Table 1. The runoff data has been collected from Mangla Dam from 1981-2012 which is mentioned in Error! Reference source not found. As Astore station is lied in Upper Indus basin, several researchers used its rainfall dataset for sub catchment of Neelum River (M. Azmat, Liaqat, Qamar, & Awan, 2017). The nine rainfall stations used namely Astore, Balakot, Muzaffarabad, Gharidopatta, Murree, Rawlakot, Plandri, Kotli and Jhelum with elevation and mean rainfall from 1981-2012 which were 2454, 975, 679, 817, 2291.2, 1638, 1400, 3000, 234m and 1.2, 4.4, 4.1 ,3.82, 4.7, 3.6, 3.7, 3.5, 2.3mm respectively. The statistics of the rainfall stations are mentioned in Table 1.

### Model Fitness Criteria

To evaluate the reliability and performance of the applied DDMs for modelling of rainfall- runoff process different performance evaluation criteria (Shoaib et al., 2018; Shoaib et al., 2015) 1) Co-efficient of determination ( $R^2$ )(Menard, 2000); (2) Normalized root mean square error (NRMSE)(Levinson & Physics, 1946); (3) Nash-Sutcliffe Coefficient of efficiency (COE)(Nash & Sutcliffe, 1970) (4) Mean square error (MSE)(Allen, 1971) were used.

$$R^2 = \frac{n(\sum xy) - (\sum x)(\sum y)}{\sqrt{[n(\sum x^2) - (\sum x)^2][(\sum y^2) - (\sum y)^2]}} \quad (1)$$

$$NRMSE = \frac{\sqrt{\frac{\sum_{i=1}^N (Q_{obs} - Q_{pre})^2}{N}}}{\sigma} \quad (2)$$

$$COE = 1 - \frac{\sum_{i=1}^N (Q_{obs} - Q_{pre})^2}{\sum_{i=1}^N (Q_{obs} - Q_{mean})^2} \quad (3)$$

$$MSE = \frac{\sum_{i=1}^N (Q_{obs} - Q_{pre})^2}{N} \quad (4)$$

Where, Qobs and Qpre are the observed and predicted flows respectively while Qmean is the mean of observed flows.  $R^2$  tells us how fit line of regression approaches the actual data in regression, value 1 illustrate that line efficiently fits the actual data. Each parameter is accessible by indicator assessed from comparison the predicted and observed values that were used in

the training and testing. The MSE can be used to quantify the difference between the average sum of squares of predicted and observed values. The lower values of MSE and NRMSE shows the precision of model.

## Research Methodology

### Gene Expression Programming (GEP)

Comprehensive explanations of Genetic Programming (GP) and Gene Expression Programming (GEP) are provided by Koza and Ferreira (C. Ferreira, 2006; C. J. a. p. c. Ferreira, 2001) respectively. GP was first suggested by Koza (Koza & Koza, 1992). It is a simplification of Genetic Algorithms (GA) (Goldberg et al., 1989). The major consistency between GP, GA and GEP is caused by the behavior of the individuals. In the GA, the entities have fixed lengths e.g. chromosomes and linear in nature. In the GP, the entities have different in shapes and sizes have non linearity behavior e.g. parse trees. In the GEP, the entities are programmed as linear series of constant length e.g. genome (C. Ferreira, 2006; C. J. a. p. c. Ferreira, 2001). GP is search system/technique that allows the problems solutions by self-creating algorithms and expressions. These algorithms are coded like a tree structure with its leaves (terminals) and functions (nodes). Basically, GP programmed the GA's by means of tree-structures. There are major five initial steps for the solution of problems using GP. These are the purpose of (1) terminals set (2) functions set (3) measure of fitness (4) control the run by quantitative variables and numerical parameters (5) the condition of describing a result and terminating a results (Koza & Koza, 1992). The first major step for the preparation of GP hypothesis is to classify the terminals set that to be used in the computer programs individually. The main types of terminal sets consist of the independent variable, state variables and the functions without arguments. Types of these terminals sets are given in the table by Koza (Koza & Koza, 1992). The second main step is to define the functions set, testing functions (IF & CASE statements) and Boolean functions (AND, OR, NOT). The third main step is measuring the fitness, which identifies the method for assessing how good a given program tackles a specific issue. Junctions in the tree are form by two components terminals and functions. The fourth main step is the selection of definite parameters to control and

governor the run. Control parameters consist of the population size and the rate of crossover. The fifth and last main step is to terminate the run. Generally, the model is considered acceptable if there is no difference in between the model results and the data. When the terminal and non-terminal operators are indicated, it is possible to set up the types (C. Ferreira, 2006; C. J. a. p. c. Ferreira, 2001). The automatic program creation is carried out by following the Darwin's evolution theory, according to this, after successive generations, new trees are produced by old trees through copy, crossover and mutation(Fuchs, 1998). On the basis of natural selection, the superlative trees will have more probabilities of being preferred to become a part of upcoming generation. Hence, where a stochastic process is established a well-modified tree is achieved(Kisi, Shiri, Tombul, & Geosciences, 2013).

## Results and Discussions

In current paper, to examine the applied DDMs performances, we considered the daily rainfall data of nine stations and daily runoff data collected from Mangla Dam, Pakistan. The input selection was the first step in rainfall- runoff modelling, different input combination C1, C2, C3, C4, C5, C6 and C7 were used in this process which were mentioned previously. The first step in modelling of rainfall-runoff process is the selection of the fitness function. The input combination was engaged with the following functions set of DTREG (a+b), (a-b), (a\*b) (a/b) and sqrt(a). Linking function of addition with 10 constants per genes, the 4 genes chromosomes with 8 S.I units of each gene length were engaged.

Amongst the other fitness function i.e  $R^2$  and MSE, RRSE was found best function with other preliminary fitness function for rainfall-runoff modelling mentioned in Error! Reference source not found. for rainfall-runoff modeling. According to the Bloat Phenomena during implementation of GEP models, without any increasing linkage to the model fitness the parse tree depth is increased (Kisi, Dailr, Cimen, & Shiri, 2012). In this study, to overcome this penalize tree depth, (More, 1978) Levenberg-Marquardt algorithm was used. Many researchers referred this algorithm in hydrological modelling i.e. (Coulibaly et al., 2000; Nourani & Kalantari, 2010; Raghuwanshi, Singh, & Reddy, 2006).

The training and testing results of with different inputs combinations C1, C2, C3, C4, C5, C6 and

C7 having selected operators in GEP mentioned in Table R<sup>2</sup> (0.89), NRMSE (280361.90 m<sup>3</sup>/sec) and MSE (-0.06) were found during training of model with input combination C1. The C6 was found poorest combination in used inputs with values R<sup>2</sup> (1.00), NRMSE (772.71 m<sup>3</sup>/sec) and MSE (0.00).

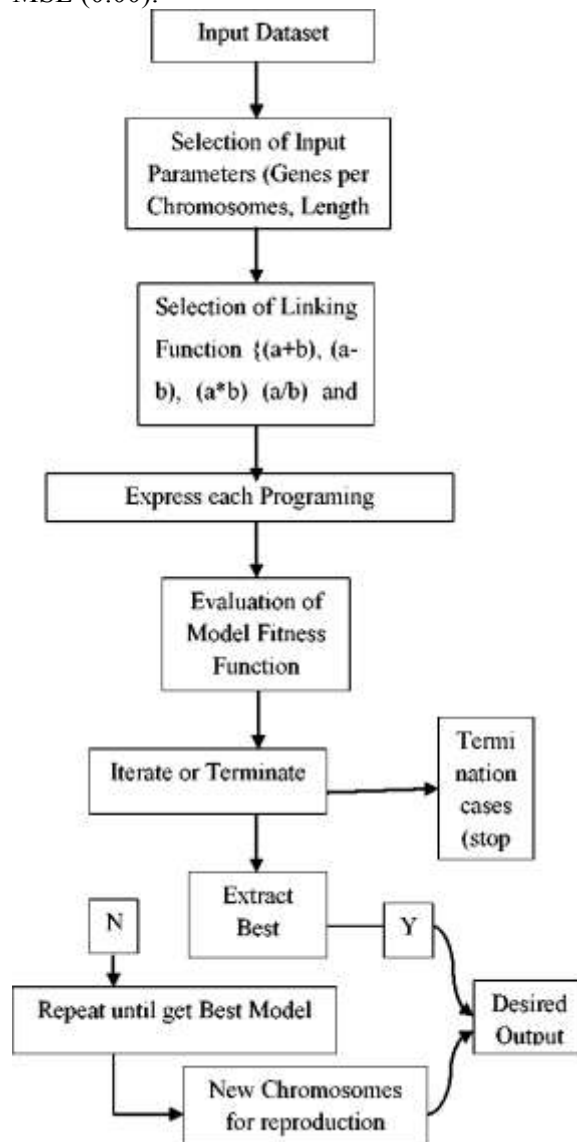


**Figure 1** Working layout of Gene Expression Programming (GEP)

While, the COE was 1.0 in overall training and testing of GEP. On the other hand, in testing of model, R<sup>2</sup> (1.00), NRMSE (1545.42m<sup>3</sup>/sec) and MSE (0.00) were detected and C2 found most efficient combination. But C5 was also has poor results R<sup>2</sup> (1.00), NRMSE (1556.95m<sup>3</sup>/sec) and MSE (117.17). Input combinations C6 and C7 also showed variations in testing. GEP has advantage over other DDMs because it is capable of giving mathematical relations between the input and outputs which is major reason of its



success (Kisi et al., 2013). Error! Reference source not found. shows the correlation between the observed runoff and predicted runoff by GEP for the Jhelum river basin for training (1981-2000) as well as testing (2001-2012) dataset respectively. During training period, there was found some irregular patterns but in testing predicted values accurately overlap with observed runoff for all input combinations (C1, C2, C3, C4, C5, C6 and C7).

## Conclusion

In this study, the prediction capability of DDM (GEP) was analyzed in modelling of rainfall-runoff process of Jhelum River basin, Western Himalaya, Pakistan a mountainous catchment. After that the prediction of runoff, observed data was evaluated by the performance evaluation criterion, Co-efficient of determination ( $R^2$ ) Normalized root mean square error (NRMSE), Nash-Sutcliffe Coefficient of efficiency (COE) and Mean square error (MSE) were used. The access the DDMs flow duration curves (FDCs) outcomes were also presented among the forecasted and observed data for each station. The conclusion of this study as follows: The results of applied DDM on the basis of model fitness criteria clearly explored that the potential of DDM for modelling of rainfall-runoff process in the Jhelum River basin. Different inputs were tried to achieve the target such as C1, C2, C3, C4, C5, C6 and C7 with lagged past daily data of rainfall and runoff. The best input combination C3 and C7 were found overall for this process which showed accurate and efficient results in training and testing respectively.

GEP has also showed good potential in modelling of rainfall-runoff process. The model fitness parameters were found  $R^2$ , COE, MSE and NRMSE, 1.00, 1.00, 0.00 and 772.71 m<sup>3</sup>/sec. Whereas, the RBF-SVM was found less accurate with results 1.00, 73.90 and 564.24 m<sup>3</sup>/sec.

## References

- Allen, D. M. J. T. (1971). Mean square error of prediction as a criterion for selecting variables. *13*(3), 469-475.
- Archer, D. R., & Fowler, H. J. J. o. H. (2008). Using meteorological data to forecast seasonal runoff on the River Jhelum, Pakistan. *361*(1-2), 10-23.
- Azmat, M., Liaqat, U. W., Qamar, M. U., & Awan, U. K. J. R. e. c. (2017). Impacts of changing climate and snow cover on the flow regime of Jhelum River, Western Himalayas. *17*(3), 813825.
- Azmat, M. J. P. P. D. T., University of Porto, Porto, Portugal. (2015). Water resources availability and hydropower production under current and future climate scenarios: The case of Jhelum River Basin, Pakistan.
- Banzhaf, W., Nordin, P., Keller, R. E., & Francone, F. D. (1998). Genetic programming: an introduction (Vol. 1): Morgan Kaufmann San Francisco.
- Bastiaanssen, W., Cheema, M., Immerzeel, W., Miltenburg, I., & Pelgrum, H. J. W. R. R. (2012). Surface energy balance and actual evapotranspiration of the transboundary Indus Basin estimated from satellite measurements and the ETLook model. *48*(11).
- Bookhagen, B., & Burbank, D. W. J. G. R. L. (2006). Topography, relief, and TRMM-derived rainfall variations along the Himalaya. *22*(8).
- Campolo, M., Andreussi, P., & Soldati, A. J. W. r. r. (1999). River flood forecasting with a neural network model. *22*(4), 1191-1197.
- Cigizoglu, H. K., & Kişi, O. J. H. R. (2005). Flow prediction by three back propagation techniques using k-fold partitioning of neural network training data. *26*(1), 49-64.
- Coulibaly, P., Anctil, F., & Bobee, B. J. J. o. H. (2000). Daily reservoir inflow forecasting using artificial neural networks with stopped training approach. *220*(3-4), 244-257.
- Dariane, A. B., & Karami, F. J. W. r. m. (2014). Deriving hedging rules of multireservoir system by online evolving neural networks. *28*(11), 3651-3665.
- Dawson, C. W., & Wilby, R. J. H. S. J. (1998). An artificial neural network approach to rainfall-runoff modelling. *42*(1), 47-66.
- Engineering, A. T. C. o. A. o. A. N. N. i. H. J. J. o. H. (2000a). Artificial neural networks in hydrology. I: Preliminary concepts. *2*(2), 115-123.
- Engineering, A. T. C. o. A. o. A. N. N. i. H. J. J. o. H. (2000b). Artificial neural networks in hydrology. II: Hydrologic applications. *2*(2), 124-137.
- Ferreira, C. (2006). Gene expression programming: mathematical modeling by an artificial intelligence (Vol. 21): Springer.
- Ferreira, C. J. a. p. c. (2001). Gene expression programming: a new adaptive algorithm for solving problems. Fowler, H., & Archer, D. J. J. o. C. (2006). Conflicting signals of

- climatic change in the Upper Indus Basin. 79(17), 4276-4293.
- Fuchs, M. (1998). Crossover versus mutation: An empirical and theoretical case study. Paper presented at the Proc. 3rd Annual Conference on Genetic Programming (GP-98).
- Goldberg, R. B., Barker, S. J., & Perez- Grau, L. J. C. (1989). Regulation of gene expression during plant embryogenesis. 26(2), 149-160.
- Hsu, K. I., Gupta, H. V., & Sorooshian, S. J. W. r. r. (1995). Artificial neural network modeling of the rainfall- runoff process. 21(10), 2517-2530.
- Immerzeel, W. W., Droogers, P., De Jong, S., & Bierkens, M. J. R. s. o. E. (2009). Large-scale monitoring of snow cover and runoff simulation in Himalayan river basins using remote sensing. 112(1), 40-49.
- Jha, M. K., Chowdhury, A., Chowdary, V., & Peiffer, S. (2007). Groundwater management and development by integrated remote sensing and geographic information systems: prospects and constraints. *Water resources management*, 21(2), 427-467.
- Kisi, O., Dailr, A. H., Cimen, M., & Shiri, J. J. J. o. H. (2012). Suspended sediment modeling using genetic programming and soft computing techniques. 420, 48-58.
- Kisi, O., Shiri, J., Tombul, M. J. C., & Geosciences. (2013). Modeling rainfall-runoff process using soft computing techniques. 21, 108-117.
- Kiş, O. J. J. o. H. E. (2009). Neural networks and wavelet conjunction model for intermittent streamflow forecasting. 14(8), 773-782.
- Koza, J. R., & Koza, J. R. (1992). *Genetic programming: on the programming of computers by means of natural selection* (Vol. 1): MIT press.
- Levinson, N. J. J. o. M., & Physics. (1946). The Wiener (root mean square) error criterion in filter design and prediction. 22(1-4), 261-278.
- Menard, S. J. T. A. S. (2000). Coefficients of determination for multiple logistic regression analysis. 54(1), 17-24.
- More, J. J. (1978). The Levenberg- Marquardt algorithm: implementation and theory. In *Numerical analysis* (pp. 105-116): Springer.
- Nash, J. E., & Sutcliffe, J. V. J. J. o. h. (1970). River flow forecasting through conceptual models part I—A discussion of principles. 10(3), 282-290.
- Nourani, V., & Kalantari, O. J. E. E. S. (2010). Integrated artificial neural network for spatiotemporal modeling of rainfall-runoff-sediment processes. 27(5), 411-422.
- Penman, H. J. W. (1961). Weather, plant and soil factors in hydrology. 16(7), 207-219.
- Raghuwanshi, N., Singh, R., & Reddy, L. J. J. o. H. E. (2006). Runoff and sediment yield modeling using artificial neural networks: Upper Siwane River, India. 11(1), 71-79.
- Shoaib, M., Shamseldin, A. Y., Khan, S., Khan, M. M., Khan, Z. M., Melville, B. W. J. S. e. r., & assessment, r. (2018). A wavelet based approach for combining the outputs of different rainfall-runoff models. 22(1), 155-168.
- Shoaib, M., Shamseldin, A. Y., Khan, S., Sultan, M., Ahmad, F., Sultan, T., Ali, I. J. W. r. m. (2019). Input Selection of Wavelet-Coupled Neural Network Models for Rainfall-Runoff Modelling. 22(3), 955-973.
- Shoaib, M., Shamseldin, A. Y., Melville, B. W., & Khan, M. M. J. J. o. H. (2015). Runoff forecasting using hybrid wavelet gene expression programming (WGEP) approach. 527, 326-344.
- Singh, P., Thakur, J. K., & Singh, U. (2013). Morphometric analysis of Morar River Basin, Madhya Pradesh, India, using remote sensing and GIS techniques. *Environmental earth sciences*, 68(7), 1967-1977.
- Smith, J., Eli, R. N. J. J. o. w. r. p., & management. (1995). Neural-network models of rainfall-runoff process. 121(6), 499-508.
- Tayfur, G., Moramarco, T., & Singh, V. P. J. H. P. A. I. J. (2007). Predicting and forecasting flow discharge at sites receiving significant lateral inflow. 21(14), 1848-1859.

## Annexures

**Table 1** Summary of basic statistics of Rainfall of individual stations in the Jhelum River basin

Rainfall Stations	Latitude (dd)	Longitude (dd)	Elevation (m)	Duration	Std.	Mean	Cv	Cs	$v_{x_{min}}$	$v_{x_{max}}$	
Astore	35.2745	35.2745	2454	1981 2012	4.43	1.2	19.66	7.72	-0.1	118.2	
Balakot	73.3532	34.5482	975	1981 2012	13.05	4.4	170.55	6.38	0	291.8	
Muzaffarabad	73.4710	34.3596	679	1981 2012	11.41	4.1	130.43	5.33	0	200.5	
Gharidopatta	73.6154	34.2256	817	1981 2012	10.45	3.81	109.36	5.66	0	214.3	
Murree	73.3943	33.9070	2291.2	1981 2012	13.11	4.7	172.04	5.54	0	255	
Rawlakot	73.7604	33.8578	1638	1981 2012	9.80	3.6	96.20	7.26	0.0	244.6	
Plandri	73.6861	33.7153	1400	1981 2012	12.13	3.7	147.25	6.74	0	260.4	
Kotli	73.9022	33.5183	3000	1981 2012	10.93	3.5	119.62	5.91	0	201.5	
Jhelum	73.7251	32.9452	234	1981 2012	9.02	2.3	81.42	6.93	-1	195.6	
Daily Runoff of Basin (Q)						1434521	50846.34	2.05E+12	71.5	25690.8	106633791

**Table 2** Primary selection for the fitness of GEP model

<b>GEP</b>			
Maximum Population Size	50	RIS Transposition rate	0.1
Genes Per Chromosomes	4	Gene Transposition rate	0.1
Gene Head Length	8	One- point Recombination rate	0.3
Maximum No. Of Generations	2000	Two-point Recombination rate	0.3
Root Relative Squared Error (RRSE)	Yes	Gene Rate	0.1
Precision Used	0.01	Linking Function	Addition
Functions Used in Programming	(a+b),(a-b),(a*b),(a/b), sqrt(a)	Constant per Gene	10
Mutation Rate	0.044	Minimum Value	-10
Inversion Rate	0.1	Maximum Iterations	1000
IS Transposition rate	0.1	Tolerance	1.00E-08

**Table 3** Training and Testing outcomes of statistics of optimal GEP model with different input combinations.

	Input Combinations/ Model Fitness criteria	C1	C2	C3	C4	C5	C6	C7
	<b>Training</b>	R <sup>2</sup>	0.89	0.84	0.77	0.82	0.84	0.72
COE		1.00	1.00	1.00	1.00	1.00	1.00	1.00
MSE		-0.06	-0.02	0.01	-0.03	2.41	-497.16	0.03
NRMSE		280361.90	261191.28	251484.86	235979.46	261191.28	251479.56	261173.40
<b>Testing</b>	R <sup>2</sup>	0.99	1.00	1.00	1.00	1.00	1.00	1.00
	COE	1.00	1.00	1.00	1.00	1.00	1.00	1.00
	MSE	-0.01	0.00	1.78	4.94	58.59	-12.96	27.46
	NRMSE	837.78	772.71	736.30	768.34	778.48	790.09	787.73

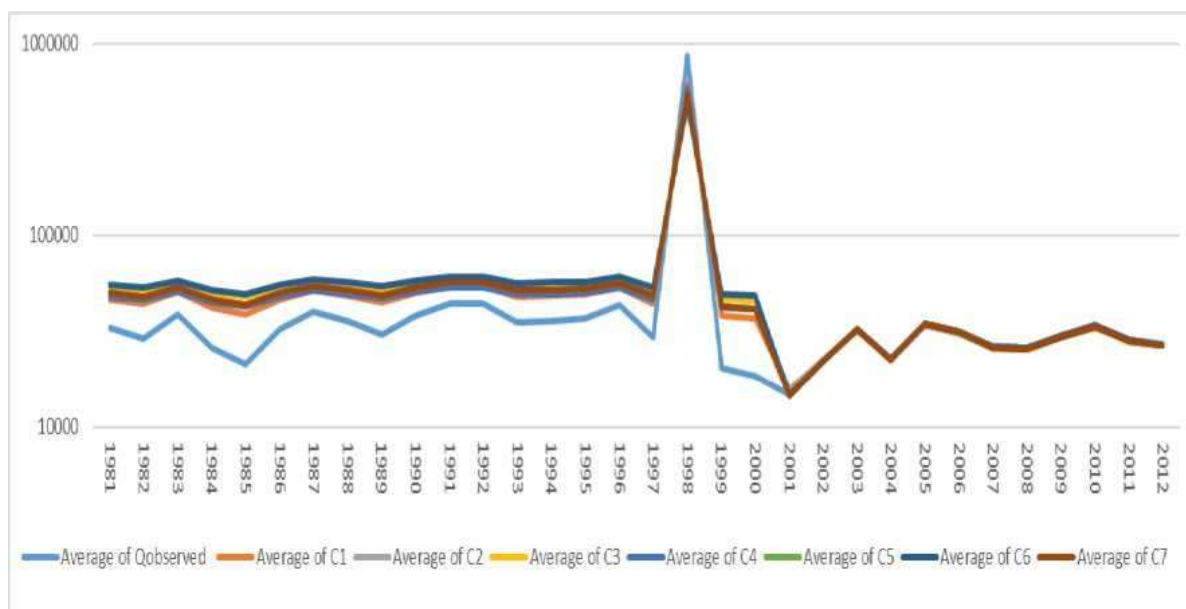


**Figure 2** Observed Vs GEP Predicted Runoff by different Input Rainfall-Runoff Combinations.

## Auto-calibration and uncertainty analysis of SWAT Model for Haro River Watershed using Sequential Uncertainty Fitting (SUFI-2) algorithm.

Saima Nauman<sup>1,2\*</sup>, Zed Zulkafli<sup>2</sup>

<sup>1</sup> Department of Civil Engineering, University of Lahore, 1-km Defence Road, Lahore 54000, Pakistan

<sup>2</sup> Department of Civil Engineering, Faculty of Engineering, Universiti Putra Malaysia, Selangor Darul Ehsan 43400, Malaysia.

Corresponding author email: [saima.engr07@gmail.com](mailto:saima.engr07@gmail.com)

**Abstract:** The study aims to utilise hydrological modelling approach to perform auto-calibration, validation, uncertainty analysis and to identify the sensitive parameters affecting the flows at Haro River watershed in Pakistan. Soil and Water Assessment Tool (SWAT) is used for the hydrological simulation of Haro River watershed. Sequential Uncertainty Fitting version 2 (SUFI-2)-an optimization algorithm in SWAT Calibration and Uncertainty Programs (SWAT-CUP) is used for calibration, validation, uncertainty analysis and sensitivity analysis of SWAT Model. The analysis shows good model performance with P factor and R factor of 0.83 and 0.88 during calibration and 0.79 and 0.84 during the validation respectively. The goodness of fit between the observed and simulated results is found to be very good with R<sup>2</sup> and NSE values of 0.82 and 0.80 respectively during calibration, and 0.77 and 0.77 during validation, respectively. For Haro River watershed, four parameters GW\_DELAY, CN2, SOL\_K and SOL\_BD out of 16 defined parameters have been found to be the most sensitive using global sensitivity analysis approach.

**Keywords:** Hydrological modelling; Haro River watershed; SWAT; SUFI-2 algorithm

### Introduction

Soil and Water Assessment Tool (SWAT) is a semi distributed river watershed model. The model was developed for evaluating the impacts on water resources that arise due to implementation of alternative management plans in river basins of large extent (Arnold et al., 2012). The model realistically simulates the key hydrological components and the relationship among them. SWAT model incorporates the parameters that are capable of demonstrating the combined effect of uncertainties found in the input data as well as in the structure of model (Abbaspour et al., 2009).

In SWAT, the river basin is distributed into sub-basins based upon varying soil, slope, land use and topography. It is a comprehensive model that utilizes the available inputs. However, large number of input parameters are required that complicates the calibration procedure and makes parameterization challenging. In 2003, Griensven and Bauwens developed an auto-calibration procedure to take care of some of these issues (Arnold et al., 2012). In the method adopted by Griensven and Bauwens the multiple objective functions were reduced to a single global criterion (Griensven and Bauwens, 2003). Later, in 2007 Abbaspour developed SWAT

Calibration and Uncertainty Program (SWAT-CUP) an auto-calibration and uncertainty program. The program merged the method presented by Griensven and Bauwens (2003) with other methods that comprised of semi-automated, multi-site inverse modeling approaches. It resulted in devising of Sequential Uncertainty Fitting Program (SUFI-2) (Arnold et al., 2012). SWAT-CUP is a generic interface that links calibration and sensitivity program with SWAT model (Tejaswini and Sathian, 2018).

The optimization algorithm SUFI-2 is used for auto calibration, uncertainty analysis and sensitivity analysis of simulated SWAT model. A series of steps is followed in SUFI-2, to progressively minimize the model parameter uncertainty as well as to achieve the criteria of calibration for prediction uncertainty. The method is applied \is applied to sets of parameters. As the method does not involve individual parameters, hence the parameter interaction is explicitly accounted in the program (Abbaspour et al., 2004).

Calibration of SWAT model is done to minimize the difference between physical observations and model simulations. This approach is followed so that the model well simulates the physical processes (Abbaspour et al., 2017). Calibration results are based upon the inputs of the model,

structure of model, calibration data and algorithms. The calibrated parameters cannot be determined uniquely, so it is pertinent to carry out uncertainty analysis to evaluate the performance of calibrated parameters of model (Abbaspour et al., 2015). Uncertainty analysis takes in account all the input uncertainties of model and propagates it to the model output. Sensitivity analysis helps in identifying the key factors influencing the model. This analysis helps in providing information about the prominent processes occurring in the study area. Sensitivity analysis can be categorized under two general types:

- 1) Local sensitivity analysis;
- 2) Global sensitivity analysis.

In local sensitivity analysis, a single parameter is changed to assess its effect on the objective function and model output, while keeping all other parameters constant. In All-at-a-time sensitivity analysis, the given parameters are changed simultaneously and then the objective function is evaluated.

The output of SUFI-2 comprises of the best range for all defined parameters that are to be used for the subsequent iterations. These parameter ranges gives best simulation results by fulfilling the below mentioned criteria, which forms the basis for successful calibration in SUFI-2.

The 95 percent prediction uncertainty (95 PPU) calculated for the output variables at the 2.5 percent and 97.5 percent levels of cumulative distribution encloses maximum measured datasets and it is given by “P factor”.

The mean distance between the two cumulative distribution levels in 95 PPU is lesser compared to the standard deviation value of given data. It is denoted by R factor and. The R factor value describes the 95 PPU band thickness. (Abbaspour et al., 2004).

The P factor and R factor evaluate the success of calibration and validation in SUFI-2. A balance between these factors is essential to achieve best-calibrated ranges of the defined parameters. Preferably, a good value of P factor ranges from 0 - 1. A P factor of 1 shows perfect model simulation with respect to uncertainty in model prediction, with 95PPU band enveloping 100% of measured data. A P factor value greater than 0.7 is considered satisfactory for discharge, while an R factor value less than 1.5 is suitable (Abbaspour et al., 2015).

In SWAT, for all HRUs, curve number (CN2), land use, soil parameters, elevation and distributed spatial parameters comprising of bulk density and hydraulic conductivity can be defined. For each simulation, the values of these parameters can be scaled by using an identifier term to the initial defined parameter estimates. The identifier codes represent the type of change that is to be introduced in the parameter.

Hagrass and Habib, also carried out a hydrological modelling study for Haro River watershed using SWAT Model, in 2017 but their study was limited to manual calibration. The current study focusses on using optimization tool to auto calibrate and further carry out uncertainty and sensitivity analysis for the hydrological parameters.

## Study area and data description

### Study Area

Haro River is the hydrological component of Potwar Plateau. It originates from the hills of Changla Gali and Nathia Gali and flows through parts of the provinces of Punjab and Khyber Pakhtunkhwa (Nauman et al., 2019) (Fig.1).

The location map of Haro River watershed is shown in Fig. 2.



**Fig. 1** Features of Haro River watershed

### Climate of the Region

The study region experiences sub-humid climatic conditions. Mean annual maximum temperature of the region varies from 17.6°C up to 40.1°C while the mean minimum temperature varies from 2.1°C to 21.6°C. The maximum temperature of 46.6°C was noted in the study area in 2005 (Zaheer et al., 2016). Precipitation and temperature strongly affects the climate of the area (Sanaullah et al., 2018).





**Fig. 2** Location of Haro River watershed

Although, precipitation in the area cannot be accurately predicted but most of it occurs from July until September. The mean annual precipitation in the nearby meteorological stations at Islamabad and Murree was recorded to be 1175 mm and 1748 mm respectively. (Zaheer et al., 2016).

#### **Data Description**

Discharge data, for the stream gauging station at Dhartian was acquired from Water and Power Development Authority (WAPDA). The daily precipitation, maximum temperature and minimum temperature data for Murree and Islamabad was obtained from Pakistan Meteorological Department. The daily relative humidity, wind speed and solar radiation data was obtained from Global Weather data for SWAT. The spatial data for SWAT Model, comprising of Digital Elevation Model, soil data, land use data and slope data was obtained from National Engineering Services Pakistan Pvt. Ltd.

#### **Research Methodology**

The hydrological simulation of Haro river watershed was done in ArcSWAT 2012. Haro River watershed was delineated into 9 sub-basins. On the basis of distinctive land use, slope and soil, the 9 sub-basins were further subdivided into 96 lumped areas or HRUs. In the weather definition data the climatic inputs including precipitation, maximum and minimum temperature, relative humidity, wind speed and solar radiation data at daily time scale were fed to the model. The model was run on a monthly time scale from 1987-2005 with a warm-up period of 2 years. The SWAT model was calibrated for the discharge at Dhartian gauge station using SUFI-2 in SWAT-CUP. Two

iterations, each consisting of 500 simulations, were performed to achieve suitable values of objective function and the performance evaluation parameters- P factor and R factor. The calibrated parameter ranges obtained from final simulation were then used for validation.

The sensitivity of the defined input parameters was assessed using global sensitivity analysis. In global sensitivity analysis, the impact of each parameter on the objective function is evaluated by carrying out large number of simulations. Although global sensitivity analysis provides more reliable outputs compared to local sensitivity analysis, the parameter ranges and the number of simulations affects the relative sensitivity of parameters.

Global sensitivity analysis employs multiple regression analysis technique. Eq. 1 is used for the quantification of parameter sensitivity.

$$g = \alpha_r + \sum_{i=1}^n \beta_i b_i \quad (1)$$

Where:  $g$  is the value of objective function,  $\beta$  is the parameter coefficient and  $\alpha_r$  is the regression constant.

In this technique, the evaluated sensitivity analyzes the average variation in objective function with simultaneously changing parameters. The t-stat is calculated in the process by division of the coefficient of parameter with its standard error. The value signifies the precision of the measured coefficient. The parameter is considered sensitive when the value of t-stat is larger than its standard error. The p-value is obtained using the t-stat values. A smaller p value depicts larger parameter sensitivity (Mehan et al., 2017). A parameter having greater absolute t-stat value and a lower p-value is regarded as most sensitive parameter (Abbaspour et al., 2017). The statistical criteria Coefficient of determination ( $R^2$ ) and Nash-Sutcliffe efficiency (NSE) depicts the model performance during calibration and validation period. An  $R^2$  value of 0 indicates no correlation between the observed and simulated data whereas a value of 1 indicates a perfect correlation between the two datasets (Krause et al., 2005). A value greater than 0.5 for  $R^2$  value is acceptable (Moriassi et al., 2007). The values of NSE in the range 0-1 show acceptable model performance. An NSE value lesser than 0 is unacceptable but a value of 1 shows perfect fit in the model simulated and observed data (Moriassi et al., 2007; Krause et al., 2005).

## Results

The parameter ranges for the calibration period were defined on the basis of absolute minimum and maximum ranges given in SWAT CUP. The initial and final parameter ranges obtained are shown in (annex-1).

The results of the calibration and validation in SWAT-CUP are given in Table 1.

**Table 1.** Performance Indicators of SWAT Model

Performance Indicator	Calibration	Validation
P-factor	0.83	0.79
R-factor	0.88	0.84
NSE	0.80	0.77
R <sup>2</sup>	0.82	0.77

During the calibration and validation phase, the model performance was found to be good with R<sup>2</sup> and NSE values of 0.82 and 0.80 respectively during calibration, and 0.77 and 0.77 during validation, respectively. The P factor and R factor were found to be 0.83 and 0.88 during calibration and 0.79 and 0.84 during the validation respectively.

The results of the global sensitivity analysis are given in Fig 3.

Based on the minimum p value and the maximum absolute t-stat value GW\_DELAY, CN2, SOL\_K and Sol\_BD are found to be the most sensitive parameters that affects discharge at Haro River watershed. This shows that all factors affecting groundwater processes, surface runoff and soil processes have the main influence SWAT Model results.

## Conclusions

The successful calibration and validation of the SWAT Model for Haro River watershed was performed using SUFI-2 in SWAT-CUP. The model showed very good performance during calibration as well as validation phase. The global sensitivity analysis in SWAT-CUP showed GW\_DELAY, CN2, SOL\_K and SOL\_BD to be the most sensitive parameters out of 16 selected parameters. These parameters are recommended to be focused for any future study on Haro River watershed and for other similar watersheds.

## Acknowledgements

The study was funded by the Ministry of Higher Education Malaysia under the Malaysian International Scholarship. The authors acknowledge with gratitude the cooperation of the Pakistan Meteorological Department, Water and Power Development Authority and National Engineering Services Pakistan for the provision of data for the research work.



**Fig. 3** Global sensitivity analysis for discharge in Haro River watershed

## References

- Abbaspour, K. C., Faramarzi, M., Ghasemi, S. S. and Yang, H., 2009. "Assessing the impact of climate change on water resources in Iran." *Water resources research*, 45(10).
- Abbaspour, K. C., Johnson, C. A. and Van Genuchten, M. T., 2004. "Estimating uncertain flow and transport parameters using a sequential uncertainty fitting procedure." *Vadose Zone Journal*, 3(4): 1340-1352.
- Abbaspour, K. C., Rouholahnejad, E., Vaghefi, S., Srinivasan, R., Yang, H. and Kløve, B., 2015. "A continental-scale hydrology and water quality model for Europe: Calibration and uncertainty of a high-resolution large-scale SWAT model." *Journal of Hydrology*, 524: 733-752.
- Abbaspour, K. C., Vaghefi, S. A. & Srinivasan, R., 2017. "A guideline for successful calibration and uncertainty analysis for soil and water assessment." A review of papers from the 2016 International SWAT Conference.
- Abbaspour, K. C., Yang, J., Maximov, I., Siber, R., Bogner, K., Mieleitner, J., ... and Srinivasan, R., 2007. "Modelling hydrology and water quality in the pre-alpine/alpine Thur watershed using SWAT." *Journal of hydrology*, 333(2-4): 413-430.
- Arnold, J. G., Moriasi, D. N., Gassman, P. W., Abbaspour, K. C., White, M. J., Srinivasan, R., ... and Kannan, N., 2012. "SWAT: Model use, calibration, and validation." *Transactions of the ASABE*, 55(4): 1491-1508.
- Hagras, M. and Habib, R., 2017. "Hydrological modeling of Haro River watershed, Pakistan." *International Journal of Research and Reviews in Applied Sciences (IJRRAS)*.
- Krause, P., Boyle, D. P. and Bäse, F., 2005. "Comparison of different efficiency criteria for hydrological model assessment." *Advances in geosciences*, 5: 89-97.
- Mehan, S., Neupane, R. P., and Kumar, S., 2017. "Coupling of SUFI 2 and SWAT for Improving the Simulation of Streamflow in an Agricultural Watershed of South Dakota." *Agricultural and Biological Engineering*, Purdue University, West Lafayette.
- Moriasi, D. N., Arnold, J. G., Van Liew, M. W., Bingner, R. L., Harmel, R. D. and Veith, T. L., 2007. "Model evaluation guidelines for systematic quantification of accuracy in watershed simulations." *Transactions of the ASABE*, 50(3): 885-900.
- Nauman, S.; Zulkafli, Z.; Bin Ghazali, A.H.; Yusuf, B. "Impact Assessment of Future Climate Change on Streamflows Upstream of Khanpur Dam, Pakistan using Soil and Water Assessment Tool." *Water* 2019, 11, 1090
- Sanaullah, M., Ahmad, I., Arslan, M., Ahmad, S. R. and Zeeshan, M., 2018. "Evaluating Morphometric Parameters of Haro River Drainage Basin in Northern Pakistan." *Polish Journal of Environmental Studies*, 27(1).
- Tejaswini, V. and Sathian, K. K., 2018. "Calibration and Validation of Swat Model for Kunthipuzha Basin Using SUFI-2 Algorithm." *International Journal of Current Microbiology and Applied Sciences (IJCMAS)*, 7(1): 2162-2172.
- Van Griensven, A. and Bauwens, W., 2003. "Multiobjective autocalibration for semidistributed water quality models." *Water Resources Research*, 39(12).
- Zaheer, M., Ahmad, Z. and Shahab, A., 2016. "Hydrological Modeling and Characterization of the Khanpur Watershed, Pakistan." *American Water Works Association*, 108(5): 262-268.

## Annex- 1

### *Description of selected parameters and their ranges*

Sr. No.	Parameters	Description	Identifier Code*	Initial Parameter Ranges		Final Parameter Ranges	
				Minimum Value	Maximum Value	Minimum Value	Minimum Value
1	CN2	SCS Runoff Curve Number	r	-0.2	0.2	-0.2	0.02
2	ALPHA_BF	Baseflow alpha Factor	v	0	1	0.32	0.98
3	GW_DELAY	Groundwater delay	v	30	450	30	278
4	GWQMN	Threshold depth of water in the shallow aquifer required for return flow to occur	v	0	2	0	1.1
5	GW_REVAP	Groundwater revap coefficient	v	0.02	0.2	0.02	0.19
6	ESCO	Soil evaporation compensation factor	v	0	1	0	0.58
7	CH_N2	Manning's "n" value for the main channel	v	0	0.15	0.07	0.15
8	CH_K2	Effective hydraulic conductivity in main channel alluvium	v	0	130	0	66
9	SOL_AWC	Available water capacity of the soil layer	r	0	1	0.3	0.9
10	SOL_K	Saturated hydraulic conductivity	r	-1	1	-1	0.17
11	SOL_BD	Moist bulk density	r	-1	1	-0.3	1
12	SFTMP	Snowfall temperature	v	-5	5	-0.25	5
13	SMFMX	Maximum melt rate for snow during year	v	1.5	7.5	4.5	7.5
14	SMFMN	Minimum melt rate for snow during the year	v	1.5	7.5	3.9	7.5
15	SMTMP	Snow melt base temperature.	v	-5	5	-0.35	5
16	TIMP	Snow pack temperature lag factor	v	0	1	0.24	0.75

## A Participatory Socioeconomic Environmental Modelling Framework for Groundwater Management

Rabeea Noor<sup>1\*</sup>, Muhammad Azhar Inam<sup>1</sup>, Qaiser Abbas<sup>1</sup>, Muhammad Asif<sup>1</sup>

<sup>1</sup> Department of Agricultural Engineering, Bahauddin Zakariya University Multan

Corresponding author email: [rabeeanoor123@gmail.com](mailto:rabeeanoor123@gmail.com)

**Abstract:** Participatory modeling connects modeling and science to stakeholder perception and expertise, thus assisting and enabling participatory decision-making when dealing with socio-economic issues. This research aims to develop a stepwise participatory modeling framework through the stakeholder built causal loop diagram (CLDs) analysis to highlight groundwater depletion in the Faizpur distributary of Bari Doab basin, Pakistan. A merged causal loop diagram is developed to represent a holistic model of the entire system to address this issue. The final merged diagram helps in understanding different system processes. Water pricing is the most effective policy among other proposed policies (e.g., water reuse, construction of dams, and change in cropping pattern). This policy will help control groundwater depletion in the study area by increasing social awareness to conserve natural resources. The case study demonstrates the effectiveness of the proposed approach in the participatory model building process. Also, the results point to social-economic aspects of groundwater management that have not been considered by other modeling studies to date.

**Keywords:** Participatory modeling, socio-economic, causal loop diagrams, groundwater management

### Introduction

Agriculture is an important sector of Pakistan's economy. This sector accounts for roughly 26 percent of the country's gross domestic product (GDP) (Rehman, Jingdong, and Du 2015). Pakistan's agricultural productivity relies heavily on the sufficient supply of irrigation water. Deficiencies in surface water supplies are now often met by farmers through the exploitation of unregulated groundwater. According to an estimate by (Qureshi et al. 2010), Pakistan is considered to be the 3rd largest groundwater extractor in the world, drawing out 10% of its groundwater resources annually (Qureshi et al. 2010); this contributes to excessive and unsustainable depletion of groundwater at the rate of 2 – 3 m per year (Shakoor et al. 2018). In Pakistan, no effective groundwater management/tube well installation policy currently exists. Due to the lack of awareness, the country's natural resources are under direct threat.

Asian countries are prime examples of sustainability failure in groundwater management. The increased production comes to increased resource demand; a dramatic increase in agricultural production has resulted in the overzealous drawdown of local and global water stores. From 1960 to 1980, a considerable amount of pumping and groundwater extraction

for irrigation began with Salinity Control and Reclamation Projects (SCARP) (Qureshi, Gill, and Sarwar 2010). From 1989 to 1993, farmers shifted toward diesel pumps (Qureshi, Shah, and Akhtar 2003), which revealed that these policies' purpose was to provide a multitude of earnings and not manage groundwater depletion. Since then, no sustainable policy was formulated, which adversely impact groundwater resources. The current study helps in bridging this gap by critically evaluating the stakeholder proposed policies.

Historical groundwater trends demonstrate a sharp decrease in the water table level and an increase in salt content in Pakistan's lower Bari Doab basin (Basharat and Basharat 2019; Latif and Ahmad 2009). This situation reinforces the urgent need for a methodological framework for sustainable groundwater management through stakeholder proposed policy evaluation. Several groundwater management studies have been performed in the Bari Doab region (a sub-catchment of the Indus River Basin) (Javed et al. 2020; Kijne 2003; Qureshi, Gill, and Sarwar 2010; Tanwir, Saboor, and Nawaz 2003), most of which indicate an increased need for sustainable groundwater management through improved policy implementation and stakeholder engagement.

Groundwater depletion is a global issue, and strategic use of regional-scale models with



global-scale analyses has dramatically enhanced awareness of the problem. All the previous groundwater policies focused on the control of waterlogging and salinity through physical modeling. However, the policies showed little interest in groundwater overexploitation investigations (Elshall et al. 2020; Van Steenberg and Oliemans 2002). Secondly, these policies were formulated without considering stakeholder participation. According to Halbe et al., (2013), it has been seen that stakeholder involvement is precious for successful policymaking. Currently, in Pakistan, the participation of stakeholders toward management and policy formulation is minimal. The approach outlined in this paper is focused on conveying the solution to this problem concerning stakeholder interviews.

The present study involves utilizing an innovative, qualitative modeling tool, i.e., Causal Loop Diagrams (CLDs), for evaluating stakeholder-defined policy scenarios (Inam et al. 2015) for sustainable groundwater management. Causal loop diagram construction is a technique used in simulation analysis to portray the simple procedure for a system dynamic hypothesis and is considered an essential step in dynamic feedback composition. It forms a bond between decisions and actions that cause system behavior. CLD development can be used for model construction and policy inspection (Binder et al., 2013).

The research will primarily focus on (1) Developing a participatory qualitative system dynamic model for groundwater management of Faizpur distributary and (2) Qualitative assessment and evaluation of stakeholder proposed policies for groundwater sustainability. The benefits of engaging the stakeholders (Motu'apuaka et al. 2015) are: (1) Recommended policy according to local conditions (2) Social awareness (3) Water balance understanding (4) Study of environmental and economic consequences (5) Qualitative model of local conditions to identify important variable for data collection (6) Provides the ease of interaction between different institutes.

The significance of this paper is related to the assessment of management policies to solve the groundwater problem, identification of the agriculture-related groundwater depletion issues and their potential solutions, bridging the gap between government departments, NGOs, and stakeholders, as well as an improved understanding of holistic system behavior and

governing processes. This research is particularly beneficial for developing countries where stakeholders have less financial support and fewer skills.

### Study area and data description

The Faizpur Distributary lies in the Bari Doab basin of Pakistan and is an offtake from the Multan Branch with full supply discharge of 8.72 m<sup>3</sup>/sec Faizpur distributary consists of three minors, i.e., Qasba Minor (HCC-55 A), Rana Minor (HCC-56 A), and Rana Minor (HCC-59 A). The study area is bounded by 29.770 N to 29.930 N latitude and 71.420 E to 71.470 E longitude. The study site lies within the Haveli central canal, and it is shown in **Fig. 1**. As indicated in the figure, Groundwater depth varies from 19.7 to 21.7 meters. Groundwater depth in 30% of the area is more than 21.7m, indicating the need for more financial resources for groundwater extraction. Currently, farmers entirely dependent on surface water supplies of the Faizpur distributary. The surface discharge may reduce in the future due to climate change and impact the area's agriculture sustainability.

The Faizpur distributary of Multan was selected due to the following reason: Groundwater is declining at a steep rate of 2 – 3 m per year (Shakoor et al., 2018). There is a need for immediate groundwater sustainability solutions to improve agriculture activities in the area. The study area lies in the agro-environmental zone, and the policies and solutions suggested through this study can be applied in other regions facing similar groundwater management issues.

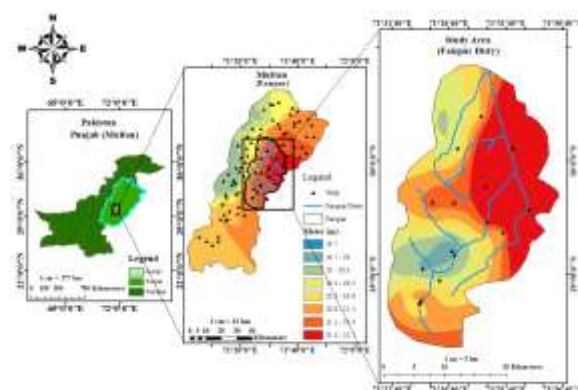


**Fig. 4** Study area (Faizpur distributary)

### Research Methodology

The methodology of the research work is explained in this section. The collaboration of stakeholders for the development of the



participatory model is essential. Reed et al., (2009) provide a comprehensive view of different stakeholder engagement techniques. The main problem faced during the interview process is the low interest of stakeholders; this is because many stakeholders might not be interested in giving the interviews and be a part of group meetings. It is due to intimidation factors; for example, they may not be able to share their real opinions, ideas, and suggestions in the presence of their seniors.

This research's suggested approach was developed to entail less time and economic resources by excluding extensive group interviews and gatherings. The overall process is based on five steps. The 1<sup>st</sup> step involves defining of problem variable, the 2<sup>nd</sup> step enlisting of stakeholders based on their roles, the 3<sup>rd</sup> step involves the conduction of stakeholder's interviews, the 4<sup>th</sup> step involves merging of causal loop diagrams of all stakeholders (i.e., expressing stakeholders' perspectives in the form of CLDs) that were built by using Vensim software and the 5th step involves the definition of policies and methods through the merged CLD. The steps that are adopted in the analysis of problem variables are given as (1) Specify the problem variable, (2) Specify the time horizon (3) Interpretation of model boundaries, and (4) Recognize the stakeholders.

After defining the problem variable, it is essential to point out the stakeholder list which plays an important role in the modeling process. The stakeholder analysis is divided into 2 stages which are as follows: (1) Specification: This stage is very important for the identification of stakeholders. (2) Prioritization: This stage is handled by examining factors (i.e., power, proximity, legitimacy, and urgency) to evaluate the stakeholder's significance (Elias, Cavana, and Jackson 2002). An extensive framework has been studied (Elias et al., 2002). This framework provides an inclusive evaluation of contrasting stakeholder views and merges the different stakeholder investigations (Freeman and McVea 2005).

After stakeholder analysis, stakeholder interviews were conducted individually to build their CLDs without any biases. An activity of interview conduction is shown in **Fig. 2**. During the stakeholder interview, the questions that were asked are: (1) When did the problem arise (Time horizon)? (2) What is the main issue you are facing now – a – days? (3) What are the effects of the problem variable? (4) What are the causes

of the problem? (5) What is the key feedback proceeding? (6) What type of policies and strategies can be acquired for resolving the problem?

Steps that help the process of CLD development include: first, define the goal and method of building a causal loop diagram through a simple example. As a developing add some sticky notes and a chart is provided to the stakeholder to generate their CLDs. After this, stakeholders attach the sticky note of the problem in the center of the chart. Then the stakeholder affixes the stick notes of causes on the left side of the chart. In the next step, direct and indirect causes are connected through casual links or connections. Then the direct and indirect consequences are affixed on the right side of the chart. Consequences, like causes, are also joined or connected through the casual loop arrows using a pencil. Eventually, causes and consequences are interlinked through feedback loops.

After stakeholder interviews, the group CLD model (as shown in **Fig. 3**) is constructed by the coordinator by merging all causal loop diagrams. The main purpose of the merged model is to represent the distinct prospects and mental models of all stakeholders related to the problem variable, its causes, its effects, feedback loops, and possible policies to address the problem variable. Identification of problem variables, causes, effects, and feedback loops are the four primary steps for the construction of the causal loop diagram. This permits for addressing the views of stakeholders and for creating a merged mental model.



**Fig. 5** Individual CLD Diagram Activity

## Results

From the literature review and the feedback from the stakeholders and experts, it was determined that groundwater depletion was the main issue in the study area. The next step is deciding whom to contact for the participatory modeling exercise,

i.e., stakeholder analysis. Initially, a stakeholder list was produced through a brainstorming process. The Provincial Irrigation Department, agricultural extension, local farmers, and farmer's organizations were considered as potential stakeholders since they have a significant role in water supply and use. Other relevant stakeholders were the Environmental Protection Department, Department of Agricultural Engineering, and its sub-departments (i.e., water management, well-drilling management, and on-farm water operations), local governments, indigenous communities, and consultants.

Further, the final stakeholder list was prioritized based on their power versus interest attributes. Eventually, on the premise of stakeholders' engagement, their dynamics analysis, power interest diagram, and stakeholder suggestion, the Irrigation Department, Agricultural Extension, local farmers, Land Reclamation Department, NGOs, Indigenous communities, and Farmers Organization were considered as potential stakeholders and were involved in the qualitative modeling exercise.

After stakeholder analysis, potential stakeholders were contacted for preparing their mental maps in the form of CLDs. Almost ten loops were incorporated into the integrated CLD (as shown in **Fig. 3**), which are discussed briefly. **Loop-1** (irrigation loop) contains causes such as groundwater pumping, growth yield, barren land, and cropland use, and consequences, e.g., cropping intensity, and recharge. Owing to a lack of groundwater, fallow (barren) loop-1 is reinforced and shows the clockwise track. **Loop-3** is the economic growth loop, and the main effective cause is the installation of tube wells. This loop shows the clockwise course, and it is balanced. Balancing loops are not very essential (compared to reinforcing loops) because these loops are self-stable and become less effective over time as compared to reinforcing loops. **Loop-5** is the cropping intensity loop, and it illustrates all causes and consequences. The dominant cause and consequence are brackish water and water availability, respectively. So, farmers may determine the seasonal crop pattern according to the area to ensure water availability. **Loop-9** is the technology loop (shown in **Fig. 3**); it contains causes such as barren land and salt contamination and consequences such as the adaptation of technology and drip irrigation development. This loop is reinforced and oriented in the counterclockwise direction. In

**Fig. 3, loop-10** is the crop productivity loop. The main causes are domestic use and deforestation. Urbanization may control the process of deforestation. Loop-10 is reinforced and depicts a counterclockwise direction.

For loops that are showing their impact on groundwater depletion, stakeholders gave their possible solutions to resolve those problems and all the given strategies were considered during the policy selection process. Some stakeholders suggested that keep interest in social awareness activities such as water wastage, (**Fig. 3** loop-9) farmers might be moved to adopt advanced technology that may help to increase crop yield. For conserving water, laser land leveling, drip, and sprinkler technologies have been recognized as short-term policies (**Fig. 3** loop-5), whilst construction of large-potential dams and pollution control in the canal were taken as long-term policies (**Fig. 3** loop-1). A few stakeholders also suggested water reuse (**Fig. 3**, loop-10). If it is possible to treat the domestic water, then the canal water can be saved out from pollution. People do not use that treated water for drinking purposes, and it could be used to irrigate the fields and fulfill the water requirements of the crop to some extent, (**Fig. 3**, loop-1); it could also reduce groundwater pumping up to some extent (**Fig. 3**, loop-1).

To control groundwater depletion, another option is the groundwater metering system/water pricing (**Fig. 3**, loop-3); upstream stakeholders were against this policy (discussed in detail later in this section). In the areas where the water level is much lower, the public might install artificial recharging wells by mutual funding or receiving a subsidy from the government to save themselves from the drought. For this purpose, awareness campaigns are necessary, and this may help to bring the groundwater level up.

The government may take all the tube wells under its charge and any redundant tube wells operating over the same area of influence might be sealed. As the metering system may boost the governmental economy, amounts may be used for the insertion of recharging wells, providing subsidies to farmers for new technology, or construction of a dam. This is a long-term policy, and it may effectively shift the current groundwater scenario. A system dynamics model will be developed for quantitative analysis of the metering system. The policy will be examined for its overall socio-economic and environmental impact on the whole system.

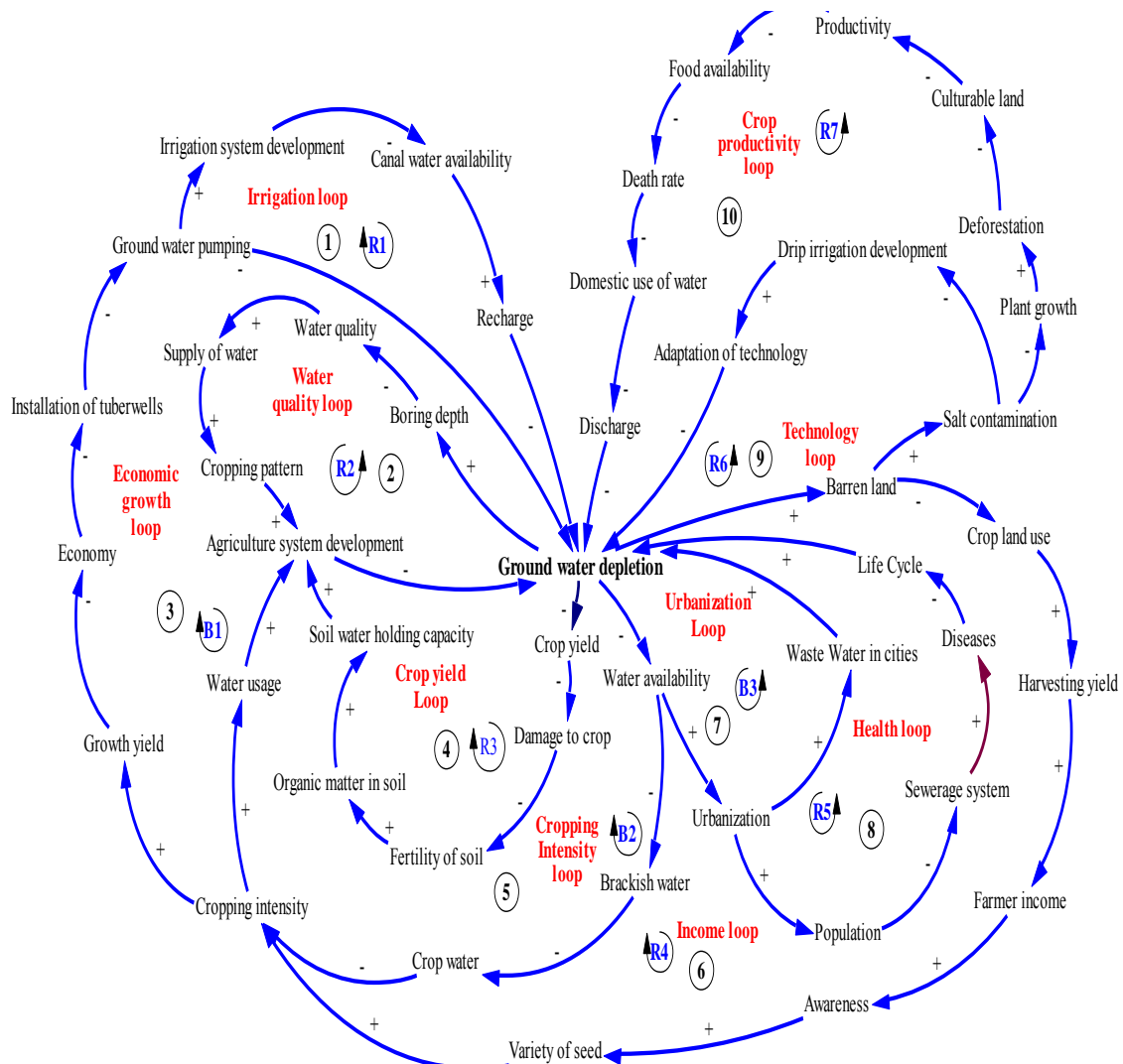


**Fig. 6** Final merged causal loop diagram from the different stakeholders

## Conclusions

This is the first research on evaluating the issue of groundwater depletion in the Faizpur distributary with the active involvement of stakeholders. The outcomes of the case imply that causal loop diagrams are a powerful and easy approach to initialize stakeholder involvement within the development of qualitative participatory models aimed towards addressing complicated troubles related to groundwater management. In the qualitative merged CLD modeling method, stakeholders recommended several policies with specific regard for economic, social, and technical steps. All stakeholders agreed that the problem of groundwater depletion in the Faizpur Distribution is attributable to the inequitable distribution of canal water sources, frequent pumping of water, low-level management activities, high agricultural needs, and lack of

social awareness. All stakeholders spotlighted the desire for a consciousness marketing campaign dealing with rainwater harvesting, irrigation scheduling, crop selection according to the area, conservation tillage, metering systems, pollution control in canals, water reutilization, laser land leveling, and drip and sprinkler technology. All voluntary case-study respondents were pleased with the participatory model that they had created and spotlighted the need to follow this approach on different agricultural issues and to construct higher expertise of complicated groundwater issues, as well as to amplify social awareness among stakeholders.

## Acknowledgments

This research was mainly supported by the Punjab Irrigation Department held by Executive Engineer Zahid Hussain as well as Agriculture Extension Department held by Agriculture

Officers Miyan Manzoor Ahmad. The farmer community and water management department are thanked for their support during the development of CLDs. Special thanks to the Department of Agricultural Engineering for providing maps to finalize the study area.

## References

- Basharat, Muhammad, and Maham Basharat. 2019. "Developing Sukh-Beas as a Potential Recharge Site during Wet Years for Bari Doab." *Applied Water Science* 9(7): 1–15. <https://doi.org/10.1007/s13201-019-1041-6>.
- Binder, Claudia R., Jochen Hinkel, Pieter W.G. Bots, and Claudia Pahl-Wostl. 2013. "Comparison of Frameworks for Analyzing Social-Ecological Systems." *Ecology and Society* 18(4).
- Elias, Arun A, Robert Y Cavana, and Laurie S Jackson. 2002. "Stakeholder Analysis for R.&D.Project Management." (September).
- Elshall, Ahmed S. et al. 2020. "Groundwater Sustainability: A Review of the Interactions between Science and Policy." *Environmental Research Letters* 15(9).
- Freeman, R. Edward Edward, and John McVea. 2005. "A Stakeholder Approach to Strategic Management." *SSRN Electronic Journal* (March 2018).
- Halbe, J., C. Pahl-Wostl, J. Sendzimir, and J. Adamowski. 2013. "Towards Adaptive and Integrated Management Paradigms to Meet the Challenges of Water Governance." *Water Science and Technology* 67(11): 2651–60.
- Inam, Azhar, Jan Adamowski, Johannes Halbe, and Shiv Prasher. 2015. "Using Causal Loop Diagrams for the Initialization of Stakeholder Engagement in Soil Salinity Management in Agricultural Watersheds in Developing Countries: A Case Study in the Rechna Doab Watershed, Pakistan." *Journal of Environmental Management* 152:251–67. <http://dx.doi.org/10.1016/j.jenvman.2015.01.052>.
- Javed, Muhammad Asif, Sajid Rashid Ahmad, Wakas Karim Awan, and Bilal Ahmed Munir. 2020. "Estimation of Crop Water Deficit in Lower Bari Doab, Pakistan Using Reflection-Based Crop Coefficient." *ISPRS International Journal of Geo-Information* 9(3).
- Kijne, Jacob W. 2003. "Water Productivity under Saline Conditions." In *Water Productivity in Agriculture: Limits and Opportunities for Improvement* (Eds), , 89–102.
- Latif, Muhammad, and Muhammad Zakria Ahmad. 2009. "Groundwater and Soil Salinity Variations in a Canal Command Area in Pakistan." *Irrigation and Drainage* 58(4): 456–68.
- Motu'apuaka, Makalapua et al. 2015. "Defining the Benefits and Challenges of Stakeholder Engagement in Systematic Reviews." *Comparative Effectiveness Research*: 13.
- Qureshi, Asad Sarwar, Mushtaq A. Gill, and Asrar Sarwar. 2010. "Sustainable Groundwater Management in Pakistan: Challenges and Pportunities." *Irrigation and Drainage* 59(2): 107–16.
- Qureshi, Asad Sarwar, Peter G. McCornick, A. Sarwar, and Bharat R. Sharma. 2010. "Challenges and Prospects of Sustainable Groundwater Management in the Indus Basin, Pakistan." *Water Resources Management* 24(8): 1551–69.
- Qureshi, Asad Sarwar, Tushaar Shah, and Mujeeb Akhtar. 2003. "The Groundwater Economy of Pakistan." (19): 31.
- Reed, Mark S. et al. 2009. "Who's in and Why? A Typology of Stakeholder Analysis Methods for Natural Resource Management." *Journal of Environmental Management* 90(5): 1933–49.
- Rehman, Abdul, Luan Jingdong, and Yuneng Du. 2015. "Last Five Years Pakistan Economic Growth Rate GDP And Its Comparison With China India And Bangladesh." *International Journal of Scientific & Technology Research* 4(1): 81–84.
- Shakoor, Aamir et al. 2018. "Groundwater Vulnerability Mapping in Faisalabad District Using GIS Based Drastic Model." *MATEC Web of Conferences* 246(January).
- Van Steenberg, Frank, and William Oliemans. 2002. "A Review of Policies in Groundwater Management in Pakistan 1950-2000." *Water Policy* 4(4): 323–44.

## Participatory Environmental Socio-Economic Modelling Complexity Issues and Solution. A case study of the Rechna Doab

Muhammad Asif<sup>1\*</sup>, Azhar Inam<sup>1</sup>, Qaiser Abbas<sup>1</sup>, Rabeea Noor<sup>1</sup>

<sup>1</sup> Department of Agricultural Engineering, Bahauddin Zakariya University Multan

Corresponding author email: [muhammadasif36304@gmail.com](mailto:muhammadasif36304@gmail.com)

**Abstract:** *The casual loop diagrams represents the variation and dynamic changes in the environment modelled systems. With the involvement of more variables in the modelling systems, directly associates with the complexity in the developed diagrams and make it complex and tedious to understand for stakeholders. This can be even more complicated during group modelling when various variables, parameters, dependent and independent factors are involved. The limited availability of the suitable methods to grip these types of complexity is also a major problem. Therefore, this manuscript suggests and proposed two methods to reduce the complexity in the casual loop diagrams. One is Endogenisation, Encapsulation and order-oriented reduction method (EEOR) which systematically helps to reduce the complexity. This method includes seven different steps which ultimately reduces the number of variables and continuously simplifying the complexity in the casual loop diagrams. The other method is the thematic maps development which methodically controls the casual loop diagrams. This method divide the grouped causal loop diagram model into the sub-models and placed the individual variables into their specific gender and discipline. This manuscript includes the comparison between the two proposed methods and found that the thematic maps development method is more suitable to simplify the casual loop diagrams. Thematic model focus on maintaining the CLD integrity and ensure the inclusion of all processes/variables. This method can be employed in any domain, where causal loop diagrams are used.*

**Keywords:** Casual loop diagram, complexity, simplification, variables

### Introduction

Increasing in environmental model complexity is a big concern that can be seen in different fields. The complexity in system includes a logical entity with specific criteria whose interaction, dynamics and elements produced structure which cannot be defined easily (Bureš, 2017). In the system dynamics, casual loop diagram (CLD) are used to capturing opinion and ideas of stakeholder for model structure. CLDs have been excellent work in policy analysis, sustainable development, natural resources management and water resources planning (Inam et al., 2015). Complexity in developed diagram is increasing due to inclusion of plenty of variables from different domain and loop in model and hence make it more sensitive and valuable. It also increased manifold during group modeling workshops where multiple perspectives are shared and complex diagrams are developed (Vugteveen et al., 2015). As the process requires multiple actors or groups, merging all their diagrams will create an extremely complex and detailed diagram. There is a well-known aphorism in the field of analyze systems: "Yet things are getting worse in detail." These details,

while making things more complicated, do little to shed light on the problem (Andersen et al., 2007). Marginal players with limited knowledge of the system can no longer contribute as the complexity of the system increases. Complex materials are difficult to understand, and can therefore allow a rapid loss of interest in the modeling exercise among the actors. Like to the definition of complexity, it is very difficult to identify a common point of view for the Reduction of the system complexity (Corbett & Smith, 2017). This is due to the strong dependence on the reduction of complexity and discipline, in which this process is managed. In particular, the methods and techniques are significantly different in specific Areas, for example, hydrology, computer science or healthcare (Diodato et al., 2014; Łapa et al., 2013). Because of this problem, a general view of the quantity of system elements and their mutual complexity correlation applies in research. Due to lack of available method which help users to finish the growth of complication, this script recommend real method. Therefore, an overall picture will be preferred for its simplicity which will allow a better later understanding of the system (Morecroft, 1982). This purposed

research comprehensively helps to simplify the complex casual loop diagram. The causal loop diagram Provide a way to map the complexity of the interest of system that includes variables, useful Links to both relationships and Polks, and the cycle of feedback (Keogh & Pearson, 2017). This research based on two method for the simplification CLDs diagrams, first one is thematic maps development and second endogeniastion, encapsulation and order-oriented reduction (EEOR) method. Both method have good potential to simplify the complication of CLDS, but both method have its own limitations and benefits. For describing the stepwise procedure these method, a case studies conducted in Rechna Doab, Pakistan(Inam et al., 2015) was used for the simplification of casual loop diagram, and merged casual loop diagram. To simplify the group diagram, each method have its own process of reduction the complexity of diagram. First one is, Endogeniastion, encapsulation and order-oriented reduction (EEOR) method. This method simplifies merged diagram by fictitious variable, identify the input and output variable, removing the exogenous variable, labelling and numbering the loops (Mesmin et al., 2016). EEOR method has certain limitation such as the system may lose its integrity by eliminating important processes. Second method is, thematic maps development. This method has an advantage over the EEOR method since it keep system details by splitting merged diagram into different sub-models. The merged diagram divided into sub-models

diagrams, in which each variable located in own sub-models with same units. But all these sub-models diagram are connected with common variable. Therefore this method is easy to understand to complex model through sub-models diagrams without losing useful information.

### **Study area**

This proposed research is applied in a case study undertaken in sub-watershed located in Rechna-Doab, Pakistan. The study area covers an area about 732.50 km<sup>2</sup> and lies between 30° 32' N and 31° 08' N latitude and 72° 14' E and 71° 49' E longitude. The study area Rechna "Doab" (two rivers) is located just above the intersection of Ravi and Chenab rivers and irrigated by the Haveli Circle Canal shown in Fig.1. The study area is good and cultivable land but 30% of the land affected due to high levels of soil salinity. The groundwater depth of study area lies in the range about 3-6 m and electrolyte concentration found in groundwater exceeding 1500 ppm in the middle portion of the basin

### **Methodology:**

#### **Thematic maps development:**

In Inam et al. (2015) all potential stakeholders were interviewed individually and their CLD were developed. Later in a following step all the individual CLDs were merged into one group model diagram.



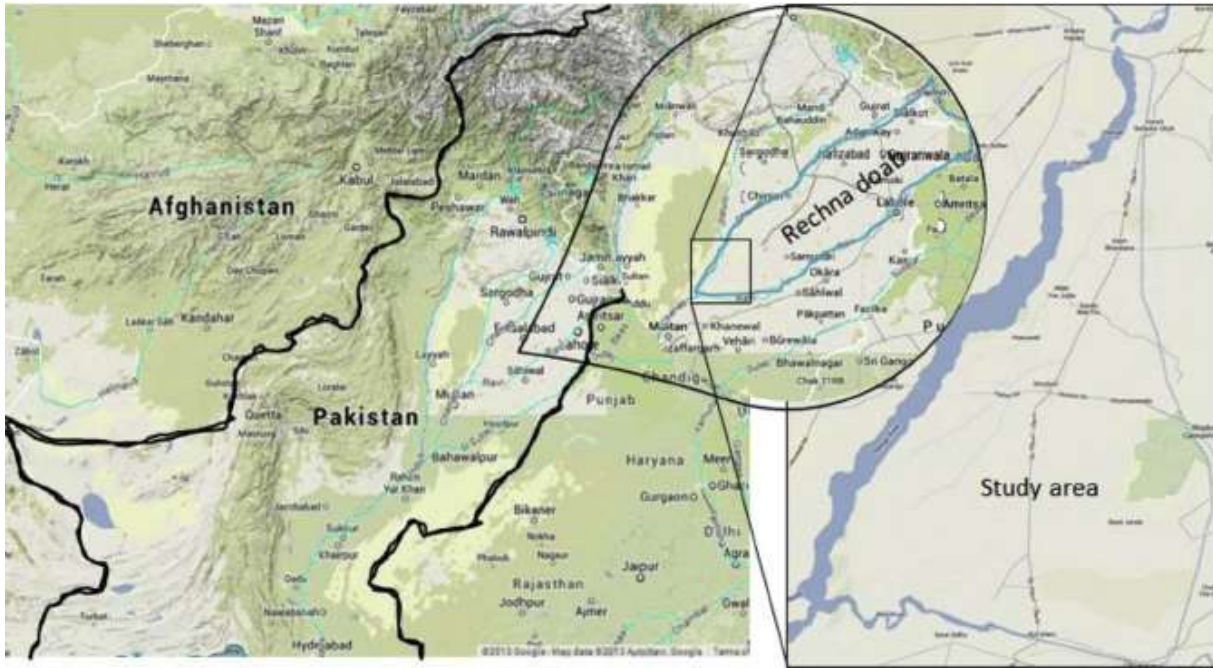


**Fig. 8.** Study area in the Rechna Doab basin, Pakistan (Inam et al., 2015)

The group merged diagram was divided into sub-thematic models represents the components of social, economic, agriculture and environmental system. This type of distribution helps to estimate the details of various aspects of isolation from other factors, and also reduce the complexity of model structure for further quantity purposes (for example, agricultural sub-model deals only those variable which have same units and related to agriculture model, while the sub-model of social system deals with change in migration, industrialization parameter and education level which completely different approach of units and quantification). It should be considered that thematic model are connected with a common variables. The different environmental sub-model (such as irrigation and groundwater) Quality, wastewater production) shows climate change conditions because of soil salinity, while the sub-model of economic dealing with government priorities in respect of government subsidies for advanced irrigation techniques and canal lining. The thematic maps strategy are used to address the complexity of diagram which takes place in four steps. In the first step, all variable

are marked according to their gender and units. The final merged CLD with classification of variables as shown in Fig 2. The all variables are replace into respective sub-models after marking. The second step is most important in which identify all overlapping variables are identified to maintain the integrity of the casual loop diagrams. They are fused together until it is decomposed into sub-models. In the third step, loops are identified. In last step, the variables were eliminated from all classes except those of interest and replace missing arrows to restore the feedback relationship.

#### **Endogenisation, Encapsulation and Order-Oriented Reduction (EEOR) Method:**

The current method is based on the three main processes: Endogenisation, Encapsulation and Order-Oriented Reduction. In fact, the approach as a whole is largely centralized supports MIMO (Multi-input, Multi-output) variables while in-degree, out-degree, and median (mediator) variables are suppressed.

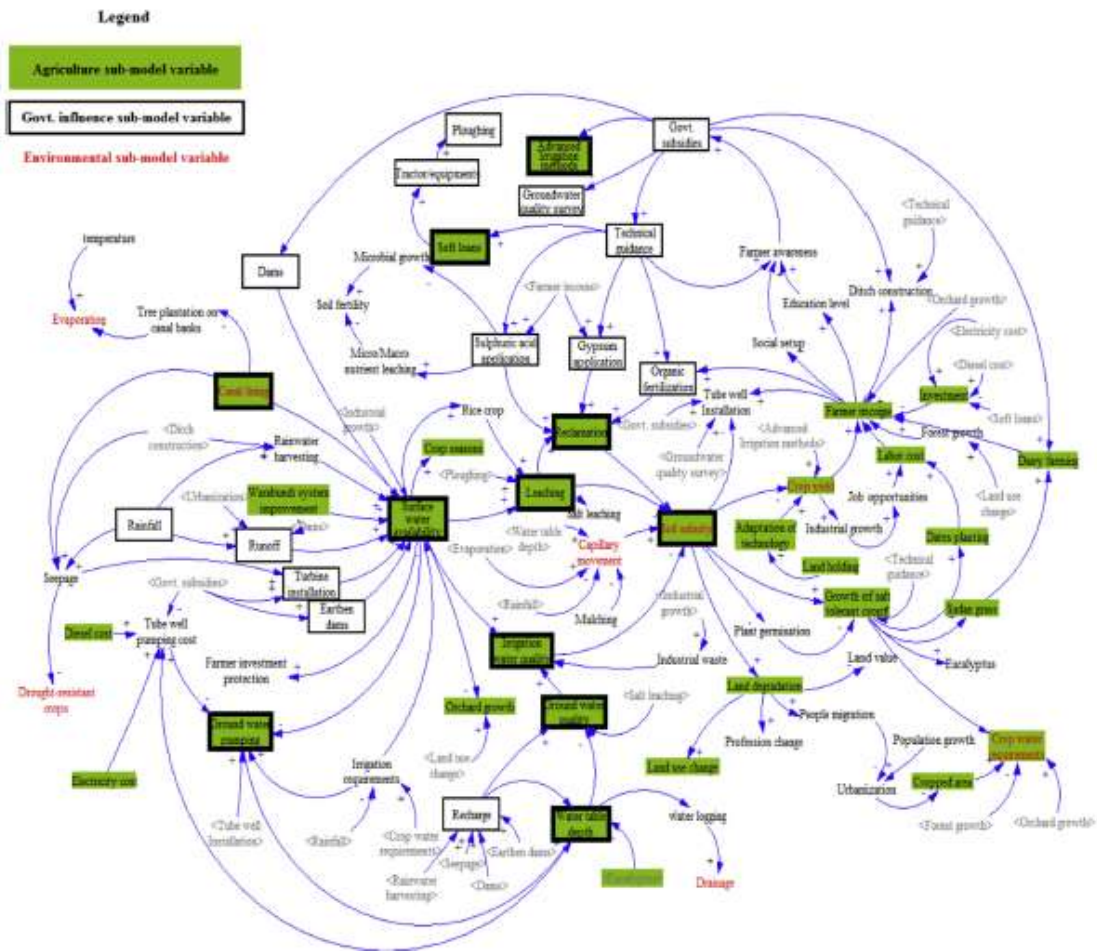
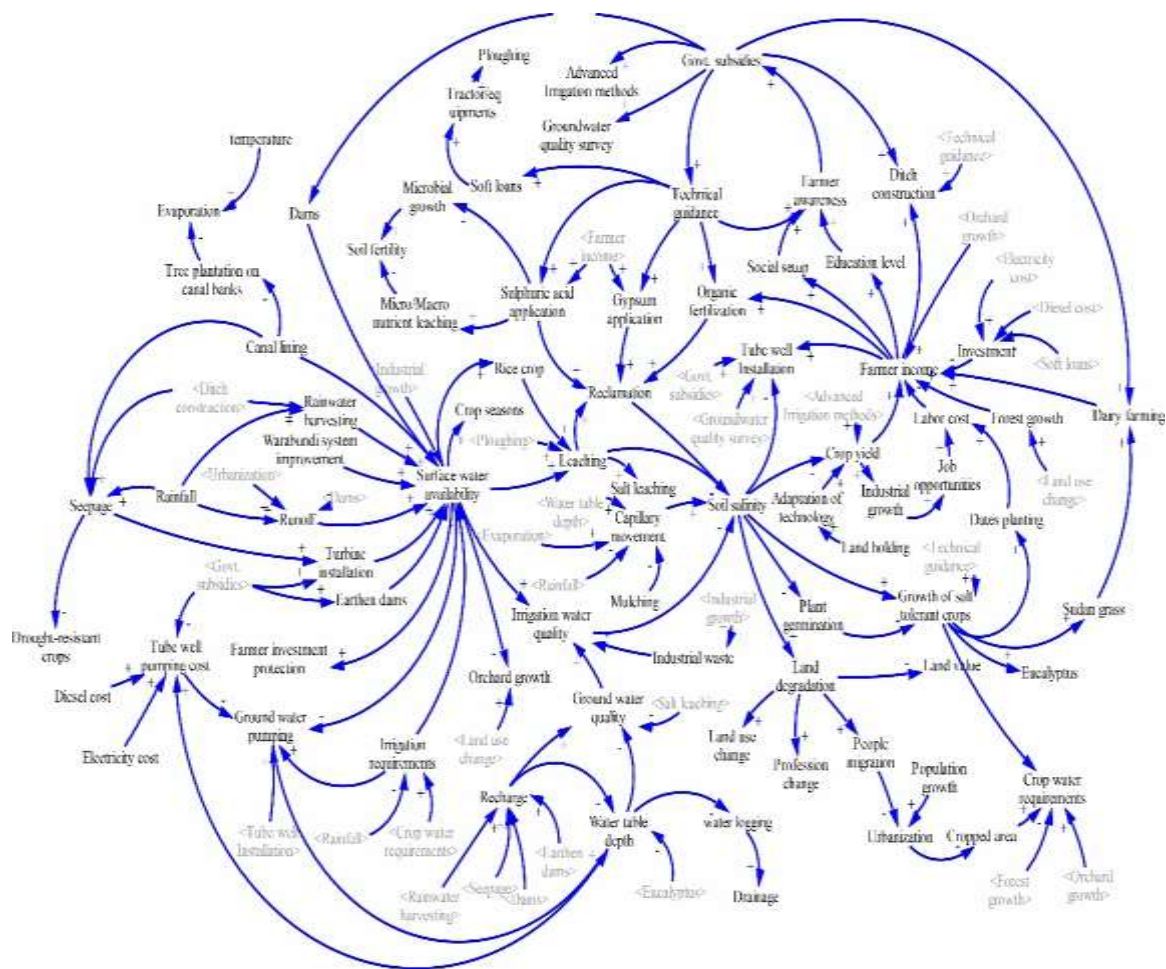


Fig. 9. Final version of merged casual diagram of all stakeholders (Inam et al., 2015)



**Fig. 10.** Complex final merged casual loop diagram(Inam et al., 2015)

The three processes listed above are grouped here according to their level of sensitive. Fig.3 shows the digitized complex diagram developed through stakeholder interviews. If endogenisation is performed first, it need to be prioritized of encapsulation. Similarly, if encapsulation can be done, it need have performed the reduction. To Ensures implementation of the procedure by sequencing the following steps.

1. Use of fictitious variables:-once the final casual loop group diagram is finalized, the cross arrows were eliminated used by using fictitious variable.to see Fig.3.
2. Label and Eliminated the exogenous input and output variables (Endogenisation):- this step takes place the Endogenisation process. It marks all exogenous input and output. Fig.4 shows the labelling and eliminating processes.
3. Elimination Single-entry-exit and Single-entry-exit double or Single entry-exit variables (Encapsulation and Order-Based Reduction):- The step 2 is repeated until attains the complexity of diagram.

4. The structure of diagram will be an endogenous nature. Fig.5 showed the behavior of established loops:- It followed the final process in which named loops and numbered Loops are corrected by merging the fictitious variables and these are named, their behavior established, and they are numbered

**Results and discussion**

The method described in the previous section can be used to simplify any complexity causal loop diagram. This section applies the method and confirms it with the help of case studies. The group (Merged) casual loop diagrams were developed intellectual capacity of individuals and obtain a complex view of the process. The creation of casual loop diagram is widely used in many research disciplines also the limitations of group modelling was presented in many studies. Though, this method shows a good source of complex casual loop diagrams, that is why it used in this study. For the most part of this method, the development of the final merged diagram



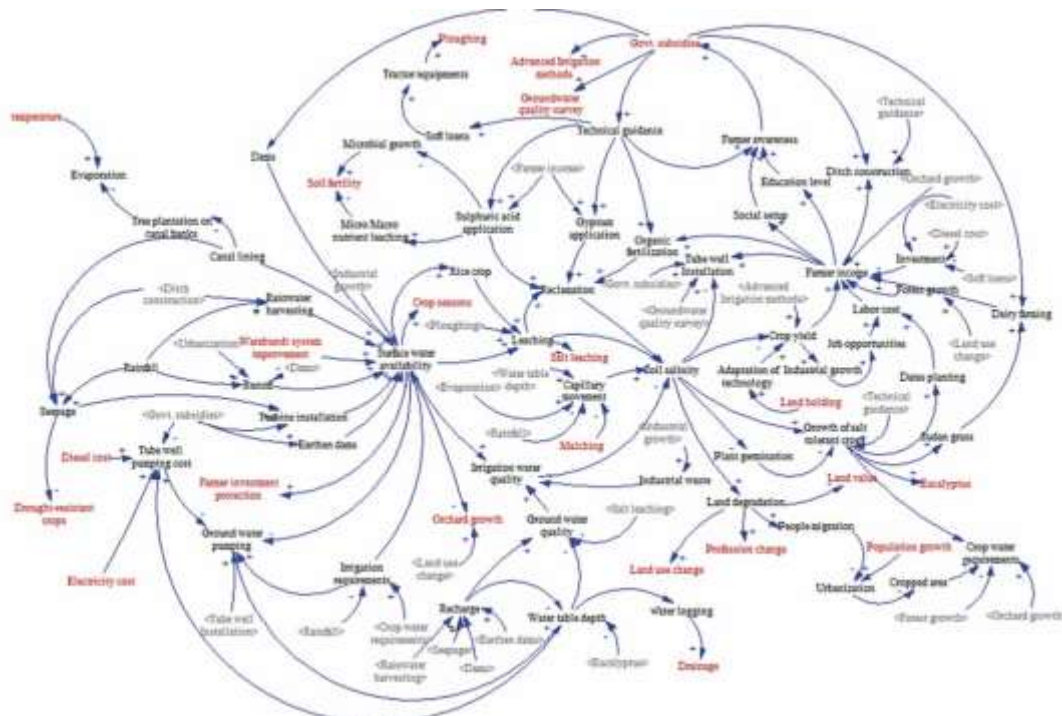


Fig. 11. Simplified the complex diagram by eliminating variables

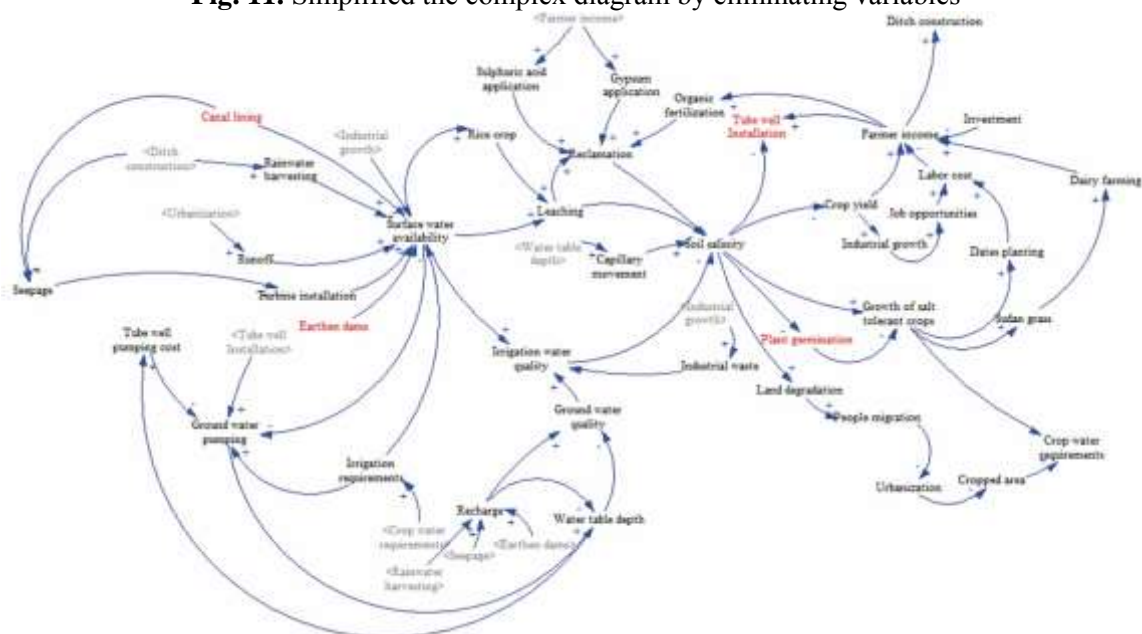


Fig. 12. Complex diagram into simplified by (encapsulation and order-based reduction) Processes

represents as complex model which includes many variable and more links. The main objective of this method is grounded used for grouping single diagrams.

The first case study demonstrates the application of the method introduced throughout the development of group casual loop diagram to show the increase complexity and reduce complexity. The first method, thematic maps development used to reduction the complexity

and divided the final merged diagram into sub-models. Fig.6 shows the sub-module addressing the themes of agriculture, for example, the agricultural thematic model was included a groundwater, farmer income, reclamation, land use/crop rotation and water availability processes. Among these thematic maps of environment, social, agriculture, and economy especially government subsidies, the agriculture thematic model is selected for the discussion and

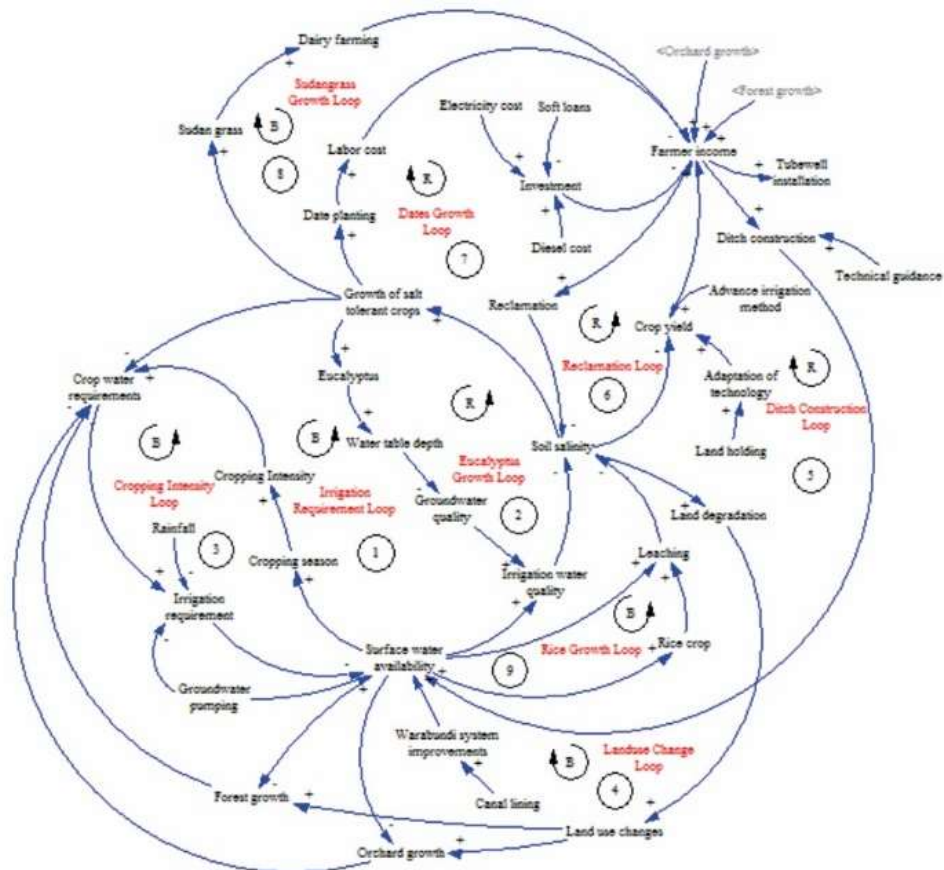


Fig. 13. Representation of thematic map of sub-model agriculture

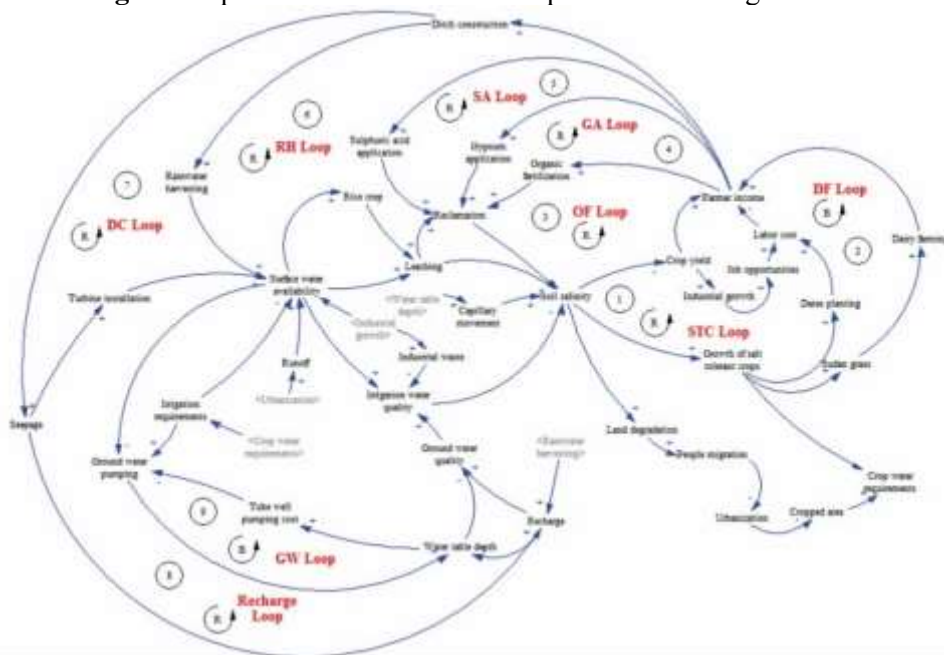


Fig. 14. Final version simplified diagram by EEOR method

it complete all physical processes relating to soil salinity management in Rechna, Doab, Pakistan. Such a separation allows the details of the different aspects of the problem to be assessed individually. In addition, this approach simplifies the structure of the model for future

use for quantification. It should be noted that these thematic models remain linked to each other through variables they have in common, and therefore, no detail is lost. In this proposed Research, the second method Endogenisation, Encapsulation and Order-Oriented Reduction

(EEOR) used same final merged diagram described in above section and the processes takes place in four steps which already described in methodology section. The fictitious variables are eventually merged. Feedback loops were completed, named, numbered, and their behavior established. The diagram that follows is much smaller than the original one, but some issues were found see Fig.7. Due to the small model structure, all possible variable feedback loops were eliminated and most of the information were mixing.

### Conclusions

A comparison was performed between the two methods. Namely as Endogenisation, Encapsulation and Order-Oriented Reduction (EEOR) and thematic maps development to reduce the complexity in the casual loop diagrams. It was found from the results that thematic maps development performed better and is more in every domain in which complex casual loop diagram is involve . This method divides the whole complex casual loop model into simplified sub-models. The flexibility of this method is that the sub models can relate to the help a common value. The main advantage of his method is that the information is not lost, no variable mixing and easily understandable.

### Acknowledgements

All stakeholder especially irrigation department, Land reclamation department, water and power development authority, and international water management institute are acknowledged for their support in the CLDs development.

### References

Andersen, D. F., Vennix, J. A. M., Richardson, G. P., & Rouwette, E. A. J. A. (2007). Group model building: problem structuring, policy simulation and decision support. *Journal of the Operational Research Society*, 58(5), 691–694.

Bureš, V. (2017). A Method for Simplification of Complex Group Causal Loop Diagrams

Based on Endogenisation, Encapsulation and Order-Oriented Reduction. *Systems*, 5(3),46. <https://doi.org/10.3390/systems5030046>

- Corbett, E. A., & Smith, P. L. (2017). The magical number one-on-square-root-two: The double-target detection deficit in brief visual displays. *Journal of Experimental Psychology: Human Perception and Performance*, 43(7), 1376.
- Diodato, N., Brocca, L., Bellocchi, G., Fiorillo, F., & Guadagno, F. M. (2014). Complexity-reduction modelling for assessing the macro-scale patterns of historical soil moisture in the Euro-Mediterranean region. *Hydrological Processes*, 28(11), 3752–3760.
- Inam, A., Adamowski, J., Halbe, J., & Prasher, S. (2015). Using causal loop diagrams for the initialization of stakeholder engagement in soil salinity management in agricultural watersheds in developing countries: A case study in the Rechna Doab watershed, Pakistan. *Journal of Environmental Management*, 152, 251–267.
- Keogh, R., & Pearson, J. (2017). The perceptual and phenomenal capacity of mental imagery. *Cognition*, 162, 124–132.
- Łapa, K., Zalasinski, M., & Cpałka, K. (2013). A new method for designing and complexity reduction of neuro-fuzzy systems for nonlinear modelling. *International Conference on Artificial Intelligence and Soft Computing*, 329–344.
- Mesmin, C., van Oostrum, J., & Domon, B. (2016). Complexity reduction of clinical samples for routine mass spectrometric analysis. *PROTEOMICS–Clinical Applications*, 10(4), 315–322.
- Morecroft, J. D. W. (1982). A critical review of diagramming tools for conceptualizing feedback system models. *Dynamica*, 8(1), 20–29.
- Vugteveen, P., Rouwette, E., Stouten, H., van Katwijk, M. M., & Hanssen, L. (2015). Developing social-ecological system indicators using group model building. *Ocean & Coastal Management*, 109, 29–39.



## Reuse of Wastewater for Irrigation Purposes in Pakistan

Asim Qayyum Butt<sup>1\*</sup>, Allah Bachaya<sup>1</sup>, Abid Latif<sup>2</sup>, Amna<sup>2</sup>, Aleeza Kainat<sup>2</sup>, Sarfaraz Ali<sup>2</sup>, Muhammad Arif<sup>2</sup>

<sup>1</sup> Civil Engineering Department, Quaid e Azam College of Engineering and Technology, Sahiwal

<sup>2</sup> Civil Engineering Department, BahauDin Zakariya University, Multan

Corresponding author email: [asimbutt7891@gmail.com](mailto:asimbutt7891@gmail.com)

**Abstract:** Agricultural field is the backbone of a Pakistan as it provides food, fiber, enhances economy which is the basic needs. To overcome the shortage of water in developing countries like Pakistan, where agriculture is major source of income, it is necessary to reuse wastewater for irrigation purpose after its treatment. The operation and maintenance are important in treatment of wastewater. In the present situation, it has become necessary for the planners to consider other additional unconventional sources of water to cope with increasing water scarcity that can be used economically and effectively for irrigation and wastewater is important for this. Therefore, use of treated municipal wastewater is introduced to prevent environmental pollution and as a source for irrigation in agriculture. The objectives of the research work are to determine the percentage reduction in different parameters of wastewater like Total Dissolved Solids (TDS), Electrical Conductivity (ECw), Sodium Absorption Ratio (SAR) Sodium, Chloride, Boron, Nitrate, Bicarbonate, pH and F Coliforms. To analyze and compare different samples for their initial raw water value, 3,5 and 10 days treatment value and find out the required Hydraulic Retention Time (HRT) so that, wastewater can be used for irrigation purposes according to FAO Irrigation Water Quality Guidelines. Sample was taken and preserved as per standards guidelines of WHO and American Public Health Association. The result clearly shows that if domestic wastewater is to be reused for irrigation purposes it must be treated by macrophytes Waste Stabilization Ponds with HRT of 10 days with slight to moderate restriction on use.

**Keywords:** Agriculture, wastewater, macrophytes, treatment, Irrigation, Hydraulic Retention Time, WHO

### Introduction:

Pakistan is an agricultural country. Economy of Pakistan tremendously depends upon agriculture. Agriculture in Pakistan directly supports country's population and accounts for 26% of gross domestic product (GDP). Total GDP is defined as sum of value added from total agriculture, industry and service sectors. Water scarcity affects around 2.8 billion people around the world at least one month out of every year. More than 1.2 billion people lack access to clean drinking water. Drinking of polluted water causes various diseases. The situation is going towards the worst water scarcity due to Indian obstruction of western rivers water. However, the most important risks associated with wastewater irrigation are related to the impact on environment and human health, safety and quality of agricultural products, salt accumulation, and water infiltration capacity of soil along with the accumulation of heavy metals and contamination caused by nutrient leaching. In the present situation, it has become necessary for the planners to consider other additional

unconventional sources of water to cope with increasing water scarcity that can be used economically and effectively for irrigation and wastewater is important for this. Therefore, use of treated municipal wastewater is introduced to prevent environmental pollution and as a source for irrigation in agriculture. Pakistan has one of the world's largest groundwater aquifer (4th after China, India and the USA). It provides more than 60% irrigation water supplies and over 90% drinking water to the people. Different research have brought their attention about waste water treatment. The methods through which aeration is introduced into the process also aid in providing constant mixing to the wastewater and flocs ("Wastewater characteristics, treatment and disposal," 2008). Activated sludge processes designed for nitrogen removal are one of the most complicated microbial systems used for engineering purposes. Activated sludge requires a high level of process control, incorporating both the quality of the flocs/sludge produced and the supply of oxygen to the flocs (Nurarif & Kusuma, 2013). To maintain a healthy floc population for effective nutrient removal, a large

portion of the mixed liquor that leaves the activated sludge process and undergoes secondary clarification is returned from the base of the secondary clarifier back to the head of the activated sludge process as return activated sludge (RAS) to re-seed the process. Mixed liquor which is not required to reseed the wastewater entering the activated sludge process is discharged into secondary clarifiers as waste activated sludge (Arun Mittal, 2011). Attached growth processes, also known as fixed film processes, involve the development and maintenance of microbial growth which attaches itself to available surfaces. This microbial growth consists of bacteria, fungi, algae and other microorganisms (collectively known as biomass) which develop on the media as a biofilm (Trikoilidou, Samiotis, Bellos, & Amanatidou, 2016). Wastewater treatment often concludes with tertiary and/or advanced treatment. For example, WAS can be treated for disposal or transport and the treated wastewater leaving secondary treatment can undergo treatment such as filtration and disinfection to achieve targeted contaminant removal e.g. pathogens, metals etc. alongside additional removal of suspended solids or nutrients. Constructed wetland are used for water reclamation, treated effluent can be reused for restricted or unrestricted irrigation of agricultural crops, toilet flush, watering of gardens, golf courses, and public parks, depending on its quality. Constructed wetlands have been increasingly used throughout the world for secondary and especially for tertiary treatment of wastewater and storm water (Mousavi et al., 2015). If well designed and maintained, their effluents can meet the high standards required for reclaiming the water. One can also partially reclaim nutrients by harvesting the aquatic vegetation or by combining wastewater treatment with aquaculture. Constructed wetlands further provide certain ancillary benefits such as wildlife habitat function, recreational facilities etc. (Yadav & Dharmendra, 2014) Large land area also required in big city land price more costly so it not suitable for large city it suitable for rural area and low population city. Its main advantage is operation and maintenance cost low and not required more skilled labor. When carefully designed and maintained, constructed wetlands can yield, at relatively low costs, an effluent suitable for reuse and concurrently provide some opportunities to recycle nutrients and to accommodate wildlife. An additional benefit gained by using wetlands

for wastewater treatment is the multi-purpose sustainable utilization of the facility for uses such as swamp fisheries, biomass production, seasonal agriculture, water supply, public recreation, wild life conservation and scientific study (Brix, 1994). Reed bed systems have many applications in developing countries, because of low Operating and Maintenance Costs. In a study with Typha beds it was concluded that local people in Tanzania could also use Typha for production of biogas, unrefined material for basket lacing and for roofing basics. However, there is a common lack of awareness of hygiene and water reusing techniques in developing countries (Dallas, Scheffe, & Ho, 2004). The role of macrophytes is to provide suitable environments for microbial growth, preventing flow and retaining solid wastes. They also stimulate the soil movement by root excretions and lessen the amount of effluent by transpiration. Moreover, the amassing of few mineral elements within the body of plant has a linear connection with the elimination of pollutants from wastewater. Macrophyte plants have produced noticeable enhancement in all aspects of wastewater quality, and reed bed systems are constantly economical per head and have low usual operational requirements (Ciria, Solano, & Soriano, 2005). Proper plants for wastewater examinations include number of species i.e. Cyperaceae, Typhaceae and Juncaceae. The chosen species should have a more production rate. Other criteria required are more oxygen transport ability, forbearance to adverse applications of pollutants, forbearance to adverse environmental conditions, resistance to diseases and simplicity of management. macrophytes species should also be chosen based on fast growth rate, ease of spread, ability for absorption of pollutants, ease of harvesting and prospective usefulness of harvested materials (Dallas et al., 2004). Constructed wetlands using plants of Triglochin, Schoenoplectus and Phragmites have been effective to remove nitrogen and phosphorous from domestic wastewaters, and that the efficiency of removal depends on the design of the macrophytes and Hydraulic Retention Time. Almost all reed beds in the United Kingdom and Europe are planted with species of Phragmites to remove heavy metals, such as zinc, lead, copper, cadmium and nickel. Conversely, Phragmites and Typha should not be used in municipal wastewater treatment systems in warm climates (Dallas et al., 2004). Moreover, macrophytes species consisting an

interior convective ventilation method have more oxygen concentrations in the roots than species depending just on the permeability of root zone. Internal transportation of oxygen in macrophytes plants generally occurs diffusion of air through pores of the plants (Ciria et al., 2005). Redistribution of biomass among different sections is necessary for existing of water altitude changes. Macrophytes species that can sustain distribution to roots without a poor effect are additional advantage. It appears that swamp macrophytes do hold elevated storage abilities and can transfer stored nutrients from one part to another. The more useful floating plants, such as Azolla, have normally more uptake abilities whereas the ability of submerged type of macrophytes is lesser. Yet, the area required for domestic wastewater treatment for phosphorus and nitrogen removal only by water hyacinths would still be more than that of submerged macrophytes (Shah, Hashmi, Ghumman, & Zeeshan, 2015). The consequences of engineered marshland methods either with Collocasia and Typhha can eliminate nitrate, sulfate, BOD, phosphorus, ammonia and COD for municipal wastewater. The average removal values for sulfate were 68–74%, for phosphorous 70%–76%, for COD 75–76%, and for ammonia 74–78%. It might therefore be concluded that the engineered marshland methods are effective in treatment of domestic sewage water. It was also concluded that marshland plants also enhanced the effectiveness of marshland system. The results also show that Engineered Wetland System with the help of plants have major performance than that of the system without plants. Furthermore, the choice of the proper species of plants for the employ in marshland may be used by its distinctiveness including its aesthetic suitability (Dhote & Dixit, 2009). There are agronomic and economic benefits of wastewater use in agriculture. Irrigation with wastewater can increase the available water supply or release better quality supplies for alternative uses. In addition to these direct economic benefits that conserve natural resources, the fertilizer value of many wastewaters is important (Anwar, Nosheen, Hussain, & Nawaz, 2010). FAO (1992) estimated that typical wastewater effluent from domestic sources could supply all of the nitrogen and much of the phosphorus and potassium that are normally required for agricultural crop production. In addition, micronutrients and organic matter also provide additional benefits.

Indirect use occurs when treated, partially treated or untreated wastewater is discharged to reservoirs, rivers and canals that supply irrigation water to agriculture. Indirect use poses the same health risks as planned wastewater use projects but may have a greater potential for health problems because the water user is unaware of the wastewater being present. Indirect use is likely to expand rapidly in the future as urban population growth outstrips the financial resources to build adequate treatment works (Nurarif & Kusuma, 2013). Contamination of surface water with pathogenic organisms in wastewater could result in the transmission of waterborne diseases for people who use the water resource for domestic and other purposes downstream. About 25% of all deaths worldwide are the result of infectious diseases caused by pathogenic microorganisms. Scientists have identified about 1400 species of microorganisms that can cause ill health, including bacteria, protozoa, protozoan parasites, parasitic worms, fungi, and viruses (Angelakis & Snyder, 2015). The major concern of wastewater discharge onto freshwater courses is the impact they have on public health. Wastewater consists of various classes of pathogens which are capable of causing diseases of various magnitude to man. Unlike some of the environmental impacts that can take a long time before they manifest, pathogens cause immediate negative health impact on people that use contaminated surface water resource for domestic, agricultural, and recreational purposes (Ilyas et al., 2019). Poorly treated wastewater can have a profound influence on the receiving watershed. The toxic impacts may be acute or cumulative. Acute impacts from wastewater effluents are generally due to high levels of ammonia and chlorine, high loads of oxygen-demanding materials, or toxic concentrations of heavy metals and organic contaminants. Cumulative impacts are due to the gradual buildup of pollutants in receiving surface water, which only become apparent when a certain threshold is exceeded. All aquatic organisms have a temperature range for their optimum function and survival. When there are sudden changes within those ranges, their reproductive cycle, growth, and life can be reduced or threatened. Owing to the organic load of wastewater, discharged effluents from wastewater treatment facilities usually contribute to oxygen demand level of the receiving water. There is increased depletion of dissolved oxygen

(DO) in surface water that receives ill-treated wastewater (Akpore & Muchie, 2011).

## Methodology

The main objectives of the research work are to determine the percentage reduction in different parameters of wastewater like Total Dissolved Solids (TDS), Electrical Conductivity (EC<sub>w</sub>), Sodium Absorption Ratio (SAR) Sodium, Chloride, Boron, Nitrate, Bicarbonate, pH and F Coliforms, so that, wastewater can be used for irrigation purposes according to FAO Irrigation Water Quality Guidelines with slight to moderate or no degree of restriction on use. And to analyze and compare different samples for their initial raw water value, 3 days treatment value, 5 days treatment value, 7 days treatment value and 10 days treatment value and find out the required Hydraulic Retention Time (HRT) for wastewater to be used for irrigation purposes. Selection of the treatment processes that are to be utilized occurs at the design stage and is based on considerations including (i) hydraulic and pollutant loading which are expected to enter the WWTP and (ii) the level of treatment required. Furthermore, WWTPs can be unique to a given site; numerous combinations of processes can be employed in a WWTP and these processes interact with one another, whereby a particular process can impact the performance of a preceding or subsequent processes (Spellman, 2003). In addition, WWTP characteristics such as scale, regulations and influent characteristics can change. For example, demographics can impact hydraulic and pollutant loading into a WWTP, generating the need for process upgrades or operational changes. These WWTPs must be flexible to change and efficiently operated to maximize existing capacity.

To study the removal efficiency of different parameters of wastewater by treating it with macrophytes (Waste Stabilization Ponds) so that wastewater can be used for irrigation purposes according to Food and Agriculture Organization (FAO) Irrigation Water Quality Guidelines. A small bench scale model was constructed and designed at a plot in Agha Pora near Delhi Gate, Multan. The domestic wastewater was collected from Nallah. The species used for the treating wastewater was Azolla (Aquatic Fern). The construction of model took place by excavating soil of dimension 10'×4'×1.5' from the mentioned spot. Plastic sheet was spreaded all

over the excavated area to control seepage. The model is illustrated in figure below:

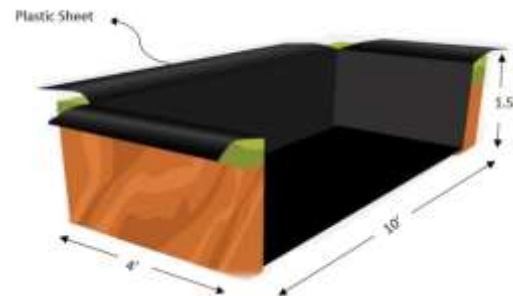


Figure 25: Section of Model



Figure 26: Physical View of Model

In balancing of Lake Ecosystem, macrophytes play a very important role. The plants macrophytes have a tendency to develop the water quality of wastewater through absorbing nutrients by the use of their efficient root system. This objective of research is to assess the usefulness of plants macrophytes in reducing the harmful parameters so that wastewater can be used for irrigation. In this research work one of the Macrophytic Species Aquatic Fern commonly called Azolla is selected for study. Following parameters of wastewater were selected to examine during the research work:

- Total Dissolved Solids (TDS)
- Electrical Conductivity (EC<sub>w</sub>)
- Sodium Absorption Ratio (SAR)
- Sodium
- Chloride
- Boron
- Nitrate
- Bicarbonate
- pH
- F Coliform

## Results and Discussions

Tests results of different parameters of wastewater which are essential for irrigation use were conducted on sewerage wastewater samples. The different parameters include Electrical Conductivity (EC<sub>w</sub>), Total Dissolved

Solids (TDS), Sodium Absorption Ratio (SAR), Sodium, Chloride, Boron, Nitrate, Bicarbonate, pH and F Coliform. The results are analyzed and tabulated in the forthcoming sections of the chapter.

The samples of wastewater were collected from the domestic sewer of Delhi Gate, Multan. After collection of samples, it was tested in laboratory PAKISTAN COUNCIL OF RESEARCH IN WATER RESOURCES, MULTAN. The results of untreated samples before the start of each trial are given below in the Table 1.

The results of untreated wastewater depicts that wastewater is of strong strength (Food and Agriculture Organization Irrigation water Quality Guidelines). All the samples of wastewater which were collected from the municipal sewer was first of all sent to primary(basic) settling tank and after screening through tank, it was distributed into lagoon having macrophytes. The specie of macrophyte taken was Azolla. The wastewater was retained for 3, 5, 7 and 10 days in model during each experimental run, and total of five runs were performed to check reduction in values of different parameters so that it can be used for irrigation purposes according to FAO (Food and Agriculture Organization) Irrigation Water Quality Guidelines. After completion of treatment from each Hydraulic Retention Time (HRT), treated wastewater samples were collected from aquatic model and tested for determination of percentage reduction in different parameters. The plants in model were yielded 2 to 3 times per week. All analysis of parameters was performed accordingly with

Standard Methods for Preservation and Examination of Wastewater (American Public Health Association). The average temperature during whole study was between 20°C and 25°C with an average of 23°C. The surface area maintained by the plants was 85 % to 95%. The average reduction of different parameters of wastewater against different Hydraulic Retention Time (HRT) during five experimental runs is given below in different tables.

Descriptive statistical data of the experimental raw municipal wastewater sample have been shown in Table 2.

The results shows the removal efficiencies of different parameters of wastewater by stabilization pond system expressed as percentage of untreated raw wastewater.

The test results of the first experiment after treatment with 10 days HRT shows a reduction of 35.54% in Electrical Conductivity (EC<sub>w</sub>), 35.54% in Total Dissolved solids (TDS), 41.73% in Soil Absorption Ratio (SAR), 30.28% in Sodium, 23.47% in Chloride, 33.68% in Boron, 31.27% in Nitrate, 48.76% in Bicarbonate, 19.57% in pH and 39.71% in F Coliform respectively.

The test results of the second experiment after treatment with 10 days HRT shows a reduction of 30.29% in Electrical Conductivity (EC<sub>w</sub>), 30.29% in Total Dissolved solids (TDS), 43.33% in Soil Absorption Ratio (SAR), 32.12% in Sodium, 21.90% in Chloride, 35.15% in Boron, 30.43% in Nitrate, 51.42% in Bicarbonate, 21.37% in pH and 42.69% in F Coliform respectively.

**Table 12** Raw water composition of different parameters during five experimental runs

Sr. #	Water Quality Parameter	Unit	Sample 1	Sample 2	Sample 3	Sample 4	Sample 5
1.	EC <sub>w</sub>	ds/m	4.471	3.731	4.120	4.325	4.948
2.	TDS	mg/L	2459	2212	2736	1958	2150
3.	SAR	No.	5.87	4.80	6.13	5.23	4.68
4.	Sodium	meq/L	11.26	12.17	10.95	10.50	11.83
5.	Chloride	meq/L	10.31	9.95	11.03	9.25	10.74
6.	Boron	mg/L	3.74	4.38	3.25	3.97	3.10
7.	Nitrate	mg/L	35.84	29.83	33.15	37.04	31.85
8.	Bicarbonate	meq/L	14.95	11.22	16.54	13.13	15.87
9.	pH	No.	8.43	8.33	8.12	8.56	8.20
10.	F Coliform	No. / 100mL	1352	1136	1378	1295	1217

**Table 13** Statistical Data of different Parameters

Sr. No	Parameter	Unit	Average value	Standard Deviation
1	EC <sub>w</sub>	ds/m	4.319	0.58
2	TDS	mg/L	2303	301.05
3	SAR	No.	5.342	0.64
4	Sodium	meq/L	11.342	0.67
5	Chloride	meq/L	10.256	0.69
6	Boron	mg/L	3.688	0.52
7	Nitrate	mg/L	25.564	9.39
8	Bicarbonate	meq/L	14.346	2.165
9	pH	No.	8.33	0.176
10	F Coliform	No./100mL	1275.6	99.01

**Table 14** Results of Sample 1

Sr. #	Water Quality Parameter	Unit	Raw Wastewater Values	Result of 3 days HRT	Result of 5 days HRT	Result of 7 days HRT	Result of 10 days HRT	% reduction after 10 days HRT
1.	EC <sub>w</sub>	ds/m	4.471	3.982	3.382	2,961	2.882	35.54%
2.	TDS	mg/L	2459	2135	1876	1668	1585	35.54%
3.	SAR	No.	5.87	5.03	4.37	3.52	2.74	41.73%
4.	Sodium	meq/L	11.26	10.67	8.93	8.19	7.85	30.28%
5.	Chloride	meq/L	10.31	9.82	9.17	8.36	7.89	23.47%
6.	Boron	mg/L	3.74	3.32	2.98	2.77	2.48	33.68%
7.	Nitrate	mg/L	35.84	31.96	29.41	26.95	24.63	31.27%
8.	Bicarbonate	meq/L	14.95	12.73	9.96	8.23	7.66	48.76%
9.	pH	No.	8.43	8.02	7.75	6.94	6.33	19.57%
10.	F Coliform	No./100mL	1352	1225	1069	982	815	39.71%

**Table 15** Results of Sample 2

Sr. #	Water Quality Parameter	Unit	Raw Wastewater Values	Result of 3 days HRT	Result of 5 days HRT	Result of 7 days HRT	Result of 10 days HRT	% reduction after 10 days HRT
1.	EC <sub>w</sub>	ds/m	3.731	3.574	3.192	2.835	2.601	30.29%
2.	TDS	mg/L	2212	2105	1923	1745	1542	30.29%
3.	SAR	No.	4.80	4.67	4.22	3.58	2.72	43.33%
4.	Sodium	meq/L	12.17	11.49	10.23	9.57	8.26	32.12%
5.	Chloride	meq/L	9.95	9.52	8.94	8.30	7.77	21.90%
6.	Boron	mg/L	4.38	4.09	3.71	3.16	2.84	35.15%
7.	Nitrate	mg/L	29.83	28.11	25.64	22.93	20.75	30.43%
8.	Bicarbonate	meq/L	11.22	9.75	8.12	6.67	5.45	51.42%
9.	pH	No.	8.33	8.12	7.65	6.92	6.55	21.37%
10.	F Coliform	No./100mL	1136	1054	892	779	651	42.69%



**Table 16** Results of Sample 3

Sr. #	Water Quality Parameter	Unit	Raw Wastewater Values	Result of 3 days HRT	Result of 5 days HRT	Result of 7 days HRT	Result of 10 days HRT	% reduction after 10 days HRT
1.	EC <sub>w</sub>	ds/m	4.120	3.892	3.551	3.182	2.740	33.50%
2.	TDS	mg/L	2736	2571	2328	2045	1819	33.50%
3.	SAR	No.	6.13	5.27	4.77	4.16	3.41	44.37%
4.	Sodium	meq/L	10.95	10.55	9.95	8.63	7.85	29.31%
5.	Chloride	meq/L	11.03	10.68	10.02	9.51	8.10	26.56%
6.	Boron	mg/L	3.25	3.04	2.76	2.39	2.18	32.92%
7.	Nitrate	mg/L	33.15	31.62	28.45	25.03	22.41	32.39%
8.	Bicarbonate	meq/L	15.54	14.84	13.12	10.97	8.10	47.88%
9.	pH	No.	8.12	8.05	7.59	6.64	6.50	19.95%
10.	F Coliform	No./100mL	1378	1236	1081	967	858	37.73%

The test results of the third experiment after treatment with 10 days HRT shows a reduction of 33.50% in Electrical Conductivity (EC<sub>w</sub>), 33.50% in Total Dissolved solids (TDS), 44.37% in Soil Absorption Ratio (SAR), 29.31% in Sodium, 26.56% in Chloride, 32.92% in Boron, 32.39% in Nitrate, 47.88% in Bicarbonate, 19.95% in pH and 37.73% in F Coliform respectively.

The test results of the fourth experiment after treatment with 10 days HRT shows a reduction of 29.82% in Electrical Conductivity (EC<sub>w</sub>), 29.82% in Total Dissolved solids (TDS), 40.71% in Soil Absorption Ratio (SAR), 28.09% in

Sodium, 19.67% in Chloride, 33.24% in Boron, 29.64% in Nitrate, 44.70% in Bicarbonate, 20.56% in pH and 44.86% in F Coliform respectively.

The test results of the fifth experiment after treatment with 10 days HRT shows a reduction of 31.66% in Electrical Conductivity (EC<sub>w</sub>), 31.66% in Total Dissolved solids (TDS), 41.23% in Soil Absorption Ratio (SAR), 29.85 % in Sodium, 24.48 % in Chloride, 31.29% in Boron, 30.76% in Nitrate, 52.17% in Bicarbonate, 18.78% in pH and 41.49% in F Coliform respectively.

**Table 17** Results of Sample 4

Sr. #	Water Quality Parameter	Unit	Raw Wastewater Values	Result of 3 days HRT	Result of 5 days HRT	Result of 7 days HRT	Result of 10 days HRT	% reduction after 10 days HRT
1.	EC <sub>w</sub>	ds/m	4.325	4.117	3.829	3.346	3.035	29.82%
2.	TDS	mg/L	1958	1782	1623	1498	1374	29.82%
3.	SAR	No.	5.23	4.86	4.34	3.77	3.14	40.71%
4.	Sodium	meq/L	10.50	10.04	9.82	8.34	7.55	28.09%
5.	Chloride	meq/L	9.25	8.79	8.21	7.93	7.43	19.67%
6.	Boron	mg/L	3.97	3.62	3.04	2.88	2.65	33.24%
7.	Nitrate	mg/L	37.04	35.31	31.58	29.17	26.06	29.64%
8.	Bicarbonate	meq/L	13.13	11.91	10.23	8.45	7.26	44.70%
9.	pH	No.	8.56	8.22	7.87	7.19	6.80	20.56%
10.	F Coliform	No./100mL	1295	1083	955	826	714	44.86%

**Table 18** Results of Sample 5

Sr. #	Water Quality Parameter	Unit	Raw Wastewater Values	Result of 3 days HRT	Result of 5 days HRT	Result of 7 days HRT	Result of 10 days HRT	% reduction after 10 days HRT
1.	EC <sub>w</sub>	ds/m	3.948	3.714	3.426	2.917	2.698	31.66%
2.	TDS	mg/L	2150	2013	1812	1607	1469	31.66%
3.	SAR	No.	4.68	4.31	3.86	3.10	2.75	41.23%
4.	Sodium	meq/L	11.83	11.07	10.33	9.21	8.28	29.85%
5.	Chloride	meq/L	10.74	9.98	9.27	8.64	8.11	24.48%
6.	Boron	mg/L	3.10	2.93	2.65	2.37	2.13	31.29%
7.	Nitrate	mg/L	31.85	28.72	25.98	23.84	22.05	30.76%
8.	Bicarbonate	meq/L	15.87	13.56	11.02	8.95	7.59	52.17%
9.	pH	No.	8.20	7.76	7.31	6.89	6.66	18.78%
10.	F Coliform	No./100mL	1217	1041	890	803	712	41.49%

**Analysis**

**Electrical Conductivity**

The range of raw value of EC<sub>w</sub> was in 3.731ds/m to 4.948ds/m. The effluent values of EC<sub>w</sub> decreases from 4.471ds/m to 2.882ds/m in experiment 1, 3.731ds/m to 2.601ds/m in experiment 2, 4.12ds/m to 2.74ds/m in experiment 3, 4.325ds/m to 3.035ds/m in experiment 4 and 3.948ds/m to 2.698ds/m in experiment 5.

The values of Electrical conductivity for all five samples fall in range of severe degree of restriction on use for irrigation purposes according to Food and Agriculture (FAO) Irrigation Water quality Guidelines. Therefore this wastewater has to be treated in order to use it for irrigation purposes. Results shows that for sample 1, 2 and 5, the values in range of slight to moderate restriction was achieved after 7 days HRT, while for Sample 3 and 4, the required value was achieved after treatment with 10 days HRT. Therefore results shows that in order to reduce the value of EC<sub>w</sub> according to FAO guidelines it should be treated with 10 days HRT. Figure 4.1 depicts the total percentage reduction at each Hydraulic Retention Time for all five experimental runs.

**Total Dissolved Solids (TDS)**

The range of raw value of TDS was in 1958mg/L to 2736mg/L. The effluent values of TDS decreases from 2459mg/L to 1585mg/L in experiment 1, 2212mg/L to 1542mg/L in experiment 2, 2736mg/L to 1819mg/L in

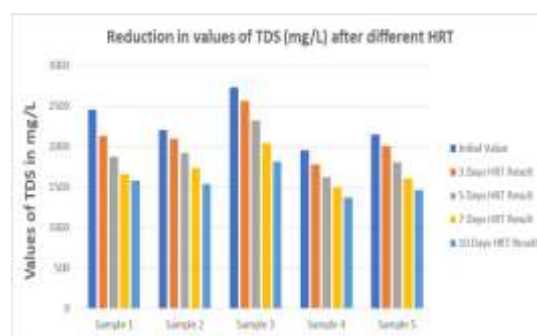


**Figure 27** Reduction of EC<sub>w</sub> during different Hydraulic Retention Time

experiment 3, 1958mg/L to 1374mg/L in experiment 4 and 2150mg/L to 1469 mg/L in experiment 5.

The values of Total Dissolved solids for sample number 1, 2, 3 and 5 fall in range of severe degree of restriction on use for irrigation purposes according to Food and Agriculture (FAO) Irrigation Water quality Guidelines, whereas sample 4 was in range of slight to moderate restriction in raw form.

Therefore this wastewater has to be treated in order to use it for irrigation purposes. But for sample 1, 2 and 5 the values were in range of slight to moderate restriction after treating with macrophytes stabilization ponds with 5 days HRT, while for sample 3, the required value was achieved after treatment with stabilization ponds with 10 days HRT. Therefore results shows that in order to reduce the value of TDS it should be treated with 10 days HRT to achieve FAO guidelines. The test results shows 35.54%, 30.29%, 33.50%, 29.82% and 31.66% reduction in sample 1, sample 2, sample 3, sample 4 and sample 5 respectively after 10 days HRT. The

severe degree of restriction on use according to FAO Guidelines is 2000mg/L.

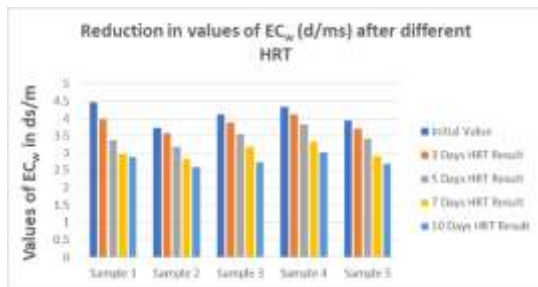


**Figure 28** Reduction of TDS during different Hydraulic Retention Times

### Sodium Absorption Ratio(SAR)

Sodium Absorption Ratio depends on three parameters i.e. Sodium, Magnesium and Calcium. The SAR is determined by using formula given below in eq 1.

$$\left\{ SAR = \frac{Na^+}{\sqrt{Ca^{2+} + Mg^{2+}/2}} \right\} \quad (1)$$

where values of sodium, magnesium and calcium are in meq/L

The values of sodium, magnesium and calcium are given in table below:

The Sodium Absorption Ratio (SAR) for wastewater was in range of 4.68 to 6.13. The ratio of SAR for treated wastewater decreases from 5.87 to 2.74 in experiment 1, 4.8 to 2.72 in experiment 2, 6.13 to 3.41 in experiment 3, 5.23 to 3.14 in experiment 4 and 4.68 to 2.75 in experiment 5. Sodium Absorption Ratio is very important parameter regarding use of wastewater for irrigation purposes. According to FAO guidelines if SAR is 0 to 3 then  $EC_w$  should be greater than 0.7ds/m in order to use it for irrigation purposes. Similarly if SAR is 3 to 6 the  $EC_w$  should be greater than 1.2ds/m in order to use it for Irrigation Purposes according to FAO criteria with no restriction on use. Corresponding value of  $EC_w$  for all five samples of SAR was greater than required value according to FAO Irrigation Water Quality Guidelines even in raw form.

**Table 19** Determination of Sodium Absorption Ratio

Sample No.	Sodium (meq/L)	Magnesium (meq/L)	Calcium (meq/L)	Sodium Absorption Ratio
Sample 1	11.26	4.00	3.36	5.87
Sample 2	12.17	6.49	6.30	4.80
Sample 3	10.95	3.07	3.30	6.13
Sample 4	10.50	3.04	5.04	5.23
Sample 5	11.83	5.62	7.20	4.68

The test results shows 41.73%, 43.33%, 44.37%, 40.71% and 41.23s% reduction in sample 1, sample 2, sample 3, sample 4 and sample 5 respectively after 10 days HRT.

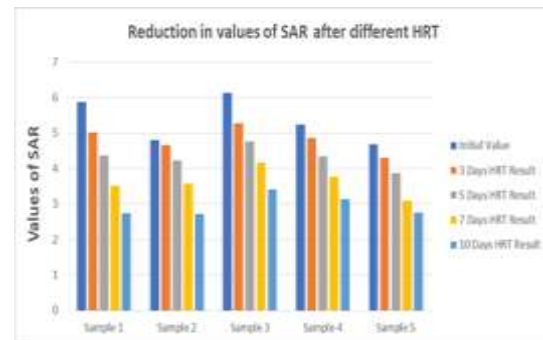


**Figure 29** Reduction SAR during different Hydraulic Retention Times

### Sodium

The raw values of Sodium were in range of 10.50meq/L to 12.17meq/L. The effluent values of Sodium decreases from 11.26meq/L to 7.85meq/L in experiment 1, 12.17meq/L to 8.26meq/L in experiment 2, 10.95meq/L to 8.63meq/L in experiment 3, 10.50meq/L to 7.55meq/L in experiment 4 and 11.83meq/L to 8.28meq/L in experiment 5.

The concentration of sodium for all five samples was greater than 3meq/L, which is required value for wastewater to be used for irrigation purposes by sprinkler method of irrigation according to FAO guidelines with slight to moderate restriction on use. Other criteria investigate to check whether wastewater can be used for irrigation purposes with respect to sodium is by checking its SAR value. The SAR value should be 3 to 9 in order to use wastewater for irrigation purposes if method of irrigation is surface irrigation. The SAR value was 3 to 6 even in raw form.

The test results shows 30.28%, 32.12%, 29.31%, 28.09% and 29.85% reduction in sample 1, sample 2, sample 3, sample 4 and sample 5 respectively after 10 days HRT.

After results of five samples, the average reduction in value of sodium after five samples is illustrated in the following graphs.

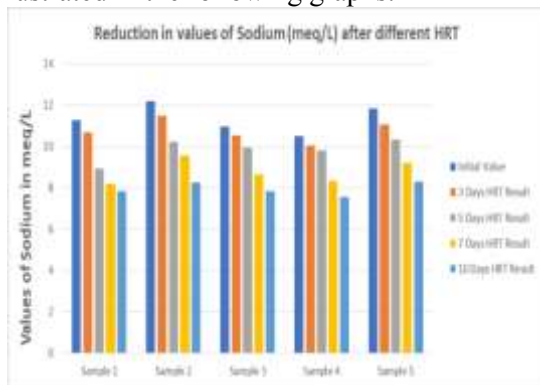


**Figure 30** Reduction of Sodium during different HRT

### Chloride

The raw values of Chloride were in range of 9.25meq/L to 11.03meq/L. The effluent values of Chloride decreases from 10.31meq/L to 7.89meq/L in experiment 1, 9.95meq/L to 7.77meq/L in experiment 2, 11.03meq/L to 8.10meq/L in experiment 3, 9.25meq/L to 7.43meq/L in experiment 4 and 10.74meq/L to 8.11meq/L in experiment 5.

The standards value of chloride according to FAO water quality guidelines is 4meq/L to 10meq/L for surface irrigation method with slight to moderate degree of restriction on use whereas for sprinkler irrigation method this value should be greater than 3meq/L with same degree of restriction on use. The concentration of chloride for sample 2 and 4 was within standards values even in raw form, while for sample 1 and 5 the required standards were achieved after treatment of wastewater in stabilization ponds with 3 days HRT. As far as sample 3 was concerned the required value was achieved after 7 days HRT. Result shows that to reduce the chloride content in wastewater according to FAO guidelines the required HRT was 7 days.

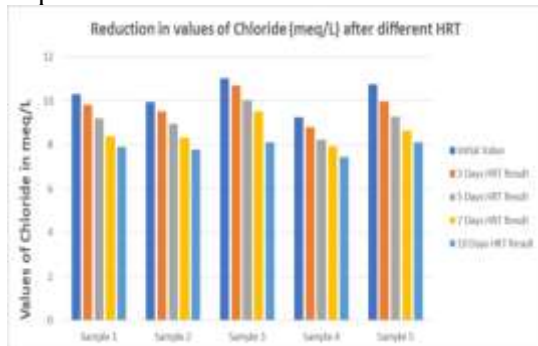


**Figure 31** Reduction of Chloride during different HRT

The test results shows 23.47%, 21.90%, 26.56%, 19.67% and 24.48% reduction in sample 1, sample 2, sample 3, sample 4 and sample 5 respectively after 10 days HRT.

### Boron

The raw values of Boron were in range of 3.10mg/ to 4.38mg/L. The effluent values of Boron decreases from 3.74mg/L to 2.48mg/L in experiment 1, 4.38mg/L to 2.84mg/L in experiment 2, 3.25mg/L to 2.18mg/L in experiment 3, 3.97mg/L to 2.65mg/L in experiment 4 and 3.10mg/L to 2.13mg/L in experiment 5. The concentration of Boron for sample 2, achieved the Food and Agriculture Organization (FAO) slight to moderate standards value i.e. 0.7mg/L to 3.0mg/L after 10 days Hydraulic Retention Time (HRT). For sample 5 the required standards of FAO was achieved by treating wastewater with stabilization ponds with even 03 days HRT, Sample 1 and 3 after 05 days HRT, and Sample 4 after 07 days HRT. Hence results shows that if wastewater is used for irrigation purposes according to FAO standards of light to moderate use, then to reduce the value of Boron it should be treated with macrophytes with HTR of 10 days.

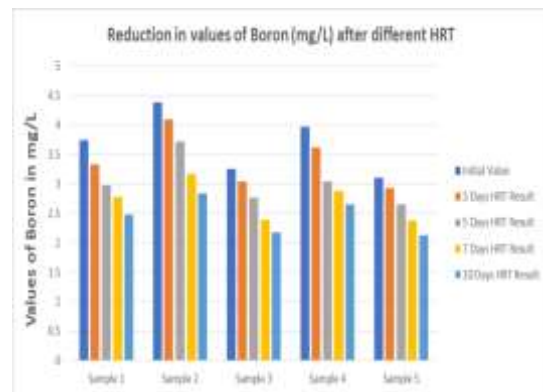


**Figure 32** Reduction of Boron during different HRT

The test results shows 33.68%, 35.15%, 32.92%, 33.24% and 31.29% reduction in sample 1, sample 2, sample 3, sample 4 and sample 5 respectively after 10 days HRT.

### Nitrate

The range of raw value of Nitrate was in 29.83mg/L to 37.04mg/L. The effluent values of Nitrate decreases from 35.84mg/L to 24.63mg/L in experiment 1, 29.83mg/L to 20.75mg/L in experiment 2, 33.15mg/L to 22.41mg/L in experiment 3, 37.04mg/L to 26.06mg/L in

experiment 4 and 31.85mg/L to 22.05mg/L in experiment 5.

The concentration of Nitrate of sample 4 achieved the FAO Irrigation Water Quality Guidelines value i.e. 5mg/L to 30mg/L after treatment with stabilization ponds with 7 days Hydraulic Retention Time (HRT). The value of 0.7mg/L to 30mg/L for sample 1 and 3 achieved the required values after treatment with 5 days HRT, and Sample 5 days after 3 days HRT while sample 2 were within values even in raw form. Therefore result shows that wastewater should be treated with HRT of 7 days to reduce the value of Nitrate in order to use it for irrigation purposes according to FAO guidelines.

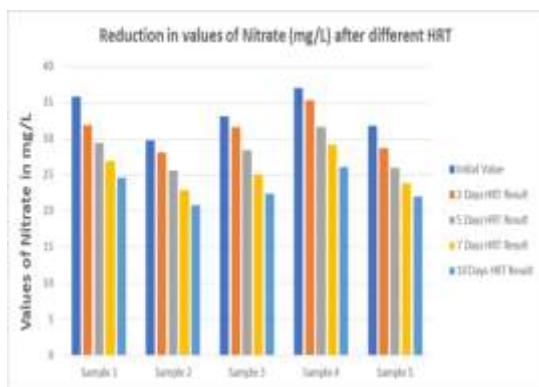


**Figure 33** Reduction of Nitrate during different HRT

The test results shows 31.27%, 30.43%, 32.39%, 29.64% and 30.76% reduction in sample 1, sample 2, sample 3, sample 4 and sample 5 respectively after 10 days HRT. The black line shows the FAO Irrigation Water Quality Guidelines value i.e. 30mg/L.

### Bicarbonate

The range of raw value of Bicarbonate was in 11.22meq/L to 16.54meq/L. The effluent values of Bicarbonate decreases from 14.95meq/L to 7.66meq/L in experiment 1, 11.22meq/L to 5.45meq/L in experiment 2, 16.54meq/L to 8.62mg/L in experiment 3, 13.13mg/L to 7.26meq/L in experiment 4 and 15.87meq/L to 7.59meq/L in experiment 5.

The concentration of Bicarbonate of sample 3 and 5, achieved the FAO Irrigation Water Quality Guidelines value i.e. 1.5meq/L to 8.5meq/L with slight to moderate use of restriction on use after treating with waste stabilization ponds with 10 days Hydraulic Retention Time (HRT). The value of 1.5meq/L to 8.5meq/L for sample 1 and 4 achieved the required values after treatment with 7 days HRT, and for Sample 2 after 3 days

HRT. This value of bicarbonate is only applicable to overhead sprinkling.

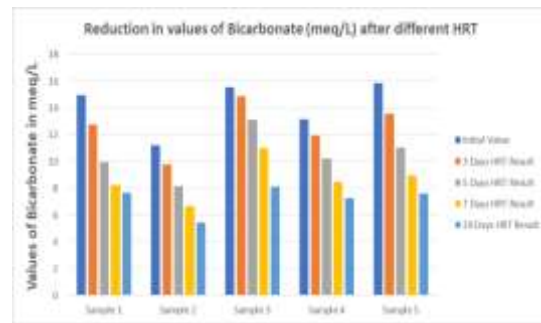


**Figure 34** Reduction of Bicarbonate during different HRT

The test results shows 48.76%, 51.42%, 47.88%, 44.70 and 52.17% reduction in sample 1, sample 2, sample 3, sample 4 and sample 5 respectively after 10 days HRT. The black line shows the FAO Irrigation Water Quality Guidelines value i.e. 8.5meq/L for over head sprinkling.

### pH

The raw values of pH were in range of 8.12 to 8.56. The effluent values of pH decreases from 8.43 to 6.33 in experiment 1, 8.33 to 6.55 in experiment 2, 8.12 to 6.50 in experiment 3, 8.56 to 6.80 in experiment 4 and 8.20 to 6.66 in experiment 5.

The concentration of pH of third and fifth sample was within the standards of FAO Irrigation water Quality Guidelines even in raw form i.e. 6.5 to 8.4, whereas for sample 1, 2 and 4, the required value was achieved after treating wastewater with stabilization ponds with 3 days HRT, therefore result shows that to reduce the value of pH, it should be treated with HRT of 03 days in order to use wastewater for Irrigation purposes.

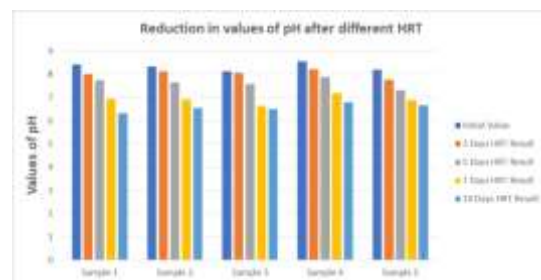


**Figure 35** Reduction of pH during different HRT

The test results shows 19.57%, 21.37%, 19.95%, 20.56% and 18.78% reduction in sample 1, sample 2, sample 3, sample 4 and sample 5 respectively after 10 days HRT.



## F Coliforms

The raw values of F Coliforms were in range of 1136 No/100mL to 1378 No/100mL. The effluent values of F Coliforms decreases from 1352 No/100mL to 815 No/100mL in experiment 1, 1136 No/100mL to 651 No/100mL in experiment 2, 1378 No/100mL to 858 No/100mL in experiment 3, 1295 No/100mL to 714 No/100mL in experiment 4 and 1217 No/100mL to 712 No/100mL in experiment 5.

The concentration of F Coliforms for sample 2,4 and 5, achieved for the required value of 1000 No/100mL according to FAO Recommended Microbiological Quality Guidelines for Wastewater use in Agriculture after 5 days HRT, whereas for sample 1 and 3 the required values were achieved after treating wastewater with stabilization ponds with 7 days HRT. Therefore result shows that wastewater should be treated with HRT of 07 days to reduce the value of F Coliform to use for Irrigation purposes.

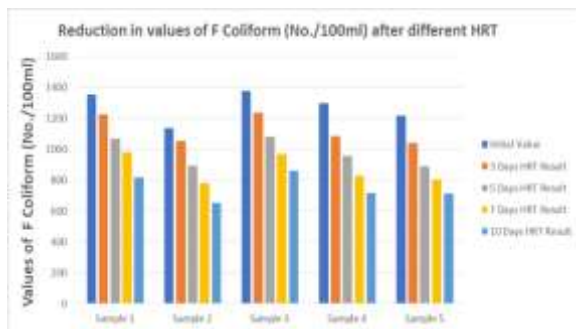


**Figure 36** Reduction of F Coliform during different HRT

The test results shows 39.71%, 42.69%, 37.73%, 44.86% and 41.49% reduction in sample 1,

sample 2, sample 3, sample 4 and sample 5 respectively after 10 days HRT. The concentration of F Coliform according to FAO Recommended Microbiological Quality Guidelines for Wastewater use in Agriculture i.e. 1000No/100mL.

## Conclusions

The result obtained after testing shows the removal efficiencies of the Waste Stabilization Pond system expressed as percentage of initial concentration and then values were compared with Food and Agriculture (FAO) Irrigation Water Quality Guidelines. The result clearly shows that if domestic wastewater is to be reused for irrigation purposes it must be treated by macrophytes Waste Stabilization Ponds with HRT of 10 days with slight to moderate restriction on use as explained in Table 5.1 below. The initial values of wastewater were in the range of severe degree of restriction on use according to FAO guidelines.

The results indicates that average reduction in values of different parameters of wastewater was 32.16%, 32.16%, 42.27%, 29.93%, 23.21%, 33.25%, 30.89%, 48.98%, 26.04% and 41.29% for EC<sub>w</sub>, TDS, SAR, Sodium, Chloride, Boron, Nitrate, Bicarbonate, pH and F Coliform respectively.

The results show higher removal efficiency for EC<sub>w</sub>, TDS, SAR, Boron, Bicarbonate and F Coliform. The results shows after three days of detention there is not much reduction in pollutant values but as the detention time

**Table 20** Different HRT required for using wastewater for Irrigation purposes

Sr. No	Water Quality Parameter	Unit	Sample 1	Sample 2	Sample 3	Sample 4	Sample 5
01	EC <sub>w</sub>	ds/m	07 days	07 days	10 days	10 days	07 days
02	TDS	mg/l	5 days	5 days	10 days	0 days	5 days
03	SAR	No.	0 days	0 days	0 days	0 days	0 days
04	Sodium	meq/l	0 days	0 days	0 days	0 days	0 days
05	Chloride	meq/l	3 days	0 days	7 days	0 days	3 days
06	Boron	mg/l	5 days	10 days	5 days	7 days	3 days
07	Nitrate	mg/l	5 days	0 days	5 days	7 days	3 days
08	Bicarbonate	mg/l	7 days	3 days	10 days	7 days	10 days
09	pH	No.	3 days	3 days	0 days	3 days	0 days
10	Facial Coliform	No./100ml	7 days	5 days	7 days	5 days	5 days



increase the reduction of pollutant in the sewage also increase.

The above table clearly shows that for each sample maximum HRT required to achieve FAO Irrigation Water Quality Guidelines is 10 days. Rate of growth of Azolla is very important. Azolla grows best in full to partial shade (25-50% of full sunlight). Growth decreases quickly under heavy shade and more than 50% of full sunlight reduces photosynthesis. The optimum relative humidity for azolla growth is between 85 and 90%. The average temperature during the trial session was kept 25 to 35 Degree Celsius. The macrophytes wastewater stabilization ponds system should be encouraged for the treatment of domestic wastewater in developing countries like Pakistan as it decreases the major toxic wastewater pollutants to a large extent and wastewater can be used for irrigation purposes as per FAO Irrigation standards. On the other hand, this is Eco-friendly, maintenance free and self-sustained also. The cost of harvesting and frequency of macrophytes need to be considered while selecting the type of macrophyte in the regions where growth rates are high to get efficient results regarding reuse of wastewater for Irrigation purposes. Different types of wastewater has different concentrations and has effect on performance of Macrophyte, therefore the initial conditions and initial values should be considered while designing the waste stabilization ponds. It is recommended that awareness should be made in farmers to utilize wastewater for Irrigation purposes after proper treatment instead of using it in polluted form. Parameter testing expenses are very high in this project. It is recommended to Government of Pakistan to establish more laboratories for testing wastewater quality so that this methodology can be applied frequently.

## References

- Nurarif & Kusuma, (2016). (2013).. In Journal of Chemical Information and Modeling (Vol. 53). <https://doi.org/10.1017/CBO9781107415324.004>
- Akpor, O. B., & Muchie, M. (2011). Environmental and public health implications of wastewater quality. *African Journal of Biotechnology*, 10(13), 2379–2387. <https://doi.org/10.5897/AJB10.1797>
- Amare, E., Kebede, F., & Mulat, W. (2018). Wastewater treatment by Lemna minor and Azolla filiculoides in tropical semi-arid regions of Ethiopia. *Ecological Engineering*, 120(April), 464–473. <https://doi.org/10.1016/j.ecoleng.2018.07.005>
- Angelakis, A. N., & Snyder, S. A. (2015). Wastewater treatment and reuse: Past, present, and future. *Water (Switzerland)*, 7(9), 4887–4895. <https://doi.org/10.3390/w7094887>
- Anwar, H. N., Nosheen, F., Hussain, S., & Nawaz, W. (2010). Socio-Economics Consequences of Reusing Wastewater in Agriculture in Faisalabad. *Pakistan Journal of Life and Social Science*, 8(2), 102–105.
- Arun Mittal. (2011). Figure 1: Aerobic Treatment Principle Figure 2: Anaerobic Treatment Principle. *Biological Wastewater Treatment*, 2–9. Retrieved from <https://www.watertoday.org/Article/Archive/Aquatech12.pdf>
- Brix, H. (1994). Functions of macrophytes in constructed wetlands. *Water Science and Technology*, 29(4), 71–78. <https://doi.org/10.2166/wst.1994.0160>
- Ciria, M. P., Solano, M. L., & Soriano, P. (2005). Role of macrophyte Typha latifolia in a constructed wetland for wastewater treatment and assessment of its potential as a biomass fuel. *Biosystems Engineering*, 92(4), 535–544. <https://doi.org/10.1016/j.biosystemeng.2005.08.007>
- Dallas, S., Scheffe, B., & Ho, G. (2004). Reedbeds for greywater treatment - Case study in Santa Elena-Monteverde, Costa Rica, Central America. *Ecological Engineering*, 23(1), 55–61. <https://doi.org/10.1016/j.ecoleng.2004.07.002>
- Dhote, S., & Dixit, S. (2009). Water quality improvement through macrophytes - A review. *Environmental Monitoring and Assessment*, 152(1–4), 149–153. <https://doi.org/10.1007/s10661-008-0303-9>
- Huntsberry, B. W. (2015). News & Observer prepares pay wall to charge users for online access. 12–14.
- Ilyas, M., Ahmad, W., Khan, H., Yousaf, S., Yasir, M., & Khan, A. (2019). Environmental and health impacts of industrial wastewater effluents in Pakistan: A review. *Reviews on Environmental Health*, 34(2), 171–186. <https://doi.org/10.1515/reveh-2018-0078>

- Mousavi, S. R., Tavakoli, M. T., Dadgar, M., Chenari, A. I., Moridiyan, A., & Shahsavari, M. (2015). Reuse of Treated Wastewater for Agricultural Irrigation with Its Quality Approach. *Biological Forum - An International Journal*, 7(1), 814–822.
- Shah, M., Hashmi, H. N., Ghumman, A. R., & Zeeshan, M. (2015). Performance assessment of aquatic macrophytes for treatment of municipal wastewater. *Journal of the South African Institution of Civil Engineering*, 57(3), 18–25. <https://doi.org/10.17159/2309-8775/2015/v57n3a3>
- Spellman, F. (2003). Handbook of Water and Wastewater Treatment Plant Operations. In *Handbook of Water and Wastewater Treatment Plant Operations*. <https://doi.org/10.1201/9780203489833>
- Trikoilidou, E., Samiotis, G., Bellos, D., & Amanatidou, E. (2016). Sustainable operation of a biological wastewater treatment plant. *IOP Conference Series: Materials Science and Engineering*, 161(1). <https://doi.org/10.1088/1757-899X/161/1/012093>
- Wastewater characteristics, treatment and disposal. (2008). In *Choice Reviews Online* (Vol. 45). <https://doi.org/10.5860/choice.45-2633>
- Yadav, M., & Dharmendra. (2014). A critical review on performance of wastewater reuse systems. *International Journal of Applied Engineering Research*, 9(1 SPEC.ISS.), 41–46.

## Application of Geostatistical Algorithms to Investigate Groundwater Quality Zones for Irrigated Agriculture

Imran Rasheed<sup>1</sup>, Aamir Shakoor<sup>1,\*</sup>, Zahid Mahmood Khan<sup>1</sup>, Hafiz Umar Farid<sup>1</sup>, Ijaz Ahmad<sup>2</sup>, Naveed Ahmad<sup>3</sup>, Qamar Iqbal<sup>1</sup>, Hafiz Muhammad Kamran<sup>1</sup> and Muhammad Abdul Wajid<sup>4</sup>

<sup>1</sup> Department of Agricultural Engineering, Bahauddin Zakariya University, Multan, Pakistan

<sup>2</sup> Center of Excellence in Water Resources Engineering, University of Engineering and Technology, Lahore

<sup>3</sup> Institute of Mountain Hazards and Environment - Chinese Academy of Sciences (IMHE-CAS), Chengdu, China

<sup>4</sup> Department of Irrigation and Drainage, University of Agriculture, Faisalabad, Pakistan

Corresponding author email: [aamirskr@bzu.edu.pk](mailto:aamirskr@bzu.edu.pk)

**Abstract:** Due to limited canal water supplies, agriculture of Pakistan heavily depends upon groundwater resources. The development of groundwater quality zones is necessary for its proper utilization and management. To evaluate the spatial groundwater quality, the present study was conducted in Lower Chenab Canal (LCC). Geostatistical analysis was performed using Gamma Design Software (GS+) and Kriging Interpolation approach of Geographic Information System (GIS) was adopted to create the maps of groundwater quality. For groundwater quality parameters i.e. electrical conductivity (EC), residual sodium carbonate (RSC) and sodium absorption ratio (SAR) to identify best fit model for different Ordinary Kriging models, Semivariogram was tested. Spherical model of semivariogram was best fitted for EC, whereas Exponential model fitted best for SAR and RSC. To create maps of combine water quality, overlay analysis was performed, according to which 17.83 and 17.30% area of LCC was depicting good quality for irrigation, 42.84 and 44.53% area was showing marginal groundwater quality, 39.33 and 38.17% area was exhibiting unsuitable quality for seasons of pre-monsoon and post-monsoon, respectively.

**Keywords:** Groundwater, GIS, Geostatistics, Kriging, Semivariogram, Gamma Design software (GS+)

### Introduction

Successful agriculture is strongly related to steady supplies of water to fulfill the demand of water for the crop. Where the canal water supplies and rainfall are insufficient, groundwater can be utilized as a replacement source to assure a high level of productivity of agricultural subject to its permissible quality. About the land of 60 million hectares exists as irrigated agricultural globally such as the USA, India, Pakistan and China register for greater than 50% of globs irrigated land (Döll & Siebert, 1999). Universally, About 60% of the production of grain is produced from irrigated agricultural by applying two-third of the world's freshwater that is extracted from groundwater. For irrigated agriculture, approximated every year about 750-800 billion cubic meters of worldwide groundwater was being utilized (Shah, 2007). With the increase of population to produce more food, in Pakistan approximate 1.2 million tube wells are working and about 62 billion cubic meter of groundwater is being pumped ,out of which greater than 90% used for agriculture purpose (Qureshi, 2012).

Geographic Information Systems (GIS) is a substantial tool that has been carried out by numerous studies to evaluate the quality of water. From the application of GIS, groundwater and natural resources have extremely benefited (Engel and Navulur, 1999). Spatial Analysis and development of Geographical Information System (GIS) assist to integrate the geographic information with laboratory investigation information and to demonstrate the spatial circulations of water quality parameters, most precisely and robustly. For public health management as a spatial decision support system and for spatial inspection of epidemiological diseases, GIS can be used as a tool. In deciding the water application strategies for different objectives, the spatial patterns of chemical ingredients are useful (Shankar et al., 2010). For various objectives, to secure sustainable protected application of these resources, monitoring and evaluation of groundwater quality is important. To assure the safe application of groundwater resources, the evaluation of groundwater quality zones is essential. The objectives of the study included: To find suitable interpolating method using

Geostatistics technique and To delineate spatial variability and determine groundwater quality zones for irrigated agriculture

### Description of study area

#### Site location

For the current study, the Lower Chenab canal (LCC) was chosen as a research site. LCC having 73°39'19" E to 72°18'54" E longitude and 32°16'14" N to 30°45'53" N latitude, is located in central-east of Punjab, Pakistan. The command area of LCC is 1.8228 million hectares (Mha) and it is further divided into seventeen (17) irrigation subdivisions as shown in Figure 1. Irrigation system of the study area is shown in Figure 2. The River Chenab flow upper side of the study area from the Northeast to the Southwest and passes through the Khanki, Qadirabad and Trimmu Headwork/barrages alongside the boundary of the study area.

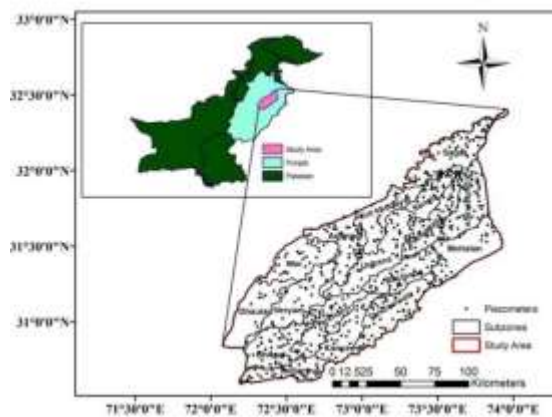


Figure 37. Location of study area

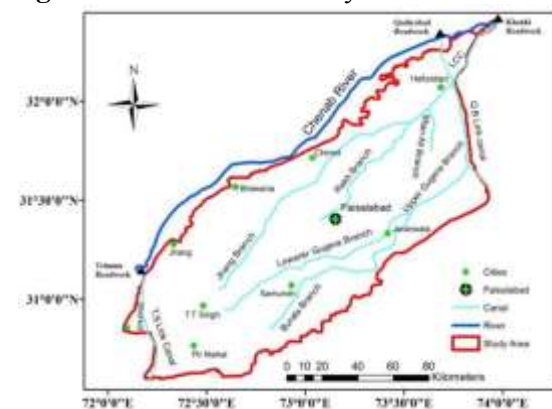


Figure 2: Canal irrigation system in LCC

### Methodology

The observed data of water quality parameters for 747 piezometric wells were acquired from

Punjab Irrigation Department (PID) Faisalabad, Pakistan. The observed data that were acquired was pre-monsoon (June) and post-monsoon (October).

### Geostatistics

Interpolation of data at various unsampled points was done using a technique that is said to be geostatistics. Deterministic and Geostatistical are two approaches used for data interpolation. Geostatistical approach that considered being most suitable is Kriging, which introduces probability during predictions of data. For Geostatistical analysis of data, Gamma Design Software (GS+, version 10), and for groundwater mapping ArcGIS 10.1 was used.

### Histogram

To check the normal distribution of observed data, histogram analysis was adopted. Different transformations such that Box-Cox and logarithmic were checked to affirm the normal distribution of observed data (Webster & Oliver, 2007). Due to positively skewed observed data of water quality parameters EC, SAR, and RSC, data was normalized through log transformation (Figure 4).

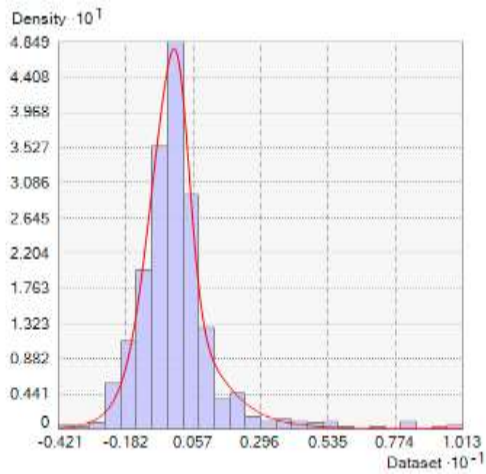
### Cross validation

To check the performance of interpolation models, the values of mean error (ME), root mean square error (RMSE), mean square error (MSE), root mean square standardized error (RMSSE) and average standard error (ASE).

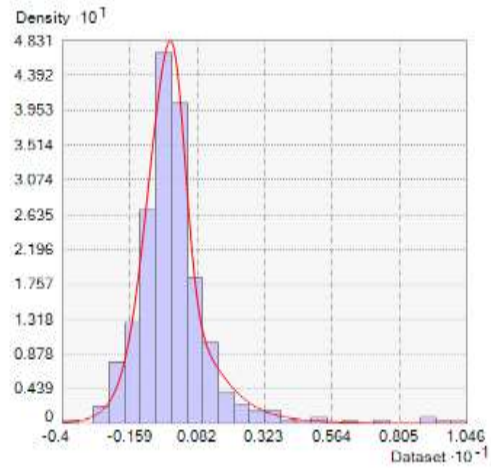
### Results and Discussion

#### Spatial autocorrelation

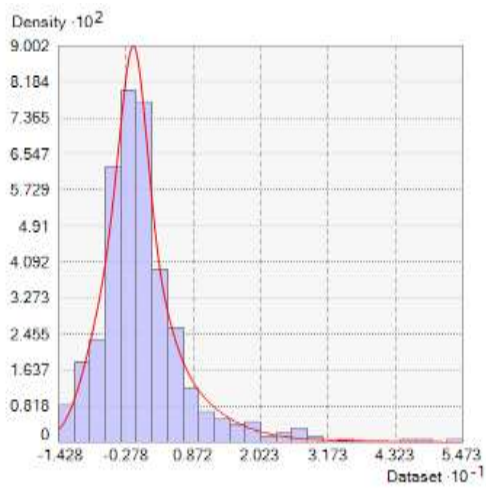
The spatial structure of variogram model between theoretical and experimental semivariogram was assessed using coefficient of determination ( $R^2$ ), residual sum of squares (RSS) and nugget to sill ratio ( $Co/Co+C$ ). The variogram model which gives highest value of coefficient of determination ( $R^2$ ) and lowest value of residual sum of squares (RSS) is best fit variogram model. The spherical model gave best results for pre-monsoon season while exponential model gave best results for



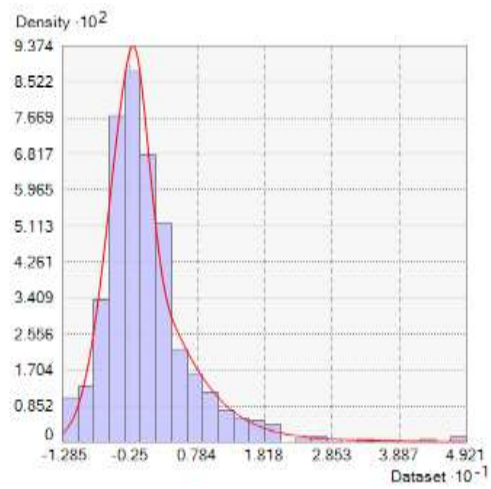
EC June



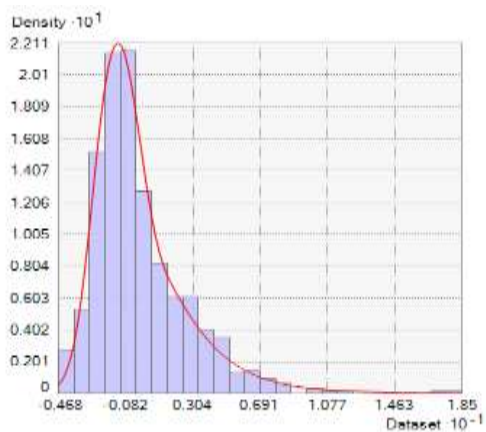
EC October



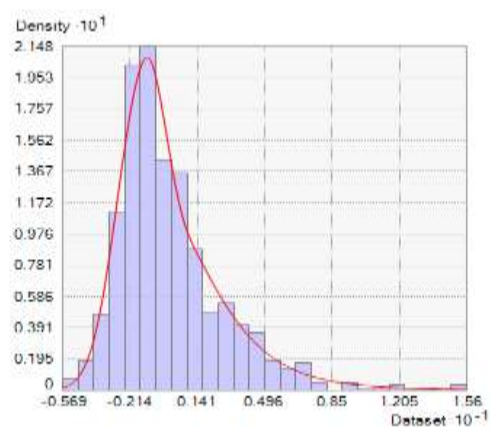
SAR June



SAR October



RSC June



RSC October

Figure 38. Histogram showing normalized data for EC, SAR and RS

post-monsoon season in case of EC. In case of SAR and RSC, the exponential model found to be best fit for seasons of pre-monsoon and post-monsoon (Figure 5).

### Cross validation results

The results of the cross validation of interpolation are shown in Table 4. The range of ME values is from -0.0229 to 0.1676; RMSE from 1.4572 to 8.0727; ASE from 1.2489 to 9.2068; MSE from -0.0153 to 0.0093; and RMSSE from 0.8238 to 1.0708. The ME values are approximately close to zero, RMSSE are close to one, which indicate the better prediction of

interpolation model. Minimum values of ASE and RMSE represent the lower and acceptable prediction error of interpolation model.

### Groundwater mapping

#### Electrical conductivity (EC)

Figure 6 reveals the analysis and variation of groundwater quality for irrigation subzones. The area (4.96%) of Kot Khudayar irrigation subdivision increased maximum under good groundwater in terms of EC succeeded. While highest area (9.94%) reduced in Wer irrigation subdivision under good groundwater.

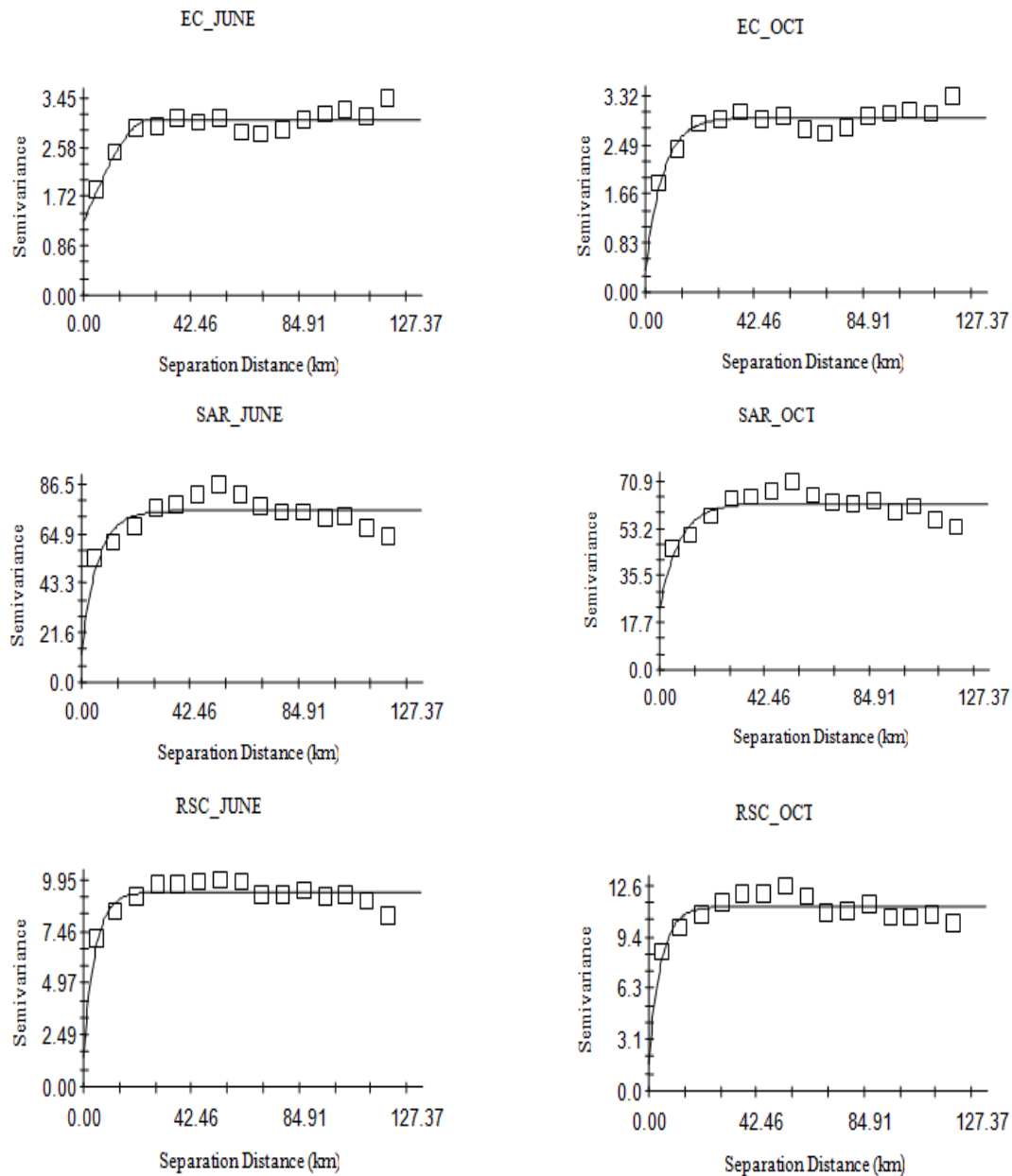


Figure 39. Experimental semivariogram model fitted best for water quality parameters



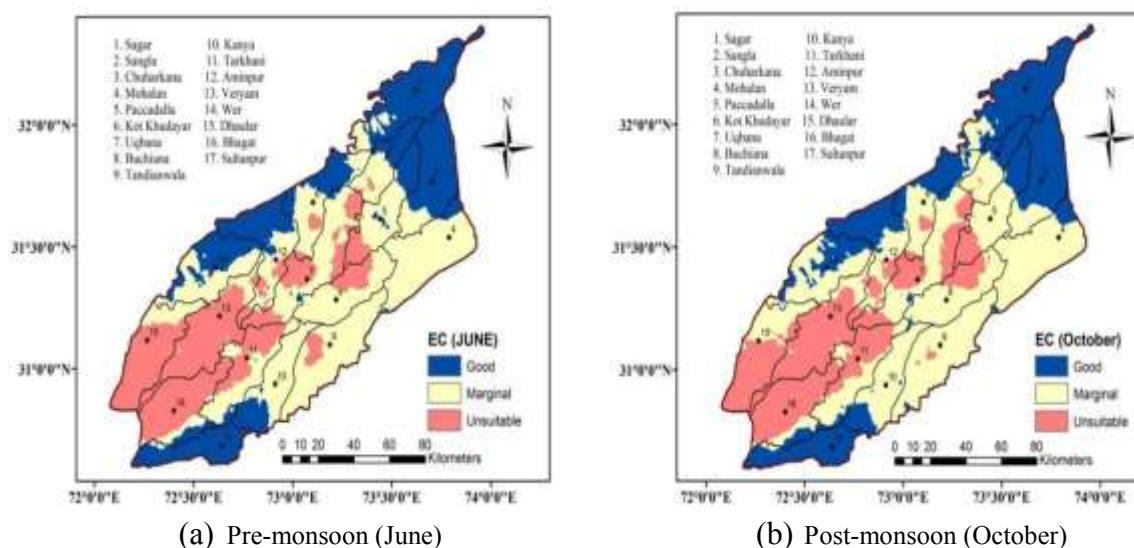
**Table 21.** Features of semivariogram models for EC, SAR and RSC

Season	Parameter	Best fit model	Nugget (Co)	Sill (Co+C)	Partial sill (C)	*Ratio $\times 100$	RSS	Model R <sup>2</sup>
Pre-monsoon	EC	Spherical	1.276	3.065	1.789	41.63	0.359	0.816
	SAR	Exponential	12.400	74.930	62.53	16.55	0.552	0.491
	RSC	Exponential	1.400	9.362	7.962	14.95	0.280	0.646
Post-monsoon	EC	Exponential	0.356	2.949	2.593	12.07	0.334	0.795
	SAR	Exponential	22.600	62.660	40.06	36.07	0.275	0.565
	RSC	Exponential	1.710	11.290	9.58	15.15	0.576	0.593

\* (Co/Co+C)

**Table 22.** Statistical outcomes of cross validation of EC, SAR and RSC

Season	Parameters	Model	ME	RMSE	ASE	MSE	RMSSE
Pre-monsoon	EC	Spherical	-0.0229	1.5037	1.4015	0.0044	0.9844
	SAR	Exponential	0.0632	8.0728	9.2068	-0.0027	0.9412
	RSC	Exponential	0.1546	2.8566	4.2552	0.0093	0.8238
Post-monsoon	EC	Exponential	-0.0355	1.4572	1.2489	-0.0153	1.0708
	SAR	Exponential	0.1676	7.1523	8.6503	-0.0023	0.8744
	RSC	Exponential	0.0923	3.0093	3.9464	-0.0024	0.8967



(a) Pre-monsoon (June)

(b) Post-monsoon (October)

**Figure 40.** Spatial distribution of EC for different subzon

The maximum increased area (14.92%) was found in Buchiana irrigation subdivision under marginal category after monsoon season. However, Kot Khudayar (4.69) has reduced the area under marginal groundwater quality. The area reduced under unsuitable quality is maximum in Buchiana (15.41%) subdivisions, whereas increased maximum in Uqbana (3.65%).

#### Sodium absorption ratio (SAR)

Table 5 and Figure 7 show the subdivisional level analysis and variation of SAR. Kanya irrigation subdivision increased the quality of groundwater with 26.86% of area under good category. Good

quality reduced by 21.64% of area in Bhagat subdivision but increased under marginal groundwater quality with an area of 12.94%. Majority part of the area reduced under marginal category after monsoon season. Unsuitable water quality decreased in almost all subdivisions except Bhagat which increased 8.70% of area after monsoon.

#### Residual sodium carbonate (RSC)

Figure 8 depict the detailed subdivision wise investigations and variation of groundwater quality of RSC. Good quality increased by 11.39% in Sangla irrigation subdivision, whereas

quality under good category has decreased unexpectedly after monsoon. Bhagat subdivision under marginal quality increased by 12.08% of area but the remaining irrigation subdivisions decreased the groundwater quality. Unexpectedly in all irrigation subdivisions, unsuitable quality increased after monsoon with maximum area of 24.75 and 22.35% in Chuharkana and Tarkhani subdivisions.

### Overall groundwater quality

Figure 9 depict the overall groundwater quality of the study area (LCC), which shows that during

pre-monsoon an area of 3249.46 km<sup>2</sup> (17.83%) of LCC has good quality of irrigation water which unexpectedly slightly decreased to 3153.62 km<sup>2</sup> (17.30%) during season of post-monsoon. An area of 7808.93 km<sup>2</sup>, i.e. 42.84% has irrigation water of marginal quality, whereas 8117.17 km<sup>2</sup>, i.e. 44.53% of marginal quality for season of pre-monsoon and post-monsoon, respectively. The area under unsuitable quality found 71699.33 km<sup>2</sup> (39.33%) of LCC during the season of pre-monsoon and 6956.74 (38.17%) during the post-monsoon

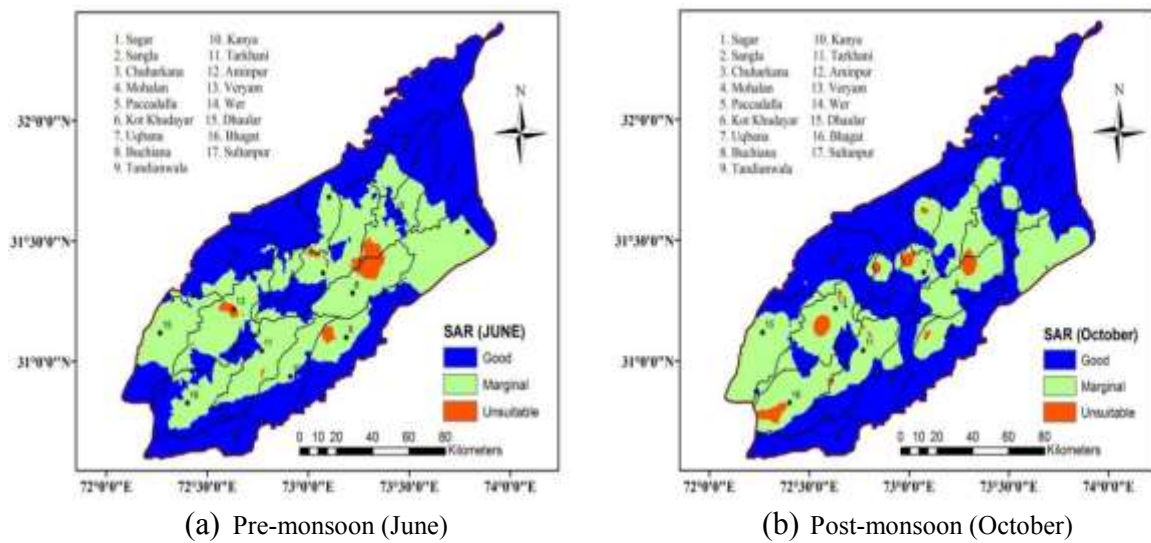


Figure 41. Spatial distribution of SAR for different subzones

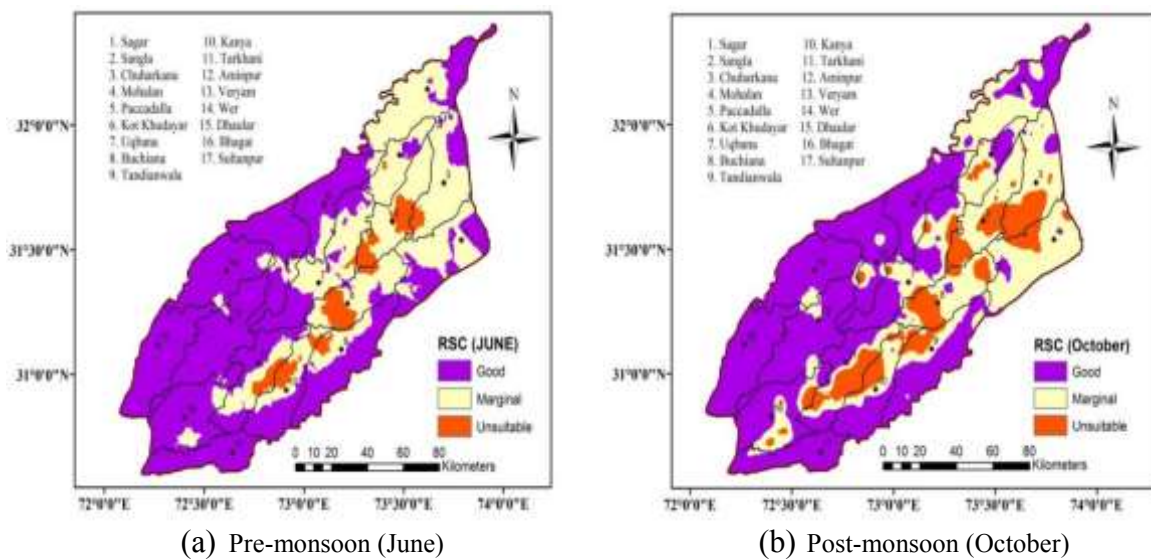
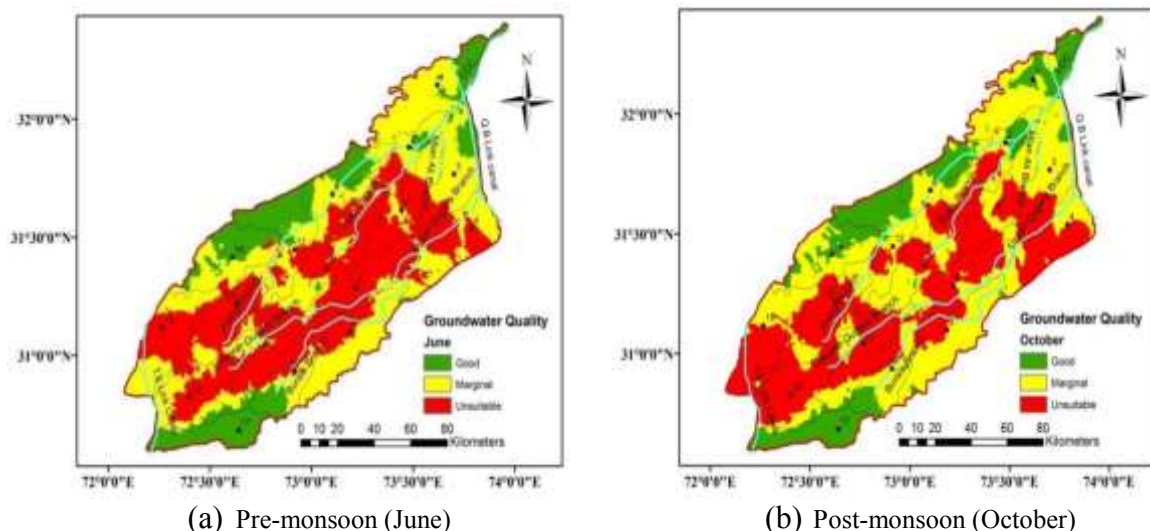


Figure 42. Spatial distribution of RSC for different subzones



**Figure 43.** Overall groundwater quality for pre-monsoon and post-monsoon

**Table 23.** Reclassification and area of each water parameter

Parameters	Quality	Range	Reclass value	Area, km <sup>2</sup> (%)	
				Pre-monsoon (June)	Post-monsoon (October)
EC (dS/m)	Good	<1.5	3	5324.89 (29.21)	5210.27 (28.58)
	Marginal	1.5-2.7	2	8165.74 (44.80)	8476.57 (46.50)
	Unsuitable	>2.7	1	4736.90 (25.99)	4540.69 (24.91)
SAR	Good	<10	3	9835.79 (53.96)	11215.10(61.53)
	Marginal	10-18	2	8026.51 (44.04)	6656.27 (36.52)
	Unsuitable	>18	1	365.22 (2.00)	356.16 (1.95)
RSC (meq/l)	Good	<2.5	3	10695.11(58.68)	9938.11 (54.52)
	Marginal	2.5-5.0	2	6534.53 (35.85)	6152.47 (33.75)
	Unsuitable	>5.0	1	997.89 (5.47)	2136.95 (11.72)
Overall quality	Good	8-9	-	3249.46 (17.83)	3153.62 (17.30)
	Marginal	6-8	-	7808.93 (42.84)	8117.17 (44.53)
	Unsuitable	3-6	-	7169.14 (39.33)	6956.74 (38.17)

## Conclusions

It was concluded from the analysis of the results that the spherical model gave best results for pre-monsoon season while exponential model gave best results for post-monsoon season in case of EC. In case of SAR and RSC, the exponential model found to be best fit for seasons of pre-monsoon and post-monsoon. Most of the area in term of salinity in LCC showed the groundwater quality of marginal category. Maximum unsuitable area with respect to EC was found in Veryam irrigation subdivision with 88.40 and 85.51% of the area for pre-monsoon and post-monsoon. The values of SAR indicate that area of LCC was less affected by alkalinity as compare to salinity and sodicity. Northeastern, northwestern and southern

parts of the study area as well as some central regions found as good groundwater quality.

Groundwater quality in LCC has a slight variation for both pre-monsoon and post-monsoon.

Groundwater quality assessed through overlay analysis, according to which good quality of groundwater was 17.83 and 17.30% of LCC area, marginal quality found 42.84 and 44.53%, whereas area of unsuitable quality was 39.33 and 38.17% for pre-monsoon and post-monsoon, respectively. Groundwater quality should be investigated for the application of drinking purpose. It is recommended that the groundwater should be artificially recharged in unsuitable quality zones for its better use in agriculture. Groundwater mapping should be applied to other irrigation regions.

## References

- Adhikary, P. P., Chandrasekharan, H., Chakraborty, D., & Kamble, K. (2010). Assessment of groundwater pollution in West Delhi, India using geostatistical approach. *Environmental Monitoring and Assessment*, 167(1–4), 599–615.
- Ahmadi, S. H., & Sedghamiz, A. (2007). Geostatistical analysis of spatial and temporal variations of groundwater level. *Environmental Monitoring and Assessment*, 129(1–3), 277–294.
- Amiri, V., Sohrabi, N., & Dadgar, M. A. (2015). Evaluation of groundwater chemistry and its suitability for drinking and agricultural uses in the Lenjanat plain, central Iran. *Environmental Earth Sciences*, 74(7), 6163–6176.
- Ayers, R. S., & Westcot, D. W. (1985). *Water quality for agriculture* (Vol. 29). Food and Agriculture Organization of the United Nations Rome.
- Baba, K., Bahi, L., & Ouadif, L. (2014). Geostatistical Analysis for delineating sterile inclusions in Sidi Chennane phosphatic series, Morocco. *Earth Sciences Research Journal*, 18(2), 143–148.
- Burrough, P. A. (2001). GIS and geostatistics: Essential partners for spatial analysis. *Environmental and Ecological Statistics*, 8(4), 361–377.
- Delgado, C., Pacheco, J., Cabrera, A., Batllori, E., Orellana, R., & Bautista, F. (2010). Quality of groundwater for irrigation in tropical karst environment: The case of Yucatan, Mexico. *Agricultural Water Management*, 97(10), 1423–1433.
- Döll, P., & Siebert, S. (1999). A digital global map of irrigated areas, report A9901. Center for Environmental Systems Research, University of Kassel, Kurt Wolters Strasse, 3, 34109.
- Eaton, F. M. (1950). Significance of carbonates in irrigation waters. *Soil Science*, 69(2), 123–134.
- Javed, Q., Arshad, M., Bakhsh, A., Shakoore, A., Chatha, Z. A., & Ahmad, I. (2014). Redesigning of drip irrigation system using locally manufactured material to control pipe losses for orchard. *Land and Water*.
- Khan, S., Rana, T., Gabriel, H. F., & Ullah, M. K. (2008). Hydrogeologic assessment of escalating groundwater exploitation in the Indus Basin, Pakistan. *Hydrogeology Journal*, 16(8), 1635–1654.
- Kumar, P. J. S., Jegathambal, P., & James, E. J. (2011). Multivariate and geostatistical analysis of groundwater quality in Palar river basin. *Int J Geol*, 4(5), 108–119.
- Latha, P. S., & Rao, K. N. (2012). An integrated approach to assess the quality of groundwater in a coastal aquifer of Andhra Pradesh, India. *Environmental Earth Sciences*, 66(8), 2143–2169.
- Liu, D., Wang, Z., Zhang, B., Song, K., Li, X., Li, J., ... Duan, H. (2006). Spatial distribution of soil organic carbon and analysis of related factors in croplands of the black soil region, Northeast China. *Agriculture, Ecosystems & Environment*, 113(1–4), 73–81.
- Mohammad, Z.-M., Taghizadeh-Mehrjardi, R., & Akbarzadeh, A. (2010). Evaluation of geostatistical techniques for mapping spatial distribution of soil pH, salinity and plant cover affected by environmental factors in Southern Iran. *Notulae Scientia Biologicae*, 2(4), 92–103.
- Qureshi, A S. (2012). Groundwater management in Pakistan: The question of balance. *Centenary Celebration (1912–2012), Paper*, (717), 207–217.
- Qureshi, Asad Sarwar, McCornick, P. G., Sarwar, A., & Sharma, B. R. (2010). Challenges and prospects of sustainable groundwater management in the Indus Basin, Pakistan. *Water Resources Management*, 24(8), 1551–1569.
- Shah, T. (2007). The groundwater economy of South Asia: an assessment of size, significance and socio-ecological impacts. *The Agricultural Groundwater Revolution: Opportunities and Threats to Development*, 7–36.
- Shakoore, A., Arshad, M., Bakhsh, A., & Ahmed, R. (2015). GIS based assessment and delineation of groundwater quality zones and its impact on agricultural productivity. *Pak. J. Agri. Sci*, 52(3), 837–843.
- Usman, M., Liedl, R., & Kavousi, A. (2015). Estimation of distributed seasonal net recharge by modern satellite data in irrigated agricultural regions of Pakistan. *Environmental Earth Sciences*, 74(2), 1463–1486.



## Revitalizing Dying Karezes of Tehsil Karezat, Balochistan, Pakistan

Hamayun Khan<sup>1</sup>, Syed Mobasher Aftab<sup>1\*</sup>

<sup>1</sup> Faculty of Engineering and Architecture, Balochistan University of Information Technology, Engineering and Management Sciences, Quetta, Pakistan.

Corresponding author email: [syed.mobasher@buitms.edu.pk](mailto:syed.mobasher@buitms.edu.pk)

**Abstract:** Karez or Qanat is an underground water canal that is connected to the ground surface with a series of upright shafts. The canal receives groundwater by natural aquifer discharge from piedmonts and flows to the valley floor by gravity. Historical Tehsil (County or Subdistrict) Karezat is specifically named for its famous centuries-old karezes selected to evaluate the geohydrological aspects. The limestones of Nisai Formation of Eocene, alluvial fans, and piedmont sediments of Quaternary are comprised of high potential groundwater zones served as recharge zones for mother-wells. In Karezat out of 106 karezes, 37 are partially active, 65 were dried-out, and 4 were demolished. Karezes were constructed during the past 25-600 years and dried in the last 3-20 years. The karezes were dried-up due to several factors including long spans of droughts that hit twice during the last two decades. Population Increase 55% in nineteen years, increase the numbers, and area cultivated with tubewells and solarization of tubewells. During the last 20 years, the area irrigated by tubewells increased 338% while by karezes declined 80% in 50 years. The total installed tubewells are 2,482 that extracted 0.37 million m<sup>3</sup> groundwater daily. The rangelands constituting 73% of the total area, supporting small ruminants, providing fuelwood to 80% of households, and generate 90% runoff. An integrated watershed management strategy has been considered to manage the watershed and to increase the natural groundwater recharge. A karez rehabilitation plan was proposed for karez extension, construction of irrigation channels, water storage ponds, and check dams.

**Keywords:** Karez, Hydrogeology, Karezat, Balochistan, Pakistan.

### Introduction

The Tehsil Karezat of Pishin District is located in the northeast of Pishin City. Hydrogeologically, Tehsil Karezat is a part of the Pishin River Basin, which is the area-wise the seventh biggest drainage basin of Balochistan. Fig. 1 represents the location Map of Balochistan with 18 River Basins and the Quetta Valley. The enlarged part of the map shows the study area of Tehsil Karezat and Union Councils (UC).



**Fig. 1** Location map, showing river basins, Quetta Valley and Tehsil Karezat.

Karez is an ancient invention, technically inclusive, sound in performance, excellent in design, and diligent in construction. The area being researched is famous for its centuries-old karez systems which are gradually moving towards the drying state. This study will help to restore, maintain and improve the conditions of the karez system. The results of this study will pave the way to explore the hydrogeological aspects of the karez system and corresponding aquifers in other regions of the province. Certain studies for the karez system have been conducted from 2007-2015 in different regions of Balochistan. The majority of the studies cover the social and economic aspects related to decreasing discharge and dying-out of karezes. In contrast, the present study is related to geohydrological and technical aspects of the karez systems. The karez is an underground canal that is connected to the ground surface with a series of upright shafts or dug-wells, Sheikh (2016). The channel of groundwater is comprised of variable lengths, ranging up to miles with numerous shafts depending on the size of the valley, Mustafa (2014). The channel collects groundwater through the natural discharge of the reservoir from alluvial-fan and flows towards the valley

floor by gravity. The karez system initiates from piedmont areas, where initial wells or shafts receiving groundwater known as mother-wells or feeding wells to karez. Karez system's function, maintenance, and management are based on local tribal laws, customary rights, and local traditions. The karez systems are constructed and planned without any technical or financial support or participation by private or public agencies, Mustafa (2007). The karez systems construction, controls, operates, manages, and maintains the country's largest community-owned systems.

The karez system uninterruptedly supplies water for irrigation and domestic use. The landowners or shareholders distribute the karez water among each other and their socioeconomic status is associated with the karez system Sheikh (2016). The sustainability of the karez system is superior to tubewells because of its long-lasting resistance from millenniums, meeting the needs of human beings and livestock. The life of the karez system is long-lasting, and the water cost is less from deep drilled tubewells. The average life of tubewells is <40 years in Balochistan and tubewells are the major cause of water level declination. Karez system has not been contributed to the declination of groundwater. The depth of the average groundwater level varies from 30-150m in most parts of Balochistan, which is declining from 1-3m per year in almost all populated river basins. The negative impact of water extraction is visible and clear that deep wells quickly extract groundwater and the migration of the people starts from the affected areas, GOB (2014).

Due to severe climatic conditions, droughts, and environmental degradation, the value of the karez system is more resilient. As it does not dry up rapidly and abstracting groundwater from aquifers slowly GOB (2011). Karezes in the small to medium size valleys effectively produce groundwater to irrigate lands. Karezes was playing the main role in fulfilling the water demands of the area for decades as they were operated without any barriers. The karez water is increasingly becoming vulnerable to reduced groundwater discharge volume over time, Mohyuddin (2012). Climate change also affected the temperatures and rainfall which influence climatic patterns. The rainfall and snow are declining continuously year by year, and dry weather conditions are high all the time. The higher rates of population growth add weight to groundwater resources, Mustafa (2007). The number of tubewells is increasing each day using

Solar Photovoltaic (PV) cells and subsidized electrical equipment without any limit on discharge, tube well depths, and operational timings. Subsequently, the groundwater level is declining in all parts of the study area. As a result, the deterioration of the water quality of karez and the threat of pollution has increased dramatically. The ultimate fact is that the decline of the groundwater table has already been dried up many karezes.

There is no significant data available from the public and private sectors to improvise the traditional heritage of the karez system. In Karezat, there is hardly any research and development activities have been conducted by the public sector. Whereas in Iran the Karez system is much more sustainable than in Pakistan. The Iranian authorities established the "International Qanat Research Center in Yazd" in collaboration with UNESCO, Laureano, and Yazdi (2012).

### **Hydroclimatology**

Several small streams and minor rivers emerged from the mountain ranges of Margha Zakaryazai (M-Zakaryazai), Churmian, and Rodh Malazai (R-Malazai) and join each other before joining the main-stream Togai Manda which flows into Surkhab Lora (River). The study area is part of the Pishin River Basin, which is flowing from Barshore in the North-East to Shorarud Valley near Burj Aziz Khan. The Pishin River water comes to the Bund Khushdil Khan Dam and the river flow heads north towards Afghanistan. The drainage area of the Pishin River Basin is 18,152 Km<sup>2</sup>, whereas the estimated surface drainage of the study area is about 1,000 Km<sup>2</sup> that located along the stream Thogai Manda and Margha-Churmian Manda. Both streams originated from the prominent Yahya Range.

The general characteristics of Karezat are mountainous and are bounded by the Salore Ghasha peak of 3,184 m, Yahya Mountain Range (MR), Churmian MR, and Rodh Malazai MR. These ranges extend from valleys western, northern and eastern margins and rise to approximately 1,966 masl. Between the comparatively steep shoulders of the mountain ranges, the flooring of the Karezat is located at topographic heights from approximately 1,550m in the northern part to approximately 3,300m in the southern part. The mountains are of similar topography and relief, elongated ridges and recurrent spurs descend.



The drainage system of Karezat is divided into small streams coming from the Rodh Malazai region and the Churmian Margha region and joins together forming Togai Manda. Churmian Margha Manda flows to Surkhab Lora near Niganda Lora and drops in Band Khusdil Khan Dam. All these streams spread their suspended and dissolved colloidal load by forming a layer of fine sediments following each flood. The locations of tubewells and karezes are marked on the map with the help of Topo Sheets No. 34 N/2, 34 N/6, and 34 N/10. The topography, drainage pattern, and hydrogeology of the area is presented in Fig. 2.

The Karezat is situated in winter territory adjacent to chilly mountain ranges experiences regular snowfall in the winter season. The winter season endures from October to March with an average temperature from 2-6°C. The summer from May to September, when the average temperature from 20-24°C. The harvesting season from September to November with an average temperature of 10°C. The climatological information of Karezat Valley across months, least and highest temperature, precipitation, humidity, sun exposure, wind speed, and Coefficient of Evapotranspiration rates are summarized in Table 1.

Karezat's climate is a local steppe climate, where the average yearly precipitation is 272 mm. Climate is considered being 'BSk' according to the Köppen-Geiger Climate Classification, Climate-data.org (2014). The average annual temperature in Karezat is 14.3°C. The climate of the Karezat is considered extreme, summer is warm, and winter is very cold. The winter experience sometimes sufficient but irregular and scanty showers. The months of January and February bring snowfall while July is considered the hottest month and temperature varies from 19°C and 35°C. The temperature drops 10-3°C usually and -14°C in January. November to May is considered wet season whereby it receives 80% of the yearly precipitation. The mean yearly snowfall is about 25% of the mean yearly precipitation. The normal precipitation in Karezat is 272 mm/year. The rainfall received in 2018 especially from January to May and at the end of November was >10 mm. The precipitation values of 2018 were analyzed to correlate with the variations of discharge quantities of karezes. The study area in 2018 received more than normal snowfall in recent history which helped to replenish declined groundwater levels. In Karezat February is the most humid and

September is the least humid months. In winters humidity ranges from 10-25% while in dry season from 28-38%, normal yearly level 20%. The minimum and maximum monthly average relative humidity vary from 28-58%, respectively. The monthly average temperature varies between 1.8 to 35.5°C and precipitation from 2-54cm. The monthly average relative humidity ranges from 28-58% and daily sunshine from 6.3-10.7 hours. The average monthly cloud intensity of the area varies from 2-20%. Based on temperature, precipitation, relative humidity, cloud cover, and solar intensity, the evaluated evapotranspiration rates vary from 2.39-10.82 mm/day.

**Table 1** Climatological data of Karezat IUCN (2011) and Climate-Data. Org, (2014).

Month	Temperature (°C)			Precipitation (cm)	Relative Humidity (%)	Daily Sunshine (hrs)	ETo (mm/d)
	Min	Max	Ave				
Jan	-4.3	7.9	1.8	54	58	6.3	2.39
Feb	-1.9	10.7	4.4	54	55	7.3	3.23
Mar	2.8	16	9.4	46	51	7.6	4.77
Apr	7.5	21.8	14.9	23	43	8.4	7.04
May	11.4	27.2	19.3	14	33	10.7	9.79
Jun	15.2	31.9	23.5	2	28	9.9	10.82
Jul	17.8	33.3	25.5	22	34	9.5	10.46
Aug	16.7	32.7	24.7	14	35	9.4	9.19
Sep	11.7	29.4	20.5	1	32	9.5	8.14
Oct	5.4	23.4	14.4	2	32	9.7	6.11
Nov	0.8	17	8.9	8	41	7.6	4.11
Dec	-2.8	11.4	4.3	32	50	7.5	2.74

## Study of Karez System

### Karez Antiquity

Karez had a first historical appearance in the mining works for draining of groundwater during the Urartu Kingdom in Northern Iran, 8<sup>th</sup> Century B.C. The collected water in ditches created drainage problems during the first millennium B.C (550-331). The karez technology spread throughout the empire to fulfill domestic needs. The karez systems were installed in Jordan, Syria, and Afghanistan. This was the start of the technology diffused to north and west into Europe, Shahid (2007). Under the rules of Arabs, the underground galleries were transferred from

the Middle East to Spain, Cyprus, Morocco, and Sicily. The Abbasids transfer karez technology from East Iran to Mecca and Central Asia. Karez system is diffused from Afghanistan to Pakistan and especially it is constructed in the border area of Pakistan-Afghanistan. It is also believed that diggers or Kahan Kash came from Afghanistan, CPAU (2011). The karez technology diffusion model is presented in Fig. 3, GOB (2014). In the world, about 60,000 Km<sup>2</sup> or about 6% of the land is irrigated by the karez system. About

half of the irrigated area is situated in Iran and the rest in Afghanistan, Pakistan, Azerbaijan, Turkmenia, Morocco, Oman, and Mexico, GOB (2014). In Balochistan, during 1904 there were 496 karezes and 1803 springs. Two-thirds of the irrigated area in Pishin and Quetta used to be irrigated by karezes and springs, Hughes-Buller (1905). Presently, there are 106 Karezes in Tehsil Karezat in 7 UCs including Balozai, Dilsora, Gawal Khanai, Gharshinan, Khanozai, M-Zakaryazai, and R-Malazai

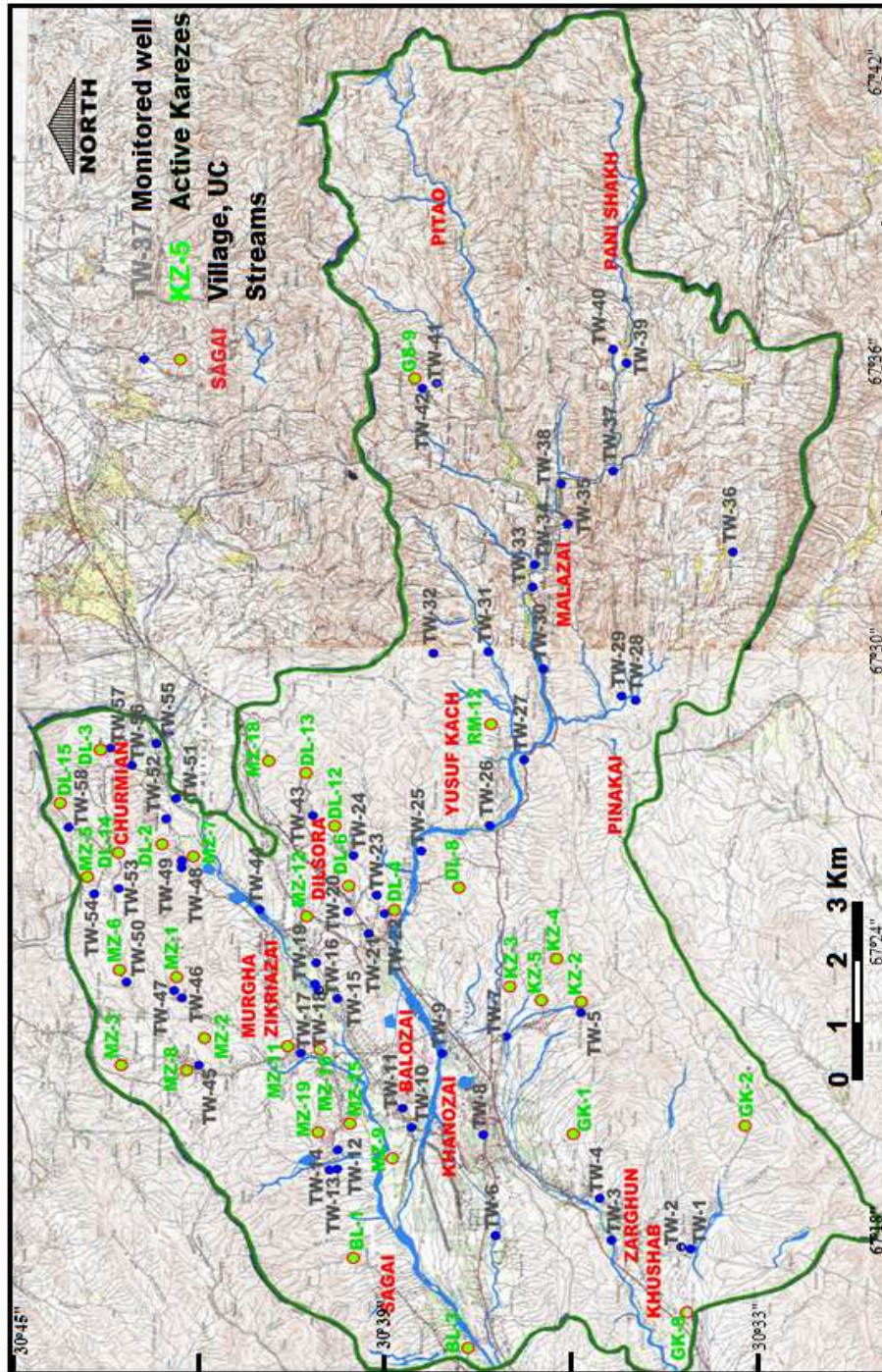
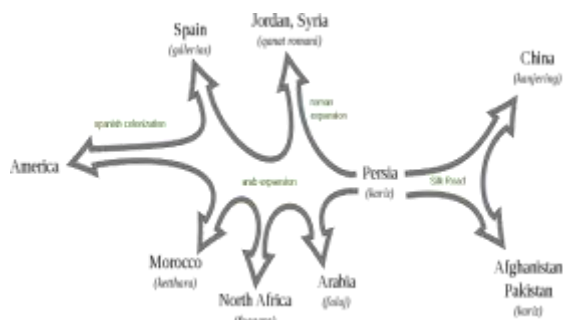


Fig. 2 Topographic Map of Karezat showing drainage pattern, location of monitored tubewells, active karezes and watershed divide line.



**Fig. 3** Karez/Qanat Technology Diffusion Model, GOB (2014).

### Karez Geometry

To understand the physical structure and geometric properties of the karez system, the construction methods and geometric types are imperative. Professionals who construct the karez system are called Kahan Kash and Muqannis or Mughannis in the local language. The basic elements in the construction of the karez system are the selection of mother wells, shafts, tunnels as well as water flooding, air circulation, and ventilation. An aerial view and cross-section of a simple karez of the study area are shown in Fig. 4. The site selection of a mother-well is done by local water experts through water dowsing, maximum depth of the mother-well range up to 100 m, depending on groundwater level. The line of shafts and depths should be precise as it uses gravitational force to flow from mother-wells to daylight point at storage ponds called outlet or dragon mouth, Maeyer, (2014).

The karez tunnels are not straight from the mother well to the outlets, but it follows natural topography and slope. Side tunnels are found which were constructed when some portion of the tunnels collapsed. There have several heads which are connecting different branches of a mother well together when less water flows from a single mother-well. A karez having only one line of shafts is called linear karez, there are different types of geometric structures of the karez system. All these systems have different methods to collect water from the mother well and convey it to the daylight point. The different geometrical types of karez systems are presented in Fig. 5.

In the study area, the minimum and maximum lengths of karez vary from 27-1,982m. Most of the Karezes have a single branch but some karezes have two branches. The mother wells of two-branched karezes are located in different directions apart from each other which joined at

a central location and discharges their water at a single day-light point. The shallow depths of the mother-wells of many karezes are among one of the major causes of drying out of karezes. It's almost impossible to rehabilitate a karez with a depth of the mother well from 3-10m. To increase the discharge of karez, it must dig down the entire underground canal from mother-well to the day-light point by several meters, which is practically not possible because of laborious work, huge costs, and the altitude of the command area.

The number of vertical shafts or wells connected to the groundwater tunnel is based on the length of the karez. In the study area, the minimum and maximum number of shafts of a karez vary from 71 to 7,106. The distance between the two shafts depending on the construction method and type of soil. The minimum and maximum shaft to shaft distance range from 15-35m, and the average distance are about 23m. The height of the underground channel or canal varies between 1.5-2.0m, and the width of the tunnel is one meter in all cases. It has also been observed that some portions of many karezes are damaged that ranges from 5-950m in lengths. The karez length, branches, depths of the mother wells, the distance between karez shafts, height, width, and damaged lengths of the underground channels are presented in Table 2.

### Existing Status of Karezes

Tehsil Karezat having 106 karezes built within different eras, the oldest one is about more than 600 years. The construction methods and equipment were changed with the passages of time but all karezes were dug by hand with human power. Every karez in the region has its own identity, history, construction stories, and pride for the community that owns it. With time karezes faced many alterations and modifications in their main design and shape. In some cases, the number of mother-wells increased and new vertical shafts added. All alterations were done for the sole reason to enhance the groundwater discharge of karezes because of increased water demands. The inventory and monitoring of the karez system represent that out of 106 karezes 37 are partially active and 65 are dried out. Four karezes are found demolished which are spoiled because of land-care from the government authorities and native communities There are seven UC in the Tehsil Karezat, the minimum and the maximum number of karezes in each UC varies from 6-30. The UC wisenumber of active



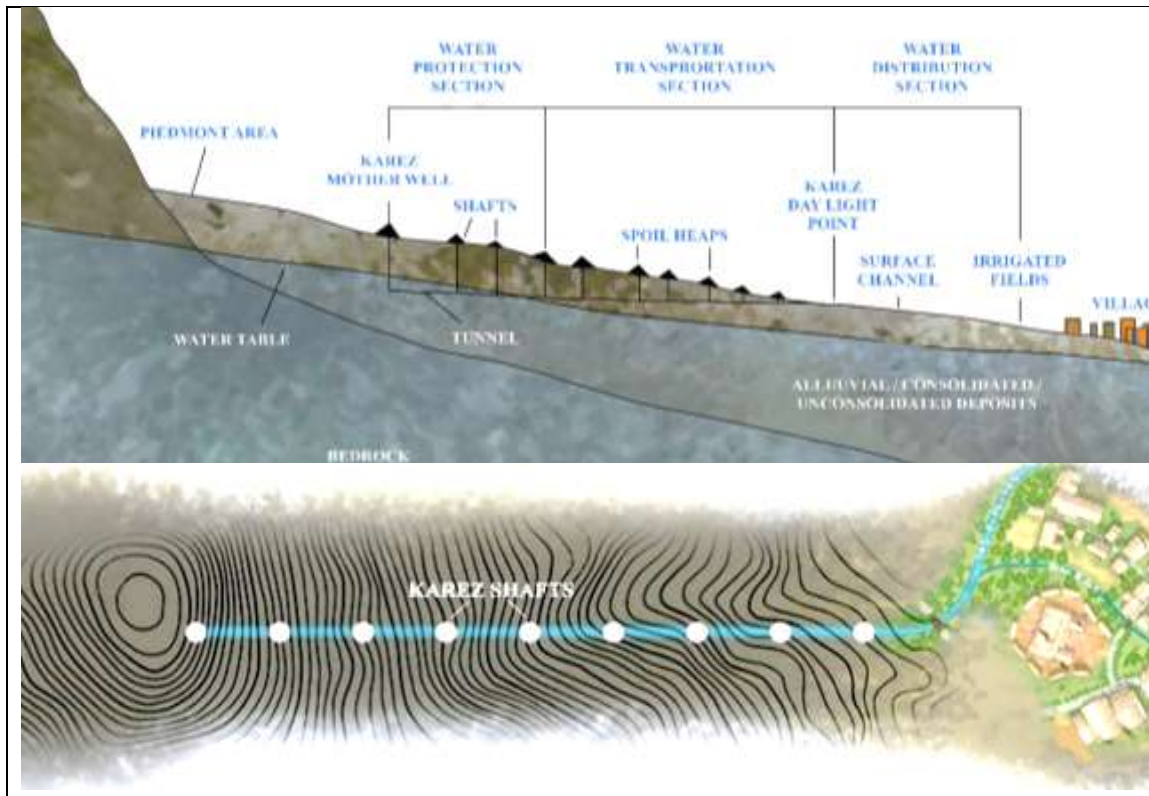


**Fig. 4** Aerial view and cross-section of a linear karez system, in Tehsil Karezat.

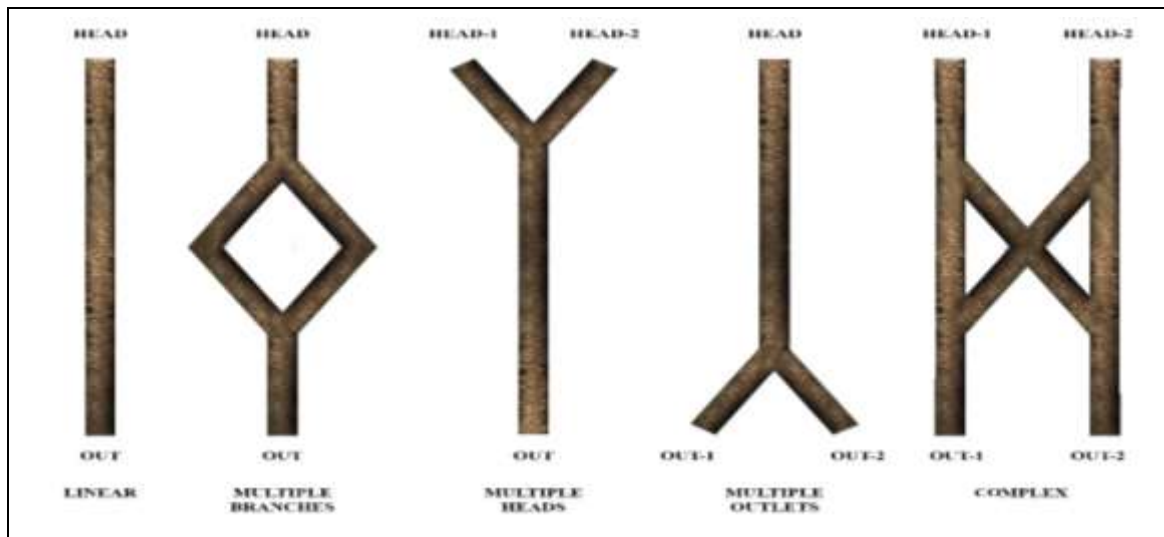


**Fig. 5** Geometrical types of karez system, Maeyer (2014).

**Table 2** Physical parameter of karezes, Tehsil Karezat.

Union Council		Total Village (No)	Karez			M-Well Depth (m)	Shafts		Underground Channel		
			Total (No)	Length (m)	Branches (No)		Total (No)	Distance (m)	Height (m)	Width (m)	Damaged Length (m)
Balozaï	Min	7	15	30	1	5	318	15	1.5	1	15
	Max			1,159	2	15		35	2.0	1	350
Dilsora	Min	13	15	27	1	5	327	18	1.5	1	5
	Max			732	1	15		33	2.0	1	150
G-Khanai	Min	10	12	83	1	5	261	5	1.5	1	5
	Max			1,982	1	23		30	2.0	1	50
Gharshinan	Min	13	9	30	1	3	315	20	1.5	1	40
	Max			1,128	2	30		30	2.0	1	90
Khanozai	Min	3	6	91	1	5	71	20	1.5	1	30
	Max			1,128	1	18		30	2.0	1	45
Margha Zakaryazai	Min	17	19	30	2	3	322	10	1.5	1	10
	Max			915	1	18		30	2.0	1	950
Rod Malazai	Min	18	30	46	1	6	1706	7	1.5	1	80
	Max			549	1	24		30	2.0	1	450

and dry karezes varies from 1-14 and 2-29 which are range from 3-67% and 26-97%, respectively. The active karezes are 35% and dried are 65% of the total. The karezes are dried during the last 3-20 years. The existing status of karezes is shown in Table 3. No proper monitoring was executed by any public sector agency. The Provincial Irrigation Department and the Public Health Engineering Department have no exact data about karez systems for any purpose. The public sector and civil society both have assumed that the age of karez is over.

Monitoring of karezes was done during field visits to the area, karezes of R-Malazai is an alarming situation. Only a single karez located in Yousaf Kach is partially active in an area of about 30 villages and almost all karezes in the area are dried out. The drying of karezes is due to different factors affecting the capacity of karezes i.e. droughts and over-mining of groundwater through mechanical means. Khanozai UC having six karezes among which four are partially active represent that the aquifer is still not over mined as compared to R-Malazai. Keeping the groundwater demands of the area it has been estimated and presumed that the residents may

have no other choice to migrate to other cities within the next 10-20 years. They have to migrate due to the unavailability of groundwater in R-Malazai if not enough precipitation is received in the coming years. Karezat having 7 Union Councils (UC) that include Balozaï, Dilsora, Gawal Khanai, Gharshinan, Khanozai, Margha Zakaryazai, and R-Malazai UCs. There are 81 villages in seven UC's varying in numbers from 3-18 with several karezes from 6-30.

Balozaï UC having a 15 karez system, the alarming situation is that 13 are dried out. Balozaï dam is contributing to recharge only two karezes which are still active and operational. Dilsora UC having a 15 karez system out of that only 9 are active used only for drinking. Gharshinan UC out of 9 karez systems 8 are dried out. Recently, Gharshinan Dam and Parheza Dams are constructed by the government which may help to revive the dry karezes. Gawal Khanai UC having a 12 karez system and 6 are active utilized for drinking purposes. Khanozai UC having a 6 karez system and 4 are active. M-Zakaryazai UC having 19 karezes out of which 14 are conveying water to daylight point which is utilized for.

**Table 3** Existing status of karezes.

UC	Karez Status (No)					Age (years)		Dried (years)	
	Total	Active	%	Dried	%	Min	Max	Min	Max
Balozaï	15	2	13	13	87	25	500	5	20
Dilsora	15	9	60	6	40	100	500	4	10
G-Khanai	12	6	50	6	50	120	450	5	16
Gharshina	9	1	11	8	89	120	350	6	17
Khanozai	6	4	67	2	33	80	400	3	16
Zakaryaza	19	14	74	5	26	50	300	5	15
R-Malazai	30	1	3	29	97	80	600	5	20
<b>TOTAL</b>	<b>106</b>	<b>37</b>	<b>35</b>	<b>69</b>	<b>65</b>	-	-	-	-

drinking. R-Malazai UC having a 30 karez system, only one of them is producing minimum discharge to daylight point at Killi Yousaf Kach. Among all karezes in the study area, not a single karez is supported by the public sector to enhance its vitality and to raise its efficiency to fulfill the needs of local farmers and residents of the area. Most of the karezes are originating from the hill toe and some are found originating from the stream bed and flows towards the command area having the main source of recharge the main flood in the stream from mountains in heavy rains or those runoff during precipitation playing the main role in recharging its aquifers.

### **Social Aspect of Karezes**

In Karezat, the Kakar Tribe of Pashtoons are living for centuries. The area is also shared by Panezai, Bazai, Essakhail, Shamozi, Ahmed Khail, Barakzai, Sulemankhail, Taran, and Sarangzai clans of the Kakar Tribe. Residence patterns of all villages are divided into tribes, sub-tribes, and lineages. All of the tribes trace their descent through a common ancestor, "Qais Abdul Rasheed". This segmentation of society plays an important role in the social organization of karezes for every karez setup, Daanish (2015). Mirabb or management committee control and solve karez related issues. The committee is elected by the shareholders based on their abilities and good relations. They are doing all this job volunteering, independently, and are not liable to any political or government officials. Mirabbs acts as a group to solve the disputes on karezes, every member has equal status, and everyone collects money from his lineage and keeps a record with themselves. At the beginning of the year, all Mirrabs get-together to have a schedule for the year.

One shareholder can take his turn after 14 days of karez water, once in the day-time and next in the night-time. Some villages have 14 Shabaroz (night and day) and some have 16 Shabaroz. The karez water is calculated as; Shabaroz = 24 Hours; Each Shabaroz = 8 Shingers; 8 Shingers = 3 hours of karez water; 1 Shingers = 8 Pals; 1 Pal= 22.30 minutes. All Shabaroz is divided among shareholders. Shareholders can exchange their water-day with each other and those having surplus water may sell their share of water. Karez is also used as a base for land ownership in the area is located. This method is applied by elders of the area and still, it is applicable by the government and the local communities. The

shareholder having more shares in karez water will have more areas of land.

People are migrating to major cities, especially those who could not afford the heavy expenses of installation deep tubewells. Migrated families are looking for an alternate source of livelihood such as day labor in mining, casual daily urban jobs. Keeping the groundwater demands of the area it has been estimated that a large segment of residents may migrate to other cities within the next 10 years. They have to migrate due to the unavailability of groundwater in Rodh Malazai if not enough precipitation is received in the coming years. Some contributing efforts economically in the hope to augment discharge, regular maintenance, and rehabilitation of karezes. Even if rainfall patterns improved, their future appeared poor. The major beneficiaries of the tubewell transition in Karezat are the large landowners who are already rich and dominant in society. The biggest losers are the small farmers who have a share in the karez system, but it goes dry. The small farmers produced nothing from the karez system, they are losing their livelihood, sense of pride, and dignity. The routine karez management and maintenance procedures kept these communities together through strong communal involvement, the drying out of the karez system weakened social bonds. Currently, the local communities are worried about the present status of the karez system. They think that to keep the karez system alive and stable for the future generation some positive steps are vital from the government side. If the same practice continues towards the karez system only remains of the ancient treasure will be left for the generations to come.

### **Population Dependent on Karezes**

Tehsil consists of populated union councils (UC) surrounding Khanozai Town having a congested population in small villages. The study area comprised 6 UCs and the population was 76,360 persons as per the 1998 census. The minimum and maximum population as per the 2017 Census of six UC's vary from 8,956 to 40,238 persons, respectively. Karezat comprises a population of 138,208 according to the 2017 census. The population ratio increased to 55% in nineteen years. The overall population density of tehsil is about 90 people/Km<sup>2</sup>. As per 2017 census figures, the urban and rural population is comprised of 40,238 and 98,042 which is 29% and 71%, respectively.



The minimum to a maximum number of families or shareholders getting their share of water from a single karez system varies from 4-130. An average of 45 shareholders or families were irrigating their lands from a single karez system. On average, there are ten family members in each shareholder than 450 inhabitants were getting benefits from a single karez. Accordingly, from 106 existing karezes a total of 48,000 inhabitants were irrigating their lands, which is about more than one-third of the total population of the area. While presently from 37 partially active karezes only around 17,000 inhabitants getting advantage from Karezes that is about 13% of the total population as per the 2017 census. The population values, minimum and maximum number of shareholders in different union councils are presented in Table 4.

### Karez Capabilities

During the span of the last 35 years, the area irrigated by the karez system is declined and reduced to 20%. It's because of quick gains by tubewells in contrast to trouble-prone karez systems. The major problems of karezes are fluctuating water tables, siltation, the collapse of roofs and shaft, and uncontrolled water supply make karez irrigation unsuitable for modern agriculture systems. During the last 20 years, the area irrigated by tubewells increased 338% while the area irrigated by karez declined 80% in the last 50 years. The transition of the karez system to dug wells and tubewells was encouraged, that cause lowering the groundwater levels and decreasing the flow of water in the karez.

The Irrigation and Power Department surveyed 1,146 karez systems in Balochistan to investigate the probability distribution of the karez command area, Irrigation Department (2014). The main objective of the survey was used to develop a probability distribution for the command area. The findings were that there is extensive variation in command area as 90% of the schemes have a command area of fewer than 1,000 Km<sup>2</sup>, 75% of the schemes have less than 670 Km<sup>2</sup>, 50% of the schemes have less than 340 Km<sup>2</sup>, and 10% of the schemes have less than 80 Km<sup>2</sup>. Table 5 provides details about these statistics.

**Table 4** UCs Population increase and the number of shareholders.

Union Council	Population (No)		Increased (%)	Shareholders (Min-Max No)
	1998	2017		
Balozai-Z	76,360	40,238	55.2	4 - 65
MC Khanozai		24,314		5 - 60
Dilsora		20,192		4 - 85
Gawal Khanai		21,250		10 - 130
Gharshinan		23,330		10 - 50
M-Zakaryazai		8,956		5 - 130
Rodh Malazai				
	<b>76,360</b>	<b>138,280</b>	<b>55.2</b>	-

**Table 5** Probability distribution of karez command area, GOB (2014).

No.	Probability (%)	Command-Area (Km <sup>2</sup> )
1	Minimum	10
2	10	80
3	25	160
4	50	340
5	75	670
6	90	970
7	Maximum	16,700

The farmers have a transition towards electric-operated deep drilled wells and diesel-operated tubewells to fulfill their field water needs. Presently, the karez water is used only for drinking water because it does not have enough quantity to irrigate fields. The 1,533 tubewells are registered with the Water and Power Development Authority (WAPDA), which are regularly paying the subsidized bills of about rupees 6,000 per month with bearing 18 hours' load shedding in seasonal cultivation. According to the WAPDA Khanozai office, there are about 955 tubewells that are logged unregistered. The area cultivated by karezes and tubewells is 20-631 Km<sup>2</sup> which is 3-97%, respectively. In the recent era, three main kinds of groundwater abstractions technologies are in common use in the study area; 1) Electric operated deep tubewells, 2) Diesel operated tubewells, and 3) Solar PV operated tubewells.

### Geological investigations

The geologic investigations of the study area were carried out to define the physical properties of the surficial and subsurface valley fill materials, including, lithology and structure of exposed geological formations. The exposed surficial formations and bedrock were examined and analyzed. The Karezat area is covered by an

alluvial cover of Recent to Sub-Recent and Bostan Formation of Pleistocene with a thickness of 750m. The regional geology and structure of Karezat are complex because of chromite and ophiolite depositions. Structurally the area is divided into, Tungi-Ahmadun Syncline, Khanozai Torakhula Ophiolite, and Murgha Zikriazai-Barshore Flysch. The Tungi Syncline is comprised of the Urak Formation of Pliocene which is included of Uzdapasha, Shinmati, and Urak Conglomerate Members. The Urak Formation is thrust by the Allozai Formation of Triassic in the north and the south by the Parh/Bibai Formation of Cretaceous. On the eastern side thrust contact with the Loralai of Jurassic, Sember, and Bibai of Cretaceous, and Dungan of Paleocene formations.

The Khanozai-Torkhula Ophiolite is overlain by Allozai Formation which is comprised of limestone and shale of Triassic that intruded by the Ultramafics. Loralai Formation of Jurassic Limestone also intruded by the Volcanics and Ultramafics during Cretaceous having chromite depositions. The Ultramafics are widely exposed are part of the Muslim Bagh Ophiolite. The Murgha Zikriazai-Barshor Flysch also named Pishin Flysch comprised Nisai Formation of Eocene, Murgha Faqirzai of Oligocene, and

Shaigalu Formation of Miocene. The Nisai Formation starts from fossiliferous limestone and shale, thick beds of shale in the middle and medium to thin-bedded sandstone, shale, and limestone at the upper part. Above the shale of the Murgha Faqirzai which is overlain by Shaigalu Formation comprised of sandstone, shale, and conglomerate. The simplified geological map of the region comprised of the study area is presented in Fig. 6, which is modified after Andrew (2015).

The exposed geological units are; the Bostan Formation; ranged in age from Sub Recent-Pleistocene. The formation is comprised of red-shale, clay, siltstone, and sandstone. The reported maximum thickness of 750m in the Pishin Basin. Siwalik Group; ranges in age from Miocene-Pliocene. The Group is comprised of Chingi, Nagri, Dhok Pathan, and Soan Formations. The name Siwalik Group including the "Sibi" and "Urak" groups, Hunting Survey Corporation (1961). The lower part of the Siwalik Group i.e. the Chingi Formation is not recognized. The Nagri Formation represents the lowermost part of the "Sibi Group" and "Urak Group" of Hunting Survey Corporation and "Uzhda Pusha Formation", Kazmi and Raza (1970).

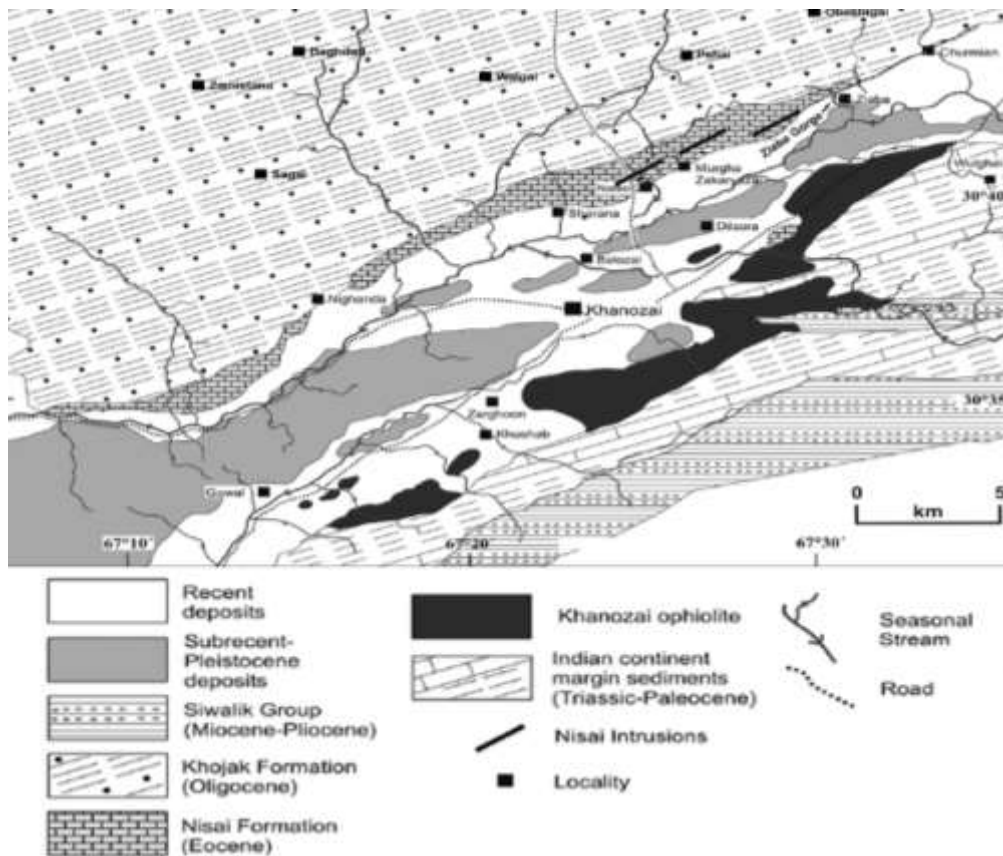


**Fig. 6** Geological map of Karezat, modified after Andrew (2015)

Nisai Intrusions; the intrusions are located within the Nisai Formation of Eocene age. The Nisai Formation is exposed towards NE of the Khanozai. The intrusions are exposed in a straight line in the lower part of the Ziaba Gorge section in the study area. Nisai Intrusions of Eocene, based on the cross-cutting of the Nisai Formation. The Nisai Intrusions formed as concordant sills, NE–SW trending, thickness ranges from 1-10m and from 20-30m apart. The intrusions are composed of basaltic to dolerites and gabbro compositions. Nisai Formation; is of Eocene age, named as Nisai Group in 1961 by Hunting Survey Corporation for dark Nummulitic Limestone. The formation later on redefined as Nisai Formation. The formation is exposed north of Nisai Railway Station, where it's more than 1200m thick. The formation comprised of limestone, marl, shale with subordinate sandstones.

Khanozai Ophiolites; range in age from Cretaceous-Paleocene, comprised of ultrabasic and basic igneous rocks. The ophiolites are composed of oceanic lithosphere and show a continuous sequence from foliated harzburgite–dunite through transition zone dunite, ultramafic–mafic cumulate, and gabbros to a sheeted dyke complex. Based on geochemical signatures and field relations, Kakar et al. (2014) proposed that this ophiolite formed in a supra-subduction-zone tectonic setting in Neotethys. Khojak Formation; of Oligocene age conformably overlies the Nisai Formation. The formation is divided into Lower Murgha Faqirzai and Upper Shaigalu Members. The formation is comprised of grey, green to brown calcareous and arenaceous shales, turbidites, laminated mudstone, and sandstone sequences.

Indian Continent Margin Sediments; ranges in age from Triassic to Paleocene. Indian passive margin sediments are found stratigraphically beneath the Bagh Complex and consist of shales and limestones, Durrani (2012). The Gwal-Bagh Thrust separates the passive margin sediments from the Bagh Complex, which is a Cretaceous sedimentary, igneous and metamorphic melange zone. The sedimentary units were deposited on the continental margin of the Indian plate, whereas volcanic units formed part of the Neotethyan Oceanic Crust. Units of the Bagh Complex were scraped off during the oblique collision and abducted onto the northwestern margins of the Indian Plate.

## Hydrogeological Investigations

Hydrogeologically, the study area of the Pishin Subbasin can be subdivided into three zones dependent on groundwater revitalize zones. The high, medium, and low potential groundwater zones. The high potential zones comprised of exposed limestone formations including the Nisai Formation of Eocene age. The Nisai Formation is comprised of limestone about 1200m thick. The secondary porosity, permeability, and solution cavities are well developed in the limestone formation that provides favorable hydrologic conditions for groundwater circulation and recharge.

The groundwater discharge from limestone formations occurs in the form of small springs with little discharge located all along with the contact of limestone and recent deposits. The alluvial fans and piedmont areas along mountain ranges are also comprised of high potential groundwater zones. These areas are comprised of sand and gravel of large to medium sizes and make it feasible to recharge for the mother-wells of the Karezes. The medium potential groundwater zones are located at basin fields in existing and dormant stream channels and courses. In these areas sand, gravel and admixture provide suitable conditions for groundwater movement and potential. Wherever conglomerate and sandstone beds are exposed to provide semipermeable zones of medium potential. The areal extent of medium potential groundwater zones differs from valley to valley depend on the size of the valley. The little to very low potential recharge zones are comprised of impermeable geographical formations including shale, silty and clayey formations. The Bostan Formation of the Sub Recent-Pleistocene age is composed of shale, clay, and siltstone. The thickness of these sediments is about 750m in the study area. The shale, clay, and siltstone from impermeable beds wherever exposed on the surface and subsurface.

## Groundwater Discharge

The discharge capacity of karezes was monitored periodically within the last four months of the year only of active karezes in all UCs. During September, the minimum and maximum measured discharge of karezes vary from 0.1-2.9 liter per second (L/s). In October, the discharge increased a little in some of the karezes and ranged from 0.1-3.2 L/s. Similarly, in the

consecutive month of November, the discharges ranged from 0.1-3.7 L/s. During the last month of December of the study period, the discharge of karezes increased from 0.1-3.9 L/s. The measured discharge quantities of karez waters represent an increase from 2.9 to 3.7 L/s in four months. The increase in the discharge of karezes is representing a positive impact of recent precipitations of the groundwater.

The number of installed tubewells in different UC varies from 107-406. The total number of tubewells is 2,363 out of that 64 were monitored to evaluate the groundwater levels. The minimum and maximum levels of groundwater vary from 1,650-2,482 masl. The groundwater table may be stabilized for long runs by controlling the tubewell discharges and by imposing a complete ban on the installation of new tubewells in the area. The number of tubewells may also be controlled by allocating a tubewell to each family with restricted depths, fixed discharge, and timings. Each community of a specific watershed may take responsibility for their groundwater to manage by themselves on scientific ground. The number of tubewells, groundwater levels, and discharge variations in the active karezes region is presented in Table 6. It has been observed that variations in the discharge of karezes are due to above-average rain and snowfall spells in the study area during the study period 2018. In the study area, the long-term cumulative average monthly precipitation ranges from 0-13 mm, while during 2018 monthly total precipitation was 0-16 mm per month. The discharge variations represent that precipitation affected the groundwater table that ultimately changes the discharge of karezes. The effect of precipitation on the discharge of karezes

was correlated by drawing and analyzing the precipitation and discharge hydrographs of karezes. Based on discharge hydrographs, the karezes may classify into four broad groups, which represent; 1) Dry karez system, 2) No increase in karez discharge, 3) Unsteady increase in karez discharge, 4) A steady increase in karez discharge. In the study area, 106 karezes are presented out of that 69 karezes are dry now which is 65% of the total karezes. The first group comprised the area with dry karezes that represent the zone with maximum depletion of the groundwater level. In this zone, the groundwater table is continuously depleting because of over-pumping. The depth of the groundwater table ranges up to 205m from the ground surface and the average level varies from 60-118m. The precipitation didn't affect the groundwater table and ultimately on the discharge of karezes. The zone is located in the middle part of the small valleys and is comprised of valley-fill fine sediments.

The second group of karezes portrays a monotonous behavior of karez discharges with no impact of precipitation. Out of 37 partially active karezes of the study area, 12 karezes had a static discharge during four months of monitoring. The minimum and maximum discharge values of karezes range from 0.1-1.9 L/s. The discharge quantities represent no change with the impact of precipitation. These karezes are located in the central to the middle part of the ranges, where recharge from the precipitation least affected.

The third group comprised karezes which represent an unsteady increase in discharges. The discharge of the karezes is increasing under the

**Table 6** Number of tubewells, groundwater level, and discharge of karezes.

Union Council	Tube Wells (No)	Monitored Tubewells (No)	Groundwater Level (masl)		Active Karezes (No)	Discharge (L/s)	
			Min	Max		Min	Max
Balozaï	406	7	Min	1810	2	Min	1.5
			Max	1891		Max	2.1
Dilsora	383	13	Min	1954	9	Min	0.1
			Max	2329		Max	3.3
G-Khanai	514	6	Min	1650	6	Min	0.5
			Max	1853		Max	3.5
Gharshinan	107	4	Min	2168	1	Min	0.4
			Max	2382		Max	0.8
Khanozai	321	3	Min	1847	4	Min	0.1
			Max	1995		Max	2.2
Zakaryazai	292	18	Min	1800	14	Min	0.1
			Max	2292		Max	3.3
R-Malazai	340	13	Min	2057	1	Min	0.3

influence of precipitation, but the increase not demonstrating a symmetrical pattern of increase and decrease. The discharge of karezes starts increasing after September and demonstrates no impact or increase after the 14 mm precipitation of November and December. These karezes are located in the middle parts of the mountain ranges. The monthly precipitation has a delayed impact on the water table and discharge quantities but a continuous declination of the water table eliminates the impact rapidly. Hydrogeologically the zone may be connected to the marl and shale formations, which impact as negative boundaries after a certain period of recharge. The unsteady karez discharges with the impact of precipitation are presented in Fig. 7.

The fourth group characterizes a continuous increase in the discharge of karezes with the effect of precipitation. The increase in discharge of karezes varies from 0.4-3.9 L/s. The minimum and maximum discharge values of karezes range from 1.1-1.3 and 2.6-3.9 L/s, respectively. The increase in discharge quantities represents a swift impact of precipitation from November on this group of karezes. The majority of these karezes are located in the upper ranges of the study area. Most of the mother-well of karezes are dug in piedmont slopes. In said ranges, the hydrogeological formations are more porous and permeable as compared to surrounding valley materials. The area with karez discharges increases; represent recharge zone under the direct influence of precipitation. The steady increase of six karez discharges with the effect of precipitation is presented in Fig. 8.

It has been concluded that precipitation is the dominant climatic factor that affected the discharge of the karez systems. Among other factors, the flood and the base flow of ephemeral streams impact karez discharge to some extent. It depends on the topography and the distance of the karez system from the streams.

### Declining of Groundwater Table

The groundwater levels in the study area are observed by the physical monitoring of 65 tubewells in all Union Councils. This is the first time that groundwater monitoring data of drilled bores for agriculture purposes have been observed. The depth of groundwater in different UCs ranges from 1,650-2,482 masl. The minimum and maximum depth of groundwater from ground-surface are 24-116m and 102-

205m, respectively. The depth of the mean groundwater level ranges from 60-118m and the standard deviation from 3.5-67.6. The depth of groundwater in different UCs of Karezat is presented in Table 7.

All monitored tubewells are found with different discharge capacity and their discharge is measured for monitoring purposes. Tehsil Karezat having 2,488 tubewells registered and recorded operational on electric power and having 6 hours of power supply to extract water for agriculture. These wells having an average discharge pipe of 8 cm in diameter. As per calculation, about 376,185.6 m<sup>3</sup> of water is extracted daily in Karezat Valley for agriculture and domestic usage.

Due to rapid population growth and technological advancement, the reducing discharge of karezes cannot meet the water requirements of large-scale agriculture practices. The introduction of new technology has been accelerating groundwater depletion which results in the abandonment of karez systems. The primary difference between the karezes and the deep well is their sustainability. With the new tubewell installations, the construction of new karezes seems to be impossible due to the time and cost of construction as compared to the drilling costs. The expenditure for the construction of a karez may be many times more than that of a tubewell. But considering the lifespan of the karez system is more sustainable than that of the bore wells.

**Table 7** The depth of groundwater level (m) in different UCs of Karezat.

Union Council	Min.	Max.	Mean	Standard Deviation
Balozai	58	168	104	34.8
Dilsora	34	183	91	49.0
G-Khanai	24	102	71	28.9
Khanozai	116	122	118	3.5
Zakaryazai	27	205	81	67.6
R-Malazai	30	104	60	27.3
Gharshinan	82	110	96	12.3

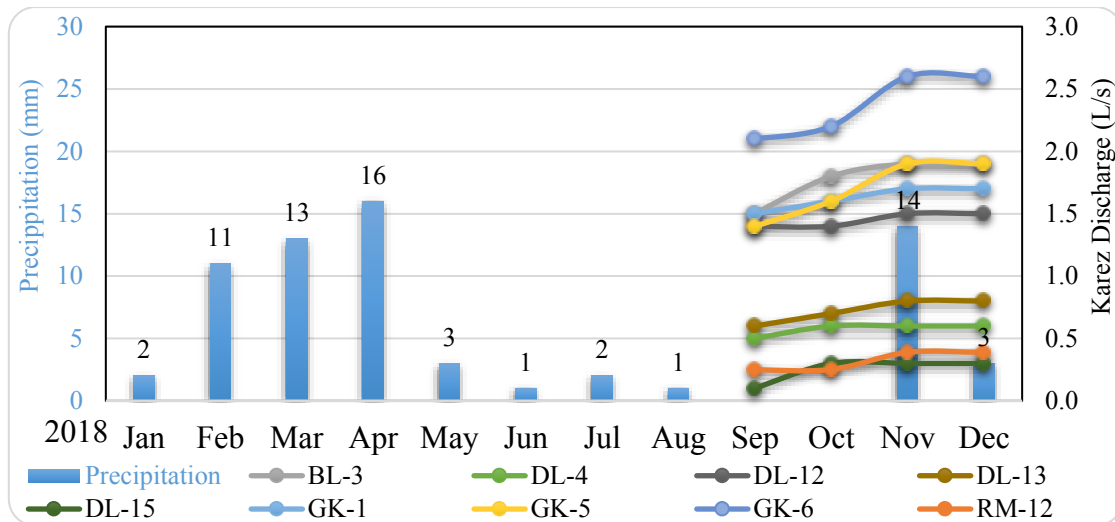


**Fig. 7** Unsteady increase in karez discharge with the influence of 2018 precipitation.

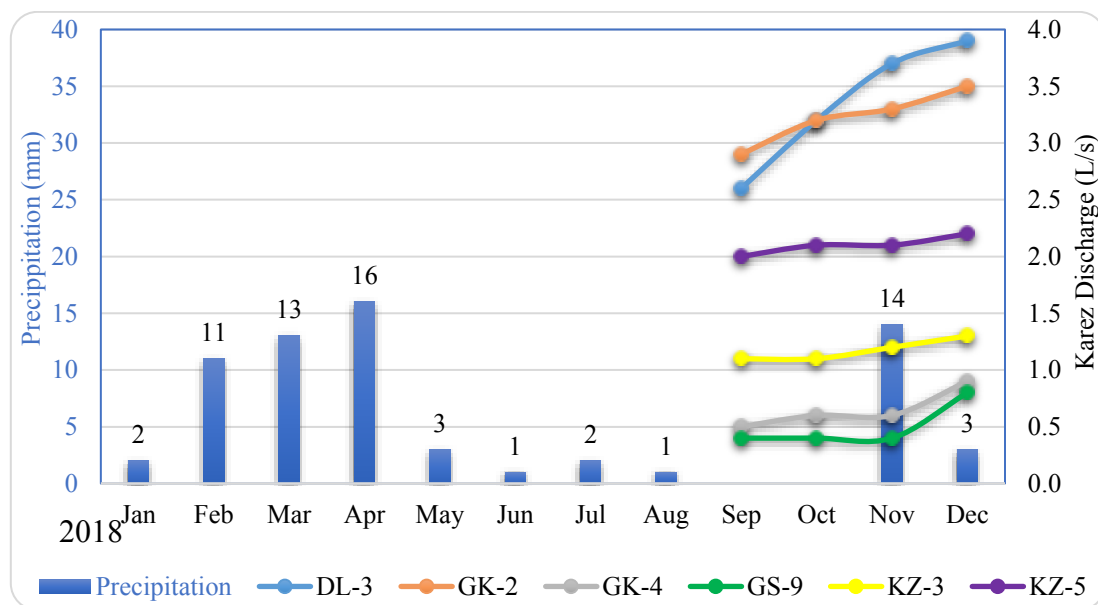


**Fig. 8:** Steady increase in karez discharge with the influence of 2018 precipitation.

**Table 8** Groundwater decline in Pishin Basin, PCRWR (2017), and Imad (2018).

#	Years		Average Decline (m)
1	1976 – 1989	13	3.97
2	1989 – 1996	7	6.40
3	1997 - 2000	3	6.71
4	2001-2004	3	4.30
5	2005-2009	4	4.00
6	2010-2014	4	7.00
7	2014-2018	4	15.00
<b>Total</b>	<b>38</b>		<b>37.08</b>

The annual recharge of groundwater in Balochistan was 2.21 billion m<sup>3</sup> on average whereas 2.66 billion m<sup>3</sup> of groundwater was

extracted during 2006-07. It is clear that almost 0.459 billion cubic meters of extra water are extracted, and it is causing an annual fall of 1 to 3 meters in the groundwater table, GOB (2014). The same is the case in Karezat where during seasonal draw down the farmer is urged to increase the depth of tubewell about 3-10 m to fulfill the water demand as the water table depth falls due to excessive drawdown.

Pumping water at a large scale has altered the hydrological regime they may not only deplete aquifers but may also dry springs and karezes and may reduce the base flow to rivers. The available groundwater monitoring data of 23 years from 1976-2000 represent that average groundwater



declined 17m in the Pishin River Basin, PCRWR (2017). The average groundwater decline values are presented in Table 8.

### **Impact of Droughts**

The severe drought of 1998-2006 put extreme pressure on already declining groundwater levels. The groundwater level declining at 0.25-1.10 m/annum as recorded as early as 1992. The absence of recharge created extra pressure on already stressed aquifers which resulted in significant reductions in karez flow and drying out of karezes. In current circumstances due to undeclared drought in these valleys communities are facing difficulties and migrating to major cities, especially those who could not afford the heavy and expensive installation of deep tubewells. For understanding the sustainability of the karez system, it is essential to view it from a much longer perspective. The karez system was sustainable for millenniums and fulfilling the needs of local communities, livestock, and nature. As per the Irrigation Department karez system and springs were affected by droughts, initially these schemes observed a reduction in water supply and then most of them dried out. The schemes were affected by depleting the water table because of the deep tubewells of large farmers in the command area of karezes. The severe droughts occurred during the last twenty years while most karezes were dried out during the last 3 to 20 years. During the same period, maximums were installed in the area. All these factors collectively affected karezes.

### **Impact of Human Activities**

The geographical area of District Pishin is 7.8 MKm<sup>2</sup> out of which 10.4% that is 0.82 MKm<sup>2</sup> is unavailable for cultivation. The potential area of 1.85 MKm<sup>2</sup> is available for agricultural crop cultivation which is 23.5%. For future growth and development, lots of advancement possibilities are available in the district. Agricultural water demand comprised the major share of total water demand based on cropping patterns. The yearly average crop water requirement for the Pishin River Basin is 658 Mm<sup>3</sup>. The forests in Pishin District are grouped into natural and artificial ones, comprising of conifers (Junipers), rangeland, artificial plantations, and other types of trees. There are seven notified natural forests which include Targhatu, Gawal, Surghund, Surkhab, Sarwat, Umai, and North Takatu; measuring 258,660

(km<sup>2</sup>), an additional 30-kilometer avenue plantation also exist in the District (GOB, 2011). The rangelands are classified as Central Balochistan Ranges. It has numerous species of indigenous trees and plants, productivity is adequate with an average production capacity of 1600 kg/km<sup>2</sup>. The rangelands have been degraded due to overgrazing and fuelwood collection, and the only remnants are less palatable plants. The degradation is aggravated by the traditional nomadic migrants.

In Karezat forests are the main source of food, timber, firewood, and shelter but also a variety of medicinal herbs. Major tree species are Shina and Obusht found in the valleys, while Ghaz in streambeds. Around karezes in mountainous regions have several trees of Shina and Obusht. It is believed that these trees are planted by inventors of the karez system, at the spot where water was found at first. Livestock in rural areas are available in huge numbers and use the water stored in earthen ponds for domestic utilization and stock watering. The water for livestock requirements is met primarily through water supply schemes. Real quantities are hard to calculate as proper farming units are not present in the study area. The basin-wide study of livestock population was around 2.4M during 2010, while projected numbers for 2020 are 3.6M. It has been estimated that the average yearly water requirement for the livestock in the Pishin River Basin is 1.2 Mm<sup>3</sup>.

### **Influences of tubewells**

Since the 1970s tubewells are successfully replacing the karez system and generally affecting and declining groundwater levels. All electric, Solar PV cells, and diesel engine-operated tubewells have been drilled in a rush without considering the location and passage of the karez system. Tubewells have a shorter life span in present circumstances 5-10 years. As compared to the karez system, which holds for centuries with proper management, GOB (2014). The percentage of the existing number of groundwater resources shown graphically in Fig. 9.

Tubewells are necessary, but these must be considered as a complementary feature to karez. Because the karez system has a long life as compared to tubewells. The primary factors of influence include the pumping rate of the well, frequency, and duration of its pumping episodes.

The distance of the tubewells located from the karez system is of prime importance.

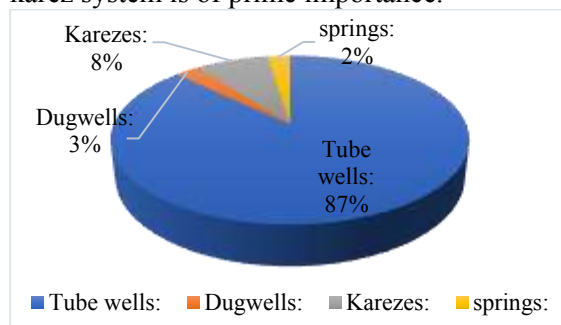


**Fig. 9** Number of water sources in Karezat.

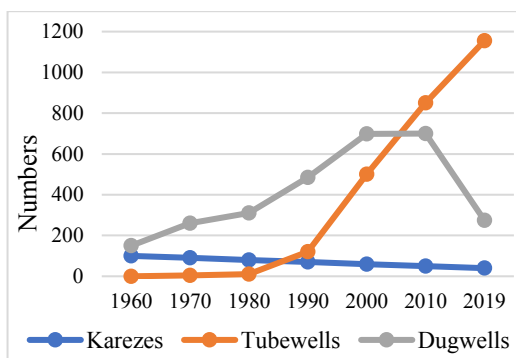


**Fig. 10** Transition of karezes into tubewells, Irrigation Department (2014).



**Fig. 11** Solar PV Panels installed on tubewells for agriculture, M-Zakaryazai, Karezat, (10 February 2019).

An active water supply well can locally lower the water table and attract the karez water from the aquifer, David (2010). The installation of tubewells happened in the early 1970s with heavy installation and operational subsidies. Under this subsidy program on tubewell operation and installation, the number of officially registered tubewells raised from 2,000 in 1970/71 to more than 14,000 in 2002/12. Despite this, there is another substantial number of private electric tubewells without a legal NOC or connection. Without NOC about 11,000 diesel-driven wells

were installed in the valleys that were not connected to the electricity grid. In Karezat, the legalized tubewells are about 1,533 which are registered with WAPDA. About 955 illegal tubewells are installed which are connected to National Grid Station. About 385 are operated through Solar Photovoltaic Cells (Solar PV Cells) and 198 are operated through diesel engines. During the recent drought span over 1998-2006, the shallow dug-wells were exaggerated worst and dropping of water table had a direct impact on the drying of shallow dug wells. As the life of tubewells in Balochistan is less than 45 years and it has dangerously affected in lowering of the water table from 30 meters to over 150 meters in many parts of the province. The number of tubewells from 1960 to 2018 increased to 1800, dug wells declined to 300 and a continuous decline of Karezes were observed. The groundwater table is declined continuously because of the increased number of tubewells. The transition of dug wells to karezes and from karezes to tubewells during the years from 1960 to 2019 is represented in Fig. 10. The large landowners have benefited the most from tubewells as they have resources, land, drill tubewells, and solarization. The solarization made it possible to fetch groundwater 8-11 hours from any depth. One of the solarized tube well systems of M-Zakaryazai UC is shown in Fig. 11.

### Physicochemical properties

The major physicochemical properties of all karezes and tubewell waters where it was available were measured. Some of the observed and measured parameters are temperature, color, odor, taste, pH, electrical conductivity (EC), and total dissolved solids (TDS). The portable meters and devices were utilized in the field to measure the groundwater quality parameters. In some countries, the guidelines aesthetic objective for drinking water quality temperature is 15°C. The temperature values of karez water in different union councils ranged from 7-14 °C with a few exceptions. While the average measured groundwater temperature of karezes is about 12.5 °C. The World Health Organization (WHO) classified the taste of drinking water based on preferable levels of TDS, WHO (2003). Karez water samples were tested at the spot and found satisfactory, the majority of the samples ranged between 300-900 mg/l. The pH ranges from 6.5 to 8.5 for drinkable water as per the WHO standard and EPA guidelines, Patil (2012). The

average pH value of Karez waters is 6.7. The measured pH values in the field have an optimal range from 6.6 to 6.9 with a few exceptions. EPA guidelines are showing the limit of Electrical Conductivity (EC) up to 2500  $\mu\text{s}/\text{cm}$ . The EC of all the karez waters is under the permissible limits of drinking water. The minimum and maximum EC values vary from 580-1240  $\mu\text{s}/\text{cm}$  and 940-1348  $\mu\text{s}/\text{cm}$ , respectively. The mean EC values range from 682-1240 and standard deviation 59-284  $\mu\text{s}/\text{cm}$ . The EC values were found under the permissible limit of drinking water 2500  $\mu\text{s}/\text{cm}$ . The minimum and maximum values of TDS in the Karez waters vary from 390-700 mg/L and 500-1000 mg/L, respectively. The mean and standard deviation values of TDS ranges from 477-700 and 6-164 mg/L, respectively. These values represent that the groundwater quality in Karezat comprised of excellent to fair. The physicochemical parameters of the water sample of active karezes were monitored and values have shown in Table 9.

### Watershed management

The overexploitation of natural resources and climate change affected the socioeconomic patterns of the communities. The low precipitation and snowfall with higher temperatures and evapotranspiration increased the intensity of droughts. The depleted water resources affected agriculture, rangelands, and livestock. The improper planning, mismanagement, and overexploitation of natural resources reduced the substantially and natural recharge to groundwater. The most important factor is the deficiency of the watershed management program in the catchment areas, Syed (2018).

The major land use of Karezat is rangelands. That constitutes about 73% of the total area of the

Karezat. Supporting the huge populations of small ruminants and providing fuelwood to more than 80% of rural households. Rangelands serve as watersheds or catchments for the valleys interspersed in mountainous areas of the Tehsil. Based on geohydrological conditions, it has been formulated that about 90% of the total runoff, which is generated after precipitation in the watersheds drains out through seasonal streams. That's not serving any beneficial purpose since the watersheds have been degraded and have lost the ability to retain and absorb water. It has been observed that water levels in the dug wells, streams, and springs, situated at the down-stream of these watersheds increases temporarily after the rainfalls but recedes very quickly. In this area, farmers do harvest and divert water for rain-fed agriculture. Due to the non-availability of financial resources and access to modern technology, they can harvest only less than 10% of total runoff.

For proper watershed management, an integrated watershed management strategy is devised for Karezat. The strategy is a development process to manage all human activities and natural resources based on the watershed. The respective communities are responsible to consider socioeconomic and environmental issues to manage the sustainability of watersheds. The sustainable development of watersheds is possible only by proper planning and management, conservation, and protection measure specific to the respective communities for all relevant sectors and subsectors. The policy and plans should be flexible and comprehensive that may be upgraded as per needs, requirements, and additional data set whenever available. The strategy may be modified with the mutual understanding, consultation, and participation of all relevant government departments, water managers, civil society, international funding

**Table 9** The pH, EC, and TDS values of karez water in different UCs.

Union Council	pH		EC ( $\mu\text{s}/\text{cm}$ )		TDS (mg/L)	
	Mean	Standard Deviation	Mean	Standard Deviation	Mean	Standard Deviation
Balozai	6.60	0.02	898	59	650	71
Dilsora	6.72	0.06	760	255	477	141
Gawal Khanai	6.77	0.16	790	269	637	141
Khanozai	6.77	0.17	1155	148	650	212
Margha Zakaryazai	6.74	0.28	894	642	581	431
Rodh Malazai	6.69	0.00	1125	0	500	0
Gharshinan	6.78	0.00	1240	0	700	0

agencies, NGOs, and relevant communities. The key issues to tackle as part of the integrated watershed management strategy are; 1). Water Governance, 2). Environmental Concerns, 3). Conservation and Sustainable Development, 4). Natural Resource Management, and 5). Community Empowerment.

### Rehabilitation of Active Karez

Different karez in Tehsil Karezat having discharge more than 1 L/s are proposed to be rehabilitated and extended. It was acknowledged that 16 such karez in the communities living in different villages depend on their karez water for drinking. These karez are poorly maintained and not having their full capacities of discharges. Karezes are selected for rehabilitation/extension and cleaning, including the establishment of water reservoirs, channel extension, and repair where required and possible. Most of the partially active karezes are located in river beds. After a detailed inspection of the karezes and discussion with the community members of all villages the following interventions are proposed; 1). Karez Extension, 2). Construction of Irrigation Channels / Pipelining, 3). Construction of Storage Ponds, 4). Check Structures for Recharge Purpose of Karezes.

The main objective of the Karez extension is to increase the water quantity by extending the horizontal tunnel and adding new vertical shafts. Karez underground galleries were manually dug along the length of a Karez toward the foothill. The vertical shafts are dug at intervals of 15 meters to remove excavated material and to provide ventilation and lighting facility and access for maintenance. The Karez reflects collective and communal work. The Karez water is stored by the user according to their water rights and applies water to their fields. The size of the proposed storage water pond is 18 meters by 18 meters and the height is two meters. This will help out the farmers to get Karez water stored for the night and farmers to irrigate their farms in the daytime.

The construction of a new water channel or laying of pipelines is proposed. The main objective of this water channel or pipelining is to reduce water conveyance losses. It would decrease the growth of weeds, to convey irrigation water under gravity from water pond to agricultural fields. The construction of the channel, ensured the essential water flow velocity to the field of the targeted communities.

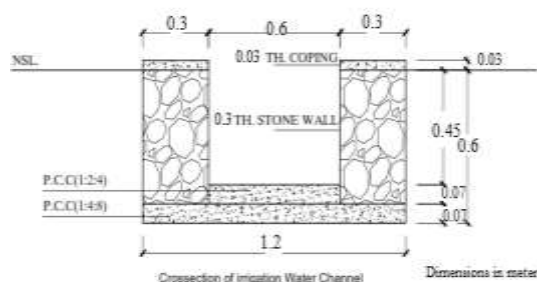


**Fig. 12** Cross-section of a proposed irrigation water channel.

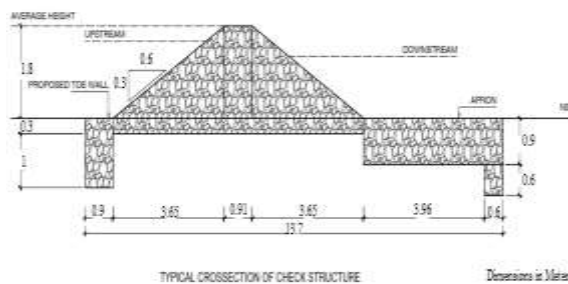


**Fig. 13** Typical cross-section of a proposed check dam for Karezat.

A standard diagram of the karez water channel is drawn as per the average discharge of karezes are presented in Fig. 12.

The check structures with dry stone pitching are proposed for the communities to store surface runoff for utilization and groundwater recharging. The proposed check structures will be constructed upstream of the karez system in the catchment area of a mother well. It would help to percolate water into the ground to recharge the aquifer to increase the base flow and to minimize the risk of flash floods. The structural design of the check dam and the daylight point chamber of Karezes are drawn based on the average discharge of Karezes, easy to maintain with minimum overall coating. A typical section of the proposed check dam is presented in Fig. 13. The proposed design of a daylight point chamber of a Karez is shown in Fig. 14.

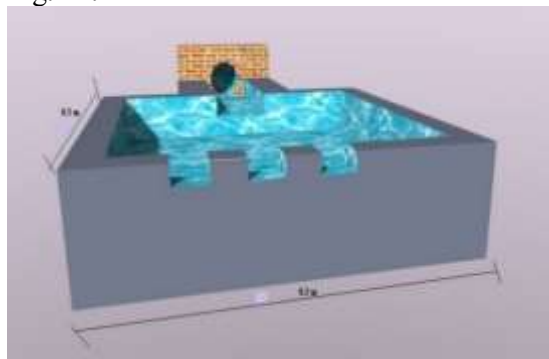


**Fig. 14** Design of a typical daylight point chamber of a karez.

## Conclusions

Hydrologically Karezat is divided into three categories dependent on high, medium, and low potential groundwater revitalize zones. The high potential zones comprised of exposed limestone including the Nisai Formation of Eocene. The groundwater discharge from limestone formations forms small springs of low discharge. The alluvial fans and piedmont sediments of Quaternary along mountain ranges are comprised of high potential groundwater zones. These are the main recharge zones for the mother-wells of the karezes.

In Karezat out of 106 karezes, 37 are partially active, 65 are dried out, and 4 demolished. The karezes were constructed from the past 25-600 years and dried during the last 3-20 years. The effect of climate change is imminent, karezes are dried due to long spans of droughts that hit twice in the last two decades from 1998-2006 and due to groundwater mining. The shallow depths of the mother-wells are among one of the major causes of drying out of karezes. In the small valleys, it's almost impossible to rehabilitate a karez with a maximum depth of the mother-well that ranges <10m.

The Karezat population was 76,360-138,208 persons as per the 1998 and 2017 census, respectively. The population increased by 55% in nineteen years.

During the last 20 years, the area irrigated by tubewells increased 338% while the area irrigated by karezes declined by 80% in the last 50 years. The karez command areas have an extensive variation as 90% of the schemes have a command area of fewer than 1,000 Km<sup>2</sup>, 50% by 340 Km<sup>2</sup>, and 10% have less than 80 Km<sup>2</sup>.

The discharge quantities of Karez waters represent an increase from 2.9 to 3.7 L/s in four months. The increase in the discharge of karezes represents a positive impact of 2018 precipitation on the groundwater. It has been estimated that on average 376,186 m<sup>3</sup> of groundwater is extracted daily by tubewells in Karezat for agriculture.

Among physicochemical parameters, the pH, EC, TDS of karez waters represent that the Karezat comprised of excellent to fair quality drinking and agricultural waters. The major land use of Karezat is rangelands that supporting the huge populations of small ruminants and providing fuelwood to rural households. Rangelands serve as watersheds that have been degraded and lost the ability to retain water.

An integrated watershed management strategy has been considered. The key components of the strategy are Water Governance; Environmental Concerns; Conservation and Sustainable Development; Natural Resource Management and Community Empowerment. For rehabilitation, sixteen karezes used for drinking are selected with community consultations. The rehabilitation comprised of Karez Extension; Construction of Irrigation Channels; Construction of Storage Ponds; and Check Dams to enhance recharge of Karezes.

## Acknowledgment

This work is part of an MS thesis in Civil Engineering submitted by Eng. Hamayun Khan to the Department of Civil Engineering, Balochistan University of Information Technology, Engineering and Management Sciences, Quetta, Pakistan. The authors are thankful and acknowledge to review the work by Professor Dr. Syed Imran Ahmed, Department of Civil Engineering, NED University, Karachi, Pakistan.

## References

- Andrew. C Kerr., 2015. Petrogenesis and tectonomagmatic significance of Eocene mafic intrusions from the Neotethyan suture zone in the Muslim Bagh–Khanozai region, Pakistan.
- Climate-data.org., 2014. <https://en.climate-data.org/asia/pakistan/balochistan/khanozai-30276/>.
- CPAU. 2011. 'Social Realities of The Karez System'. Wardak, Afghanistan: Organization.
- Daanish Mustafa, 2015. "Karez versus Tube Well Irrigation: The Comparative Social Acceptability and Practicality of Sustainable Groundwater Development in Baluchistan, Pakistan.
- Danish Mustafa, 2007. The Transition from Karez to Tubewell Irrigation: Development, Modernization, and Social Capital in Baluchistan, Pakistan. *World Development*, 35 (10), 1796-1913.
- David., 2010. The interaction between ground water and surface water.
- Durrani., 2012. Petrology and provenance of the sandstone channel succession within the Jurassic Loralai Formation, Sulaiman Fold-Thrust Belt, Pakistan. *Journal of Himalayan Earth Sciences*, 45, 1–16.

- OB, Planning & Development. 2011. District Development profile Pishin. Quetta: GOB.
- GOB, Planning & Development. 2014. Water of Balochistan. supporting implementation of IWRM Policy in Balochistan G.O.B - ADB & Royal govt of Netherlands. (pp. 11-12). Quetta: Government of Balochistan.
- Hamayun Khan, 2019. Hydrogeological Study of Karez System in Tehsil Karezat, Balochistan, Pakistan. MS thesis in Civil Engineering. Balochistan University of IT, Engineering and Management Sciences, Quetta Pakistan. Unpublished.
- Hunting Survey Corporation, 1961. Reconnaissance geology of part of West Pakistan, Toronto, Canada.
- Imad Ali and Syed M Aftab, 2018. Impact of Climate Change and Human-Induced Factors on the Quaternary Aquifer of Quetta Subbasin, Pakistan. Unpublished MS Thesis, BUIITEMS, Quetta, Pakistan.
- Irrigation Dept, GOB (2014). Water Resources Development in Balochistan. Quetta: Govt of Balochistan.
- Muhammad Ishaq Kakar, Mehrab Khan, Khalid Mahmood, Andrew C. Kerr, 2014. Facies and distribution of metamorphic rocks beneath the Muslim Bagh ophiolite, (NW Pakistan): Tectonic implications. *Journal of Himalayan Earth Sciences* 47(2):115-124.
- Kazmi, A., Reza, S. Q. 1970. Water supply of Quetta Basin, Balochistan, Pakistan. *Geol. Surv. Pakistan Rec.*, 20, 97-138.
- Meayer Philippe de. 2014. "Creating a Database System for Managing and Analyzing the Karez I System in Xinjiang.
- Mohyuddin. 2012. Social Organization of a Karez In Balochistan. *World System Analysis in Anthropology Perspective*.
- Mustafa, D. 2014. The Necessity of Karez Water Systems in Baluchistan Department of Geography -.
- Patil. P.N., Sawant. D.V, Deshmukh. R.N. (2012). Physico- Chemical Parameters for Testing of water-A review. *International Journal of Environmental Sciences*, 3, no 3., 1196-1203.
- Pietro Laureano and M. H. Papoli Yazdi, 2012. Evaluation Report, the first five years performance of International Centre on Qanats and Historic Hydraulic Structures (ICQHS) under the auspices of UNESCO. *Topographical Maps of Pishin, Quetta and Ziarat Districts, Fourth Edition, Scale 1:50,000 comprising Toposheet No. 34N/2, 34N/6 and 34N/10, Survey of Pakistan, Islamabad.*
- Shahid, A. 2007. "Karez - A Cultural Heritage of Natural and Agricultural Sectors and An Interminable System of Harvesting Groundwater in Baluchistan.
- Shaikh M. Atif, 2016. Karez Irrigation in Balochistan. Do something before it is too late. April 2016, Pak Affairs, Research Report. *Jahanger's Monthly Magazine World Repot.*
- Syed M. A., 2018. Strategies to Manage Aquifer Recharge in Balochistan, Pakistan: An overview. 2018 IOP Conf. Ser.: Mater. Sci. Eng., 414.
- World Health Organization, 2003. Total dissolved solids in Drinking-water Background document for development of WHO Guidelines for Drinking-water Quality. WHO/SDE/WSH/03.04/16.



## Subsurface investigation for Groundwater formation in District Rahim Yar Khan (Pakistan) using Vertical Electrical Techniques

Hafiz Umar Farid<sup>1\*</sup>, Akhtar Ali<sup>1</sup>, Zahid Mehmood Khan<sup>1</sup>, Ijaz Ahmad<sup>2</sup>, Aamir Shakoor<sup>1</sup>

<sup>1</sup> Chairman, Department of Agri. Engineering, Faculty of Agri. Sciences and Technology, Bahauddin Zakariya University, Multan, 60800 Pakistan.

<sup>2</sup> Centre of Excellence in Water Resources Engineering, University of Engineering and Technology, Lahore 54890, Pakistan

Corresponding author email: [hufarid@bzu.edu.pk](mailto:hufarid@bzu.edu.pk)

**Abstract:** The electrical resistivity survey technique is most widely used to explore the groundwater because it is a quick and less expensive and reliable geophysical tool. The vertical electrical soundings were carried out at 80 locations in the district Rahim Yar Khan, Punjab, Pakistan, using resistivity meter (ABEM Terrameter SAS 4000, Sweden). The Schlumberger electrode configuration was used with the half current electrode spacings (AB/2) ranging from 2 to 180 m and potential electrode spacings (MN) 1 to 40 m. The collected field data were interpreted using the Computer Software "Interpex 1X1D". The outputs of VES interpretations were verified by using the borehole data collected at various six locations selected from the district. Using the combination of VES results along with borehole data, longitudinal conductance values of the first and second layers were estimated in the range of 0.03-0.48 Siemens and 0.004-29 Siemens respectively. That indicated the presence of fresh groundwater of good quality in second layer. Moreover the fresh groundwater having aquifer resistivity of more than 40  $\Omega$  m was found in the North-West side of the district Rahim Yar Khan along with the Indus River Bank and thickness of fresh groundwater layer was in the range of 10-100m below the ground surface which can be pumped to minimize the secondary salinization where as the brackish groundwater was found in desert area of the district and this brackish water may produce salinity effects throughout the area.

**Keywords:** Resistivity Surveys, Groundwater, Aquifer characteristics, Borehole, Irrigation.

### Introduction

Groundwater is considered to be a most reliable resource and is used for irrigation, drinking as well as for industrial purposes all over the world. It is used mostly for drinking purposes. In Pakistan, ground water is a rich source of irrigation. Groundwater pumping and use on commercial scale began since 1960's by launching of Salinity Control and Reclamation Projects (SCARPs). The pumped ground water was inserted into canal system for conjunctive use of groundwater along with canal water to increase the irrigation supplies (Qureshi et al, 2008). It is estimated that 62 billion cubic meter of groundwater is being pumped annually to supplement surface water supplies (WAPDA, 2009). At this time about 1 million small capacities private tubewells are in operation in the country including 0.85 million in Punjab (PES, 2012).

Since there are no definite rules of groundwater management, each farmer can install a tubewell in his land without getting permission and prior investigation. This uncontrolled and unregulated

use of groundwater affects the aquifer potential. Moreover huge no. of dug wells have become dry, yet the water table is declining and ground water quality is deteriorating. Depletion of ground water is noticed seriously in non-canal command areas of the province Punjab and where canal supplies are very poor and irrigation is completely relied on fresh groundwater (Qureshi et al, 2008). The monitoring of groundwater level shows a decreasing behavior of water table. It should be necessary to get an overview of groundwater conditions before the design and planning of water related projects. Mostly farmers and other related persons have no information about modern techniques of investigation. Often the traditional methods are being used for investigations, which are too expensive, laborious, time taking and only provide information in discrete points. The resistivity survey method may be used for the exploration of groundwater to estimate its behavior (Khalil et al, 2009). It is considered to be a best alternative of hit and trial boring to some extent. It would be the most economical, quick and reliable source of estimating the groundwater characteristic. Therefore on the

basis of groundwater conditions and problems, the current research work has been designed to explore the groundwater aquifer to assess the groundwater quality of the study area to develop the guidance for tubewell installation of the farmers of study area.

### Methodology

#### Study Area

The study was conducted at various villages and towns of district Rahim Yar Khan, Punjab. The district lies between  $27^{\circ}40'$ - $29^{\circ}16'$  towards North as well as  $60^{\circ}45'$ - $70^{\circ}01'$  towards East. The general weather of the district Rahim Yar Khan (study area) is hot as well as dry, during the season of summer whereas cold and dry during the winter season. The duration of summer season is continued between the months of April and October where as the winter months are started from November and remained continued up to March. The average rainfall is approximately 100 millimeters (3.9 inch). The district Rahim Yar Khan has three main geographic portions; The Riverside area of the

district covers the southern side of the Indus River. Its major portion belongs to river bed. The canal-irrigated area is situated on the south and is isolated by Minchan Bund. The Cholistan area is found on the south of the irrigated area and continued up to the Indo-Pak border.

### Resistivity Survey Method

Electrical resistivity survey, a geophysical survey technique has proved to be an effective and reliable tool in locating viable aquifers for continuous and regular water supply (Todd and Mays, 2005). The instrument used to measure the Vertical Electrical Sounding (VES) was Terrameter SAS 4000 (ABEM, Sweden). The meter is the property of Department of Agricultural Engineering, Field Wing, District Rahim Yar Khan, Govt. of Punjab. The targeted sites were investigated with contribution of this department. The Schlumberger electrode technique was employed for the measurement of Vertical Electrical Sounding (VES) at 80 different locations at the study area. In this method all the four electrodes were placed

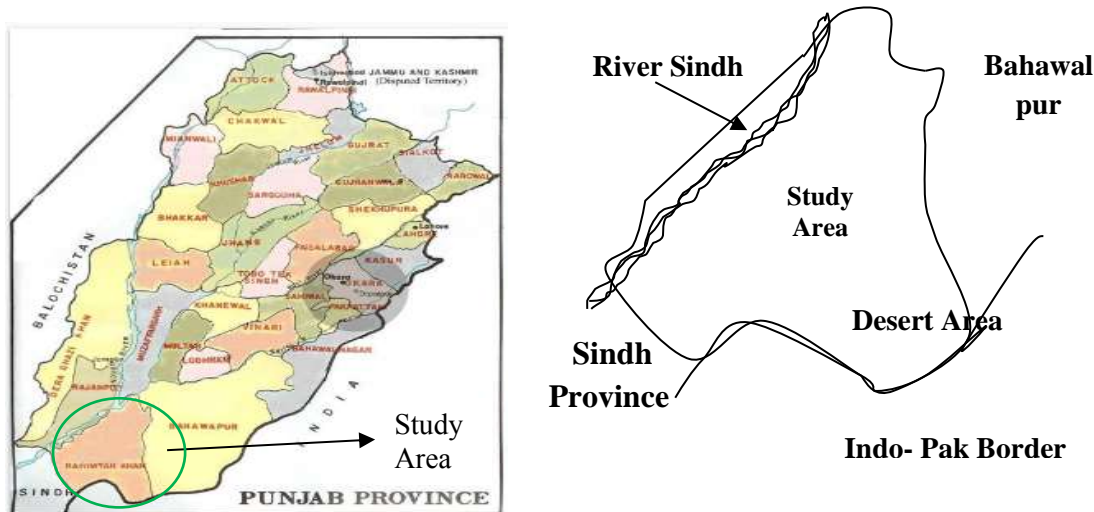
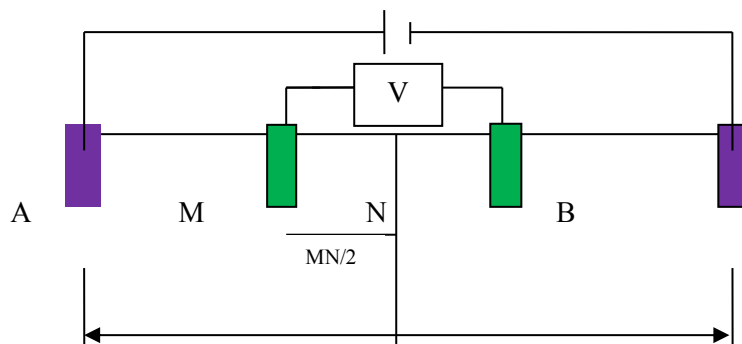


Figure 1. Location of Study area



**Fig. 2.** Layout of Schlumberger electrode Array

in a straight line and distance between inner electrodes was fixed at some stations while the distance between the outer electrodes was changed for each measurement (Fig. 2). In resistivity survey, Schlumberger electrode array was selected, keeping current electrode gap (AB/2) of 2, 4, 8, 10, 15, 20, 25, 25, 30, 35, 40, 45, 50, 50, 60, 70, 80, 90, 100, 100, 120, 140, 160, 180 and 200 meter. The increment in potential electrode spacing was made at similar spacings of 25, 50 and 100 m. In overlapping as well as extending over segments, mostly the Schlumberger data are employed because at each station of electrode spacing (AB/2), the resistivity meter shows poor sensitivity (P. Sikandar 2009). So in this situation the MN gap was increased and measuring the two values for the same AB/2 was taken, one reading at the shorter and other at the larger MN spacing. The spacings between the potential electrodes (MN/2) were increased step wise at 0.5, 5, 10 and 20 meters. The resistance of earth at separate spacings was estimated using resistivity meter at different electrode spacings in district Rahim Yar Khan. The values of apparent resistivity of the medium below the electrodes can be obtained by multiplying the earth resistance with the geometric constant (K). In case of Schlumberger electrode arrays the value of geometric constant (K) can be calculated as (Arshad et al 2007, P.Sikander 2009).

$$\rho_a = K * R \quad (1)$$

where:

$\rho_a$ = Apparent Resistivity in Ohm meter ( $\Omega$  m),  
V=Voltage, potential drop, in milli-Volt (mV)

I = Current in milli-ampere (mA) and K = Constant of proportionality

$$K = \pi \frac{(AB/2)^2 - (MN/2)^2}{MN} \quad (2)$$

Where:

AB = Spacings between two outer electrodes (m)  
and MN= Spacings between two inner electrodes (m)

### Aquifer Parameters

Formation factor is very important parameter and is computed by the following expression;

$$F = \rho_a / \rho_w \quad (3)$$

F is known as the formation factor and its value remains same for pure sand. F was calculated by the layer wise values of groundwater and aquifer resistivity. The layer wise hydraulic conductivity

can also be computed using following relationship given by Yadav, (1995).

Where:

$$F = 21.18F - 4.48 \quad (4)$$

Longitudinal conductance and transverse resistance are two the most important parameters regarding the aquifer characteristics. These elements were also estimated through VES resistivity survey data. The transverse resistance was determined using:

$$TR_i = \rho \times Hi \quad (5)$$

The longitudinal conductance was also determined using:

$$LC_i = EC \times Hi \quad (6)$$

## Result and Discussions

### Electrical Resistivity Survey data collection and Processing

The resistivity survey data was interpreted by the use of the 1-D inversion technique (IX1D, Interpex, USA). The software gave the output in the form of resistivity model which fits the obtained field data with the least possible root mean square (RMS) error between the synthetic data of model and actually observed data. In order to obtain the least and constant fitting errors between synthetic model curve and field data, the method of iteration was used.

With the help of computer software (1X1D), the field data were interpreted by plotting the true resistivity against electrode spacing shown in figure 3. The model output also gave the thickness, depth of all interpreted layers. These results were correlated/compared with borehole data at all selected six sites. The resistivity survey results and soil samples collected from drilled boreholes at six sites (RYK1, RYK2, RYK29, RYK33, RYK50, and RYK62) are given in figure 4. A total of six well logs (one at each site) were prepared up to 90m, 90m, 90m, 100m, 100m and 90m depth. The results from the analysis of borehole data and VES data interpretation results are matched closely with each other. The first layer had resistivity value of 155  $\Omega$  m at RYK1, correlates to the top soil (loam) which extends up to the depth of 5m from the ground surface. Between 5- 13 m depth, the resistivity increased to 936  $\Omega$  m, indicating coarse sand. The third layer from 13-78 m, shows decreasing trend in resistivity of 85  $\Omega$  m where as fourth layer from

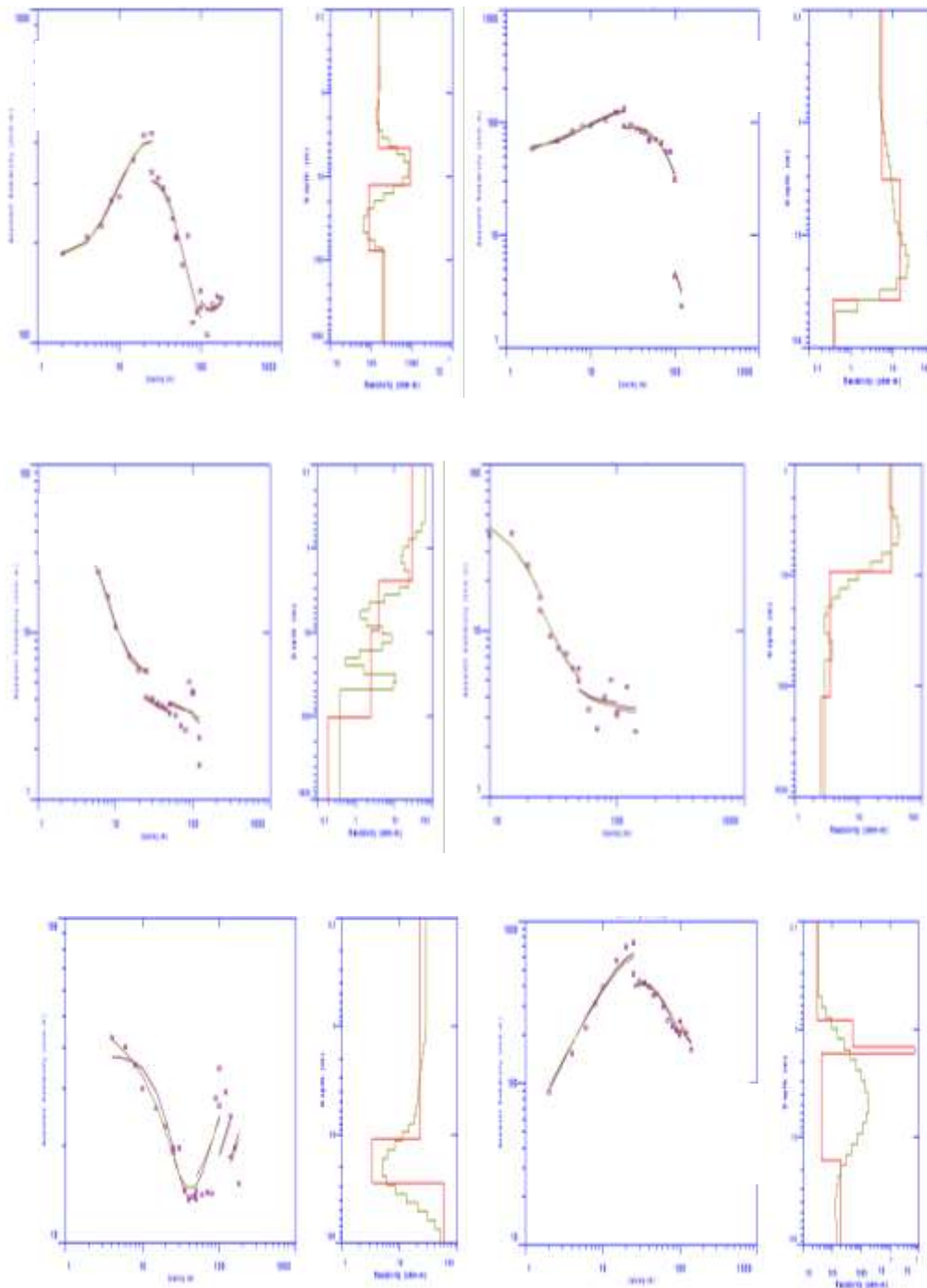


**Fig. 3.** Model Output of 1X1D Computer Software at Six sites

78m depth shows resistivity of 212  $\Omega$  m, represent the coarse sand with alternate thin layer of clay containing good quality fresh groundwater. Similarly a close agreement was also found in other selected sites and shown by the figure below.

The aquifer resistivity obtained from the interpretation of VES data and the associated values of EC, SAR and RSC obtained from the hydro chemical analysis of water samples

collected from the borehole drilling are shown in table (1). The table shows that EC values generally increases by increasing the depth below ground surface. However, the irrigation water suitability criteria developed by WAPDA (1977), shows that resistivity values more than 20  $\Omega$  m, EC values less than 2.5 dS/m and SAR values less than 13 indicate fresh groundwater. The values of electrical conductivity (EC) of the water samples collected from all six sites (RYK1,

RYK2, RYK29, RYK33, RYK50 and RYK62) were correlated with the aquifer resistivity obtained from the interpretation of the apparent resistivity data at the same sites. The values of aquifer resistivity ( $\Omega$  m) of all the selected sites were plotted along X- axis and water quality (dS/m) of the corresponding layers along Y-axis to get the relationship between the aquifer resistivity and groundwater quality (figure 5). This curve gave the value of coefficient of determination,  $R^2 = 0.911$  and shown in figure (5).

Thus using the relation developed between EC of groundwater and aquifer resistivity, the fresh and saline groundwater layers were identified on the basis of the criteria developed by WAPDA. So the groundwater layer having resistivity values more than  $40\Omega$ m was declared as fresh groundwater zone whereas resistivity values less than  $40\Omega$ m shows saline/brackish water zone.

#### Aquifer Parameters

The values of aquifer resistivity ( $\rho_a$ ), groundwater resistivity values ( $\rho_w$ ) and their corresponding values of formation factors (F) at

six sites are given in table 1. From the table, it is evident that values of formation factor vary greatly depending upon the variation in the resistivity values. The more value of formation factor shows the presence of the resistive particles in the soil of larger diameter indicating the sand and gravel particles, the low values of formation factor indicate the presence of finer particles of soil. The hydraulic conductivity values computed from formation factor 'F' was 13554.96m/day, 525.13m/day, 2643.02m/day, 237.40m/day, and 405.78m/day and 3266.45m/day of RYK1, RYK2, RYK29, RYK33, RYK50 and RYK62 respectively. The transverse resistance (TR=Layer thickness x resistivity) was determined using equation (5), while the longitudinal conductance (LC = Layer thickness/ resistivity) was also determined using equation (6) and interpreted layer parameters were taken from table (2). The higher values of transverse resistance represent the aquifer layer having more values of resistivity thickness, while the more values of longitudinal conductance are representing low resistivity values that indicate the poor quality of groundwater.

**Table 1.** Formation factor

Name of VES	Thickness Ti(m)	VES Resistivity ( $\Omega$ m)	Remarks	Groundwater Resistivity ( $\Omega$ m)	Formation Factor (F)
RYK1	5	155	Unsaturated	0.80 0.77	1170 110.4
	8	936	Saturated		
	65	85	Saturated		
		212			
RYK2	3	6	Unsaturated	0.32 0.32	46.88 3.13
	35	15	Saturated		
		1	Saturated		
RYK29	2	30	Unsaturated	0.04 0.021	100 150
	7	4	Saturated		
	95	3	Saturated		
		0			
RYK33	9	33	Saturated	1.68 1.25	19.64 3.2
	116	4	Saturated		
		3			
RYK50	11	23	Saturated	0.71 0.63	32.39 6.35
	17	4	Saturated		
		58			
RYK62	1	30	Unsaturated	0.86 0.77	79 229.87
	2	512	Unsaturated		
	7	1871	Unsaturated		
	27	68	Saturated		
		177	Saturated		

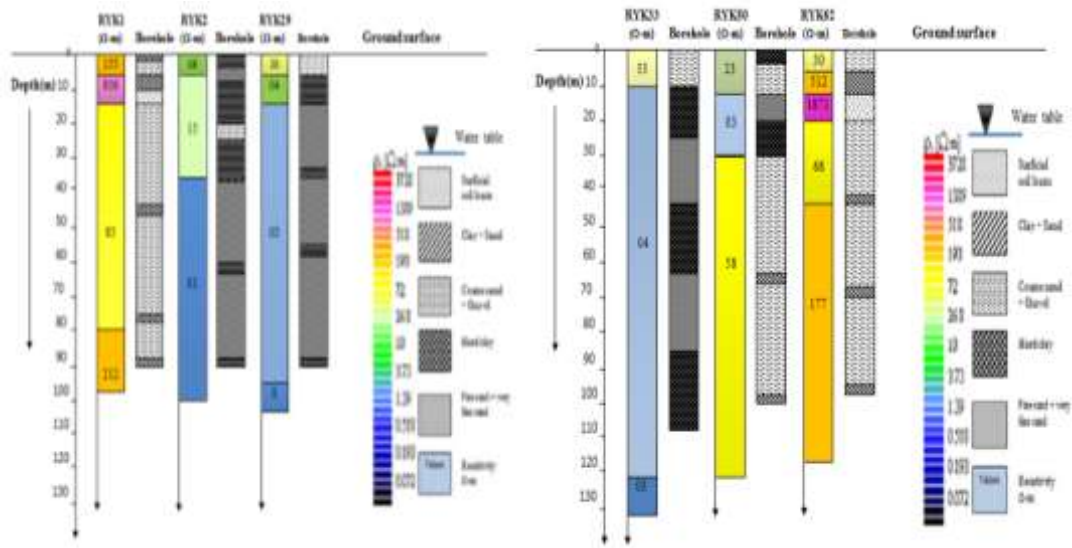


**Fig. 4.** Correlations of Resistivity Results with Subsurface Lithology

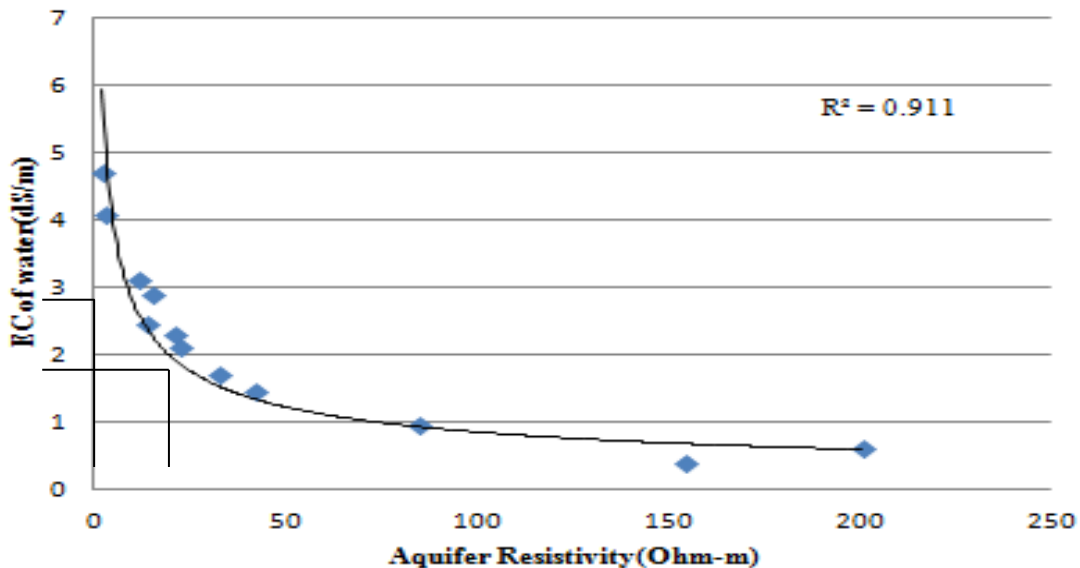


**Fig.5.** Relations between Aquifer Resistivity and Electrical Conductivity (EC) of Groundwater

The longitudinal conductance values of the first and second layers were estimated (table.2) in the range of 0.03-0.48 Siemens and 0.004-29 Siemens respectively where as values of transverse resistance were in the range of 18-775Ωm<sup>2</sup> and 28-7488Ωm<sup>2</sup> respectively. The greater value of transverse resistance in the second layer shows that fresh groundwater of good quality is available in that layer.

**Conclusions**

Following conclusions are drawn on the basis of geological data interpretation:

1. It was observed that the resistivity survey technique has the potential to detect fresh groundwater layers and subsurface lithology at the study area because evaluation based on the borehole data has close agreement with the resistivity survey data.
2. The aquifer characteristics such as longitudinal conductance and transverse resistance were computed by using aquifer resistivity ( $\rho$ ) and thickness of respective layers. The longitudinal conductance values of the first and second layers were estimated in the range of 0.03-0.48 Siemens and



**Table 2.** Longitudinal Conductance and Transverse Resistance

Name of VES	Thickness Ti(m)	VES Resistivity ( $\Omega$ m)	Remarks	Longitudinal Conductance (Siemens)	Transverse Resistance ( $\Omega$ m <sup>2</sup> )
RYK1	5	155	Unsaturated	0.03	775
	8	936	Saturated	0.009	7488
	65	85	Saturated	0.76	5525
		212		Undefined	Undefined
RYK2	3	6	Unsaturated	0.5	18
	35	15	Saturated	2.33	525
		1	Saturated	Undefined	Undefined
RYK29	2	30	Unsaturated	0.07	60
	7	4	Saturated	1.75	28
	95	3	Saturated	31.67	285
		0		Undefined	
RYK33	9	33	Saturated	0.27	297
	116	4	Saturated	29	464
		3		Undefined	Undefined
RYK50	11	23	Saturated	0.48	253
	17	4	Saturated	4.25	68
		58		Undefined	Undefined
RYK62	1	30	Unsaturated	0.03	30
	2	512	Unsaturated	0.004	1024
	7	1871	Unsaturated	0.004	1309
	27	68	Saturated	0.40	1836
		177	Saturated	Undefined	Undefined

0.004-29 Siemens respectively where as values of transverse resistance were in the range of 18-775 $\Omega$ m<sup>2</sup> and 28-7488 $\Omega$ m<sup>2</sup> respectively. The greater value of transverse resistance in the second layer shows that fresh groundwater of good quality is available in that layer. The hydraulic conductivity values computed from formation factor 'F' was 13554.96m/day, 525.13m/day, 2643.02m/day, 237.40m/day, and 405.78m/day and 3266.45m/day of RYK1, RYK2, RYK29, RYK33, RYK50 and RYK62 respectively.

- The empirical relationship between resistivity of interpreted subsurface layers and electrical conductivity (EC) of groundwater samples gave value of  $R^2=0.911$ , these informations may be helpful for further studies of resistivity survey in district Rahim Yar Khan.
- The fresh groundwater having aquifer resistivity of more than 40  $\Omega$ m was found in the North-West side of the district Rahim Yar Khan along with the Indus River Bank. It was also noted that the thickness of fresh groundwater layer was in the range of 10-100m below the ground surface which can be pumped to

minimize the secondary Salinization. On the other hand the brackish groundwater was found in desert area of the district and this brackish water may produce salinity effects throughout the area.

- On the basis of the results obtained of the research work, it is recommended that North West side of the district Rahim Yar Khan along with the Indus River Bank is suitable for tubewell installations regarding the pumping of fresh groundwater for irrigation purposes.

### References

- Arshad, M. J. M. Cheema and S. Ahmad. 2007. Determination of lithology and groundwater quality using Vertical Electrical Sounding (VES) resistivity surveys. International Journal for Agri. Biol. 9(1):143-146.
- ESP. 2010. Economic Survey of Pakistan. Government of Pakistan, Islamabad. PP.17.
- H.U.Farid, 2009. Determining the Aquifer Characteristics Using Resistivity Survey and Pumping Test Techniques.

- Khalil, M.A., A. Fernando and S. Monterio. 2009. Influence of degree of saturation in the electric resistivity–hydraulic conductivity relationship. *Surv. Geophys.* 30:601-615.
- M. Arshad, A. Shakoor, 2013. Hydraulic transmissivity determination for groundwater exploration using Vertical Electrical Sounding (VES) Method in comparison to the Traditional Methods, *Pak. J. Agri. Sci.* , Vol. 50(3), 487-492.
- PES. 2012-13 Pakistan Economic Survey. Govt. Pakistan, Islamabad.
- P. Sikandar, A. Bukhsh, T, Ali, M. Arshad (2010). Vertical Electrical Sounding (VES) resistivity survey technique to explore low salinity groundwater for tube well installation, Chaj Doab, *Journal for Agriculture Research* (2010), 48(4).
- Qureshi, A.S. M.N. Asghar, S.Ahmad, I. Masih, 2004. Sustaining crop production under saline groundwater conditions: A case study from Pakistan. *Australian Journal for Agricultural Sciences*. Vol. 54(2): 421-431.
- Qureshi. 2008. Groundwater Management in Pakistan, the Question of the Balance Paper No. 717, P- 210
- Selvam. S, Sivasubramanian. P (2012) Groundwater potential identification using geoelectrical surveys: A case study from Medak district, Andhra Pradesh, India. *International Journal of Geomatics and Geosciences*, Volume 3, No.1, 2012.
- Shah. T., 2007. The groundwater economy of South Asia: An assessment of size, significance and socio-ecological impacts: In Giordano, M and Villhoth, KG. (Editors), *The Agricultural Groundwater Revolution: Opportunities and Threat to development*. CABI Publications. 7-36 pp.
- WAPDA. 2009. Water resources and hydropower development vision-2025. Planning and Design Division, WAPDA, Pakistan.
- WAPDA. 1977. Report on soil salinity survey and research division. Vol.1, Water and Power Development Authority (WAPDA) - Lahore.
- Yadav, G.S. 1995. Relating hydraulic, geoelectric parameters of the Jayant aquifer, India. *J. Hydrol.* 167, 23- 38

## Assessment of Groundwater Vulnerability and Aquifer Protective Capacity Using Vertical Electrical Resistivity Method

Muhammad Rizwan Shahid<sup>1</sup>, Hafiz Umar Farid<sup>1</sup>, Zahid Mahmood Khan<sup>1</sup>, Muhammad Naveed Anjum<sup>2</sup>, Saddam Hussain<sup>1</sup>

<sup>1</sup> Department of Agricultural Engineering, Bahauddin Zakariya University, Multan-Pakistan

<sup>2</sup> Department of Land and Water Conservation Engineering, PMAS Arid Agriculture University, Rawalpindi.

Corresponding author email: [hufarid@bzu.edu.pk](mailto:hufarid@bzu.edu.pk)

**Abstract:** This study was conducted in district Multan to evaluate the subsurface lithology, groundwater vulnerability and aquifer protective capacity. This information will help to assess the quality of fresh groundwater depth and position. A total of 68 vertical electrical sounding surveys carried out. The data was interpreted by helped of iterative interpretation using 1-D inversion technique software. 1X1D interpreted data was used to prepare spatial distribution maps. These Maps were prepared using ArcGIS 10.5. The study examined that a major's part of the study area had three and four subsurface geo-electric layers. The spatial distribution maps for AR showed that the fresh groundwater quality was present on the north-western and north-eastern sides of the study area for the layer 3rd and 4th layers. About 42% of the study area has poor protective capacity, 21% weak protective capacity and 33% moderate protective capacity. The result showed a higher yield potential of groundwater in the north-eastern part compared to the southern side. Overall analysis showed that these maps will be helpful in the future for assessing quality, protective capacity and groundwater vulnerability in the region. The obtained data will help in understanding vulnerable area of study area.

**Keywords:** VES, Apparent resistivity, APC and groundwater vulnerability

### Introduction:

Agriculture sector of Pakistan consider backbone in development and growth of economy. The majority of the population is dependent on this sector, directly or indirectly. It accounts for about 24% of the Gross Domestic Product (GDP) and accounts for half of the labour force employed, making it the largest source of foreign exchange earnings (Pakistan Economic Survey 2017-18). The agricultural sector reported strong growth of 2.67 percent, significantly higher than the growth of 0.58 percent achieved in the previous year. Rice output increased by 2.9 percent to 7,410 million tones and maize output by 6.0 percent to 7,236 million tonnes with respect to 'Kharif' crops, while cotton production decreased by 6.9 percent to 9,178 million bales. The crop water requirement ranging from 1260 mm to 2850 mm for varieties of crops depend upon the climatic condition of country. Groundwater is a core element of our livelihood system and substantially contributes to economic development (ran Masoud Saatsazet al. 2011) (Jia et al., 2019). Water shortages and emissions have become a significant global issue in recent decades. The use of groundwater has increased dramatically in recent decades. Over two

thousand people worldwide depend for their drinking water needs on groundwater (Kurunthachalam et al. 2014). Roughly 90% of Pakistan's population uses the aquifer for their household purpose (A. Memon et al., 2020) (Watto & Mugeru, 2016). Contribution of GW to irrigated agriculture has doubled in last the last decades from 27 to 54 MAF. A rapidly increase population is adding stress to groundwater. Numbers of tube wells are increasing yearly because every year more tubewells are installed to meet the citizen's demands for water. Excessive usage has led in the intrusion into the fresh aquifers of saline (brackish) groundwater in a few places, thereby making it unusable. In 1970th per capital available water was less than 1700 cubic meters (000). This situation becomes critical in 2000th as per capita available were less than 1000 cubic (Coventry et al. 2001). Common techniques are often conducted to determine the groundwater resources are geophysical and hydro-geological investigations. Geophysical investigations, while often overflowing with uncertainty and perception complexities, offer a fast and cost-effective way of collecting dispersed information on subsurface hydrogeology. Latest techniques geophysical, has significantly increased over the few years

back in both mapping groundwater resources and water quality measurements that is because of the innovation in numerical simulation solutions. Thanks to significant developments in electronic technologies. (Metwaly et al., 2010) (Mpofu et al., 2010). Co-efficient electrical resistance is often used in environmental studies because parameters such as fluidity, matrix consistency, porosity, permeability, temperature, refractive index, granule scale, cementation degree, rock and weather are measured for electrical resistance of earth materials. As we discussed before that many techniques were available in accessing groundwater, but resistivity method is a common approach as it ease of operation, low cost compare to other method and its reliability. This technique is very efficient in those areas also with high resistance, such as between the bedrock and weathered overburden. Groundwater vulnerability might be characterized as a deterioration of natural groundwater quality that is artificially induced. Pollution is primarily caused by the disposal of waste water after the use of water for a wide range of purposes. Wide ranges of sources and causes can adjust groundwater quality, going from septic tanks to irrigated farming separated from domestic and industrial waste. VES method were used to see the behaviour of groundwater vulnerable area in this study.

### Objective of Study:

- The following objectives of the study were;
- To determine the aquifer protective capacity of area.
- Assessment of groundwater vulnerability of aquifer using geo-electrical method.
- To determine potential of groundwater.

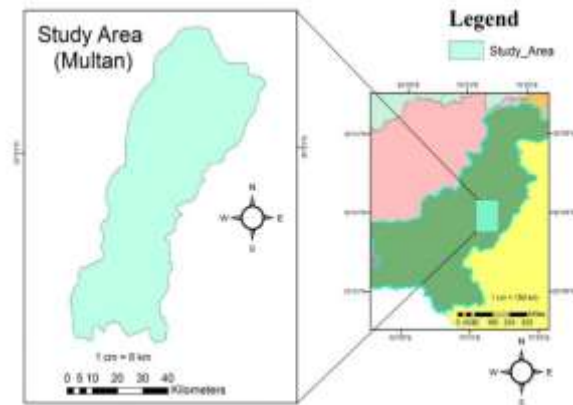
### Material and Methodology:

#### Study Area and Geographical Location:

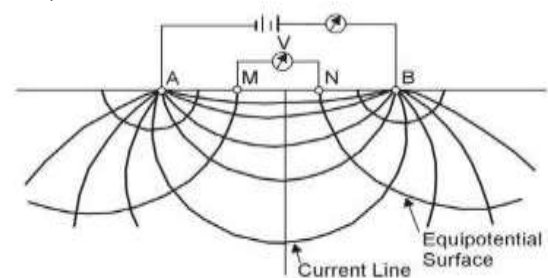
This research was carried out in district Multan Punjab Province, Pakistan. Its area is plane and is located between latitude 30.19 and longitude 71.47. The Multan District is bordered by Khanewal, Vehari and Lodhran. River Chenab is the main source of surface and groundwater recharge. Bahawalpur and Rahim Yar Khan is the Major city which closet to Multan.

### Electrical Resistivity Method:

VES is easiest and most broadly used. This techniques used for unravelling subsurface structure groundwater investigation, deciding depth to bedrock, aquifer system and reasonable site for landfill etc. Electrical Resistivity is directed as either soundings or profiles.

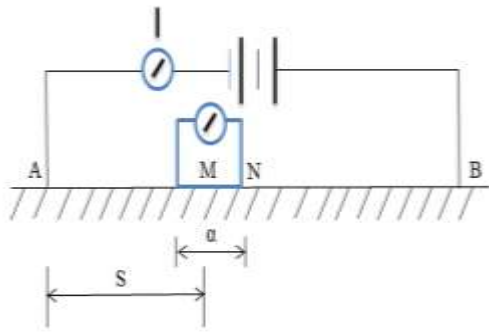


A sounding is a technique that is used to determine depth by changing resistivity. It's consisting of four electrodes, two of them are current electrodes and two of them are potential electrodes. The current electrodes are placed in outer side of and potential electrodes at inner sides. The current electrodes inject the current into the ground and their resultant potential (V) is measured. As the current electrodes distance increases, the deeper the investigation. (Han & goleman, daniel; boyatzis, Richard; Mckee, 2019)



### Electrode Configuration Methods:

There are many electrode configuration are used for various purpose mainly depend on the objective. Wenner, dipole-dipole, Lee-partitioning, pole-dipole, buried bipole-pole, Mise-aal-masse. Wenner array and the Schlumberger array are the two main array configurations.



Schlumberger Configuration was used in this study. 4 electrodes are placed in one line. Outer electrode spacing is kept more usually five times than the inner electrodes. Current electrodes are relocated with each measurement, holding the potential electrodes at the same positions. Positioning of potential electrode is changed when the signal becomes too weak to measure.

#### Computation of Dar Zarrouk Parameters:

Fresh water aquifers are invaded by salt water. It's necessary to explore and separation of fresh water aquifers from saline water aquifers. Parameters of Dar-Zarrouk were computed namely transverse unit resistance (TR), longitudinal unit conductance (LC). Dar-Zarrouk were computed to assess the aquifer protective capacity and their critical application in the resolving of fresh and saline water aquifers. Longitudinal Conductance LC (mho) is expressed as  $LC_i = h_i / AR_i$  and TR is represented as  $TR_i = AR(h_i)$ . (Farid et al., 2017)

**Table 1** Aquifer Protective Capacity Rating (Alile et al., 2008)

Serial No.	Longitudinal Conductance ( $\Omega^{-1}$ )	Protective Capacity Rating
1	>10	Excellence
2	5–10	Very good
3	0.7–4.9	Good
4	0.2–0.69	Moderate
5	0.1–0.19	Weak
6	0.1	Poor

#### Assessment of Groundwater Vulnerability:

The most commonly techniques are being used in assessing aquifer vulnerability spontaneous Potential methods and ground penetrating radar. Assessing the vulnerability of aquifer using electrical resistivity is a well promising technique. It relatively easy, offers relatively

rapid areal coverage and penetration depth are low. Groundwater contamination is vigorous process. But the hydrological cycle may result in pollutants being transported in various directions through the soil, groundwater aquifer and/or surface water streams. The groundwater quality based on the AR values. Higher values indicate good water quality. The longitudinal conductance and thickness values obtained showed how much it's protected against contamination.

#### Data Collection:

A total of 68 surveys data were collected from district Multan. Electrical resistivity method was used, which introduced current into ground to get resistance. The Schlumberger configuration was implemented to determine AR data. AR of mean, minimum and maximum values of 68 locations are given in Table in next slide. The Dar Zarrouk parameter were used to get values of TR and LC. The Arc GIS 10.5 was used to prepare maps of these parameters.

#### 1D Software Interpretation:

The understanding of the gathered data was interpreted by helped iterative interpretation using 1-D inversion technique software. The software can sum up the resistivity information in the form of subsurface layer by mean of apparent resistivity measured by vertical electrical sounding. This model has ability to generalize the resistivity data by fitting observed field data information with least root mean error (RMSE) between the measured data and anticipated resistivity data.

#### Preparation of Spatial Distribution Maps:

Spatial distribution maps was prepared using Arc GIS. A total of 68 survey were conducted and their locations were obtained (latitude & Longitude) using a GPS receiver. For the first, second, third, and fourth layers, spatial distribution maps were prepared. The spatial analyst tool has been used to obtain the spatial distribution of Parameters of the aquifer, such as aquifer AR, layer thickness, LC, and TR in the study area. Ordinary Kriging technique was used from Arc Gis for preparation of maps. It assists with gaps between known points of information. This surface would then be able to be utilized even in territories without information to estimate risk. Kriging is a best technique for



spatial interpolation that assessments values at unknown points dependent on values at known points. (Sholichin & Prayogo, 2019) (Polidori, 2020).

## Result and Discussion

### Interpreted Data of Geoelectric Parameters Using 1X1D Software

The gathered data was interpreted by helped iterative interpretation using 1-D inversion technique software. The software can sum up the resistivity information in the form of subsurface layer. A brief report of all data interpretation of the resistivity survey at different sites in the district, Multan was summarised in the table. The interpreted 1X1D (Interpex, USA) model's geoelectrical parameter are shown in table. We saw that layer thickness expanded from Layer 1 to Layer 4, showing the more noteworthy homogeneity of aquifer material as it moved downward. LC and TR values also increased from layer 1 to layer 4.

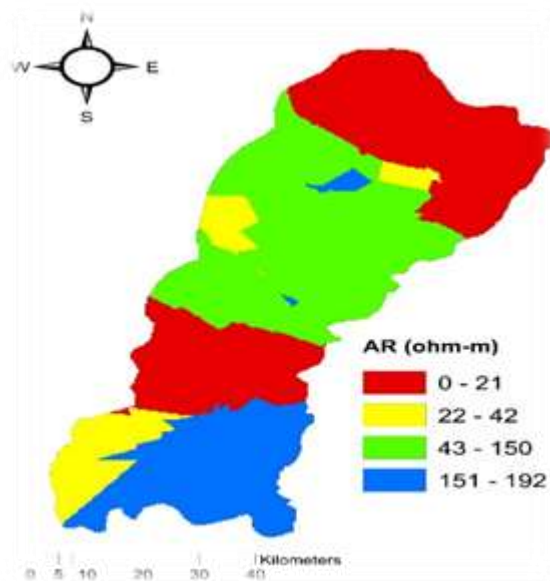
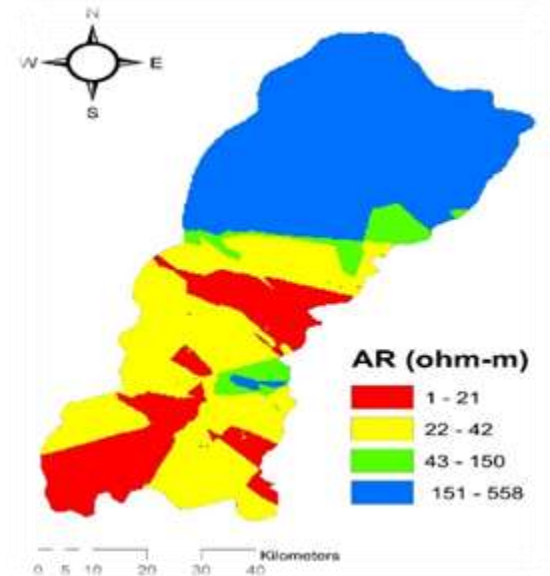
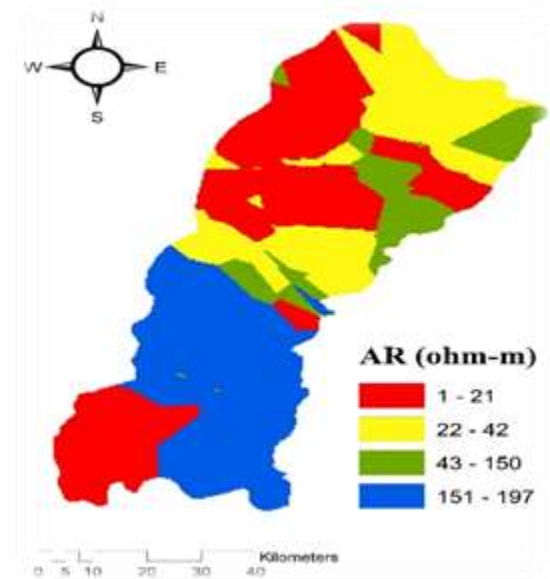
### Assessment of Groundwater Vulnerability on the basis of Groundwater quality mean of Apparent Resistivity

#### Spatial Distribution Maps of Apparent Resistivity

Spatial distribution maps of for four layers were prepared. These maps of groundwater quality prepared on the base of interpreted data (AR values). AR values were characterized on the basis of quality which indicated condition of groundwater quality.

Apparent Resistivity (ohm- m)	Condition of Quality
<21	Not Suitable for irrigation
21-42	Marginally Suitable
>42	Good Quality
>156	Very Good Quality

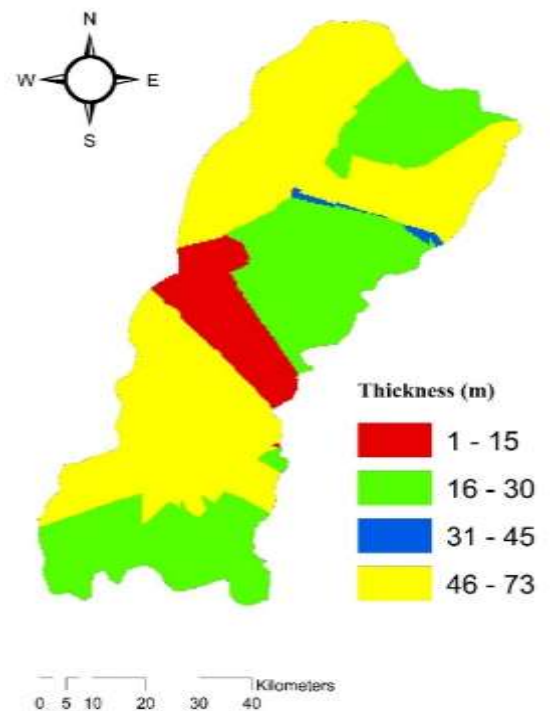
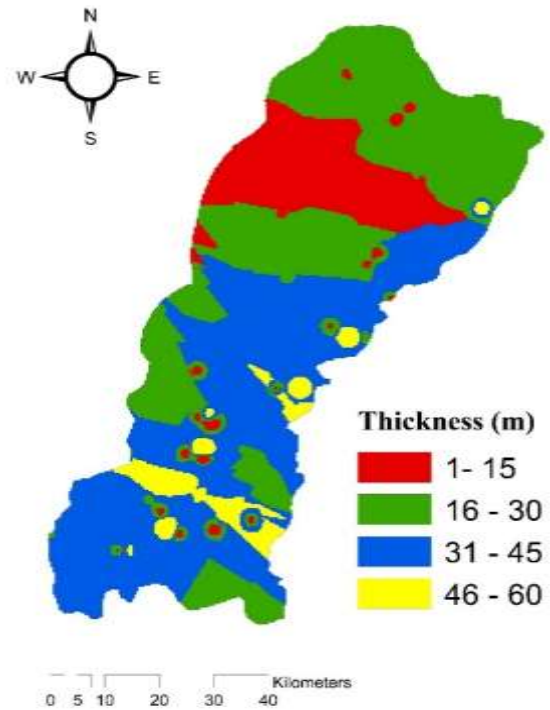
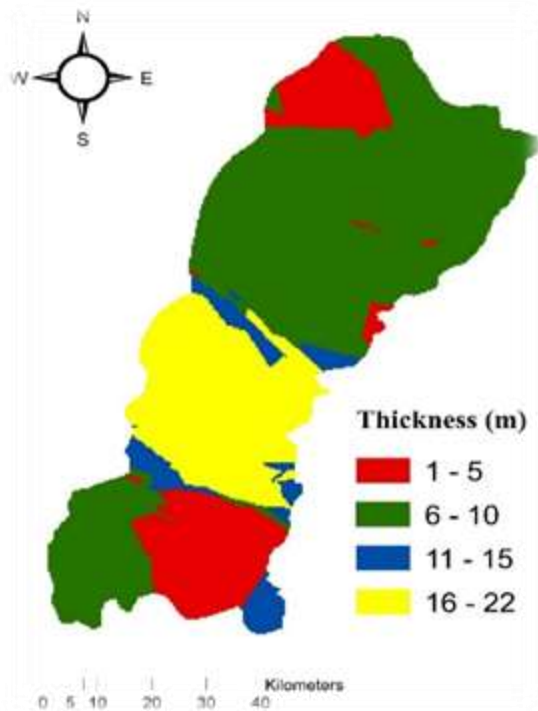
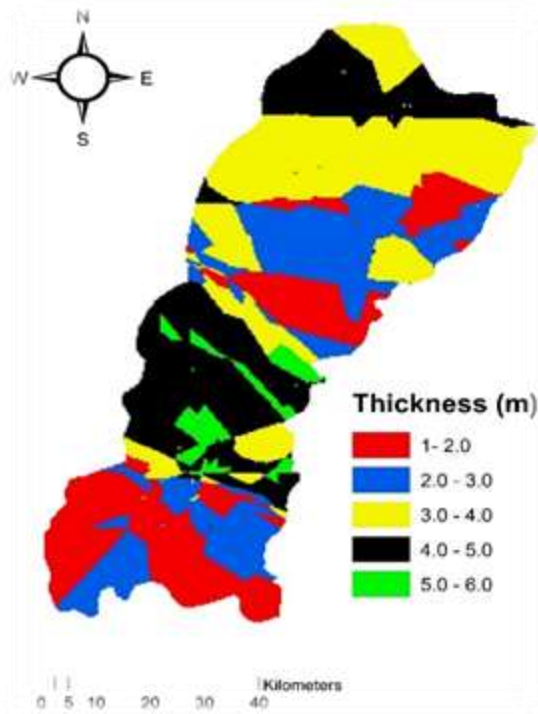
(Of et al., 2003; Lashkaripour et al., 2005; Farid et al. 2017)





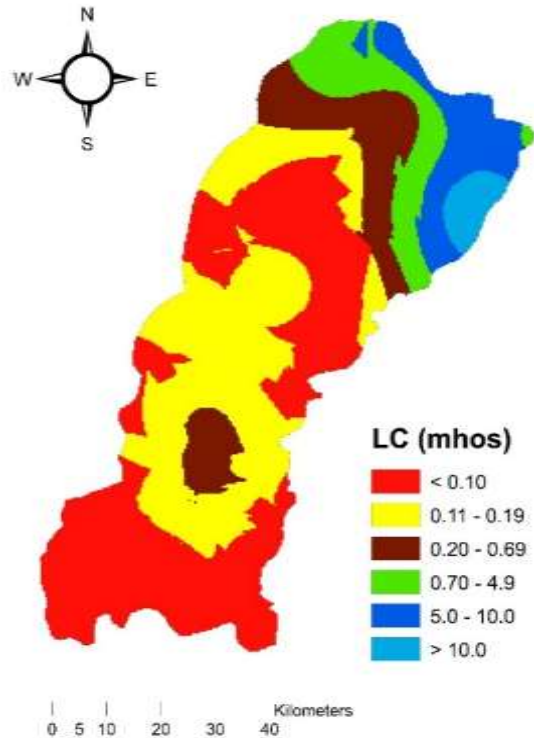
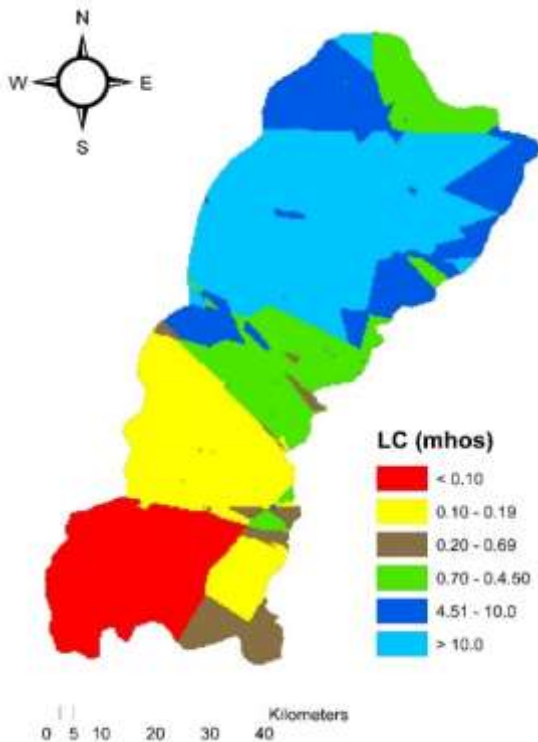
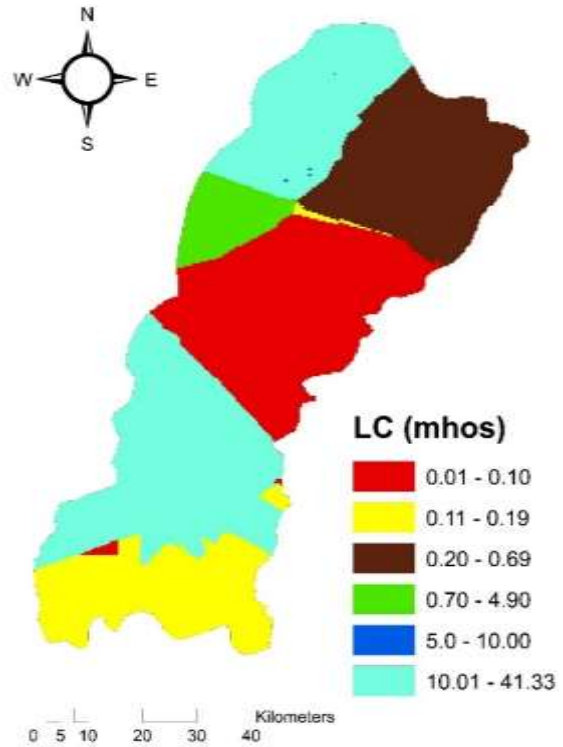
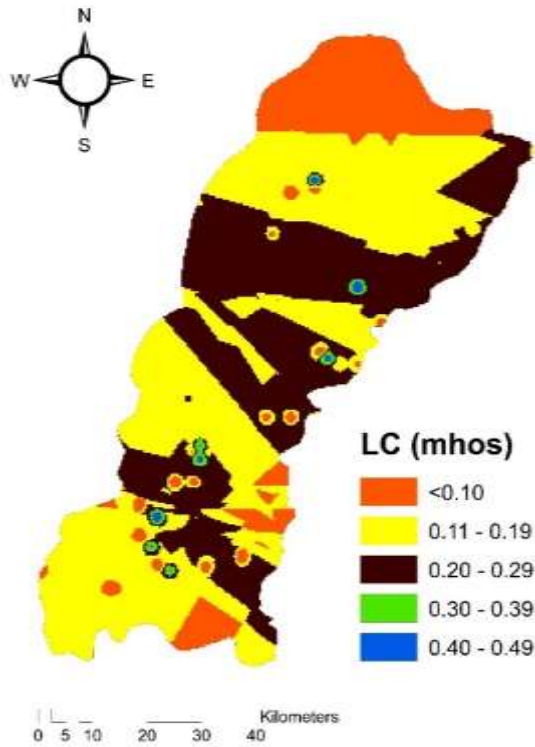
The quality of underground water was quite variable with regard to irrigation purpose. Layer 3 north-west and north-east in upper part and Layer 4 in the east-west side in center and east to south side of the study area showing good quality of water can be pumped.

**Spatial Distribution Maps of Layer Thickness:**



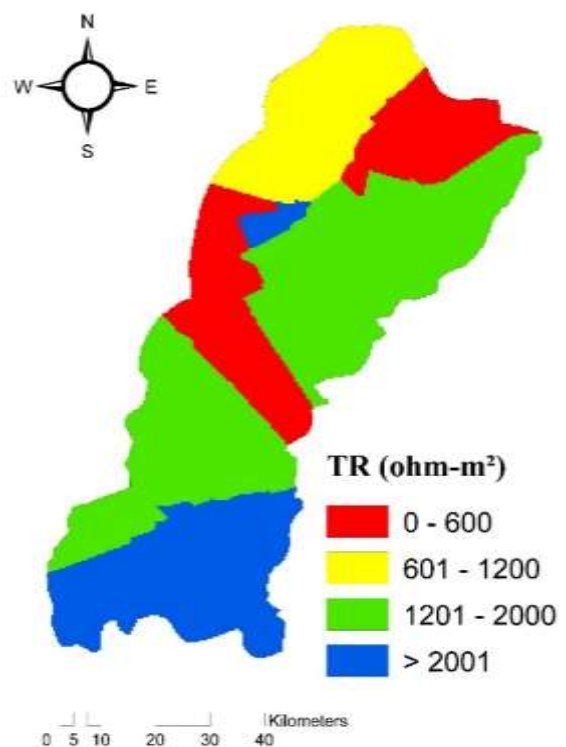
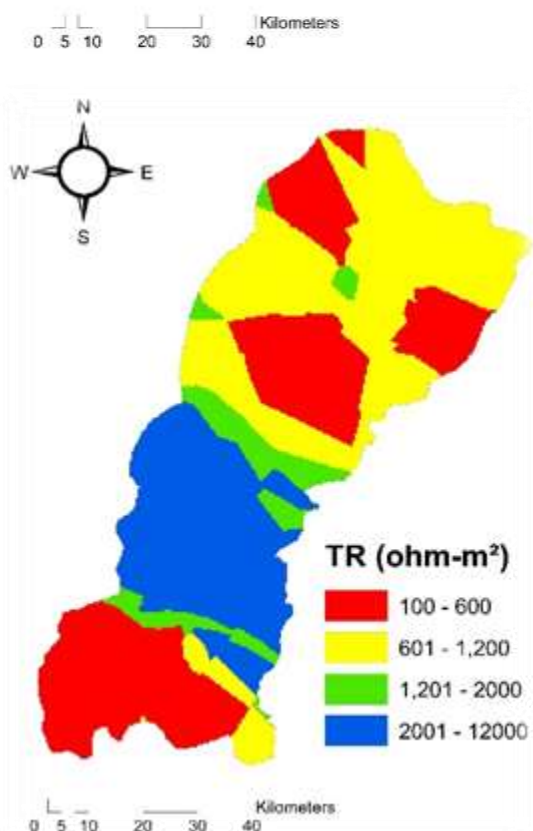
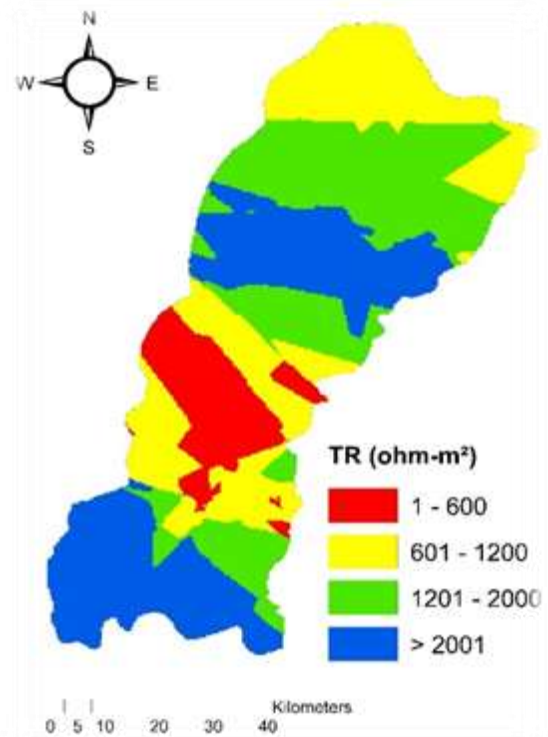
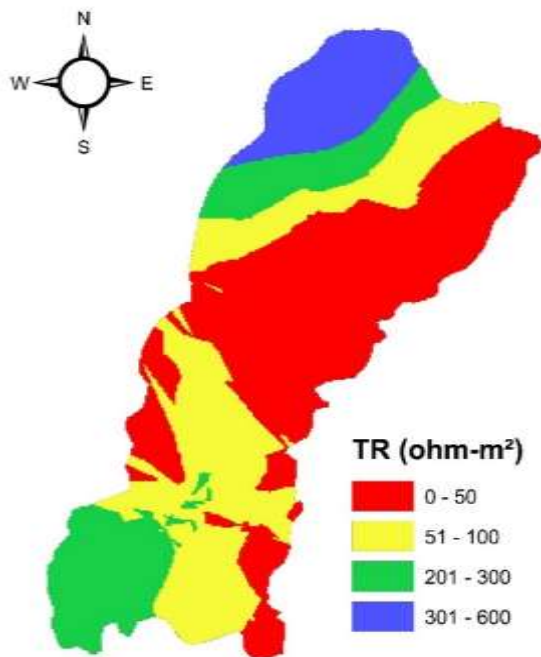
Good layer thickness were present in the 2<sup>nd</sup> layer between 16-22 m, 3<sup>rd</sup> layer with major portion between in range 16-45 m and fourth layer other than center part east to west in range between 16 to 73 m. The effluents discharged into fresh water and in open drains caused contamination of groundwater into the shallow aquifer.

### Spatial Distribution Maps of Longitudinal Conductance



These maps showing protective capacity of layers. Top layer is more important as it allows seepage through it. The protective of top layer is poor and weaker as its values lower than the 0.19, 2<sup>nd</sup> layer has 60% poor and 3<sup>rd</sup> layer has 54% poor protective capacity thus allowed contaminate to infiltrate through it.

## Spatial Distribution Maps of Transverse Resistance



Transverse resistance values indicated the potential of aquifer zone as well as salinity behaviour of whole study area. In layer 3<sup>rd</sup> the lower boundary and the portion above the center part was observed in the transverse resistance values greater than 2001 ohm-m<sup>2</sup>. Above the center part, the transverse resistance values in the range of 1200-2000 which have mixed up saline

and fresh water layers. The TR map for layer 4 showed that study area of higher yield in east to south and west direct in lower part as its value greater than the 2001 ohm-m<sup>2</sup>. The result revealed that higher transverse resistance value which indicated the higher yield potential was observed in different layers of the study area.

### Conclusions

- The results revealed that VES method and spatial distribution maps are effective tools.
- These provide information about the aquifer vulnerability, protective capacity, and groundwater potential for exploitation of groundwater in better quality and quantity.
- The average layer thicknesses of 2.51, 5.71, 24.73, and 22.44 m were recorded for Layers 1-4, respectively.
- The higher average layer thickness for Layer 3 (24.73 m) also indicated that the area of thick subsurface formation was expected to have higher groundwater potential aquifer as it has higher TR values.
- About 42% of the study area has poor protective capacity, 21% weak protective capacity and 33% moderate protective capacity.
- This indicates that the top-most geoelectric layers in the area are mostly pervious geologic materials through which surface and near-surface contaminants can infiltrate.

### Recommendations

- Groundwater monitoring for its sustainable development.
- Promote Skimming Well Technology
- Public awareness about the dwindling status of groundwater.
- Well spacing is also helped in to arrest the groundwater draw downs and keep it at a minimum level.
- To make small ponds or water reservoir either in or near River for water storage during flooding.
- To develop an early warning system for forecast groundwater quality and quantity trends.

### Reference:

Water, J. (2011). The application of groundwater modelling to simulate the behaviour of

groundwater resources in the Ramhormooz Aquifer, Iran Masoud Saatsaz \*

- Jia, X., O'Connor, D., Hou, D., Jin, Y., Li, G., Zheng, C., Ok, Y. S., Tsang, D. C. W., & Luo, J. (2019). Groundwater depletion and contamination: Spatial distribution of groundwater resources sustainability in China. *Science of the Total Environment*, 672, 551–562. <https://doi.org/10.1016/j.scitotenv.2019.03.457>
- Kurunthachalam, S. K. (2014). Water Conservation and Sustainability: An Utmost Importance. *Journal of Waste Water Treatment & Analysis*, 05(02), 1–4.
- Memon, A., Ansari, K., Soomro, A. G., Jamali, M. A., Naeem, B., & Ashraf, A. (2020). Estimation of groundwater potential using GIS modeling in Kohistan region Jamshoro district, Southern Indus basin, Sindh, Pakistan (a case study). *Acta Geophysica*, 68(1), 155–165. <https://doi.org/10.1007/s11600-019-00382-3>
- Watto, M. A., & Muger, A. W. (2016). Groundwater depletion in the Indus Plains of Pakistan: imperatives, repercussions and management issues. *International Journal of River Basin Management*, 14(4), 447–458. <https://doi.org/10.1080/15715124.2016.1204154>
- Coventry, D. (2001). World Resources 2000–2001: People and Ecosystems: The Fraying Web of Life. *Agriculture, Ecosystems & Environment*, 86(1), 109–110. [https://doi.org/10.1016/s0167-8809\(01\)00142-6](https://doi.org/10.1016/s0167-8809(01)00142-6)
- Metwaly, M., El-qady, G., & Massoud, U. (2010). Integrated geoelectrical survey for groundwater and shallow subsurface Integrated geoelectrical survey for groundwater and shallow subsurface evaluation: case study at Siliyin spring. August 2015. <https://doi.org/10.1007/s00531-009-0458-9>
- Mpofu, V., Manatsa, D., & Muchuveni, E. (2010). Mapping groundwater aquifers using dowsing, slingram electromagnetic survey method and vertical electrical sounding jointly in the granite rock formation: a case of Matshetshe rura ... January 2014.
- Han, E. S., & Goleman, Daniel; Boyatzis, Richard; Mckee, A. (2019). 濟無No Title No Title. *Journal of Chemical Information and Modeling*, 53(9), 1689–1699.

- Alile, O. M., Amadasun, C. V. O., & Evbuomwan, A. I. (2008). Application of vertical electrical sounding method to decipher the existing subsurface stratification and groundwater occurrence status in a location in edo North of Nigeria. *International Journal of Physical Sciences*, 3(10), 245–249
- Farid, H. U., Mahmood-Khan, Z., Ali, A., Mubeen, M., & Anjum, M. N. (2017). Site-specific aquifer characterization and identification of potential groundwater areas in Pakistan. *Polish Journal of Environmental Studies*, 26(1), 17–27. <https://doi.org/10.15244/pjoes/64645>.
- Polidori, L. (2020). *Methods : A Critical Review*.
- Sholichin, M., & Prayogo, T. B. (2019). FIELD Identification Of Groundwater Potential Zone By Ves Method In South Malang , Indonesia. 10(02), 999–1009.
- Lashkaripour, G. R., Ghafoori, M., & Dehghani, A. (2005). Electrical resistivity survey for predicting Samsor aquifer properties , southeast Iran. 7.



## Evaluation of Low Impact Development (Lids) Drainage Control Measures Using Pcswm in an Urban Watershed

Qaiser Abbas<sup>1\*</sup>, Muhammad Azhar Inam<sup>1</sup>, Rabeea Noor<sup>1</sup>, Muhammad Asif<sup>1</sup>

<sup>1</sup> Department of Agricultural Engineering, Bahauddin Zakariya University Multan, Pakistan

Corresponding author email: [qaiser8201@gmail.com](mailto:qaiser8201@gmail.com)

**Abstract:** Personal computer storm-water management model (PCSWMM) was applied to analyze the use of the low impact development (LID) for urban storm water management. Increase of urbanization in Multan City has led to increase the generation of storm water runoff. Increase of storm water runoff in the city is changing Multan into a flood prone area during monsoon season. In Wahdat colony (Multan) storm of mild intensity generate significant runoff during monsoon season due to which storm water stagnant over the land surface. This study involves the control of urban storm water and evaluation of different types of LIDs. This project employed geographic information system (GIS) to make a shapefile of the catchment area, rainfall analysis to establish storm water scenario, DEM to determine terrain attributes such as elevation and slope of terrain. Finally, PCSWMM was simulated for 24hr rainfall event and the data was recorded at each 15mint interval. Maximum and minimum water depths were observed as 1m and 0.25 m respectively. The modeling results successfully replicate the observed field data. The modeling results helps in identifying the appropriate LIDs as per site conditions. We concluded that the existing drainage system is insufficient to cater the flow of Multan region and there is a need of management practices.

**Keywords:** Personal computer storm water management model; Low impact development; Geographic information system

### Introduction:

As urbanization increases, it has badly affected the drainage system and related issues arises, such as human health problems, infrastructural issues, etc. In urbanize areas of Pakistan, drainage condition is very poor. As a result, gutters over-spill as flooded roads cause agony among the people of that area and they had to pass through dirty water. The major cause of floods in Pakistan is high intensity rainfall in the river catchments, which sometimes supplemented by snowmelt flows, generally result into floods in rivers during the monsoon season. During the last seventy one years in Pakistan more than 12,000 people lost their lives, almost 20 million people were affected by it while direct flood damages in Pakistan occur to infrastructure, agricultural crops, damage to urban and rural property and public utilities (Aslam, 2018).

Multan is the 7<sup>th</sup> largest metropolitan city of Pakistan and it faces storm water drainage problems in the monsoon season. In addition, People put their solid waste in the sewerage system, which may cause sewerage system blockage. In Multan city water and sanitation agency (WASA) controls storm water runoff by

using heavy duty dewatering pumps and desilting of sewerage lines (Soncini et al., 2014). The study area (Wahdat colony) is urbanized and densely populated. Hence, the existing drainage structure/drainage facilities cannot be retrofitted. The specific objectives of this study are: (1) to identify critical locations of study area to apply LIDs. (2) to identify different LIDs according to site conditions. (3) to evaluate LID technology with reference to urban storm water management. (4) Create social awareness in flood hazard areas.

Stormwater Management Model (SWMM) is a dynamic rainfall-runoff model capable of continuous simulation of runoff quantity and quality and PCSWMM is distinctly useful in representing flow (Zhang et al., 2010) (Zhang et al., 2013). PCSWMM software was used to analyze the condition of our study area in the rainy season, by using the available data, so that we can predict the best management practices (BMP) for the critical locations in the study area to overcome the drainage problems. LID is the method that uses a system of practices allocated across a development site which is designed to control stormwater runoff and terminating the need for substantial storm sewer systems. Studies have demonstrated the effectiveness of LID



techniques and its controlment of runoff from small and moderate rainfall events, and for limiting pollution exportation from residential developments (Dietz & Clausen, 2008)(Zhang et al., 2013). Main Goals of LID practices includes runoff reduction, infiltration increase, groundwater recharge, and water quality improvement through pollutant control processes. (Line et al., 2012). LIDs such as rain garden, infiltration trenches, rain barrels, porous pavements and vegetative covers can be simulated through PCSWMM. These LIDs were evaluated for the study area. Rain barrels can be installed at the buildings downspout of wahdat colony catchment to reduce the peak runoff(Center, 2014). Rain gardens can be made where water stands in the pervious ponding areas and these are depressed areas in the landscape designed to store water which later can be used for gardening or other purposes (Peterson, 2008)(Water, n.d.). Infiltration trenches are shallow (1 to 4m) excavations that are lined with filter fabric and filled with stones to create underground reservoirs for storm water(Quality, 2001). The runoff gradually percolates through bottom and sides of the trench into the surrounding subsoil over a period of days and rain barrels can be installed at buildings downspout. LID practices have been successfully utilized in urban areas for encouraging environmental sensitive planning and design, and effective management of water resources (Shafique & Kim, 2015)(Marchildon & Kassenaar, 2013).

### Methodology:

This Project is related to drainage problems caused by the intense rainfall and municipal discharge in wahdat colony catchment. Main causes of water accumulation on the site are clogging and lack of maintenance of sewerage lines, Improper slope of surface, flow of solid waste material in sewerage lines, less discharge capacity of sewerage line and deposits of sediments in the drains. Water accumulation causes problems to buildings and roads, Human health problems and difficulty in moving from pounding sites. To overcome these problems, PCSWMM Software is used to control storm water runoff by applying Low Impact Development (LIDs) in that area. The area of Wahdat colony is selected from the preliminary survey and some critical locations are identified where we can apply LID technologies. The study

area is situated in Multan, Punjab, Pakistan as shown in Fig. 1. The study area lies between 30°12'20" North and 71°29'50" East. The land in our study area is used for residence, commercial, educational and religious purposes. As it includes schools, mosques, houses and playing grounds. It covers 40.2ha (99.3acres) of area. Most of the area is affected by the storm water pounding and the pounding depth ranges between 0.25-1m. Current drainage capacity of sewerage lines is 0.44cumec.



**Fig. 15** Layout of study area

Rainfall data is collected from MNSUAM (Muhammad Nawaz Shareef University of Agriculture Multan), design discharge and existing drainage design from WASA (Water and Sanitation Agency), DEM of 30\*30m resolution is downloaded from Google. ArcGIS is employed to prepare the shapefile of Wahdat colony catchment. Rainfall data of 15minute interval is collected from MNSUAM (Muhammad Nawaz Shareef University of Agriculture Multan) for an event of 26.2 mm occurred on 23<sup>rd</sup> June, 2019. This event is selected on the basis of data availability for the study purpose only.

Unfortunately, no flow records are available for the study area. Hence, the design discharge of the sewerage lines as reported by WASA is used for analysis purpose. In order to account for sewage clogging and maintenance issue 60% of the design discharge is assumed for drainage calculation purpose.



**Fig. 16** Sewerage layout plan

There are three main holes in the area. Sewerage layout plan is shown in Fig: 2. Design discharge is determined as 0.9 cumecs, actual discharge is 0.44 cumecs and water present on the surface is 0.46cumecs. So, the existing drainage system is insufficient to cater the flow and there is a need of management practices. Land use plan of Wahdat colony catchment is prepared on AutoCAD software and converted into shapefile by employing ArcGIS software. We have analyzed that permeable area is 18.75% and impermeable area is 81.25% in the catchment. Permeable area includes playing grounds and free space while impermeable area includes the area for roads, buildings and houses. Shapefile of wahdat colony catchment is shown in **Fig. 3**.

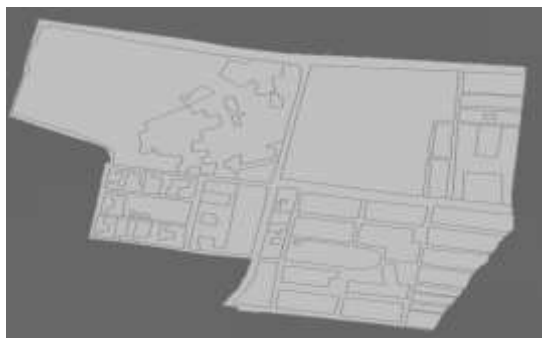


**Fig. 17** Shapefile of Wahdat colony catchment

Comparisons with and without LID controls are made between the peak runoff and total runoff volume for the selected event. It is expected that the LID would reduce both peak runoff and total runoff volume.

### Results and discussion

From the above discussion it is obvious that rainfall generate a significant amount of runoff during monsoon season and convert the wahdat colony (study area) into flood prone area due to clogging of sewerage lines and improper drainage system. The people of wahdat colony faced human health problems as well as damage to buildings and roads. DEM is used to highlight the places in depression, water accumulates in lower elevation areas in rainy season. Moreover, water came from the surroundings and accumulate to a depth of 0.25 to 1 m in lower elevation area. The area has maximum and minimum elevation of 125.30m and 121.64m respectively from MSL. The elevation difference is 3.66m. Design discharge is 0.9cumecs, actual discharge is 0.44cumecs and water present on the surface is 0.46cumecs. So, the existing drainage system is insufficient to cater the flow of this

particular region and there is a need of management practices, keeping in view the urbanization nature of the city, we have proposed LIDs. PCSWMM is used to predict and improve the storm water management using LIDs according to the site condition. We have shown some proposed locations where we can apply rain barrels, rain gardens and infiltration trenches in **Fig. 4**.

Rain barrels are proposed to install at the building's downspout of wahdat colony catchment to reduce the peak runoff. Rain barrels are proposed to install at 3 buildings. Areas of buildings are  $30*8m^2$ ,  $25*10m^2$  and  $20*10$  respectively. Volume of water obtained from roof top is 6288liter (1662 gallons), 6550liter (1730 gallons) and 5240liter (1384 gallons) respectively. Size of rain barrel is calculated by considering area of buildings and rainfall occurred on the selected event ( $26.2mm = 0.0262m$ ). Four rain barrels of capacity 420 gallons are proposed to install at each of building1 and building2. Three rain barrels of capacity 460 gallons are proposed to install at building 3. Two rain gardens are proposed in the porous ponding areas. Size of rain gardens is calculated by determining the runoff of most intensive rainfall from the historical record. Areas of rain garden sites is optimized as  $(100*30 m^2)$   $3000m^2$  each. For this estimation approximately two rain gardens around  $8.5*6*1.5$  cubic meter(length\*width\*depth) are required. Infiltration trenches are proposed to be made along the roadside areas to remove the water present on the roads. Ten infiltration trenches are proposed to capture 4500 cubic meter water. Size of infiltration trenches is determine as 550cubic meter. The conveyance systems can handle design storms of 25-years. From the above calculations almost all the water present on the site is removed by the proposed LIDs. The absence of flow data and calibration may introduce significant uncertainties to the model. However, it has been showed that the PCSWMM model can produce relatively accurate results even when there is a lack of data to calibrate the model.

### Conclusion:

PCSWMM is used to predict and improve the storm water management using LIDs in the Wahdat colony catchment of area 40.2 ha. It is observed that drainage capacity of sewerage lines



**Fig. 18** Critical location for LIDs

is not sufficient to drain out the water generated by the intense rainfall event and water stands on the surface due to clogging problems of drainage lines. Damage to infrastructure and severe human health problems are arises due to the stagnant water. Therefore, LID practices are proposed to control the storm water damages to the urban infrastructure. PCSWMM is simulated for 24hr rainfall event and the data was recorded at each 15mint interval, maximum and minimum water depths are observed as 1m and 0.25m respectively. Water drainage capacity is  $0.44\text{m}^3/\text{s}$  and water present at the surface is  $0.46\text{m}^3/\text{s}$ . The modeling results replicate the field data analysis. After simulation, PCSWMM have shown the pounding sites in the catchment area and the maximum depth of the pounding is 1m. BMPs are proposed for the pounding sites to drain out accumulated water. Rain gardens, rain barrels and infiltration trenches are evaluated in the critical locations. Eleven rain barrels, 2 rain gardens and ten infiltration trenches are proposed to capture the surplus water. By applying these LID practices, peak runoff is reduced significantly, and drainage problems are resolved.

#### **Acknowledgement:**

Research and data support from WASA and MNSUA are acknowledge for this research.

#### **Reference:**

Aslam, M. (2018). Flood Management Current State, Challenges and Prospects in Pakistan: A Review. *Mehran University Research Journal of Engineering and Technology*, 37(2), 297–314. <https://doi.org/10.22581/muet1982.1802.06>  
 Center, T. E. (2014). How to build a Rain Gauge. 1.

Dietz, M., & Clausen, J. (2008). Stormwater Runoff and Export Changes With Development in a Traditional and Low Impact Subdivision. *Journal of Environmental Management*, 87, 560–566. <https://doi.org/10.1016/j.jenvman.2007.03.026>  
 Line, D. E., Brown, R. A., Hunt, W. F., & Lord, W. G. (2012). Effectiveness of LID for commercial development in North Carolina. *Journal of Environmental Engineering (United States)*, 138(6), 680–688. [https://doi.org/10.1061/\(ASCE\)EE.1943-7870.0000515](https://doi.org/10.1061/(ASCE)EE.1943-7870.0000515)  
 Marchildon, M., & Kassenaar, D. (2013). Analyzing Low Impact Development Strategies Using Continuous Fully Distributed Coupled Groundwater and Surface Water Models. *Journal of Water Management Modeling*, 6062, 319–336. <https://doi.org/10.14796/jwmm.r246-17>  
 Peterson, W. (editor). (2008). *Rain Gardens: Iowa Rain Garden Design and Installation Manual*. 1–28.  
 Quality, W. (2001). *Infiltration Systems Infiltration Trenches Infiltration Systems Infiltration Trenches*. 169–180.  
 Shafique, M., & Kim, R. (2015). Low impact development practices: A review of current research and recommendations for future directions. *Ecological Chemistry and Engineering S*, 22(4), 543–563. <https://doi.org/10.1515/eces-2015-0032>  
 Soncini, A., Bocchiola, D., Rosso, R., Meucci, S., Pala, F., & Valé, G. (2014). Water and Sanitation in Multan, Pakistan. In *Research for Development* (pp. 149–162). [https://doi.org/10.1007/978-3-319-02117-1\\_12](https://doi.org/10.1007/978-3-319-02117-1_12)  
 Water, S. (n.d.). Frequently Asked Questions about Rain Gardens. 1–12. [www.clearchoicescleanwater.org](http://www.clearchoicescleanwater.org)  
 Zhang, G., Hamlett, J. M., Reed, P., & Tang, Y. (2013). Multi-Objective Optimization of Low Impact Development Designs in an Urbanizing Watershed. 2013(December), 95–108.  
 Zhang, G., Hamlett, J. M., & Saravanapavan, T. (2010). Representation of Low Impact Development Scenarios in SWMM. *Journal of Water Management Modeling*, 6062(Lid), 183–198. <https://doi.org/10.14796/jwmm.r236-12>

# Management of Surface Water Resources to Mitigate the Water Stress in Karachi

Muhammad Tayyab<sup>1\*</sup>

<sup>1</sup> Senior Engineer, National Engineering Services Pakistan (NESPAK), Lahore, Pakistan

Corresponding author email: [tayyab222@outlook.com](mailto:tayyab222@outlook.com)

**Abstract:** Karachi is the largest, most populous city and economic backbone of Pakistan but, unfortunately, is presently facing the worst water crisis of the history. Pakistan has the natural endowment of extensive water resources but harnessing of these assets requires a paradigm shift in water policy and management [1]. The situation in Karachi is the small-scale replica of what is expected to be a national scenario if imminent efficient water management strategies are not adopted. History of water crisis in Karachi is spanned over a period of three decades and the situation seems to be getting worse with each passing day with no immediate solution in sight. This study assesses the potential available in surface water resources (especially Indus River) to meet the additional water demand of 650 MGD (260+390) [2] by Karachi Water & Sewerage Board (KW&SB). Indus river is the largest source of fresh water for Karachi and the water availability in the river varies seasonally; the entire system comes under pressure during dry season whereas, plentiful flows are available during the wet season. Hence, Indus river flows at Kotri barrage have been analysed for their magnitude and temporal availability as to support the system in meeting the requisite demand. The additional flows available at Kotri downstream have been proposed to be diverted to Kalri Baghar Feeder Upper (KBFU) system and store in Keenjhar lake for further transmission to Karachi. Synthetic augmented inflow series have been devised and scenario-based integrated reservoir operations of the three lakes (Keenjhar, Haleji & Hadero) have been carried out to assess the system potential. Due consideration has been given to the environmental flow requirements of lower riparian and that of irrigation flows requirements of KBF system. Further, potential water management approaches have been proposed and an action plan has also been devised to meet the requisite water demands.

**Keywords:** Water Crisis, Surface Water Resources, Indus River, KW&SB, Kotri Barrage, KBFU Canal, Synthetic Inflows, Keenjhar Lake, Reservoir Operations, Water Management, Environmental Flow.

## Rationale

Water security is one of the biggest challenges in Pakistan for its sustained development. Providing adequate water for human consumption, agriculture and industry is very exigent task for the authorities on the face of ever-increasing water-stress, rapidly dwindling water reserves and a sleeping giant of climate change. Food and water security are the biggest threat to Pakistan's economy. The issue of food and water security in Pakistan is quite tricky as poorly managed water resources and inefficient irrigation practices bear more than 60% losses and that too with one of the least crop yields per unit of water in the world [3]. Hence, all the pressure happens to be shifting on already stressed water resources due to which domestic water availability has been largely suffered.

Karachi is the largest, most populous city and economic backbone of Pakistan serving as a financial (15% contribution to GDP), trading and industrial hub (housing 60% of the industries). Notwithstanding, the city is suffering the worst

water crisis of the history. Foregoing above, the water availability situation in Karachi is expected to be getting worse if no immediate steps are taken. It is very well established that there are certain issues on management side in addition to the meagreness of available water resources yet, this paper highlights the water availability potential in Indus river to mitigate the water stress and proposes the management strategies to address the looming water crisis in Karachi.

## National and Regional Water Profiles

Water availability scenario in Pakistan directly impacts the water available for Karachi as it is situated at tail of the Indus River. Hence, nationwide utilization of water influences the flows being received at Kotri barrage (last structure on the Indus river). Water availability, sectoral utilization, history of water supply schemes development in Karachi and present availability & demand scenarios have been discussed in forthcoming sections.



## National Scenario

Pakistan derives its water resources largely from precipitation and snow/ glaciers melt. Two spells of rainfall are observed i.e. monsoon during summer and, winter rainfalls. The precipitation is distributed quite unevenly both in time and space; almost 60% of the rainfall is received from July-September and magnitudes vary from less than 100 mm in Sindh and Balochistan to a value of more than 1500 mm in the wet mountains. 92% of the geographic area of Pakistan is classified as semi-arid / arid and extreme variability in rainfall patterns has direct impacts on river flows [4] [5] [6]. Indus being one of the longest rivers in the world is considered to be the backbone of Pakistan as almost all the water sources are derived from Indus basin. The annual flows in Indus river varies from 92.65 to 207.70 MAF. Another major source of water is groundwater that has annual potential of around 55 MAF and more than 90% of which is utilized every year. *Figure 1* presents the share of each source and sectoral uses. Irrigation sector is the largest consumer of water in Pakistan [7] [8] [9].

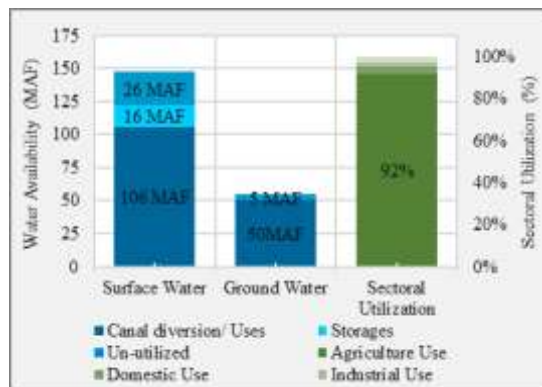


**Figure 44:** Water Availability and Sectoral Utilization in Pakistan (UNDP 2016)

Over the past few decades, Pakistan's water profile has changed drastically from being a water abundant country (5260 cubic meters per year in 1950), to one experiencing water stress (under 1000 cubic meters per capita at present) [10] [11] [12]. Per capita designed live water storage capacity available in Pakistan is 121 m<sup>3</sup> which is only higher than that of Ethiopia. Pakistan has a storage capacity of mere 30 days whereas, Colorado river in USA stands at 900 days [13]. The water stress levels along with the main causative factor i.e. population growth is presented in *Figure 2*. Water stress on surface water sources led to rapid groundwater depletion posing serious threat to its sustainability and

alarmingly, Pakistan is ranked among top ten countries having least access to the clean water. As per findings of the 2006 UN report "there is enough water for everyone and water insufficiency is due to mismanagement, corruption, lack of appropriate institutions, bureaucratic inertia and shortage of investment in both human capacity and physical infrastructure" [14].

Water availability and water security are key issues driving the national security & safety and also have potential in transcending national boundaries as limited water resources results in general destabilization increased trends of migration. Prioritizing water resources in policy matters at domestic and global levels is becoming indispensable.

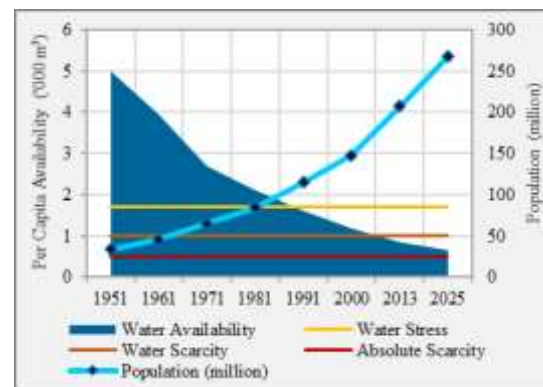


**Figure 45:** Historic Water Availability and Population Trends in Pakistan [15] [16]

## Regional Scenario

Karachi city is located in the south-west of Pakistan and has metropolitan area of about 3,530 km<sup>2</sup>. Mlair and Liyari rivers pass through the city whereas, Indus river flows in south-east side where exists infrastructure for supplying water to Karachi via Keenjhar lake which is fed from Kotri barrage through Kalri Baghaar Feeder Upper (KBFU) canal and associated water transmission system. The climate of the city falls under that of specific to arid regions with high temperature (35 °C to 10 °C) and small magnitude average annual rainfall (around 85 mm).

### Water Sources and Availability at Karachi

Surface and ground water are the two major sources of water supply in Karachi. Indus river (via KBFU canal and Keenjhar lake) is the main source along with contributions from Hub dam whereas, ground water sources (Dumlotte wells) contribute in very small percentage because of its poor quality. Some of the water sources

development works undertaken over the period of last one and a half centuries are [17] [18] [19] [20]:

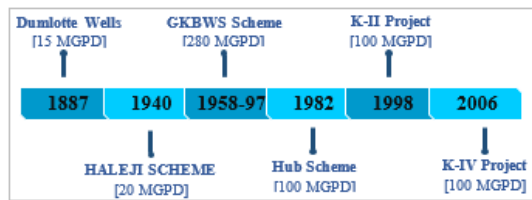


**Figure 46:** Development of Water Supply Schemes for Karachi

Cumulatively from various sources, at present, authorities manage to provide approximately 665 MGD water against the demand of 1200 MGD, resulting in a shortfall of 535 MGD. Moreover, estimates suggest that 35% of the water is lost in transmission hence, available water drops to a mere 433 MGD [21]. Recent projections suggest that Karachi's population will grow by 30% from year 2017-30 (Euromonitor, London) hence, increased pressure on demand side is imminent.

### Water Transmission System from Indus River to Karachi

Water transmission system from Indus to Karachi has been developed since 1940 with the construction of Haleji lake [22]; which was fed from an inundation canal called Baghar canal. Water from Haleji was conveyed to Gharo pumping station via Haleji conduit for onward transmission to Karachi. After completion of

Kotri barrage in 1955 the inundation canal was converted to perennial supply. At the same time, provision was made to supply water to Karachi directly from the barrage by taking water from Keenjhar lake through KG canal. Karachi Development Authority (KDA) canal receives water from the KG canal and supply water to Dhabeji pumping station, for transmission to Karachi. After commissioning of the Kotri barrage system, the use of Haleji lake was not viable, except for use it as an emergency storage. The Line diagram of entire system is presented in *Figure 5*.

### Keenjhar Lake Feature

Keenjhar lake had been formed by embanking the eastern side of two lying marshy areas, "dhands", and the remainder of the perimeter being formed by the foothills of Kirthar Range. As per latest bathymetry by NESPAK, the Lake is 32 km long, has surface area of 132 sq. km and live storage capacity of 0.339 MAF at present Maximum Conservation Level (MCL) of 16.45 m asl (54.00 ft) [23]. The intake level of K-IV is planned at 11 m where an additional live storage capacity of 0.119 MAF shall be achieved [24]. Presently, there are two outlet regulators on the lake; the PQ fall regulator (irrigation supplies to Thatta) and KG canal regulator (water supply to Karachi). The lake also receives runoff from catchment area of about 700 square miles. *Figure 4* presents the layout of the scheme.

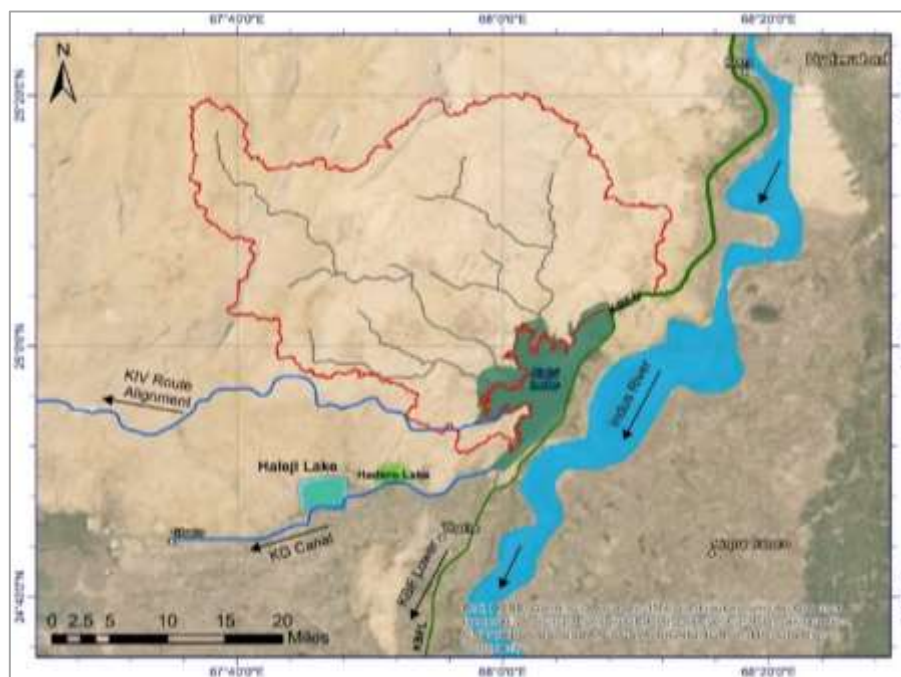


**Figure 47:** Study Area Features and Scheme Layout



## Beyond Urban Water Security The vulnerabilities of Intermittent Water Supply

Water unavailability is considered to be one of the major factors that handicap the business continuity and economic growth as it poses serious threat to sustainable development and human wellbeing. It has been understood that water availability in Indus River is seasonal and there is very little water available during the winter season, that's the time when role of storages come into play. Presently, Keenjhar lake is being relied on for meeting domestic water needs of Karachi. Intermittent water supply is the condition under water stress where water is supplied for a fixed period of time that is more costly, exacerbating inequalities among users, weaker people-govt social contract and contributes to conflict, violence, or migration. Hence, not only water availability but a consistent supply for domestic usage to Karachi city is indispensable.

### Scope of The Paper

The present study has been carried out to: evaluate the potential available at Indus river to meet the escalating water demands of Karachi; to suggest an action plan for meeting additional demands; assess the feasibility of the integration of additional storages into the system; and hydrological modelling in order to ascertain the storage and depletion pattern of the storages.

### Materials and Methods

Since, the entire project area falls under the command of KBFU canal system, flow data of the entire system (**Figure 5**) has been collected from Irrigation Department for the last 20 years. Reported gate openings and water levels have been translated into discharge using hydraulic formulae. The major data collection points include (but not limited to): Kotri barrage, KBFU head, -2.4 RD Keenjhar & KBFL regulators, bathymetric survey of Keenjhar, Haleji & Hadero lakes and previous studies on the lake (s). Moreover, climatic data of the study area have also been collected from relevant agencies. A simple but efficient approach has been adopted to check consistency & homogeneity in data, to find abnormalities and correct them before using in further analyses. The entire water transmission system, from Kotri to Karachi, has been analysed for the magnitude and trends of historic flow

pattern. System water balance and present operation has been studied at length. Moreover, to manage the additional flows, water availability at Kotri has been analysed, potential in flood spills d/s Kotri (considering environmental flows provisions) to meet the additional demand and operational management of the storages (lakes operations) has also been studied.

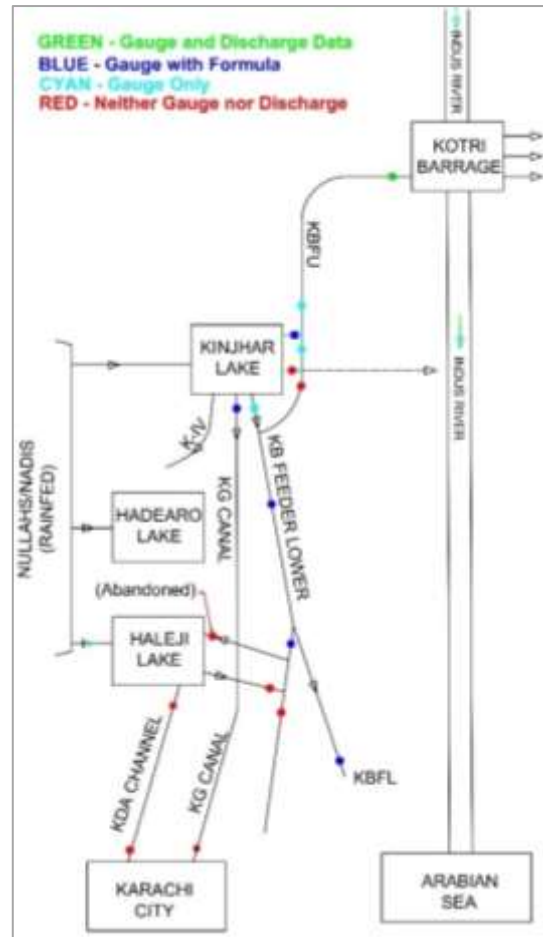


**Figure 48:** Line Diagram of KBFU and Keenjhar Lake System

### Climatic Indices of the Study Area

Collected daily rainfall (1970 to 2019) and temperature data of Hyderabad show very scarce rainfall around the year i.e. 07 inches on average annual basis and high temperatures round the year. Evaporation data of Pakistan Council of Research in Water Resources (PCRWR) regional office at Drip campus Tando Jam (1996 to 2017) shows average annual evaporation rates of 2,290 mm (90 inch). Climatic trends of the study area presented in **Figure 6**.

## Water Balance and Operations of Keenjhar Lake

Flow series at key structures have been developed to analyse the historic flows magnitudes & pattern for devising the water management strategy. Flow series at KBFU head, Keenjhar lake, KBF lower, PQ Fall and KG canal regulators have been developed for studying water balance (presented in *Figure 7*).

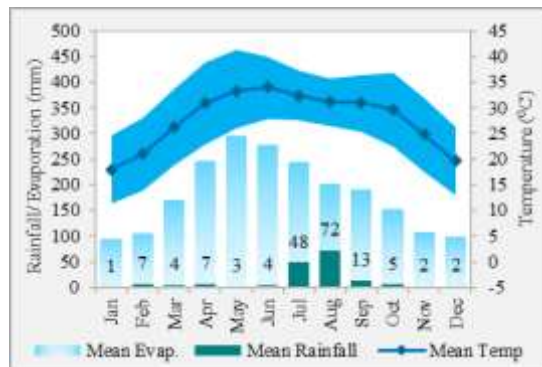


**Figure 49:** Monthly Rainfall, Temperature and Evaporation Trends in the Study Area

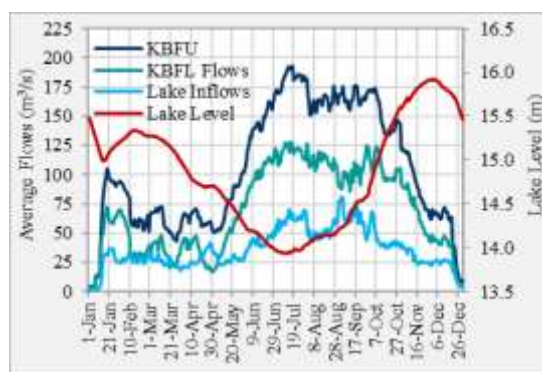


**Figure 50:** Average Flow Series at KBFU, KBFL & Lake Regulators and Lake Historic Levels

The data of offtakes from KBFU has been collected and rainfall-runoff analysis of the streams draining into the lake (having catchment area of 1,800 sq. km (700 sq. miles)) has been carried out. Further, evaporation losses from the system have also been incorporated in water balance study. Reservoir operation study of the lake (s) has been carried out to ascertain the requirement of additional supplies in view of available flows. An excel worksheet model has been developed; lake inflows, outflows and change in storage are the major components of the operation. Inflows are fed from lake regulator with occasional runoff from the streams; KG canal, PQ Fall and evaporation losses are considered as outflows whereas fluctuation in lake levels has been taken as change in storage.

Adopted components of the water balance are presented in *Figure 8*. Since, additional water supply to Karachi shall be managed through K-IV therefore, phased operation of K-IV (260 MGD for 1<sup>st</sup> and 390 MGD for 2<sup>nd</sup> phase) [25] has been considered in the operation.

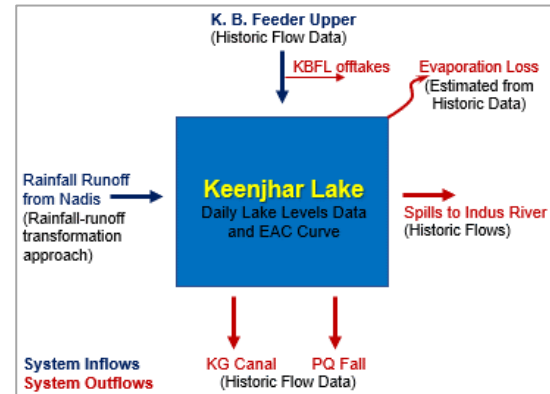


**Figure 51:** Components of Water Balance

## Present Operational Scenario of Keenjhar Lake

Existing operational scenario of the lake has been replicated using reported inflow data series and model generated lake levels have been checked with that of reported lake levels. It has been ascertained that the system in its present operation shall not be able to meet any additional demand as the system tends to produce shortage under present inflows. Hence, additional supplies to the system are indispensable. The results of the operations are presented in *Figure 9* and show that the lake reaches to its dead storage before onset of next wet season hence, necessitating the increased inflows to the lake. Extra flows shall help in continuous direct supply of water with small contribution from the lake and the lake filled in during the wet season may be utilized in dry season.

## Proposed Management Approach

The proposed approach suggests the action plan for managing additional flows and storage/depletion pattern of the lake for uninterrupted water supply. Since, it has been established that additional flows to the existing system are indispensable, the problem can be approached in two different ways: the ideal case would be of adding all the additional required water into the system and then take it out at K-IV, which is impossible on the face of scarce/ seasonal availability of water resources. The other feasible option is the utilization of excess flood flows

during wet period; tapping those flows at Kotri, feeding into KBFU and then storing at available storages, which may be utilized year-round. Hence, magnitude and time distribution of flows at Kotri has been studied. Moreover, historic data of KBFU shows that it has never been operated at its design discharge of 9,100 ft<sup>3</sup>/s so, restoration of KBFU to its design is indispensable for it to carry additional flows. Next challenge is formulating a trade-off between available excess flows, volume of available storages and the volume of water required to be stored till the next wet season is at the door. The analysed scenarios are: a) availability of additional flows in the system (Sindh accorded allocations and share in flood spills); b) increasing the inflows to the system; and c) evaluation of system capacity to carry/store the additional flows for the complete year.

### Evaluation of Additional Supplies at Kotri Barrage

Water availability at Kotri d/s (in addition to environmental flows) has been studied and the analyses of flows at Kotri barrage (**Figure 10**) suggest that the water has always been plentiful during the summer flood period starting from July to mid-September, with flows reducing during the recession towards end of the year with expected occasional small rise near April. Irrigation water demand at Kotri Barrage is far greater than Karachi's requirements, so the total water requirement at Kotri is very seasonal. Historic data at Kotri shows that that plentiful amount of water (average of 26 MAF) is being wasted into the sea almost every year. Hence, wastages at Kotri minus the environmental flows of 5,000 cfs, have been analysed in consideration

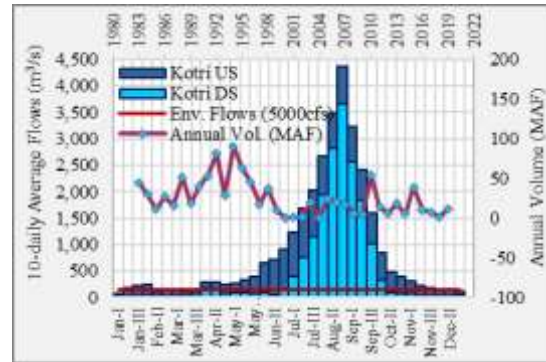


**Figure 52:** Flows Availability at Upstream and Downstream of Kotri Barrage (WAPDA)

of KBFU system carrying capacity and available storages volume. Revamped KBFU shall be operated at its design of 9,100 cfs whenever excess flows are available at Kotri.

### Scenarios Development

For the operation of Keenjhar lake, various scenarios have been developed by adopting synthetic inflow series and phased demand of 260 and 650 MGD. The adopted scenarios are:

1. Augmenting the lake inflows by lining KBFU; and
2. Diverting flood spills from Kotri downstream (in excess of environmental flows).

In scenario-1, the excess water saved from seepage recovery has been diverted into the lake and in scenario-2, lined KBFU has been operated at its design discharge of 9,100 cfs, whenever excess flows are available at Kotri. Whereas, KBF lower canal has been operated at its historic discharge. The comparison of synthetic inflow series is presented in **Figure 11**. The additional flows available for each scenario are 0.13 MAF

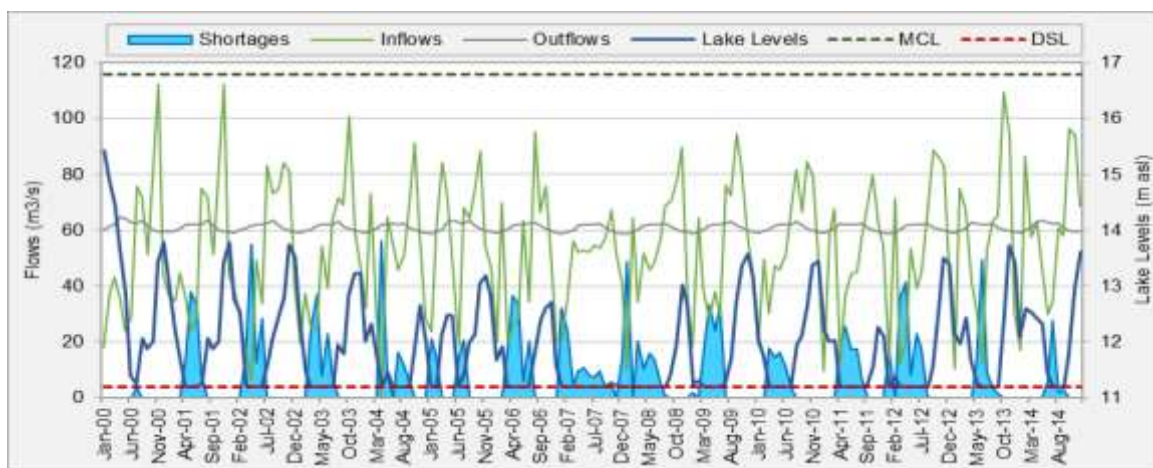


**Figure 53:** Keenjhar Lake Operation under Present Inflows for Phase-1 of K-IV (260 MGD)



and 0.74 MAF annually, respectively. The results of operational scenario are presented in following section.

### Scenario-1: Present Inflows

Keenjhar lake operation has been carried out for adopted three scenarios of inflow conditions i.e. present flows and two additional inflow series as discussed above. The results show that the system in its present flows is unable to meet any additional demands. Average volume of the shortages encountered equals to 0.20 MAF whereas maximum annual volume equals to 0.33 MAF. Results of the operation are presented in Figure 12.

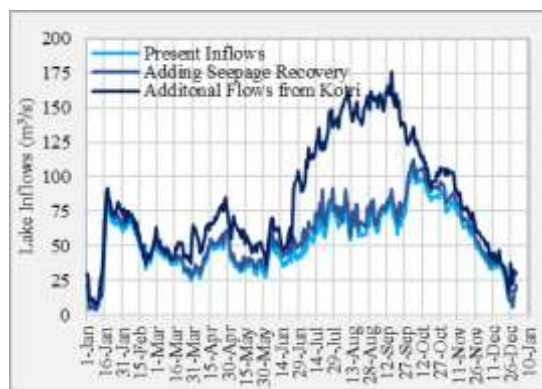


Figure 54: Present and Synthetic Inflow Series

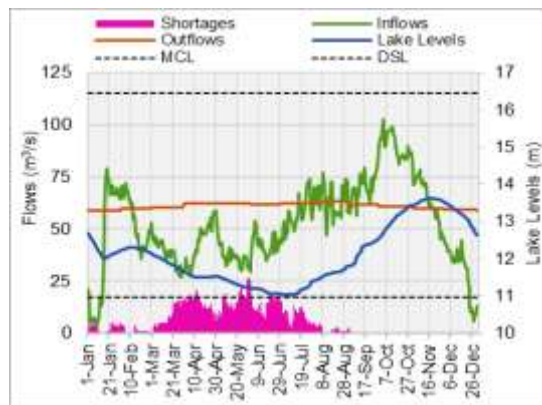


Figure 55: Operation with Present Inflows for 260 MGD Demand

### Scenario-2: Additional Inflows into the lake (Lined KBFU)

Additional flows of 0.14 MAF saved from seepage have been fed into the lake. In this scenario shortages days and volumes have been reduced whereas, the system is still unable to fully meet the demand of 260 MGD and furnished the average annual shortages volume of 0.110 MAF (maximum = 0.237 MAF) and 0.612 MAF for 650 MGD demand. Hence, increased flows are required to meet the water demands.

### Scenario-3: Additional Inflows into the lake (Support from Kotri d/s Flood Spills)

Increased flows from Kotri barrage, in excess to environmental flows of 5,000 cfs, have been diverted into KBFU and fed into the lake. In this scenario the system meets the demand of 260 MGD whereas, for 650 MGD demand (Figure 13) additional flows of 0.284 MAF are required.

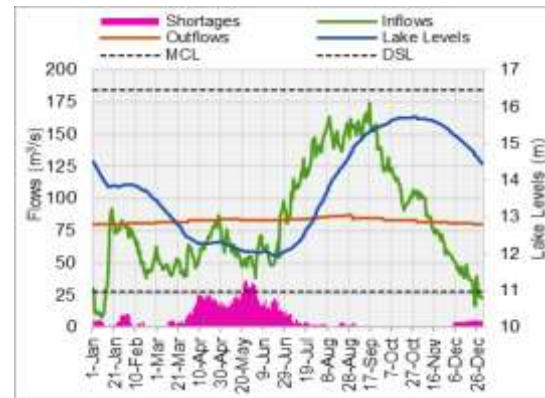


Figure 56: Operation with Additional Flows from Kotri and 650 MGD Demand

### Integrated Reservoir Operations

Three lakes have been integrated to minimize the shortages at Keenjhar lake. EAC of the lakes developed from bathymetric survey suggests that the live storage capacity of Haleji and Hadero lakes is about 0.054 MAF and 0.027 MAF, respectively. The lakes have been operated with the inflows managed from Kotri barrage and having filled the lakes during wet season. The results show that integrating both the lakes (with the operation of Keenjhar lake) provides additional dependence for 14 days and shortages volume of 0.284 MAF reduces to 0.203 MAF for 650 MGD.

### Suggestions for Operation of Existing Storages

In view of above analyses, tentative operation of existing storages has been summarized below:

- i. Keenjhar Lake should be filled while River Indus is in flood, if it is to be properly used for primary storage of the excess flood water.
- ii. The period of the greatest water shortages is during the months of May and June; it is during this period that the Kharif flood is expected to rise and, although the flood rise can occur at any time from the beginning of April onwards it can also be delayed until the end of June.
- iii. The flood rise is unpredictable and one of the primary purposes of Keenjhar Lake should be to provide security to Karachi water supply during May and June. One mode of operation of the lake

would therefore be to fill the lake during the period July to mid-September and not deplete the lake until February; from February until June the lake could be depleted only for supplying Karachi.

iv. The proposed rules for operating Keenjhar Lake can be summarized as follows:

<b>July to mid-September</b>	Fill the lake to normal retention level to provide water to Karachi and manage all irrigation through link canal.
<b>Mid-September to end of December</b>	Irrigation indents to be placed at Link canal and supply water for Karachi from the lake.
<b>January to February</b>	Refill the lake during this period in addition to supplying water to Karachi and manage all irrigation through Link canal.
<b>March to June</b>	Basic irrigation flows may be managed through Link canal. Short term fluctuations arriving from KBFU may be fed to the lake. Provide a supplement to the irrigation flows through the Link canal from the lake by PQ Fall regulator. Provide Karachi's water supply by depleting the lake.
<b>June</b>	If the river flows are rising and it is expected that there will be sufficient supply by the mid of June, provide additional irrigation water by depleting the lake.

### Conclusions and Recommendations

The conclusions and findings of the study are formulated as below:

1. Present system is unable to meet any additional demand for Karachi hence, additional supplies to the lake are indispensable;
2. Lining and restoration of KBFU to its design discharge of 258 m<sup>3</sup>/s (9,100 ft<sup>3</sup>/s) is very crucial as it will minimize the seepage losses and shall have capacity to carry additional flows;
3. Additional supplies to the lake may be managed either by i) occasionally compromising irrigation supplies to ensure continuous additional supply of 260/650 MGD or ii) managing flows from Kotri barrage flood spills;
4. Managing all required flows from Kotri is the ideal case which practically isn't possible due to fixed indents of all four canals off taking from Kotri and also the fact that no excess flows are available except during the wet season.

Hence, excess flows during wet season have been diverted to KBFU system, stored, managed and supplied to Karachi;

5. The study formulated the various synthetic inflow series in an attempt to divert maximum amount of excess flows from Kotri in consideration of the system carrying capacity and the volume of available storages;
6. Analyses of flows at Kotri downstream suggest that the flows have always been plentiful during the wet season (July through October). As of historic data, the average annual flows being wasted into the sea are of the magnitude of around 29 MAF whereas, environmental flows requirement is of mere 3.6 MAF;
7. Revamping KBFU to its design and diverting additional flows enabled the system to meet the demand of 260 MGD whereas, occasional shortages have been observed for 650 MGD;
8. Integration of Haleji and Hadero lakes into the system provides very little support provided the fact that they have very small storage capacities, have shallow depths and escalating evaporation rates make them run dry very quickly. Hence, the proposals for raising both these lakes or merging all these lakes into a large single storage volume may add to the benefits;
9. Further, it is also suggested to rise the Keenjhar lake by 2 ft up to the level 56 ft. as the historic data suggest that the lake spillway has never been operated. Rising shall provide additional volume of 0.07 MAF;
10. Since, the command area of KBFU is, mostly, water-logged therefore, efforts should be made to line the irrigation network. The water saved by lining may add up to the available useable flows.
11. There is much room available for optimizing the irrigation demands. A changed and improved cropping pattern on the face of prevailing waterlogging and water stress scenario shall do a great favour. For example; oil seed crops may be adopted instead of high-water requirements crops of sugarcane etc.
12. First-hand site information suggests that the system suffers substantial losses in terms of water theft and transmission losses etc. therefore, authorities should make maximum efforts to moderate such losses in irrigation and domestic supplies.
13. KW&SB efficiency may be enhanced by:
  - a. Reducing planned and unmanaged water thefts in the form of tanker mafia.
  - b. Improving and replacing the old and leaking water supply network.
  - c. Unaccounted for and non-revenue water (45-50%) may be reduced as per international practices (6%).

- d. Unmetered water supply and private/illegal connections by boring into the KWSB main lines should be discouraged.

## References

- EPRI, Taylor T, Goldstein, R. (2010). "Sustainable Water Resources Management, Volume 3: Case Studies on New Water Paradigm". EPRI, Palo Alto, CA and Tetra Tech 2009:1020587.
- Osmani & Company (pvt) Limited (2015). "Detailed Design and Construction Supervision of Greater Karachi Bulk Water Supply Scheme K-IV"
- Prinz, D. & Malik, A.H (2002). "More Yield with Less Water – How Efficient Can be Water Conservation in Agriculture?" Proceedings, 5th Internat. EWRA Conference on Water Resources Management in the Era of Transition, Athens, Greece, 4-8 September 2002, (pp 18 - 35).
- FAO AQUASTAT Survey (2011). "Irrigation in Southern and Eastern Asia in Figures", FAO Water Reports, ISSN 1020-1203.
- FAO. (2003). "Review of World Water Resources by Country"
- Flint RW (2004). "The Sustainable Development of Water Resources". Water ResUpdate Issue 127:41–51.
- UNDP (2016). "Development Advocate Pakistan, Water Security in Pakistan: Issues and Challenges" (Volume 3, Issue 4).
- Daanish Mustafa, Majed Akhter, and Natalie Nasrallah (2013). "Understanding Pakistan's Water-Security Nexus, United States Institute of Peace"
- Siegmann, K. A., & Shezad, S. (2006). "Pakistan's Water Challenges: A Human Development Perspective". Sustain Dev Policy Instit (SDPI).
- Mustafa, K. (2012, 09 23). "Pakistan's Per Capita Water Availability Dwindling". The News.
- Birdsall, N., Kelley, A. C., & Sinding, S. W. (Eds.). (2001). "Population Matters: Demographic Change, Economic Growth, and Poverty in the Developing World". Oxford University Press, DOI: <https://doi.org/10.1093/0199244073.001.0001>
- Brown RR, Keath N, Wong THF (2009). "Urban Water Management in Cities: Historical, Current and Future Regimes". Water Sci Technol 59(5):847–855. <https://doi.org/10.2166/wst.2009.029>
- The World Bank Group (2019). "Pakistan Getting More from Water", Contributors: William J. Young, Arif Anwar, Tousif Bhatti, Edoardo Borgomeo, Stephen Davies, William R. Garthwaite III, E. Michael Gilmont, Christina Leb, Lucy Lytton, Ian Makin, and Basharat Saeed.
- Human Development Report (2006). "Beyond Scarcity: Power, Poverty and the Global Water Crisis", ISBN 0-230-50058-7, Published for the United Nations Development Programme (UNDP), <http://hdr.undp.org>.
- Annual Report of State Bank of Pakistan (2016-2017). (though draft national water policy).
- Lt. Col. Islam-ul-Haque, Jawad Falak (2018), "Water Resources Management Karachi: The Uroos-ul-Bilaad". Centre for Peace, Security and Development Studies.
- Ahmad, M., & Burki, S. J. (2015, 07 05). "Water Crisis in Karachi: Old Issues Needing a New Look. Business Recorder"
- Bhutta, M. N., Ramzan, M., & Hafeez, C. A. (2002). "Groundwater Quality and Availability in Pakistan". In Proceedings of seminar on strategies to address the present and future water quality issues. Islamabad: Pakistan Council of Research in Water Resources.
- Hasan, S. (2013). "The 12 Remaining Dumlottee Wells". Dawn News.
- Hasan, S. (2015). "Hub Dam Water Level Rises to 289 feet". Dawn News.
- WWF (2019). "Situational Analysis of Water Resources of Karachi", A Project Funded by the European Union.
- MMP & ACE (1988), "Study of Kalri Baghaar Feeder System-Draft Final Report"
- NESPAK (2015). "Feasibility Study of Present Network of Kalri Baghaar Feeder and Keenjhar Lake and Suggesting Measures for Up-Gradation of the Same to Enhance Water Requirement from Keenjhar Lake to Karachi Water and Sewerage Board (KW&SB)"
- NESPAK (2019). "Third Party Design Review of the Greater Karachi Bulk Water Supply Scheme K-IV Project"
- Kazmi, S. J. H., Shaikh, S., Tamiz, I., Khan, S., Arsalan M. H., (2015). "EIA of K-IV Project", Jointly Conducted by University of Karachi, Osmani & Company and KW&SB. Karachi: EIA of K-IV project: jointly conducted by KW&SB and OCL.



## Comparison of Treaties/Agreements Signed Between Major Transboundary River Basins

Faraz ul Haq<sup>1\*</sup>, Ijaz Ahmad<sup>1</sup>, Noor Muhammad Khan<sup>1</sup>

<sup>1</sup> Centre of Excellence in Water Resources Engineering, University of Engineering and Technology Lahore, Pakistan

Corresponding author email: [engrfaraz@uet.edu.pk](mailto:engrfaraz@uet.edu.pk)

**Abstract:** Rivers do not follow political borders while flowing through their natural courses. The way in which transboundary waters are managed affects sustainable development within and beyond a country's borders. Transboundary rivers can be the cause of water conflict between nations. Internationally several water disputes are reported around transboundary river basins and various water treaties and agreements have been signed to resolve these conflicts and issues. The present study aimed at comparative analysis of treaties and agreements signed across major transboundary river basins e.g. Indus, Danube, Mekong, Ganges Brahmaputra-Meghna, Nile etc. The outcomes of this work will be helpful to learn from the best practices of Managing Transboundary river basins.

**Keywords:** Transboundary rivers; Indus; Mekong; Danube; Nile; Ganges basin

### Introduction

Water is essential to ensure the continuance of life. Even a positive action can have a negative reaction. For instance, a unilateral move by one country to adapt to climate change by building a dam could drastically reduce a river's flow downstream in another country. The way in which transboundary waters are managed affects sustainable development within and beyond a country's borders. Transboundary rivers can be the cause of water conflict between nations. Rivers do not follow political borders while flowing through their natural courses. Several transboundary river basins (e.g., River Nile, Sanaga, Helmand River and Indus, etc) in the world are shared by different countries. Internationally several water disputes are reported around these transboundary river basins and various water treaties (e.g. Kosi treaty, Mahakali treaty and Indus water treaty) and agreements have been signed to resolve these conflicts and issues.

However, due to the increase in world population, water scarcity, variation in precipitation, over abstraction of groundwater, climate change and distress in water supplies, conflicts may further arise between these countries over limited freshwater resources. Therefore, it is important to provide the information related to transboundary conflicts,

issues, treaties and future concerns to the researchers and policy makers.

The present study aimed at comparative analysis of treaties and agreements signed across major transboundary river basins e.g. Indus, Danube, Mekong, Ganges Brahmaputra-Meghna, Nile etc. This work will be helpful to learn from the best practices of Managing Transboundary river basins.

### Indus river basin

The Indus river basin is one of the world's largest transboundary river basin with a total drainage area of about  $1.08 \times 10^6$  Km<sup>2</sup>, shared by Pakistan (56%), India (26.6%), China (10.7%) and Afghanistan (6.7%) (Wolf et al., 2007), which makes it a geopolitically intricated region. The Indus river originates from Mansarovar lake in the Tibetan plateau and flows through Jammu, Kashmir, and Pakistan before draining into the Arabian Sea. Indus river basin is shown in Figure 1.



**Figure 1:** Map of Indus river basin

IWT comprises of twelve articles and eight (A-H) annexures. According to article 1, all the waters of eastern rivers i.e. Sutlej, Beas, and Ravi will be offered to India. According to article 3 (I), Pakistan shall accept unobstructed use of all waters of western rivers. While in article 3 (II) it is stated that India shall be under responsibility to let the flow of all the waters of the western rivers, except for controlled uses provided in annexure C&D. In article 4 and annexures C, D, E of IWT, conditions for the use of waters of the western river to India are listed i.e. for drinking purpose, agriculture, hydro-power development, etc.

### Ganges Brahmaputra Meghna Basin

The salient features of Ganges Brahmaputra Meghna basin are:

Area: 1,086,000 Km<sup>2</sup>

Shared between: India, Bangladesh, Nepal, Tibet

Population: more than 500 Million.

This basin is shown in Figure 2.



**Figure 2.** Map of Ganges Brahmaputra Meghna Basin

The main issues of this basin are Irrigation development in India & Climate change in the Himalaya, Irrigated agriculture in Bangladesh (**Kulna Jessore**), Stability of river systems in Bangladesh and **Sundarbans** protected brackish water wetlands in Bangladesh. Ganges

treaty (1996) is signed between Bangladesh and India for dispute resolution. Its main points are:

- The sharing between India and Bangladesh of the Ganga / Ganges waters at Farakka.
- Joint Committee from both governments, submit yearly reports (Article-VI)
- Joint committee followed by Indo-Bangladesh Joint Rivers Commission and mutual discussion of both governments (Article- VII)
- Review after five years interval or earlier, two years initial review (Article-X)
- For thirty years, can be renewed (XII).

### Mekong River Basin

The area of Mekong river basin is 795,000 km<sup>2</sup> with a length of 4,350 km. it is shared between China (21%) Myanmar(3%), Laos (25%), Thailand (23%), Cambodia (20%), and Vietnam (8%). The map of Mekong river basin is shown in Figure 3.



**Figure 3.** Map of Mekong river basin

The Agreement on Mekong River Basin (Mekong River Commission) was signed in 1995. Its salient features are:

- Signed on 5 April 1995, between: Cambodia, Laos, Vietnam and Thailand.
- Protection of the environmental and ecological balance (Article 3)
- Mekong River Commission (Council, Joint Committee, Secretariat- Article 12)
- Rules for Water Utilization and Inter- Basin Diversions (Article 26)
- Conflict resolution by Commission followed by governments (Article 34,35)

## Danube River Basin

The area of Danube river basin is 80,000 Km<sup>2</sup> which constitutes 10% of Europe and is shared between 19 Countries. The map of Danube river basin is shown in Figure 4.



**Figure 4.** Map of Danube river basin (Gerhard Sigmund, 2002)

Danube River Protection Convention (ICPDR) was signed between countries with the following salient features:

- Signed on June 29, 1994, in Sofia, Bulgaria, Came into force in October 1998.
- The conservation, improvement and rational use of surface waters and groundwater
- Measures to reduce the pollution loads entering the Black Sea from sources in the Danube River Basin
- Exchange of Information (Article-12)
- Water resources protection measures (Article-6)
- Information to the public (Article- 14)
- Research and development (Article-15)

## Nile River basin

This basin is 6,700 kilometers long and is shared between ten countries Rwanda, Burundi, Democratic Republic of the Congo (DRC), Tanzania, Kenya, Uganda, Ethiopia, South Sudan, Sudan and Egypt. Its main issues are Irrigation development in Sudan and Egypt and Hydropower and reservoir development in Ethiopia. Egypt has historically threatened war on Ethiopia and Tanzania over the Nile river. The map of Nile river basin is shown in Figure 5.



**Figure 5.** Map of Nile River basin

The Agreement on Nile River Basin was signed in 1959 with following features:

- Signed on November 8, 1959, at Cairo, between the then United Arab Republics (Egypt) and Sudan for full utilization of Nile Waters.
- Technical cooperation between the two republics i.e., Permanent joint technical commission (Article-IV)
- Sudan agreed to give a water loan to United Arab Republic for agriculture expansion (Annex-I)
- No share for other riparian, however, both parties will take join stance if other countries will claim water of Nile

## Findings

- Partial Treaties: Indus, Ganga, Mekong, Nile
- Focus on Water Division: Indus, Ganga, Nile
- Focus on Sustainable Development and Protection of Basin: Danube, Mekong, thus
- Have Technical Committees and Secretariate to develop and carryout Development Plans
- Effective Conflict Resolution Mechanism: Indus, Mekong, Danube.

## Way Forward

- Develop or adopt Legal Framework for Sustainable development and protection of waters, environment, and population of all basins, especially TRANSBOUNDARY river basins.
- Improvement of Legal Frames works (if already existing) to include:
- the principles of “Not to cause Significant Harm”,
- “Principle of Cooperation” and
- “Principle of Sharing Data”

## References

- Conflict and Cooperation Over International Freshwater Resources: Indicators Of Basins At Risk, By *Shira Yoffe, Aaron T. Wolf, And Mark Giordano* (2003), In Journal Of The American Water Resources Association American Water Resources Association, October 2003
- International Waters: Identifying Basins at Risk, By Aaron T. Wolf, Shira B. Yoffe And Mark Giordano, in *Water Policy* 5 (2003) 29–60,
- Water Conflict Chronology, by Dr. Peter H. Gleick of Pacific Institute for Studies in Development, Environment, and Security, 2008.
- UNEP-DHI and UNEP (2016). Transboundary River Basins: Status and Trends, Summary for Policy Makers. United Nations, Environment Programme (UNEP), Nairobi.
- Wolf, A. T. (2007). Shared Waters: Conflict and Cooperation. *Annual Review of Environment and Resources*, 32(1),241–269.  
<https://doi.org/10.1146/annurev.energy.32.041006.101434>



## Optimization of Water Allocation Based on Irrigation Water Supply and Demand in Chaj Doab, Pakistan

Muhammad Abdul Wajid<sup>1\*</sup>, Syed Hamid Hussain Shah<sup>1</sup>, Aamir Shakoor<sup>2</sup>, Hafiz Umar Farid, Ijaz Ahmad<sup>3</sup>, Naveed Ahmad<sup>4</sup>, Muhammad Adnan Shahid<sup>1</sup>, Aroosa Jabeen<sup>1</sup>

<sup>1</sup> Department of Irrigation and Drainage, University of Agriculture, Faisalabad, Pakistan

<sup>2</sup> Department of Agricultural Engineering, Bahauddin Zakariya University, Multan, Pakistan

<sup>3</sup> Center of Excellence in Water Resources Engineering, University of Engineering and Technology, Lahore

<sup>4</sup> Institute of Mountain Hazards and Environment - Chinese Academy of Sciences (IMHE-CAS), Chengdu, China

Corresponding author email: [mabdulwajid2@gmail.com](mailto:mabdulwajid2@gmail.com)

**Abstract:** Sustainable management of the canal water resources through optimum water allocation is the need of the modern world due to the rapid rise in water demand and climatic variations. So, the present research was conducted at Chaj doab, Indus Basin-Pakistan, with the primary aim to estimate effective and productive water management allocation using calibrated WEAP (Water Evaluation and Planning) model. Six different scenarios were developed and the results showed that the current available surface water is not sufficient to meet with the demand for agricultural water. LJC (Lower Jhelum Canal) command area is more sensitive to water scarcity, as this area is more than twice the UJC (Upper Jhelum Canal) command area with less LJC design discharge as compared to UJC. The future climate change scenarios for RCP 4.5 and 8.5 showed a percent decrease in catchment reliability up to 26.80 and 26.28 for UJC as well as 27.56 and 27.31 for LJC catchment, respectively. It is concluded that scenario-3 was much sufficient to reduce canal water deficit to optimize canal water allocation. The improvement in the irrigation system and cropping area should be optimized for efficient canal water management.

**Keywords:** Climate Change, Indus Basin, Irrigation Canals, Water Demand, Allocation, Water Evaluation and Planning.

### Introduction

The economy of Pakistan is primarily depending on irrigated agriculture, and it uses more than 95% of the total freshwater resources to irrigate 80% of the cultivatable land which generates 90% of nutrition and fodder (Abbas et al., 2021). The contribution of the agriculture sector in the GDP of Pakistan is almost 19% and providing jobs to 42% of people (Culas & Baig, 2020). Hence, water availability has direct influence on country in terms of its socioeconomic growth. In Pakistan, water is under stress with susceptible irrigation. An increase in future food demands more water to produce food but there is no additional water available (Archer et al., 2010). Even not only in Pakistan, globally water scarcity has risen in preventing plant development as a necessary constraint of environment in most of the regions (Moriani et al., 2002; Tognetti et al., 2006). Inadequate supply of surface water to crop is one of the major reasons of low crop production in the country and it can increase the difference between demand and supply of agricultural production (Latif & Pomee, 2003).

This trend is worsened by the inequality of water allocation among water users at the head, middle and tail reaches of the irrigation system (Hussain, 2005; Rinaudo et al., 1997). To overcome on water shortages, it is necessary to consider water management alternatives for both water demand and supply sides (Griggs & Noguera, 2002; Khalid & Khan, 2016; Tanaka et al., 2006).

WEAP (Water Evaluation and Planning) (Sieber et al., 2005) have been used for the analysis of water demand, water resource systems, water planning, and management, water balance and water allocation policies (Mugatsia, 2010). WEAP model combines the approach related to demand and supply preference in order to define rules of operation for making water allocations towards demand sites (Blanco-Gutiérrez et al., 2011; Yates et al., 2005). The impact of divergent management strategies and possible shortages can be determined by performing scenario analysis and simulation of variation in demand and supply variables (Yates et al., 2005).

Pakistan is considered to be the most threatened country in terms of climate change vulnerability (Ashraf et al., 2019). It is predicted that crop



production is profoundly affected by the different variations in temperature and rainfall in Pakistan (Mahmood et al., 2019; Raza et al., 2019). Optimization of water allocation is not only necessary to reduce canal water deficit but also crucial in terms of mitigating climate change impacts. Hence, the WEAP model has been introduced because it not only performs water allocations but also predicts impacts of future climatic variations, which could be helpful in policy reforms for future planning and management of current water resources. The aim of the research was to estimate irrigation water demand based on irrigation water supply and to optimize the water allocation to the demand sites under different scenarios using the WEAP (Water Evaluation and Planning) Model to reduce water deficit in canals. Furthermore, to develop strategies for effective water resource utilization under changing climate.

## Materials and Methods

### Study area

The present study was performed for an area bounded by rivers Jhelum and Chenab, known as Chaj Doab, Punjab Province of Pakistan, as shown in Figure 1. It ranges between longitudes from 72°10'E to 74°22'E and latitudes from 31° 11' N to 32° 58'N. The study area altitude varies from 150 to 250 m above mean sea level. The

total area of Chaj Doab is almost 5,854 km<sup>2</sup> consisting of 4 districts, i.e., Gujrat, Mandi Bahauddin, Sargodha, and some part of Jhang. The irrigation system of Chaj Doab is largely comprised of two main canals named Upper Jhelum Canal abbreviated as (UJC), and Lower Jhelum Canal called as (LJC). Two branch canals such as Gujrat branch and Phalia branch originates from UJC, while six branch canals originate from LJC, i.e., Shahpur branch, Northern branch and feeder, Southern branch, Southern feeder, Sulki branch, and Khadir feeder. Rice, sugarcane, wheat, citrus, and fodder are the main crops grown in this area (Ashraf & Zeeshan, 2012).

### Data collection and analysis

A large number of data set is required to develop a hydrological model and for its processing. The detailed summary of input data type, description, source and format, as well as methodology applied, are presented in Table 1.

### Model development

In this present study, Water Evaluation and Planning (WEAP), developed by Stockholm Environment Institute was used to acquire the required objectives. It is one of the commonly used tools for modeling, planning, and management of the water resources all over the world. It is a modeling package based on the

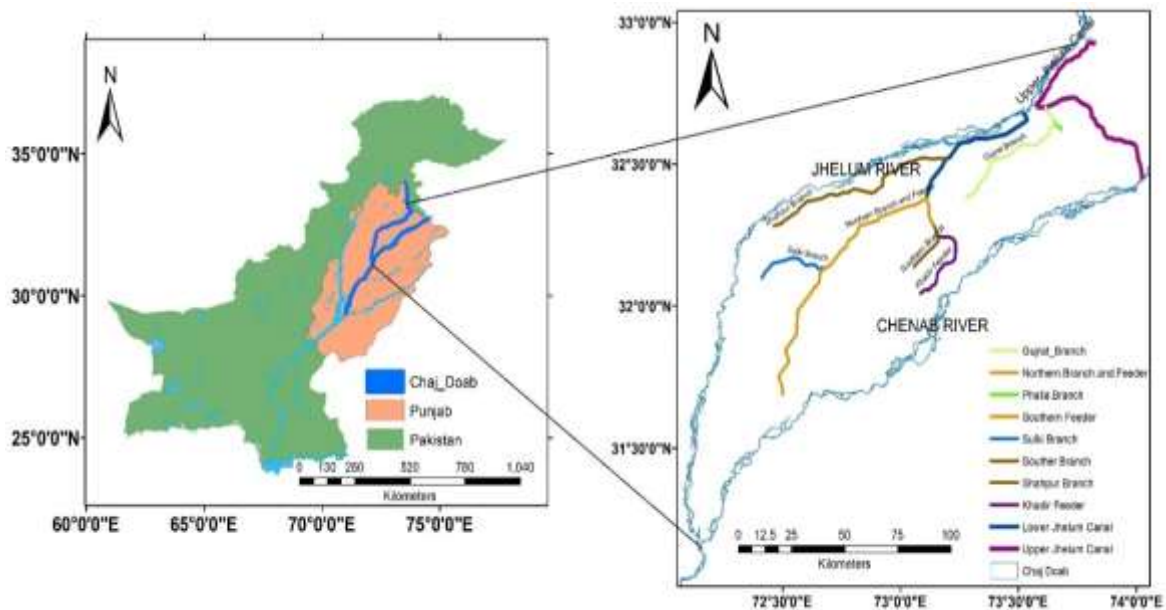


**Figure 57** Irrigation system in the study area

**Table 24:** Input data for the development of the Water Evaluation and Planning (WEAP) model

Sr. No.	Data type & description	Frequency	Duration	Data Source and Format
1	Head Discharge data (Mangla Dam, Jhelum River, LJC & UJC (Main canals) )	Daily Basis	2006 – 2016	Excel files from Punjab Irrigation Department, Lahore, Government of Punjab, Pakistan
2	Climatic Data (Max. temperature and Min. temperature, Rainfall, Wind Speed Humidity, Sunshine Hours and Latitude, Longitude)	Monthly Basis	2006 – 2016	Notepad files from Regional Meteorological Department, Lahore, Govt. of Punjab, Pakistan
3	Soil Data (Soil type of Upper Jhelum Canal (UJC) & Lower Jhelum Canal (LJC) command area)	FAO developed world soil map	Soil map for both command areas in Chaj Doab	Soil map Shapefiles in (.shp) format From FAO website (www.fao.org/geonetwork/srv/en/metadata.show?id=14116)
4	Land use & land Cover Data	Rabi & Kharif season	2013-2014	Faculty of Agricultural Engg. & Tech. University of Agriculture Faisalabad, Pakistan
5	Agricultural data (Crop Planting date, Crop Co-efficient, etc.)	Yearly Basis	2006-2016	Yearly online published Reports (concerned Agri. Departments) & FAO. 56
6	Shapefiles (River Jhelum, UJC & LJC and its Command areas)	-----	-----	(.shp) format From Punjab Irrigation Department, Lahore Govt. of Punjab, Pakistan

object-oriented program (Blanco-Gutiérrez et al., 2011). GIS-based shapefiles of the Chaj doab irrigation system were added into the projected area to build the command area (Figure 2).

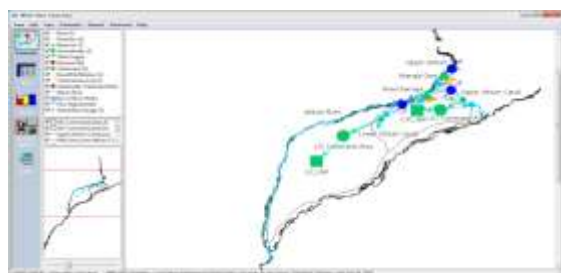


**Figure 58** Schematic view of the Chaj Doab in WEAP Model

The MABIA method was used for simulation, which involves the daily basis simulation for different parameters i.e., irrigation water demand, evaporation and transpiration, growth of crops, irrigation scheduling, crop yield, and also contain elements like calculation of soil water capacity and reference evapotranspiration. This method further used the dual ‘K<sub>c</sub>’ method, where

K<sub>c</sub> value consists of two components, including basal crop coefficient (K<sub>cb</sub>) and soil evaporation K<sub>e</sub>. The formula for actual ET<sub>a</sub> is given in Equation (Error! Reference source not found.)

$$ET_a = (K_s \times K_{cb} + K_e)ET_{ref} \quad (1)$$

Where ET<sub>ref</sub> is reference evapotranspiration, and K<sub>s</sub> is soil stress co-efficient.

Total available water or available water capacity can be determined by subtracting a wilting point from field capacity, and it can be represented by the Equation (Error! Reference source not found.) as:

$$TAW = F.C - W.P \quad (2)$$

Where, TAW stands for total available water, and WP named as a wilting point while FC represents the field capacity of the soil. For reference evapotranspiration cropwat model was used.

### Scenarios

The impact of six different scenarios were tested on unmet demand and reliability of the system against reference scenario (2007-2070). The

current account year was 2006 and it was extended up to 2070 to simulate reference scenario for the purpose of comparison, analysis and evaluation of other future scenarios. The efficiency of different irrigation system was consider as follows; drip irrigation efficiency 80-91 % (Battikhi & Abu-Hammad, 1994) and sprinkler 54-80% (Zalidis et al., 1997). All the scenarios were developed under reference scenario based on findings from water demand and supply simulation as shown in Table 2

### Model Calibration

Nash-Sutcliffe efficiency (NSE) and Percent bias (PBIAS) were calculated using Equations **Error! Reference source not found.** and **Error! Reference source not found.**, respectively for calibration and validation of the model results (Moriassi et al., 2007).

### Nash-Sutcliffe efficiency (NSE)

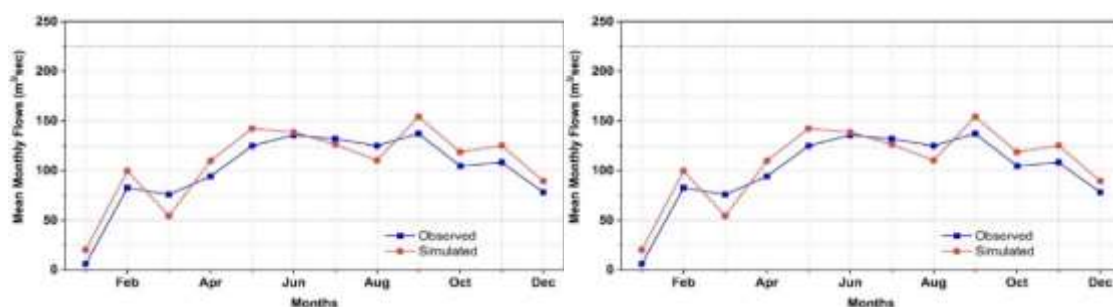
$$NSE = 1 - \frac{\sum_{i=1}^n (Q_o - Q_s)_i^2}{\sum_{i=1}^n (Q_o - \bar{Q}_s)^2} \quad (4)$$

### Percent bias (PBIAS)

$$PBIAS = 100 \times (\sum_{i=1}^n (Q_o - Q_s) / \sum_{i=1}^n (Q_o)_i) \quad (5)$$

**Table 25:** Representation of all the scenarios

Scenarios	Strategies implementation
<b>Scenario-1:</b> (Irrigation System Improvement)	Increase in irrigation efficiency (85%) using drip and sprinkler technologies, and Seepage losses reduction through canal lining (50%)
<b>Scenario-2:</b> (Changing Crop Area)	Reduction in area of High delta crop and replacement with low water delta crops (50%)
<b>Scenario-3:</b> ombination of Scenario 1 and 2)	Irrigation Efficiency (85%), Seepage losses reduction (50%), area reduction of high delta crops and replacement (50%)
<b>Scenario-4:</b> Canal Capacity Enhancement	Increasing canal capacity through canal maintenance i.e. silt removal and increase in canal diversions (20%)
<b>Scenario-5:</b> Climate Change with RCP 4.5	Future climate change impact (Temperature & Rainfall data) with RCP 4.5 up to 2070
<b>Scenario-6:</b> Climate Change with RCP 8.5	Future climate change impact (Temperature & Rainfall data) with RCP 8.5 up to 2070



Where,  $Q_o$  represents observed flow and  $Q_s$  shows simulated flow,  $\bar{Q}_s$  is mean of the simulated flow and  $n$  is the number of observations.

## Results and Discussion

### Simulated and observed streamflow

A comparison was made between mean monthly observed and simulated flows from 2006 to 2010 for calibration and 2011 to 2016 for validation. The study graph established by the model indicates the deviation of the simulated flow with respect to observed flow as well as its height of deviation in Figure 3-4.

### Model calibration and validation

The WEAP model was subjected for calibration from years 2006 to 2010 and for validation from years 2011 to 2016, as presented in Figures 5-6. The statistical parameters such as  $R^2$ , NSE coefficient, PBIAS were tested to observe model

**Figure 59** Streamflow for calibrated years at UJC and LJC

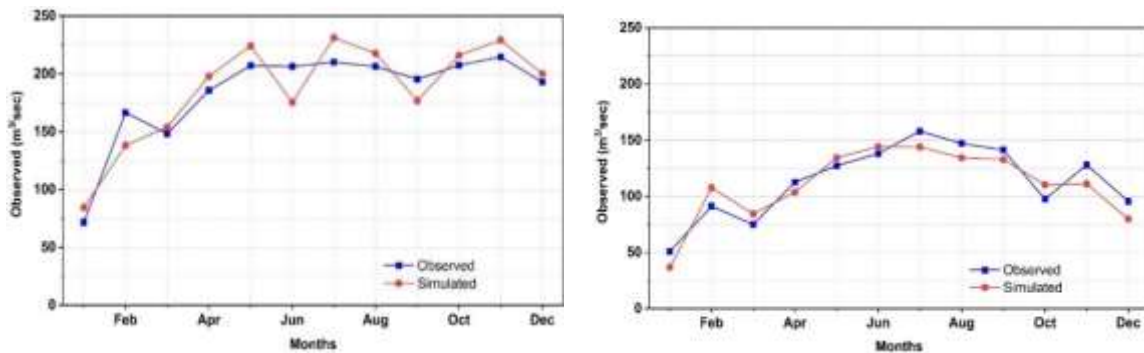


**Figure 60** Streamflow for validated years at UJC and LJC

calibration and validation on observed and simulated average monthly streamflow as shown in Table 3. The negative sign indicates that the simulated flow is lower than the observed flow. For the satisfactory performance of the model, the values of PBIAS should be in range of  $\pm 25\%$  in case of streamflow. NSE should be  $>0.50$  and the range for  $R^2$  is between 0 and 1 with 1 is an indication of perfect match between simulated and observed flows and 0 shows a very bad

comparison (Moriassi et al., 2007). The resulted statistical values are clearly showing a good match between the measured and simulated flows.

**Canal water deficit**

The WEAP model results for irrigation water requirement, unmet demand and water supplied for both of the UJC and LJC command area are presented in Figures 7-9. The overall water

**Table 3:** Model calibration and validation results

Statistical Parameters	Calibration		Validation	
	Upper Jhelum Canal (UJC)	Lower Jhelum Canal (LJC)	Upper Jhelum Canal (UJC)	Lower Jhelum Canal (LJC)
<b>NSE</b>	0.91	0.83	0.8	0.83
<b>PBIAS</b>	-2.92	-7.01	-1.48	-2.97
<b>R<sup>2</sup></b>	0.93	0.87	0.83	0.85

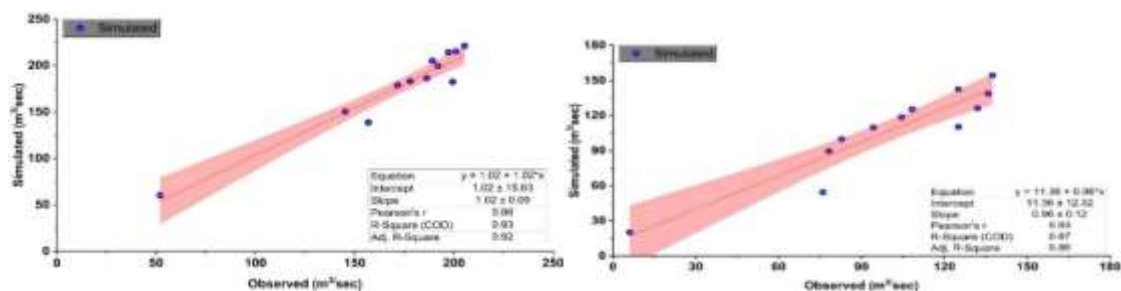


**Figure 61** Calibration results for UJC and LJC flows

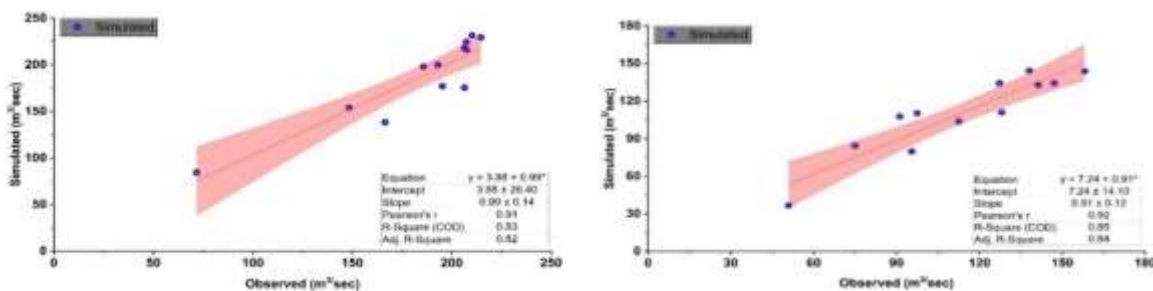




**Figure 62** Validation results for UJC and LJC flows

demand of both the canal command areas (Upper Jhelum canal and Lower Jhelum Canal) were 4086 MCM and 10607 MCM, respectively. LJC has more culturable command areas as compared to UJC thus have more water demand. The volume of water delivered to UJC and LJC command area was 1888.8 MCM and 2066.4 MCM, respectively.

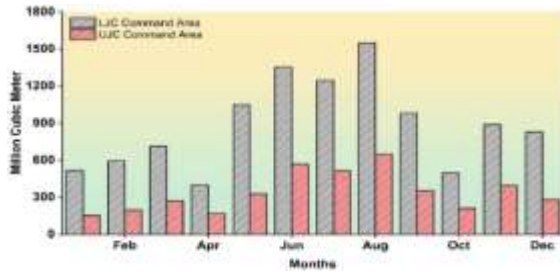


**Figure 63** Water demand for both canal catchments

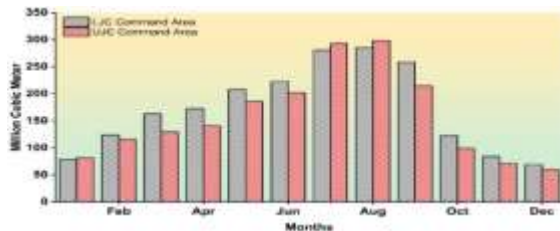


**Figure 64** Supply delivered for both canal catchments

It is clear from the results that the supplied volume of water is not enough to fulfill water demand. The mean annual unmet demand for UJC Command area and LJC command areas were 2197.2 MCM and 8540.6 MCM, respectively, as shown in Figure 14.

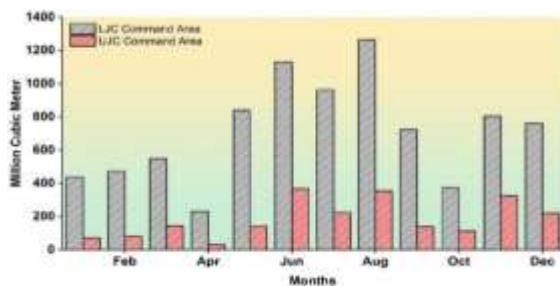


**Figure 65** Unmet demand for both canal catchments

### Canal catchment reliability

The results of model showed that the reliability of canal catchment is decreasing such as 61.15% of reliability in Upper Chenab canal area and 46.41% in Lower Jehlum canal area (Figure 10). Less percentage of reliability shows an enlarged

water shortage in canal command areas for irrigation water.

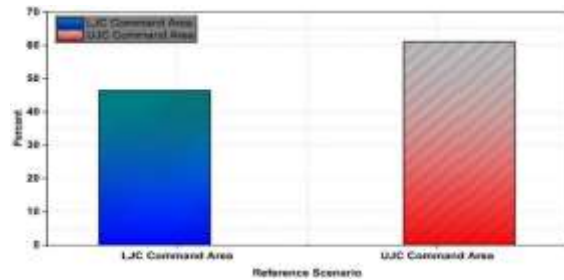


**Figure 66** Reliability Comparison of both Canals catchments under reference scenario

### Future Water Allocation Scenarios Development

Scenario analysis was performed to optimize the allocated water to the demand sites in order to reduce canal water deficit. The effect of these scenarios was checked on the reliability of the demand sites. Demand site reliability for all the scenarios were compared with reliability of the reference scenario as shown in Figure 11 and Figure 12. Results showed that with the implementation of first scenario, the reliability of the UJC command area could be increased from 61% to 75%. On the other hand, LJC command area reliability would improve from 46% to 50%.



**Figure 67** Representation of all future scenarios for UJC command area

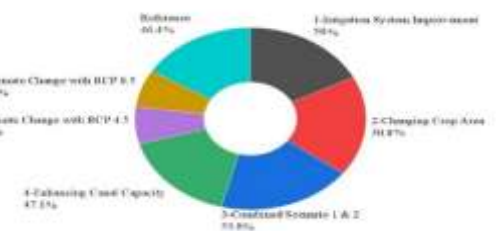


**Figure 68** Representation of all future scenarios for LJC command area

The results of percent reliability change between reference and other scenarios are presented in Table 4. Results depicted that by implementing second scenario, reliability of the UJC and LJC



**Table 4** Reliability change (%) comparison between reference and other scenarios

Scenario Types	Change in Reliability (%)	
	Upper Jhelum Canal	Lower Jhelum Canal
<b>Reference Scenario</b>	No Change	No Change
<b>Scenario-1:</b> (Irrigation System Improvement)	+13.46	+3.59
<b>Scenario-2:</b> (Changing Crop Area)	+9.49	+4.36
<b>Scenario-3:</b> (Combination of Scenario 1 and 2)	+22.82	+7.44
<b>Scenario-4:</b> Canal Capacity Enhancement	+2.31	+0.64
<b>Scenario-5:</b> Climate Change with RCP 4.5	-26.80	-27.56
<b>Scenario-6:</b> Climate Change with RCP 8.5	-26.28	-27.31

Note: Where (+) sign indicates the percentage increase in demand site reliability and (-) sign shows percentage decrease in demand site reliability as compared to reference scenario.

catchment could be enhanced from 61 to 71% and 46 to 51%. Under Scenario 3, results highlighted that the demand site reliability for Upper Chaj Doab (UJC command) could be maximized up to 84% from 61% showing a 23% increase in reliability. For Lower Chaj Doab (LJC command), the reliability will rise from 46% to 54% which is an indication of 8% rise. So, this strategy is seeming to be too effective especially in the UJC area. Under scenario 6, Results showed that after water allocation, the reliability for UJC demand site would be increased from 61 to 64% while for LJC it would increase from 46 to 47%. Results for scenario 5 showed that the demand site reliability for Upper Chaj Doab will decrease from 61 to 34.36% while for Lower Chaj Doab, it will also decrease from 46 to 18.8%. Results for scenario 6 also showed decrease in reliability for both catchment area such as in UJC from 61 to 34.87% and in LJC 46 to 19.10%

### Proposed strategies

Based on current study results and scenario analysis, different strategies are proposed for efficient and effective utilization of the present water resources. The scenario-3 which includes combined application of improving irrigation system and reduction in area of high-water requiring crops with less water consuming crops should be practically implemented. Operate canal at full supply level and proper maintenance should be enforced. Based on future climate change, respective alternate water regulation policies should be revised and re-planned based on the crop types, its area covered and on field water requirement for efficient water allocation

### Conclusions

In this research, Water Evaluation and Planning Model (WEAP) was used for hydrological simulation of the Chaj Doab area to estimate irrigation water demand and to develop respective allocation optimization strategies under multiple future climatic scenarios analyses for reducing canal water deficit to manage currently available water resources efficiently. Currently, available surface water is not sufficient to meet with the demand for agricultural water. LJC command area is more sensitive to water scarcity, as this area is more than twice the UJC command area with less LJC design discharge as compared to UJC. It is concluded that the scenario-3 (a combination of scenario 1 and 2) were found to be much practical approach in reducing canal water deficit because the implementation of this scenario maximized the system reliability approximately up to 84 and 54% for UJC and LJC command areas, respectively. The future climate changes may double the unmet demand, and particularly the LJC command area is seriously going to face water scarcity situations if not properly managed. Additionally, WEAP can be used as a useful hydrological modeling tool for efficient water resources management, and planning for the researchers and respective guidelines for policymakers will have fruitful outcomes.

### References

- Abbas, G., Ali, A., Khan, M., Mahmood, H. Z., Wahab, S. A., & Amir-ud-Din, R. (2021). The Transition from Arid Farming Systems to Agroforestry Systems in Pakistan: A Comparison of Monetary Returns. *Small-scale Forestry*, 1-26.

- Allen, R. G., Pereira, L. S., Raes, D., & Smith, M. (1998). Crop evapotranspiration-Guidelines for computing crop water requirements-FAO Irrigation and drainage paper 56. Fao, Rome, 300(9), D05109.
- Archer, D. R., Forsythe, N., Fowler, H. J., & Shah, S. M. (2010). Sustainability of water resources management in the Indus Basin under changing climatic and socio economic conditions. *Hydrology and Earth System Sciences*, 14(8), 1669–1680.
- Ashraf, M. Q., Khan, S. A., Khan, R., & Iqbal, M. W. (2019). Determinants of Adaptation Strategies to Climate Change by Farmers in District Sargodha, Pakistan. *International Journal of Economic and Environmental Geology*, 16–20.
- Ashraf, M., & Zeeshan, A. B. (2012). Diagnostic analysis and fine tuning of skimming well design and operational strategies for sustainable groundwater management-indus basin of pakistan. *Irrigation and Drainage*, 61(2), 270–282.
- Battikhi, A. M., & Abu-Hammad, A. H. (1994). Comparison between the efficiencies of surface and pressurized irrigation systems in Jordan. *Irrigation and Drainage Systems*, 8(2), 109–121.
- Blanco-Gutiérrez, I., Varela-Ortega, C., & Flichman, G. (2011). Cost-effectiveness of groundwater conservation measures: A multi-level analysis with policy implications. *Agricultural Water Management*, 98(4), 639–652.
- Culas, R. J., & Baig, I. A. (2020). Impacts of irrigation water user allocations on water quality and crop productivity: The LCC irrigation system in Pakistan. *Irrigation and Drainage*, 69(1), 38–51.
- Griggs, D. J., & Noguer, M. (2002). Climate change 2001: the scientific basis. Contribution of working group I to the third assessment report of the intergovernmental panel on climate change. *Weather*, 57(8), 267–269.
- Hussain, I. (2005). Pro-poor intervention strategies in irrigated agriculture in Asia: poverty in irrigated agriculture: issues, lessons, options and guidelines: Bangladesh, China, India, Indonesia, Pakistan and Vietnam. Final synthesis report. International Water Management Institute.
- Khalid, I., & Khan, M. A. (2016). Water Scarcity-A Major Human Security Challenge to Pakistan. *South Asian Studies*, 31(2), 143.
- Latif, M., & Pomee, M. S. (2003). Irrigation management turnover: an option for improved utilization of limited water resources in Pakistan. *Irrigation and Drainage: The Journal of the International Commission on Irrigation and Drainage*, 52(3), 261–272.
- Mahmood, G. G., Rashid, H., Anwar, S., & Nasir, A. (2019). Evaluation Of Climate Change Impacts On Rainfall Patterns In Pothohar Region Of Pakistan. *Water Conservation & Management (WCM)*, 3(1), 1–6.
- Moriana, A., Villalobos, F. J., & Fereres, E. (2002). Stomatal and photosynthetic responses of olive (*Olea europaea* L.) leaves to water deficits. *Plant, Cell & Environment*, 25(3), 395–405.
- Moriasi, D. N., Arnold, J. G., Van Liew, M. W., Bingner, R. L., Harmel, R. D., & Veith, T. L. (2007). Model evaluation guidelines for systematic quantification of accuracy in watershed simulations. *Transactions of the ASABE*, 50(3), 885–900.
- Mugatsia, E. A. (2010). Simulation and scenario analysis of water resources management in Perkerra catchment using WEAP model. M Asters Thesis, Department of Civil and Structural Engineering, School of Engineering, Moi University, Kenya,(December).
- Raza, M. H., Bakhsh, A., & Kamran, M. (2019). Managing climate change for wheat production: An evidence from southern Punjab, Pakistan. *Journal of Economic Impact*, 1(2), 48–58.
- Rinaudo, J.-D., Strosser, P., & Rieu, T. (1997). Linking water market functioning, access to water resources and farm production strategies: example from Pakistan. *Irrigation and Drainage Systems*, 11(3), 261–280.
- Sieber, J., Yates, D., Huber Lee, A., & Purkey, D. (2005). WEAP: a demand priority and preference driven water planning model: Part 1, model characteristics. *Water International*, 30(4), 487–500.
- Tanaka, S. K., Zhu, T., Lund, J. R., Howitt, R. E., Jenkins, M. W., Pulido, M. A., Tauber, M., Ritzema, R. S., & Ferreira, I. C. (2006). Climate warming and water management adaptation for California. *Climatic Change*, 76(3–4), 361–387.
- Tognetti, R., d'Andria, R., Lavini, A., & Morelli, G. (2006). The effect of deficit irrigation on crop yield and vegetative development of *Olea europaea* L.(cvs. Frantoio and Leccino).

- European Journal of Agronomy, 25(4), 356–364.
- Yates, D., Sieber, J., Purkey, D., & Huber-Lee, A. (2005). WEAP21—A demand-, priority-, and preference-driven water planning model: part 1: model characteristics. *Water International*, 30(4), 487–500.
- Zalidis, G., Dimitriadis, X., Antonopoulos, A., & Gerakis, A. (1997). Estimation of a network irrigation efficiency to cope with reduced water supply. *Irrigation and Drainage Systems*, 11(4), 337–345.

## Application of Multispectral images using R-Studio package to Estimate Canal Water Deficit: A comprehensive study of Multan Irrigation Zone

Qamar Iqbal<sup>1</sup>, Aamir Shakoor<sup>1,\*</sup>, Zahid Mahmood Khan<sup>1</sup>, Hafiz Umar Farid<sup>1</sup>, Ijaz Ahmad<sup>2</sup>, Muhammad Awais<sup>3</sup>, Imran Rasheed<sup>1</sup>, Hafiz Muhammad Kamran<sup>1</sup>, Muhammad Abdul Wajid<sup>3</sup>

<sup>1</sup> Department of Agricultural Engineering, Bahauddin Zakariya University, Multan, Pakistan

<sup>2</sup> Center of Excellence in Water Resources Engineering, University of Engineering and Technology, Lahore

<sup>3</sup> Department of Irrigation and Drainage, University of Agriculture, Faisalabad, Pakistan

Corresponding author email: [aamirskr@bzu.edu.pk](mailto:aamirskr@bzu.edu.pk)

**Abstract:** The timely and accurate utilization of Land Use Land Cover (LULC) information in irrigated agricultural area can help to manage canal water according to the crop water requirements. In this respect, a study was carried out to map the LULC of command area of Multan Irrigation Zone (MIZ) of Pakistan for the estimation of canal water adequacy (CWA) using R-Studio. In R studio, MODISsp and MODISTool packages were used and the tiles of area of interest were obtained from MODIS tiles tool. Multispectral images of MODIS satellite (Aqua and Terra) were acquired for both Rabi and Kharif seasons for year 2016-2017. The unsupervised classification of Normalized Difference Vegetation Index (NDVI) was constituted on LULC of the command area. Initially, total 46 classes were created with maximum likelihood and finally these classes were merged into 7 classes, based on field knowledge. The error matrix method was applied to assess the accuracy assessment with overall accuracy of 83.33, 77.36, 81.25% and the total cropping area of major crops was 31751, 103212 and 106144 hectares for Haveli, Mailsi and Nili Bar circles, respectively. The volume of water required for cropped area was estimated from the LULC and crop evapotranspiration. The canal water adequacy was determined from the amount of water required to cropping area and canal water supply during the season. It was found that the average canal water adequacy for Haveli, Mailsi and Nili Bar canal was 1141 (58%), 235 (51%), 312 (50%) Mm<sup>3</sup>year<sup>-1</sup>, respectively.

**Keywords:** MODISsp, MODISTool, LULC, Aqua, Terra, CROPWAT, NDVI, crop evapotranspiration

### Introduction

The success of irrigated agriculture in highly depends upon the canal irrigation system and unconstrained supply to the farmer's field. This is only possible when there is exact estimation of crop acreage and total amount water required in each cropping season in the canal command area. Satellite information can be used to identify suitable areas for continued irrigated cropping by using the maps created from the data. Irrigation potential can be calculated from vegetation indices and analysis of demand-supply curve in irrigated command areas of Pakistan. In the analysis of NDVI times series types of vegetation are considered using phenological disparity (Defries & Townshend, 1994). With the use of NDVI and AVHRR data, different techniques have been established to differentiate the types of crop. If the land cover and land use classes are mixed on the similar map, then it is known as Land Use and Land Cover (LULC) classes. For many states, precise land use maps are not easily accessible (Wood *et al.*, 2000). To create strategies for worldwide food security and to

predict shortcomings, mapping of cropland is needed with enough accuracy through open, replicable and quick techniques (Thenkabail, 2009). Agricultural land use planners, policymakers, donor organizations and crop insurance firms require timely access to precise agricultural LULC maps for a multitude of reasons (Khan *et al.*, 2010).

MODIS is a vital tool which aboard two satellites Terra (EOS AM-1) and Aqua (EOS PM-1). The rotation of both satellites is perfectly timed so that Terra passes north to south pole across the equator in the morning, in the meantime Aqua orbits the earth from south to north pole over the equator in the afternoon. Two vegetation indices are derived from atmospherically accurate reflection in the red, near-infrared and blue wavebands; the uniform vegetation difference index (NDVI), which provides consistency with NOAA's AVHRR NDVI time series record for historical and climate applications; and the enhanced vegetation index (EVI), which minimizes canopy-soil differences and enhances sensitivity over dense soil applications. These

two entities describe the global range of states and processes of vegetation more effectively. Keeping in view the better water resource management of an irrigated command area, the objectives of this research work were i) to determine the cropping area of major crops from multispectral images using R-Studio package in the command area of Multan Irrigation Zone, ii) to estimate the actual crop water requirement of major crops using metrological data and iii) to determine the canal water deficit.

## Material and Methods

### Study area

The study was conducted on the regional basis and area for this study was the command area of the Multan Irrigation Zone. It lies between 29°24'58.45" and 31°17'8.24"N and 71° 5'42.46" and 73°53'49.51"E at an average elevation above sea level is 156m (512 ft). Multan irrigation zone was constructed since 1968 and consists of three canal circles i.e. Mailsi Canal Circle, Haveli Canal Circle and Nili Bar Canal Circle (Figure 1).

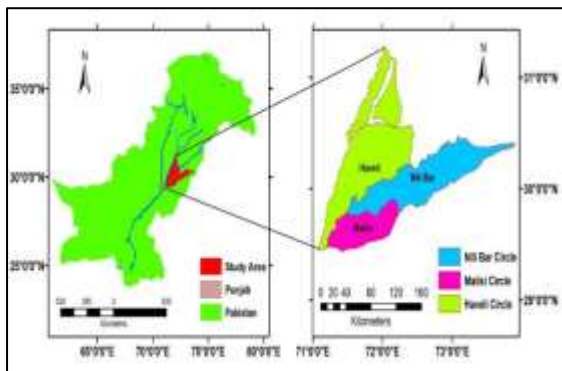


Figure 1: Map of the Multan Irrigation Zone

### Data acquisition

The methodology flow chart to conduct this research for estimating of canal water deficit is showing in Figure 2. For research purpose, different type of data sets such as satellite images, irrigated command area, soil type, climate, crops, crop calendar and discharge data were used to get the result and information about the study area. Irrigation discharge data on daily basis were acquired from online data source of Punjab Irrigation Department, Lahore-Pakistan.

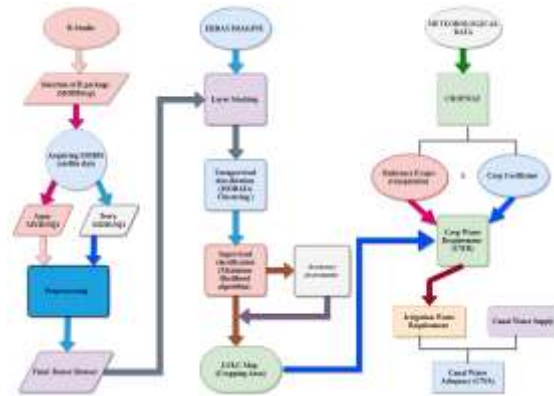


Fig. 2: Methodology layout

MODIS (Moderate Resolution Imaging Spectroradiometer) data set of multispectral images were used due to their high spatial and temporal resolution on regular basis. This satellite products (Aqua and Terra) having spatial resolution of 250m and data was free of charge. The discharge data of daily basis for each distributary which was modified according to the need of the research study.

### Acquiring of Satellite data

There were two methods for acquiring MODIS satellite data 1) MODIS official website or Earth data center website 2) R-Studio. R Programming language is a powerful programming tool for statistical analysis and implementing the graphical techniques such as linear and nonlinear modelling, time series analysis, classical test of statistics, classification of satellite data. This is an object-oriented programming language (R Core Development Team, 2013). High quality of graphs can be made from this programming language due to easy interface of the language. It uses command-line interpreter and support matrix arithmetic like MATLAB and APL.

### MODISstp

There were different options tab given, and then filling the required information raster images of MODIS were acquired. The next step was the selection of layers, which were processed according to research requirement. 16-day NDVI average layer was selected and saved the information for next step. In this tab, the Earthdata (<https://earthdata.nasa.gov/>) username and password was put. The purpose of this function was to connect the MODISstp to Earthdata server and download the raster data sets. Spatial extent data was given in view of AOI and Tiles data obtained from MODIS\_tiles tool.



### Irrigation water demand

Irrigation water requirement and total water demand for specific crop is determined from the equation (1):

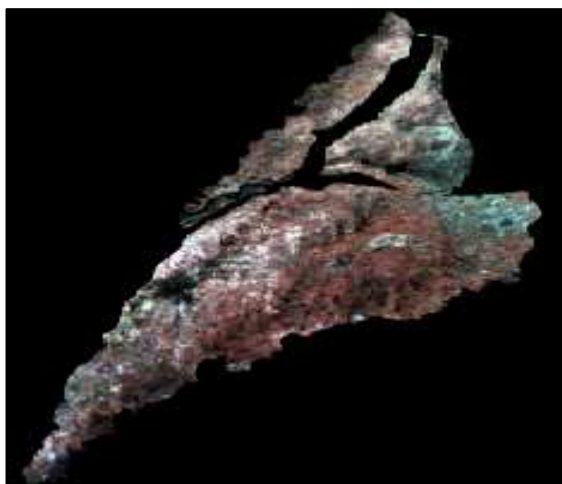
$$IWR = \sum \text{Area of crop} \times \text{CWR} \quad (1)$$

Total irrigation water requirement was calculated from the product of crop acreage determined from satellite data and crop water requirement of specific crop in study area.

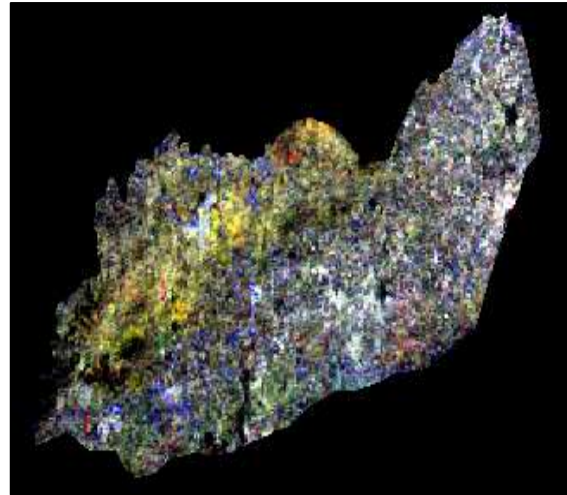
### Results and Discussion

#### Mapping of Land Use

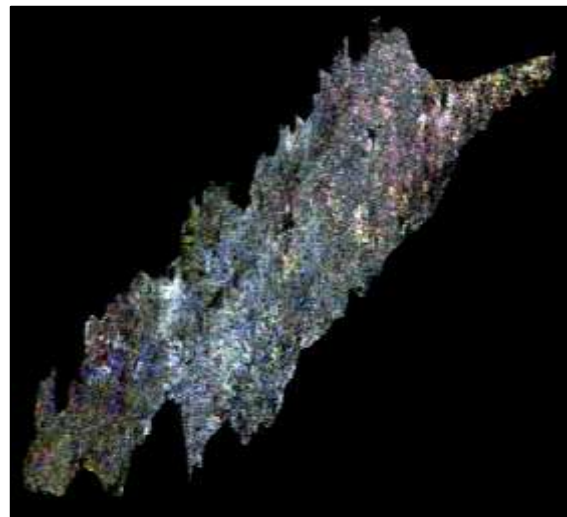
The area of study was divided into three zone such as Haveli circle, Mailsi circle and Nili Bar circle (Figure 3). These images were the stacked images of Haveli, Mailsi and Nili Bar circle which was used in unsupervised classification to make the LULC map. MODIS multi temporal NDVI images having 250m resolution exhibited better potential for detecting and developing crop related mapping of LULC, periods of crops, types of crops, rotation of crops at larger scale e.g. regional and command level. MODIS has moderate spatial, high temporal, good spatial resolution and good global coverage which enables this product to cover large area. Wardlow & Egbert, (2010) found that MODIS has high temporal and spatial resolution which covered larger area.



(a)



(b)



(c)

**Figure 3:** Stack images of (a) Haveli, (b) Mailsi and (c) Nili Bar circle

#### Accuracy assessment analysis

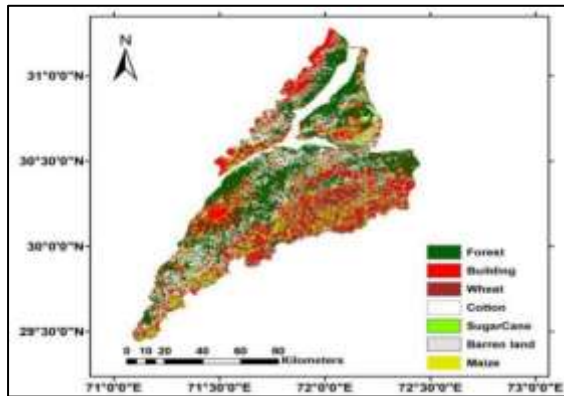
During the process of accuracy assessment, 125 points were used which were recorded in ground truth survey and Google Earth pro was also used in ground truthing of LULC map.

The error matrix algorithm which was performed on Haveli LULC map gave the overall classification accuracy of 83.33% and good of value of Kappa coefficient 0.79, overall classification of LULC classification of Mailsi circle was recorded 77.36% and 0.72 Kappa coefficient and accuracy of LULC map of Nili Bar was recorded 81.25% and 0.61 of Kappa coefficient.

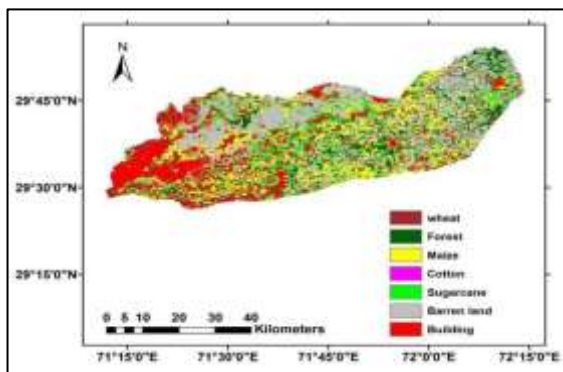
#### Cropping area

The cropping area of major crops in Haveli circle were shown in Table (3.6). The area of

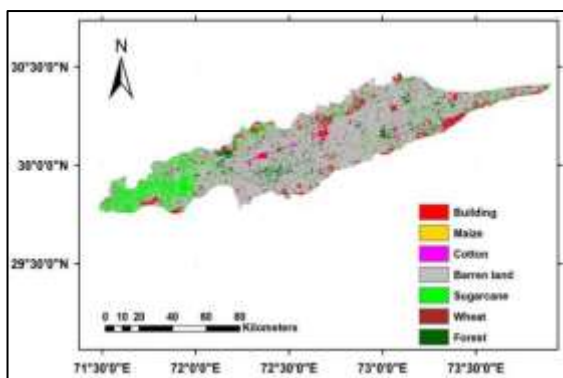
sugarcane, wheat, cotton and maize was 9391, 5043, 15157 and 2160 hectares of in Haveli circle, respectively. The area of sugarcane, wheat, cotton and maize was 20537, 40581, 41681 and 413 hectares of in Mailsi circle, respectively. The area of sugarcane, wheat, cotton and maize was 61162, 18525, 15438 and 7719 hectares of land cultivated in Nili Bar circle, respectively.



(a)



(b)



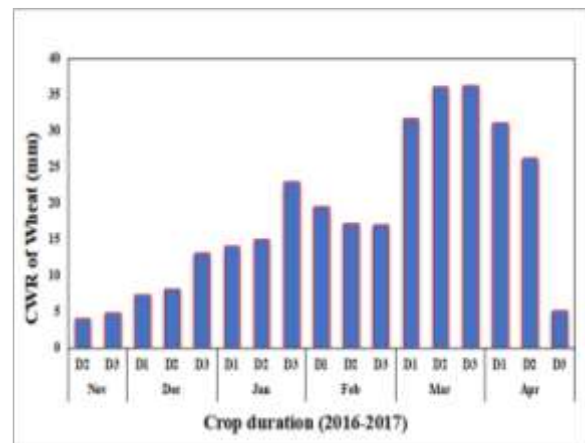
(c)

**Figure 4** LULC map of (a) Haveli, (b) Mailsi and (c) Nili Bar

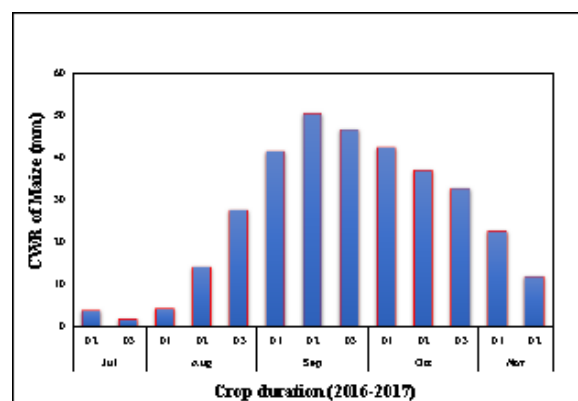
### Irrigation water requirements

Irrigation water requirement of major crops were calculated on 10-days monthly basis intervals

(D1, D2 and D3) and represented in Figures 5 and 6. The minimum value of crop water requirement of wheat crop was 9 mm in the month of November, maximum value was 104.1 mm in the month of March and the total CWR of wheat crop was estimated 310 mm season<sup>-1</sup>. The minimum value of CWR of maize was 5.5 mm in the month of July, the maximum value in the month of September was 139 mm and total CWR of maize crop was estimated 336 mm season<sup>-1</sup>. The recorded minimum value of crop water requirement of cotton was 25.1 mm in the month of November, the maximum value in the month of September was 157 mm and total CWR of cotton crop was estimated 605 mm season<sup>-1</sup>. The crop water requirement of sugarcane was minimum 2.3 mm in the month of December, the maximum value was 272 mm in the month of May and total CWR of sugarcane crop was estimated 1580 mm season<sup>-1</sup>.

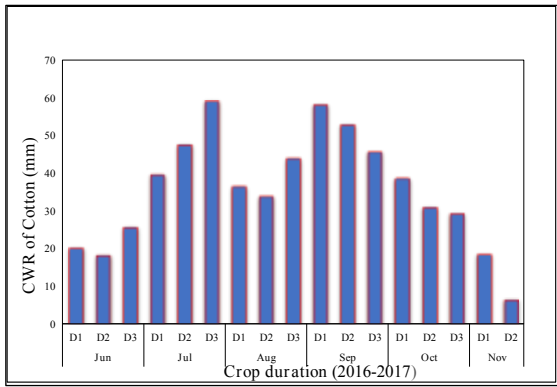


(a)

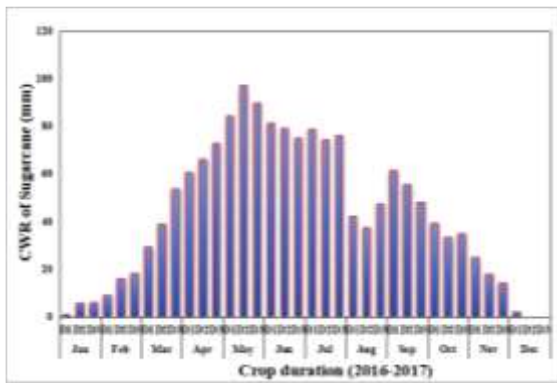


(b)

**Figure 5** (a) Wheat and (b) maize crop water requirement on 10-days interval



(a)



(b)

**Figure 6** (a) Cotton and (b) Sugarcane crop water requirement on 10-days interval

**Seasonal irrigation water requirement**

Irrigation water requirement of major crops of study were calculated using CROPWAT 8.0 model. This model used the Penman-Monteith equation to calculate the  $K_c$  values of different crops with the help of  $ET_o$  and growth stages data of different crops. The data were used for corresponding years of 2016-2017. The Figure (7) showed the irrigation water requirement of Rabi crops i.e. wheat 310mm and Kharif crops i.e. cotton 605mm and maize 336mm, respectively. While, sugarcane crop covered whole cropping season and had irrigation water requirement of 1580mm The IWR of Rabi crops were low due to low temperature which effects the  $ET_o$  values. While in Kharif season, due to heat of summer, the value of  $ET_o$  was higher which increased the irrigation water requirement.

**Canal water deficit**

The Figure (8) showed the comparison of CWR for Rabi and Kharif season in Haveli, Mailsi and Nili Bar circle, respectively. The CWR in Rabi season was recorded as 898, 288 and 567

$Mm^3year^{-1}$  in Haveli, Mailsi and Nili Bar circle, respectively and in Kharif was recorded as

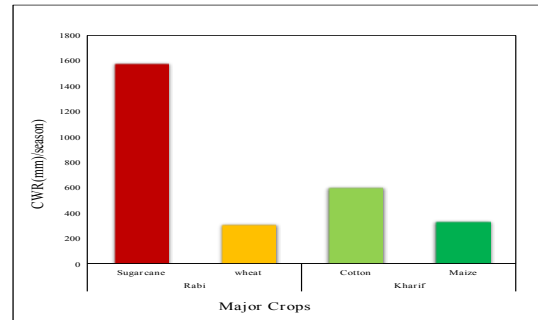


**Figure 7** Irrigation water requirement for Rabi and Kharif crops

1731, 428 and 629  $Mm^3year^{-1}$  in Haveli, Mailsi and Nili Bar circle, respectively. The volume of canal water needed to irrigated crops in Haveli, Mailsi and Nilibar were 2536, 587 and 779  $Mm^3year^{-1}$ , respectively. In Pakistan, a lot of irrigation water is lost before it becomes available to crop for irrigation. The conveyance efficiency is 60% (IDP, 2019). It was meant that only 60% of volume of canal water available to crops. In which canal water deficiency was recorded as 1141 (58%), 235 (51%) and 312 (50%)  $Mm^3year^{-1}$  in in Haveli, Mailsi and Nili Bar circle, respectively (Figure 9). The groundwater was used to fill the demand and supply gap of canal water.

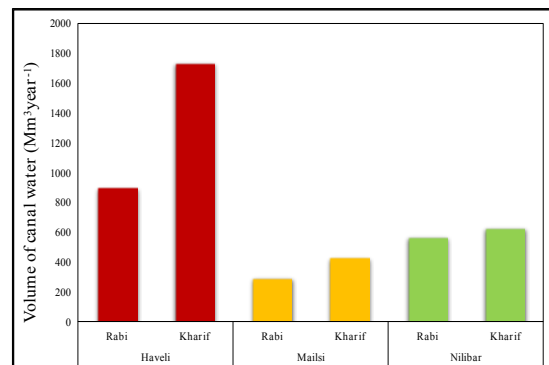


**Fig.8:** CWR of Rabi and Kharif crops

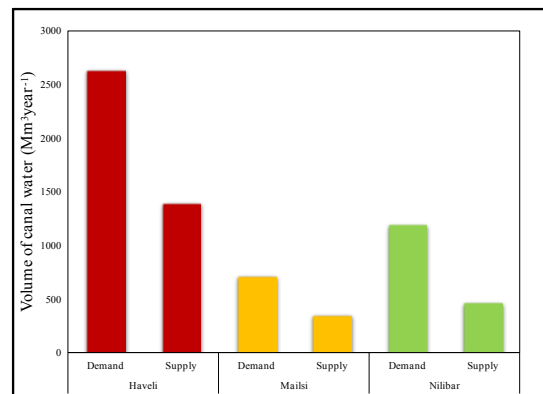


**Fig.9** Seasonal irrigation demand and supply

## Conclusions

In this research work, R programming language was used to acquire MODIS 250 NDVI layer for whole growing season (2016-2017). The estimated cropping area was compared with the reported area of crop reporting department and different Government agencies and their result was good. Certain classes showed low accuracy which is due to small size of field as compared to size of pixel of crop. CROPWAT model was used to estimate the crop water requirement of study area. It was found that 64149, 72276 and 10292 hectares, respectively in Multan Irrigation Zone (MIZ). Crop water requirement of sugarcane, wheat, cotton and maize crop was determined as 1580, 310, 605 and 336 mm season<sup>-1</sup>, respectively. It was found that May and June

## References

- Ahmad, S. (1993). Viability of agriculture resource base: A critical appraisal. *Agricultural Strategies in the 1990s: Issues and Options*. Pakistan Association of Agricultural Social Scientists, Islamabad, 449–466.
- Allen, R G, Smith, M., Pereira, L. S., & Pruitt, W. O. (1997). PROPOSED REVISION TO THE FAO PROCEDURE FOR ESTIMATING CROP WATER REQUIREMENTS. *Acta Horticulturae*, (449), 17–34. <https://doi.org/10.17660/ActaHortic.1997.44.9.2>
- Allen, Richard G, Pereira, L. S., Raes, D., Smith, M., & Ab, W. (1998). Guidelines for computing crop water requirements-FAO Irrigation and drainage paper 56. *Crop Evapotranspiration*, 1–15. <https://doi.org/10.1016/j.eja.2010.12.001>
- Balakrishnan, P. (1986). Issues in water resources development and management & the role of remote sensing. Indian Space Research Organisation.
- Bastiaanssen, W. G. M., Molden, D. J., & Makin, I. W. (2000). Remote sensing for irrigated agriculture: Examples from research and possible applications. *Agricultural Water Management*, 46(2), 137–155. [https://doi.org/10.1016/S0378-3774\(00\)00080-9](https://doi.org/10.1016/S0378-3774(00)00080-9)
- Bruzzone, L., & Prieto, D. F. (2001). Unsupervised retraining of a maximum likelihood classifier for the analysis of multitemporal remote sensing images. *IEEE Transactions on Geoscience and Remote Sensing*, 39(2), 456–460. <https://doi.org/10.1109/36.905255>
- Chaudhry, Q. Z., & Rasul, G. (2004). Agro-climatic classification of Pakistan. *Science Vision*, 9(3–4), 59–66.
- Cheema, M. J. M., & Bastiaanssen, W. G. M. (2010). Land use and land cover classification in the irrigated Indus Basin using growth phenology information from satellite data to support water management analysis. *Agricultural Water Management*, 97(10), 1541–1552. <https://doi.org/10.1016/j.agwat.2010.05.009>
- Cosgrove, W., Rijsberman, F., & Water, C. (2000). *World Water Vision: Making Water Everybody's Business*.
- Defries, R. S., & Townshend, J. R. (1994). N-dvi-Derived Land Cover Classifications At a Global Scale. *International Journal of Remote Sensing*, 15(17), 3567–3586. <https://doi.org/10.1080/01431169408954345>
- FAO. (2019, December 12). CHAPTER 3: CROP WATER NEEDS. Retrieved from FAO: <http://www.fao.org/3/s2022e/s2022e07.htm>
- Foerster, S., Kaden, K., Foerster, M., & Itzerott, S. (2012). Crop type mapping using spectral-temporal profiles and phenological information. *Computers and Electronics in Agriculture*, 89, 30–40. <https://doi.org/10.1016/j.compag.2012.07.015>
- Government of Pakistan. (2010). *Agricultural Census 2010: Pakistan report*. 59.
- were observed peak water demanding months having 272 mm and 236 mm crop water requirement, respectively. Crop water requirement of different crops of area of study was obtained for both growing seasons. Rabi season had 39% and Kharif season had 61.4% requirement of canal of water for different crops for the growing season of 2016-2017. Canal water deficiency was recorded as 1141 (58%), 235 (51%) and 312 (50%) Mm<sup>3</sup>year<sup>-1</sup> in in Haveli, Mailsi and Nili Bar circle, respectively. It is recommended that the cutting edge technology like R Programming language should be used by think tanker for better management of canal water resources.

- IDP. (2019, December Monday). Salient Features of Multan Irrigation Zone. Retrieved From Irrigation Department Punjab: <https://irrigation.punjab.gov.pk/page/1040>
- Khan, S. B., Sobia Sadaf, M., Raja, H., & Kashif, K. P. O. (2010). Publication Team.
- Larkin, K. (2010). Pakistan faces long-term damage to irrigation system. *Nature*. <https://doi.org/10.1038/news.2010.424>
- Lawley, V., Lewis, M., Clarke, K., & Ostendorf, B. (2016). Site-based and remote sensing methods for monitoring indicators of vegetation condition: An Australian review. *Ecological Indicators*, 60, 1273–1283. <https://doi.org/10.1016/j.ecolind.2015.03.021>
- Lobell, D. B. (2013). The use of satellite data for crop yield gap analysis. *Field Crops Research*, 143, 56–64. <https://doi.org/10.1016/j.fcr.2012.08.008>
- Massey, R., Sankey, T. T., Congalton, R. G., Yadav, K., Thenkabail, P. S., Ozdogan, M., & Sánchez Meador, A. J. (2017). MODIS phenology-derived, multi-year distribution of conterminous U.S. crop types. *Remote Sensing of Environment*, 198, 490–503. <https://doi.org/10.1016/j.rse.2017.06.033>
- Mingwei, Z., Qingbo, Z., Zhongxin, C., Jia, L., Yong, Z., & Chongfa, C. (2008). Crop discrimination in Northern China with double cropping systems using Fourier analysis of time-series MODIS data. *International Journal of Applied Earth Observation and Geoinformation*, 10(4), 476–485. <https://doi.org/10.1016/j.jag.2007.11.002>
- Myneni, R., Hoffman, Y., & Knyazikhin. (2002). Global products of vegetation leaf area and fraction absorbed PAR from one year of MODIS data. *Remote Sensing of Environment*, 76, 139–155.
- Nagler, P. L., Cleverly, J., Glenn, E., Lampkin, D., Huete, A., & Wan, Z. (2005). Predicting riparian evapotranspiration from MODIS vegetation indices and meteorological data. *Remote Sensing of Environment*, 94(1), 17–30. <https://doi.org/10.1016/j.rse.2004.08.009>
- Naheed, & et al. (2013). Seasonal Variation of Rainy Days in Pakistan. *Pakistan Journal of Meteorology*, 9(Jan 18, 2013), 9–13.
- Naheed, G., & Mahmood, A. (2009). Water Requirement of Wheat Crop in Pakistan. *Pakistan Journal of Meteorology*, 6(11), 89–97.
- PBS. (2020). Approved Crop Calendar. Retrieved from Pakistan Bureau of Statistics, Government of Pakistan: <http://www.pbs.gov.pk/content/approved-crop-calendar-0>
- R Core Development Team. (2013). R: A language and environment for statistical computing. R Foundation for Statistical Computing, Vienna, Austria. URL <http://www.R-project.org/>. R Foundation for Statistical Computing, Vienna, Austria.
- R Core Team. (2018). R: A language and environment for statistical computing. R Foundation for Statistical Computing, Vienna, Austria. URL <http://www.R-project.org/>.
- Ray, S. S., Dadhwal, V. K., & Navalgund, R. R. (2002). Performance evaluation of an irrigation command area using remote sensing: A case study of Mahi command, Gujarat, India. *Agricultural Water Management*, 56(2), 81–91. [https://doi.org/10.1016/S0378-3774\(02\)00006-9](https://doi.org/10.1016/S0378-3774(02)00006-9)
- Rwanga, S. S., & Ndambuki, J. M. (2017). Accuracy Assessment of Land Use/Land Cover Classification Using Remote Sensing and GIS. *International Journal of Geosciences*, 08(04), 611–622. <https://doi.org/10.4236/ijg.2017.84033>
- Thenkabail, P. S. (2009). Water productivity mapping using remote sensing data of various resolutions to support “more crop per drop.” *Journal of Applied Remote Sensing*, 3(1), 033557. <https://doi.org/10.1117/1.3257643>
- Vasiliades, L., Spiliotopoulos, M., Tzabiras, J., Loukas, A., & Mylopoulos, N. (2015). Estimation of crop water requirements using remote sensing for operational water resources management. *Third International Conference on Remote Sensing and Geoinformation of the Environment (RSCy2015)*, 9535(June), 95351B. <https://doi.org/10.1117/12.2192520>
- Wardlow, B. D., & Egbert, S. L. (2010). A comparison of MODIS 250-m EVI and NDVI data for crop mapping: A case study for southwest Kansas. *International Journal of Remote Sensing*, 31(3), 805–830. <https://doi.org/10.1080/01431160902897858>
- Wood, S., Sebastian, K., & Scherr, S. J. (2000). Pilot analysis of global ecosystems: agroecosystems. World Resources Institute.



- Waqas, M.M., Awan, U.K., Cheema, M.J.M., Ahmad, I., Ahmad, M., Ali, S., Shah, S.H.H., Bakhsh, A. and Iqbal, M., (2019). Estimation of canal water deficit using satellite remote sensing and GIS: a case study in lower chenab canal system. *Journal of the Indian Society of Remote Sensing*, 47(7), 1153-1162.
- Molden, D.J. and Gates, T.K. 1990. Performance measures for evaluation of irrigation-water-delivery systems. *J. Irrig. Drain. Eng.*, 116, 804–823.

## Formulation of Precision Input Management Strategy for Wheat using Handheld Crop Sensor

Huzaifa Shahzad<sup>1</sup>, Hafiz Umar Farid<sup>1\*</sup>, Zahid Mahmood Khan<sup>1</sup>, Aamir Shakoor<sup>1</sup>, Rana Muhammad Asif Kanwar<sup>1</sup>, Khawar Abbas<sup>1</sup>

<sup>1</sup> Department of Agricultural Engineering, Bahauddin Zakariya University, Multan 60800, Pakistan

Corresponding author email: [hufarid@bzu.edu.pk](mailto:hufarid@bzu.edu.pk)

**Abstract:** The precise monitoring of nitrogen (N) is an effective strategy to develop and enhance the crop yield per unit of land. Precision control of nitrogen (N) is a useful approach to improving the productivity of land and crops, but it involves field-level spatial variability data. The primary objective of this study was to formulate the precision input management strategy for wheat to achieve maximum productivity per unit land using the Green Seeker handheld crop sensor. The spatial variability in the field was identified based on soil sampling of 80 samples at a depth ranging from 0 cm to 30 cm. The spatial pattern was analyzed for the Soil pH, Soil EC, Soil sodium ion ( $\text{Na}^+$ ), Soil nitrogen (N), Soil organic matter (O.M) and carbon (O.C), and Soil available potassium (AK) and phosphorus (AP). A total of 8 treatments were applied by applying a randomized complete block design (RCBD) with four total replications. The extent of variability was confirmed by CV (%) which was > 30% for all the soil parameters except for pH having CV = 4.1 (%). The spatial analysis indicated maximum grain yield in the right corner of the North-East zone extending from the center of the study area to the South-east zone due to high values of soil N, O.M & O.C in the study area. The  $(\text{PNAR})_{G.S}$  was identified 90-100 kg/ha that yields 3699 kg/ha and the  $(\text{PNAR})_{S.B}$  was 110-117 kg/ha that yields 3231 kg/ha. The average nitrogen requirement ( $N_{rea}$ ) was 0.027 kg/kg and 0.021 kg/ka based on the Green Seeker application rate. The results indicated strong linear relation of BY ( $R^2 = 0.85$ ) and GY ( $R^2 = 0.80$ ) with GS\_NDVI. The calibrated models predicted effectively the BY, GY, and Plant N-uptake with  $R^2 = 0.85, 0.84, \text{ and } 0.81$ , respectively. The predicted models were evaluated based on low RMSE of 412.3 kg/ha, 307.9 kg/ha, and 0.06% for BY, GY, and N uptake, respectively. The results recommended the use of precision nitrogen management strategies originated from crop sensors and soil analysis to reduce field variabilities and provide a sustainable environment that enhances crop productivity for small landholders.

**Keywords:** Green Seeker, Spatial Variability, NUE, RCBD, RMSE, PFP

### Introduction

Application of fertilizer and pesticide inputs conferring to the necessity of field and crop at the right place can be achieved by most efficiently by precision farming practices. The operation of the innovative management practices in various farming systems involves the knowledge of spatial variability in soil and crop pattern. An ideal amount of N fertilizer must be received by agriculture land to attain increasing nitrogen effectiveness and maximum productivity return, higher crop yield. The patterns of crop growth and crop yield of agricultural land are extremely affected by the over-fertilization and under fertilization due to conventional farming practices. To overcome these negative impacts produced, the use of an optimal N rate on the agricultural land is very compulsory. Thus, for the adaptability of precision farming in agriculture, the practice of innovative proximal sensing and remote sensing methods seems a

vilifying solution [1]–[3]. Nitrogen management decisions can be critically enhanced by nitrogen use efficiency (NUE) [4]. NUE can be increased through an improved choice of management practices (e.g. application rate and timing of nitrogen, sowing date), crop genetic improvement, and crop growing environment (e.g. climate and type of soil) [5]. [6] projected that only 33% of N fertilizer recovered at the end of the crop while the rest of 67% N fertilizer leads to environmental contamination and economic losses. However, the amount of available N minerals declines temporally because of spatial variabilities influenced by the optimum in-season rate of N-fertilizer [7]. However, the precision N-management approaches are necessary to be optimized over the lands facing nutrient deficiencies and low N use efficiencies. This may not only removes the risk of environmental contamination but also increases yield per unit land of cereal crops [8], [9]. Sustainable agricultural development

practices are required to be promoted to overcome growing food demands and declining natural food resources. Small landholders need to focus on these development approaches to maximize per unit land productivity. Hence, precision agriculture approaches are the fruitful method to uphold the declining natural resources by applying inputs only at the right time of need [10].

Additionally, keeping in mind the changing spatial behaviors of physiochemical soil parameters, Variable rate technologies could be the productive method to apply fertilizer [11]. [12] reported precision agriculture techniques in combination with the variable rate technology are the most effective way to make N-management strategy based on the spatial variability. Moreover, N-management strategies can also be developed using a handheld sensor providing real-time variable fertilizer rates over the field. These sensors are the key tools to boost the crop yield per unit land of less fertile soils [7], [13]. However, the crop N sensor never provides the actual amount of required fertilizer, rather the actual N status of plants analyzed through vegetation indices through these crop N sensors. One of the most common and effective indices is the Normalized difference vegetation indices (NDVI) that assist in making in-season N requirement algorithms [14]. Depending upon the developed N algorithms, plant N needs can be calculated easily to meet the requirement of crop nutrient level in the entire field [15].

## Materials and Methods

### Study Area

The experimental field for the study was selected at Agriculture Research Farm of the Department of Agricultural Engineering, Bahauddin Zakariya University, Multan. The study area lies between 71.7389°E and 30.4358°N which covers an area of 1.00 ha. The study area is located in District Multan, Punjab Pakistan. The district Multan lies between 71.5247° E and 30.1575° N. The total covered area of Multan is 286 km<sup>2</sup> with an elevation of 124 meters above the mean sea level. The climatic conditions of Multan are arid with sweltering summer and cold winters. The temperature of the city is usually high in the summer season. All for seasons can be seen in Multan i.e., Summer (alongside monsoon), Winter, Spring, and Autumn. The climate in Multan is called a desert climate. There is

virtually no rainfall during the year in Multan. The average annual temperature is 25.6 °C in Multan. In a year, the average rainfall is 175 mm. Triticum Astivum L. (Wheat) was selected to be sown on the site based on its importance of providing energy, protein, and fiber to the world's population.

### Sampling and Treatment preparation

A total of 80 soil samples from the top of the soil in the field, collected using soil augurs at a depth ranging from 0-30 cm. Each of the sample were taken to library to access spatial variability for soil pH, EC, Na<sup>+</sup>, OM, OC, AP and AK. Overall, 32 plots were prepared with 8 treatments from T1 to T8. All the treatments were applied using RCBD design with four total replications mainly to control the variation in the field.

### Green Seeker measurements and plant sampling

The GS\_NDVI were recorded timely at the growing stages of wheat germination, 3-feeekes, 5-feeekes, booting stages and before the harvesting of the crop mainly to develop the nitrogen fertilizer optimization algorithm. The plant sampling was performed during the growing stages of wheat to analyze the plant N-uptake by Kjeldahl's method.

### Data analysis

The collected data was analyzed statistically using the software Statistix 10.0. The descriptive statistical analysis was conducted to check the (minimum, maximum, mean, SD, Kc, Ks and CV) of all physiochemical soil parameters. The Pearson's correlation analysis was conducted using Statistix 10.0 to analyze the relationship among the soil parameters. The regression analysis was performed for plant N uptake vs GS\_NDVI and Grain yield vs GS\_NDVI. The observed yields were plotted against the calibrated prediction model equations. To validate the generated equations, the models were tested to determine the goodness of fit among the observed and predicted data for wheat.

$$RMSE = \sqrt{\frac{\sum_{i=1}^n (P_i - A_i)^2}{n}}$$

Where, P<sub>i</sub> and A<sub>i</sub> are the predicted and actual yield values and n represents the total no of observations. The goodness of fit for the model is confirmed if the obtained RMSE value was less.

$$NRMSE = \frac{RMSE}{A_{vi}} \times 100$$

Where  $A_{vi}$  represents the average actual yield. The goodness of fit for calibrated model is considered excellent if the NRMSE less than 10%, good if more than 10% and less than 20%, fair if more than 20% and less than 30%, and poor if more than 30% [16].

## Results and Discussions

### Descriptive Statistics

The variability among the soil physio-chemical soil parameters were analyzed based on the coefficient of variation. [17] defined criteria to identify the variability existing in the physiochemical properties of soil parameters. Depending upon CV a parameter has low variability when the CV is less than 10% ( $CV < 10\%$ ), medium variability when CV ranges between 10% to 20% ( $10\% \leq CV \leq 20\%$ ), high variability when it ranges between 20% to 30% ( $20\% \leq CV \leq 30\%$ ), and very high variability when the CV is greater than 30% ( $CV > 30\%$ ). The observed results indicated very high variability ( $CV > 30\%$ ) among the parameters except for soil pH ( $CV < 10\%$ ). The maximum value for GY was observed 4000.3 kg/ha whereas the minimum value was 540 kg/ha. The observed skewness results indicated the soil pH and GY were negatively skewed while the other parameters represented the positive skewness. The descriptive statistics is shown in the Table 1.

### Pearson's Correlation

The strength of linear relationship between the two parameters were determined by Pearson's

correlation. The results indicated the highest correlation was observed between the organic carbon and organic matter, significant at  $p = 0.05$ . A strong positive correlation relation of nitrogen (N) was indicated with organic matter and organic carbon. [18] reported the organic matter acts as an agent that boost up many soil properties like the structure of the soil, water holding capacity of the soil, and nutrient supply. The soil organic matter and organic carbon have a strong bond to deal with the supply of crop N and the demand for the crop N. Similarly, soil pH and soil EC indicated a positive correlation between them. [19] reported higher the value of pH, the higher it will associate with the increasing values for soil EC. The Pearson's correlation of the soil parameters is shown in Table 2.

### Wheat Grain Yield (Kg/ha)

The regression analysis was performed using MS Excel. The relationship between grain yield and GS\_NDVI. The relationship is shown in the Figure 1. The regression analysis was performed by following linear, polynomial, quadratic, exponential, power and logarithmic equations. The linear model was selected based on the best coefficient of determination value  $R^2 = 0.85$ . The maximum grain yield was observed 4000.3 kg/ha against the GS\_NDVI value 0.73.

**Table 1** Descriptive statistics for physiochemical properties of soil parameters

Parameters	Min	Max	Mean	SD	Kc	Ks	C.V
pH	8.600	10.300	9.432	0.389	-0.557	-0.351	4.124
EC (dS/m)	0.390	2.800	1.364	0.477	0.817	0.631	34.995
Na <sup>+</sup> (mmol/100g)	0.600	5.900	2.815	1.044	0.291	0.591	37.085
OM (%)	0.050	0.730	0.275	0.151	1.305	1.250	55.191
OC (%)	0.029	0.423	0.159	0.088	1.305	1.250	55.191
N (%)	0.003	0.046	0.017	0.009	1.239	1.344	52.923
AP (ppm)	1.000	13.00	4.200	3.289	1.078	0.151	78.319
AK (ppm)	210	640	411.32	124.54	0.176	-0.978	30.27
GY (kg/ha)	540.54	4000.3	2666	783.28	-0.430	-0.403	38.908

**Table 2** Pearson's Correlation between soil physiochemical parameters

	pH	EC (dS/m)	Na <sup>+1</sup> (mmol/100g)	OM (%)	OC (%)	N (%)	AP (ppm)	AK (ppm)
<b>pH</b>	1.000							
<b>EC</b>	0.346*	1.000						
<b>Na<sup>+1</sup></b>	0.457*	0.502**	1.000					
<b>OM</b>	-0.342*	0.031 <sup>NS</sup>	0.038 <sup>NS</sup>	1.000				
<b>OC</b>	-0.342*	0.031 <sup>NS</sup>	0.038 <sup>NS</sup>	1.000**	1.000			
<b>N</b>	-0.396*	-0.028 <sup>NS</sup>	0.012 <sup>NS</sup>	0.920**	0.920**	1.000		
<b>AP</b>	-0.545*	-0.176 <sup>NS</sup>	-0.074 <sup>NS</sup>	0.418*	0.418*	0.427*	1.000	
<b>AK</b>	-0.197 <sup>NS</sup>	0.343*	0.170*	0.336*	0.336*	0.282*	0.222*	1.000

Here (\*) represents the values or "r" are significant at 0.05 level, (\*\*) represents the values or "r" is significant at 0.01 level and "NS" describes the value or "r" are not significant at any level.

### Plant N uptake (%)

Similarly, the relationship between plant N uptake and the fertilizer treatment levels was plotted using MS Excel. The power function regression model was selected based on the  $R^2 = 0.91$ . The maximum plant N uptake was observed for the N fertilizer rate 90-110 kg/ha.

The observed plant N-uptake was higher for the N fertilizer level as suggested by  $(PNAR)_{G,S}$  (Figure 2). The other treatments were observed with less plant N uptake due to the over and under supply of N-fertilizer. This further confirms the growth of plants relies on the optimum supply of nitrogen fertilizer to carry out the nitrogen cycle.

### Effect of nitrogen on crop attributes

The effect of N-fertilizer on crop attributes were found significant at  $p \leq 0.05$ . The mean grain yield was observed increasing up to the  $(PNAR)_{G,S}$  and declines because of the excess supply of the N fertilizer. The over fertilizer application after reaching the optimum level tends to reduce the grain yield, however the biological yield still may increase due to the excess N-fertilizer supply [20]. Similarly, it was analyzed that with an increase in the application of N fertilizer, the absorption of plant N

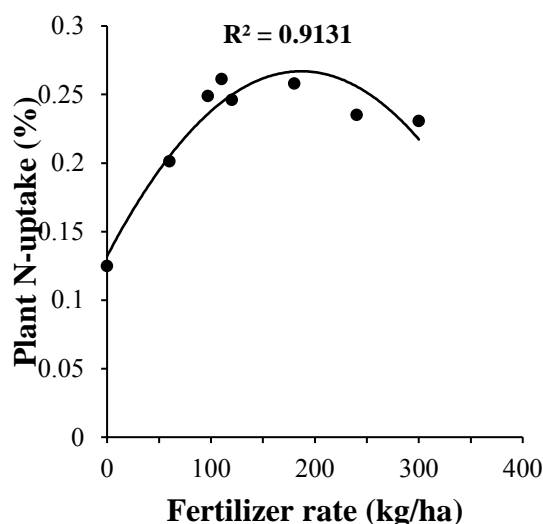


**Figure 1** Relationship between GY and  $GS\_NDVI$

improved substantially. The highest values of plant N uptake were observed at 0.261 % against the treatment T7. However, the lower value of N uptake was recorded for the treatment T1, with no fertilizer application. [21] reported in his research, that the pattern for plant N uptake was influenced by the changing application of N fertilizer. [22] stated the enhancement of both N uptake by plants and grain yield by applying the precise amount of N fertilizer. The effect of N-fertilizer on crop attributes is shown in the Table 3.



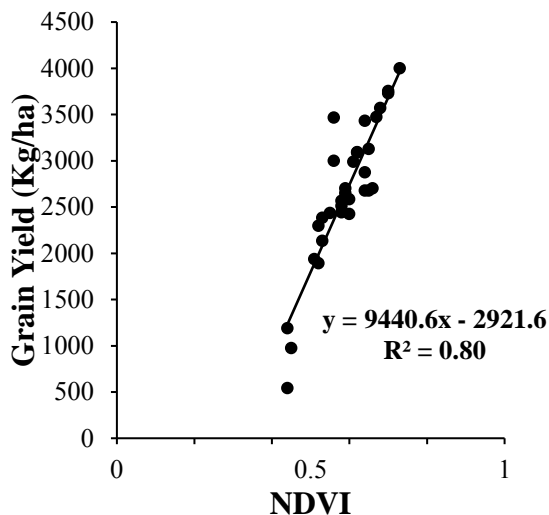


**Figure 2** Relationship between plant N-uptake and Fertilizer rate

**Table 3** Effect of N-fertilizer on crop attributes

Treatments	Fertilizer (kg/ha)	Mean GY (kg/ha)	N-uptake
T1	0 (C.A)	764.1 <sup>F</sup>	0.125 <sup>E</sup>
T2	60	2058.7 <sup>DE</sup>	0.201 <sup>CD</sup>
T3	120	2874.6 <sup>B</sup>	0.246 <sup>BC</sup>
T4	180	2367.9 <sup>B</sup>	0.258 <sup>AB</sup>
T5	240	2170.5 <sup>CD</sup>	0.235 <sup>ABC</sup>
T6	300	1960.6 <sup>DE</sup>	0.230 <sup>BC</sup>
T7	110-117	3231.7 <sup>C</sup>	0.261 <sup>A</sup>
T8	90-100	3699.4 <sup>DE</sup>	0.249 <sup>BC</sup>

C.A: Control application, Different letters in the same columns indicate the level of significance at  $p \leq 0.05$ .

### Prediction of GY and N uptake

The prediction models were calibrated by the help of wheat crop data obtained from the previous year. The regression analysis was performed, and the linear function equations were selected based on their coefficient of determination values. The values of  $R^2$  for calibrated linear relation were observed 0.803 and 0.809 for grain yield and plant N uptake, respectively. The predicted and the actual values for grain yield were plotted against each other. The results indicated the  $R^2$  for the grain yield was 0.84 among the predicted and actual values of the grain yield. The comparison of predicted and actual grain yield is shown in the Figure 3. Similarly, the predicted and the actual values for grain yield were plotted and the  $R^2$  of 0.81 were observed. The comparison of predicted and

actual plant N uptake is shown in the Figure 4. The selected equations are given below:  
 $Y$  (Grain yield) =  $6925$  (GS\_NDVI) -  $1756.7$   
 $Y$  (N-uptake) =  $0.8232$  (GS\_NDVI) -  $0.2273$

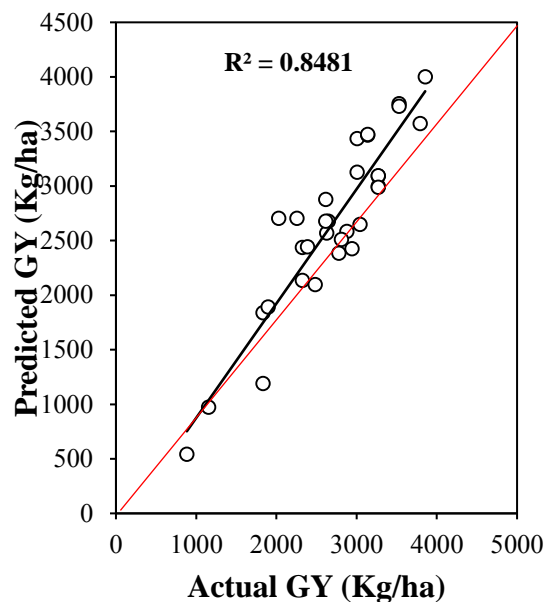


**Figure 3** Comparison of predicted and actual grain yield (kg/ha)

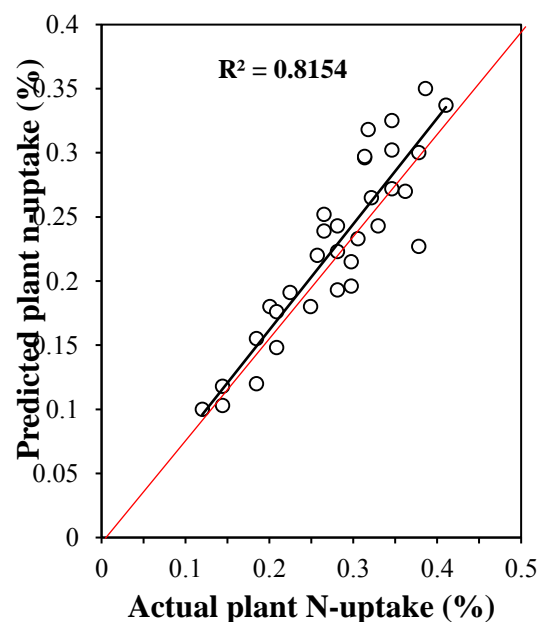


**Figure 4** Comparison of actual and predicted plant N uptake

### Validation of prediction models

The calibrated models were validated by the help of RMSE (kg/ha) and NRMSE (%). The results indicated the RMSE of grain yield and plant N uptake were 307.9 kg/ha and 0.06% which were lower to validate the model. Similarly, the

observed NRMSE for grain yield and Plant N-uptake were greater than 10% and less than 20% indicated good performance of predicted model (Table 4).

**Table 4** Performance evaluation of models

Crop Attributes	RMSE (Kg/ha) & (%)	NRMSE (%)
Grain Yield	307.93	11.59
N-uptake	0.06	14.23

### Nitrogen Fertilizer Optimization Algorithm (NFOA)

Following algorithm was developed based on our analysis:

1. Predicting the grain yield using GS (NDVI) before topdressing N fertilizer application.
2. Grain yield (kg/ha) = 9440.6 \* (GS\_NDVI) - 2921.6
3. The average nitrogen requirement ( $N_{req}$ ) for grain yield was 0.021 and 0.027 kg/kg for yield ranges of 3231 kg/ha and 3699 kg/ha based on (PNAR)<sub>S.B</sub> and (PNAR)<sub>G.S</sub> application rate.
4. Calculate the final precision nitrogen uptake (FPNU) through N-requirement and predicted yield:

$$FPNU \text{ (kg N/ha)} = N\text{-requirement} \times \text{yield}$$

5. Predicting the early season plant N-uptake (EPNU) using GS\_NDVI before topdressing: EPNU(kg N/ha)=0.8232\*(GS\_NDVI)- 0.2273
6. Determination of topdressing nitrogen requirement using the formula:

$$NR \left( \text{kg} \frac{N}{\text{ha}} \right) = \frac{FPNU - EPNU}{\text{Nitrogen use efficiency (NUE)}}$$

The NUE value was set to 40 %.

### Conclusions

Following conclusions has been drawn from our research:

1. Each of the soil parameter (soil EC,  $Na^+$ , OM, OC, AP and AK) and GY except for soil pH showed higher soil variability based of the coefficient of variation (CV), which was above the acceptable limit  $CV > 20\%$ .
2. The higher grain yield was observed 3699 kg/ha and 3231 kg/ha for the treatment levels based on (PNAR)GS and (PNAR)SB respectively, as compared to the other N-fertilizer levels showed better yield with the application of precision N management strategies. Each level was found significant at  $p \leq 0.05$ .
3. The grain yield was observed increasing with N-fertilizer application from 0 kg/ha up to the (PNAR)GS, but declined above the PNAR showed over-application of N-fertilizer reduced crop productivity per unit land.

4. The optimal N rate determined for (PNAR)GS and (PNAR)SB were 90 kg/ha and 110 kg/ha, which indicated the precision N management strategies can help to reduce the fertilizer application cost.
5. The average N requirement for grain yield was 0.021 kg/kg and 0.027 kg/kg for (PNAR)SB and (PNAR)GS which indicated for the smaller and larger areas, the instant application of N fertilizer precisely by handheld crop sensors.
6. The relation of plant N uptake with GS\_NDVI showed that the requirement for application of in season N-fertilizer can be determined by using the NDVI data for the management of field N losses.
7. Overall results of this study found that the rate of Precision N-fertilizer application increased crop yield. Therefore, the precision N management practices needed to be focused based on soil basis and N assessment by handheld crop sensors to mitigate the spatial variabilities of study area.

### References

- [1] Q. Cao, Z. Cui, X. Chen, R. Khosla, T. H. Dao, and Y. Miao, "Quantifying spatial variability of indigenous nitrogen supply for precision nitrogen management in small scale farming," *Precis. Agric.*, vol. 13, no. 1, pp. 45–61, 2012, doi: 10.1007/s11119-011-9244-3.
- [2] L. Quebrajo, M. Pérez-Ruiz, A. Rodriguez-Lizana, and J. Agüera, "An approach to precise nitrogen management using handheld crop sensor measurements and winter wheat yield mapping in a mediterranean environment," *Sensors (Switzerland)*, vol. 15, no. 3, pp. 5504–5517, 2015,
- [3] T. Oksanen, *Estimating operational efficiency of field work based on field shape*, vol. 4, no. PART 1. IFAC, 2013.
- [4] S. Asseng, N. C. Turner, and B. A. Keating, "Analysis of water- and nitrogen-use efficiency of wheat in a Mediterranean climate," *Plant Soil*, vol. 233, no. 1, pp. 127–143, 2001,
- [5] M. A. Semenov, P. D. Jamieson, and P. Martre, "Deconvoluting nitrogen use efficiency in wheat: A simulation study," *Eur. J. Agron.*, vol. 26, no. 3, pp. 283–294, 2007, doi: 10.1016/j.eja.2006.10.009.
- [6] W. R. Raun and G. V. Johnson, "Improving nitrogen use efficiency for cereal production," *Agron. J.*, vol. 91, no. 3, pp. 357–363, 1999,

- [7] N. R. Kitchen et al., "Economic and environmental benefits from canopy sensing for variable-rate nitrogen corn fertilization," *Am. Soc. Agric. Biol. Eng. Annu. Int. Meet. 2009, ASABE 2009*, vol. 8, no. 09, pp. 4774–4790, 2009,
- [8] J. F. Shanahan, N. R. Kitchen, W. R. Raun, and J. S. Schepers, "Responsive in-season nitrogen management for cereals," *Comput. Electron. Agric.*, vol. 61, no. 1, pp. 51–62, 2008, doi: 10.1016/j.compag.2007.06.006.
- [9] F. Solari, J. Shanahan, R. Ferguson, J. Schepers, and A. Gitelson, "Active sensor reflectance measurements of corn nitrogen status and yield potential," *Agron. J.*, vol. 100, no. 3, pp. 571–579, 2008, doi: 10.2134/agronj2007.0244.
- [10] 2010 Godfray et al., "Godfray, H.C.J., Beddington, J.R., Crute, I.R., Haddad, L., Lawrence, D., Muir, J.F., Pretty, J., Robinson, S., Thomas, S.M. and Toulmin, C., 2010. Food security: the challenge of feeding 9 billion people. *science*, 327(5967), pp.812-818.," *sciencemag.org*, 2010.
- [11] R. K. Roberts, B. C. English, and S. B. Mahajanashetti, "Evaluating the Returns to Variable Rate Nitrogen Application," *J. Agric. Appl. Econ.*, vol. 32, no. 1, pp. 133–143, 2000,
- [12] J. Van Loon, A. B. Speratti, and B. Govaerts, "Precision for smallholder farmers: A small-scale-tailored variable rate fertilizer application kit," *Agric.*, vol. 8, no. 4, 2018,
- [13] Y. Yao et al., "Active canopy sensor-based precision N management strategy for rice," *Agron. Sustain. Dev.*, vol. 32, no. 4, pp. 925–933, 2012, doi: 10.1007/s13593-012-0094-9.
- [14] A. C. Tagarakis and Q. M. Ketterings, "Proximal sensor-based algorithm for variable rate nitrogen application in maize in northeast U.S.A.," *Comput. Electron. Agric.*, vol. 145, no. August 2017, pp. 373–378, 2018,
- [15] B. S. Tubaña et al., "Adjusting midseason nitrogen rate using a sensor-based optimization algorithm to increase use efficiency in corn," *J. Plant Nutr.*, vol. 31, no. 8, pp. 1393–1419, 2008,
- [16] K. Loague and R. E. Green, "Statistical and graphical methods for evaluating solute transport models: Overview and application," *J. Contam. Hydrol.*, vol. 7, no. 1–2, pp. 51–73, 1991,
- [17] 2002 Gomes and Gracia, "Pimentel-Gomes, F. and Garcia, C.H., 2002. *Estatística aplicada a experimentos agronômicos e florestais: exposição com exemplos e orientações para uso de aplicativos (Vol. 309)*. Piracicaba: Fealq."
- [18] R. Hijbeek, "On the role of soil organic matter for crop production in European arable farming. ."
- [19] I. Kisić and I. Jurisic, "INFLUENCE OF WILDFIRE AND FIRE SUPPRESSION BY SEAWATER ON SOIL PROPERTIES," vol. 13, no. 4, pp. 1157–1169, 2015.
- [20] M. Ghobadi and M. Ghobadi, "Effect of Anoxia on Root Growth and Grain Yield of Wheat Cultivars," undefined, 2010.
- [21] H. Sun, H. Zhang, J. Min, Y. Feng, and W. Shi, "Controlled-release fertilizer, floating duckweed, and biochar affect ammonia volatilization and nitrous oxide emission from rice paddy fields irrigated with nitrogen-rich wastewater," *Paddy Water Environ.*, vol. 14, no. 1, pp. 105–111, 2016,
- [22] Z. Wen, J. Shen, M. Blackwell, H. Li, B. Zhao, and H. Yuan, "Combined Applications of Nitrogen and Phosphorus Fertilizers with Manure Increase Maize Yield and Nutrient Uptake via Stimulating Root Growth in a Long-Term Experiment," *Pedosphere*, vol. 26, no. 1, pp. 62–73, 2016,

## Role of oblique vegetation in flood mitigation

Shahbaz Khalid<sup>1\*</sup>, Ghufraan Ahmed Pasha<sup>1</sup>, Usman Ghani<sup>1</sup>, Afzal Ahmed<sup>1</sup>, Muhammad Asghar<sup>1</sup>,  
Ammar Sabir<sup>1</sup>

<sup>1</sup> Department of Civil Engineering, University of Engineering and Technology Taxila

Corresponding author email: [shahbazkhalid.02@gmail.com](mailto:shahbazkhalid.02@gmail.com)

**Abstract:** Universally, floods are known as the most destructive natural hazard, resulting in loss of lives and a huge loss of property. The inimitable climatic condition of Pakistan renders its susceptibility to different types of floods, throughout the year. In the monsoon season, heavy rainfall and flash floods in northern areas pose severe problems to the people. Structural damage due to water-based disasters such as floods is the main problem of peoples living near flooding areas. This paper discusses a series of experiments where energy loss, hydrostatic forces, and hydrodynamic forces on the house of varying porosity are investigated for oblique vegetation. Water surface profiles for different orientations of vegetation are examined. The results show that the percentage increase in the house porosity decreases the hydrostatic force contrarily increases in hydrodynamic force. The maximum loss of energy is observed for oblique vegetation with an angle of 30°.

**Keywords:** Flood control; hydrodynamic loading; oblique vegetation; hydrostatic force

### Introduction

Flood is considered the most devastating natural hazard. During the last three decades, the frequency of flood disaster loss is increased in both economic and structural damages. Thus, there is a rising consent that climate-changing is leading to an increase in floods' magnitude and frequency. A past study of floods shows that Pakistan has been badly affected by sixteen major floods, which resulted in huge loss of lives and structural destruction. (Commission, 2009) It is observed that most of the river basins in Punjab and Sindh are severely affected by the floods. Since 1947 Pakistan has lost US\$ 6 billion due to the floods. Over the six decades, more than 7693 Pakistani have lost their lives, and more than 1,00,654 villages are affected by floods (Commission, 2009). Research findings found that flood dynamic loading and impact load caused by wooden debris plays a vital role in structure destruction (Cuomo *et al.*, 2009; Palermo, Nistor and Al-faesly, 2012; Como and Mahmoud, 2013). There is a need to propose such reforms to mitigate the dynamic effects of floods. Many researchers have worked to find such methods to minimize flood energy using both natural (soft) and artificial (hard) methods (Tanaka, 2012; Nateghi *et al.*, 2016; Rahman, Schaab and Nakaza, 2017) worldwide, natural method is being used as flood mitigation (Pasha and Tanaka, 2017). A combined effect of vegetation to dissipate the flood energy was

observed (Ahmad *et al.*, 2020; Asghar *et al.*, 2020; Tariq and Pasha, 2020). The effect of oblique vegetation is not yet considered.

The susceptibility of a building structure is generally dependent on both flow rate and the water depth. Empirical investigation derived from the historical floods is relatively minimal (Saatcioglu, Ghobarah and Nistor, 2006). So, it is necessary to account for several queries related to such phenomenon provoke for recent positioning proceeding the traditional and deterministic approach to risk valuation. Post-flood-survey reports have exposed that coastal forests worked to reduce the disastrous effect of the floods. Thickness and density of vegetation both help to increase water upstream of the vegetation. (Rahman, Schaab and Nakaza, 2017) Vegetation work as energy mitigation, trapping debris, providing an easy escape route to flood water. It is determined experimentally and numerically, flood force reduction due to the coastal forest is greatly dependent on the geometry and density of the forest. It is experimentally determined that by increasing the aspect ratio of vegetation, both the water level and the velocity at the downstream side of the vegetation are greatly decreased. Declination in both water level and velocity of flow at the downstream side is observed while increasing the aspect ratio of vegetation (Rahman, Schaab and Nakaza, 2017).

Flow characteristics also depend on the geometry of the coastal forest. The occurrence of the hydraulic jump, energy loss phenomenon, and

the flow pattern show a considerable effect of the vegetation pattern. Experiments were conducted to evaluate the energy loss through the vegetation of varying thickness, density and under dissimilar flow conditions. Different patterns of hydraulic jumps were also analyzed (Pasha and Tanaka, 2017; Rahman, Schaab and Nakaza, 2017). After colliding with vegetation, flood water loses its power and strikes the house with minimum energy. Due to energy loss, the probability of washout of the house becomes smaller (Tanaka and Ogino, 2017; Asghar *et al.*, 2020). The past studies recognized that by increasing the opening of the house, a linear reduction in hydrostatic force is observed (Wüthrich *et al.*, 2018). A combined effect of vegetation and the house model to mitigate the flood energy has also been examined (Asghar *et al.*, 2020), but the role of oblique vegetation was not considered. This research will help to understand the behavior of oblique vegetation against the catastrophic flood. A series of experiments is performed to observe the behavior of oblique vegetation on the house of varying porosity to mitigate the flood energy. An experimental study comprising of opening in the house and its response to oblique vegetation is also investigated in this paper.

### Forces on building due to flood

The fragility of the building structure (structure stability of buildings) depends on both of capacity and loading of the building. This paper focuses on the loading on structures induced by the flood. During extreme floods, buildings are suspected to both hydrostatic and hydrodynamic loads.

#### Hydrostatic force.

Horizontally acting hydrostatic force ( $F_{hs}$ ) mainly depends on the change in the upstream and downstream water level of the house. FEMA P-55 (Bass and Koumoudis, 2012)

$$F_{h,static} = \frac{1}{2} \rho g (h_{us}^2 - h_{ds}^2) \quad (1)$$

In the given equation, " $\rho$ " is the density of water " $g$ " is gravitational acceleration " $h_{us}$ " and " $h_{ds}$ " are the upstream and downstream water levels of the house, respectively.

#### Hydrodynamic force

The hydrodynamic load results from the combination of drag and inertia. Hydrodynamic force ( $F_{hd}$ ) mainly depends on the kinematics

characteristic of flow and dynamic properties and geometry of the structure.

Hydrodynamic force induces by the flood depends on the water level on the upstream wall of the house and the velocity of the flowing water.

In practice, the simplified formula FEMA P-55 (Bass and Koumoudis, 2012) is used to calculate the hydrostatic force per unit length.

$$F_{h,dynamic} = c_d \cdot \rho \cdot g \cdot h \cdot u^2 \quad (2)$$

Where " $C_d$ " is the drag coefficient, " $\rho$ " is the density of water, " $g$ " is the gravitational acceleration. " $h$ " is the water level on the upstream side of the house, which depends on the flow condition and geometry of the structure, and " $u$ " is the velocity of water orthogonal to the object,

### Flume characteristics and experimental procedure

Experiments were conducted in a glass-sided flume of constant bed slope (1/500), 11m length, 0.30m wide, and height of 0.34m at Water Resource Engineering laboratory of University of Engineering and Technology, Taxila under different conditions of the house model and vegetations. A schematic diagram showing the arrangement of vegetation and the house model is shown in Fig.1.

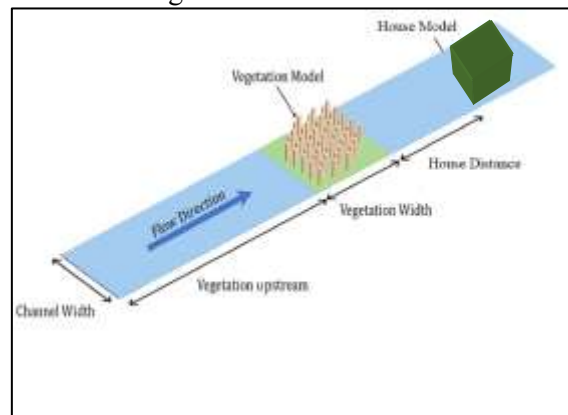


**Fig.1** The schematic diagram of the water channel

A model of house with varying porosity ( $P$ ) (0 – 20) % is shown in Fig. 2, which was used to perform experiments under different conditions. Fig. 2 (a), (b), (c) represent the the house model (HM) with 0%, 10%, 20% porosity of the house respectively. This house model with an equal height of 15cm, length of 10cm, and a width of 10cm of the real house was designed with a small scale of (1/45). It provides the equal height of a real building 675cm, width 457cm, and length 475cm.





(a)



(b)



(c)

**Fig.2** The house model with different porosities (a) 0% porosity, (b) 10% porosity, and (c) 20% porosity.

These experiments were performed with oblique vegetation and varying porosity of the house model. Equations mentioned above were used to calculate the hydrostatic and hydrodynamic forces on the house. Vegetation with different orientations (angles) is shown in Fig. 3. Vegetation is shown in Fig. 3 (a, b, c, d) represent the orientation(VA) of  $0^{\circ}$ ,  $15^{\circ}$ ,  $30^{\circ}$  and  $45^{\circ}$  respectively. A digital camera was used to observe the velocity direction and the reaction of the building against the flood intensity. Table 1 contains the experimental condition of vegetation and flowing water

**Table 1** Experimental Condition

<b>Case No</b>	1
<b>Initial Froude Number (<math>Fr</math>)</b>	1.56
<b>Vegetation Density (<math>G/d</math>)</b>	1.09
<b>Vegetation Thickness (<math>dn</math>)</b>	180
<b>Vegetation Length (m)</b>	0.6
<b>Vegetation Type</b>	Transition
<b>Building Distance (m)</b>	1m



(a)



(b)



(c)



(d)

**Fig. 2** Vegetation with different orientation (a) perpendicular to flow ( $0^\circ$ ), (b) at  $15^\circ$ , (c) at  $30^\circ$ , (d) at  $45^\circ$

## Results and Discussion

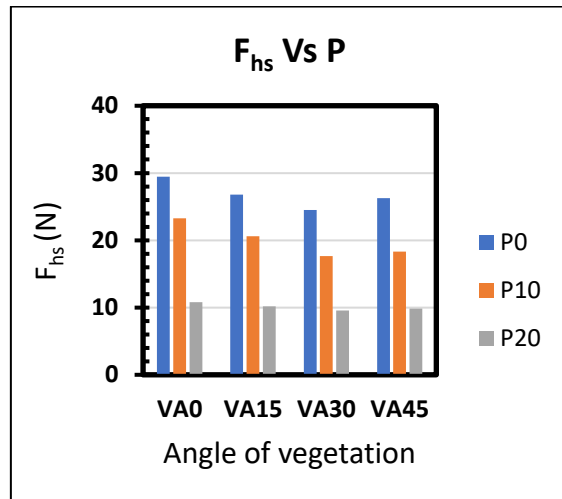
### Hydrostatic and Hydrodynamic Forces.

Fig.3 shows the results of experimentally determined values of hydrostatic and hydrodynamic forces, which are obtained by using the equations (1, 2) mentioned above.

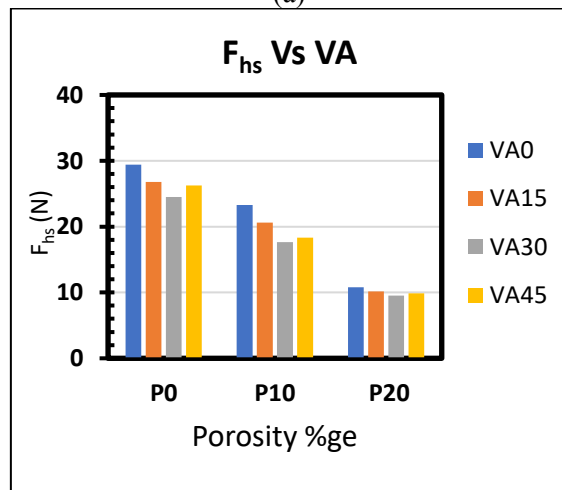
Fig. 3 (a) shows that for any oblique vegetation, hydrostatic force is linearly decreased with a linear increase in porosity ( $P$ ) of the house. The hydrostatic force depends on the water level at the upstream side of the house, so as we increase the porosity, more water passes through the house, and the upstream water level decreased as compared to a solid wall. The same trend is followed for each angle of vegetation.

Fig 3(b) shows that for each porosity of the house hydrostatic force is minimum for  $VA30^\circ$ . Experimental results revealed that by changing the angle of vegetation from  $0^\circ$  upto  $30^\circ$ , water level downstream of the house is increased, and

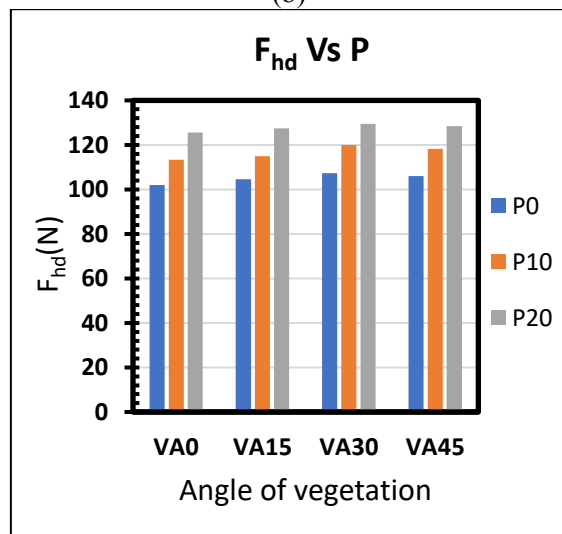
hydrostatic force decreased. But when the vegetation angle is changed from  $30^\circ$  to  $45^\circ$  water level at the downstream wall of the house decreased, and hydrostatic force ( $F_{hs}$ ) increased, as shown in Fig.3(b).



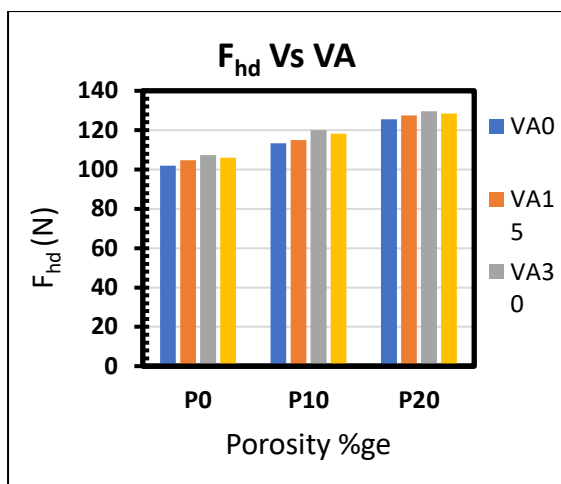
(a)



(b)



(c)



(d)

**Fig. 3** Experimentally derived hydrostatic force (a) Fhs Vs P (b) Fhs Vs VA

and hydrodynamic. (c) Fhd Vs P (d) Fhd Vs VA Fig. 3(c) explains the behavior of oblique vegetation against the house model of varying porosity. For each vegetation angle hydrostatic force is linearly increased by increasing the house porosity. Experimentally derived hydrodynamic results for different orientations of vegetation show similar results, as explained in the past study (Wüthrich *et al.*, 2018).

Fig.3 (d) shows that for the same porosity of the house, hydrodynamic force changes as the orientation of the vegetation is changed from 0° to 30° hydrostatic force increases and as the orientation is changed from 30° to 45° hydrodynamic force decrease. Hydrodynamic force is maximum at VA30°.

### Energy Dissipation

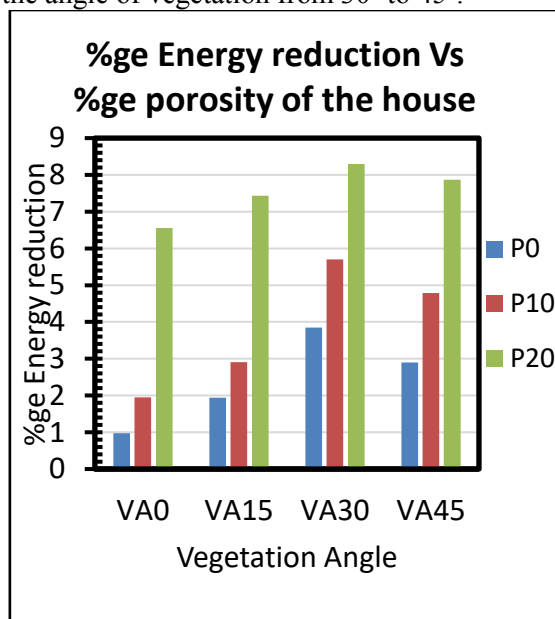
Specific energy  $E$ , in term of  $v$  and  $y$ , Velocity of flow and depth of water respectively can be written as chow (Chow, 1959)

$$E = y + \frac{v^2}{2g} \quad (3)$$

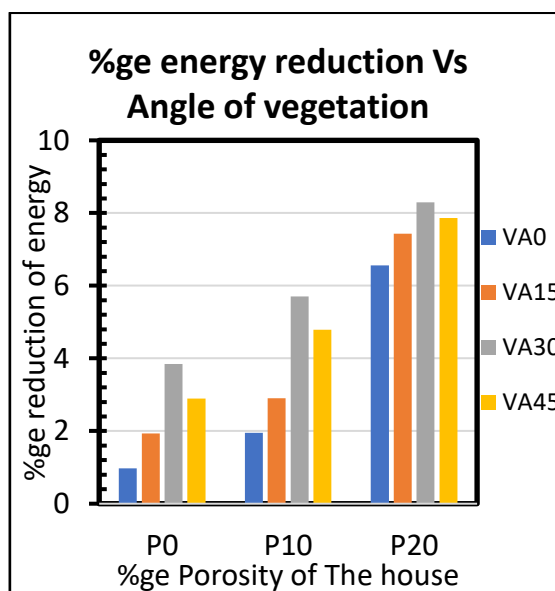
Where  $g$  is the gravitational acceleration. In this research, we find the total energy loss on the front wall of the house model in term of  $\Delta E = (E_1 - E)$  where  $E_1$  is the total energy at the upstream wall of the house without vegetation and  $E$  represent the energy at the upstream wall of the house in the presence of oblique vegetation at angle 0°, 15°, 30°, and 45°. Relative loss of energy is calculated as  $\Delta E/E$ .

Fig.4 (a) represents the percentage of relative energy loss for different angles of vegetation for different porosity of the house. For any angle of

the vegetation, by increasing the porosity of the house %ge loss of relative energy is increased. Percentage loss of energy is maximum for the house porosity of P20. By increasing the porosity the upstream water level is decreased so the percentage loss of energy is increased. The same trend is followed for each angle of vegetation. Fig.4 (b) shows that for each porosity of the house, the percentage loss of energy is increased as we increase the angle from 0° to 30°, but a little decrease in energy loss is observed by increasing the angle of vegetation from 30° to 45°.

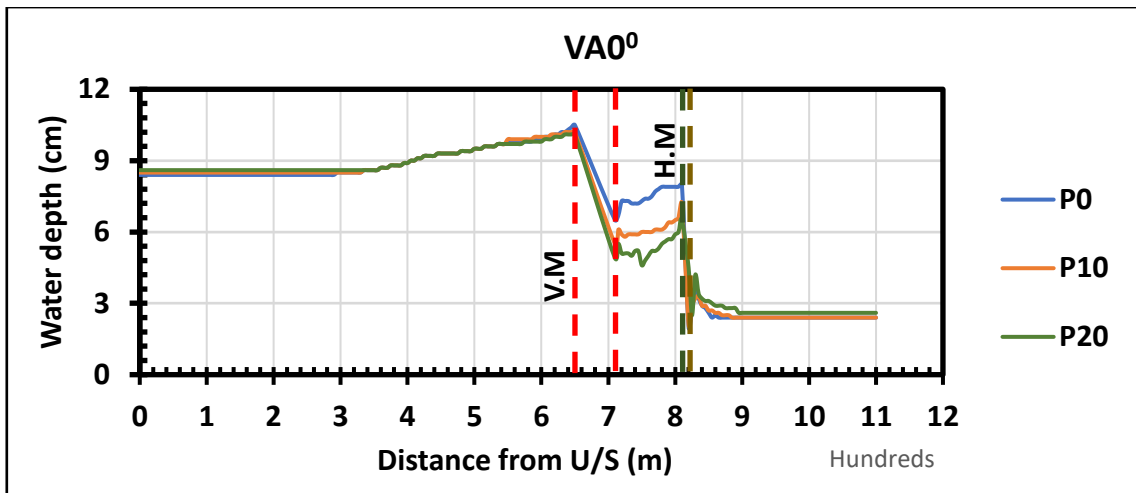


(a)

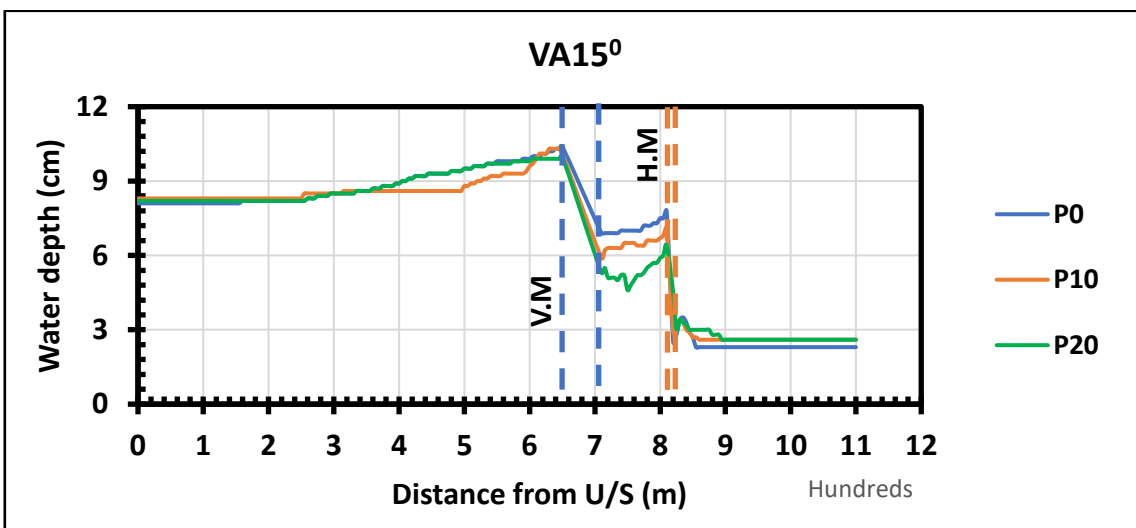


(b)

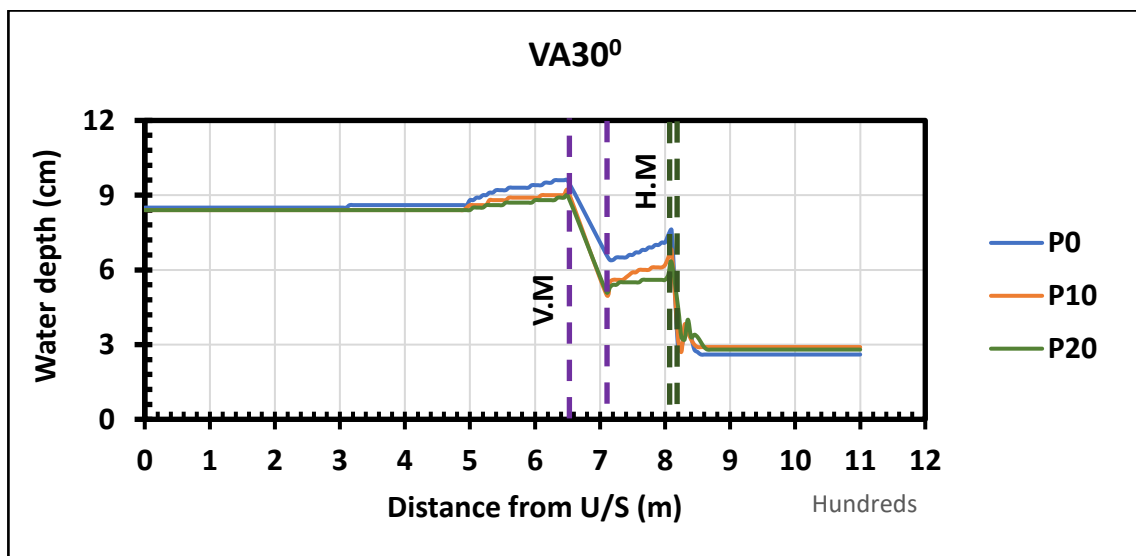
**Fig.4** percentage Relative loss of energy due to oblique vegetation



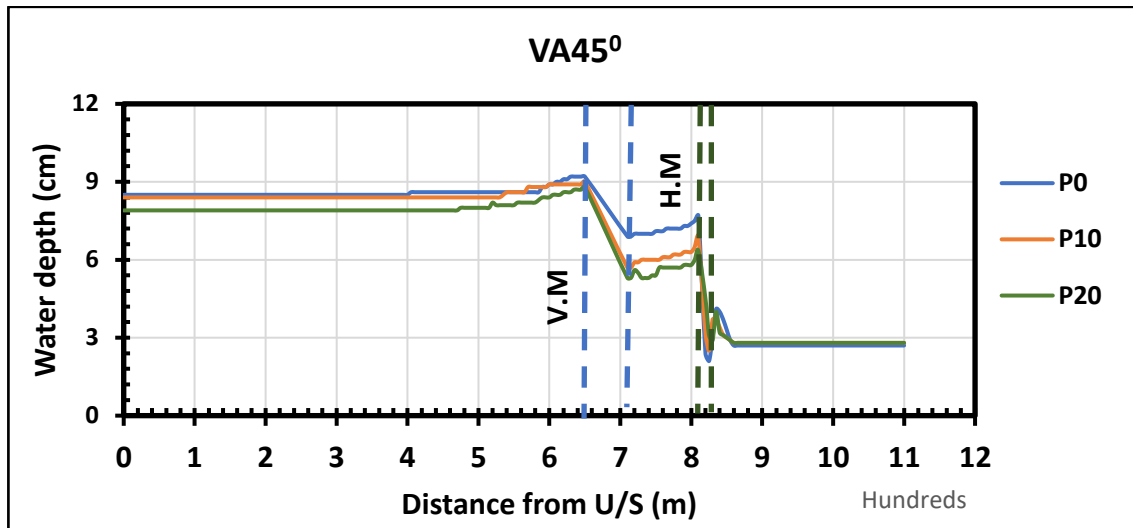
(a)



(b)



(c)



(d)  
**Fig.5:** Water profiles for oblique vegetation at different angles

### Water surface profile

Water surface profile against each angle of vegetation angle was observed. Fig. 5 (a, b, c, d) represents the water surface profiles for vegetation angle  $0^\circ$ ,  $15^\circ$ ,  $30^\circ$ , and  $45^\circ$  respectively for different porosity of the house. It was observed that the effect of the hydraulic jump generated by vegetation was nullified by the backwater rise of the house model. The hydraulic jump was observed on the downstream side of the house model. A large jump was observed in the case of a non-porous house model, while a shorter jump was observed in the highly porous case. Backwater rise was highest in the non-porous case.

### Conclusion

In evaluating the flood-induced risk structure stability is the main concern in flood-prone areas. Structures designed without considering the Dynamic loading are badly affected by the flood dynamics. Experimental results conclude that maximum energy is dissipated in case  $VA30^\circ$ . Moreover, as the porosity of the house is increased, energy dissipation is also increased. This will help to design the porous house in the flood-prone area.

### Acknowledgment

The authors would like to thank the Department of Civil Engineering, University of Engineering and Technology Taxila Pakistan for providing

excellent research facilities in Hydraulics Lab to accomplish this research.

### Reference

- Ahmad, M. et al. (2020) 'Investigating the Flow Hydrodynamics in a Compound Channel with Layered Vegetated Floodplains', 6(5), pp. 860–876.
- Asghar, M. et al. (2020) 'Investigating multiple debris impact load and role of vegetation in protection of house model during floods', in 2nd Conference on Sustainability in Civil Engineering (CSCE'20). Islamabad, pp. 1–7.
- Bass, D. and Koumoudis, V. (2012) 'FEMA's Coastal Construction Manual Update—Flood-Resistant Design', in Advances in Hurricane Engineering. Reston, VA: American Society of Civil Engineers, pp. 128–135. doi: 10.1061/9780784412626.012.
- Chow, V. (1959) 'T. 1959 Open-Channel Hydraulics', McGraw Hill.
- Commission, F. F. (2009) 'Flood management in Pakistan. Annual Flood Report', p. 44.
- Como, A. and Mahmoud, H. (2013) 'Numerical evaluation of tsunami debris impact loading on wooden structural walls', Engineering Structures, 56, pp. 1249–1261.
- Cuomo, G. et al. (2009) 'Hydrodynamic loadings of buildings in floods', in Coastal Engineering 2008: (In 5 Volumes). World Scientific, pp. 3744–3756.
- Nateghi, R. et al. (2016) 'Statistical analysis of the effectiveness of seawalls and coastal forests in mitigating tsunami impacts in



- Iwate and Miyagi prefectures’, *PloS one*, 11(8), p. e0158375.
- Palermo, D., Nistor, I. and Al-faesly, T. (2012) ‘Impact of Tsunami Forces on Structures: The University of Ottawa Experience Impact of Tsunami Forces on Structures: The University of Ottawa Experience’, (May 2014).
- Pasha, G. A. and Tanaka, N. (2017) ‘Undular hydraulic jump formation and energy loss in a flow through emergent vegetation of varying thickness and density’, *Ocean Engineering*, 141, pp. 308–325.
- Rahman, M. M., Schaab, C. and Nakaza, E. (2017) ‘Experimental and numerical modeling of tsunami mitigation by canals’, *Journal of Waterway, Port, Coastal, and Ocean Engineering*, 143(1), p. 4016012.
- Saatcioglu, M., Ghobarah, A. and Nistor, I. (2006) ‘Performance of structures in Indonesia during the December 2004 Great Sumatra earthquake and Indian Ocean tsunami’, *Earthquake Spectra*, 22(SUPPL. 3), pp. 295–319. doi: 10.1193/1.2209171.
- Tanaka, N. (2012) ‘Effectiveness and limitations of coastal forest in large tsunami: conditions of Japanese pine trees on coastal sand dunes in tsunami caused by Great East Japan Earthquake’, *Journal of Japan Society of Civil Engineers, Ser. B1 (Hydraulic Engineering)*, 68(4), p. II\_7-II\_15.
- Tanaka, N. and Ogino, K. (2017) ‘Comparison of reduction of tsunami fluid force and additional force due to impact and accumulation after collision of tsunami-produced driftwood from a coastal forest with houses during the Great East Japan tsunami’, *Landscape and Ecological Engineering*, 13(2), pp. 287–304.
- Tariq, K. and Pasha, G. A. (2020) ‘Development of ecosystem-based flood mitigation approach – investigations by experiments and numerical simulation’, 0, pp. 1–19. doi: 10.1111/wej.12662.
- Wüthrich, D. et al. (2018) ‘Experimental study on forces exerted on buildings with openings due to extreme hydrodynamic events’, *Coastal Engineering*, 140, pp. 72–86.

## Comparative Study of Total Dissolved Solids (TDS) Between Sand Absorption Media and Silica Absorption Media for Ganglion Trap of Non-Aqueous Phase Liquid (NAPL), Using Flow Visualization Channel.

Musaab Habib Bangash<sup>1\*</sup>, Naeem Ejaz<sup>2</sup>, Muhammad Zeeshan Ahad<sup>1</sup>, M. Mahboob Alam<sup>3</sup>

<sup>1</sup> Iqra National University Peshawar

<sup>2</sup> University of Engineering and Technology Taxila

<sup>3</sup> City University of Sciences and Information Technology, Peshawar

Corresponding author email: [mousabbangash@yahoo.com](mailto:mousabbangash@yahoo.com)

**Abstract:** The growing Anthropogenic activities has lead human kind dependent more on resources and materials. One of the main element of hydrocarbon which is known as non-aqueous phase liquid (NAPLs) has been investigated in flow visualization tank of specifications and standards. The ganglion trapped of Non Aqueous Phase Liquid (NAPLs) has been selected for dissolved behavior studies in which the dissolved behavior study was compared between sea sand and silica sand medium. The Total dissolved solids show different results and different behavior with different medium inserted between flow. These two absorption medium were placed exactly in the mid of flow visualization tank This pilot study of ganglion trapped in soil medium with different medium shows different results. The medium of sea sand and silica sand reduces total dissolved solids up to some permissible limits. The behavioral study of dissolved particles endorsed the interpretation of surface and subsurface contamination of water which can further be utilized in ground water characteristics and properties.

**Keywords:** Non- Aqueous Phase Liquid(NAPLs), Flow Visualization Channel, Sand Medium.

### Introduction

The World population is increasing each day. The increase in world population has increased anthropogenic activities. These anthropogenic activities have lead the inhabitants to face contamination on surface and undersurface. One of the Hydrocarbons family component Non Aqueous Phase Liquid(NAPLs) that exist as separate and non-homogeneous matter when it is surrounded by water or air. (G.Huling, 1995).The variation between chemical and physical properties between NAPLs and water acts as catalyst to separate both fluids from mixing. (G.Huling, 1995).These residual segment of organic liquid also known as ganglia, detached from main flow of the fluid and are kept in aquifers inside pore spaces. These liquids may transfer through saturated zone of water while the residue may left behind in their flow path as ganglia. (G.T.Geller:J.R.Hunt, 1993).The trapped liquids can migrate to water table and ultimately rest in the water saturated zone as remainder ganglia, which is occupied in pores. (Ioannidis:I.Chatzis, 2002).The dissolution of these ganglion trapped and removal is much needed effort activity. (Ioannidis:I.Chatzis, 2002).These ganglion trapped in pores needed proper dissolution studies and behavioral studies.

The behavior of these ganglion traps are the reason for the water contamination which flows over the residual and is responsible for ground water contamination. These hydrocarbons elements remain on the soil for a long time. (A.Atekwana & D.Legall, 2004).The contamination level may be controlled if some sort of adsorption media is involved in between them where it flow in the direction towards media. The total dissolved solids test can be used to find out that how much impurities has been removed or has been settled down due to adsorption media. The media may not even provide the transparency to clear all flow in it but some extent to. These dissolved and not dissolved scenario make us able to give some picture about further ill effects of contamination to surface and subsurface. The media introduce sand or silica gel study in flow channel may give us result to differentiate between total dissolved solvents and non-dissolved solvents. The study done by (Qiu, 2017) states that for velocity distribution and for other behavioral studies it was necessary to take stainless steel tank which is further kept to be aligned centrally and level for the investigation, for the uniform flow behavior study protocols has been kept in practice and observe maximum possible correct result of flow behavior.

The Study was conducted to analyze and interpret the behavioral flow of water in flow visualization channel. To study ganglion (trapped in pores) behavior the small pilot study arrangements of porous box comprises of earth material and in between one of the family member of hydrocarbons i.e motor mobile oil (Shell 10w-40) has been inserted in between the pores of soil sample so that the soil samples may comprises of ganglion trapped in pores of soil. The trapped elements are studies under flow of water in channel. In this attempt the medium used between the flow was the sand and other was silica gel to observe the behavior of dissolved solvents in water.

### Purpose

The Context of paper includes evaluation of the water in fluid visualization channel, in rectangular shape with one major lump of study sample besides by filtration medium. The arrow indicates the direction of the flow of fluid sample with in the middle of the channel is the study sample with filtration media and then after observation of the sample there is the collection tank to continue the flow further process is continued by electric pumps. The investigation was through the visualization techniques of experimental hydrodynamic flow in vertical channel.

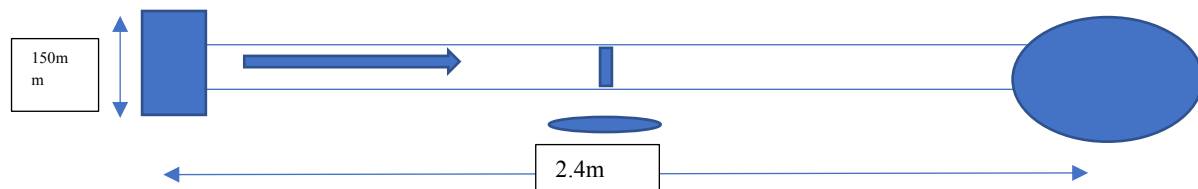


**Figure 1:** Diagram of Flow Visualization Channel

### Approach and Methodologies

The dissolved behavioral examination comprises the approach we took a flow visualization channel size of 150mm high and 2.4 m long with approximate 60litre capacity. The transparent box of channel shows steam line of the flow easily observable and it may easily measure the flow elements and fluid properties. For the study of Non Aqueous Phase Liquid (NAPLs) element Ganglion Trapped on surface and subsurface one of the hydrocarbon family motor mobile oil (Shell 10w-40) is used as sample which is molded in soil surrounding and bounded by porous box of size (40mm X 40mm). The usage

of box for the hardened soil filled with motor oil considered as ganglion trapped is considered for pilot study. The sample box was inserted in the middle of the channel with slope of 3% for which it was found the discharge flowed fluently with no interruption and barriers. The water flow with smooth flow towards the end of storage tank, the medium used between the flow is utilized to know the dissolved solids of sample. The study sample placed between is the characterized in such a way that it presents itself in ganglion which is trapped in soil medium and is derivative of Non Aqueous Phase Liquid NAPLs hydrocarbon element.

For total dissolved solids measurements pre calibrated TDS meter is used to find out the dissolved solids in water which is being passed by the sample of ganglion trapped and then by sea sand or silica sand. The count of desolation variates according with the filtration medium placed. For the experimental observations flow starts with switching On the button of flow and then controlling the flow with control valve. The TDS value was noted for each segment ten times with a gap of 2mins. The TDS meter was kept soaked in sample for at least 10secs while recording each value. The value of each segment discharge was disturbed while controlling the control valve and each discharge value was noticed with individual TDS value. Introducing sea sand medium in front of soil

sample and then noting the reading of required parameters and then putting silica medium in front of soil sample and noting the reading of required parameters made us able to study comparative behavior of dissolved solids of ganglion trapped as non-aqueous phase liquid in two different filtration medium.

**Table:** Comparative Total Dissolved Solids parameters between Sea Sand Media and Silica Sand Media

S.No	Medium	T.D.S	Medium	T.D.S	Discharge
1	Sea Sand	810mg/L	Silica Sand	732mg/L	0.015m <sup>3</sup> /s
2	Sea Sand	921mg/L	Silica Sand	620mg/L	0.010m <sup>3</sup> /s
3	Sea Sand	1021mg/L	Silica Sand	721mg/L	0.035m <sup>3</sup> /s
4	Sea Sand	753mg/L	Silica Sand	901mg/L	0.016m <sup>3</sup> /s
5	Sea Sand	834mg/L	Silica Sand	872mg/L	0.027m <sup>3</sup> /s
6	Sea Sand	939mg/L	Silica Sand	832mg/L	0.045m <sup>3</sup> /s
7	Sea Sand	760mg/L	Silica Sand	756mg/L	0.082m <sup>3</sup> /s
8	Sea Sand	898mg/L	Silica Sand	801mg/L	0.032m <sup>3</sup> /s
9	Sea Sand	699mg/L	Silica Sand	601mg/L	0.044m <sup>3</sup> /s
10	Sea Sand	834mg/L	Silica Sand	701mg/L	0.021m <sup>3</sup> /s

## Results

The Result obtained from the experimental observation makes us able to come towards some point of comparative studies between two filtration media. As a result, we have observed and experimentally recorded that for each segment of different discharge shows variation with respect to medium applied. For the sea sand and silica sand medium of different discharges each for 10sec first segment contains TDS 810mg/L,921mg/L for second,1021mg/L for third, 753mg/L for fourth, 834mg/L for fifth,939mg/L for sixth,760mg/L for seventh,898mg/L for eighth,699mg/L for ninth,834mg/L for tenth in sea sand media beside soil sample. Similarly, for silica sand

Medium TDS value for first was found 732mg/L,620mg/L for the second,721mg/L for third,901mg/L for fourth,872mg/L for fifth,832mg/L for sixth,756mg/L for seventh,801mg/L for eighth,601mg/L for ninth,701mg/L for tenth.

The different behavior leads us between two media is that both of them shows TDS varying result when placed in sample water way. The comparative studies show us that silica medium resist more solvents as compare to other medium of sand which when placed after the sample of ganglion trapped in soil of box. The silica sand medium developed between the flow of water and storage shows when it is placed may work as better filtration media in the water way as compare to common sand. During the flow of water both shows some resistance and that resistance results in the formation of dissolved activities.

For the worksheet plotted different discharge were observed by controlling different velocities so that it may qualify different parameters of

examination of required studies. The examination was purely worked on obtained result of TDS meter. The behavioral result of silica sand was more prone to resistivity which lead the water to slowly discharge. These non-aqueous phase behaviors of residual captured is founded to monitored for stream flow level when placed in between a medium exists and the subsurface may also exist some media so that these dissolved solids behavior may be made pilot studied a ground water contamination behavior. The segmental studies for ten seconds of each phase with instrument ushered us to take decision between the behavior of dissolved solids between both the medium.

## Conclusions

In the conclusion it has been concluded that ganglion trapped of NAPLs can produced sedimentation in the further flow way. These residuals may be trapped with some media of adsorption. The adsorption media of sea sand and silica sand both of them plays role for these residuals to resist in some manner. These filtrations may be produced in the way to flow for which took up some residuals in their pores spaces. The silica medium shows more efficient result in absorption as compare to other common sand media. The desolation of residuals gives the hints that that ganglion trapped in non-aqueous phase liquids may result in impurities in subsurface which may lead to depletion of aquifer and other ground water impurities. The silica medium shows more dissolved solids in the flow trapped in non-aqueous phase liquid which may be further interpret that the filtration media may be introduced in theses hydrocarbons impurities remaining on soil towards water table towards surrounding subsurface. These total dissolved solids parameters can also abled us to

recognized the other behavioral aspects of sediments deposited by these non-aqueous phase liquids (NAPL).

### Reference

- A.Atekwana, E., & D.Legall, E. A. (2004). The relationship of total dissolved solids measurements to bulk electrical conductivity in an aquifer contaminated with hydrocarbon. 56(281-294).
- G.Huling, C. J. (1995). Ground Water Issue. Oklahoma: Superfund Technology Support Center for Ground Water.
- G.T.Geller:J.R.Hunt. (1993). Mass Transfer From Nonaqueous Phase Organic Liquids in Water Saturated Porous Media . 29(4).
- Ioannidis:I.Chatzis, N. S. (2002). Dissolution of residual non-aqueous phase liquid in porous media:pore scale mechanism and mass transfer rates. 25.
- Qiu, S.-Q. Y.-C. (2017). Investigation of Velocity Distribution in Open Channel Flows Based on Conditional Average of Turbulent Structures. Mathematical Problems in Engineering.



## Laboratory measurements of velocity and hydrodynamic force over coarse fixed rough bed

Muhammad Zain Bin Riaz<sup>1\*</sup>, Shu-Qing Yang<sup>1</sup>, Muttucumaru Sivakumar<sup>1</sup>

<sup>1</sup> School of Civil, Mining and Environmental Engineering, University of Wollongong, Wollongong, Australia

Corresponding author email: [mzbr518@uowmail.edu.au](mailto:mzbr518@uowmail.edu.au)

**Abstract:** In natural flows, bed sediment particles are entrained and moved by the fluctuating forces, such as lift and drag, exerted by the overlying flow in the particles. To develop a better understating of these forces and the relation of the forces to the local flow, the horizontal and vertical components of force on near bed fixed particles and of fluid velocity above of them were measured synchronously. Measurements were made for a spherical test particle fixed at various heights above fixed rough bed. Fixed ball experiments involving simultaneous measurements of hydrodynamic forces and velocity on the particle at entrainment conditions revealed the significance of impulse in initiating sediment entrainment such that an optimum combination of force and duration is required to produce the threshold impulse. Short duration lift forces of magnitudes greater than the submerged weight are thought to be responsible for partial lifting of the completely shielded particle. Quadrant analysis of the dominant hydrodynamic force reveal the higher probability of occurrence of high-magnitude force induced by ejection ( $Q_2$ ) and sweep ( $Q_4$ ) events.

**Keywords:** Incipient motion; Hydrodynamic forces; Quadrant analysis; Force sensor

### Introduction

Predicting the initiation and evolution of bed forms produced by water flowing over loose sediment beds requires a relation giving the transport of the sediment in terms of the motion of the fluid. The relationships typically proposed are empirical or semi empirical, with the fluid motion generally characterized by spatially or temporally averaged quantities, such as mean fluid velocity or bed shear stress. In most cases these relations also incorporate a condition for initiation of sediment motion, such as a critical bed shear stress below which no significant movement occurs. According to this, the movement of sediment particles is related to factors that are reasonably easy to measure and predict.

The entrainment and movement of particles is due to the changing forces such as lift and drag that are exerted directly by the flow on the particles and not due to bed shear stress nor any other average characteristic of the flow (Riaz et al., 2020). Parameterization of the fundamental physical processes that cause sediment erosion, transport, and deposition can be best provided by the average flow parameters.

This idea is not new and many theoretical models are built for sediment particle motion in turbulent flow by many researchers (Anderson and Hallet, 1986; Niño and García, 1994; Sekine and

Kikkawa, 1992; Wiberg and Smith, 1985; Yang, 2019). The models, however, all proceed from assumptions about how the forces on sediment particles originate and, more importantly, how they should be treated. Unfortunately, the physically accurate model of bed particle motion remains hypothetical because only a few actual data are available on the details of these forces and their association to the flow. For better understanding, more models are not required; instead cautious experimental measurements are needed to outline the flow particle association accurately so that the model that is created can be somewhat realistic.

The terms drag and lift are used for the streamwise and vertical components, respectively, of the hydrodynamic force. In steady flows, many studies applied visual techniques such as photography and videography (Niño and García, 1998; Sumer and Oguz, 1978) while some studies used a force sensor to measure the forces to examine the bed load motion (Detert et al., 2010; Dwivedi et al., 2011; Schmeckle et al., 2007). The measured the direct fluctuating forces and velocities to understand the phenomena responsible for sediment entrainment due to coherent structures. If the plane of possible ( $u'$ ,  $v'$ ) combinations is divided in four quadrants, the velocity vector for a shear flow falls mainly in quadrants two and four ( $Q_2$  and  $Q_4$ ). Names for

the quadrants in the  $(u', v')$  plane have been given according to certain smooth wall coherent structures in the bursting cycle: sweeps ( $Q_4$ ) and ejections ( $Q_2$ ). These names are often used for flows over rough beds as well, or for nonequilibrium flows (Nelson et al., 1995; Raupach and Shaw, 1982). The magnitude and frequency of occurrence of ejection ( $Q_2$ ) and sweep ( $Q_4$ ) events change over the height of the flow (Raupach and Shaw, 1982).

Hofland and Booij (2004) concluded that the particle movement was associated with periods of high streamwise velocity, with the initial movement often caused by fluctuating vertical velocities. The fluctuating vertical velocities were found to be associated with clockwise vortices (Alfadhli et al., 2014; Yang, 2019). Cameron (2006) concluded that the start of particle motion corresponds to the tail end of the hairpin vortex and the high streamwise velocity reaching the particle. In contrast to those of Hofland and Booij (2004), where ejection flow events were indicated to provide the initial particle uplift before sweep entrainment, Cameron's entrainment experiments did not indicate an ejection flow event. Rather, the particle started to move only when a sweep flow structure reached the particle. Detert (2008) carried out experiments in a laboratory flume, roughened with spheres and gravel. In a streamwise vertical plane, large-scale wedge-like flow structures were observed, where in the sense of a sweep event, a zone of faster fluid rolls over a zone with slower fluid.

Various mechanisms proposed by researchers regarding the role played by coherent structures in entraining the sediment particles reveal a lack of consensus, with scope for further research. This paper describes an investigation of the role of instantaneous fluctuating velocities using laboratory experiments and their effect on hydrodynamic forces responsible for the inception of sediment motion and verification of laboratory setup.

### Research Methodology

The inception of sediment motion was physically investigated in a relatively large recirculating flume at the Faculty of Engineering and Information Sciences, University of Wollongong, Australia in which water was supplied from a head tank (Fig. 1). The test section was 10.5 m long, 0.4 m deep and 0.3 m wide with glass side walls.

The flow of the flume was generated using a 50 L/s pump connected to the head tank. At the

upstream inlet to the open channel section, a series of baffles in the header tank and honeycomb at the inlet of the open channel were installed to straighten the flow (Fig. 1). For monitoring the flow rates in the channel, an electromagnetic flow meter (F-2000 from Blue White Industries Ltd) was fixed to the plumbing system. The flow rate through the flume was controlled by the pump with a variable frequency drive. The water depths were measured using rail mounted pointer gauges and Ultrasonic displacement meters (UDM) at different location in flume. The acoustic displacement meters were calibrated in steady flow using the pointer gauges.

The spheres of average diameter of 38 mm were fixed by glue into a Perspex sheet in a hexagonal shaped structure over a 10m length of the flume. A false bed was created to compensate for the height of the force sensor by introducing river pebbles over the flume bed. In the test section, a target ball of 36.6 mm diameter was surrounded by a group of 3D printed balls filled with small steel spheres which were not glued (Fig. 1), so they would remain in place under their own weight. Adjacent to the target ball, a mobile bed was placed for 0.5m length to capture the movement of movable particles, covered by the river pebbles which were sieved between 3 mm to 5 mm.

The three-dimensional (3D) force sensor (BesTech Force Sensor specially built and calibrated for this study) was used to measure the load imposed on metal foil strain gauges and was sealed with silicone gel sealant to make it waterproof. The strain gauge signals were connected to the external amplifier (specially made for the strain gauge base force sensor and calibrated for this force sensor) and signal conditioning equipment through the sensor cable. In the external electronic system, the sensor signals were amplified and combined to produce signals representing the forces. The sensitivity of the sensor is 0.88 mN in the x direction and 1.5 mN in the z direction. The crosstalk from x to y and y to x is 0.5 % of full scale. The top surface of the sensor is the sensing face and is precisely machined to be extremely flat. To transfer the loads from the sphere to the force sensor, through the cylindrical supporting rod, a 6 mm thick circular steel plate was machined perfectly flat and attached to the top face of the sensor.

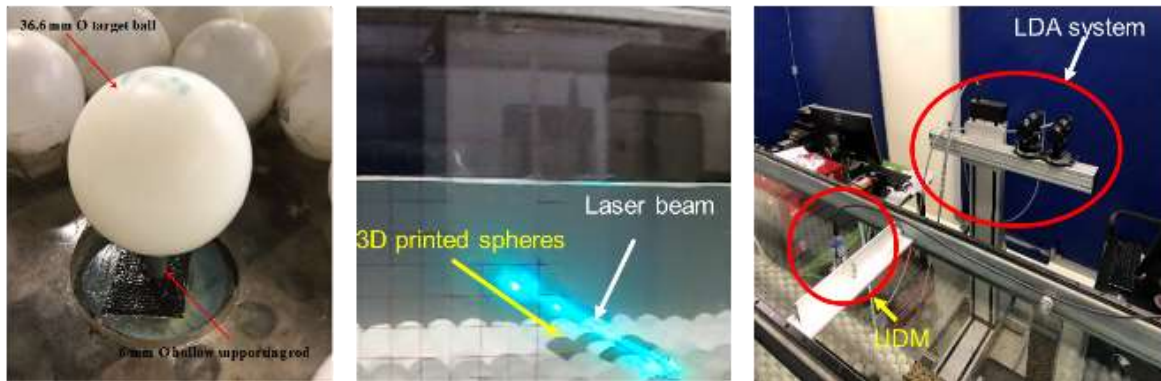
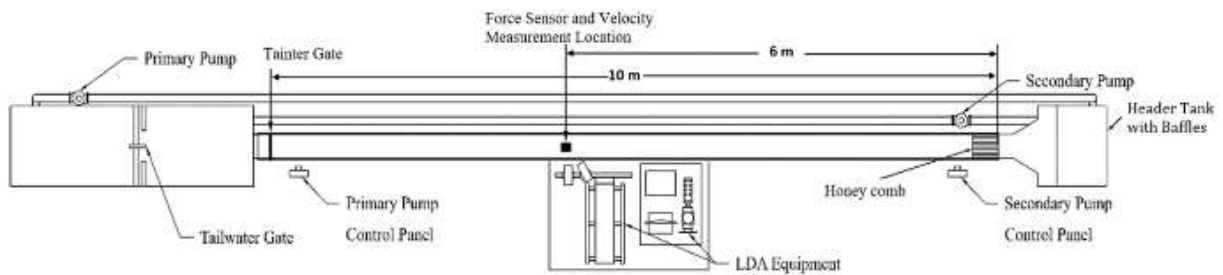


**Fig. 1** Schematic diagram of the laboratory flume, view of target ball, false bed preparation for force sensor and LDA system

The circular plate was tightened to the sensitive face of the sensor. While tightening the captive button head bolts specific care was taken. The bolts were tightened with a hex key through the bolt holes. One at a time, each bolt was turned a few times and then the next bolt was turned until the sensor mounting surface became flat. The 6 mm diameter supporting hollow brass rod was then attached to the 5 mm thread on the steel plate. At the other end of the 6 mm hollow supporting brass rod a target sphere was attached (Fig. 1). A box was made from Perspex sheet to cover the sensor body, with a 7 mm diameter hole at its centre, to waterproof the force sensor. Between the sensor body and the Perspex box, a space of 2 mm was kept all around. With a 5 mm diameter thread on the steel plate, the hole (on the box) provided a clearance of 1 mm all around the thread. Except for the circular hole at the centre of the box, all the open joints surrounding the bolts and edges were made waterproof using high-performance silicone complimented by petroleum jelly, which offers exceptional adhesion and long-life reliability. The major challenge was to prevent the inflow of water through the gap between the circular hole at the centre of the box and the supporting rod (see Fig. 1) since inflow of water through this gap could impart a false force reading from the sensor. A small amount of white petroleum jelly was applied in the gap, thus sealing the gap perfectly and allowing flexibility for small movement of the

threaded rod. The arrangement of the supporting rod and target sphere attached to it was done in accordance with preventing them from touching the surrounding particles. According to this setup, the force sensor recorded the hydrodynamic forces on the sphere due only to flow of the water.

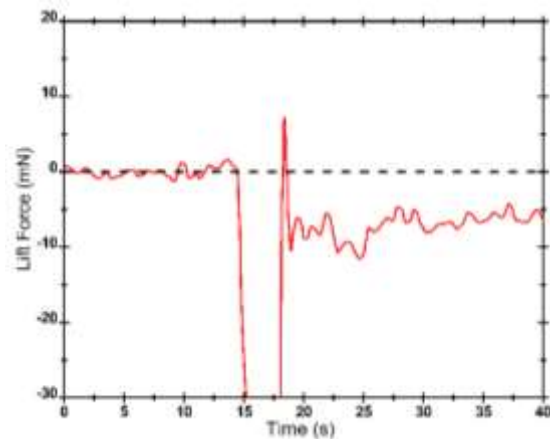


**Fig. 2** Response of the force sensor in the y direction due to loading and unloading of a gram mass in the downward y direction  
The performance of the sensor when installed in the flume was checked by applying known weights to the sensor in the x and y directions. Figures 2 & 3 shows the response of the sensor in x and y directions on application of a weight of 0.00981 N (1 g) in the negative y direction. Peaks observed between 22 and 25 s were due to the manual loading of the weight on the force sensor.

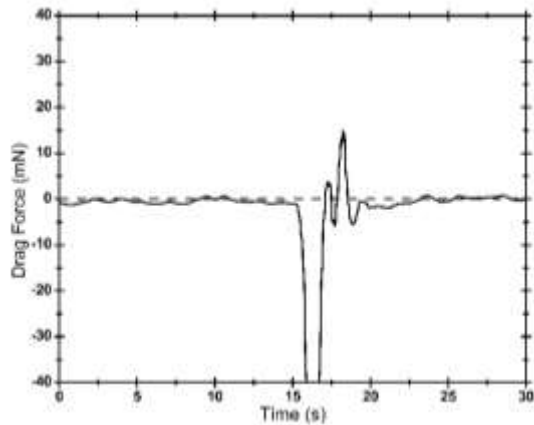


**Fig. 3** Response of the force sensor in the x direction due to loading and unloading of a gram mass in the x direction

The voltage data obtained were multiplied by the calibration matrix provided by the manufacturer, and the resulting time series was transformed into the frequency domain using fast Fourier transformation. The filtered time series of drag sampled at 500 Hz is shown in Fig. 4. Analysis shows that virtually all of the output is at frequencies below 20 Hz. During all the experiments, the force sensor was fixed at 200 Hz to acquire the data.

The laser Doppler anemometer (LDA) was used to measure point velocity and turbulence. For a brief description of the principles of LDA, see (Buchhave et al., 1979; Durst et al., 1977; Yang et al., 2020). This is a two component LDA used in backscatter mode with a 60 mm fibre optic probe and a front lens with a 400 mm focal length (Fig. 1). The system consists of a 280 mW continuous wave Argon-Ion laser and transmitting optics that include a beam splitter, Bragg cell and signal processors. Laser beams of  $\lambda=514.5$  nm, green light and  $\lambda=488$  nm, blue light were used to measure the horizontal and vertical velocity component respectively. The LDA was operated with a 40 MHz frequency shift to enable the measurement of positive and negative flows along either axis. The flow was seeded with 20  $\mu\text{m}$  diameter PSP seeding particles, which provide an excellent source of scattering centres, yielding data rates of between 180 and 250 (normally 200 Hz) and the velocity range was set 1.0 m/s using BSA flow in this study. The LDA was run with DANTEC Burst Spectrum Analyser processor (BSA) software which was used for signal processing and which was connected to an oscilloscope and a PC. The BSA processor operates on a correlation type process, and signals were validated only when Doppler bursts of

sufficient threshold were recorded on both channels. The oscilloscope converts the electrical signals into velocity data and the BSA processor software performed initial post processing of raw data. During all experiments, removal of communication errors, low signal to noise ratio (by default set as 0 dB using software) were done by the BSA processor software.

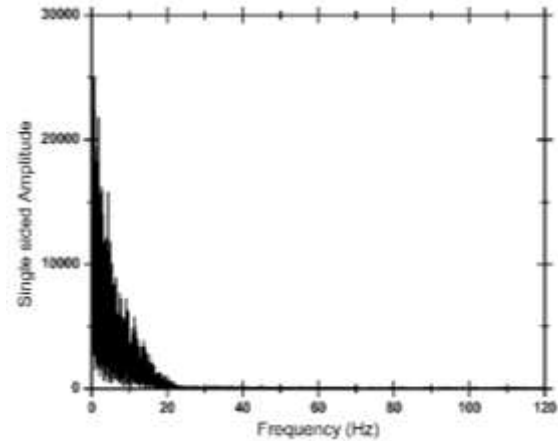


**Fig. 4** Real part of the Fourier magnitude versus frequency relationship of drag

The measurements were conducted between  $x = 6$  and 7 m and video movies were recorded with a handy camera Zoom™ (60 fps). Two separate processors (computers) were used to record LDA data and National Instrument data (for force sensor and Ultrasonic displacement meter) to avoid any loss of LDA data by using a single processor. It was essential to synchronize all the recordings. An analog pulse signal was sent from the LDA system to the National Instrument, to start the force sensor and UDM for acquiring the data. The camera was physically synchronized with the LDA by introducing a green light in front of the camera frame. All the instruments were synchronized within  $\pm 0.5$  ms.

## Results and Discussion

This study consider rough boundary flows of relative submergence,  $H/D=2.76$  to 4.12 (where H is the depth of flow and D is the particle diameter). The experiments were undertaken for a range of mean velocity Reynolds numbers ( $R=4m\bar{U}/\nu$ ) from  $99 \times 10^3$  to  $134 \times 10^3$ . All flows have Froude numbers less than unity, indicating a subcritical flow environment. Three different particle exposure (e) and three flow depths (H) were tested. The flow properties for the exposures and flow depths tested are shown in Table 1.

The basic data from the experiments consist of 45 time series of paired measurements of the

horizontal and vertical components of velocity and force. Example of two typical time series are shown in Figure 5. Figs. 5a and 5b show a 25 sec time history of synchronize velocity and force components recorded for  $H=015$  mm and  $e=0$  and 8 mm, respectively. It is interesting to note that for  $e=0$  the peaks and troughs are significantly less correlated between the measured force and velocity data. However for  $e=8$  mm the velocity and force data are well correlated. It is important to note that the scale are not same in Figs. 5a and 5b.

**Table 1** Flow properties from fixed bed experiments

$e$ (mm)	$H$ (mm)	$\bar{U}$ (m/s)	$Re$ ( $\times 10^3$ )	$Fr$
0	105	0.58	99.1	0.57
	132	0.76	129.8	0.67
	157	0.79	134.9	0.64
4	105	0.54	92.2	0.53
	132	0.71	121.3	0.62
	157	0.69	117.8	0.55
8	105	0.49	83.6	0.48
	132	0.55	93.9	0.48
	157	0.61	104.2	0.49

Figs 6 & 7 are showing normalized instantaneous fluctuating velocity and force plots. The normalized velocity plots confirm the occurrence of an ejection ( $Q_2, u < 0, v > 0$ ) and a sweep ( $Q_4, u > 0, v < 0$ ) events during the entrainment of particle at different exposure. Similar observations were made for other exposures and flow depth investigated but are not shown here for brevity.

In order to investigate the effect of duration and magnitude of the dominant hydrodynamic force on the particle, impulse (product of duration and magnitude) was estimated from the time history record of force. The duration of force causing impulse was calculated from consecutive positive fluctuations of force recordings. Three distinct events corresponding to positive fluctuations of force can be identified from the dominant lift force time history record and are plotted in Fig. 6 for  $e=0$  mm and  $H=105$  mm: (1) the event of maximum duration (Fig. 6a) of magnitude 25 mN lasting for 0.21 s (Impulse = 5.2 mN s), (2) the event of maximum force (Fig. 6b) of magnitude 45 mN of duration 0.14 s (impulse = 6.3 mN s), and (3) the event of maximum impulse, which coincided with event 2 in this study.

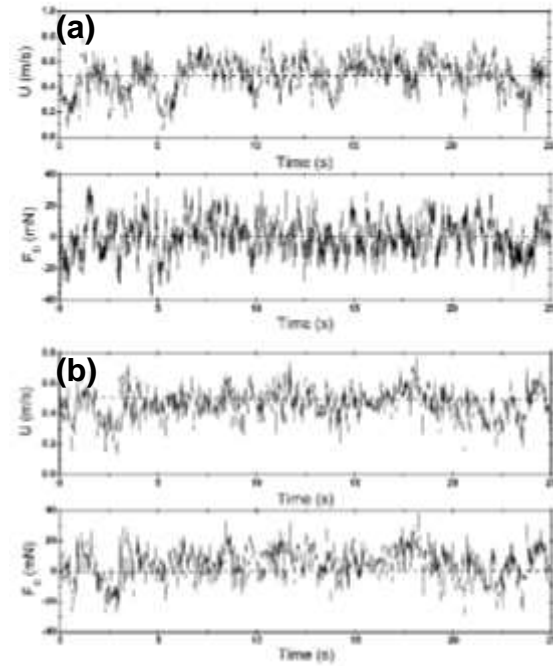


**Fig. 5** Synchronous time history of velocity and drag force for  $H=105$  mm and (a)  $e=0$  mm (b)  $e=8$  mm

Event 2 and 3 occurred at the same instant, signifying the importance of higher lift force for generating the necessary impulse required for sediment entrainment at lower exposures. The magnitude of the lift force at event 2 is almost 20 % more than that at event 1 and just equal to the submerged weight of the target sphere used in this study. The duration of occurrence of event 2 is almost the same as event 1, implying that a completely shielded particle can only be entrained by a lift force of magnitude greater than its submerged weight and of sufficient duration to be eject away by the ejection event. A high-magnitude lift force of short duration (around 0.05 s) can cause partial lifting up of the completely shielded sphere before it falls back down to its position of rest, as observed frequently in this study.

For the higher exposure particle instead of lift force drag force is more important. Figure 7 shows events for  $e=8$  mm and  $H=105$  mm using the dominant drag force time history instead drag. The magnitude of the drag force at event 2 is more (20 mN versus 38 mN) than that at event 1. Therefore, an optimum combination of drag and duration, not necessarily maximum individually, is necessary to produce the impulse required for sediment entrainment at higher exposures. Plots of time history recorded for velocity in Fig. 7 show that



the three events mentioned above are caused by the presence of a strong sweep event.

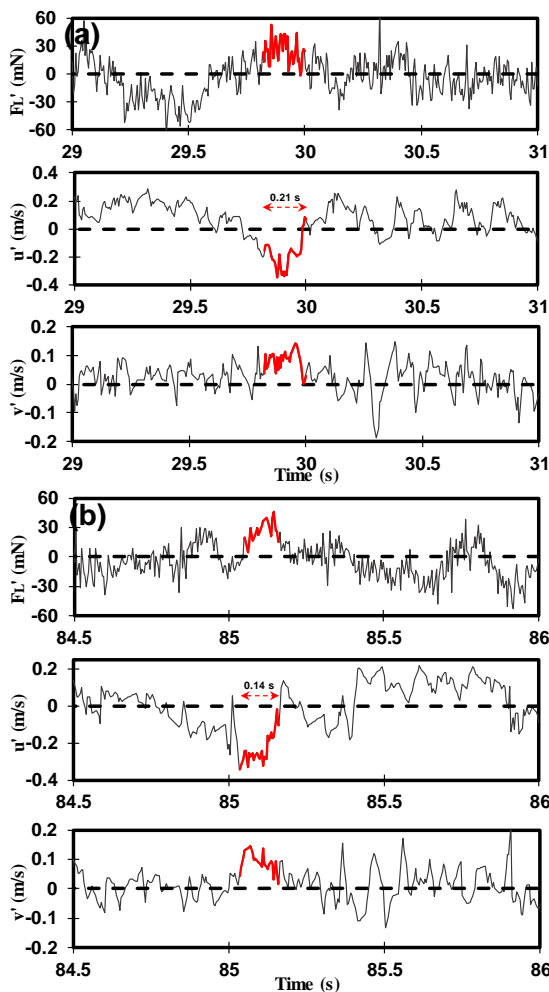
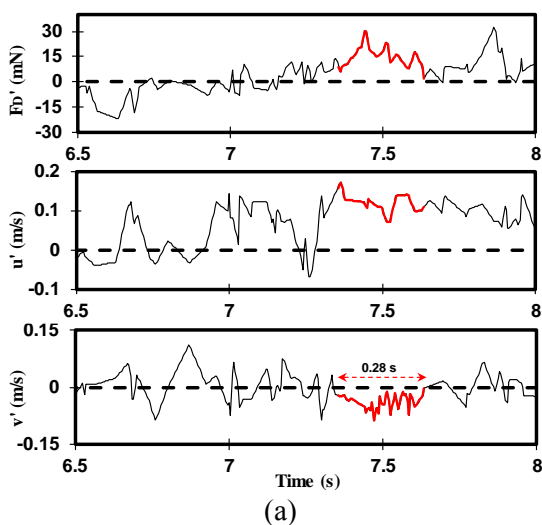


**Fig. 6** (a) Event of maximum force and impulse,  $u'$  and  $v'$  and (b) event of maximum duration,  $u'$  and  $v'$  in the lift force time history record for  $e=0$  mm and  $H=105$  mm.



(a)

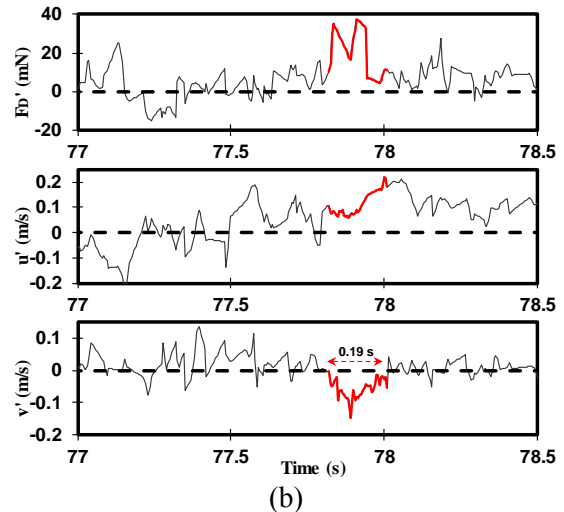


**Fig. 7** (a) Event of maximum force and impulse,  $u'$  and  $v'$  and (b) event of maximum duration,  $u'$  and  $v'$  in the lift force time history record for  $e=8$  mm and  $H=105$  mm.

In order to investigate the role of the coherent flow structures responsible for entrainment, probabilistic analyses of drag for  $e = 8$  mm and lift force for  $e = 0$  mm were carried out. The extreme forces responsible for entrainment mainly corresponded to the occurrence of  $Q_2$  and  $Q_4$  events because of their higher probability of occurrence. This indirectly implies that  $Q_2$  and  $Q_4$  events have a higher probability of generating the impulse required for entrainment through an optimum combination of force and duration.

## Conclusions

An experimental investigation of the effect of hydrodynamic forces and velocities responsible for inception of sediment motion has been carried out using a laboratory flume with LDA used to record the flow velocity along with simultaneous force measurement. Impulse is found to be an important factor in initiating sediment entrainment such that an optimum combination of force and duration is required to produce the threshold impulse. Short duration lift forces of magnitude exceeding the submerged weight of the completely shielded particle are thought to be responsible for partial uplift and resettlement of the particle in its cavity. Ejection and sweep events are found to be mainly responsible for occurrence of high force magnitudes.

## Acknowledgements

The authors acknowledge the technical assistance of Gavin Bishop, Travis Marshall and Jordan Wallace. Furthermore, Peter Ihnat's assistance in

LabView programming for data collection and synchronization is highly appreciated and the financial support provided by the Higher Education Commission (HEC) of Pakistan and the University of Wollongong, Australia.

## References

- Alfadhli, I., Yang, S.-q. and Sivakumar, M., 2014. Influence of vertical motion on initiation of sediment movement.
- Anderson, R.S. and Hallet, B., 1986. Sediment transport by wind: Toward a general model. *Geological Society of America Bulletin*, 97(5): 523-535.
- Buchhave, P., George Jr, W.K. and Lumley, J.L., 1979. The measurement of turbulence with the laser-doppler anemometer. *Annual Review of Fluid Mechanics*, 11(1): 443-503.
- Cameron, S.M., 2006. Near-boundary flow structure and particle entrainment, University of Auckland.
- Detert, M., 2008. Hydrodynamic processes at the water-sediment interface of streambeds. Ph.D. thesis Thesis.
- Detert, M., Weitbrecht, V. and Jirka, G.H., 2010. Laboratory measurements on turbulent pressure fluctuations in and above gravel beds. *Journal of hydraulic engineering*, 136(10): 779-789.
- Durst, F., Melling, A., Whitelaw, J. and Wang, C., 1977. Principles and practice of laser-doppler anemometry. *Journal of Applied Mechanics*, 44: 518.
- Dwivedi, A., Melville, B.W., Shamseldin, A.Y. and Guha, T.K., 2011. Flow structures and hydrodynamic force during sediment entrainment. *Water resources research*, 47(1).
- Hofland, B. and Booij, R., 2004. Measuring the flow structures that initiate stone movement. *River Flow 2004*: 821-830.
- Nelson, J.M., Shreve, R.L., McLean, S.R. and Drake, T.G., 1995. Role of near-bed turbulence structure in bed load transport and bed form mechanics. *Water resources research*, 31(8): 2071-2086.
- Niño, Y. and García, M., 1994. Gravel saltation: 2. Modeling. *Water resources research*, 30(6): 1915-1924.
- Niño, Y. and García, M., 1998. Experiments on saltation of sand in water. *Journal of Hydraulic Engineering*, 124(10): 1014-1025.
- Raupach, M.R. and Shaw, R., 1982. Averaging procedures for flow within vegetation canopies. *Boundary-layer meteorology*, 22(1): 79-90.
- Riaz, M.Z.B., Yang, S.-Q. and Sivakumar, M., 2020. Simultaneous measurement of horizontal and vertical velocities and forces beneath a tidal bore, Coastlab20. IAHR, Zhoushan, China, pp. 8.
- Schmeeckle, M.W., Nelson, J.M. and Shreve, R.L., 2007. Forces on stationary particles in near-bed turbulent flows. *Journal of Geophysical Research-Part F-Earth Surfaces*, 112(F2): 1-21.
- Sekine, M. and Kikkawa, H., 1992. Mechanics of saltating grains. II. *Journal of Hydraulic Engineering*, 118(4): 536-558.
- Sumer, B.M. and Oguz, B., 1978. Particle motions near the bottom in turbulent flow in an open channel. *Journal of Fluid Mechanics*, 86(1): 109-127.
- Wiberg, P.L. and Smith, J.D., 1985. A theoretical model for saltating grains in water. *Journal of Geophysical Research: Oceans*, 90(C4): 7341-7354.
- Yang, S.-Q., 2019. Formula for sediment transport subject to vertical flows. *Journal of Hydraulic Engineering*, 145(5): 04019013.
- Yang, S.-Q., Riaz, M.Z.B., Sivakumar, M., Enever, K. and Miguntanna, N.S., 2020. Three-dimensional velocity distribution in straight smooth channels modeled by modified log-law. *Journal of Fluids Engineering*, 142(1).

## Experimental study of soil erosion on steep hills with varying tree patterns

Walli Ahmed<sup>1\*</sup>, Ghufran Ahmed Pasha<sup>2</sup>, Usman Ghani<sup>2</sup>, Afzal Ahmad<sup>2</sup>

<sup>1</sup> University of Engineering and Technology, Taxila, Punjab, Pakistan

<sup>2</sup> Faculty of Civil and Environmental Engineering, Department of Civil Engineering, University of Engineering and Technology, Taxila, Pakistan

Corresponding author email: [walliahmed32@gmail.com](mailto:walliahmed32@gmail.com)

**Abstract:** The effectiveness of vegetation (trees) on hill slopes to minimize erosion depends on hill inclination and vegetation pattern. Vegetation with wide gaps does not reduce flow velocity, and sometimes it becomes the source of flash floods. This paper summarizes a series of laboratory experiments investigating the effects of different vegetation patterns on hill slope erosion. Two densities of vegetation (sparse and intermediate) were used to study the erosion phenomenon against two different bed slopes (10 and 15 degrees). The results showed that erosion was reduced by increasing the vegetation density and reducing the slope.

**Keywords:** Erosion, hill slopes trees density, Energy loss

### Introduction

Pakistan is a developing country, and most of the revenue of the country depends on agriculture. The total cultivated area of the country is 21.1 Mha, out of which 16.2 Mha of that cultivated area is irrigated through canals and available ground water resources. In comparison, the remaining 4.9 Mha (about 23.22% of the total cultivated land) is irrigated through natural resources like rain water (Ahmad, 2016). Due to mismanagement of available resources and an increase in population, the country faces a shortage of water. The decrease in water surface supplies from 5260m<sup>3</sup>/capita in 1951 to 1032m<sup>3</sup>/capita in 2013 is only due to the increasing population of the country (WAPDA, 2013). Hill slopes become unstable due to anthropologic activities like deforestation and cultivation. Moreover, landslides occur due to excessive rainfall especially in the monsoon season. Due to such man-made activities, the slopes become highly vulnerable to top soil erosion. To address such a problem, an eco-friendly and sustainable system of covering the land with vegetation canopy needs to be adopted. Hydraulic resistance and reflection of water by trees can reduce the energy of flowing water, inundation depth, inundation area, and hydraulic force behind the vegetation. (Iimura & Tanaka, 2012) investigated the effects of vegetation density both experimentally and analytically and concluded that the vegetation density is one factor responsible for reducing the level and velocity of the water behind the vegetation.

However, there are not so many studies on the effect of vegetation patterns on upstream of hills and energy reduction up till now. The purpose of this study is to investigate the different trees densities on the hill slopes which can reduce erosion and dissipate the energy of high velocity flows.

### Research Methodology

#### Experimental setup

A glass-sided flume having a total length of 20m and width of 0.96m was used to perform experiments. The slope model was placed 1.5 m from inlet. The slope model was 1 m in length. For a slope of 10 degrees the upstream bed was 0.27m high, and the downstream bed was 0.17m high. For the case of 15 degrees slope, the upstream bed was 0.36m high, and the downstream bed was 0.17m high.

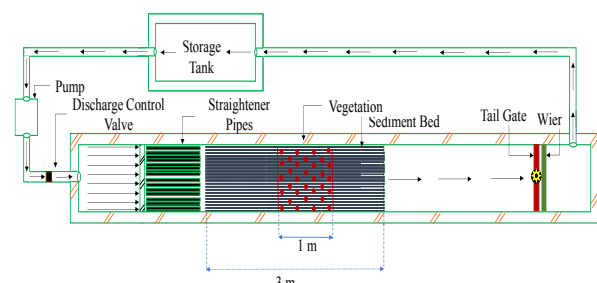


Fig- 1



Fig- 2(a)



Fig- 2(b)

### Hydraulic Condition

Sub-critical Froude number is selected for given studies, and velocity is adapted accordingly. Initially, the lower range of Froude number was selected. Actually, with a higher Froude number, the length of hydraulic jump increase thus the lower values of Froude number was used.

### Vegetation conditions

There are normally 430 species of trees in Pakistan, but the most common type present in the hilly areas of Pakistan is the pine trees. Their further types are blue pine (*Pinus wallichiana*), chir pine (*Pinus roxburghii*), which are the most common trees. Their specifications are used same as that of Ali (2019), and the specifications were (average tree height = 15 m and trunk diameter = 0.4 m) and the trees can be considered as circular cylinders (Tanaka et al., 2014). The trees can be taken as circular cylinders (Tanaka et al., 2014). As suggested by (Takemura & Tanaka, 2007), flow structures depend on their  $G/d$  arrangement of their vegetation model where  $G$  represents the spacing between each cylinder in a cross-stream direction, and  $d$  is the diameter of a cylinder. The selected vegetation densities are sparse and intermediate. For the selected scale of 1/50 the cylinders have diameter of 0.008m. The experimental conditions are given in Table 1.

### Experimental conditions

The selected width of vegetation is infinite. The water levels at every 10–20 cm intervals

Table 1

Case no	1	2	3	4
Slope (degrees)	10	15	10	15
Vegetation Condition	Sparse	Sparse	Intermediate	Intermediate
Flow condition	0.02	0.02	0.02	0.02
Vegetation density	2.13	2.13	1.09	1.09
C/C distance b/w cylinders (D) cm	5.008	5.008	3.3	3.3

(depending on the water surface variation) measured at the center line of the channel throughout the sediment bed of the channel. Before placing the vegetation model in the channel, the discharge was measured using discharge equation of trapezoidal weir. As a trapezoidal weir is installed at the tail end of flume. Final discharge values ( $m^3/s$ ) were calibrated by using both the discharge values. In Table. 1, where  $D$  is the center to center distance between cylinders and  $W$  is the width of the vegetation model. (Pasha& Tanaka, 2017). The experimental setup with  $G/d$  values 1.09 and 2.13 show intermediate and sparse tree arrangement respectively Ali (2019).

As  $dn$  (No. cm) which is expressed as a function of summed tree diameter. It is defined as a product of the diameter of a tree ( $d$ ) at breast height and the number of trees ( $n$ ) in a rectangle with a frontage of unit length and depth equal to the width of the forest ( $W$ ), (Shuto, 1987). Their values are selected as used by Ali (2019) by using the equation:

$$dn = 2/(\sqrt{3} D^2) W d \times 50$$

The parameter “50” in the above equation adjusts a unit in Shuto's definition of  $dn$  (No. cm) on a 1:50 scale, because  $d$ ,  $D$ , and  $W$  are in centimeters. In the present studies the selected value of  $dn$  is 180 (Pasha& Tanaka, 2017). The following parameters can be understood by considering the Fig. 3.

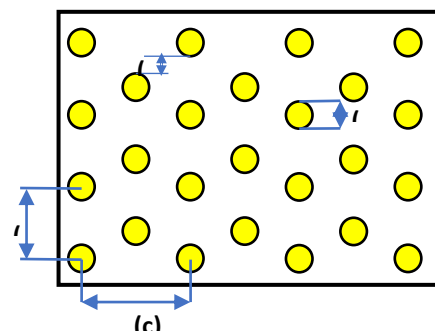
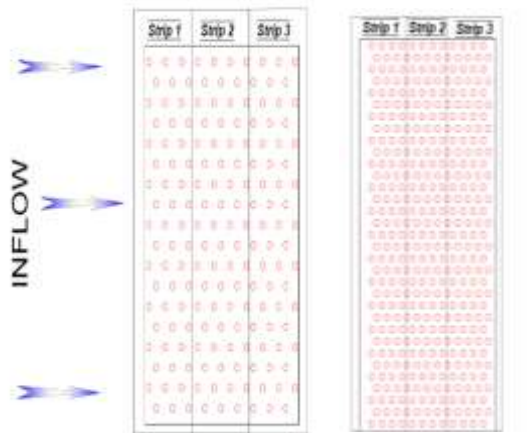


Fig- 3

## Results and discussion

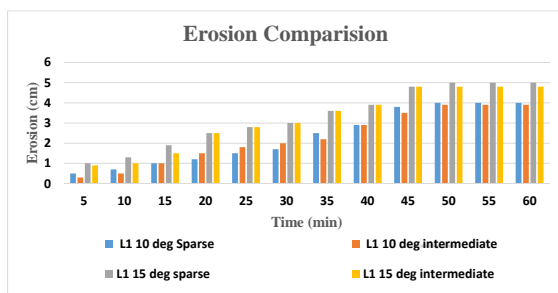
In this Experimental study, the cases are performed with two different tree densities (e.g. Intermediate and Sparse) with different bed slopes including (10 and 15 degrees). The water depth is selected according to Froude number. As in this study, the whole under mentioned working area is divided into three sections. Section A, the upstream strip. Section B, the middle strip and Section C, the downstream strip of the slopy area.



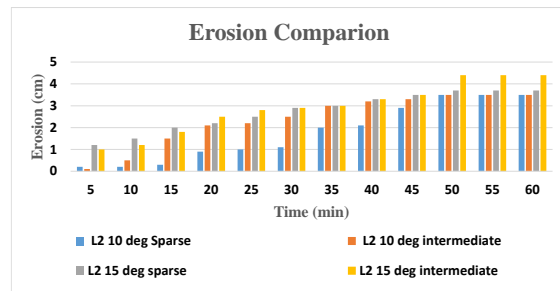
**Fig 4(a)** Sparse Arrangement (b)Intermediate Arrangement

### Erosion comparison among different strips

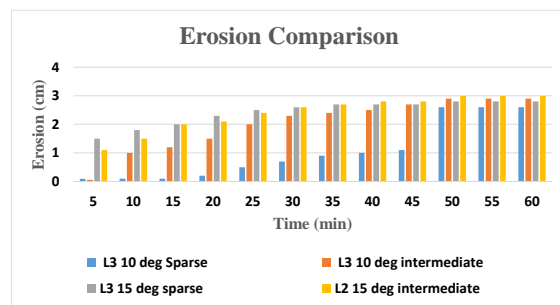
As erosion pattern is discussed under different vegetation arrangements, thickness, and densities. The hill gradient also impacts the erosion values as with the increase in gradient, the value of erosion also increases and the velocity of flowing water also increases which speeds up the soil detachment mechanism. The comparative analysis of erosion in each strip is given in Fig. 5.



(a)



(b)



(c)

**Fig-5** Erosion among different strips. (a) represents the top strips erosion. (b) represents the middle strips erosion. (c) represents the bottom strips erosion

As in Fig. 5, it can easily be said that the value of erosion increased with slope. The reason is that with an increase in slope, the water accelerates which increases erosion. Moreover, the erosion in sparse case is more than in that of intermediate case because in intermeidate case the spaces among vegetation are less, which retards the flow and causes less erosion. As investigated by (Noarayanan et al., 2012), that the flow resistance increase with flow velocity, vegetation density and elastic properties of material.

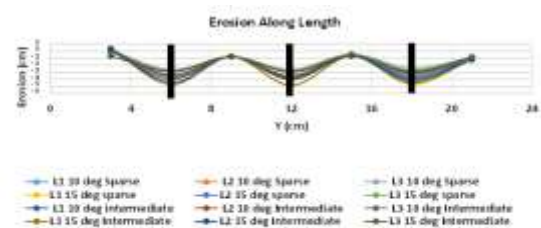


**Fig- 6** vegetation along length

In Fig. 6, the analysis of all layers w.r.t slopes is given. Black cylinders shows vegetation along length. The average of erosion is taken along length wise in each strip. This investigation shows that minimum erosion occurs in intermediate case as compared to sparse case; the reason is that vegetation plays an important role in giving stability to these slopes. The stability of these



slopes depend on the mechanical stability of trees roots (Chirico et al., 2013).

### Erosion Patterns

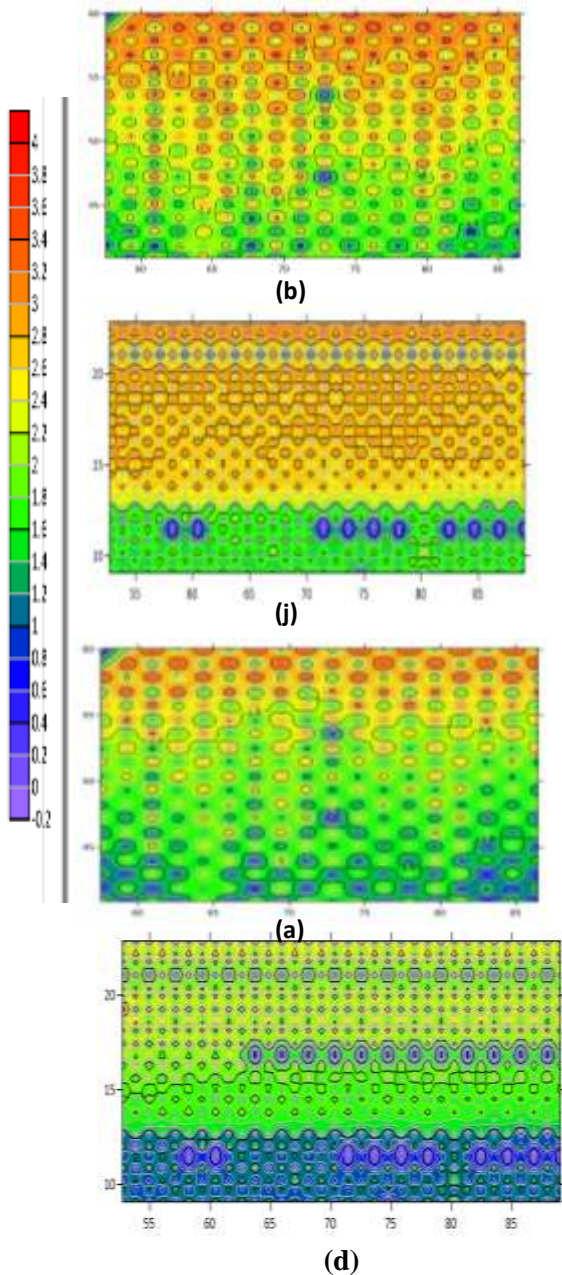


**Fig- 7** (a) 10 degree slope sparse case (b) 10 degree slope intermediate case (c) 15 degree slope sparse case (d) 15 degree slope intermediate case

In Fig. 7, the scour patterns of all 4 cases are mentioned; the flow direction is from top to bottom. The average of erosion is taken, which can be seen in Fig. 7. The orange and reddish areas show maximum erosion and the bluish and purple area in contours show minimum erosion. It signifies that erosion at upstream is maximum in

every case as when water moves on hill slopes, the upstream side has to face the maximum energy of incoming water which results in maximum erosion. On the other hand, on downstream face the erosion is minimum as the flow energy of water is dissipated on upper strips, as investigated by (Chow, 1959) that the energy of the flow is dissipated as the resistance offered by the channel increase.

**Table-2**

G/d	Slope (degree)	Location	Percentage reduction
2.13	10	Top strip	33
		Middle strip	41
		Bottom strip	56
1.09	10	Top strip	65
		Middle strip	58
		Bottom strip	51
2.13	15	Top strip	15
		Middle strip	61
		Bottom strip	53
1.09	15	Top strip	20
		Middle strip	41
		Bottom strip	53

As given in Table. 2, percentage reduction of each strip w.r.t time. This investigation shows that top strip of each case has maximum value of erosion. Overall, erosion reduction in intermediate case with 10 degree slope is maximum as compared to other cases.

### Conclusions

The following experimental study performed under given conditions and it was concluded that:

- 1- Minimum erosion occur with intermediate vegetation density, the reason is that intermediate vegetation dissipate the energy of water flow behind the vegetation , so water with less energy causes less erosion.
- 2- Maximum erosion is observed on higher slopes, higher slopes accelerates incoming water.
- 3- In each case, top strip shows maximum erosion. The reason is that incoming water strikes with that portion with maximum energy.

### Acknowledgements

I would like to express my gratitude to my advisor Dr. Ghufraan Ahmed Pasha for providing his beneficial comments, suggestions and

guidance. Moreover, I am thankful to Laboratory supervisors for allowing me to use the hydraulic flume to finish my experimental research.

## References

- Ahmad, E. M. (2016). Optimal management of water resources in selected hill torrent command of area
- Ahmed, G., Graduate, P., Tanaka, N., & Society, R. (2020). Characteristics of a Hydraulic Jump Formed on Upstream Vegetation of Varying Density and Thickness. 1–28. <https://doi.org/10.1142/S1793431120500128>
- Ahmed, G., & Tanaka, N. (2017). Undular hydraulic jump formation and energy loss in a flow through emergent vegetation of varying thickness and density. *Ocean Engineering*, 141(June), 308–325. <https://doi.org/10.1016/j.oceaneng.2017.06.049>
- Chirico, G. B., Borga, M., Tarolli, P., Rigon, R., & Preti, F. (2013). Role of Vegetation on Slope Stability under Transient Unsaturated Conditions. *Procedia Environmental Sciences*. <https://doi.org/10.1016/j.proenv.2013.06.103>
- Chow, V. T. (1959). *Open Channel Hydraulics*. McGraw-Hill Company. Erlangga : Bandung.
- Imura, K., & Tanaka, N. (2012). Numerical simulation estimating effects of tree density distribution in coastal forest on tsunami mitigation. *Ocean Engineering*. <https://doi.org/10.1016/j.oceaneng.2012.07.025>
- Kells, J. A., Balachandar, R., & Hagel, K. P. (2001). Effect of grain size on local channel scour below a sluice gate. *Canadian Journal of Civil Engineering*. <https://doi.org/10.1139/101-012>
- Noarayanan, L., Murali, K., & Sundar, V. (2012). Performance of flexible emergent vegetation in staggered configuration as a mitigation measure for extreme coastal disasters. *Natural Hazards*. <https://doi.org/10.1007/s11069-012-0089-5>
- Shuto, N. (1987). The Effectiveness and Limit of Tsunami Control Forests. *Coastal Engineering in Japan*. <https://doi.org/10.1080/05785634.1987.11924470>
- Takemura, T., & Tanaka, N. (2007). Flow structures and drag characteristics of a colony-type emergent roughness model mounted on a flat plate in uniform flow. *Fluid Dynamics Research*. <https://doi.org/10.1016/j.fluiddyn.2007.06.001>
- Tanaka, N., Yasuda, S., Imura, K., & Yagisawa, J. (2014). Combined effects of coastal forest and sea embankment on reducing the washout region of houses in the Great East Japan tsunami. *Journal of Hydro-Environment Research*. <https://doi.org/10.1016/j.jher.2013.10.001>

## Soil Mapping of Inaccessible Sites using Remote Sensing and GIS

Tariq Ahmed Awan<sup>1\*</sup>, Muhammad Usman Arshid<sup>1</sup>

<sup>1</sup> Civil Engineering Department, University of Engineering and Technology Taxila, Pakistan

Corresponding author email: [tariqawan02@gmail.com](mailto:tariqawan02@gmail.com)

**Abstract:** Geotechnical investigation in hilly areas for the low-rise projects becomes troublesome and costly process. Owing the difficulties in mobilization and setting up the drilling equipment on the rolling terrains. The current study aimed at development of digital soil maps using emerging geographical information systems for a renowned hilly area in Pakistan. The research work included collection and processing of available geotechnical data followed by georeferencing and digitization of acquired soil properties. Inverse Distance Weighting (IDW) and Kriging method of spatial interpolation was applied for preparation of thematic maps of soil class. The accuracy of maps developed was evaluated using linear regression method in which predicted soil class from developed maps and actual soil class are compared. Considering the maximum anticipated depth of foundation for low rise projects thematic maps of soil class were developed up to 20 feet depth with 5 feet interval in using colour contours. IDW maps gave better representation of soil variation then Kriging because IDW determines the soil type at unsampled location using linearly weighted method.

**Keywords:** Geographical Information System (GIS)1; Murree 2; Interpolation 3; Thematic Maps 4

### Introduction

Nowadays, with the advances in computer technologies, geographic information system (GIS) is widely used for spatial data management and manipulation. GIS was used for the visualization of geotechnical properties of soil such as SPT-N value, Uniaxial compressive strength and soil class of Eskisehir City, Turkey[1]. GIS was used in many projects of geotechnical engineering for capturing, analyzing, and displaying georeferenced data. In this research GIS is used to identify potential barriers in project and GIS was also used to interpolate the soil characteristics at inaccessible site[2]. A geotechnical analysis usually requires a large amount of spatial data for which GIS is the best tool. It can analyze data in very short period. A paramount feature of the GIS is its capability to create new data by combining and analyzing available data[3]. A comprehensive study was done by developing of engineering geological maps by GIS for landslide susceptibility[4]. The identification of soil type helps the geotechnical engineers to know the suitability of soil type for the certain type of foundation. Geotechnical engineers have been trying hard to predict the variation of soil and its properties by sketch maps and manual diagrams, which need lot of cost and effort by which it becomes uneconomical. GIS was used for localizing peat in the Surfers Paradise soil by categorizing geotechnical properties.

Geotechnical data was used to make micro zonation maps of study area and areas having peat was identified[5]. GIS based technology provides an easy and economical way in the field of geotechnical engineering for developing soil thematic maps i.e. soil class map. Soil Maps are extremely useful at reconnaissance level specially in mountainous region where it is impossible to setup equipment of borehole such as top of hill or a bottom of valley. The basis of this study is to determine the spatial variability of soil type thus predict soil type of an area at unsampled locations especially inaccessible sites with the help of different spatial interpolation methods like Inverse Distance Weighted (IDW) and Kriging Interpolation. The different spatial interpolation techniques like IDW, Kriging & Spline to map the Geotechnical Properties of Udham Singh Nagar District using GIS[6]. In this study soil class maps are made by using interpolation techniques in which each soil class is assigned a value in ascending order according to their gradation size and interpolated to develop thematic soil class map. For preparation of soil maps using GIS data availability is the key. Available data gives results in seconds by using GIS which is very useful innovation in soil engineering. The production of thematic maps based on soil classification gives geotechnical engineers idea about construction site and help them in deciding the soil suitability for the designed structures. A research was conducted

this study to measure soil properties and its spatial variabilities of Sulaimani City using conventional analytical and geostatistical method. In this study Atterberg limits, undrained shear strength of soil is focused using ArcGIS mapping[7]. The use of GIS in geotechnical engineering is very common nowadays in similar way a study was done to develop maps which shows the subsurface characteristics of soil and rock formation to indicate the swelling characteristics of clay in that area along Sheikh Zayed canal using GIS[8]. The mapping of geotechnical data is done by natural neighbor interpolation tool in GIS. In past study area on which study is performed in Hassan Usman Katsina Polytechnic Nigeria. The data of test pits were tested in laboratory and incorporated in ArcGIS 10.2.1, which gives output data in the form of Index and geotechnical properties of soil[9]. Web base GIS system was developed to locate and purchase boreholes of interest, to view boreholes and cross sections that are generated online, to provide downloadable data in a standard format for downstream analysis and perform geotechnical queries using a geotechnical search engine (GSE)[10]. Regional geotechnical maps using Kriging interpolation in have been appraised showing creditable accuracy for the Pothohar plateau in Pakistan[11]. In geotechnical soil surveys, the geotechnical properties of soil layers must be known to the required depth. The depth needed for this study is up to 20 feet. This study aims to prepare soil maps for Tehsil Murree, Punjab, Pakistan up to 20 feet depth. The soil maps are prepared to determine the foundation soils' suitability in residential areas and other project related to Geotechnical engineering.

### **Study area and data description**

Murree is the subdivision of Rawalpindi and located at 33.9078°N and 73.3915°E and at an altitude of approximately 7500 feet. DEM (Digital Elevation Model) is used to find elevation at any point of the area. DEM of the study area is shown in Figure 1a and location of the study area is shown in Figure 1b.

The neighbouring districts at the northern and western side of Murree are Haripur and Abbottabad Khyber Pakhtunkhwa, at the eastern side Jhelum River.. In contrast, on the southern side of Murree, Kotli Satian is present. Murree Formation is also as lower Miocene, which is mostly Continental sandstone and claystone. The sandstone is usually reddish gray to purple gray,

fine to medium grained, thick bedded, micaceous, cross bedded, jointed, and calcareous in that area[12].

Murree is present in the sub-Himalayan mountain region. Murree is in the earthquake zone 3 according to the earthquake zoning map of Pakistan, which is considered as moderate hazard area. Ministry of Housing and Works Pakistan prepared these zones for Building codes provision. In Murree area, the hill slopes are reasonably steep and vary from 17° to 30°. An increase in slope steepness results in the decreasing of shear strength of the material that causes landslides. The rapid urbanization like formation of road networks, disturbed slopes and immature geology is the reason for landslides in Murree[13]. So, land sliding is a periodic phenomenon in those areas where the slopes are steep along streams, roads and disturbed slopes, as noticed during a field survey. The soil is typically clayey loamy and shallow, their development is restricted by the steepness of slopes. The locator map and digital elevation map of the study have been shown in Figure 1

### **Research Methodology**

The methodology used in this study comprised of eight phases. The flowchart of all the steps involved in this research is shown in Figure 3. The first phase of this study is soil survey and field observation. In which study area is visited and surveyed to inspect the study area visually. In the second step, Landsat images of the study area were downloaded from USGS site. In the third step, it was classified by a supervised classification technique to determine the landcover use. Earlier research was held to assess Land use land cover (LULC) patterns in Murree to show the urban expansion[14]. DEM (Digital Elevation Model) was also incorporated to find the elevation data at any point of the study area. In the next step, available geotechnical data is collected from different soil laboratories which is exploratory soil data obtained from various construction projects in Murree. So, in this respect total 205 boreholes data is collected up to 20 ft depth which is in the form of soil class. In these boreholes, data soil class is reported at different intervals of depth. The available data was available in different locations forms. The soil classification of the collected geotechnical data was based on the Unified Soil Classification System (USCS)[15]. Next, data has been tabulated using MS Excel to make it accustomed

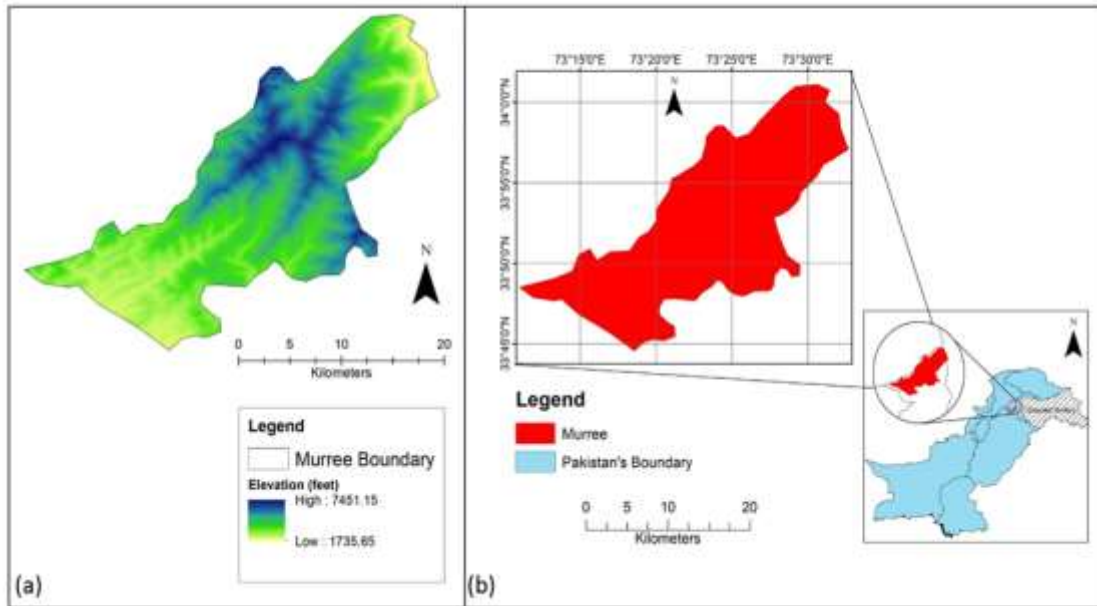


**Figure 69-**(a) Digital Elevation of study area Murree (b) Map showing study area position in Pakistan

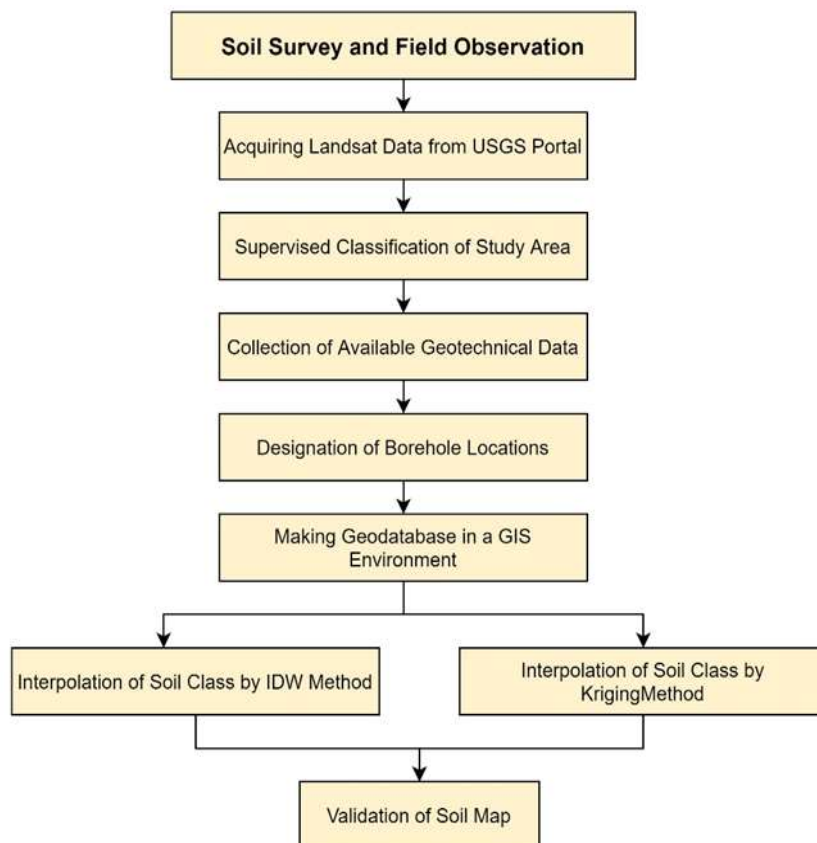


**Figure 70-** Flowchart of methodology



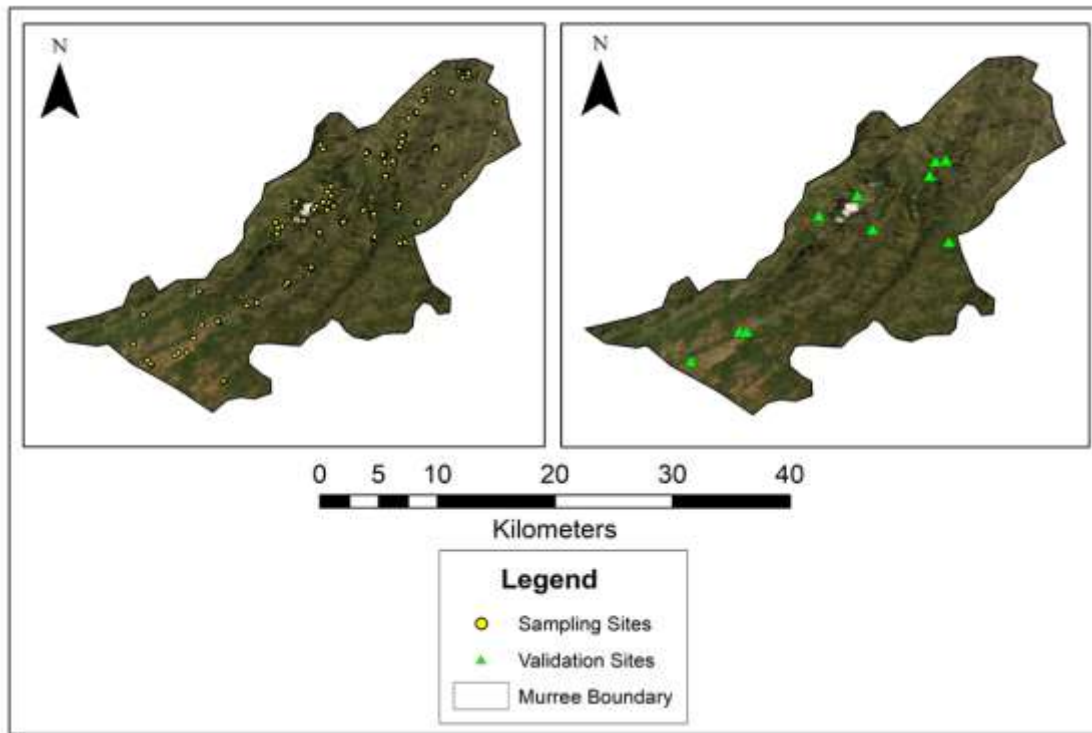


**Figure 71-**Map of sampling sites and validation sites (borehole locations)

to the GIS environment. The spatial locations in which longitude and latitude does not exist, boreholes have been designated by using Google Maps and Google Earth actual locations on each project's site.

Figure 4 shows the procedure of obtaining the boreholes coordinates from a project site. After that the geotechnical data has been horizontally tabulated in MS Excel sheet to be compatible with the GIS setting. The table below show the values assigned to soil classes.

**Table 1:** Soil sample classes and assigned values to be used in GIS environment

Soil Class	Assigned Values	Soil Class	Assigned Values
MH	1	GC-GM	9
CL	2	GM	10
CL-ML	3	GW	11
ML	4	GP-GM	12
SC	5	GW-GM	13
SC-SM	6	Shale	14
SM	7	Sandstone	15
GC	8		

Using geodatabase spatial interpolation techniques which are applied with the help of Arc Map 10.3. The interpolation techniques

examined were (1) IDW interpolation (2) Kriging interpolation.

According to the field investigations, inverse distance weighting (IDW) method appears to be the adequate method to present the study area. The IDW method is also one of the most used predetermined models in spatial interpolation by researchers in geosciences [16]. The IDW can be expressed in term of equation (1).

$$Z_{x,y} = \frac{\sum_{i=1}^n Z_i W_i}{\sum_{i=1}^n W_i} \quad (1)$$

Where  $Z_{x,y}$  is the point to be estimated,  $Z_i$  represents the control value for  $i$ th sample point, and  $W_i$  is a weight that determines the relative importance of individual control point  $Z_i$  in the interpolation procedure.

Kriging method can also be adequate to show the spatial variability in geotechnical engineering. Geostatistical methods such as kriging can produce predictions based on spatial autocorrelation and cross-correlation but are always accompanied by average smoothing effects; a local singularity created by nonlinear geo-processes, therefore, requires special methods to be properly evaluated [17]. The kriging can be defined as equation below.

$$\check{z}(s_0) = \sum_{i=1}^N \lambda_i Z(s_i)$$

As, interpolation can be done on the basis of values, so values were assigned to each soil class according to gradation size. Interpolation resultant values are manually set as values assigned to soil class and reclassified to get desired maps. The interpolation is a procedure used to predict the soil class at certain locations that lack sampled points.

### Results and Discussions

Supervised classification of Landsat image is done to show the landcover use of study area. The study area is classified into Barren Land, Urban Area, Grassland/Forest, and Water. The result of supervised classification shows that most of the study area is covered by Grassland and Forest, so there is a large area that still needs to be developed. Murree is a hill station and is mostly surrounded by high mountains and valleys which are usually inaccessible sites.

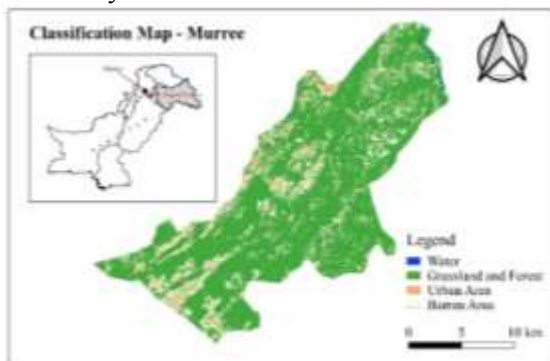


**Figure 72:** Map showing classification results of Tehsil Murree

Taking samples at every position in the study area for investigation of soil type can be very expensive. As a substitute, a measure of the soil type of the representative sample at investigated locations and then predicting the soil type in all other locations using the interpolation tool of GIS can save cost and time. In this respect, Eight GIS-based interpolated soil maps have been developed for the study area at depths up to 20 ft (Figure 6 and 7). Soil maps show the distribution of the soil type over the study area. The various colors ranges indicate the number of soil types present in the area. As depth interval of each map is 5ft so 10 maps for both IDW and Kriging interpolation techniques are developed. Different soil types are present in different areas but in study area mostly soil is clayey soil and silty clay soil. There is a different thickness of layers of soil which ranges from 5 ft to 20 ft. As depth increases variation of soil decreases.

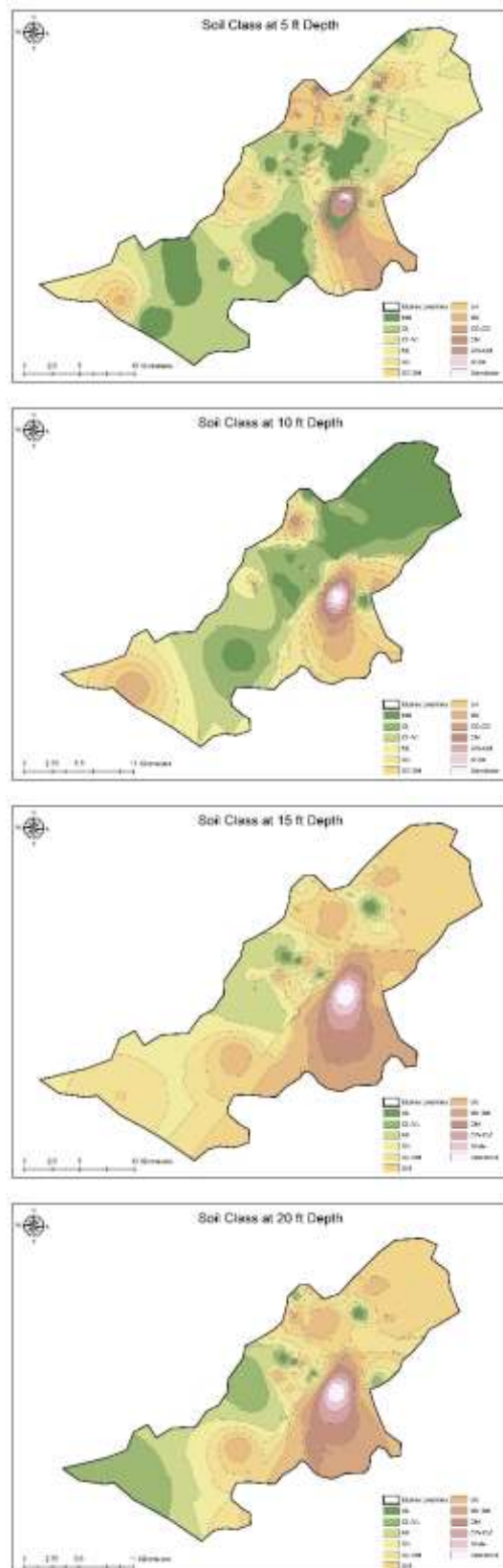


**Figure 73:** Soil type maps prepared by IDW interpolation technique. (graph) validation results

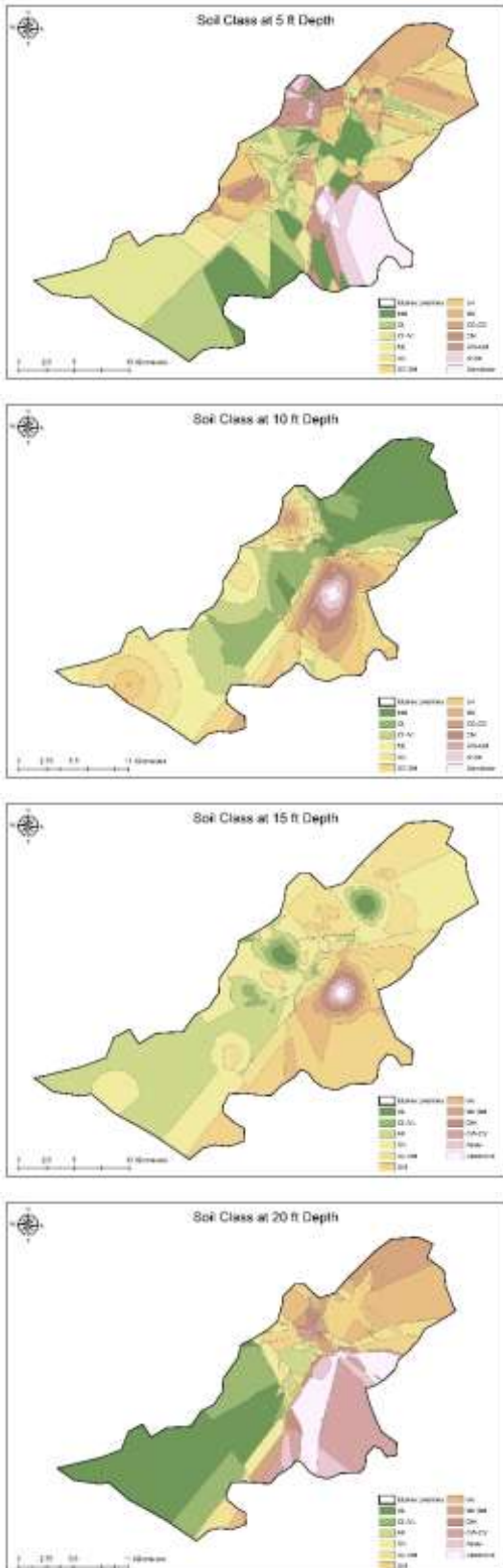


**Figure 74:** Soil type maps prepared by Kriging interpolation technique. (graph) validation results

## Validation and Prediction Accuracy

The basic of interpolation is the prediction of values of attributes at unsampled locations. In order to provide spatial heterogeneity of the soil class in the study area, interpolation can also be used to prepare continuous maps of soil class maps from data obtained from sampled locations. Validation was performed to calculate the difference between the expected values and the residual values observed. In this analysis, validation using MS Excel was performed using the linear regression process.

Validation of the data is carried out by comparing the calculated values with the original values, in which values are assigned to soil class in ascending order according to their gradation size. In result of validations, IDW method gave us better result than Kriging Interpolation method because maps developed by IDW interpolation methods are continuous. Moreover, in IDW interpolation method, the sample points are weighted during interpolation so that the influence of one point relative to another decrease with distance from the unknown point you want to create.

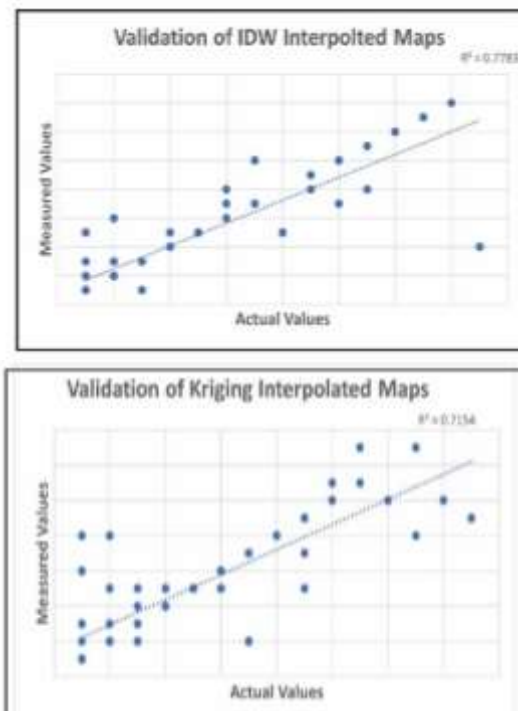


**Figure 75:** illustrations showing validation of results

## Conclusion and Recommendation

This paper described a novel approach that integrates GIS and the soil investigation data such as soil type to develop thematic soil maps

that can be used by the construction industry. To conclude, two interpolate techniques have been used to develop the soil maps of the study area. The Inverse Distance Weighting (IDW) technique within the Spatial Analyst in ArcMap 10 showed a better representation for the soil type variation with a certain parameter. Since the study area is an attractive hill station of Pakistan and development is needed to create charm for international tourist. The proposed thematic soil maps can serve as a valuable guide to evaluate the suitability of areas to be developed and also to determine if further precautions are needed for safer planning actions or remediations for existing structures. These maps can be used to keep the construction within budget and schedule especially at a reconnaissance level. By these maps sub-surface at depth interval of 5ft was visualized so GIS can be used effectively in geotechnical engineering applications. As mentioned above prepared illustrations are useful for generalized landuse planning purposes and to check the suitability of site for a certain type of structure.

#### **Acknowledgement**

The authors are grateful to Geotechnical Engineering Laboratory of UET Taxila and M/S SWISS TECH Consultancy (Rawalpindi, Pakistan) to their support and providing necessary data.

#### **References**

- Orhan, A. and H.J.E.E.S. Tosun, Visualization of geotechnical data by means of geographic information system: a case study in Eskisehir city (NW Turkey). 2010. 61(3): p. 455-465.
- Singh, A., et al., GIS applications in geotechnical engineering some case studies. 2015. 5(2).
- Dai, F., C. Lee, and X.J.E.g. Zhang, GIS-based geo-environmental evaluation for urban land-use planning: a case study. 2001. 61(4): p. 257-271.
- Chacón, J., et al., Engineering geology maps: landslides and geographical information systems. 2006. 65(4): p. 341-411.
- Al-Ani, H., et al., Categorising geotechnical properties of surfers paradise soil using geographic information system (GIS). 2013. 5(2): p. 690-695.
- Khatri, S. and S. Suman, MAPPING OF SOIL GEOTECHNICAL PROPERTIES USING GIS. 2019.
- Ahmed, C., et al., Geostatistics of strength, modeling and GIS mapping of soil properties for residential purpose for Sulaimani City soils, Kurdistan Region, Iraq. 2020: p. 1-15.
- Labib, M. and A.J.A.S.E.J. Nashed, GIS and geotechnical mapping of expansive soil in Toshka region. 2013. 4(3): p. 423-433.
- Adam, J., et al., Mapping of Soil Properties Using Geographical Information System (GIS): A Case Study of Hassan Usman Katsina Polytechnic. 2018. 8(4): p. 544-554.
- Kunapo, J., et al., Development of a Web-GIS based geotechnical information system. 2005. 19(3): p. 323-327.
- Arshid, M.U. and M.J.A.S. Kamal, Regional Geotechnical Mapping Employing Kriging on Electronic Geodatabase. 2020. 10(21): p. 7625.
- Critelli, S. and E.J.S.G. Garzanti, Provenance of the lower Tertiary Murree redbeds (Hazara-Kashmir Syntaxis, Pakistan) and initial rising of the Himalayas. 1994. 89(3-4): p. 265-284.
- Khan, A.N., A.E. Collins, and F.J.N.H. Qazi, Causes and extent of environmental impacts of landslide hazard in the Himalayan region: a case study of Murree, Pakistan. 2011. 57(2): p. 413-434.
- Kausar, R., et al., Spatio-temporal land use/land cover analysis of Murree using remote sensing and GIS. 2016. 6(3): p. 50-58.
- Craig, R.F., Craig's soil mechanics. 2004: CRC press.
- Lu, G.Y. and D.W. Wong, An adaptive inverse-distance weighting spatial interpolation technique. Computers & geosciences, 2008. 34(9): p. 1044-1055.
- Wang, C. and H. Zhu, Combination of Kriging methods and multi-fractal analysis for estimating spatial distribution of geotechnical parameters. Bulletin of Engineering Geology and the Environment, 2016. 75(1): p. 413-423.



## Quantifying Potential Impact of Temperature Variations on Water Demand in Multan Irrigation Zone

Hafiz Muhammad Kamran<sup>1</sup>, Aamir Shakoor<sup>1,\*</sup>, Zahid Mahmood Khan<sup>1</sup>, Hafiz Umar Farid<sup>1</sup>, Ijaz Ahmad<sup>2</sup>, Hafiz Muhammad Awais<sup>3</sup>, Qamar Iqbal<sup>1</sup>, Imran Rasheed<sup>1</sup>, Muhammad Abdul Wajid<sup>3</sup>

<sup>1</sup> Department of Agricultural Engineering, Bahauddin Zakariya University, Multan, Pakistan

<sup>2</sup> Center of Excellence in Water Resources Engineering, University of Engineering and Technology, Lahore

<sup>3</sup> Department of Irrigation and Drainage, University of Agriculture, Faisalabad, Pakistan

Corresponding author email: [aamirskr@bzu.edu.pk](mailto:aamirskr@bzu.edu.pk)

**Abstract:** In the hydrological cycle reference evapotranspiration ( $ET_o$ ) is the major component. The impact of climate change on  $ET_o$  in the Southern Punjab, Pakistan was determined using CROPWAT model. Detailed analysis of historical weather data (1984–2018) helped in creating baseline data to compare with regression analysis for the regional level. In this research, ordinary least square regression (OLS) technique is used for investigating the  $R^2$  and variable sensitivity that are affecting  $ET_o$  in the study area. While future predictable average temperature according to PMD PRECIS scenario for the years of 2019 to 2050 would be 28°C and according to PMD regCM4 scenario for the years of 2019 to 2050 would be 27.5°C. SNHT results showed that change point occurred at year 2001. After 2001 temperature trend suddenly increased. Based on data of the year 2017 cropping area of two major crops (wheat and maize) future water demand is projected. PMD PRECIS scenario data was used for the projection of future water demand. According to the year 2017 water demand was 7540Mm<sup>3</sup> while according to PMD PRECIS scenario in future average water demand could be increased up to 7978Mm<sup>3</sup>. Projection says that in future average water demand could be increased up to 438Mm<sup>3</sup> which is an alarming situation.

**Keywords:** Temperature, Reference Evapotranspiration, Crop water requirement, Water demand

### Introduction

The shortage of fresh water has become a more alarming situation in most parts of the world. In most parts of the world, water disputes have created in conflict and crises situation (Hoekstra et al., 2012). The demand for freshwater in the entire world is increasing; in the 21<sup>st</sup> century, it can be considered as a serious challenge. Freshwater usage rose up to six-fold globally from 1900 to 1995. The crisis of water has turned into a severe condition around the globe considered that the gap between widened demands and available water resources has been extended. Generally, the utilization of fresh water for agricultural production is about 70% (Xiong et al., 2010; Fader et al., 2011). The climate change impact on the World's hydrological cycle is anticipated to reshape the standard of demand and methods to getting water for both rain-fed and irrigated agriculture around the globe (Ohmura and Wild, 2002; FAO, 2011).

Any changes in climatic components over a significant time is defined as climate change which may affect crop yield, water requirement, irrigation requirement and consequently

freshwater resources either positively or negatively (Wheeler and Von Braun 2013). To calculate the available water, ET and precipitation are the main component of the water cycle (Sabziparvar and Tabari, 2010). Direct measurement of ET is a very difficult procedure, therefore, to calculate its different variety of models has been used (Gad and El-Gayar, 2010). Four weather parameters are majorly affecting the ET including temperature, humidity/vapour pressure, wind speed and solar radiation (Isikwue et al., 2014). Crop evapotranspiration will be increased due to increasing temperature, which causes the variations in crop yield and water production (FAO, 2011). The impact of temperature variations on water resources is affecting the whole irrigation system of Pakistan (Wescoat, 1991). In most of the developing countries, like Pakistan, the agriculture department is growing. Pakistan's economic system is agriculture-based and more depends upon the massive scale Indus basin irrigation system. Because of climate change in Pakistan annual water demand will rise by 10% whereas in the total water availability no significant



change is expected but declining water availability is predicted.

Keeping in view the above facts the following objectives of the current research were selected.

1) to analyze climatic parameters and determine the most influencing parameter, 2) to develop the correlation between most influencing parameter and reference evapotranspiration and 3) to predict crop water requirement of major crops in the region using different future climatic scenarios

## Materials and Methods

### Study Area

The focus of this study is Multan Irrigation Zone, a part of the Punjab province of Pakistan. The latitude and longitude of the Multan district is 30.1575° N, 71.5249° E. The Multan Irrigation was started on 25.03.1968. This zone is consisting of 03 Canal Circles and 01 Development Circle namely, Haveli Canal Circle, at Multan, Mailsi Canal Circle, at Multan, Nili Bar Circle, at Sahiwal and Development Circle, Multan Zone, at Sahiwal.

### Climatic Data Collection

In this study wind, relative humidity, minimum and maximum temperature data values for the area of study for the period 1983 to 2017 was obtained from Global Weather Data for SWAT (<https://globalweather.tamu.edu/>) and these data were arranged according to requirement. Sun (hr) data was obtained from world-timedate.com website. Future temperature data (daily) for prediction were collected from Pakistan Metrological Department. Four scenarios PRECIS, regCM4, RCP4.5 and RCP8.5 were selected for future prediction for the selected study areas.

### Data processing protocol and statistical analysis

ET<sub>o</sub> Calculation/ Computation of reference evapotranspiration

In this study to compute the value of ET<sub>o</sub>, FAO Penmen- Monteith method was used. For determining ET<sub>o</sub> values, this equation has been widely used (Allen et al., 1998). This equation can be writes as;

$$ET_o = \frac{(0.408\Delta(Rn - G) + (\gamma \frac{900}{T + 273})u_2(es - ea))}{\Delta + (\gamma(1 + 0.34u_2))}$$

The FAO Penman-Monteith equation requires air maximum and minimum temperature, humidity, and wind speed and radiation data. The average monthly climatic data of the selected stations were used. For analysis, daily station data were collected from PMD.

### Determination of CWR

Crop water requirement is the product of crop coefficient (K<sub>c</sub>) and reference evapotranspiration (ET<sub>o</sub>) (FAO).

$$CWR = (K_c \times ET_o)$$

Where, CWR = Crop Water Requirement, K<sub>c</sub>=Crop co-efficient; ET<sub>o</sub>=Ref. Evapotranspiration and K<sub>c</sub> (crop coefficient)

### Trend analysis and most Influencing parameters

Standard Normal Homogeneity Test (SNHT) was developed by Alexandersson in 1986 to detect a change in a series of rainfall data. SNHT is applied to a series of ratios that compare the observations of a measuring station with the average of several stations. Standard normal homogeneity test (SNHT) has been performed using XLSTAT software for trend analysis. Most influencing parameters were determining using data analysis regression techniques.

### Model validations

The statistical parameters such as Mean error, Mean Absolute Error, Root mean squared error and Modeling efficiency were used for model validation.

### Future scenarios

Group method of data handling (GMDH) is also known as statistical and Polynomial Neural Networks. For predictive analytics solutions and chain planning GMDH is a global innovative provider. Four types of tools were used for data analysis: Time series forecast, Regression (Synthetic dataset), Curve fitting (Polynomial Model) and Frequency analysis.

## Results and discussion

### Most influencing parameters

Most influencing parameters were determine using data analysis regression technique. According to results, it was found that temperature and wind are the most influencing parameters (Table 1).

**Table 1:** Data analysis regression results

	Coefficients	Standard Error	t Stat	P-value
<b>Intercept</b>	1.165209671	13.31915367	0.0874838	0.930888290
<b>Avg.Temp</b>	0.071350724	0.011552619	6.1761516	9.8349E-07*
<b>Humidity</b>	-0.188976699	0.187505248	-1.007848	0.321863440
<b>Wind</b>	1.068730904	0.043494009	24.571911	5.7961E-21*
<b>Sun</b>	0.714525267	0.703938395	1.0150395	0.318481240
<b>Rad</b>	-0.440994346	0.573914689	-0.768397	0.448463850

\*Highly-significant

In this research ordinary least square regression (OLS) model was used for investigating the world's controlling factors that are affecting  $ET_0$  in China. Geographic weighted regression (GWR) model is used for exploring the spatial relationship between climatic variables and  $ET_0$ . Depending upon the GWR results, the most influencing climatic variable affecting  $ET_0$  is temperature.

### Trend analysis using SNHT

The results of Standard Normal Homogeneity Test (SNHT) for temperature trend analysis are shown in Figure 1. The results show that temperature change point occurred at year 2001 and showed sudden increased.

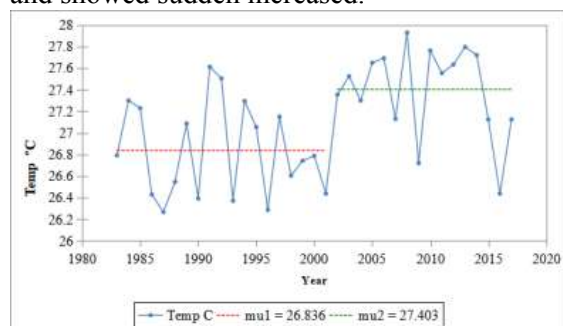


**Figure 1:** Standard Normal Homogeneity Test (SNHT)

### Relationship between Min, Max and Avg. Temperature for Estimating $ET_0$

Three types of relations were developed for estimating  $ET_0$  using minimum, maximum and average temperatures. These relationships gave the idea about best fit temperature for measuring  $ET_0$  (Table 2). According to RMSE and MEF results there is no such a big difference among the results values, but average temperature results are more precise. So average temperature is the best fit temperature that can be used for estimating  $ET_0$ .

**Table 2:** Relationship b/w min, max and avg. temp. for estimating  $ET_0$

Temperature	RMSE	Modeling Efficiency (MEF)
Minimum	0.449429	0.994659
Maximum	0.459315	0.995439
Average	0.45	0.995719

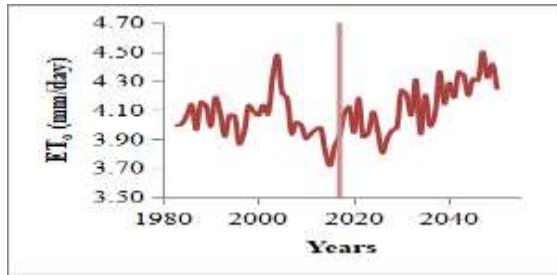
### Validation results

#### Correlation & validation between temperature & $ET_0$

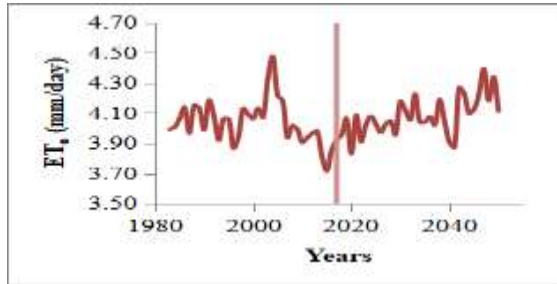
The climatic data of 35 years from 1984 to 2018 were used to develop the relations using excel regression techniques. Yearly analysis shows that polynomial regression technique is best which gave the highly precise results as shown in Table 3 while seasonally analysis shows that the linear regression technique is best which gave highly precise results. Monthly analysis shows that the linear regression technique is best which gave highly precise results. Best fit equations and validation results of mean error, mean absolute error, root mean square error and modeling efficiency on yearly, seasonally and monthly basis.

#### Analysis of reference evapotranspiration ( $ET_0$ ):PRECIS and regCM4 scenario

$ET_0$  data for the years 1984 to 2050 are presented in Figure 2. The graph indicated that the range of  $ET_0$  is in between 3.7 to 4.5mm/day.  $ET$  increases due to high temperature and dry hot wind while  $ET$  decreases due to high precipitation and moist cold wind.



(a)



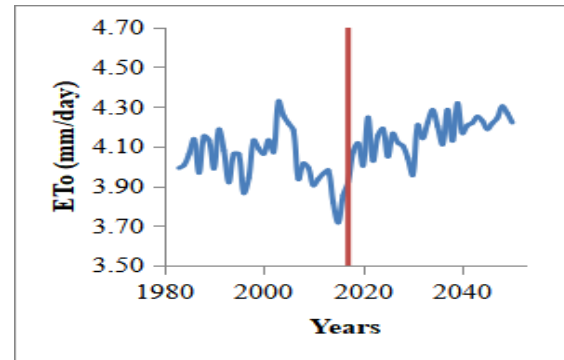
(b)

**Figure 2:** results of (a) PRECIS and (b) regCM4 scenarios

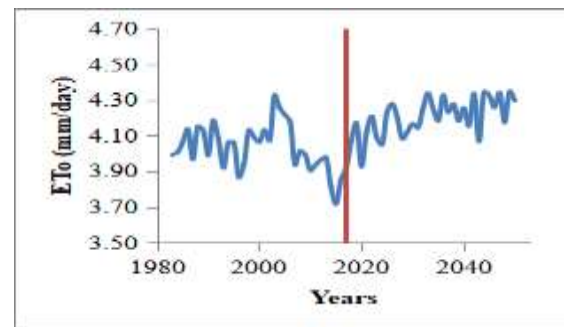
### RCP 4.5 and RCP 8.5 scenario

ET<sub>0</sub> data for the years 1984 to 2050 are presented in Figure 3. ET<sub>0</sub> was presented in millimeter per day (mm/day). The graph indicated that the range of ET<sub>0</sub> is in between 3.7 to 4.3mm/day. ET increases due to high temperature and dry hot wind while ET decreases due to high precipitation and moist cold wind. The water vapour holding capacity

of air can be enhanced by increasing temperature and affects evapotranspiration. By increasing temperature, the saturation pressure increases as well and can cause dryness and also enhance ET.



(a)



(b)

**Figure 3:** Results of (a) RCP 4.5 and (b) RCP 8.5 scenarios

**Table 3:** Correlation and validation between temperature & ET<sub>0</sub>.

Duration	Equations	ME	MAE	RMSE	MEF
Yearly	$ET_0 = 0.001T^2 + 0.052T + 1.288$	-0.08	0.39	0.47	0.986227
<b>Seasonally</b>					
Rabi	$ET_0 = 0.148T + 0.197$	0.01	0.28	0.35	0.986806
Kharif	$ET_0 = 0.197T - 1.770$	-0.18	0.38	0.46	0.990915
<b>Monthly</b>					
January	$ET_0 = 0.039T + 1.720$	0.01	0.10	0.13	0.996129
February	$ET_0 = 0.062T + 1.916$	0.01	0.12	0.15	0.996954
March	$ET_0 = 0.062T + 2.398$	0.00	0.11	0.14	0.998508
April	$ET_0 = 0.038T + 3.484$	0.00	0.14	0.17	0.998544
May	$ET_0 = 0.070T + 2.692$	0.01	0.20	0.29	0.996601
June	$ET_0 = 0.238T - 3.616$	0.02	0.31	0.39	0.994706
July	$ET_0 = 0.101T + 2.008$	0.03	0.36	0.42	0.994452
August	$ET_0 = 0.171T - 0.812$	0.02	0.34	0.42	0.993709
September	$ET_0 = 0.210T - 2.549$	0.02	0.24	0.32	0.994239
October	$ET_0 = 0.044T + 2.141$	0.02	0.15	0.19	0.996398
November	$ET_0 = -0.019T + 3.030$	-0.01	0.15	0.19	0.994343
December	$ET_0 = 0.067T + 1.214$	0.01	0.13	0.17	0.993964

## PMD scenarios results

Figure 4 shows the  $ET_o$  data for the years of 1984 to 2050 using past data and PMD scenarios (PRECIS, RegCM4, RCP4.5 and RCP8.5).  $ET_o$  was presented in millimeters. The graph indicated that the range of  $ET_o$  is in between 1440 to 1537 mm. PRECIS has high  $ET_o$  value as compared to regCM4 while RCP 8.5 has high  $ET_o$  value as compared to RCP 4.5. Some climatic factors affect the sensitivity of ET, including temperature variations, wind speed, sun hours and humidity (Mamassis et al., 2014).

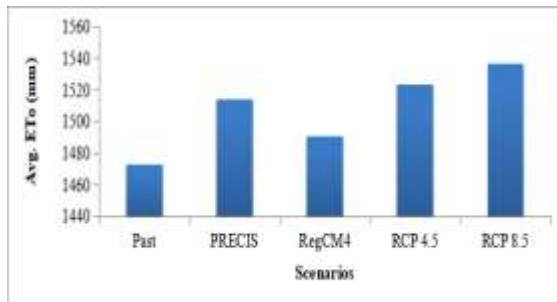


**Figure 4:** PMD scenarios results

## Group Method of Data Handling (GMDH) analysis

### Time series forecast

Time series forecast results using GMDH model are shown in Figure 5. Time series forecast is a technique that is used for the prediction of events through a sequence of time. Historical data examine by the analysts and check for four patterns of time decomposition, such as trends, seasonal patterns, cyclic patterns and regularity. Basically, this technique is used for predicting future events by analyzing the past trends based on the assumption that in future trends will be similar to the historical trends.

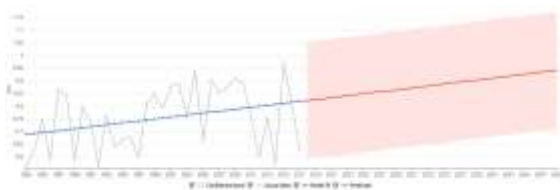


**Figure 5:** Results of Time series forecast analysis

### Curve fitting (Polynomial model)

Curve fitting (Polynomial model) results using GMDH model are shown in Figure 6. The

process of constructing a curve is called curve fitting. In this technique behind the process mathematical functions have worked that gave the best-fit series of data points, possibly subject to constraints.

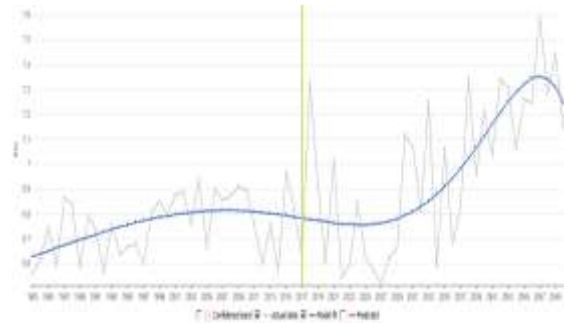


**Figure 6:** Curve fitting (Polynomial model)

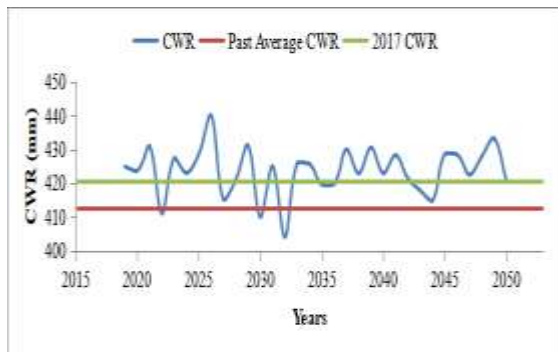
Regression (synthetic dataset) results using GMDH model are shown in Figure 7. Regression (synthetic dataset) is a repository of data technique in which data is generated programmatically. Regression (synthetic dataset) data is not collected by any real-life survey or experiment.



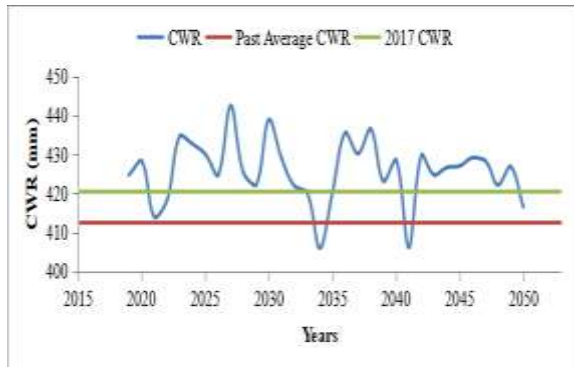
**Figure 7:** Regression (synthetic dataset)

## Analysis of crop water requirement: Wheat under RCP4.5 and RCP 8.5 scenario

Analysis of CWR for wheat in the region is present in Figure 8. Trend analysis indicates that in past years the average CWR for wheat was 412mm and in 2017 the average CWR for wheat was 420mm. Based on this projection, in future CWR would be in between 404 to 440mm and 406 to 442mm according to RCP4.5 and RCP 8.5 scenarios respectively. In future for wheat, CWR is highly increasing as compared to the past average value. This is because the winter season is shrinking every year.



(a)

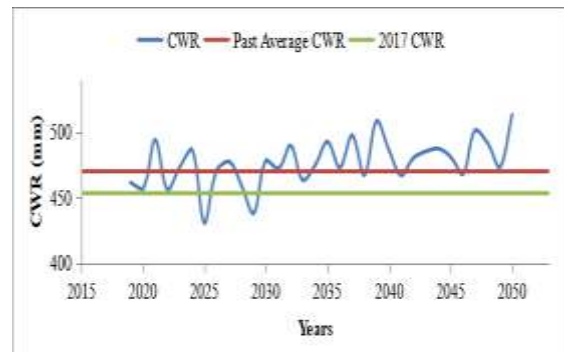


(b)

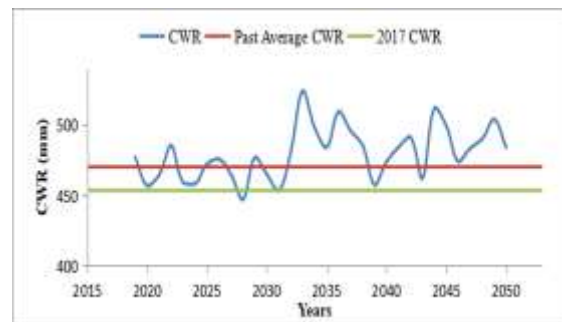
**Figure 8:** Analysis of CWR for wheat under (a) RCP 4.5 and (b) 8.5 scenarios

#### Analysis of CWR for Maize under RCP 4.5 and RCP 8.5 scenario

Analysis of CWR for wheat in the region is present in Figure 9. Trend analysis indicates that in past years the average CWR for maize was 470mm and in 2017 the average CWR for maize was 457mm. Based on the projection, in future CWR would be in between 431 to 513mm and 447 to 524mm according to RCP4.5 and RCP 8.5 scenarios, respectively. In future for maize, CWR is increasing at a moderate rate as compared to the past average value. This is due to increasing evapotranspiration by increasing temperature. Climate change would carry modifications into hydrological parameters like variations in temperature, precipitation and evapotranspiration (Jain and Kumar, 2012). 1°C increasing temperature will produce 40mm an average increase in annual potential evapotranspiration is the western U.S (George et al., 1993).



(a)



(b)

**Figure 9:** Analysis of CWR for maize under (a) RCP 4.5 and (b) 8.5 scenarios

#### Change analysis of crop water requirement

##### Change analysis of CWR for wheat under RCP 4.5 and RCP 8.5 scenario

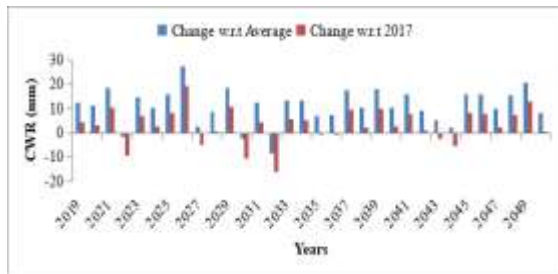
Change analysis of past trend and projection of CWR of wheat for the region is present in Figure 10. According to past average data, change is higher as compared to data of 2017. According to past average data and data of the year 2017 projected CWR is increasing up to 28 and 20mm in RCP 4.5 scenario while 30 and 22mm in RCP 8.5 scenario respectively. According to data of year 2017 CWR is slightly decreasing in some years. Decreasing  $ET_0$  would be due to Uneven and unusual precipitation trend while Increasing  $ET_0$  would be due to the increasing temperature which will increase the water demand.

##### Change analysis of CWR for Maize under RCP 4.5 and RCP 8.5 scenario

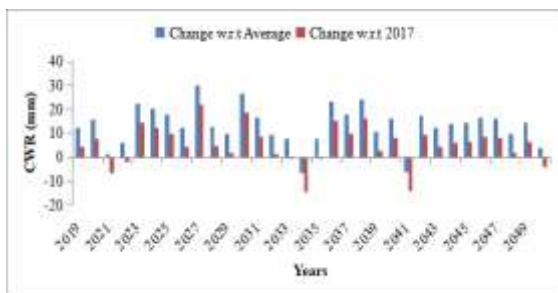
Change analysis of past trend and projection of CWR of maize for the region is present in Figure 11. According to past average data change is lower as compared to data of 2017. According to past average data and data of the year 2017 projected CWR is increasing up to 43 and 60mm in RCP 4.5 scenario while 54 and 70mm in RCP 8.5 scenario respectively. According to past



average data CWR is decreasing in some years. Decreasing  $ET_0$  would be due to Uneven and unusual precipitation trend while Increasing  $ET_0$  would be due to the increasing temperature which will increase the water demand.

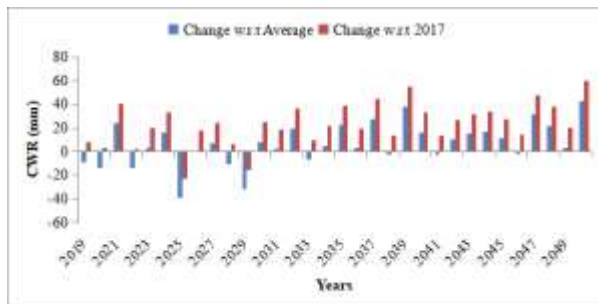


(a)

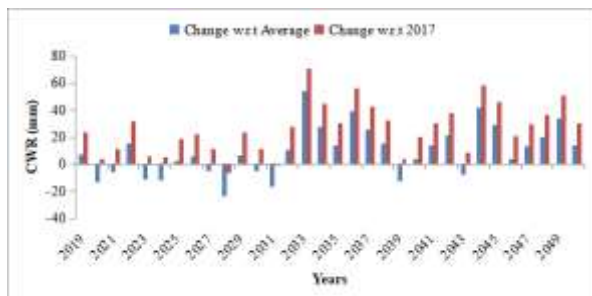


(b)

**Figure 10:** Change analysis of CWR for wheat under (a) RCP 4.5 and (b) 8.5 scenario



(a)



(b)

**Figure 11:** Change analysis of CWR for Maize under (a) RCP 4.5 and (b) 8.5 scenario

## Future water demand

Future crop water requirement represents the future water demand in agriculture of Multan irrigation zone. Based on data of the year 2017 cropping area of wheat and maize future water demand is projected for these two major crops. PMD PRECIS scenario data were used for the projection of future water demand (Figure 12).

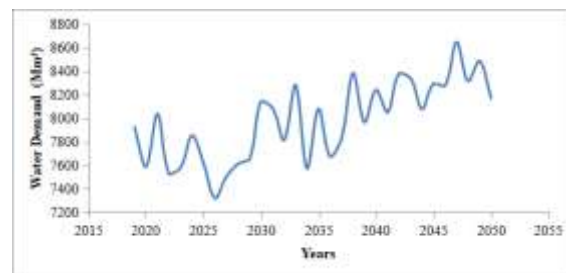


**Figure 12:** Future water demand

According to the year 2017 water demand was  $7540\text{Mm}^3$  while according to PMD PRECIS scenario in future average water demand could be increased up to  $7978\text{Mm}^3$  as shown in Figure 4.26. Projection says that in future average water demand could be increased up to  $438\text{Mm}^3$  up to 2050 as shown in Figure 4.27 which is an alarming situation.

## Conclusions

The following conclusion were drawn from the reported research study. It has been found that significant change point occurred in 2001 based on SNHT analysis. Temperature and wind are most influencing parameters among four parameters (Temperature, wind, relative humidity and sunshine hours) to determine  $ET_0$ . Correlation analysis showed that monthly analysis has best results among the yearly, seasonally and monthly correlation analysis. Increase in wheat CWR under RCP 4.5 scenario is up to 27.5mm while under RCP 8.5 scenario is up to 30mm till 2050. Increase in maize CWR under RCP 4.5 scenario is up to 43mm while under RCP 8.5 scenario is up to 54mm till 2050. Temperature variations are not same in all over the region so spatial data should be used for more accurate results. CWR calculator is limited within Multan region. It should be widened up to large scale using more climatic data. Relationships are developed on based on regression and correlation techniques. The latest techniques (ANN, soft computing) should be used for better accuracy.

## References

- Allen, R.G., L.S. Pereira, D. Raes and, M. Smith. 1998. 'Crop evapotranspiration – Guidelines for computing crop water requirements'. FAO Irrigation and drainage :56. Food and Agriculture Organization. Rome, Italy.
- Bates, B.C., Z.W. Kundzewicz, S. Wu, J.P. Palutik. 2008. Climate Change and Water, Technical Paper of the Intergovernmental Panel on Climate Change.33–48.
- Fader, M., D. Gerten, M. Thammer, J. Heinke, H. Lotze-Campen, W. Lucht and W. Cramer. 2011. Internal and external greenblue agricultural water footprints of nations, and related water and land savings through trade. *Hydro Earth Syst Sc* 15: 1641-1660.
- FAO, 2011.Climate change, water and food security. Food and Agriculture Organization of the United Nations, Land and Water Development Division, Rome.
- FAO, 2011.Climate change, water and food security. Food and Agriculture Organization of the United Nations, Land and Water Development Division, Rome.
- Gad, H.E., S.M. El-Gayar. 2010. Effect of solar radiation on the crops evapotranspiration in Egypt. In: The 14th International Water Technology Conference. Cairo, Egypt: IWTC, 769–783.
- Ghosh, S. and C. Misra. 2010. Assessing hydrological impacts of climate change modeling techniques and challenges. *The Open Hydrology Journal* 4, 115–121.
- Hoekstra, A.Y. and P.Q. Hung 2002. Virtual water trade: A quantification of virtual water flows between nations in relation to international crop trade. Value of Water Research Report Series No. 11, UNESCO-IHE, Delft, The Netherlands.
- Isikwue, C.B., O.M. Audu and O.M. Isikwue. 2014. Evaluation of evapotranspiration using FAO penman–monteith method in Kano Nigeria. *International Journal of Science and Technology*, 3(11): 698–703.
- Mamassis, N., D. Panagoulia and A. Novcovic. 2014. Sensitivity analysis of Penman evaporation method. *Global Network for Environmental Science and Technology*, 16(4): 628–639.
- Ohmura, A. and M. Wild. 2002. Climate change: is the hydrological cycle accelerating? *Science* 298: 1345-1346.
- Ohmura, A. and M. Wild. 2002. Climate change: is the hydrological cycle accelerating? *Science* 298: 1345-1346.
- Sabziparvar, A.A. and H. Tabari. 2010. Regional estimation of reference evapotranspiration in arid and semiarid regions. *Journal of Irrigation and Drainage Engineering*, 136(10): 724–731.
- Wescoat, J. and L. Jr. 1991. Managing the Indus River basin in light of climate change: four conceptual approaches. *Global Environmental Change*. 1, 381-395.
- Wheeler, T. and J. von Braun. 2013. Climate change impacts on global food security. *J. Sci.*, 341: 508–513.
- Xiong, W., I. Holman, E. Lin, D. Conway, J. Jiang, Y. Xu and Y. Li. 2010. Climate change, water availability and future cerealproduction in China. *Agric. Ecosyst. Environ.* 135 (1–2), 58–69.
- Xiong, W., I. Holman, E. Lin, D. Conway, J. Jiang, Y. Xu and Y. Li. 2010. Climate change, water availability and future cerealproduction in China. *Agric. Ecosyst. Environ.* 135 (1–2), 58–69.

## Climate Change Impact Assessment on Irrigation Water Supply and Demand in Rechna Doab, Pakistan

Aroosa Jabeen<sup>1\*</sup>, Syed Hamid Hussain Shah<sup>1</sup>, Aamir Shakoor<sup>2</sup>, Muhammad Abdul Wajid<sup>1</sup>,  
Muhammad Adnan Shahid<sup>1</sup> and Hafiz Umar Farid<sup>2</sup>

<sup>1</sup> Department of Irrigation and Drainage, University of Agriculture, Faisalabad, Pakistan

<sup>2</sup> Department of Agricultural Engineering, Bahauddin Zakariya University, Multan, Pakistan

Corresponding author email: [aroosajabeen34@gmail.com](mailto:aroosajabeen34@gmail.com)

**Abstract:** Water Evaluation and Planning (WEAP) model was applied to predicts the impact of climatic variability and increased withdraws of the irrigation on the accessible amount of water. Six scenarios were performed to predicts the climate change impact on water demand and irrigation system reliability. Results displayed that mean annual water demand for Upper Rechna doab and lower Rechna doab was about 14765 and 20654 million cubic meter (MCM), respectively. The demand site reliability for UCC (Upper Chenab canal), RB (Raya branch), Jhang, Gugera, Haveli canal and MR (Marala Ravi) were found to be 40.25%, 41.05%, 41.05%, 18.53%, 93.17% and 91.05%, respectively. Irrigation demand of Rechna doab were predicted to be increased from 5902 MCM (Scenario 3) to 5963 MCM (Scenario 6), in comparison to baseline period.

**Keywords:** WEAP, Climate change, Water demand, Irrigation system reliability

### Introduction

Climate change can have extreme effects on the hydrological cycle by evapotranspiration, soil moisture and precipitation with increasing temperature (Kahsay et al., 2018). The rainfall pattern is prospectively changing around the world due to initiation of global warming and climate change (Paul et al., 2018). Climatic changes such as variation in weather configurations as well as floods and droughts, intensified population, escalation of human water demand and its misuse are major causes of the water scarcity. The hydrologic structures are widely studied on the basis of climate change effect in all over world (Brown et al., 2019; Nauman et al., 2019).

Due to poor substructure and less familiarization, Pakistan is mainly affected by climate change (Stocker et al., 2013; Sithiengtham, 2019). From the past many years, Pakistan is facing huge floods due to deviations in levels of temperature on seasonal and daily basis (Chohan et al., 2015; Nauman et al., 2019). For example, at Chenab river; there was a continuous heavy flood of 0.96 million cusecs in 2010. Similarly, deposition of silt, sand and water was major cause of prolonged substantial destruction to rice paddies (Chohan et al., 2015).

The large gap among water demand and water supply has enlarged manifolds because of enormous rise in agriculture activities and

reduction of the river flow in Pakistan. This gap usually extends in growing season of summer than winter growing season. In Pakistan, production of agriculture is largely dependent on irrigation system and climatic conditions (Sadozai et al., 2019). Therefore, there is a dire and urgent need to develop an approach oriented real time system which can give irrigation water in an adaptable form particularly where needed. WEAP model can be used for determining water demand like real time water demand which based on crop water requirement. WEAP Model can also establish future climatic scenarios on the basis of current account year and also determine that how much climatic change has sufficient impact on future irrigation water demand and reliability. WEAP model is mostly used for estimating the effect of climate change in future (Mehta et al., 2013; Santikayasa et al., 2015; Sithiengtham, 2019) and can also be used to develop multiple scenarios or other alternatives on different water resources (Wilby et al., 2007; Joyce et al., 2011).

Therefore, there is dire need to use hydrological modeling tools to manage surface water resources under future climate scenarios. Thus, the research study was conducted with these key objectives 1) to assess current irrigation water demand in Rechna doab using satellite data, 2) to estimation of the impact of climate change on future irrigation demand under different climate change scenarios and 3) to build and calibrate

WEAP model to develop guidelines for effective management of canal water resources.

16.7 % Sialkot and 16.6% Sheikhupura (Khan et al., 2008).

## Materials and Method

### Data collection and pre-processing

#### Study area

The research data were collected for period of 2006-2016 includes Climate data, Soil data, Discharge data and Agriculture data (Table 1).

The study area consists of Rechna Doab, Punjab province of Pakistan that lies between Ravi and Chenab rivers in core of Indus basin irrigation system (Figure 1). Overall farm area of Rechna doab is 2.30Mha from which 15.3 percent situated in Faisalabad district and remaining is allocated in other districts such as 8.9 % Toba-Tek Singh; 25.1 % Jhang; 17.5% Gujranwala;

#### Rechna doab schematization

The GIS map of study area manipulated in WEAP as reference background of schematic river networks, principal groundwater bodies, sub-catchments and other physical components of Rechna Doab catchment.

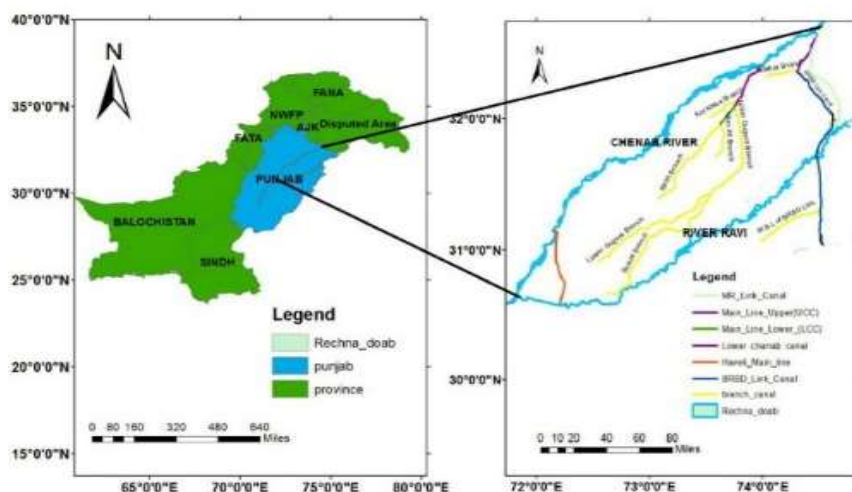


Figure 76: Location of Rechna Doab and irrigation system (Main, Link and Branch Canals)

Table 26: Data collection of study area from different sources

Inputs	Time period and specification of Input data	Sources of data	Description of parameters
Monthly basis Meteorological Data	2006-2016	Regional Meteorological Department, Lahore, Government of Punjab, Pakistan	Latitude, Longitude, Wind Velocity, Relative Humidity, Precipitation, Maximum and Minimum temperature, Sunshine Hour
Daily basis Discharge	2006-2016	Punjab Irrigation Department, Lahore, Government of Punjab, Pakistan	Barrages and Head works, River Chenab and Ravi, Main, Link and Branch Canals
Soil Data	Soil map of all command areas of Rechna Doab	FAO-website ( <a href="http://www.fao.org/geonetwork/srv/en/metadata.show?id=14116">http://www.fao.org/geonetwork/srv/en/metadata.show?id=14116</a> )	Jhang, Gugera, RB area, H link Area, Marala Ravi area,
Agricultural Data	2006-2016	Concerned Agricultural Department (Yearly online published Reports & FAO. 56)	Crop Coefficient, Crop Planting Date, Irrigation Scheduling
Shape files of command area	-----	Punjab Irrigation Department, Lahore Government of Punjab, Pakistan	River Chenab and Ravi, Main, Link and Branch Canals
Land Use Land Cover Data	2013-2014	Faculty of Agricultural Engineering and Technology. Uni. of Agri. Faisalabad.	Seasonal crops of Canal command areas in Rechna Doab

In WEAP model, MABIA method was used which can calculate transpiration, evaporation, time of irrigation and amount of water for irrigation, crop growth time along with yields amount for each crop (Ahmed et al., 2015). The time-step of MABIA method is obtained daily after computing transpiration, infiltration, evaporation, runoff and requirements of irrigation, and the results can be accumulated to a monthly step (Esteve et al., 2015). The reference evapotranspiration was calculated using Penman-Monteith equation in Cropwat model.

### Proposed climate change scenarios

Six climate change scenarios (Table 2) were proposed in WEAP in order to determine future climatic change on irrigation water demand of Rechna Doab. The design scenarios were based on GCM data which used in AR4 (4<sup>th</sup> assessment report) by IPCC (Intergovernmental Panel on Climate Change) (Meehl et al., 2007) and collected from PMD website as shown in Table 2.

### Model calibration and validation

The monthly stream flow data at discharge gauges and canals were used for calibration and validation (Obahoundje et al., 2017; Hussien et al., 2018). The NSE (Nash et al., 1970) is dimensionless and scaled version of MSE for the value range between 0 and 1 but 1 for a perfect model because it gives a much well defined elevation for the model results and performance (Obahoundje et al., 2017). Volumetric efficiency ranges between 0-1 and 1 for an absolute agreement among observed and simulated stream flow values. As shown in equation (1) and (2),  $Q_{st}$  and  $Q_o$  are the values of simulated stream flow and observed stream flow and N is total numbers of observations.

Volumetric Efficiency (Moriassi et al., 2007):

$$VE = 1s - \frac{\sum_{i=1}^N |Q_{st} - Q_o|}{\sum_{i=1}^N (Q_o)} \quad (1)$$

Nash-Sutcliffe Efficiency (Moriassi et al., 2007):

$$NSE = 1 - \frac{\sum_{i=1}^N (Q_o - Q_{st})_i^2}{\sum_{i=1}^N (Q_o - \overline{Q_s})_i^2} \quad (2)$$

## Results and Discussion

### Calibration and validation of WEAP model

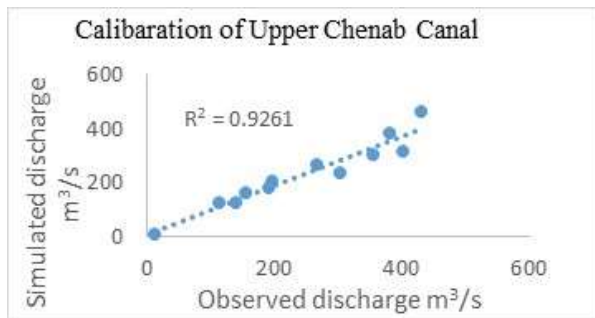
The values of  $R^2$  and NSE display the relationship between monthly observed and simulated stream flow of Upper Chenab Canal and Lower Chenab canal. The monthly average values for duration of 2006-2010 were used for the calibration as shown in Figure 2 where  $NSE=0.92$  and  $R^2$  is 0.93 in Upper Chenab canal (UCC) and  $NSE=0.77$  and  $R^2 =0.88$  in Lower Chenab Canal. The volumetric efficiency of Upper Chenab canal and Lower Chenab canal were 0.94 and 0.90, respectively.

**Table 27:** Six climate change scenarios

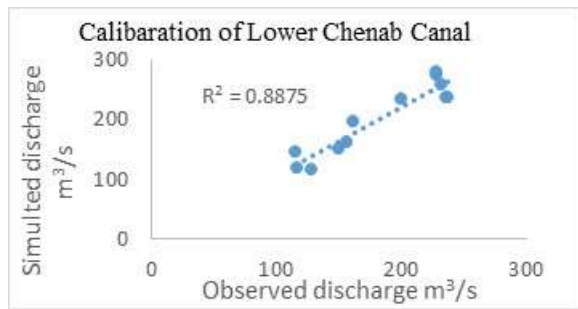
Scenarios	Approaches
<b>Scenario-I:</b> Precipitation-RCP 4.5 Scenario	Future climate change effects (Rainfall data) with RCP 4.5 up to 2099
<b>Scenario-II:</b> Temperature-RCP 4.5 Scenario	Future climate change effects (Temperature data) with RCP 4.5 up to 2099
<b>Scenario-III:</b> Combine effect of prep and temp-RCP 4.5 Scenario	Future climate change effects (Temperature & Rainfall data) with RCP 4.5 up to 2099
<b>Scenario-IV:</b> Precipitation-RCP 8.5 Scenario	Future climate change effects (Rainfall data) with RCP 8.5 up to 2099
<b>Scenario-V:</b> Temperature-RCP 8.5 Scenario	Future climate change effects (Temperature data) with RCP 8.5 up to 2099
<b>Scenario-VI:</b> Combine effect of precip. and temp-RCP 8.5 Scenario	Future climate change effects (Temperature & Rainfall data) with RCP 8.5 up to 2099

After the calibration step, a validation was performed for period of 2011-2016. For the degree of accuracy, the modeling results were measured at monthly timescale by using performance indicator NSE and  $R^2$  and VE. Streamflow of Upper Chenab canal and Lower Chenab canal were simulated reasonably well with  $NSE= 0.94$  and  $0.88$  and  $R2 =0.94$  and  $0.92$  as shown in Figure 3 and  $VE=0.98$  and  $0.84$ .



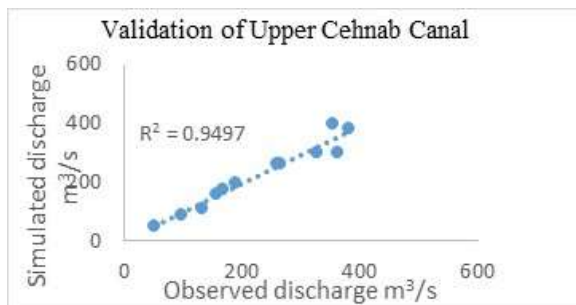


(a)

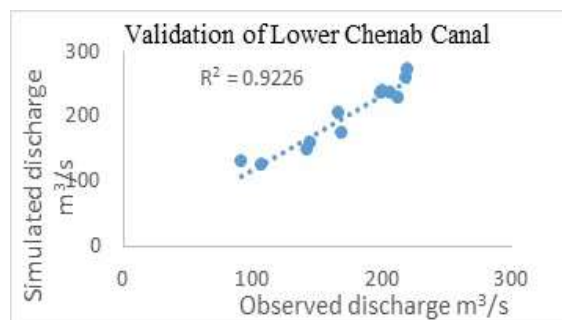


(b)

**Figure 2:** Calibration of (a) Upper Chenab canal and (b) Lower Chenab canal for period of 2006-2010



(a)



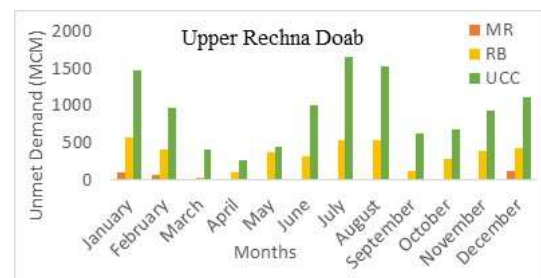
(b)

**Figure 3:** Validation of (a) Upper Chenab Canal and (b) Lower Chenab canal for the time period 2011-2016

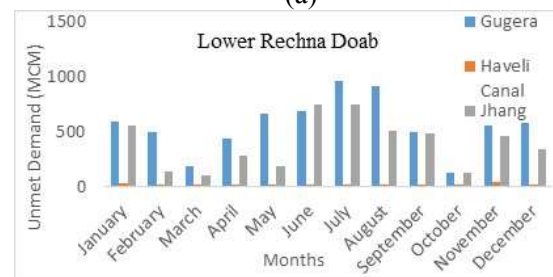
### Estimation of unmet demand

For the period of 2006-2016 unmet demand for sub-catchment areas of Upper and Lower Rechna Doab was estimated by WEAP. For WEAP

model, the unit of unmet demand was selected in million cubic meters (MCM). Unmet demand is the amount of water which cannot be substantially distributed from river in a section of year. That condition is prospective to decline in future because of rise in water demand if no methods would be adopted to address them. Unmet demand curve of canal catchment areas (MR area, RB area, UCC area, Jhang, Gugera, and Haveli Canal area) is extraordinary high in months of Dec, Jan, Feb, June, July and August as compared to other months such as March, April, May, October and November as shown in Figure 4.



(a)



(b)

**Figure 4:** Unmet demand for (a) Upper Rechna Doab and (b) Lower Rechna Doab

### Future Climate Change Scenario Analysis

Six climate scenarios were evaluated in terms of current water demand and reliability which was estimated by using RCP 4.5 and RCP 8.5 of monthly temperature and precipitation data for time period of 2007-2099. These climate change scenarios are described in detail below.

#### Precipitation-RCP 4.5 scenario

In this scenario we used the GCM data of precipitation RCP 4.5 in order to estimate the impact of precipitation on irrigation system reliability. The Figure 5 shows that the trend of future system reliability which attained from this scenario is reduced as compare to the existing reliability of system. This scenario is predicting a decrease in precipitation over the next century. The results highlights that the total crop water

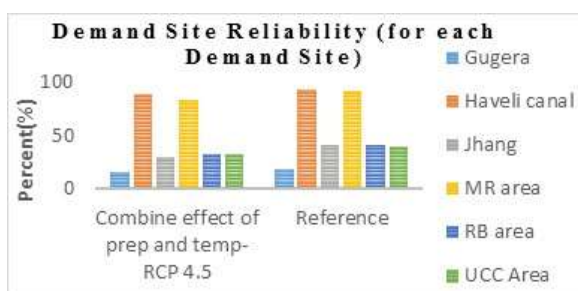
requirement is not fulfilled from the available water supply. Moreover, canal catchment areas are also facing water shortage due to decreasing precipitation in future.



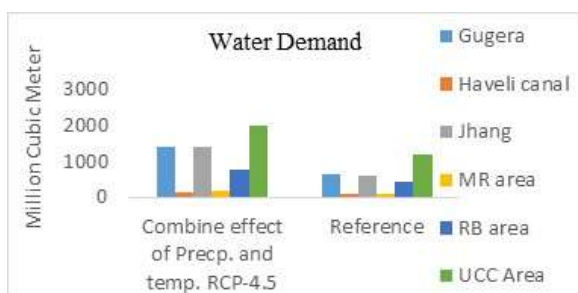
**Figure 5:** Reliability in precipitation - RCP 4.5 scenario

### Combine effect of precipitation and temperature-RCP 4.5 scenario

The RCP4.5 monthly data of precipitation and temperature was used in this scenario for the assessment of the combine effect of maximum temperature and precipitation on the irrigation system and water demand of canal catchment areas. The reliability is reduced in this scenario as compared to the reference scenario such as existing reliability of all canal catchment area which is an indication that the system would be under more stressed condition in future because of increased temperature and decreased precipitation as shown in Figure 6. On the other hand, the results of this scenario show an increasing trend of water demand as in Figure 6.



(a)



(b)

**Figure 6:** Demand site reliability and Water demand for combine effect of prep and temp-4.5 scenario and reference

### Precipitation RCP-8.5 scenario

The RCP 8.5 monthly data of precipitation was used in this scenario for determining the demand site reliability. Figure 7 shows that the reliability is decreasing because of decline in precipitation. This also predicts the decrease in stream flow and its impacts on agriculture irrigation system.

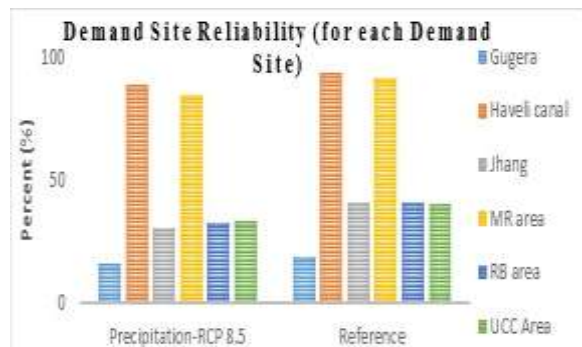
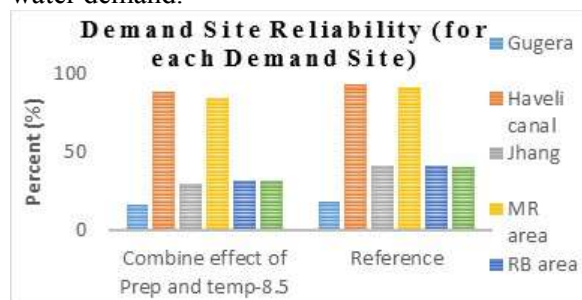


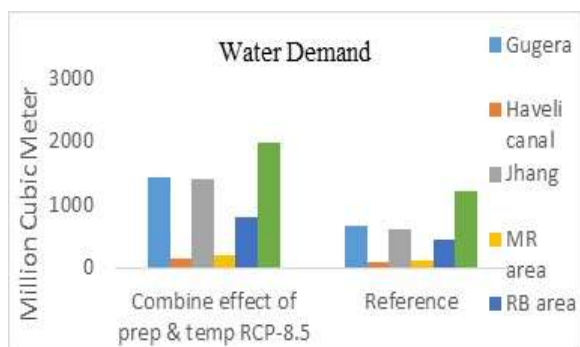
**Figure 7:** Reliability of precipitation RCP-8.5 and reference for all canal command areas

### Combine scenarios of RCP 8.5

The monthly data of precipitation and temperature RCP 8.5 used to determine the irrigation system reliability. The result shows that the reliability trend is decreasing for all canal command areas (Figure 8). The water demand is expected to rise under future climate compared with current condition or reference scenario as shown in Figure 8 because of the lower surface runoff and rates of groundwater recharge linked by enlarged evapotranspiration. Increased temperature and decreased precipitation results in increasing evapotranspiration (ET) and lessening soil moisture. The ET is increasing in large vegetative areas while lower ET values exist in less vegetative areas. There is a negative effect of climate change on the reliability and water demand.



(a)



(b)

**Figure 8:** Irrigation system reliability and Water demand of all canal command areas for combine effect of prep and temp-RCP 8.5 scenarios

### Comparison of climatic scenarios results

Different Scenarios were projected. These scenarios were developed to evaluate impacts of feasible future climate changes on availability of current water resources for all canal command areas. As we showed in the Table 3, where reliability of all canal catchment areas is

decreasing and all scenarios have a negative impact on system reliability. Lower percentage of reliability shows the possibility of system failure and decrease of water supply in all canal command areas in future. The reliability of UCC is decreased up to 17.75% in the scenario of combine effect of prep and temp-RCP 4.5. Similarly, reliability is also decreasing in all scenarios.

The water demand trend is increasing in both future climatic scenarios because the precipitation is decreasing and maximum temperature is increasing. As shown in the Table 4, 68.1% water demand of Haveli canal will increase in future. The unsolved problems were identified which need to be focused according to the overall results. Therefore, it is not suitable to give the recommendations of water based technologies and cropping patterns without concerning overall effects of climate change and water demand of the irrigated agriculture.

**Table 28:** Results comparison of irrigation system reliability for each canal command areas

Name of Scenarios	Reliability (%)					
	Gugera	Haveli canal area	Jhang	MR area	RB area	UCC area
References	No change	No change	No change	No change	No change	No change
Precipitation-RCP 4.5	-12.3%	-5.4%	-28.19%	-8.95%	-19.95%	-16.85%
Temperature-RCP 4.5	-5.1%	-2.4%	-3.98%	-2.65%	-2.15%	-3.47%
Combine effect of prep and temp-RCP 4.5	-11.5%	-5.2%	-27.55%	-9.05%	-20.54%	-17.75%
Precipitation-RCP 8.5	-12.2%	-5.1%	-26.51%	-7.01%	-19.86%	-16.58%
Temperature-RCP-8.5	-8.5%	-3.7%	-3.55%	-2.55%	-1.85%	-4.25%
Combine effect of Prep and temp-8.5	-11.8%	-5.4%	-26.80%	-6.85%	-22.15%	-20.75%

**Table 29:** Results comparison of Irrigation water demand

Canal -catchment areas	Water Demand	
	Combine effect of prep and temp-RCP 4.5	Combine effect of prep and temp-RCP 8.5
References	No change	No change
Gugera	+47.8%	+46.5%
Haveli canal	+68.1%	+67.1%
Jhang	+42.5%	+41.7%
MR area	+52.6%	+52.8%
RB area	+55.4%	+55.1%
UCC Area	+60.5%	+60.5%

## Conclusion

In this research, WEAP model was used to explore the potential impacts of climate change and increased irrigation water demand on available and future water resources in Rechna doab. The objective of study was to establish the modeling framework that can be used for measuring the climate change impacts on the water stressed regions of Rechna doab. Therefore, the future water demand of Gugera was found to be increased about +47.8% and +46.5% in the combine effect scenarios of RCP 4.5 and RCP 8.5. In combine effect scenario of RCP 8.5, the irrigation system reliability of Jhang and Upper Chenab canal were found to be decreased about -26.80% and -20.7%. Results showed the quantitative variation in precipitation or rainfall because of very less precipitation during dry seasons and excessively large precipitation during rainy seasons. Reduction of canal water supply in the canals downstream results in the increase of groundwater pumping causing the increase in irrigation cost leading towards reduction in income and productivity of canals downstream irrigators. The model results displayed that average monthly unmet water demand of Rechna doab will considerably increase in the future decades. Results also showed that both water use and risks of flood in study areas would increase in future because of continuous climate change impacts. The results for Precipitation-RCP 8.5 scenario showed that the irrigation system reliability of Rakh branch area will decrease to almost -19.85%. There is dire need to develop feasible methods and approaches in order to cope with low productivity and hidden impacts of climate change.

## References

- Ahmed, N., Mahmood, S., & Munir, S. (2015). Estimation of potential and actual crop evapotranspiration using weap model. *Science International (Lahore)*, 27(5), 4373-4377.
- Brown, T. C., Mahat, V., & Ramirez, J. A. (2019). Adaptation to future water shortages in the united states caused by population growth and climate change. *Earth's Future*, 7(3), 219-234. <https://doi.org/10.1029/2018EF001091>
- Chohan, K., Ahmad, S. R., ul Islam, Z., & Adrees, M. (2015). Riverine flood damage assessment of cultivated lands along chenab river using gis and remotely sensed data: A case study of district hafizabad, punjab, pakistan. *Journal of Geographic Information System*, 7(05), 506. <https://doi.org/10.4236/jgis.2015.75041http://www.climate-science.gov/Library/sap/sap2-1/finalreport/default.htm>
- Esteve, P., Varela-Ortega, C., Blanco-Gutiérrez, I., & Downing, T. E. (2015). A hydro-economic model for the assessment of climate change impacts and adaptation in irrigated agriculture. *Ecological Economics*, 120, 49-58. <https://doi.org/10.1016/j.ecolecon.2015.09.017>
- Hussen, B., Mekonnen, A., & Pingale, S. M. (2018). Integrated water resources management under climate change scenarios in the sub-basin of abaya-chamo, ethiopia. *Modeling Earth Systems and Environment*, 4(1), 221-240. <https://doi.org/10.1007/s40808-018-0438-9>
- Joyce, B. A., Mehta, V. K., Purkey, D. R., Dale, L. L., & Hanemann, W. (2011). Modifying agricultural water management to adapt to climate change in california's central valley. *Climatic Change*, 109(1), 299-316. <https://doi.org/10.1007/s10584-011-0335-y>
- Kahsay, K. D., Pingale, S. M., & Hatiye, S. D. (2018). Impact of climate change on groundwater recharge and base flow in the sub-catchment of tekeze basin, ethiopia. *Groundwater for Sustainable Development*, 6, 121-133. <https://doi.org/10.1016/j.gsd.2017.12.002>
- Khan, S., Rana, T., Gabriel, H. F., & Ullah, M. K. (2008). Hydrogeologic assessment of escalating groundwater exploitation in the indus basin, pakistan. *Hydrogeology Journal*, 16(8), 1635-1654. <https://doi.org/10.1007/s10040-008-0336-8>
- Meehl, G.A., Covey, C., Delworth, T., Latif, M., McAvaney, B., Mitchell, J. F., ... & Taylor, K. E. (2007). The wcrp cmip3 multimodel dataset: A new era in climate change research. *Bulletin of the American Meteorological Society*, 88(9), 1383-1394. <https://doi.org/10.1175/BAMS-88-9-1383>
- Mehta, V.K., Haden, V. R., Joyce, B. A., Purkey, D. R., & Jackson, L. E. (2013). Irrigation demand and supply, given projections of climate and land-use change, in yolo county, california. *Agricultural water management*, 117, 70-82. <https://doi.org/10.1016/j.agwat.2012.10.021>

- Moriasi, D. N., Arnold, J. G., Van Liew, M. W., Bingner, R. L., Harmel, R. D., & Veith, T.L. (2007). Model evaluation guidelines for systematic quantification of accuracy in watershed simulations. *Transactions of the ASABE*, 50(3), 885-900. <https://doi.org/10.13031/2013.23153>
- Nash, J. E., & Sutcliffe, J. V. (1970). River flow forecasting through conceptual models part i—a discussion of principles. *Journal of hydrology*, 10(3), 282-290. [https://doi.org/10.1016/0022-1694\(70\)90255-6](https://doi.org/10.1016/0022-1694(70)90255-6)
- Nauman, S., Zulkafli, Z., Bin Ghazali, A. H., & Yusuf, B. (2019). Impact assessment of future climate change on streamflows upstream of khanpur dam, pakistan using soil and water assessment tool. *Water*, 11(5), 1090. <https://doi.org/10.3390/w11051090>
- Obahoundje, S., Ofose, E. A., Akpoti, K., & Kabo-bah, A. T. (2017). Land use and land cover changes under climate uncertainty: Modelling the impacts on hydropower production in western africa. *Hydrology*, 4(1), 2. <https://doi.org/10.3390/hydrology4010002>
- Paul, N., & Elango, L. (2018). Predicting future water supply-demand gap with a new reservoir, desalination plant and waste water reuse by water evaluation and planning model for chennai megacity, india. *Groundwater for Sustainable Development*, 7, 8-19. <https://doi.org/10.1016/j.gsd.2018.02.005>
- Sonia, Sadozai, K. N., Khan, N. P., Jan, A. U., & Hameed, G. (2019). Assessing the impact of climate change on wheat productivity in khyber pakhtunkhwa, pakistan. *Sarhad Journal of Agriculture*, 35(1). <http://dx.doi.org/10.17582/journal.sja/2019/35.1.284.292>
- Santikayasa, I. P., Babel, M. S., & Shrestha, S. (2015). Assessment of the impact of climate change on water availability in the citarum river basin, indonesia: The use of statistical downscaling and water planning tools. In: *Managing water resources under climate uncertainty*. Springer: pp. 45-64. [https://doi.org/10.1007/978-3-319-10467-6\\_3](https://doi.org/10.1007/978-3-319-10467-6_3)
- Sithiengtham, P. (2019). Projecting water demand and availability under climate change through the application of weap in the nam ngum downstream area, laos. Flinders University.
- Stocker, T. F., Qin, D., Plattner, G. K., Tignor, M. M., Allen, S. K., Boschung, J., Nauels, A., Xia, Y., Bex, V., & Midgley, P. M. (2013). *Climate change 2013: The physical science basis*. Cambridge University Press Cambridge.
- Wilby, R. L., & Dawson, C. W. (2007). *Sdsm 4.2-a decision support tool for the assessment of regional climate change impacts*. User manual, 1-94.



## Spatiotemporal Variations in Snow Cover using Google Earth Engine in Gilgit-Baltistan, Pakistan

Hania Arif<sup>1\*</sup>, Syed Amer Mehmood<sup>1</sup>, Hafiz Haroon Ahmad<sup>1</sup>

<sup>1</sup> University of the Punjab, Lahore, Pakistan

Corresponding author email: [sandokan\\_nice@hotmail.com](mailto:sandokan_nice@hotmail.com)

**Abstract:** Snow and Glacier in the mountain ranges of Hindu-Kush, Karakoram, and Himalayas (HKH), are supposed to be shrinking. In the result, serious significances occurs in respect of water accessibility for inhabitants of down streams. This investigation is an effort to identify the temporal variation in tendency of snow cover in the Gilgit Baltistan (GB), northern Pakistan. For the calculation of the Normalized Difference Snow Index (NDSI) and estimation of snow covered area (SCA) MODIS images for the period of 2000 to 2020 were used. Hunza, Astore, Gilgit, Diamir, Shyok, Ghanche, Sakardu and Shigar are major sub-basins lying in Gilgit Baltistan (GB) and Hunza and Sakardu are mostly glaciated which are lays in GB. Annual fluctuation in snow cover within GB was 10 to 80%. In accumulation season that is from December to February, snow cover was almost 80% while in melting season that is from July to September this area was reduced 65-75%. The maximum and minimum SCA detect in 2009 was almost 57687.85 km<sup>2</sup> and 12083.40 km<sup>2</sup> respectively. The results show that there has been a very slight fluctuation in SCA with the passage of time. Mann Kendell trend shows the fluctuation on snow. But Mann Kendell negative trend on glacier peaks but positive trend on glacier surge and somehow foot of glaciers.

### Introduction:

Pakistan has a large number of Glaciers which have almost 5000 glaciers and glaciers cover area is almost 13680 km<sup>2</sup>. Pakistan has second largest glacier which known as Siachen glacier [Rasul, at al., 2011]. Glaciers are known as fresh water tower. In Pakistan, Glaciers play an important role in irrigation system and server as a major resource of fresh water. Snow and glaciers are preserved the fresh water in winter season and due to the melting of snow in summer season which feed the rivers and northern area of Pakistan. Economy of Pakistan is mainly reliant on agricultural, that contributing the 21% in GDP [Government of Pakistan, 2016].

In past few years, water super vision has converted a severe worldwide problem and water supply is decreasing as per capita. This condition is increasing with increasing population mainly in heavily colonized area like Asia. In Pakistan, mainly water usage is divided into three area of whole country i) 92% of water is used in agriculture, ii) 6% is used in household and iii) 2% consumption is based on industrial [Hussain at al., 2005]. HKH mountain ranges are the main sources of fresh water supply where this water system fulfill the needs of people which known as most populated area on earth and millions of people lives depend on it also in the lower area of this region [Rees at al., 2006; Immerzeel at al.,

2010]. The climatic condition of this area is semiarid especially in downstream, the supply of water from glaciers is already necessary for the crop production in this area [Nüsse at al., 2012]. In climate change, glaciers are considered the primary indicator.

About 90% of the Indus River flow originates from the hilly areas of the Western Himalayas, Karakoram and Hindu Kush [Liniger at al., 1998]. According to the IPCC (Inter-Governmental Panel on Climate Change) report in 2007, reduction in snow area throughout the last decades; as a result water availability is reduce and the seasonal variation of runoff has been observed [IPCC, 2007]. According to a study, snow and glacial melting is the major source of fresh water especially in arid and semi-arid area [Gurung at al., 2011]. Almost 17% population of the whole world is dependent upon snow melting for the sake of fresh water. [Barnett at al., 2005]. In 2013 of IPCC report, average temperature increase was detected in HKH region because of global warming [IPCC, 2013]. Remote sensing is playing a vibrant part of assessing the SCA in whole world [Shrestha at al., 2010]. MODIS products of snow-cover is an important development in snow cover evaluation especially in remotely area and these product change the traditional techniques. (Tahir et al., 2011).

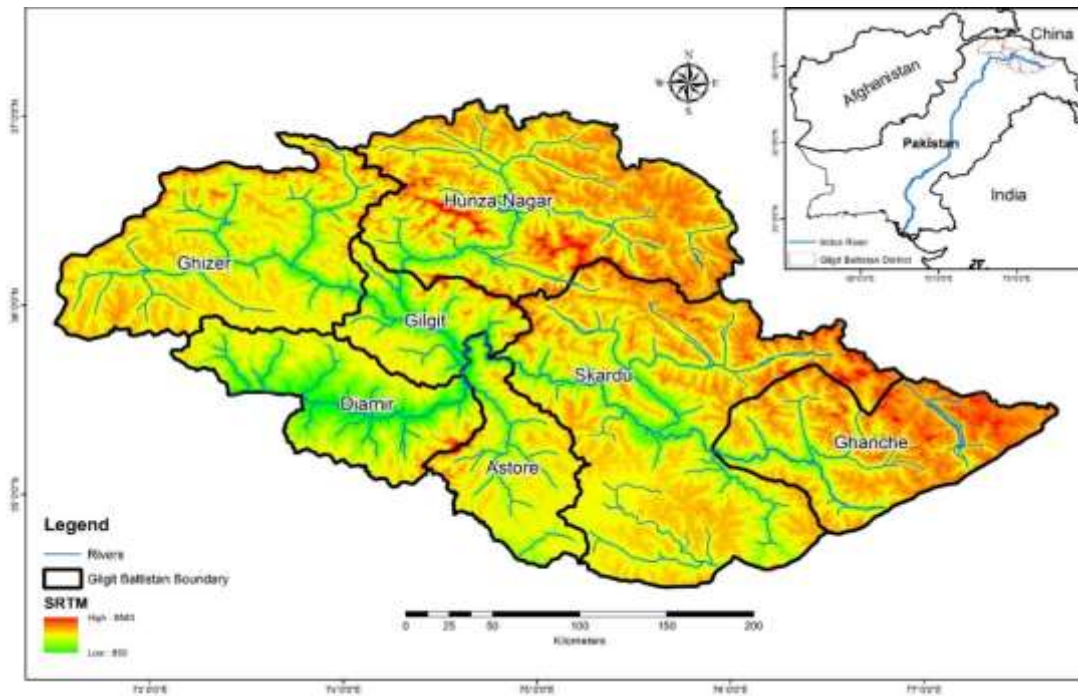


**Figure. 1** Location Map of GB

Pakistan is a developing country which economy majorly depends on food production that is more susceptible for climate changes. Pakistan does not have suitable monitoring structures for the forecast of extreme events, or the evaluation of fluctuations in weather patterns.

## Materials and Methodology

### Satellite Data

The Moderate Resolution Imaging Spectroradiometer (MODIS) dataset with spatial resolution of 500 m has been extremely appropriate for appraising snow cover of any basin which have 10,000 km<sup>2</sup> or larger area. MODIS 8-Day snow products were selected to calculate the snow cover area. Satellite datasets (MOD09A1) from 2000 to 2020 were used through Google Earth Engine (GEE). Digital Elevation Model (DEM) of Shuttle Radar Topography Mission (SRTM) having 30 m resolution was used to define topography, delineation of the watershed boundaries and elevation analysis. The SRTM DEM tiles were acquired from online USGS data portal. Study area covers the seven districts of GB in Pakistan (Figure 1).

### Methodology

The snow-product of MODIS used in this study was having spatial resolution of 500m and projected onto Universal Transverse Mercator (UTM) Zone 43N projection with WGS-1984

datum. The SCA was estimated by using 8 daily MODIS snow-products. Satellite datasets (MOD09A1) from 2000 to 2020 were used through GEE. Snow detection usages the Normalized Difference Snow Index (NDSI) approach using GEE from 2000 to 2020 that is an actual way to distinguish snow from other features. In other words snow cover area seen as more enhanced.

$$\text{NDSI} = \frac{\text{Band 4} - \text{band 6}}{\text{Band 4} + \text{band 6}} \quad (1)$$

Band 4 = Green (sur\_refl\_b04)

Band 6 = SWIR (sur\_refl\_b06)

NDSI is used to observe the extent of SCA. This behavior of snow helps in differentiating between snow and clouds in remotely sensed data. Moreover, NDSI gives the strength to results of multiple band combinations, as, its value less than 0.4 (<0.4) indicates the presence of snow. The Snow Covered Area (SCA) is been estimated using the Snow cover products of MODIS for the period 2000–2020 periods using google earth engine. The monthly SCA data is develop, taking the average of 8-day data in every month for GB area. The analysis is carried out for mean monthly and an annual of SCA of study area. Using the SRTM DEM of the study area, extracted for detailed analysis of snow cover distribution and all work done through programming in GEE.

In 2000, the snow trend of GB as basin wise shows in (Figure 2). In Figure 3, snow variation

represents through remote sensing data and these images represent the monthly variation of snow in GB area where August and September is having maximum snow free area, February is having maximum snow area and January images are not available in 2000 because MODIS launched in 18 February 2000.

In 2020, the snow trend of GB as basin wise shows in (Figure 4). In Figure 5, snow variation represents through remote sensing data and these images represent the monthly variation of snow in GB area where August and September is having maximum snow free area, January February is having maximum snow area.

Melting of Ice-sheet and snow is continuous and major contributor of river flow in Pakistan. 85% annual flow in Indus River comes from snow and glacier melting (Hewitt et al. 2005). The trend of spatiotemporal variation in SCA at annual basis was similar in all sub basins lying within GB.

In Figure 6, trend shows that snow cover area in GB is decreases and increases simultaneously. Indus River (IR) and its streams originate from Karakoram and Himalayan region beside the north eastern and northern border of Pakistan. The Indus River system create a relationship among two natural reservoirs, 1<sup>st</sup> one is snow in mountainous region and 2<sup>nd</sup> one is groundwater that contained alluvium in Indus of the Punjab and Sindh Provinces of Pakistan. IR and its tributaries water is main source for agricultural area and water supply for 130 million people. Owing to melting of snow in the summer season (July, August and Sept) the huge volume of water is accessible in IR.

### Benefits using GEE

MODIS data in the GEE has various advantages especially for large area and long time series mapping (Johansen et al., 2015, Patel et al., 2015). Furthermore, it is very easy to integrate annual and mean monthly NDSI time series and develop the classification accuracy. As more remote sensing data and machine learning algorithms are integrated through GEE and data collection, we extract the information from remote sensing data to be shortened even for further use. GEE makes data management easier as all set of remote sensing data can be called through one or two lines of code. Most of RS products are already processed. A great advantage is we didn't download the remote sensing products when we are working on long term analysis. Basic functionality of GEE, time and space is save as compare to when we are working manually. In GEE, we have done statistical analysis on satellite images. Mann Kendall trend shows the fluctuation on snow. But Mann Kendall negative trend on glacier peaks but positive trend on glacier surge and somehow foot of glaciers (Figure 7).

Mann Kendall trend shows the fluctuation on snow. The Mann–Kendall test model is applied on the NDSI data, and the results are shown in Figure 7. In summary, the z-score and tau-value for the entire NDSI time series period (2000–2020) are found to be  $-0.95$  and  $0.84$ , respectively. Negative values show the negative trend on glaciers and positive values shows positive trend foothill of glaciers.

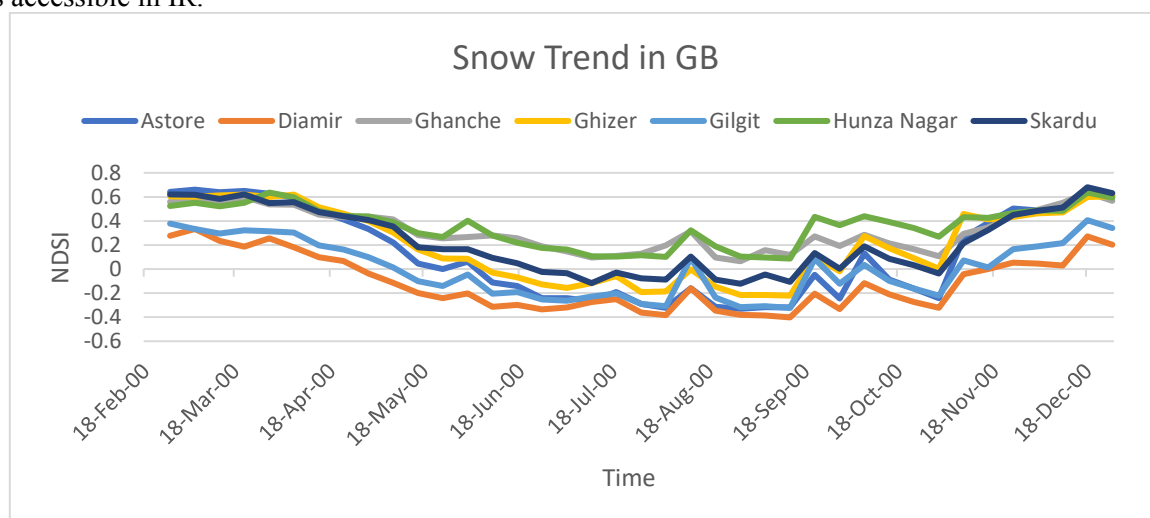
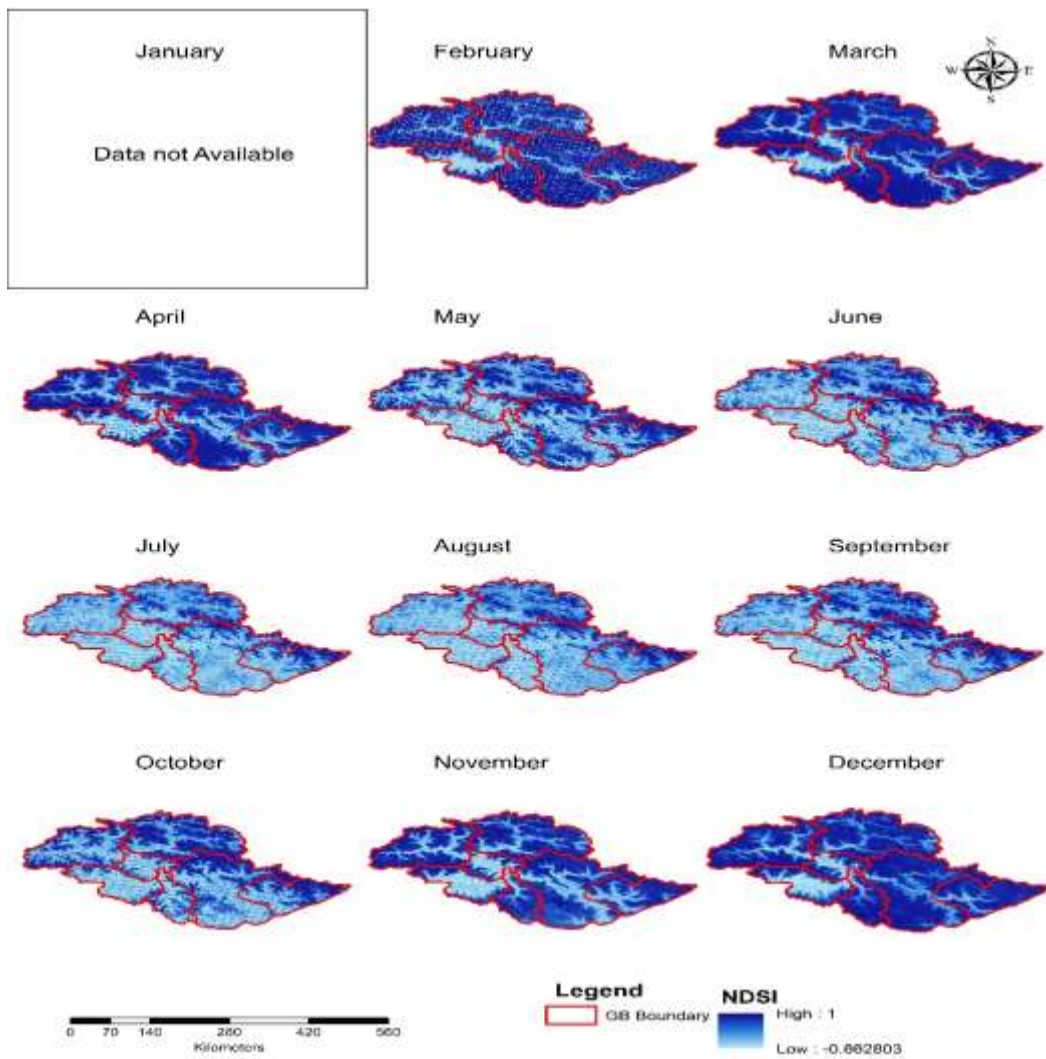
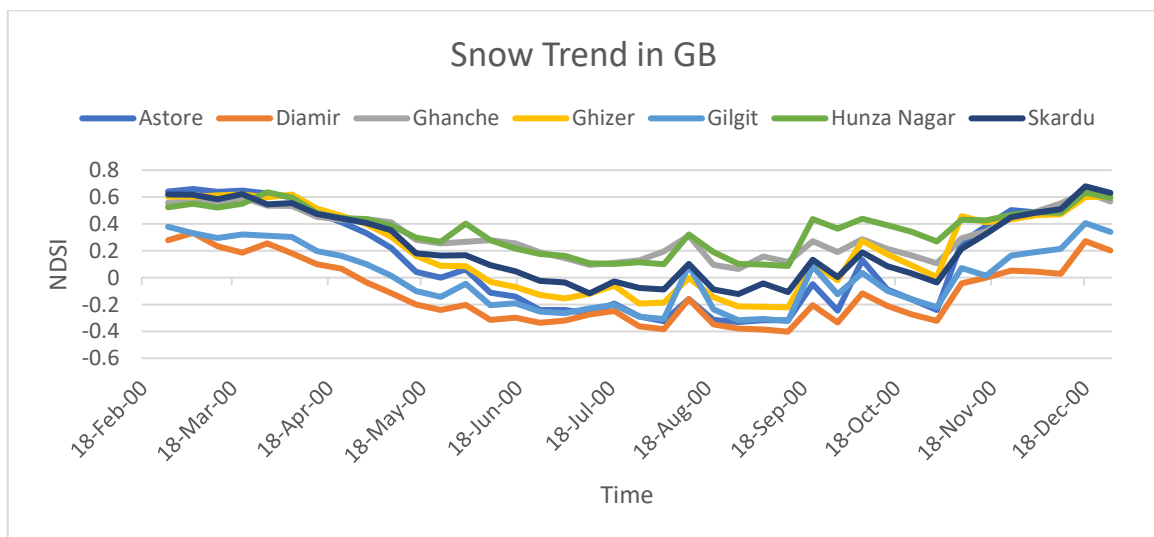


Figure 2: In 2000 Snow Trend of GB



**Figure. 3** NDSI of 2000



**Figure 4:** In 2020 Snow Trend of GB



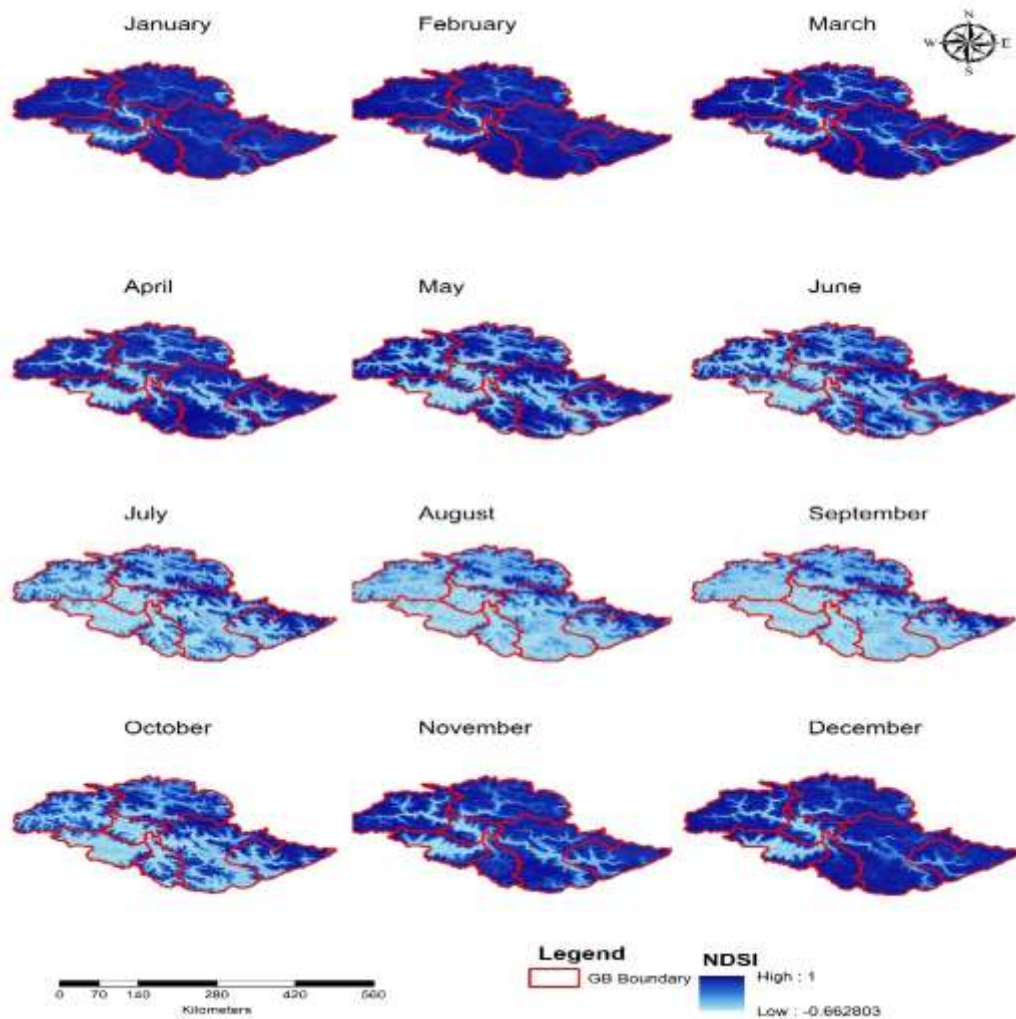


**Figure 5: NDSI of 2020**

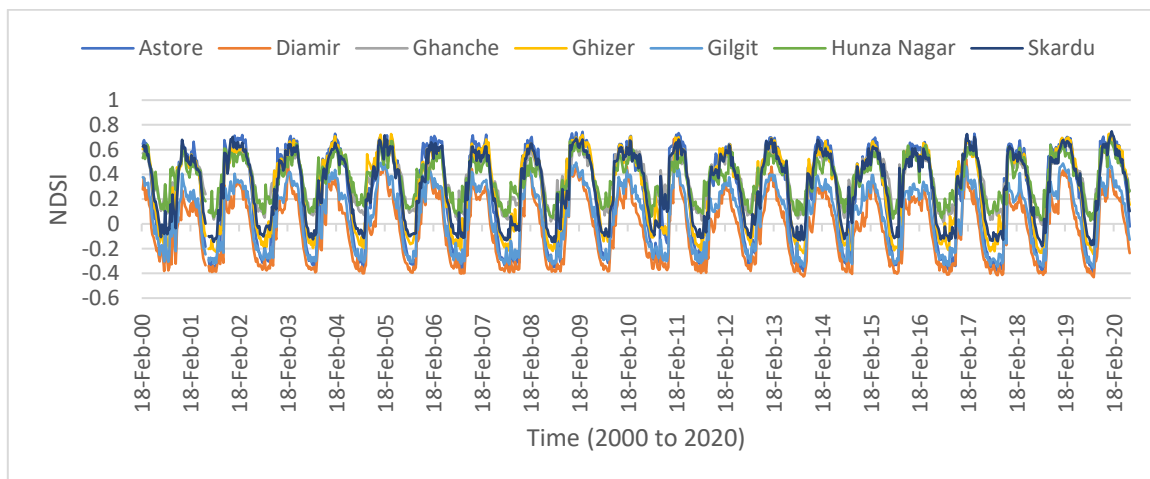


**Figure 6: NDSI Spatio-temporal distribution in Gilgit Baltistan for the period of 2000 to 2020**



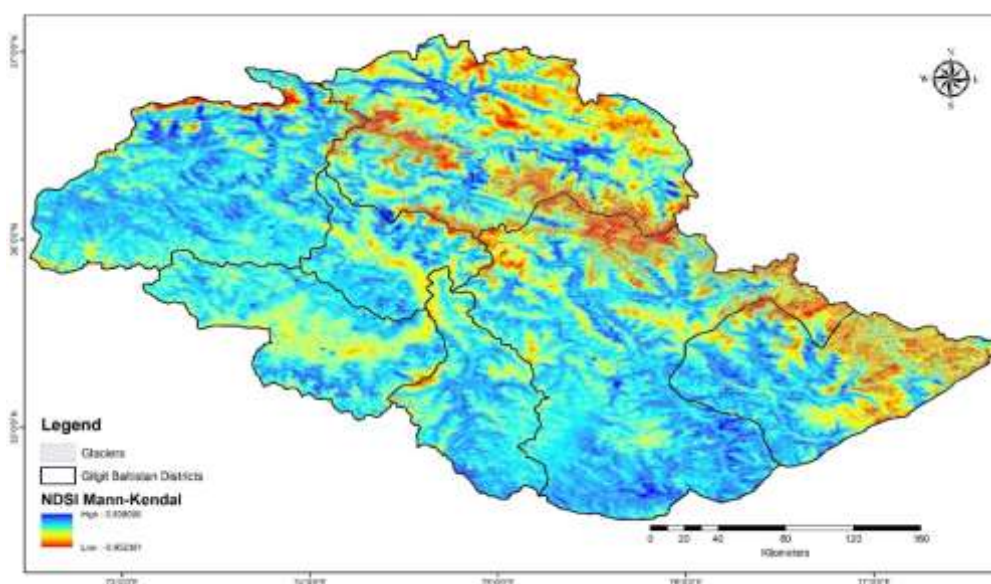


**Figure 7:** Mann Kendell trend show the NDSI changes in GB

### Conclusion

Snow cover dynamic plays a vital role in hydrological characteristics of any basin in terms of annual, seasonal depletions and accumulation. Snow cover dynamic and associated altitudinal variability of a basin determine the fresh water availability during summer season. In this investigation, we detected the snow cover area patterns in GB Pakistan over the past two decades by examining the snow index (NDSI). Based on the processing and analysis of MODIS images acquired from 2000 to 2020 using GEE. It was found that in GB, there is fluctuation trend in snow cover. However, this trend was observed decreasingly while analyzing the data for the month of July and August each year. Mann Kendell trend showed the fluctuation on snow. But Mann Kendell negative trend on glacier peaks but positive trend on glacier foothills. Remote sensing and GIS technologies are highly helpful in identification, mapping, estimation and exploitation of SCA spread over spatial domain.

### References

- Archer, D.R. and Fowler, H.J., Spatial and temporal variations in precipitation in the Upper Indus Basin, global teleconnections and hydrological implications, *Hydrol. Earth Syst. Sci.*, 2004, vol. 1, no. 8, pp. 47–61.
- Bajracharya, S.R., Maharjan, S.B., and Shrestha, F., *The Status of Glaciers in the Nepal Himalayas*, 2011, ICIMOD.
- Barman, S. and Bhattacharjya, R.K., Change in snow cover area of Brahmaputra river basin and its sensitivity to temperature, *Environ. Syst. Res.*, 2015, vol. 1, no. 4, pp. 1–10.
- Barnett, T.P., Adam, J.C., and Lettenmaier, D.P., Potential impacts of a warming climate on water availability in snow-dominated regions, *Nature*, 2005, vol. 7066, no. 438, pp. 303–309.
- Dirk Scherler, Bodo B. & Manfred R. S., Spatially variable response of Himalayan glaciers to climate change affected by debris cover, *Nature Geoscience*, 2011 vol. 4, pages 156–159.
- Government of Pakistan, *Pakistan Economic Survey 2015-16*, Ministry of Finance, Islamabad, Pakistan, 2016.
- Gurung, D.R., Giriraj, A., Aung, K.S., Shrestha, B., and Kulkarni, A.V., *Snow-Cover Mapping and Monitoring in the Hindu Kush-Himalayas*, Kathmandu: ICIMOD, 2011.
- Hewitt, K., Young, G.J., and David, C. Hydrological investigations at Biafo Glacier, Karakoram Range, Himalaya; An important source of Water for the Indus River, *Annals of Glaciol.*, 1989, vol. 13.
- Hewitt, K., The Karakoram anomaly? Glacier expansion and the “elevation effect,” *Karakoram Himalaya, Mount. Res. Develop.*, 2005, vol. 4, no. 25, pp. 332–340.
- Hussain, S.S., Mudasser, M., Sheikh, M.M., and Manzoor, N., Climate change and variability in mountain regions of Pakistan implications for water and agriculture, *Pakistan J. Meteorol.*, 2005, no. 2, vol. 4.
- Immerzeel, W.W., Droogers, P., de Jong, S.M., and Bierkens, M.F.P., Large-scale

- monitoring of snow cover and runoff simulation in Himalayan river basins using remote sensing, *Remote Sens. Environ.*, 2009, vol. 113, pp. 40–49.
- Immerzeel, W.W., van Beek, L.P.H., and Bierkens, M.P.F., Climate change will affect the Asian water towers, *Science*, 2010, vol. 5984, no. 328, pp. 1382–1385.
- IPCC 2007. Climate change 2007: an assessment of the intergovernmental panel on climate change, Assess Rep 446 (November), pp. 12–17.
- Kasper Johansen, Stuart Phinn, Martin Taylor, “Mapping woody vegetation clearing in Queensland, Australia from Landsat imagery using the Google Earth Engine, *Remote Sensing Applications: Society and Environment*, Volume 1, 2015, Pages 36-49, ISSN 2352-9385, <https://doi.org/10.1016/j.rsase.2015.06.002>.
- M. Akhtar, N. Ahmad, M.J. Booij, “The impact of climate change on the water resources of Hindukush–Karakorum–Himalaya region under different glacier coverage scenarios”, *Journal of Hydrology*, Volume 355, Issues 1–4, 2008, Pages 148-163, ISSN 0022-1694, <https://doi.org/10.1016/j.jhydrol.2008.03.015>.
- Mountains of the World: Water Towers for the 21st Century. Mountain Agenda for the Commission on Sustainable Development (CSD), Liniger, H., Weingartner, R., and Grosjean, M., Eds., Berne, 1998.
- Nüsser, M., Schmidt, S., and Dame, J. Irrigation and development in the Upper Indus Basin, *Mt. Res. Dev.*, 2012, vol. 1, no. 32, pp. 51–61.
- Patel, S.S., Ramachandran, P. A Comparison of Machine Learning Techniques for Modeling River Flow Time Series: The Case of Upper Cauvery River Basin. *Water Resource Manage* 29, 589–602 (2015). <https://doi.org/10.1007/s11269-014-0705-0>
- Rees, H.G. and Collins, D.N., Regional differences in response of low in glacier-fed Himalayan rivers to climatic warming, *Hydrol. Process.*, 2006, vol. 2169, pp. 2157–2169.
- Shrestha, A.B., Wake, C.P., Mayewski, P.A., and Dibb, J.E., Maximum Temperature Trends in the Himalaya and Its Vicinity: An Analysis Based on Temperature Records from Nepal for the Period 1971–1994, *J. Climate*, 1999, vol. 12, pp. 2775–2786.
- Shrestha, R.K., Ahlers, R., Bakker, M.B., and Gupta, J., Institutional dysfunction and challenges in flood control along the trans-boundary Koshi River: A case study of the Kosi Flood 2008, *Econom. Polit. Weekly*, 2010, vol. 45, pp. 45–53.
- Sirguey, P., Mathieu, R., Arnaud, Y., and Fitzharris, B.B., Seven years of snow cover monitoring with MODIS to model catchment discharge in New Zealand, *IEEE Int. Geosci. Remote Sensing Sympos. (IGARSS, 2009)*, Cape Town, pp. II-863–II-866.
- Tahir, A.A., Chevallier, P., Arnaud, Y., Ahmad, B., and Umer, E., Snow cover dynamics and hydrological regime of the Hunza River basin, Karakoram Range, Northern Pakistan, *Hydrol. Earth Syst. Sci.*, 2011, no. 15, vol. 7, pp. 2275–2290.
- Tahir, A.A., Chevallier, P., Arnaud, Y., Ashraf, M., and Bhatti, M.T., Snow cover trend and hydrological characteristics of the Astore River basin (Western Himalayas) and its comparison to the Hunza basin (Karakoram region), *Sci. Total Environ.*, 2015, vol. 505, pp. 748–761.

## Impact of climate variation on hydrological behavior of snow fed catchment in Chitral basin, Pakistan

Muhammad Muneeb<sup>1</sup>, Muhammad Waseem<sup>1,\*</sup>, Muhammad Awais Zafar<sup>1</sup>, Faraz ul Haq<sup>1</sup>

<sup>1</sup> Centre of Excellence in Water Resources Engineering, University of Engineering and Technology, Lahore 54890 Pakistan.

Corresponding author email: [dr.waseem@uet.edu.pk](mailto:dr.waseem@uet.edu.pk)

**Abstract:** A major portion of the snow in the Pakistan is accumulated in the Indus basin watershed. Discharge is the combination of glacier melt and snow in the upper Indus basin UIB. Impact of snowmelt to runoff is very critical in the mountainous region. It is therefore essential to ascertain snow melt runoff for better water resource management in Pakistan. The study is aimed to assess the hydro-meteorological parameters in Chitral catchment by using historical data and their impact on flows. Further SRM model was used to examine the hydrological behavior of snow fed catchment in response to climatic variation. The results revealed that during historical period (1981-2015),  $T_{max}$  is increasing at  $0.61\text{ }^{\circ}\text{C/decade}$  while  $T_{min}$  is increasing at  $0.23\text{ }^{\circ}\text{C/decade}$ .  $T_{max}$  is increasing more as compared to  $T_{min}$ . Annual precipitation is increasing at  $39.2\text{mm/decade}$ . Stream flow of the catchment is increasing  $32.42\text{ m}^3/\text{s}$  per decade over a 1991-2015 period possibly due to an increase in temperatures and summer monsoon precipitation. The study results suggest that Chitral basin undergoes an annual snow cover change of about 40% - 80% where SCA is 70% - 90% in the winter whereas, SCA is 17% - 25% in the summer. The hydrological behavior of the Chitral basin was analyzed by considering the hydrological and climatological data on Chitral basin. High correlation was found between SCA, temperature and flows indicating that Chitral basin is highly dependent on snow fed and glacier fed catchment. Trend in snow cover area and flows in Chitral basin both zone wise and basin wide show an increasing trend which shows that stream flows of Chitral basin is largely dependent on snowmelt and temperature seasonality. Study of climate change is very important factor for examining water resource management in Pakistan and all over the world.

**Keywords:** Spatial-temporal snow cover trend, Upper Indus River Basin, Hydrological behavior, Water resources management, snow melt runoff model SRM, Snow Cover Area SCA

### Introduction

Precipitation, temperature, runoff, and extreme events due to climate change has become more attractive and important topic now a days as they are directly and indirectly impacting the water resources, food security, live stocks, crops, hydropower generation, sediment issues and industrial sectors. [10]. From 1880 to 2012 temperature of the globe has increased  $0.65\text{ }^{\circ}\text{C}$  to  $1.06\text{ }^{\circ}\text{C}$ . Mean yearly precipitation has inclining in the middle part of northern half of the world. From the commencement of industrial period concentration of  $\text{CO}_2$  has risen dramatically which causes Global warming. Reason of global warming causing declining in magnitude of Arctic ice from 1979 to 2012. The rate at which Arctic ice is declining is  $3.8\%$  per decade. [5] A lot of stream in upper Indus basin is contributed by its snow and glacial melt. Evaluation of snow cover and its spatial and temporal variation is an imperative factor to comprehend the better water asset management. The Indus basin is a locale having marginally

expanding pattern of SCA in the southern and northern parts. The Greater Karakoram Range situated in upper Indus basin UIB, has a broad arrangement of snow. The directions given by Wapda were straightened out amid watershed outline. The hypsometric bend was utilized to appraise the mean rises and their regarded zones. [18]

Snow and glacial melt are a vital source of water. It is vital for the two meteorologists and nearby locals. Modis information, Aphrodite temperature and release information were utilized to ponder the variety for the four bowls. Solid relationship was seen among SCA, temperature and release portraying high arrangement between them. In the locale diminishing propensity was watched for SCA. Converse connection was created among temperature and SCA. Similarly backwards connection was seen among streams and SCA. For the sake of modis information examination Himalayan area encounters decrease in SCA. Negative connection among's temperature and SCA indicates drift is an aftereffect of expanding

temperature. [9]. Similarly, the majority in the ice sheets withdrawing and of perceptions appear, on the normal, a speeding up of such reaction since 1990. Notwithstanding, icy masses in the Karakoram Range have highlighted sporadic conduct since quite a while, demonstrating adjusted spending plans amid the most recent decade [8]

The performance of hydrological models in northeastern china was evaluated and downscaled the outputs of general circulation model GCM. Variation in streamflow was analyzed by using different hydrological models. The results revealed that it's very important to use different hydrological models for better water resource management in Songhua river basin SRB region. [6]. Glacier modelling was integrated into hydrological modelling and put forth an important consideration in glaciers since they are vital source of water, irrigation and for power generation. Glaciers and snow melt are important factors to be considered for climate change. They are continuously changing due to warming trend of globe. The coupled model that was used for runoff estimation have very good model efficiency results. [13]

The future impact of climate was studied on scarcely gauged basin in northern Pakistan. As streamflow are fundamental factor for water resources; therefore, it's very essential to quantify the climate variation and their impact on streamflow's for better water strategic management in highly mountainous region. HEC-HMS and SRM model were used for hydrological modelling to examine the impact of climate variation on flows of Jehlam basin. After calibration and validation of these two models result revealed that temperature and flows are increasing linearly possibly due to early glacier melting and maximum amount of snow in high altitudes. [5]

The sensitivity of SRM was studied by assessing SCA and temperature. Snow is vital source for the fresh water. snowmelt runoff modelling basically predicts the magnitude of snowmelt and runoff. Modis snow products were used to analyze snow cover area. The results of study suggest that SRM model is more sensitive to high elevation and location of temperature gauges at station, the findings of the result will be beneficial for snow melt runoff modelling and water planning and management. [11]

The runoff prediction was evaluated by using SRM model in Gilgit basin. There is as serious issue of global warming in glacierized region

especially in the Himalaya region therefore its essential to forecast runoff caused by glaciers and snowmelt in Gilgit river. The SRM model was calibrated for four years 2007,2008,2009 and 200 respectively with good model efficiency results. The future climate change scenarios were generated by using precis model for better prediction of flows. The result suggested an increase in Gilgit streamflow's which demands better management of water resources and power generation in Indus basin for future period. [1]

The flows in Chitral were estimated under different scenarios generated by glaciated ice cover. the rapid increase in global warming due to rise in temperature lead to glacier melting, mostly the rivers which flows throughout the year originates from the glaciers. Pakistan as an agricultural country; glaciers are of extreme importance. The major rivers of Pakistan originate from HKH Hindu- Kush Himalaya region; it's quite clear that future of Pakistan is associated with glacier melt. therefore, estimation of flows with respect to glacier melting in Chitral is of great importance. [15]

A study is focused in China to approximation the influence of change in climate at temperature, rainfall and overflow for Songhua River Basin, using SWAT model. It is observed that future temperature will increase for both scenarios RCP's 4.5 and RCP's 8.5. But the precipitation will decrease for some sub basins and will increase for some sub basin. And stream flow also will decrease in future [12]

Spatial - temporal trends in Chitral basin were estimated and the hydro-climatological behavior was examined. Annual and seasonal SCA was assessed by using modis snow products from 2001-2016; in order to ascertain the climatic variation and their response to water supplies. Trend analysis of snow cover area SCA and hydro-climatic variables were carried out by using Mann - Kendall test. The results revealed significant increasing trend in SCA both basin wide and zone wise a slightly decreasing trend in mean temperature and summer flows was observed. Streamflow of Chitral basin is largely dependent on snow melt and temperature seasonality as estimated by SRM model. [2]

The comparative assessment of spatiotemporal variation in snow cover area and its impact on hydrological behavior was studied on Gilgit, Hunza and Astore river basins. Upper Indus basin UIB is located in the HKH Hindu- Kush Himalaya region which supply most of the water that is used in Pakistan mostly for the irrigation

purpose. The study results revealed that different glacier coverage has significant impact on the flows of upper Indus basin. [19]

For the river of Brahmaputra, it is estimated that runoff for the higher tributary of the river will reduce by 20% and evapotranspiration will increase in future. Glacier melting rate will increase till 2040. After 2040 melting rate will reduce. Peak runoff will be more. Peak flow of the river Ganges will growth in future due to climate change. Water availability may reduce by 17% and mean annual runoff will be more in future [17]

According to change in Climate scenario by 1°C incline in temperature lead to 15% decline in glaciated extent. For upper Indus Basin that deals with special effects of variation in climate on Resources of water, in this study Mann-Kendall assessment has practices to see the changes due to climate according to his studies temperature and runoff has increasing pattern but precipitation has no consistent trend. It is estimated that temperature will have grown of 0.9°C in Pakistan by the 2020 [20]

According to another studies annual temperature is rising. Mean annual temperature is increasing in spring, autumn and winter but decreasing for summer for Mangla watershed. Precipitation is decreasing throughout watershed. Mean annual runoff of Jahlem River has decreased during 1961 to 2010. [22]

The snowmelt runoff modelling in hunza basin Pakistan was evaluated by using SRM model.as major contribution in flow is due to glacier and snow melt located in Karakorum range that's why it's important to estimate snowmelt runoff caused by snow fed catchment. The results calculated suggest that srm mode can be efficiently used in snow fed catchment of UIB. [18]

The aim of my study is ascertainment of Climate variation in snow fed catchment i.e. (Chitral basin), assessment of the snow cover and its spatial-temporal variation and to examine the hydrological behavior of snow fed catchment in response to snow cover and climate variation.

## Study Area

Chitral, (latitude 35° 51' 48" & longitude 71° 47' 15") is situated in Khyber Pakhtunkhwa, Pakistan (Fig. 1). The city has an average elevation of 1,500 m (4,921 ft.), having catchment area of 13126 km<sup>2</sup>. Approximately, 13% of the catchment area has an elevation above 5000 m ASL. The Chitral DEM was classified into different elevation zones by using reclassify command from 3D-analyst Tool. The DEM was classified into eight elevation zones. The zone 1 is of low elevation (1473-2000m) and zone 8 is of high elevation (5000-7603 m). Mean hypsometric elevation (havg) of Chitral catchment was determined using Arc GIS. Key characteristics of the catchment area are given in Table 1 and 2.

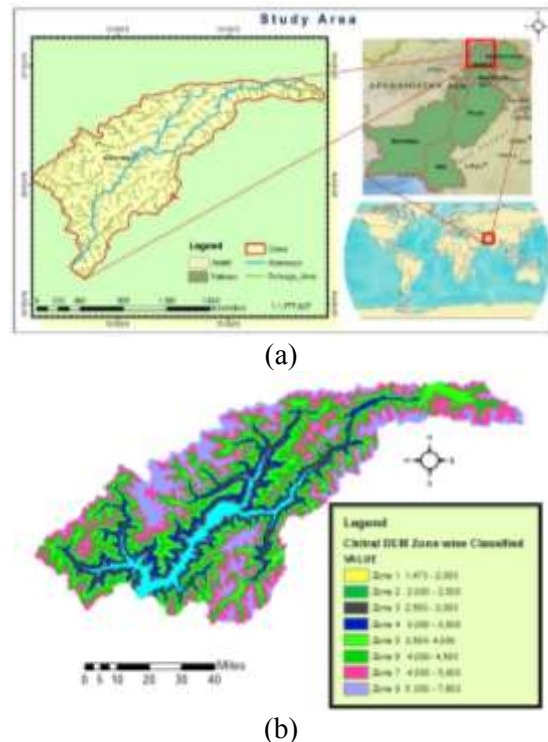


**Fig. 77.** (a). Study Area, (b) DEM of Chitral

**Table 0.** Key Characteristics of the Study Area.

Catchment	Chitral River basin
River flow gauging station	Chitral hydrometric station
Latitude	35° 50' 46" North
Longitude	71° 47' 55" East
Elevation of gauging station	1500 m
Drainage area	12400 km <sup>2</sup>



Glacier-covered area	1650 km <sup>2</sup> (~12.5% of watershed area)
Area above 5000 m	1710 km <sup>2</sup> (~13% of watershed area)
Mean elevation	4100 m ASL

**Table 2.** Catchment Areas under Different Elevation Zones

Zone	Elevation Bands	Mean Elevation (m)	Area Km <sup>2</sup>	Cumulative area	Area of each zone (%)
1	1473-2000	1736	150.1	150.1	1.1%
2	2001-2500	2500	555.2	705.3	4.2%
3	2501-3000	2750	991.6	1546.8	7.6%
4	3001-3500	3250	1492.0	2483.6	11.4%
5	3501-4000	3750	2166.6	3658.6	16.5%
6	4001-4500	4250	2814.1	4980.6	21.4%
7	4501-5000	4750	2899.2	5713.3	22.1%
8	5000-8000	6500	2057.6	4956.8	15.7%

Hypsometry means relative proportion of an area at different elevations within a region and hypsometric curve depicts distribution of area with respect to altitude. The hypsometric curve was used to estimate the mean elevations and their respected zones.

## DATA

### Climatic Data

Observed daily meteorological data of two climate stations (maximum temperature, minimum temperature, and precipitation) was collected from Pakistan Meteorological Department (PMD) for the period 1980-2015.

### Discharge Data

Stream flow measurements in Chitral watershed was collected from the Water and Power Development Authority Surface Water Hydrology Project (WAPDA-SWHP) for the period 1990-2015 on daily basis.

### Spatial Data

The modis (MOD10A2) snow products were used for the period of January 2010 to December 2015 to assess the snow cover extent. The digital elevation model DEM was downloaded from

website of NASA located at National Snow and Ice Data Centre (NSIDC). The DEM represents maximum, minimum and mean elevation; in our case chital has minimum, mean and maximum elevation of 1463m, 4100m and 7603 m respectively. To avoid this manually (time consuming) downloading of daily tiles R-Script has been developed which will do all the processes by its own and desired daily MODIS tiles can be downloaded. R-Script has been developed which can do all the downloading process automatically by use of script 'myScriptdownload.R'

### Snow cover

In order to calculate the actual snow cover area at of the day, cloud cover should be eliminated in the image, for this purpose R-Script 'cloud\_eliminator\_loopy.R. R' was used. It works wherever the cloud cover is present; it will automatically see the image before or after the cloud image/tile and interpolate the snow values (presence of snow under cloud cover).

To snow cover was analyzed by calculating the snow cover area at each elevation zone. For this purpose, R-Script snowcover\_analysis.R. R was used to generate the cover area zone wise. This

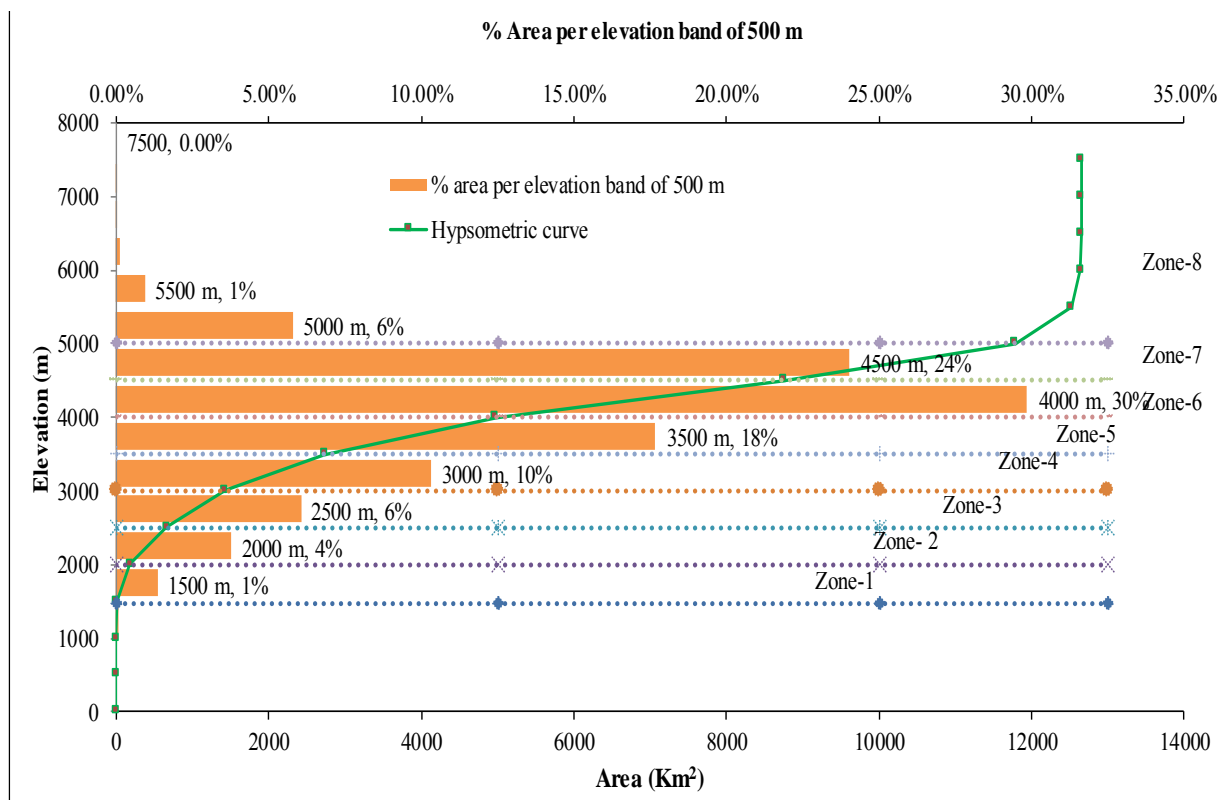


Fig. 2. Hypsometric curve of Chitral basin

Table 3. Database and Source

Data Type	Source	Resolution	Description
Climatic data	Pakistan Metrological Department (PMD)	Daily	Rainfall, Temperature, (1981-2015)
Hydrological data	Water and Power Development Authority (WAPDA)	Daily	Streamflow's (1991-2015)

snow cover analysis script read the snow and no snow pixel from the cloud free image in file format of \*.tiff, and tabulate each the snow cover area over each elevation zone. For this purpose, MODIS cloud free tiles which were generated from above script 'cloud\_eliminator\_loopy.R. R' and elevation zones file which were produced by using 'Ez\_generator.R'. The R-Script has been developed which will use the snowcover.txt file and interpolate the missing snow and no snow values. It works wherever the cloud cover is present, it will automatically see the image before or after the cloud image/tile and interpolate the snow values (presence of snow under cloud cover).

## Methodology

### Trend Analysis of Hydro-climatological Data

Trend analysis of flows, precipitation and temperature were carried out by non-parametric Mann-Kendall test. before applying this test, auto correlation test was applied to homogeneity of data by using SNHT Standard normal homogeneity test.

The Mann-Kendall equation is given by following equation:

$$Z_{MK} = \begin{cases} \frac{S-1}{\sigma_s} & \text{if } S > 0 \\ 0 & \text{if } S = 0 \\ \frac{S+1}{\sigma_s} & \text{if } S < 0 \end{cases} \quad (1)$$

### SRM Model Description

Model Structure of snow melt runoff model is given below:

$$Q_{n+1} = [c_{Sn} \cdot a_n(T_n + \Delta T_n)S_n + c_{Rn}P_n] \left(\frac{10000}{86400}\right) A(1 - k_{n+1}) + Q_n k_{n+1} \quad (2)$$

SRM can be applied both by basin-wise and zone wise. Basin wise application is easy due to easy calibration while zone wise calibration is difficult. Following Steps are followed:

1. First, set up your SRM Project. Reference elevation means elevation of your stream gauging station in (m) and its latitude and longitude and means hypsometric elevation is mean of minimum and maximum elevation.

2. Then go to edit simulation and a dialogue box will be open. It is better to use daily average temperature as input data in SRM. Select metric units. Select the start and end period of simulation. In the initial runoff, put the value of for example 31 December 2010 runoff if you have the plan to run SRM for the year 2011.
3. The main thing in SRM simulation is an adjustment of its parameter, the Main sensitive parameter is DDF, Cr, Cs and recession coefficients x and y. The correction selection of parameter is necessary.
4. So, parameter values of nearby catchment where SRM was applied and then you can modify those parameters values afterward. After optimization following parameters were used in SRM model at Chitral basin.

Zone ID	Zone Area (km <sup>2</sup> )	Hypsometric Mean Elevation (m)	% NE Aspect	Avg Elevation, NE Aspect (m)	% SE Aspect	Avg Elevation, SE Aspect (m)	% NW Aspect	Avg Elevation, NW Aspect (m)
1	150.10	1736.00	0	0	0	0	0	0
2	555.29	2500.00	0	0	0	0	0	0
3	991.69	2750.00	0	0	0	0	0	0
4	1492.34	3250.00	0	0	0	0	0	0
5	2166.30	3750.00	0	0	0	0	0	0
6	2814.00	4250.00	0	0	0	0	0	0

Basin Area (km<sup>2</sup>): 13126.22

Fig. 3. SRM project

Table 4. Parameters used in SRM

Parameters	Parameter values used
DDF (cm. °C-1d-1)	0.5
Lag Time (hrs)	18
Lapse rate (°C/100m)	0.64
Teric (°C)	0
Cs	0.0350 -0.2
Cr	0.08-0.12
RCA	1 (June-August) 0 (September-May)

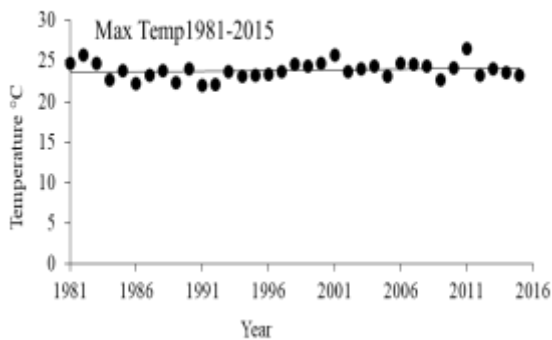
Xc	0.85 (June-September) 1.07 (October-May)
Yc	0.02

### Results and Discussion

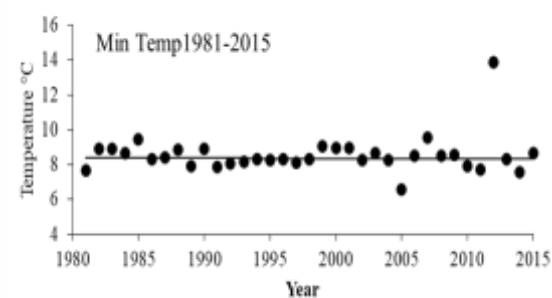
Trend analyses to assess the climate variation in snow cover area (SCA) and hydro-climatic variables (runoff, temperature and precipitation) was carried out using Mann-Kendall's trend test. The details about outcomes are as described below.

## Hydro Meteorological Data Analysis

The annual maximum temperature for Chitral station showed an increasing trend. The maximum temperature is increasing 0.61 °C/decade as shown in (Fig. 4). The annual average max temperature from (1981-2000) is increasing at 0.56 °C/decade while from (2000-2015) is decreasing at 0.92°C/decade



(a)



(b)

**Fig. 4.** Trend of Annual Average (a) Max and (b) Min Temp. of Chitral (1981-2015)

### Annual Variation in Rainfall

The historical trend of precipitation showed that annual and summer rainfall is increasing. The rainfall is increasing more in 1981-2000 at rate of 44.5mm/decade, while from 2000-2015 it is Increasing 30.6mm/decade. Annual precipitation is increasing at 39.2mm/decade.

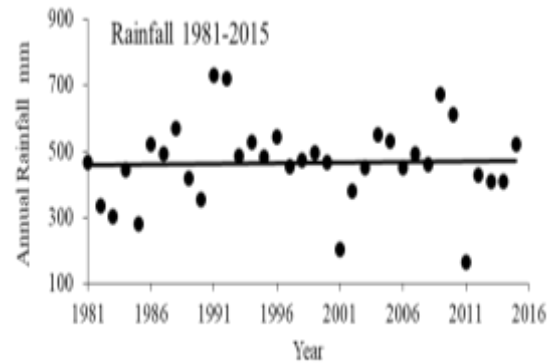


**Fig. 5.** Trend of Annual Rainfall of Chitral (1981-2015)

### Variation in Stream flows

Stream flow of the catchment is increasing 32.42 m<sup>3</sup>/s per decade over a 1991-2015 period possibly due to an increase in temperatures and summer monsoon precipitation

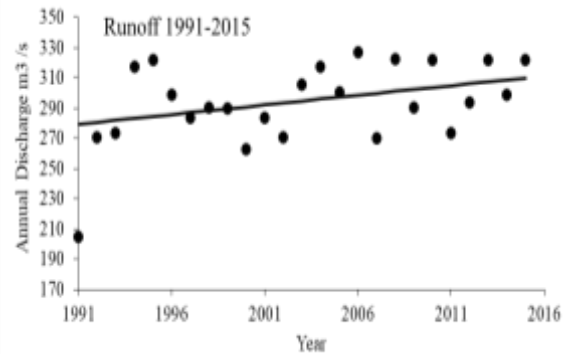
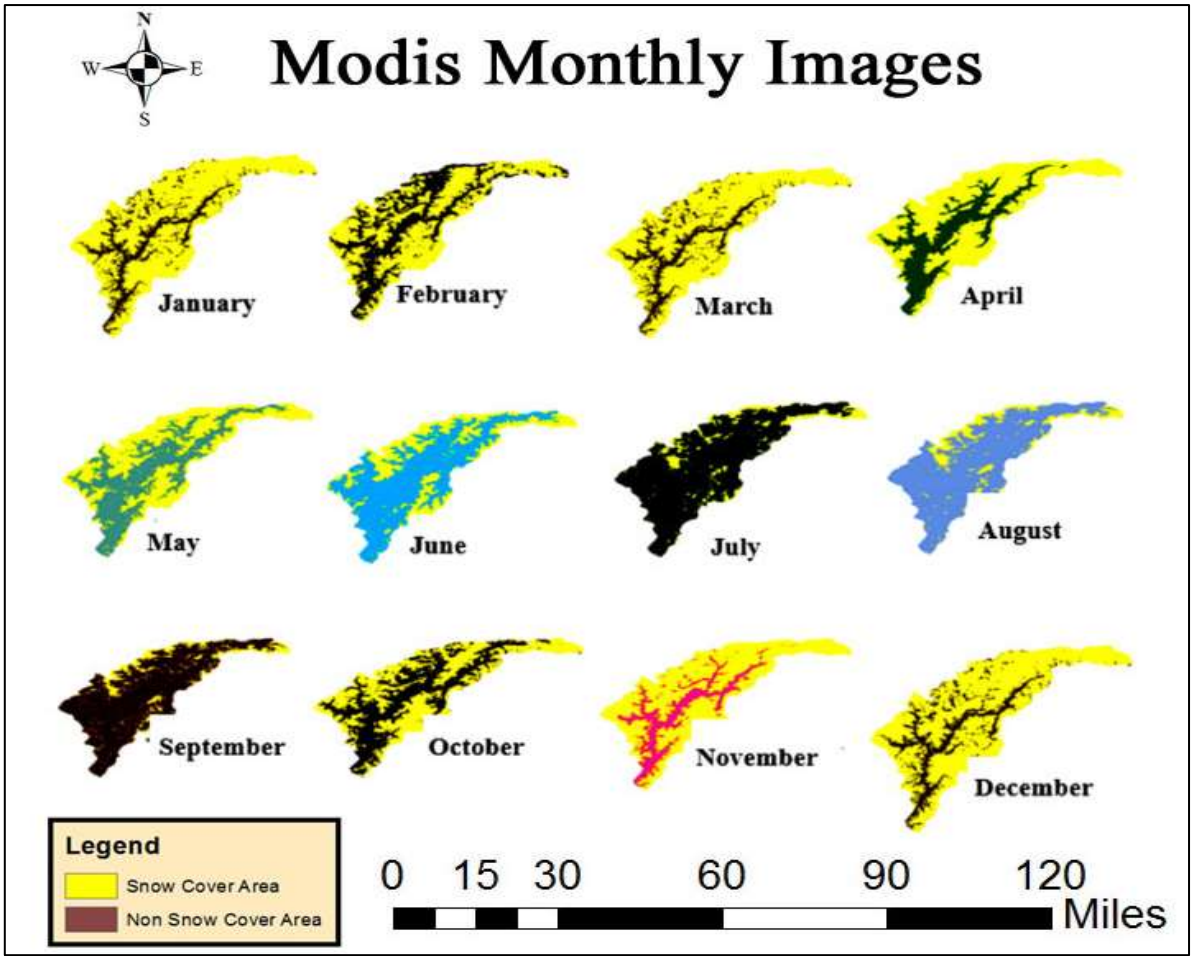


**Fig. 6.** Trend of Annual Runoff of Chitral station (1981-2015)

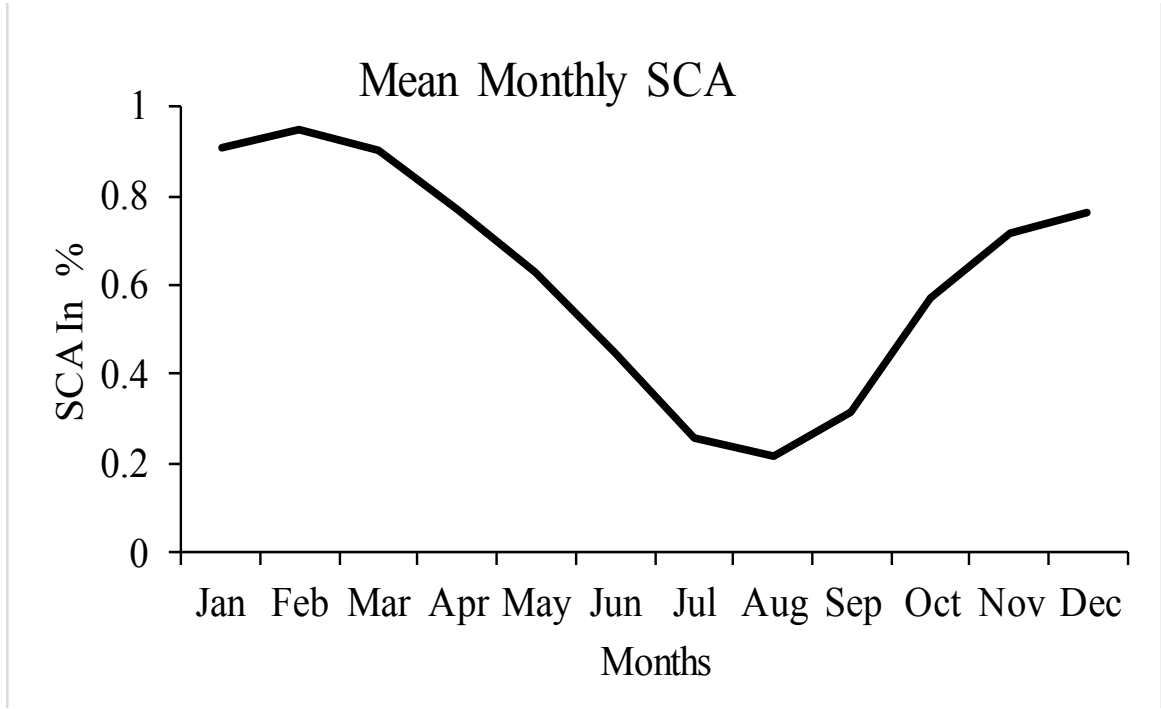
### Variation in Snow Cover Area (SCA)

#### Temporal Variation of Snow Cover Area SCA

The Snowmelt period starts in early April and the minimum snow cover is observed during August and September when the snow cover area drops in a range of 17–25%. This study explains that the Chitral basin undergoes a snow cover change of about 40% - 70% where SCA is 70% - 90% in



(a)



(b)

**Fig. 7.** (a). MODIS (MOD10A2) satellite images presenting the average snow cover area for each month in the Chitral River basin over the year 2015. (b). Mean monthly SCA in the Chitral basin.



the winter (snow accumulation period), whereas, SCA is 17% - 25% in the summer (snowmelt period). The expansion in snow cover area of the Chitral River basin may be the result of a decreasing trend in the mean temperatures and an increasing trend in the catchment's annual precipitation.

### Spatial Variation in snow cover area (SCA)

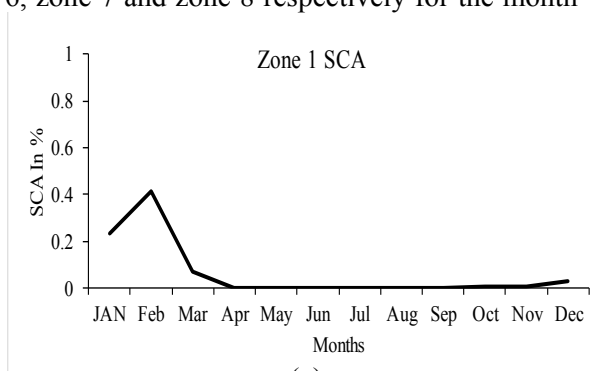
The mean variation in spatial extent of SCA in Chitral basin is as shown (Fig. 8). Variation in spatial extent of SCA is also presented for the eight zones (1 to 8) for the Chitral basin. The SCA varies from 20-65% in zone 1 and zone 2 for the period of January and February, while SCA varies from 2-18% in zone 1 and zone 2 for the month of December. The mean SCA is maximum in the winter season especially in the months of January and February while mean SCA is minimum in the summer season especially in the months of August and September. The SCA varies from 68-85 % in zone 3, zone 4 and zone 5 respectively for the month of January and February, while SCA varies from 30-58% in zone 3, zone 4 and zone 5 respectively for the month of November and December. The SCA varies from 88-98 % in zone 6, zone 7 and zone 8 respectively for the month

of January and February, while SCA varies from 60-94 % in zone 6, zone 7 and zone 8 respectively for the month of November and December.

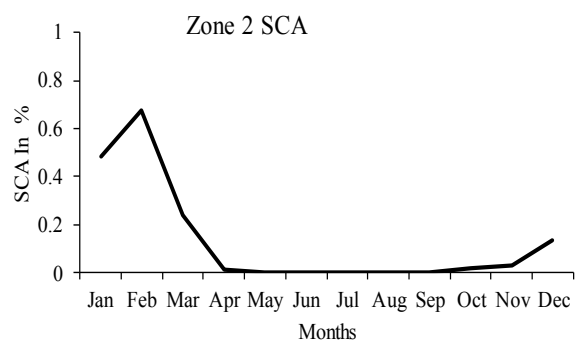
It is to be noted that maximum SCA is achieved approximately in the higher zones especially in zone 6, 7 and zone 8 respectively. This effect may be attributed to the westerlies circulation which may cause more snow at higher altitudes, and maximum snow cover area SCA is observed in the high altitudes. Changes in precipitation and temperature significantly influences the hydrological behavior of Chitral basin but snowmelt has more influence on the stream flows rather than temperature and rainfall.

### SRM Model Calibration and Validation

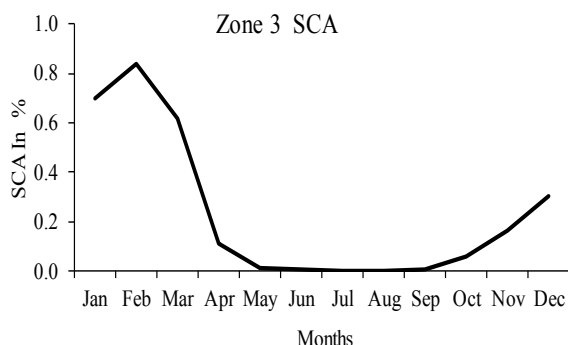
The model was calibrated for 2009-2010 using the daily data of runoff recorded at the outlet of the watershed. The observed and simulated values were plotted against each other in order to determine the coefficient of determination ( $R^2$ ) for runoff. The ( $R^2$ ) values for daily time span 2009-2010 were 0.80, 0.82. For 2014-2015 were 0.88, 0.89. Validation proves the performance of the model for simulated flows in periods different from the calibration periods, but without any



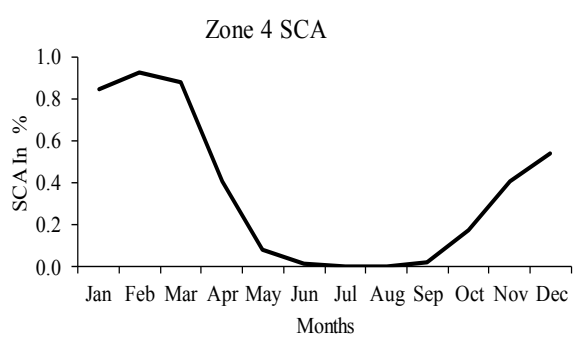
(a)



(b)



(c)



(d)

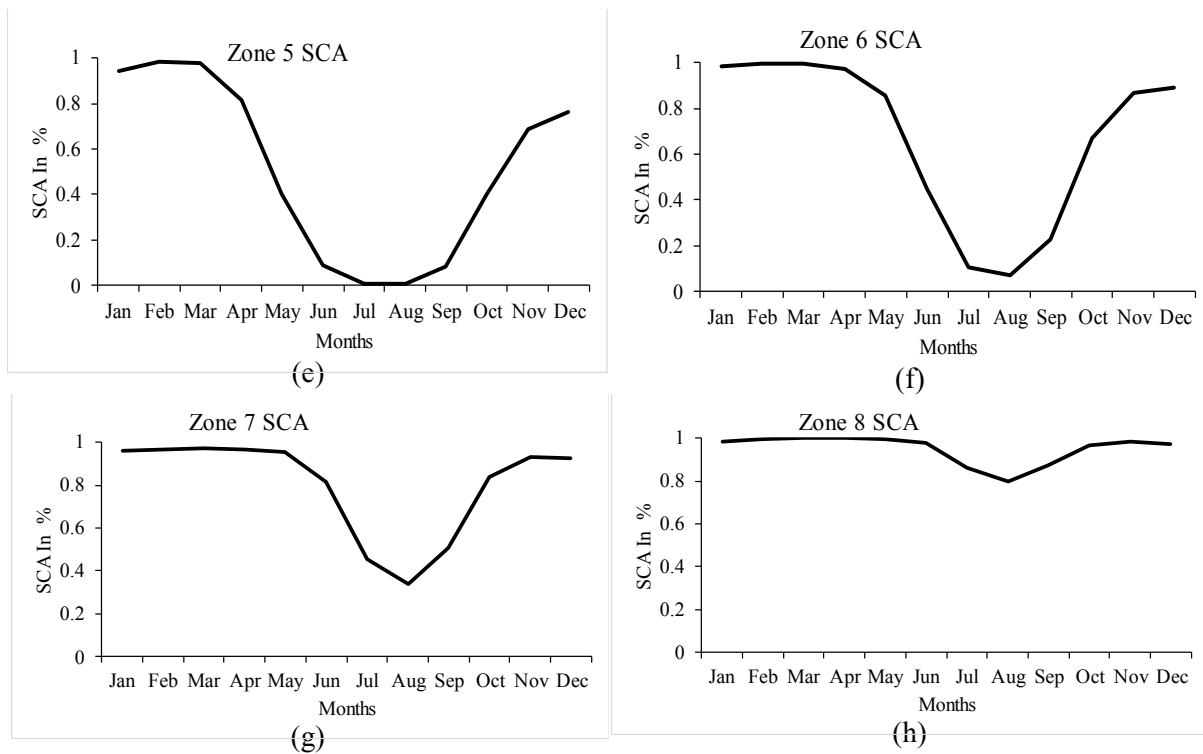
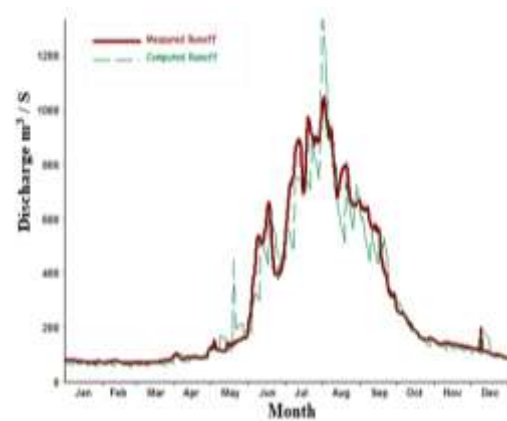


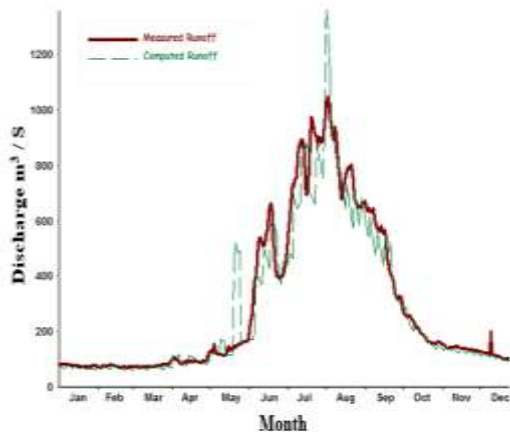
**Fig. 8.** Zone Wise Spatial Variation of SCA over study period (2010–2015)

further adjustment in the calibrated parameters. SRM model was validated for 2014-2015. It demonstrates that the reproduced hydrographs sensibly coordinate with the calibrated model. The hydrological behavior of Chitral basin shows that in the winter season when the snow accumulation is maximum the discharge is minimum but in summer season when the snow melt is maximum runoff is maximum, means there is inversely correlation between SCA and Q which is -0.81, and correlation between T and SCA -0.84, because when mean temperature is maximum snow melt will be maximum due to which snow cover area SCA will be minimum.

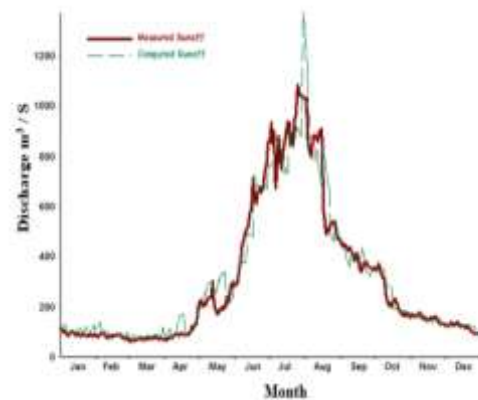


(b)

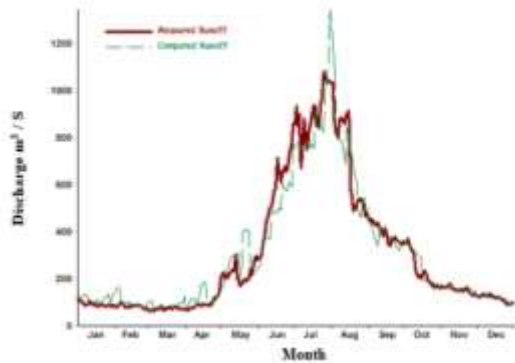
**Fig. 10.** SRM calibration a.2009, b.2010



(a)



(a)



(b)  
**Fig. 9.** SRM Validation a. 2014, b.2015

### Correlation Results

The correlation results show that stream flow is showing a positive correlation with temperature, means with the increase in temperature discharge is maximum, while discharge is showing an inverse correlation with snow cover area SCA, it's obvious that in winter snow is maximum but discharge is minimum but in summer its vice versa. Similarly, with the increase in precipitation snow cover area is maximum. Correlation values indicate that the stream flow of Chitral basin is largely dependent on the snowmelt and temperature seasonality.

**Table 5.** Summary of the Correlation Results

correlation between Q & T	0.77
correlation between Q & P	-0.07
correlation between SCA and Q	-0.81
correlation between T and SCA	-0.84
correlation between P and SCA	0.14

### Impact of Climate Change on Hydrological Behavior

It is obvious from the hydrograph (Fig. 12) that the flow in Chitral River starts to rise in spring season when the snow accumulated during precedent season starts melting and finds its highest in peak summer season when snow and glacier melt is at its maximum. The river flow in Chitral basin depends on seasonal snowmelt and rainfall. So, the stream flow was simulated using the SRM model, a physically based distributed hydrologic model that uses a GIS interface and readily available input data such as Digital Elevation Model (DEM) and climate data. The future stream flows were also simulated based on future developed climate change scenario using calibrated SRM model. Pakistan is an agriculturally based country and its major contribution of flows is obtained from the upper Indus basin UIB. The high-altitude glaciers feeds water supply of UIB. SRM model has effectively simulated the flows with good model efficiency results.

### Conclusions

The results of the study revealed a significant increasing trend in seasonal (winter and summer) precipitation in Chitral basin. The past trend showed that annual precipitation is increasing at 38.1 mm/decade. The highest warming trend was observed at rate of 0.56 °C per decade. On the other hand, the maximum temperatures have decreased significantly by 0.92°C per decade from (2000-2015). Stream flow of the catchment is increasing 32.42 m<sup>3</sup>/s per decade over a

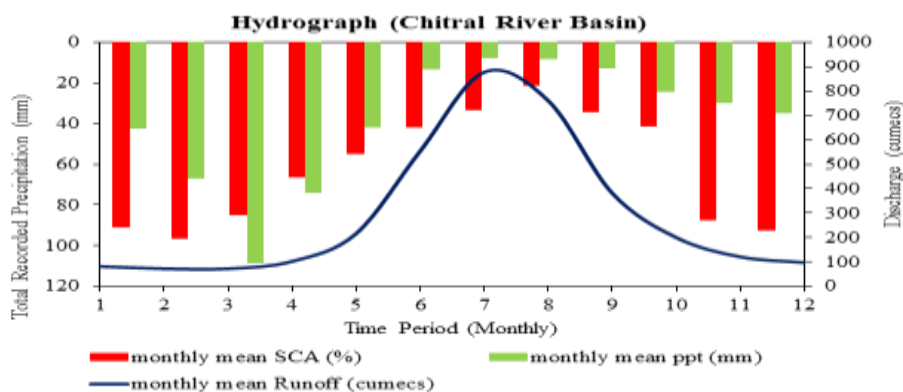


**Fig. 10.** Hydrograph of Chitral catchment

1991-2015 period possibly due to an increase in temperatures and summer monsoon precipitation. Chitral basin undergoes a snow cover change of about 40% - 70% where SCA is 70% - 90% in the winter whereas, SCA is 17% - 25% in the summer. The variation in temperature and precipitation also exist in seasons. On the whole temperature, precipitation and snow melt rate is increasing. Snow and glacier melt are estimated to contribute more than 80% of the total flow in the Chitral river, evaluated by SRM model. The hydrological behavior of the Chitral basin was analyzed by considering the hydrological and climatological data on Chitral basin. High correlation was found between SCA, temperature and flows indicating that Chitral basin is highly dependent on snow fed and glacier fed catchment. SRM+G model could be used for better assessing the contribution of glaciers in snowmelt in snow fed catchments and its impact on stream flows. It's very essential to quantify the climate variation and their impact on streamflow's for better water strategic management in highly mountainous region

## References

- Adnan, M., Nabi, G., Poomee, M.S. and Ashraf, A., 2017. Snowmelt runoff prediction under changing climate in the Himalayan cryosphere: A case of Gilgit River Basin. *Geoscience Frontiers*, 8(5), pp.941-949.
- Ahmad, S., Israr, M., Liu, S., Hayat, H., Gul, J., Wajid, S., Ashraf, M., Baig, S.U. and Tahir, A.A., 2018. Spatio-temporal trends in snow extent and their linkage to hydro-climatological and topographical factors in the Chitral River Basin (Hindukush, Pakistan). *Geocarto International*, pp.1-24.
- Azizullah, A., Khattak, M.N.K., Richter, P. and Häder, D.P., 2011. Water pollution in Pakistan and its impact on public health—a review. *Environment international*, 37(2), pp.479-497.
- Azmat, M., Qamar, M.U., Huggel, C. and Hussain, E., 2018. Future climate and cryosphere impacts on the hydrology of a scarcely gauged catchment on the Jhelum river basin, Northern Pakistan. *Science of the Total Environment*, 639, pp.961-976.
- Bates, B., Kundzewicz, Z. and Wu, S., 2008. *Climate change and water*. Intergovernmental Panel on Climate Change Secretariat.
- Faiz, M.A., Liu, D., Fu, Q., Li, M., Baig, F., Tahir, A.A., Khan, M.I., Li, T. and Cui, S., 2018. Performance evaluation of hydrological models using ensemble of General Circulation Models in the northeastern China. *Journal of Hydrology*, 565, pp.599-613.
- Fowler, H.J. and Archer, D.R., 2005. Hydro-climatological variability in the Upper Indus Basin and implications for water resources. *Regional Hydrological Impacts of Climatic Change—Impact Assessment and Decision Making*, 295, pp.131-138.
- Gardelle, J., Berthier, E. and Arnaud, Y., 2012. Slight mass gain of Karakoram glaciers in the early twenty-first century. *Nature geoscience*, 5(5), p.322.
- Gurung, D.R., Maharjan, S.B., Shrestha, A.B., Shrestha, M.S., Bajracharya, S.R. and Murthy, M.S.R., 2017. Climate and topographic controls on snow cover dynamics in the Hindu Kush Himalaya. *International Journal of Climatology*, 37(10), pp.3873-3882.
- IPCC. 2012. *Report: Changes in Climate Extremes and Their Impacts on the Natural Physical Environment*. A Special Report of Working Groups I and II of the IPCC, Annex II managing the Risks of Extreme Events and Disasters to Advance Climate Change Adaptation. Cambridge University Press, Cambridge, UK.
- Kult, J., Choi, W. and Choi, J., 2014. Sensitivity of the Snowmelt Runoff Model to snow covered area and temperature inputs. *Applied Geography*, 55, pp.30-38.
- Li, F., Zhang, G. and Xu, Y., 2016. Assessing climate change impacts on water resources in the Songhua River basin. *Water*, 8(10), p.420.
- Li, H., Beldring, S., Xu, C.Y., Huss, M., Melvold, K. and Jain, S.K., 2015. Integrating a glacier retreat model into a hydrological model—Case studies of three glacierised catchments in Norway and Himalayan region. *Journal of Hydrology*, 527, pp.656-667.
- Menon, S., Koch, D., Beig, G., Sahu, S., Fasullo, J. and Orlikowski, D., 2010. Black carbon aerosols and the third polar ice cap. *Atmospheric Chemistry and Physics*, 10(10), pp.4559-4571.
- Naeem, U.A., Hashmi, H.N. and Shakir, A.S., 2013. Flow trends in river Chitral due to different scenarios of glaciated extent. *KSCE*

- Journal of Civil Engineering, 17(1), pp.244-251.
- Robinson, D.A. and Frei, A., 2000. Seasonal variability of Northern Hemisphere snow extent using visible satellite data. *The Professional Geographer*, 52(2), pp.307-315.
- Shen, Z.Y., Chen, L. and Chen, T., 2012. Analysis of parameter uncertainty in hydrological and sediment modeling using GLUE method: a case study of SWAT model applied to Three Gorges Reservoir Region, China. *Hydrology and Earth System Sciences*, 16(1), pp.121-132.
- Tahir, A.A., Chevallier, P., Arnaud, Y., Ashraf, M. and Bhatti, M.T., 2015. Snow cover trend and hydrological characteristics of the Astore River basin (Western Himalayas) and its comparison to the Hunza basin (Karakoram region). *Science of the total environment*, 505, pp.748-761.
- Tahir, A.A., Adamowski, J.F., Chevallier, P., Haq, A.U. and Terzago, S., 2016. Comparative assessment of spatiotemporal snow cover changes and hydrological behavior of the Gilgit, Astore and Hunza River basins (Hindukush–Karakoram–Himalaya region, Pakistan). *Meteorology and Atmospheric Physics*, 128(6), pp.793-811.
- Tahir, A.A., Chevallier, P., Arnaud, Y., Neppel, L. and Ahmad, B., 2011. Modeling snowmelt-runoff under climate scenarios in the Hunza River basin, Karakoram Range, Northern Pakistan. *Journal of hydrology*, 409(1-2), pp.104-117.
- Tahir, A.A., Hakeem, S.A., Hu, T., Hayat, H. and Yasir, M., 2017. Simulation of snowmelt-runoff under climate change scenarios in a data-scarce mountain environment. *International Journal of Digital Earth*, pp.1-21.
- Yaseen, M., Nabi, G. and Latif, M., 2016. Assessment of climate change at spatio-temporal scales and its impact on stream flows in mangla watershed. *Pakistan Journal of Engineering and Applied Sciences*.



ISBN: 978-969-8670-06-01



Centre of Excellence on Water Resources  
Engineering  
UET, G.T. Rd, Lahore- Pakistan. 54890  
Tel: +92 42 99250257  
Fax: +92-42-99250259  
Email: [cewre@cewre.edu.pk](mailto:cewre@cewre.edu.pk)  
[www.cewre.edu.pk](http://www.cewre.edu.pk)

For orders, please contact:  
Conference Organizing Committee  
Tel: +92 42 99250257  
Email: [cewre.media@gmail.com](mailto:cewre.media@gmail.com)

 Printed on recycled paper.

© 2021 Centre of Excellence on Water Resources Engineering,  
UET Lahore-Pakistan.

All rights reserved. Published 2021.